Living with Two X Chromosomes: of Mice and Women

Studies on the initiation mechanisms of X chromosome inactivation in stem cells and mouse models, and the role of RNF12 herein

Tahsin Stefan Barakat

Cover shows a collection of pictures obtained from immunofluorescence and fluorescence *in situ* hybridization experiments performed throughout this thesis work.

ISBN: 978-94-6182-154-6
Cover and layout design: Tahsin Stefan Barakat

The work described in this thesis was performed at the Department of Reproduction and Development, Erasmus MC - University Medical Center, Rotterdam, The Netherlands

Printing of this dissertation has been kindly supported by:
Department of Reproduction and Development, Erasmus MC - University Medical Center, and Erasmus University Rotterdam
Teckelkennel "Vom Eschenweg", Jutta Barakat

Living with Two X Chromosomes: of Mice and Women

Studies on the initiation mechanisms of X chromosome inactivation in stem cells and mouse models, and the role of RNF12 herein

Leven met twee X chromosomen: over muizen en vrouwen

Onderzoek naar de initiatie mechanismen van X chromosoom- inactivatie in stamcellen en muismodellen, en de rol van RNF12 daarin

Thesis

to obtain the degree of Doctor from the
Erasmus University Rotterdam
by command of the
rector magnificus
Prof.dr. H.G. Schmidt
and in accordance with the decision of the Doctorate Board

The public defence shall be held on
Wednesday 12th September 2012 at 13:30 hrs

by

Tahsin Stefan Barakat

Born in Meerbusch, Germany

Doctoral Committee

Promotors: Prof.dr. J. H. Gribnau
Prof.dr. J. A. Grootegoed

Other members: Prof.dr. E. Heard
Prof.dr. F. Grosveld
Dr. R. J. H. Galjaard

CONTENT

CHAPTER 1 ..... **9**

PART 1: INTRODUCTION ON X CHROMOSOME INACTIVATION 9
PART 2: THE X CHROMOSOME, X CHROMOSOME INACTIVATION AND ITS IMPLICATIONS FOR HUMAN DISEASE 45
SCOPE OF THIS THESIS 83

CHAPTER 2 ..... **85**

RNF12 IS AN X-ENCODED DOSE DEPENDENT ACTIVATOR OF X CHROMOSOME INACTIVATION 85

CHAPTER 3 ..... **117**

PRECISE BAC TARGETING OF GENETICALLY POLYMORPHIC MOUSE ES CELLS 117
A RESTRICTION FRAGMENT LENGTH POLYMORPHISM BASED BACTERIAL ARTIFICIAL CHROMOSOME TARGETING STRATEGY FOR EFFICIENT AND FAST GENERATION OF KNOCKOUT ALLELES IN POLYMORPHIC MOUSE EMBRYONIC STEM CELLS 131

CHAPTER 4 ..... **165**

X-CHANGING INFORMATION ON X INACTIVATION 165

CHAPTER 5 ..... **179**

RNF12 ACTIVATES *XIST* AND IS ESSENTIAL FOR X CHROMOSOME INACTIVATION 179
ADDENDUM: MICE DELETED FOR *XIST* INTRON 1 DO NOT SHOW AN X CHROMOSOME INACTIVATION PHENOTYPE 207

CHAPTER 6 ..... **213**

RNF12 INITIATES X CHROMOSOME INACTIVATION BY TARGETING REX1 FOR DEGRADATION 213

CHAPTER 7 ..... **239**

INITIATION OF X INACTIVATION IS REGULATED BY TRANS-ACTING ACTIVATORS AND CIS-ACTING ELEMENTS: NO EVIDENCE FOR A FUNCTIONAL INVOLVEMENT OF X-PAIRING 239

CHAPTER 8 ..... **269**

LOSS OF RANDOM AND IMPRINTED XCI IN *RNF12* MUTANT MICE 269

CHAPTER 9 ..... **285**

X INACTIVATION IN HUMAN IPS AND ES CELLS 285

CHAPTER 10 ..... **311**

GENERAL DISCUSSION 311

REFERENCES **327**

APPENDIX 367

ABBREVIATIONS 368
SUMMARY 369
SAMENVATTING 373
CURRICULUM VITAE 377
LIST OF PUBLICATIONS 379
PHD PORTFOLIO 381
ACKNOWLEDGEMENTS 383

Für meine Mutter

Chapter 1

Part 1: Introduction on X chromosome inactivation

Parts of this chapter have been published in

Tahsin Stefan Barakat and Joost Gribnau (2010)
"X chromosome inactivation and embryonic stem cells"
Adv Exp Med Biol 695: 132-154
&
Tahsin Stefan Barakat and Joost Gribnau (2012)
"X chromosome inactivation in the cycle of life"
Development 139: 2085-2089

Sex determination, sex chromosomes and their evolution

Sexual reproduction represents one of nature's most ingenious inventions during evolution [1], facilitating exchange of genes located on homologous chromosomes in the generated offspring, providing important variation for natural selection. To enable sexual reproduction, a difference in sex between individuals is a prerequisite, and several ways of sex determination have evolved in different species. In species like crocodiles, lizards and turtles, the sex is determined by the incubation temperature of the egg [2-3]. However, in many species, the sex of an individual is genetically determined by genes located on sex chromosomes [4]. Mammals are heterogametic, in which the female nucleus contains two X chromosomes and a male nucleus one X chromosome and one Y chromosome. Almost 100 years ago, Herman Muller proposed that in *Drosophila melanogaster*, the X and Y chromosomes originated from a common pair of autosomes [5]. This idea was later applied by Susumu Ohno to vertebrates, who argued that the X chromosome remains conserved, whereas the Y chromosome degenerates during evolution [4]. Now it is generally accepted that sex chromosomes originated from a pair of autosomes, and divergence of these autosomes in proto-X and proto-Y chromosomes was initiated, in the ancestor of marsupials and placental mammals, by the emergence of the key male sex determining gene *Sry*, which evolved from the ancestral *Sox3* gene on the proto-Y chromosome [6-11]. In subsequent steps the proto-Y chromosome acquired male beneficial genes, resulting in a genomic region which was non-homologous with the X chromosome. It is thought that the absence of homology initiated degeneration of the Y chromosome. Nowadays the Y chromosome contains less than a 100 single copy and multicopy genes, of which are 78 male specific, most of them involved in male fertility and sex determination [12-13]. The X chromosome is still able to recombine in meiosis in the female germ line, which prevented degradation, and which contributed to the maintenance of a large chromosome containing more than a thousand genes, involved in a plethora of biological functions, varying from brain development to metabolism and fertility [4, 14].

The human X chromosome is approximately 155 Megabase (Mb) in length, and harbors around 1098 genes (**Figure 1**). With its 7.1 genes per Mb, the gene density of the X chromosome is among the lowest of all chromosomes [14]. Although the X chromosome contains the longest human gene known, the dystrophin (DMD) locus, spanning more than 2 Mb, the average gene length of X chromosomal genes is lower compared to the other human chromosomes [14]. Only around 1.7% of all nucleotides of the human X chromosome are being transcribed into protein coding transcripts, whereas the remainder is composed of repetitive sequences, pseudogenes and genes encoding non-coding RNAs [14]. Among the genes on the X chromosome, there is an accumulation of so-called cancer-testis antigen genes, which are characterized by their expression in certain cancers, whereas in physiological conditions, their expression is predominantly found in testis [14-19]. Interestingly, the same low gene density and accumulation of testis-specific genes is found in the chicken Z chromosome [20]. In the chicken, sex is determined by the ZW system in which the females are heterogametic. Although the human X and chicken Z chromosome evolved from different ancestral chromosomes, expansion of the one sex chromosome that has a homologous pairing partner in either female (XX in mammals) or male (ZZ in birds)

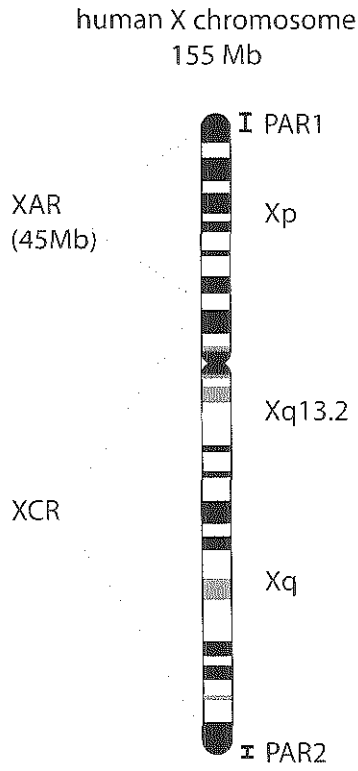

Figure 1: The human X chromosome
Schematic of the human X chromosome, showing the short (Xp) and long arm (Xq), with the pseudoautosomal regions (PAR), and the X added (XAR) and X conserved regions (XCR). The X inactivation center, located at Xq13.2 is indicated as well.

meiosis, by accumulation of intergenic regions and repetitive areas like LINE repeats, together with acquisition of testis-specific genes on the larger chromosome X or Z seem to be a common theme in the evolution of sex chromosomes [20].

The evolution of the mammalian X chromosome started more than 165 million years ago (MYA), long after the divergence of the mammalian and avian lineages. Alignment comparison between the human X chromosome and the chicken genome has shown that a large block of homology can be found between the long arm of the human X chromosome (Xq) and chicken chromosome 4p [14]. This so-called X conserved region (XCR) can be found in all three mammalian groups - the placental mammals (Eutheria), the marsupials (Methateria) and the egg-laying mammals (Prototheria, monotremes) – and is therefore a descendant from a proto-X chromosome present before the divergence of the

mammalian lineages 150 MYA [7, 14]. Another block of homology can be found between chicken chromosome 1 and the short arm of the human X chromosome (Xp). This region is not conserved in marsupials and monotremes, and must have been added to the proto-X chromosome before radiation of the placental mammals around 100 MYA, and after separation from the marsupial lineage 150 MYA, and is referred to as the X added region (XAR) [7, 14, 21].

Although the emergence of *Sry*, some 160 MYA, has initiated the divergence of the proto-X and Y chromosomes, and prevention of recombination between the X and Y has resulted in degeneration of the Y chromosome, some small parts of our sex chromosomes are still homologous to each other, and still recombine during male meiosis [22]. Intriguingly, these so-called pseudoautosomal regions are not remnants of the original autosomal progenitor, but are added later during evolution to both the X and the Y chromosomes. The 2.7 Mb pseudoautosomal region located at the short arm of the human X and Y chromosomes, called PAR1, appears to be crucial for proper sex chromosome pairing and subsequent chromosome segregation during male meiosis [22-23], and was added 80 to 100 MYA. Around 24 genes being expressed from both the X and the Y chromosomes are mapped to the PAR1, including 7 well defined genes affecting energy metabolism and growth. Another, 330 kb small, pseudoautosomal region (PAR2) is located at the distal tip of the long arm of the human sex chromosomes. This region of the X and Y chromosomes seems to be primate specific, as its addition took only place 4 to 10 MYA [14, 24-25], and does not seem to be crucial for male fertility [26].

The X chromosome and the need for dosage compensation

Both sexes contain an equal number of autosomal chromosomes, and a balanced dosage of X linked genes is needed to accomplish functional cell physiology [27-29]. In heterogametic species, the evolution of a single gene-rich X and gene-pore Y chromosome in males results in a potential dosage problem, as in males only a single X chromosome is responsive for the same functions as two X chromosomes in females. Many genes act in a dose-dependent manner, and therefore during the attrition of the proto-Y, the monosomy of the proto-X chromosome in males is believed to be compensated by an up-regulation of gene transcription from the newly formed X chromosome, thereby restoring the equilibrium between autosomal and X-linked genes [4]. For females, this up-regulation of X-linked gene transcription would further disrupt the desired equilibrium, as the presence of two, and highly transcribed, X chromosomes would disrupt an equal gene dosage between the autosomes and sex chromosomes in females. To prevent this potential problem, in placental mammals, dosage compensation of X-linked genes between both sexes is achieved by inactivation of one of the two X chromosomes in females, in a process called X chromosome inactivation (XCI) [4, 30-32]. XCI occurs during early female development, and results in functional heterochromatinization and silencing of the X chromosome, which is maintained during subsequent cell divisions throughout life [33]. XCI leads to mono-allelic expression of most X-linked genes, with the exception of genes located in the pseudo-autosomal region(s) and a number of other genes escaping from inactivation [34-

35]. These latter genes often have X-degenerate counterparts on the Y chromosome, which also carries a pseudo-autosomal region homologous to that of the X chromosome. As a result, beside these escaping genes, only one X chromosome is functionally active in both sexes. Since expression of X-encoded genes from this chromosome and the single X in male cells is two-fold up-regulated compared to autosomes, the proper dosage of X-encoded genes is restored, thereby complying to Ohno's hypothesis [4].

The first experimental evidence for this hypothesis has come from studies involving the chloride channel gene *Clc4*, which is X-linked and subject to XCI in the mouse strain *Mus spretus*, but autosomal in different laboratory mouse strains [36]. Quantification of allele specific gene expression in crosses of hybrid mice has shown that the autosomal copy of *Clc4* is expressed at around half the level of expression compared to the X-linked copy, providing evidence that indeed the transcription of the X chromosome is up-regulated compared to autosomes [36]. Micro-array studies investigating whole genome wide expression of genes have consolidated the idea that the X chromosome is up-regulated [37-40]. Although, recently, an RNAseq study has claimed to reject Ohno's hypothesis [41-42], reporting no up-regulation of the X chromosome and a resulting X-to-autosome expression ratio of 0.5 in both human and mouse. Subsequent studies have shown that this result can be explained by the fact that low and tissue-specifically expressed genes were taken into consideration in this study [43-44]. When only genes showing moderate to high expression were compared, an up-regulation of the X chromosome was found, bringing the X-to-autosome ratio to 0.7 [43-44]. The reason that the X-to-autosome ratio did not increase to 1, as would be expected if up-regulation of X-linked genes would be complete, might be related to the fact that RNAseq might result in noisy data [43]. Alternatively, this might indicate that only certain dosage sensitive genes show up-regulation, whereas other genes do not. Evidence for this has recently been obtained in a study which focused on X-linked genes, whose gene products are involved in multi-protein complexes [45]. Indeed, for X-linked genes encoding proteins being part of large protein complexes, an X-to-autosome ratio of 1 has been found [45]. This might indicate that Ohno's hypothesis mainly holds true for dosage sensitive genes.

In different species, the problem of dosage compensation has been differently solved (**Figure 2**). In *Drosophila melanogaster*, males harbor a single X chromosome, and a Y chromosome which is not related to the human Y chromosome, whereas females have two X chromosomes. A difference in X-linked dosage of genes is prevented in this species by sex-specific up-regulation of gene transcription from the single X chromosome only in males [29, 46-48]. Since the X chromosomes in females are not being hypertranscribed, there is no need for a further dosage compensation mechanism in female flies. In the nematode *Caenorhabditis elegans*, hermaphrodites have two X chromosomes, whereas males have a single X chromosome and no Y chromosome. Here it are the hermaphrodites, which reduce the X-linked transcription, to achieve a similar transcription level between the sexes [49-50]. Since de facto in both sexes of this worm species only one X chromosome is active, also here an up-regulation mechanism has evolved, comparable to the situation in placental mammals.

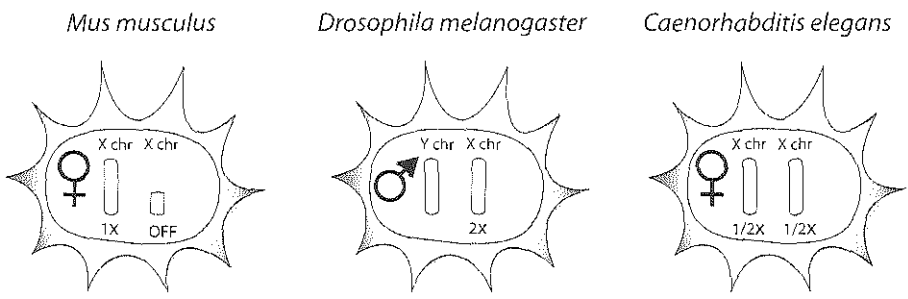

Figure 2: Dosage compensation in different species
In mice and other placental mammals one X chromosomes in females is inactivated during early embryonic development to achieve an equal dosage of X-linked genes between both sexes. In the fly, the single X chromosome in males becomes two-fold up-regulated. In worms, hermaphrodites reduce expression from their two X chromosomes, to equalize expression from a single X chromosome in males.

X chromosome inactivation in the mouse: development and timing in the cycle of life

In mice, two forms of XCI exist. Imprinted XCI (iXCI) of the paternally inherited X chromosome (Xp) is initiated very early during female embryonic development, around the two- to eight-cell stage [51-52], and is maintained in the extra-embryonic tissues and its derivatives, including the fetal placenta [53] (**Figure 3**). The Xp is reactivated in the inner cell mass (ICM) of the developing female embryo [54]. Then, at around day 5.5 of embryonic development, a second round of XCI is initiated in the embryo proper developing from the epiblast, which is random with respect to the parental origin of the future inactive X chromosome (Xi) [30]. This random inactivation (rXCI) is also observed for female mouse embryonic stem (ES) cells, when these ES cells are induced to differentiate.

ES cells are derived from the ICM of a blastocyst. They are characterized by the ability of self renewal and are pluripotent with the capacity to form all cell types of the embryo proper and the adult organism upon development or differentiation [55-56]. Besides potential applications for regenerative medicine, ES cells are an ideal study system for early mammalian development from the pre-implantation period onwards [57-58]. Female mouse ES cells retain two active X chromosomes (Xa) and upon differentiation these cells initiate random XCI, making them the prevailing model system to study XCI [59-60]. This points to a link between rXCI and the transition of cells from a pluripotent state to more differentiated cell types. Besides simulating early development in an

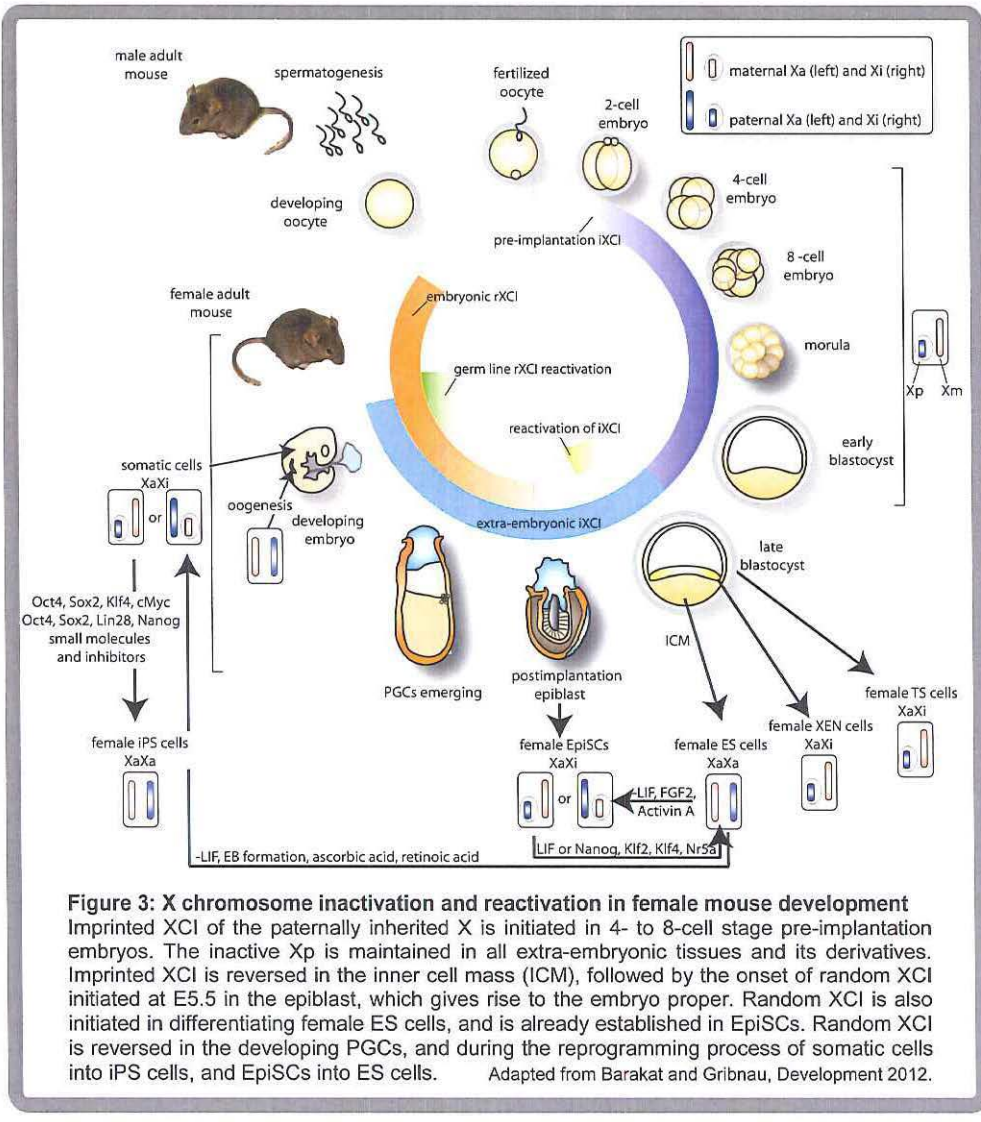

Figure 3: X chromosome inactivation and reactivation in female mouse development Imprinted XCI of the paternally inherited X is initiated in 4- to 8-cell stage pre-implantation embryos. The inactive Xp is maintained in all extra-embryonic tissues and its derivatives. Imprinted XCI is reversed in the inner cell mass (ICM), followed by the onset of random XCI initiated at E5.5 in the epiblast, which gives rise to the embryo proper. Random XCI is also initiated in differentiating female ES cells, and is already established in EpiSCs. Random XCI is reversed in the developing PGCs, and during the reprogramming process of somatic cells into iPS cells, and EpiSCs into ES cells. Adapted from Barakat and Gribnau, Development 2012.

experimental setting, XCI in ES cells is important to accomplish proper cell function and developmental potential of these cells in culture or when transplanted back to an embryo. The recent discovery of induced pluripotent stem (iPS) cells, which have ES cell characteristics and are derived from somatic cells by reprogramming with defined pluripotency factors [61-66], has reemphasized the importance of studying initiation, maintenance and reversibility of XCI in this type of cells. Among others, the active status of X chromosomes in ES and iPS cells can be used as a pluripotency marker, as during iPS

reprogramming the inactivated X chromosome (Xi) from somatic cells becomes reactivated in mouse iPS cells [67-68].

After initiation of rXCI, the transcriptional silent state is maintained through inheritance of epigenetic modifications, so that the choice of the Xi is maintained in dividing cells. As a consequence, female tissues are a mosaic of cells expressing either Xp or the maternally derived Xm. This is nicely demonstrated by female (or XXY male) calico cats, carrying red and brown hair color genes on the two X chromosomes.

Although rXCI is a very stable form of epigenetic gene silencing, it is reversed in the germ line, in primordial germ cells (PGCs), around the time when also the genomic imprints are erased [69]. Hence, oocytes contain two active X chromosomes. In remarkable contrast, the single X chromosome in spermatocytes is silenced, in the form of an XY body, through a meiotic sex chromosome inactivation (MSCI) mechanism which targets unpaired chromatin regions which are not engaged in homologous meiotic recombination [70]. Progressive loss of homologous recombination between X and Y is interlinked with the evolution of the heterologous XY chromosome pair from a pair of autosomes. To cope with the consequences of this evolution, MSCI likely is as important as XCI. However, the mechanism leading to MSCI is different from that leading to XCI.

Cis acting factors involved in regulation of X chromosome inactivation

Transcriptional silencing of a whole chromosome during development has fascinated biologists for decades, and in recent years a considerable amount of knowledge has been acquired which now contributes to our understanding of the molecular mechanisms involved in such silencing, among others in mammalian XCI. Genetic studies in mice and humans with X-to-autosome translocations have revealed that a major X-linked control locus, the X inactivation center (Xic in mice and XIC in humans) is necessary for XCI to occur [71-74]. Early studies in humans had raised the idea that the XIC must be located on the long arm of the X chromosome close to the centromere, based on the observations that abnormal X chromosomes with the presumed XIC present in two copies have a bipartite Barr body morphology, and isochromosomes containing the short arm of the X chromosome are not present in the population, presumably because such chromosomes are unable to inactivate because of a lack of the XIC [75-77]. Further studies of abnormal patient X chromosomes revealed that only one XIC can be present, and this must be located between Xq11.2 and Xq21.1 [78]. By studying human and primate mitotic metaphase chromosomes, it was noticed that a female specific bend is present at Xq13.3-q21.1, which was likely to be the visible manifestation of the condensation process of the Xi [79-80], starting at the XIC. By making use of somatic cell hybrids containing rearranged X chromosomes, and another set of abnormal patient cells with X chromosomes which retained the possibility to be inactivated, the minimal region of overlap, the XIC, was further delineated to Xq13 [81], as this region was always present in cells able to undergo XCI. Similar studies in mice identified the Xic [71, 73, 82], which encompasses more than 1 Mb on the mouse X chromosome [83], and has been shown to contain 13 genes of which

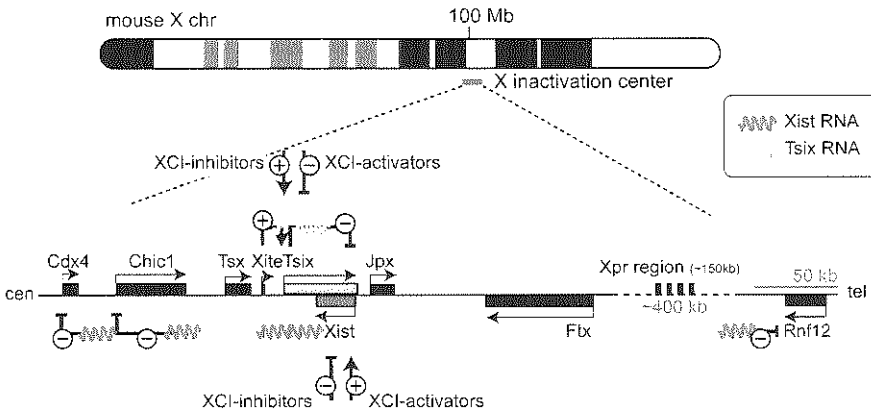

Figure 4: The X inactivation center
Three non-coding X-linked genes, located within the X inactivation center, are important for the XCI process. *Xist* coats the Xi in *cis*, recruiting chromatin modifiers involved in silencing the Xi. *Tsix* and *Xite* are transcribed anti-sense to *Xist*, and repress *Xist*. *Xist*, *Tsix* and *Xite* are regulated by *trans*-acting X-encoded activators of XCI, and autosomally-encoded repressors of XCI. Adapted from Barakat and Gribnau, Development 2012.

at least 3 genes are involved in the process of XCI. These genes, *Xist*, *Tsix* and *Xite*, are non-coding, and represent the master switch locus involved in silencing of the X chromosome in *cis* (**Figure 4**).

The first gene which has been found to map to the XIC/Xic is the X-inactive specific transcript (*Xist* in mice, *XIST* in humans) [74, 84-85]. *Xist* is the only known gene which is specifically expressed from the Xi. *Xist* is a non-coding gene, consisting of 7 exons in the mouse and 8 exons in human, producing a poly-adenylated RNA molecule (17 kb in human and 15 kb in mouse), which is subject to alternative splicing [86-87] and has a half-life of approximately 4 to 6 hours [88-90]. *Xist* RNA is tightly associated with the Xi [91-92], and it is required for XCI to occur in *cis*, as knockout studies in female ES cells and mice have shown that X chromosomes bearing a deletion of the *Xist* gene are unable to inactivate the mutated X [93-95]. In case of the knockout mice, an *Xist* deleted allele can be transmitted trough the maternal germ line, resulting in healthy male offspring, or females in which always the non-mutated allele is inactivated. In case of paternal transmission, female offspring is not born, due to a failure of initiation of imprinted XCI which results in a virtual absence of placental tissues [93-94]. During XCI, expression of *Xist* is up-regulated from the future Xi [89, 96]. *Xist* RNA molecules spread from the Xic across the X chromosome in *cis*, and cover the Xi completely. By spreading along the Xi, *Xist* RNA induces heterochromatinization of the X chromosome by attracting chromatin modifiers involved in gene silencing [97-99].

In the mouse, two DNAseI hypersensity sites and 7 footprints characterize the primary *Xist* promoter (P1), which is located directly upstream of the gene [100-102]. Footprint II is a putative TATA box, although this site does not seem to be a direct TATA-binding protein (TBP) binding site. At the transcriptional start site, where footprint 1 is

located, a putative YY1 binding site has been found. In addition, binding of the transcription factors E2F, AP1, SP1 and CBP has been found in the region of the minimal promoter [101]. Further upstream of *Xist*, 5 additional footprints have been identified, but their function remains to be determined [103-104]. A recent study which makes use of a panel of 12 different reporter constructs containing different parts of the *Xist* promoter has identified three enhancer and three silencing elements in the *Xist* promoter, and found putative binding sites for the estrogen receptor, retinoic acid receptor, SRY, and the transcription factors C/EBP, NFY and NFAT [105].

Another promoter, the P2 promoter, is located +1503 bp of the *Xist* transcriptional start site [106]. Transcripts derived from this promoter lack the A-repeat which is crucial for silencing, but seem to be more abundantly present in female somatic cells [106]. The functional relevance of these transcripts is not clear. The P0 promoter, located upstream of P1 was proposed to result in unstable *Xist* transcripts [88, 106], but this turned out to be an artefact, representing the 3' termination site of antisense transcription through the *Xist* locus [89, 107].

In human, the *XIST* promoter has been shown to bind the common transcription factors SP1, YY1 and TBP, and seems to be constitutively active in reporter constructs [108], which indicates that, prior to XCI and after XCI initiation, *XIST* must be actively repressed on the Xa. This repression might include repressive histone modifications, and DNA methylation [109-114].

One of the most characteristic features of the produced *Xist* RNA is the presence of 6 highly conserved tandem repeats, termed repeat A to F [86-87, 115-116]. The A-repeat, located in *Xist* exon 1, seems to full fill a crucial role in the gene silencing capability of *Xist*, and consists of 7.5 copies of a direct repeat unit, constant CG rich and variable AT rich, which harbors two short inverted repeats that might fold into a secondary structure comprising two stem loops. This stem loop structure is believed to be able to interact with putative proteins, thereby contributing to the silencing function of this repeat. The B-repeat is transcribed from a microsatellite tract (CCCCAG) n which is present in many species, but the function of this repeat is unknown. The C-repeat, transcribed from a sequence located 3 kb downstream of the A-repeat, consist of 14 tandem repeats of a C-rich sequence in the mouse, and has been implicated in the *cis* localization of the *Xist* RNA. Only one copy of this 11 bp monomer is present in humans. Repeat D is the largest of all repeats, but its monomers are less conserved during evolution, resulting in a large variability between species. Repeat E also shows a high degree of variability, with a small monomer length between 25 and 30 bp, and like the D-repeat, its functions are unclear. Finally, the F-repeat is transcribed from sequences located at the start of the P2 promoter, and contains a binding site for the cell cycle factor E2F [117]. Therefore, this repeat, with a 19 bp motif, might be important for the regulation of *Xist* transcription.

Another non-coding gene located within the mouse Xic is *Tsix*, which is transcribed antisense to *Xist* [118]. *Tsix* contains four exons and at least two transcriptional start sites, producing a 40 kb transcript, which only localizes to the Xic, as determined by RNA-FISH experiments. The *Tsix* gene fully overlaps with the *Xist* gene in mice, and *Tsix* was shown to negatively regulate expression of *Xist*, as a deletion of *Tsix* leads to up-regulation of *Xist* transcription, and near exclusive inactivation of the mutated X chromosome in female cells [119-120]. Prior to XCI, expression of *Tsix* is from both X

chromosomes in a 10- to 100-fold excess compared to *Xist*, and expression is continued, transiently after initiation of XCI, on the future Xa [121]. On the Xi, transcriptional shutdown of *Tsix* is accompanied by chromatin changes at the *Tsix* promoter [122]. The exact mechanisms involved in *Tsix*-mediated silencing of *Xist* are unknown. Since expression of *Tsix* transcripts is found in a gradient along the *Xist* gene, with more transcripts in the 5' portion of *Tsix* relative to the 3' portion of the gene, a role for transcriptional interference as a mechanism to suppress *Xist* has been proposed [89, 121, 123]. Another possible mechanism by which *Tsix* might suppress *Xist* transcription is via RNA-mediated silencing. It has been shown that *Tsix* regulates the methylation status and thus the activity of the *Xist* promoter, via *de novo* methyltransferase 3a (DNMT3A) [89, 124]. Also, active chromatin marks are more abundant at the *Xist* promoter in cells with a deficient *Tsix* gene in *cis*, whereas marks of repressed chromatin are reduced [111, 125-127]. Antisense transcription through the *Xist* promoter itself seems to be crucial for the establishment of repressive chromatin marks, as a truncation of *Tsix* to 93% of its normal length failed to induce *Xist* silencing [112]. Also deletion of the *Dxpas34* element, which is a CpG island located downstream to the major *Tsix* promoter and also initiates antisense transcription, abrogates *Xist* silencing in *cis*, thereby further emphasizing the importance of antisense transcription in *Tsix*-mediated silencing of *Xist* [127-129]. Furthermore, the methylation status of this CpG island coincides perfectly with antisense transcription through *Xist* [130-131]. *Xist* and *Tsix* transcripts are partially overlapping, and a possible role for an RNAi-mediated mechanism regulating XCI therefore cannot be excluded [132]. Small xiRNAs, ranging in size from 25 to 42 nucleotides, have indeed been detected from different regions within the *Xist* gene, and a mutation of the endonuclease *Dicer* resulted in a loss of xiRNA formation and decreased methylation of *Xist*, implicating a role for *Dicer* in XCI. This is disputed by others, who found that *Dicer* null-ES cells show normal XCI, and that the effects on Xa are mediated by a decreased activity of *de novo* methyltransferases rather than a direct effect of *Dicer* [133-134]. Therefore, at present the exact role of small RNAs in XCI initiation is unclear. Also, over-expression in *cis* of *Tsix* cDNA in a cell line with abrogated endogenous *Tsix* transcription did not result in restoration of *Tsix*-mediated *Xist* silencing, which argues against an RNAi-mediated process [135].

The third non-coding gene involved in XCI is *Xite*, for X chromosome intergenic transcript element [136]. This gene is located approximately 10 kb upstream of *Tsix*, and its expression and methylation pattern during XCI is similar to that of *Tsix*. *Xite* is believed to be the positive regulator of *Tsix* [137]. Deletion of *Xite* results in reduced antisense transcription of *Tsix* through the *Xist* locus, implying a similar role for *Xite* in inhibiting *Xist* expression as for *Tsix* and *Dxpas34* [131, 136].

Beside *Xist*, *Tsix* and *Xite*, the Xic harbors several other genes (**Figure 5**), most of unknown function. An involvement of these genes in the regulation of XCI was unknown at the start of this thesis research. At its centromeric site, a neuron-specific gene called nucleosome assembly protein 1-like 2 (*Nap1l2*, also known as *Bpx*) is located, which encodes a protein of 460 amino acid residues [138-139]. This gene is entirely located in the last intron of *Ppnx*, which is transcribed in the same orientation [140]. *Ppnx* is highly expressed in undifferentiated ES cells, and seems to be a testis-specific gene in adult mice, where expression is found in germ cells having entered meiosis [140]. *Ppnx* does not seem

to be conserved in human. *Ppnx* has different splice variants, and since *Ppnx* and *Nap1l2* have a different expression pattern, transcriptional interference between these two genes is likely to be prevented [140]. Also centromeric, *Cdx4*, a small gene with three exons, belonging to the caudal family of homeobox genes, encodes a 282 amino acid protein which is highly conserved amongst species [140-141]. *Chic1* is located upstream of *Cdx4*, spanning 40 kb in mouse, and 163 kb in human [140]. Also known as BRX, CHIC1 belongs to the familiy of cysteine-rich, hydrophobic proteins, and is specifically expressed in brain tissues [142]. Between *Chic1* and *Xite*, another testis-specific gene is located, which is called *Tsx* [140, 143]. *Tsx* spans 10 kb in the mouse, and encodes a 156 amino acid, highly acidic protein without homology to any other protein [140, 144]. Immunostaining showed exclusive expression of *Tsx* in pre-meiotic germ cells in pre-pubertal mouse testes, whereas in adult mice *Tsx* mRNA has been found in Sertoli cells, the somatic cells supporting spermatogenesis. *Tsx* is not expressed in the female germ line, but expression can be found from the 2-cell stage onwards throughout pre-implantation development [145]. *Tsx* has become a pseudogene in humans [140]. The region upstream of *Xist*, is characterized by the presence of *Jpx* and *Ftx*, two genes transcribed into non-coding RNAs of unknown function [140]. *Jpx*, also called *Enox*, is located 10 kb upstream of *Xist*, is transcribed in the opposite direction, and is well conserved among species, implicating a potential function for this non-coding RNA. *Jpx* expression does not seem to be sex-specific or developmentally regulated, is ubiquitously expressed in somatic tissues [140], and partially escapes XCI [146-147]. *Ftx* is transcribed in the same orientation as *Xist*, and its expression is found in multiple tissues [140]. Yet another testis specific gene, *Cnbp2*, is located 150 kb upstream of *Xist* [140]. It encodes a 170 amino acids protein which has a high similarity to cellular nucleic acid binding protein (CNBP), a zinc-finger DNA binding protein. Since *Cnbp2* has only one exon, but is conserved amongst species, it is likely to be a retrogene derived from *Cnbp* [140]. Its function is unknown. Finally, around 300 kb upstream of *Xist*, the gene *Xpct*, encoding X-linked PEST box containing transporter, is located, which is also known as *Slc16A2* or *Mct8* [148-149]. *Xpct* covers 147 kb in the mouse, and 117 kb in humans, and its 6 exons are highly conserved amongst all eutherians. The 565 amino acid XPCT protein is a member of the monocarboxylate cotransporter family that mediates movement of lactate and pyruvate across membranes, and is involved in thyroid hormone transport [149-150]. Hence, mutations in *XPCT* cause a human mental retardation syndrome [151-152]. *Xpct* is subject to XCI, as only expression from the Xa has been observed [148-149, 153]. *Xpct* is highly expressed in liver and kidney, at lower levels in heart, brain and lung, and its expression is low or absent in spleen, testis, skeletal muscle [149] and undifferentiated ES cells [154]. Homozygous knockout mice show abnormal thyroid hormone metabolism, but are born at expected Mendelian frequencies [155].

Interestingly, the region upstream of *Xist*, including *Jpx*, *Ftx*, *Cnbp2* and *Xpct*, displays several chromatin features of the inactive X chromosome, including enrichment of H3K9me and H3K27me3, prior to differentiation [156-157]. The functional relevance of this so-called heterochromatic hotspot remains to be determined.

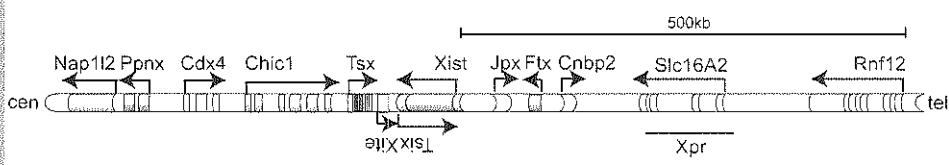

Figure 5: The X inactivation center on the mouse X chromosome
Shown are all 13 genes known to map to the X inactivation center. See text for details.

Counting the number of X chromosomes and the initiation of random X chromosome inactivation

A long standing question in XCI research involved the counting and choice mechanisms regulating initiation of XCI, leading to inactivation of the proper number of X chromosomes. How does a cell sense the number of X chromosomes present in a nucleus, and how many of them need to be inactivated? A number of clinical observations in patients with an aberrant number of X chromosomes have shed some light on this question. In patients with a supernumerary number of X chromosomes, like so-called 47,XXX super females or 47,XXY Klinefelter patients, all but one X chromosome become inactivated [158-160]. In Turner syndrome patients, the single X chromosome present in these females does not undergo XCI, whereas in tetraploid female embryos two inactivated X chromosomes are found [161-162]. From this, the general rule has been deduced that XCI results in one Xa per diploid genome [163].

Several models, with increasing complexity and partially overlapping mechanisms, have tried to explain the XCI counting and initiation mechanisms (**Figure 6**). The blocking factor (BF) model predicts the presence of an autosomally encoded factor which is present in one entity in a diploid nucleus [72-73]. The BF is thought to act through binding to a DNA element, called counting element, and only interacts with one X chromosome, thereby rescuing this X from XCI in *cis*. Since there is only enough BF in a diploid nucleus to prevent XCI on one X chromosome, all additional X chromosomes will become silenced. The related symmetry breaking model states that the BF is not a single entity, but consists of several autosomally encoded molecules which assemble on the future Xa, thereby preventing XCI [164-165]. Since the Xic is necessary for XCI to occur, as XCI is initiated only in the presence of more than one Xic in a diploid nucleus, it seems likely that the postulated counting element must be located within the Xic. Several studies made use of transgenes and deletions, to identify the counting element, reasoning that when an additional counting element would be introduced into male ES cells, this should be able to titrate away the limiting BF and induce counting. Therefore, XCI should also occur on the endogenous X chromosome, which is now no longer protected by the BF.

Indeed, in several transgenic male ES cell lines with autosomally integrated transgenes covering *Xist* and *Tsix*, or *Xist* alone, ectopic XCI occurred on the single endogenous X chromosome [166-171]. Autosomal *Xist* expression and silencing of autosomal genes adjacent to the integration site was also observed. The transgenes used to

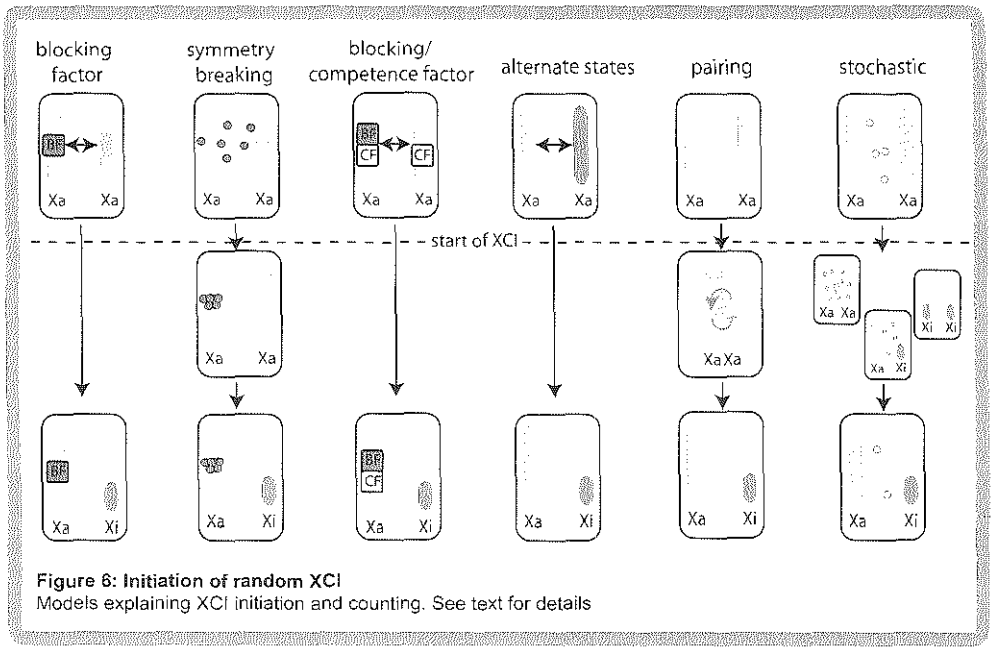

Figure 6: Initiation of random XCI
Models explaining XCI initiation and counting. See text for details

generate these ES cell lines varied from large YACs carrying >500 kb to small cosmids of only 35 kb covering only *Xist* and flanking regions [167]. These studies therefore indicated that factors involved in counting may be located within the sequences covered by the transgenes. However, other related studies did not show induction of counting using similar transgenes [172-174], or showed that only multicopy transgenes are able to induce counting [175]. Interestingly, studies involving a deletion of *Xist* on one X chromosome in female ES cells, which had shown that *Xist* is necessary for XCI to occur in *cis*, also revealed that *Xist* transcription and the deleted part of the *Xist* gene are not involved in counting, as XCI is normally initiated on the wild type X chromosome [93-95, 104, 176-177]. In contrast, different male *Tsix* mutant ES cells, some already generated prior to the identification of *Tsix*, displayed initiation of XCI on the single X chromosome, which suggested a role for the deleted sequences in the counting process [120, 123, 127, 129, 178]. Deletion of these sequences, however, did not disturb the counting process in female cells, but resulted in preferential inactivation of the mutated allele, showing that *Tsix* mediates silencing of *Xist* in *cis* [119]. These findings could be explained through a mechanism whereby the respective mutations disrupt the counting element, preventing BF binding. However, a heterozygous deletion of a region including *Xist*, *Tsix* and *Xite* (ΔXTX), in female ES cells and mice, did not result in a disturbed counting process, as the wild type X chromosome was normally inactivated [179]. This finding indicated that *Xist*, *Tsix* and *Xite* are not required for the counting process, and locate the counting element outside the deleted region, although studies with *Xist* transgenes suggest that overlapping sequences may be involved which play a redundant role in counting and initiation of XCI.

In contrast to all previously reported *Tsix* mutations, one described *Tsix* mutation (ΔCpG), which involves a deletion of the *Dxpas34* region, did not result in aberrant XCI in male cells [180]. Interestingly, female cells with a homozygous ΔCpG *Tsix* mutation showed chaotic XCI, with many cells initiating XCI on both X chromosomes. Based on this finding an X-encoded competence factor (CF) was hypothesized, involved in activation of XCI. One model comprising the combined action of a BF and CF postulates that the abundantly present CF inactivates all X chromosomes but not the one to which BF is bound [177]. Another hypothesis states that also the X-encoded CF is limiting and is titrated away by one 'copy' of the autosomally-encoded BF, which corresponds to a single X chromosome [180]. When more than one X chromosome is present in a diploid nucleus, the extra copies of CF will not be titrated by the BF, and will inactivate the remaining unprotected X chromosome(s).

The model of alternate states proposes that the two X chromosomes in an XX cell are already different prior to XCI [181]. This model is supported by the fact that cohesion of sister chromatids has been shown to be differentially regulated between two X chromosomes in undifferentiated ES cells. Also differences in DNA methylation and the chromatin state may play a role. Therefore, this model involves a putative epigenetic difference between two genetically identical chromosomes, existing prior to the initiation of XCI. However further experimental validations for these observation are needed.

A different model explains counting and choice in XCI by transient transvection or direct pairing of the two Xic's present in a female diploid nucleus [182-183]. This model is supported by observations that in early differentiating ES cells, there is a non-random spatial distribution of the Xic's in the nucleus, at which the Xic's move closer to each other prior to the onset of XCI [184]. These transient *trans*-interactions are only found in early differentiating cells which have started to express *Xist*, but have not yet recruited EZH2 or H3K27me3 [183].This transient pairing event may therefore play a role in the regulation of counting and choice. Pairing is facilitated by *Tsix* and *Xite* sequences, and it seems to be dependent on the action of CTCF [185]. The stem cell transcription factor OCT4 and ongoing transcription catalyzed by RNA polymerase II are also crucial for the pairing events [185-186]. A genomic region covering part of the *Slc16A2* gene, located 250 to 350 kb telomeric to *Xist* has been identified, which also mediates pairing of the X chromosomes at the onset of XCI [187], and was proposed to play a role in the activation of XCI. At present, it is unclear whether pairing has a functional role in XCI, or is a consequence of transcriptional activation of the Xic on both X chromosomes which may result in relocation of the Xic's close together in the nucleus. In line with this, the majority of Xic co-localizations occur in close proximity to the nuclear envelope [182]. Interestingly, pairing appears not to be required for initiation of XCI, as XCI is initiated in $XX^{\Delta 65kb}$ ES cells with a deletion distal to *Xist*, removing *Tsix* and *Xite* sequences, which abolish the XCI pairing event [182-183]. Therefore additional studies are needed to clarify the role of pairing in XCI.

Many of the above-discussed models assume that the XCI process is deterministic and mutually exclusive, in which always the correct number of X chromosomes are inactivated in female cells. However, *in vitro* studies with diploid and tetraploid ES and ICM cells revealed a significant percentage of cells with too many or too few Xi's [162, 179, 188], suggesting a stochastic mechanism directing the XCI process, with an

independent probability for every X chromosome to initiate XCI [179]. Comparison of the relative number of cells that initiated XCI between different diploid, triploid and tetraploid ES cells indicated that the X-to-autosome ratio determines the probability for an X chromosome to be inactivated [189] (**Figure 7**). The probability is the resultant of different factors: X-encoded XCI-activators and autosomally-encoded XCI-inhibitors that promote or repress *Xist* accumulation, respectively. Upon development or differentiation, the concentration of the XCI-activators will rise and/or the concentration of the XCI-inhibitors will decrease, and in female cells this will be sufficient to generate a specific probability in time for enough *Xist* to accumulate and start to spread in *cis* (**Figure 8**). XCI-inhibitors are involved in setting up a threshold that has to be overcome by *Xist* to accumulate. Because the XCI-activator gene is X-linked, spreading of *Xist* will down-regulate the XCI-activator gene in *cis*, preventing the second X chromosome from inactivation. In this model, initiation of spreading is a stochastic event, so that the chance for silencing of the XCI-activator gene on either X is equal. In male cells the concentration of the XCI-activator will not be sufficient to break the threshold and initiate XCI. Therefore, female specific initiation of XCI is obtained through a sex-dependent dosage difference in X-encoded XCI-activators that promote *Xist* RNA accumulation. Female cell lines and mice that harbor *Xist* or *Tsix* mutations that affect the transcription rate of either one of these genes indicate that *Xist* and *Tsix* are the major players in setting up the probability, and that the XCI-activators and XCI-inhibitors are likely to act through these genes.

Trans acting factors in the regulation of X chromosome inactivation

How are *Xist*, *Tsix* and *Xite* regulated? Deletion of the complete *Xist*, *Tsix* and *Xite* region in female ES cells still allows initiation of XCI on the wild type, unmutated X chromosome [179]. This, together with results obtained using single copy transgenes harboring *Xist* and *Tsix* sequences [175], has indicated that other factors are likely to be involved in the regulation of X chromosome inactivation, and have led to the stochastic X chromosome initiation model described above [179, 189]. In the present XCI activator/inhibitor model, the XCI-inhibitors are autosomally encoded *trans*-acting factors which act against the XCI-activators in setting up the threshold for XCI to be initiated. Interestingly, most of the inhibitors of XCI which have been identified thus far appear to be factors which are also involved in maintaining ES cell homeostasis by generating an ES cell specific transcription factor network. These findings link repression of XCI to the pluripotent state of a cell, as was first proposed more than 30 years ago [190]. In pluripotent ES and ICM cells, it appears to be the pluripotency factors which repress XCI, either by stimulating expression of *Tsix* or by repressing *Xist* expression [191-192]. The latter can be direct or indirect through repression of activators of *Xist*. One of the pluripotency factors coming into play is OCT4, which has been shown to be crucial for the regulation of *Tsix* expression, by binding to the *Xite* promoter and *Tsix* regulatory regions [186]. REX1, a repressor of genes involved in cell differentiation and a key marker of ES cell pluripotency, has also been shown to regulate *Tsix* expression, by binding to the *Tsix* regulatory *Dxpas34* region [192]. Binding

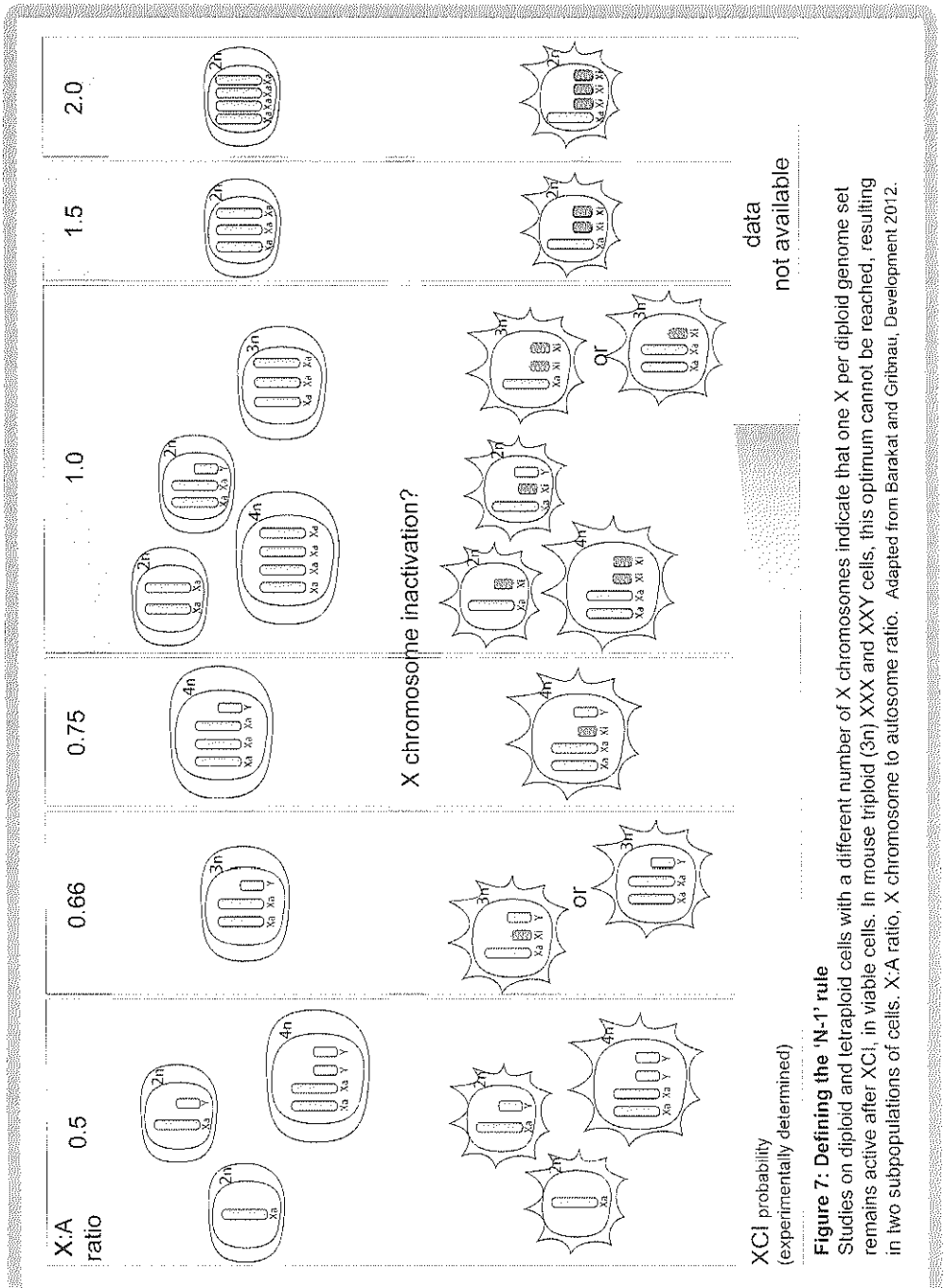

Figure 7: Defining the 'N-1' rule
Studies on diploid and tetraploid cells with a different number of X chromosomes indicate that one X per diploid genome set remains active after XCI, in viable cells. In mouse triploid (3n) XXX and XXY cells, this optimum cannot be reached, resulting in two subpopulations of cells. X:A ratio, X chromosome to autosome ratio. Adapted from Barakat and Gribnau, Development 2012.

of REX1 in this region involves complex formation in which also the reprogramming associated factors KLF4 and cMYC, and the ubiquitously expressed factors CTCF and YY1 take part [192-193]. The binding of these factors to the *Dxpas34* region seems to facilitate the recruitment of the transcriptional machinery to the *Tsix* promoter, leading to efficient initiation and elongation of *Tsix* transcription. SOX2 and KLF4 also bind to the *Xite* region, thereby possibly enhancing the positive regulation of *Xite* on *Tsix* transcription.

Direct suppression of *Xist* by pluripotency factors in ES cells has been proposed to involve NANOG, OCT4 and SOX2 recruitment to a region in *Xist* intron 1 [191]. ChIP sequencing studies revealed two other pluripotency factors, PRDM14 and TCF3, that bind to the same region within intron 1 of *Xist*, suggesting a putative role also for these factors in repression of *Xist* [194-195]. In support of this, genetic depletion of *Nanog* in ES cells resulted in up-regulated *Xist* expression, and rapid down-regulation of *Nanog*, *Oct4* and *Sox2* gene expression is accompanied by ectopic *Xist* accumulation [191].

Although an involvement of pluripotency factors in the *Xist* repression seems to be straightforward, as XCI initiation is coupled to cellular differentiation, release of *Xist* repression by loss of pluripotency factors alone cannot explain female specific initiation of XCI, as both in male and female cells pluripotency factors are believed to be down regulated upon differentiation. Therefore it will be interesting to test whether genetic ablation of pluripotency factor binding sites within the *Xist* locus is sufficient, to result in XCI initiation. Alternatively, redundant mechanism might be in place, where pluripotency factors not only repress *Xist* directly, but might also play a role in suppression of XCI-activators prior to differentiation. Since XCI-activators are believed to be X-linked, such a delicate interaction of multiple factors might explain the apparent crucial role of pluripotency factors in regulation of XCI in female cells. At the start of this thesis research, the identity of XCI-activators was unknown, and identification of these factors was considered to be crucial for the further understanding of control of XCI initiation.

The identification of XCI-activators and XCI-inhibitors, and the subsequent functional studies on the regulatory roles of these factors, will most likely highlight that the network regulating XCI involves intricate relationships between multiple factors, often acting in a dose-dependent manner, and on various target genes. Down-regulation of most autosomally encoded XCI-inhibitors occurs in both male and female differentiating ES cells, but only the female cells will initiate random XCI, based on sex-specific differential expression of X-linked XCI-activator genes (**Figure 8**). Initiation of random XCI will result in silencing of the X-linked XCI-activator genes in *cis*, providing a feedback mechanism preventing initiation of XCI on the second X chromosome. When *Tsix* is silenced in *cis*, this results in a drop in the threshold for sustained *Xist* expression, so that *Xist* remains expressed on the Xi, despite decreased XCI-activator activity. On the Xa, silencing of *Xist* involves *Tsix* transcription-mediated recruitment of chromatin remodelers and the *de novo* methyl transferase Dnmt3A to the *Xist* promoter. All these regulatory mechanisms might allow an efficient and robust initiation of rXCI.

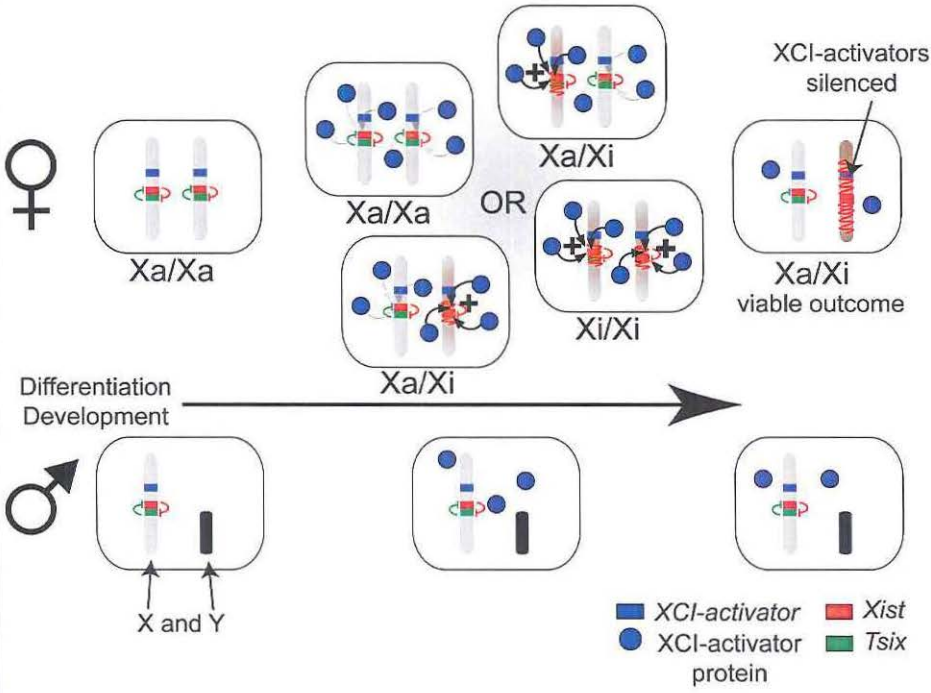

Figure 8: A stochastic model for XCI
A stochastic model for XCI postulates that initiation of XCI is dependent on X-encoded activators of XCI and autosomally encoded inhibitors of XCI. Upon differentiation or during development the nuclear concentration of the XCI-activator(s) (blue) increases, whereas the concentration of XCI-inhibitors such as NANOG, OCT4 and SOX2 decreases (not shown), or remains constant in time (YY1 and CTCF, not shown). XCI-activators are X-encoded, and therefore only in female cells the balance in the nuclear concentration of these factors is sufficient to generate an independent and continuous probability to initiate XCI (grey and black arrows), and results in cells that do not initiate XCI, or initiate XCI on one or both X chromosomes (+). Initiation of XCI results in spreading of *Xist* and silencing of XCI-activator genes in *cis*, resulting in down-regulation of the XCI-activator concentration, which prevents XCI on the remaining Xa. Adapted from Barakat and Gribnau, Adv Exp Med Biol 2010

X chromosome silencing and maintenance of silencing

Once XCI is initiated, a series of events takes place which changes the euchromatin of the active X chromosome into the tightly packed inactive heterochromatin of the Xi, which can be recognized as the Barr body in female somatic cells [196-197]. The first step in this cascade of events is the transcriptional up-regulation and spreading of RNA transcribed from *Xist* on the future Xi [74, 84] (**Figure 9**). The *Xist* transcript contains several repeats, of which the A repeat, located in the 5' portion of the *Xist* RNA, is involved in the silencing process [115]. Coating of the future Xi with *Xist* RNA leads to a rapid deprivation of RNA

polymerase II and associated transcription factors, which leads to an immediate reduction of gene transcription on this chromosome, and the creation of a silent, repetitive nuclear compartment [198-199]. This silent compartment is initially mainly composed of repeat sequences, but upon further differentiation, as silencing occurs, genes are moved into this compartment [198]. One of the earliest events after *Xist* accumulation are specific chromatin changes, including the loss of active chromatin marks like H3K9 acetylation and H3K4 mono- and di-methylation [52, 156, 200], as well as a gain of silent chromatin marks like H3K27 tri-methylation (H3K27me3) [97-98, 122, 201], H3K9 di-methylation (H3K9me2) [156-157, 202-204], H4K20-mono-methylation (H4K20me1)[205] and mono-ubiquitylation of histone H2A on lysine 119 (H2AK119ub1) [206-207], followed by the incorporation of histone variants including macroH2A [208] and changes in DNA methylation and replication timing [209-211] (**Figure 10**).

To initiate the establishment of chromatin changes and silencing, *Xist* RNA needs to accumulate and spread along the X chromosome. The exact mechanism involved in *Xist* spreading is not clear. Studies using inducible expressed *Xist* transgenes harboring several deletions in ES cells have shown that several regions within the *Xist* RNA are capable of chromosomal binding, but non of them seems to be essential and absolutely required for chromosomal localization [115]. The lack of conserved motifs within these binding regions has made it difficult to discover a unique binding sequence involved in chromosomal localization of the *Xist* RNA. A recently generated hypomorphic *Xist* allele in mice, with an inversion within *Xist* from approximately 5 kb into the first exon until exon 5 ($Xist^{INV}$) [212], shows compromised *Xist* localization in *cis*. This allele leads to female embryonic lethality relatively late during embryonic development (E9.5-10.5), and is characterized by partial chromosomal silencing, based on the assessment of chromosome-wide histone modifications. Although it seems difficult to decipher which feature of the inverted *Xist* RNA is responsible for the failure of proper localization, this study indicates that several structural features of the *Xist* RNA might be crucial for its proper localization.

Further evidence points to a crucial role for exon 1 in localising *Xist* to the X chromosome [115]. Screens using peptide or locked nucleic acid (PNA or LNA) oligonucleotides have shown that probes binding to the C-repeat located in *Xist* exon 1 disrupt proper *Xist* localization [213-214]. The C-repeat consists of 14 tandem repeats of a C-rich sequence in mice [86], and targeting of these repeats leads to an immediate displacement of *Xist* RNA from the Xi, including loss of PRC2 [214] and macroH2A [213] from the Xi, which is only recovered after *de novo Xist* RNA synthesis. In human only one C-repeat is present [87], which might explain why targeting of the human C-repeat in 293 cells did not result in *Xist* displacement [214]. In agreement with a role of exon 1 in *Xist* localization, it has been found that the nuclear scaffold protein SAF-A (also known as hnRNPU or SP120) is a crucial component in the mechanism which defines *Xist* localization [215-216]. SAF-A has been characterized as a DNA/RNA binding protein and is a putative component of the nuclear scaffold involved in regulation of gene expression and DNA replication. SAF-A was found to be enriched on the Xi, and its enrichment is dependent on the RNA binding domain of SAF-A [217], and *Xist* transcription [218]. UV cross-linking and immunoprecipitation experiments have shown that SAF-A has a high binding affinity for a region in *Xist* exon 1, implicating that SAF-A might directly bind to this region of *Xist*, thereby facilitating the chromosomal localization of *Xist*, as RNAi-

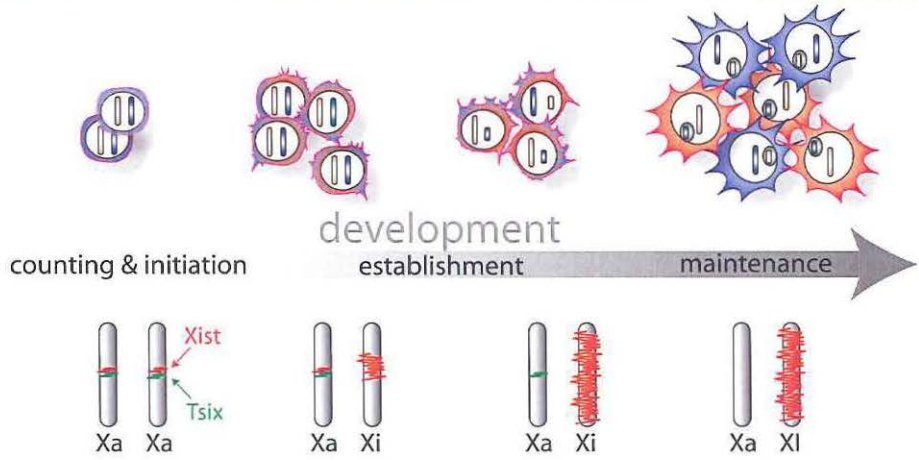

Figure 9A: Random XCI
The random XCI process can be divided in three phases; counting and initiation, establishment and maintenance. *Xist* is initially expressed at low levels, but then is up-regulated on the future Xi and remains expressed thereafter. *Tsix* represses *Xist* in *cis* on the Xa, and is silenced when the Xi is established.

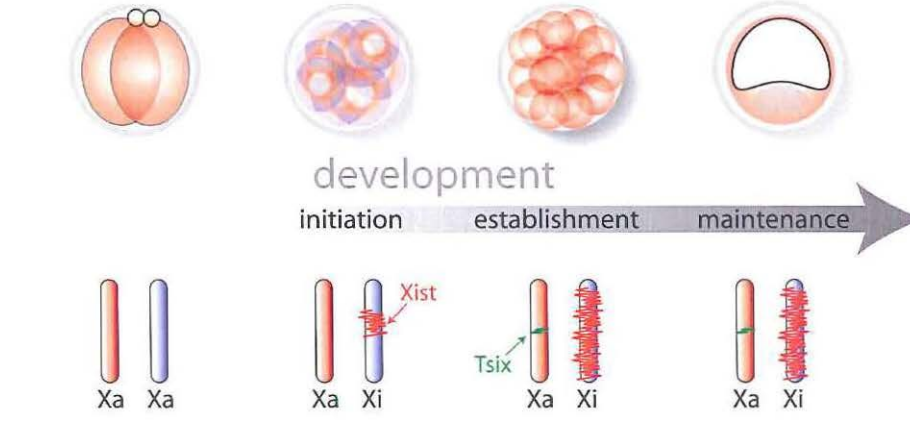

Figure 9B: Imprinted XCI
Imprinted XCI is initiated in the mouse cleavage stage embryo, and results in the exclusive inactivation of the paternal X chromosome. Imprinted XCI starts with up-regulation of *Xist* expression from the Xp (blue). At later stages *Tsix* expression is required to repress *Xist* on the Xm (red).
Adapted from Barakat and Gribnau, Development 2012.

mediated knock-down of SAF-A results in disrupted *Xist* cloud formation in both somatic and ES cells [216]. In line with this, homozygous SAF-A knockout mice are embryonic lethal at around E6.5, although it is at present not clear whether females are more affected compared to males due to the failure of XCI initiation [219]. This first interaction between *Xist* and a nuclear scaffold protein might indicate that an interaction between *Xist* and the nuclear scaffold is crucial for *Xist* to localize in *cis* over the X chromosome from which it is transcribed. This would be in agreement with earlier studies, which showed that *Xist* RNA remains associated with the nuclear scaffold after removal of chromatin [91].

Another protein which has recently been proposed to interact with *Xist* RNA is the DNA-binding protein YY1 [220]. YY1 was shown to be a bivalent protein, capable of binding both RNA and DNA trough different sequence motifs. As YY1 is able to bind both the *Xist* RNA (through an interaction involving the aforementioned C-repeat transcribed from *Xist* exon 1) and the DNA, YY1 was proposed to tether the *Xist* RNA to the X chromosome in *cis*. Although this docking hypothesis is intriguing, at present it is not clear how *Xist* RNA docking to the *Xist* locus is compatible with the *Xist* spreading itself. Thus, future studies are needed to address how, under this scenario, *Xist* is able to translocate along the chromosome.

Recruitment of *Xist* RNA to the Xi may also be facilitated by BRCA1, a protein involved in many pathways including checkpoint activation and DNA repair. Association of BRCA1 with the Xi was found in a small percentage of cells, and reconstitution experiments indicated a role for BRCA1 in *Xist/XIST* localization [221-222]. Nonetheless, this claim is disputed by others, and the exact role of BRCA1 in XCI remains to be determined [223-224].

Beside proteins directly or indirectly interacting with *Xist* RNA, sequence specific characteristics of the X chromosome might help in the *Xist* spreading. Studies on X-to-autosome translocations and autosomally integrated *Xist* transgenes have indicated that *Xist* spreading on autosomal regions is not complete, which indicated that X-chromosomal sequences are needed for efficient spreading [72, 168, 225-228]. Booster elements or way stations have been hypothesized to facilitate the *Xist* transmission along the X chromosome [229], and LINE-1 retrotransposons were postulated to be the most likely candidate for being these booster elements [230-233], as they are one of the most common repetitive sequences in mammalian genomes and are enriched on the X chromosome compared to autosomes [234-237]. Regions on the X chromosome that undergo XCI have a higher LINE-1 density than regions surrounding genes that escape inactivation [14, 236-241], and the density of LINE-1's on the fused autosome in X-to-autosome translocations seems to correlate with the amount of *Xist* spreading [226-228, 239, 242-246]. However, also other sequences may be important for the *Xist* spreading, as others did not find a correlation between LINE-1 density and spreading, or suggested a less critical role [122, 140, 240, 247-249]. How *Xist* interacts with these sequences during the spreading process, and whether these interactions are direct or mediated by other molecules is at present not clear. In mice, LINE repeats are also transcriptionally active on the Xi at early stages of XCI [250], and small RNAs, which might be produced from these active LINE repeats have been implicated in enhancing the silencing efficiency of certain X-linked genes. Based on

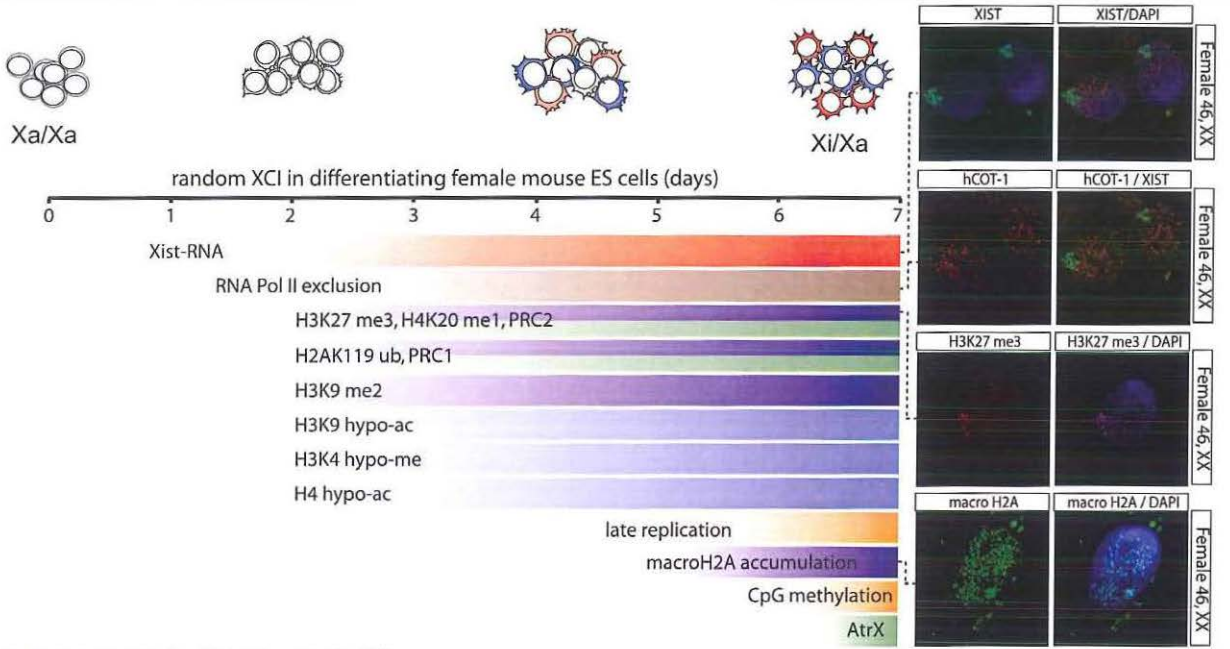

Figure 10: Epigenetic changes on the Xi
Initiation of random XCI is induced upon differentiation of female ES cells. The first change on the future Xi is spreading of *Xist* RNA in *cis* (red), followed by exclusion of RNA polymerase II (brown), the loss of active chromatin marks (blue), and gain of chromatin marks or incorporation of histone variants specific for inactive chromatin (purple). These chromatin changes are accompanied by accumulation of proteins and protein complexes (green), and other epigenetic changes including a shift to late replication in S phase and CpG methylation (orange). The right panels show female human fibroblast subjected to *XIST* RNA FISH, RNA FISH with a Cot probe detecting RNA Polymerase II transcribed repetitive regions, an immuno staining with anti H3K27 me3 antibody, and an immuno staining with anti macroH2A antibody. Each cell contains one *XIST* signal coating the Xi, which corresponds with a Cot negative area, accumulation of H3K27 me3 and incorporation of macroH2A.

their methylation, LINE repeats on the Xi also differ from LINEs located on autosomes [251]. Further studies are needed to clarify the role of LINE repeats both in the initiation of XCI, and spreading of *Xist* along the X chromosome.

After *Xist* accumulation, one of the first histone modifications detected on the Xi is H3K27me3. This modification is dependent on the Polycomb repressive complex PRC2, which accumulates on the Xi and consists of the proteins EED, RbAp46/48, SUZ12 and EZH2, of which EZH2 is a methyl transferase implicated in H3K27 tri-methylation [98, 252-253]. Recently, a direct interaction between EZH2 and the A-repeat of *Xist* has been reported, and *Ezh2* knockdown studies in female ES cells indicated a role for PRC2 in establishment of the Xi in random XCI [99, 254-255]. These studies also found an interaction between the A-repeat and SUZ12. Interestingly, a knockout of EED resulting in a non functional PRC2 complex and the genome wide depletion of H3K27me3 reveals only a defect in imprinted XCI in mice [256], with re-activation of the Xi in extra-embryonic tissues. Despite defects in embryonic development due to the absence of EED, random XCI was not affected in the embryo [257], which contrasts with results obtained after knock-down of *Ezh2 in vitro* [99]. A different study, employing autosomally integrated inducible *Xist* transgenes, indicated that H3K27me3 did not accumulate in the absence of EED, and in addition some components of the PRC1 complex (MPH1 and MPH2) do not localize to the *Xist* coated autosome. However, recruitment of RING1B, which is part of the PRC1 complex, and *Xist* mediated silencing of autosomal sequences were not affected [258]. Accumulation of H2AK119ub1 (mono-ubiquitylation of histone H2A on lysine 119) on the Xi is dependent on RING1B [206-207], but a homozygous *Ring1b* mutation did not affect *Xist*-mediated silencing of an autosome with a transgenic insertion of *Xist* [258]. These findings indicate that PRC1 and PRC2 are dispensable for random XCI, which does not exclude the possibility that these complexes are involved in redundant mechanisms in the establishment and maintenance of the Xi.

As mentioned before, the A-repeat seems to be important for the silencing capability of *Xist*. Inducible *Xist* transgenes lacking the A-repeat are deficient in silencing [115], and interactions between the A-repeat and PRC2 components could suggest that the A-repeat is important for PRC2 recruitment to the Xi, thereby explaining its role in silencing [99, 254-255]. To investigate the role of the A-repeat in the endogenous *Xist* locus, two independent A-repeat knockouts have been generated in ES cells [259-260], and one line of knockout mice has been derived [259]. In both cases, deletion of the A-repeat did result in absence of XCI initiation from the mutated allele [259-260]. In mouse studies, transmission of the mutated allele through the maternal germ line resulted in female pups with completely skewed XCI, in which always the non-mutated allele was inactivated, whereas transmission trough the paternal germ line resulted in absence of viable female offspring, due to a failure of initiation of imprinted XCI on the paternal X chromosome [259]. Surprisingly, this lack of XCI initiation was not caused by the spreading of a mutated *Xist* RNA which is unable to silence, but instead was explained by the total absence of *Xist* transcription from the mutated allele. In both ES cells and *in vivo*, higher *Tsix* expression levels have been found emanating from the X chromosome harboring the A-repeat deletion. Although one study explains the lack of *Xist* production from the A-repeat deleted allele by a failure of proper *Xist* splicing, which is supported by the fact that an interaction between

the A-repeat and the splicing factor ASF/SF2 is found [260], the lack of *Xist* production is more likely to be explained by the increased *Tsix* level [259]. Apparently, A-repeat deficient *Xist*, unable to recruit PRC2, is unable to silence *Tsix* in *cis*, which will result in the high *Tsix* level observed. The increased *Tsix* level might therefore explain the aberrant methylation of the *Xist* promoter which has been found on the mutated allele, which will result in transcriptional silencing of that allele [259]. This explanation would be in line with the results obtained from studies using inducible *Xist* transgenes lacking the A-repeat, since in that case both *Tsix* is missing in *cis*, and the endogenous *Xist* promoter is replaced by an inducible promoter [115, 261]. Therefore, in this situation, A-repeat deficient *Xist* RNA will still be expressed from the transgene, in contrast to the mutated *Xist* RNA from the endogenous locus in the A-repeat mutant. In addition, inducible *Tsix* expression has recently been shown to result in *Xist* silencing *in vivo* in extra-embryonic tissues, which was also found to be caused by aberrant methylation of the *Xist* promoter [124].

Although it seems clear that the A-repeat performs an important role in the silencing function of *Xist*, there has also been evidence for silencing capability independent of this well conserved repeat. A recently generated 16 bp insertion of an unrelated sequence into exon 1 of *Xist* (*Xist* ^{IVS}), which does not disrupt the A-repeat, leads to X chromosome coating in *cis* in mouse embryos and establishment of some histone modifications associated with the Xi, including H3K27me3 and H4 hypoacetylation. However, gene silencing seems to be compromised in these mice, as this hypomorphic *Xist* allele leads to female specific lethality during mid and late gestational stages [262]. Evidence for A-repeat independent modes of gene silencing also comes from transgene studies in ES cells which express A-repeat deficient *Xist* [205, 258]. Although with less efficiency, in the absence of this repeat, still recruitment of polycomb group repressive (PcG) complexes has been found [205, 258]. Expression of the same transgene in already differentiated cells, did not result in PcG recruitment, which further supports the presence of a window of opportunity in which silencing can occur [261]. Studies have indicated that *Xist* needs to be expressed within the first 48 hours of differentiation of female ES cells to accomplish proper silencing. Interestingly, transient expression of the A-repeat mutant *Xist* for a short time during early differentiation imparted a memory to the chromosome, which allowed PcG recruitment upon re-expression of the transgene after 9 days of differentiation. This could argue against a direct recruitment of PcG complexes by *Xist*, and might indicate that at least a redundant pathway may exist, in which PcG complexes are recruited to the Xi based on a chromosomal mark which functions as a memory [205]. Using the same transgene, it was recently found that A-repeat deficient *Xist* is able to induce chromosome-wide histone H4 hypoacetylation and H3K4 hypomethylation, which are also both associated with gene silencing [218]. H4 hypoacetylation persisted after transient transgene expression, and therefore it is tempting to speculate that this mark may represent the above mentioned memory, which needs to be in place to attract PcG complexes [218].

Next to the questions regarding the presence of epigenetic memory on the X chromosome, another interesting question remains how the silencing window is determined [261]. As PcG complexes are abundantly present both in undifferentiated ES cells and their differentiated progeny, but correct silencing occurs only after early *Xist* expression, it could be that co-factors are needed to accomplish proper PcG recruitment or function. Alternatively, post-transcriptional modification of either the PcG complexes or the *Xist*

RNA might be necessary. As either these modifications or the required co-factors might be developmentally regulated, this could confine the window in which *Xist* is able to induce proper silencing. Candidate co-factors for PcG-RNA interactions include JARID2 [263-265] and PCL2 [266]. Both proteins are present at high levels in ES cells and during early differentiation, and expression levels decline during later differentiation. Although both proteins do not have a defined RNA-binding domain, knock-down of *Pcl2* results in a significantly reduced PRC2 recruitment to the Xi [266]. However, both these candidate co-factors cannot explain the recruitment of PRC1 to the Xi. Early studies had shown that PRC1 is recruited by H3K27me3, a mark which is generated by the PRC2 complex, thus linking function of both complexes together in a hierarchical order [267-269]. PRC1, however, was also found to be recruited to the Xi in a PRC2 deficient background [258, 270]. This discrepancy can now likely be explained by the identification of the RYBP-PRC1 complex, involved in histone H2A monoubiquitylation [271]. RYPB was found to be enriched on the Xi in trophoblast stem cells [272], and co-localization of H2AK119ub1 and RYPB was found in EED-deficient ES cells, which suggests that in response to accumulation of *Xist* RNA, RYPB-PRC1 can be recruited to the Xi, accounting for the H3K27me3-independent histone H2A monoubiquitylation [271].

Besides co-factors and complexes involved in installing repressive chromatin modifications on the Xi, other proteins might be involved in setting up an appropriate developmental context in which *Xist* RNA can induce silencing. By making use of the same inducible *Xist* transgenes which delineated the XCI window of opportunity in ES cells [261], it has been found that inducible expression of *Xist* is able to silence genes in B- and T-cell precursors in adult mice [273]. This indicates that in these cells, the factors involved in *Xist* mediated gene silencing are transiently reactivated. By making use of a T-cell lymphoma model in which gene expression of parental and *Xist*-resistant tumor cells were compared, *SatB1* and its closely related homolog *SatB2* were identified as factors which define the developmental context for gene silencing by *Xist* [274]. These cancer associated genes encode nuclear proteins, which act as genome organizers and gene regulators [275]. Knock-down studies of *SatB1* and *SatB2* showed a partial defect in silencing of the X chromosome in differentiating female ES cells, suggesting a direct role for these nuclear scaffold proteins in heterochromatinization of the Xi [274]. These are most likely redundant functions, as single disruption of the genes encoding these proteins is compatible with female development in mice [276-278].

Even more proteins have been implicated in establishment and maintenance of the Xi. An E3 ubiquitin ligase complex consisting of the speckle-type POZ protein SPOP and CULLIN3 has been shown to be involved in the regulation of macroH2A deposition on the Xi [279]. SPOP and CULLIN3 ubiquitinate both BMI1, a component of the PRC1 complex, and macroH2A. Ubiquitination of macroH2A appears crucial for the recruitment of macroH2A to the Xi, and RNAi-mediated knock-down of either SPOP or CULLIN3 results in diminished macroH2A staining on the Xi. RNAi-mediated knock-down of either macroH2A or SPOP/CULLIN3 in combination with demethylation and deacetylation inhibitor treatment, resulted in reactivation of an Xi-linked reporter gene. Reactivation was not found with demethylation and deacetylation inhibitor treatment alone, indicating a role for macroH2A in the maintenance of the silent Xi state. The silencing function of macroH2A might be indirectly established by recruitment of the Poly (ADP-ribose)

polymerase 1, PARP1 [280]. PARP1 is a nuclear enzyme involved in modulating chromatin structure, sensing DNA damage and regulation of gene expression [281-283]. MacroH2A is able to recruit PARP1 to the Xi, and to inhibit the catalytic activity of PARP1. Enzymatically inactive PARP1 is able to bind nucleosomes and inhibits transcription [284]. Depletion of PARP1 in combination with demethylation and deacetylation inhibitor treatment leads to reactivation of an Xi-linked reporter gene. Hence, macroH2A might collaborate in gene silencing by modulating the enzymatic activity, and thus the ability of PARP1 to silence X-linked genes. Interestingly, despite the clear evidence of macroH2A recruitment to the Xi [208, 285-288], knockout of macroH2A1 does not lead to female specific lethality [289-290], which might be caused by the redundancy between different isoforms and variants of macroH2A [285, 291-292]. However, also simultaneous knock-down of macroH2A1 and macroH2A2 in ES cells is compatible with normal differentiation and initiation of XCI [293], although a combined knockout of both genes will be necessary to specify the involvement and requirement of macroH2A in the silencing and maintenance of the Xi.

One of the last events in the stabilization of the inactive state of the Xi is the methylation of CpG islands in promoter regions and within genes [209]. Relative to the active X chromosome, the Xi is hypomethylated in gene-poor regions, but hypermethylated in gene-rich regions [294-296]. DNMT1 (a maintenance methyl transferase) has been shown to be crucial for the stable maintenance of the Xi during embryonic development, as a mutation in DNMT1 leads to failure of gene silencing and associated embryonic lethality at E9.5 [297]. In contrast, DNMT3A and DNMT3B, which are important for the *de novo* establishment of methylation marks, are not required for XCI in mice [298]. This indicates that DNA methylation is required mainly for stable maintenance of the Xi. The protein SMCHD1 also associates with the Xi, where it is involved in maintenance of methylation of CpG islands of genes subject to XCI [299-300]. SMCHD1 contains a SMC-hinge domain which is found in proteins involved in cohesion and chromosome condensation. *SmcHD1* knockout mice show defects in maintenance of the Xi in embryonic and extra-embryonic tissues. Notably, in plants, a SMC-hinge domain containing protein has been identified as a factor involved in RNA-mediated DNA methylation [301]. It seems plausible that if such a mechanism is conserved between plants and animal species, mammalian SMCHD1 might have a related function in the regulation of methylation in XCI.

Analysis of *Atrx* heterozygous female knockout mice implicated a role for ATRX, a chromatin remodeling protein named alpha-thalassaemia and mental retardation on the X chromosome, in imprinted XCI [302]. Female mice inheriting a mutated allele through the female germ line fail to inactivate the paternal X in extra-embryonic tissues, suggesting a failure in imprinted XCI. Interestingly, at later stages of ES cell differentiation, ATRX also associates with the Xi, supporting a role in maintenance of the Xi [303]. One more protein to add to the list would be the Trithorax group protein ASH2L, which is enriched on the Xi in the maintenance phase of XCI [218]. It is believed that this protein is recruited as a structural component of the Xi and might interact with PcG complexes. Its precise function needs to be determined.

Once the Xi is established, expression of *Xist* is no longer necessary for the maintenance, as a conditional deletion of *Xist* does not lead to reactivation of silenced genes [95, 261, 304]. Furthermore, many of the above-mentioned histone modifications and

specific protein enrichments to the Xi disappear upon deletion of *Xist*, with the notable exceptions of histone H4 hypoacetylation and DNA methylation of promoters, which seem to be associated with stable and *Xist*-independent maintenance of XCI. However, what is also clear is that apparently multiple redundant proteins and epigenetic layers are involved in the establishment and maintenance of the Xi. Together, they ensure that the Xi is stably silenced and propagated, leading to persistent dosage compensation.

The pseudo-autosomal region (PAR) of the X is not silenced. In addition, a limited number of X-linked genes outside the PAR escapes from XCI mediated silencing, as investigated in the mouse. In human, mole, cow and elephant, even more escapees have been identified [305-310]. Therefore, in different species, the completeness and robustness of silencing appears to differ, which might be caused by a differential evolutionary need for dosage compensation between species. The genes which escape dosage compensation, and do not have Y-chromosomal homologues, are thus differentially expressed between males and females, and may play a role in establishing differences between both sexes. In addition, the X-degenerate genes on the Y chromosome have become different from the X-chromosomal paralogs, meaning that several X- and Y-linked genes may contribute to genetic differences between the sexes even when an X-chromosomal escapee has a Y-chromosomal paralog. Most of the X-linked escapees are located on the XAR of the short arm of the X chromosome, which might reflect their younger evolutionary age and perhaps a lower constraint for dosage compensation [240, 305, 308, 310] (**Figure 1**). However, some escapees are also located in the XCR, and are showing different levels of escape in different tissues and species. For example, the mouse *Atrx* gene escapes XCI sporadically in the trophoblast [302], and in 40% of ear fibroblasts, but not in other cell lines. However, in human and elephant, this gene does not show such an escape [305, 311-312]. The chromatin environment and nuclear organization of the gene locus seems to be important for the probability of a gene to escape, as escaping genes are located outside the *Xist* territory which forms a repressive compartment [198], and correlation has been found between the level of escape and the presence of repeat sequences in the gene environment [238, 240, 313]. Furthermore, escapees seem to be concentrated in clusters, at least in human [240], which has lead to the hypothesis that escaping domains are delimited by boundaries [314]. The multifunctional insulator protein CTCF [315] has been found to bind to several boundaries between escaping genes and genes subject to XCI [316]. In agreement with this, the *Jarid1c* gene in mice is surrounded by CTCF binding sites, and is escaping XCI [316]. However, the artificial flanking of a transgene by insulators containing CTCF sites did not result in escape of XCI of the transgene [317]. Therefore, CTCF binding alone cannot explain all behavior related to escape of XCI. However, what seems clear from additional transgene studies is that intrinsic features of gene loci are important to determine whether a gene can escape, as four different locations of the same BAC transgene on the X chromosome in mice all resulted in escaping expression of transgenic *Jarid1c* [318].

In summary, many different redundant epigenetic layers and only partly understood complex interactions between RNAs, proteins, modified histones and DNA are involved in the silencing and maintenance of the silent state of the X chromosome. Although many investigations have studied various mechanisms, only the first steps have been made towards a complete understanding of the underlying processes involving silencing and maintenance of XCI. More factors and interactions with a role in the initiation

and maintenance of XCI silencing are anticipated to be discovered, as illustrated by the recent genome wide RNAi screen using reactivation of an X-linked GFP transgene in MEFs as a readout, which yielded a list of 32 new candidate proteins involved in maintenance of XCI, including the ORC2 and HP1α proteins [319]. Their precise function in keeping the X chromosome silent needs to be determined.

Evolution of X chromosome inactivation and the X inactivation center

As discussed above, the evolution of the mammalian sex chromosomes is an ongoing process which started more than 160 MYA, and has resulted in the presence of two X chromosomes in female placental mammals, and one X and one Y chromosome in their male counterparts. To compensate for the monosomy of X-linked genes in males, initial up-regulation of X-linked gene transcription was necessary in males, conferring a more severe dosage problem on females, which now had to deal with a higher dosage of X-linked genes being transcribed from both of their X chromosomes. The solution for this problem was the start of X chromosome inactivation, and taking a look at our closest related mammalian relatives will teach us more about the evolution of this important process and aid us to identify the molecular players involved, since the two main mammalian groups, the marsupials and the placental mammals, share the same origin of the X chromosome [4].

The third group of mammals, the egg-laying monotremes, consists only of the platypus and two species of echidna, diverged at the base of the mammalian branch 166 MYA [320-322]. These species have a complex and not well understood mechanism of sex determination, involving multiple X and Y chromosomes, which form a chain during meiosis [323-325]. Several of these X chromosomes have homology to the chicken Z chromosome (rather than to the X of marsupials and placental mammals) [326], and whether the monotreme X chromosomes are subject to dosage compensation is a matter of debate [323]. A recent study of epigenetic modifications characteristic of the inactive X chromosome did not find any difference between male and female platypus sex chromosomes, strongly arguing against the presence of a chromosome-wide, epigenetic dosage compensation mechanism in monotremes [327]. Instead, X-linked gene expression in monotremes might be, at least partially, regulated on a gene-by-gene basis [328-329].

Marsupials have evolved an X-linked dosage compensation mechanism which involves a chromosome wide silencing mechanism, comparable to that in eutherians [330]. Although XCI in marsupials is far from being resolved, several important differences have been identified between XCI in marsupials and placental mammals. In marsupials, XCI is always imprinted, rendering the paternal X chromosome inactive [331-334]. Furthermore, XCI in marsupials seems to be more incomplete, less stable [335] and less tissue specific [328], compared to placental mammals. The inactive X in marsupials is late replicating [332, 336], shows underacetylation of histones [337-339] and repressive histone modifications [327], comparable to the eutherian Xi, but no DNA methylation differences have been observed [340-341]. Most strikingly, an *Xist* gene has not been found in marsupials [116, 342-343]. Therefore at present, it is not clear how a chromosome-wide

silencing mechanism is achieved in marsupials, although the presence of a not yet identified non-coding RNA mimicking the *Xist* function of eutherians cannot be excluded. A candidate for this is the recently identified *Rsx* RNA, which seems to have *Xist*-like properties [344].

The absence of chromosome-wide dosage compensation in monotremes, and the presence of such a mechanism in marsupials despite the absence of *Xist*, can help to understand the evolutionary age and origin of the current eutherian X inactivation center (Xic). Since the marsupial lineage diverged 148 MYA, and *Xist* dependent X inactivation is the active mechanism in all investigated placental mammals with a XX/XY female/male karyotype [21, 339, 345], and must thus have evolved prior to the major radiation in the eutherian lineages starting some 100 MYA, *Xist* evolution can be traced back to a window of 48 million years [320, 346]. *Xist* is present only in placental mammals, so that sequence alignment of *Xist* with other, non-eutherian species cannot help deciphering the evolutionary origin of the Xic. However, four protein-coding genes, namely *Cdx4*, *Chic1*, *Slc16a2*, and *Rnf12* which are flanking the Xic, are well conserved between different vertebrate classes, including birds and amphibians. As the linkage of these genes is conserved, it can be assumed that this genomic locus represents the orthologous region of the Xic in non-eutherian species, referred to as the Xic Homologous region (XicHR) [342]. Interestingly, this region is located near the *Sox3* gene, in birds [347]. In the common ancestor of marsupials and placental mammals, one *Sox3* allele gave rise to the *Sry* gene, on the proto-Y chromosome, signifying the beginning of the mammalian X and Y chromosomes. Since *Sox3* is a dosage sensitive gene [11], and up-regulation of *Sox3* expression from the proto-X chromosome might have been crucial for males to compensate for loss of one allele, and hence for females to conquer, it seems plausible that genes located in close proximity of *Sox3* on the ancestral X chromosome were recruited first in the evolution of the XCI machinery [347].

In both chicken and frog (*Xenopus sp.*), the XicHR region contains 5 protein coding genes, namely *Fip1/2*, *Lnx3*, *Rasl11c*, *UspL* and *Wave4*, which do not have detectable orthologs in eutherians. Comparative sequence analysis instead has shown that the present day Xic genes *Tsx*, *Xist*, *Jpx* and *Ftx* have evolved from the XicHR genes *Fip1/2*, *Lnx3*, *UspL* and *Wave4*, respectively [116, 342, 345]. The *Rasl11c* gene seems to have become a pseudogene in eutherian species, and no sequence homology is detectable in rodents. Interestingly, the same region of the XicHR is disrupted in marsupials, where both the *Cdx4-Chic1* part and the *Slc16A2-Rnf12* part are located in different places on the long arm of the X chromosome, the former being located close to the centromere, whereas the latter is located much more distal [343, 348-349]. Also in platypus (a monotreme), the *Cdx4-Chic1* and *UspL-Wave4-Slc16A2-Rnf12* blocks are separated, located at different positions on chromosome 6p [343]. This chromosomal linkage is interesting, since several eutherian X-linked genes are located on platypus chromosome 6, which shows strongly enriched staining for H3K9m3 and H4K20me3, and depletion for H3K27me at the satellite regions [327]. A link between accumulation of these modifications and regulation of gene expression of these pre-Xic genes has still to be addressed. The fact that both in monotremes and marsupials the orthologs of the protein-coding genes of the XicHR can be found is in agreement with the absence of *Xist* in these lineages. Interestingly, the fact that the XicHR seems to be disrupted in both monotremes and marsupials, whereas the order of

gene derivatives is conserved in eutherians, implies that the disruption of this region must have occurred twice during evolution, since monotremes diverged from the therian lineage some 18 million years before the marsupials diverged from the placental mammals [343].

The chicken *Lnx3* gene is most likely the progenitor of the modern day eutherian *Xist* gene [116, 342]. In chicken, *Lnx3* encodes a PDZ domain-containing ring finger 1 protein, with E3 ubiquitin ligase activity [350]. Sequence comparison between *Xist* and *Lnx3* has shown that some exons and introns of *Xist* are remnants of *Lnx3* exons, but numerous point mutations and deletions suggest that during evolution *Lnx3* lost its protein-encoding capacity. However, *Lnx3* did not become a pseudogene. Rather, insertions of transposons and other mobile elements into *Lnx3* has contributed to the development of the *Xist* gene which is transcribed into the non-coding but functional *Xist* RNA. Among others, ancient mobile elements like the L3CR element are present in all eutherian *Xist* orthologs, suggesting that these insertions have occurred early during evolution [116]. Also many of the sequences transcribed into functional tandem repeats of the *Xist* RNA, including the *Xist* exon 1 sequence transcribed into the A-repeat, are derived from mobile elements, in this case from endogenous retroviruses [116]. Furthermore, several species specific mobile elements can be found in the different *Xist* orthologs amongst different species, for example Alu repeats in primates and B1 and B2 repeats in rodents [116, 345], thereby explaining differences in gene structure amongst species. Based on their high similarity, it has been proposed that *Xist* exon 4 has retained some regulatory elements of *Lnx3* exon 4 [342]. *Xist* exon 4 is highly conserved among eutherians, and is predicted to be transcribed into RNA forming a stable secondary structure representing a structural domain within the *Xist* RNA [310, 351]. The same secondary structure however is absent from chicken *Lnx3* mRNA, making a functional similarity between these regions unlikely [343]. Also the A-repeat of *Xist* RNA, important for the silencing capacity, is missing in *Lnx3* [116, 343], and *Lnx3* shows a variable expression both in male and female chickens in different tissues [342]. Therefore it seems likely that during evolution, *Xist* originated from *Lnx3* and in time acquired new regulatory cues and functional properties.

As mentioned before, *Xist* has evolved between 148 and 100 MYA in the eutherian lineage. What happened since then, to the *Xist* gene and the Xic locus? Comparative sequence analysis has been obtained for the Xic region and the *Xist* gene in mouse, human and bovine [140], rat, mouse, bovine, dog, vole and human [116, 310], different families of rodents [117], and recently for different primate species [352]. What is clear from these studies is that, in the majority of eutherian species, the overall organisation and gene content of the Xic is conserved. Clustering of genes in the Xic region might be important, since it is well known that genes with similar expression characteristics are often found within the same gene neighborhoods [353], and are regulated by similar mechanisms. However, some differences might be as important, and also have implications for improving our understanding of the X chromosome inactivation mechanism(s). For example, compared to the rodent Xic, the XIC in humans is considerably expanded, likely due to insertions of species specific repeats. The *Tsx* gene seems to be conserved in rodents, but in the primate lineages it has become a pseudogene [140]. *Slc16A2* is highly conserved between all placental mammals, but its orientation is reversed between rodents and humans [140]. Whereas *Tsix* appears to play a crucial role in the regulation of XCI in mice [118, 180, 354], *TSIX* may have lost such a role in primates [117, 140, 352]. The 3' end of *TSIX*,

which is overlapping with the *XIST* gene being transcribed from the opposite strand, is conserved, but other areas of *TSIX* show repeat element insertions and even large scale deletions in human, and also in other primates [352]. Also the *DXPas34* region and the *Xite* gene, which seem to be crucial for *Tsix* expression in rodents, are not conserved at a sequence level in primates, reinforcing some of the distinct differences between primate and rodent XCI [128, 352].

The *Xist* gene structure is fairly well conserved among eutherian species [140, 345]. In particular the promoter region of *Xist* shows a higher level of conservation among species [116-117]. However, there is only a low level of similarity of the transcribed *Xist* sequence. The *Xist* exons show 66% sequence identity between mouse and human, and 62% identity between mouse and bovine [140], a figure which is close to the average conservation of untranslated regions of ortholog protein-coding genes between mouse and human. Although in most species the number of *Xist* exons is identical, the exon-intron structure differs significantly [116, 140, 352], and the length of the gene shows some dramatic variability amongst species, most likely due to species-specific insertions of repetitive regions and amplification of repeats [116]. Interestingly, comparison among six different primate species has shown that the overall size of the ancestral primate *Xist* locus is very similar to the present day human *XIST* locus, indicating that during the last 80 million years only small, lineage specific changes occurred within the *XIST* gene [352]. One of these small changes seems to involve the D-repeat, which is transcribed from *Xist* exon 1. Whereas the A-repeat, crucial for the silencing capability of the *Xist* gene [115] is highly conserved among all species studied, the D-repeat shows some variation among species, and is even missing in certain primates, including lemurs [352]. Whether this has a functional consequence for XCI in these species remains to be addressed.

XCI and human ES cells

Studying X chromosome inactivation in humans is challenging. Due to ethical reasons, the use of early human embryos for research purposes has been widely restricted. Similarly, data on XCI in great apes and other primates are not available. Most of the obtained knowledge on human XCI has come from studies which made use of different model systems, including mouse-human cell hybrids, human embryonal carcinoma and tumor cell lines [147, 355] and human transgenes integrated in mouse ES cells [170, 174, 356-358]. The derivation of human ES (hES) cells promised the availability of a potent study model for human XCI, comparable to mouse ES cells. Different studies explored XCI in hES cells, with varying and conflicting results [359-364]. Most of the female hES cell lines display an inactivated X chromosome already in the undifferentiated state, characterized by *XIST* expression, *XIST* RNA coating, and accumulation of markers of heterochromatin on the Xi. Other undifferentiated female cell lines have two active X chromosomes, and have the potential to inactivate one X during differentiation, comparable to mouse ES cells (**Table 1**). Interestingly, certain cell lines behave different in distinct laboratories, with some sub-clones showing random XCI upon differentiation, whereas others show XCI hallmarks prior to differentiation. In a survey of 11 characterized hES cell lines, Silva et al. (2008) identified three different classes of hES cells with regard to XCI [361]. The first class only

	mouse			human
	ES cells	EpiSC	mEpiSC	ES cells
XaXa	+	+	-	+/-
XaXi	-	-	+	+/-
Xist/XIST	-	-	+	+/-
H3K27 me3, Cot exclusion	-	-	+	+/-
bFGF, Activin/Nodal sign.	-	-	+	+
Lif/Stat3 signalling	+	+	-	-
diff. in extra embr. tissue	-	-	+	+

Table 1: Characteristics of mouse and human pluripotent stem cells
Comparison of XCI characteristics and growth conditions of different reported human and mouse pluripotent female stem cells. Indicated are the presence (+) or absence (-) of an Xi and epigenetic changes associated with XCI in the different pluripotent stem cells described. Also shown are the tissue culture conditions required to maintain these stem cells (+), and the potential to differentiate in extra-embryonic tissues (+).

displays XCI characteristics upon differentiation. The second and third classes have an inactive X chromosome in the undifferentiated state, but in the third group *XIST* expression is lost. Although this last category does no longer express *XIST*, other XCI markers are still present, like the exclusion of Cot1 RNA from the X chromosome. Interestingly, in these cells, H3K27 tri-methylation is also lost, which indicates that H3K27 tri-methylation is dispensable for the maintenance of XCI. These results support previous findings that in mice and human recruitment of H3K27 tri-methylation is *XIST* dependent [97].

How can the differences between hES and mouse ES cells regarding XCI be explained? In mice, cells of the ICM show two Xa's prior to differentiation. A species-specific difference in the time window in which XCI occurs could explain why hES cells, which are also derived from the ICM, display XCI characteristics prior to differentiation. Does random XCI in human embryos already occur at an earlier stage, and do hES cells therefore display an Xi? Alternatively, reactivation of the Xi established during the early cleavage stages might occur later in humans compared to mouse. In mouse embryos, imprinted XCI occurs prior to implantation, and causes inactivation of the Xp [51-53, 365-366]. Imprinted XCI is maintained in the extra-embryonic tissues, but is reversed in the cells of the ICM (**Figure 3**), by reactivating the Xp, likely initiated by NANOG expression in cells of the epiblast [367]. Although XCI in human embryos is also initiated during the early cleavage divisions according to one report [368], it is unclear whether human XCI is imprinted [369-378]. According to another study, *XIST* accumulation in human blastocyst is often found on two X chromosomes, whereas silencing has not occurred yet at this stage [379]. In addition it is unclear at what stage the Xi is reactivated, if reactivated at all, and

hence, if XCI in undifferentiated hES cells could be due to persistence of XCI initiated in the early pre-implantation embryo, rather than representing precocious initiation of random XCI. In support of this, a highly skewed XCI pattern has been observed in female hES cells with a preference for one of the two X chromosomes to be inactivated [360, 380]. If an imprinted form of XCI would exist in humans, favoring inactivation of one of the parental X chromosomes, a lack of reactivation could explain these findings. Unfortunately, the paternal origin of the inactivated X chromosome was not determined in these studies.

Next to the above-described variations in the XCI timing between mouse and human, the observed differences in XCI between undifferentiated human and mouse ES cells could reflect more fundamental differences [381-382]. Human and mouse ES cells differ significantly in morphology, clonogenicity, molecular profile and culture requirements. For example, hES cells need bFGF and activin / Nodal signalling for their self renewal, whereas mouse ES cells depend on LIF / Stat3 signalling [383-384], and both cell types are characterized by a genome wide difference in occupancy of gene promoters by pluripotency factors [385]. Although both cell types have the potential to differentiate *in vitro* into cell types of all germ layers, and to form teratomas *in vivo*, only for mouse ES cells the capability to contribute to the germ line and to generate an entire animal has been tested. For obvious ethical reasons, this will not be studied for hES cells, so that this piece of evidence whether hES cells are indeed the human equivalent of mouse ES cells will never be obtained. In mice, an additional pluripotent cell population has been isolated from the post-implantation mouse epiblast using culture conditions including bFGF and activin, in the absence of LIF [386-387]. These so-called EpiSCs (post-implantation epiblast derived stem cells) express the pluripotency factors OCT4, SOX2 and NANOG, but differ in morphology and in the expression of certain transcripts from mouse ES cells, making them more comparable to hES cells [388]. Although these cells can differentiate *in vitro* into cells of all germ layers and extra-embryonic trophectoderm, they are extremely inefficient in contributing to chimaeras, and germ line transmission has not been reported. Female EpiSCs have undergone XCI, leaving one X chromosome active. Therefore, it is possible that XCI observed in hES cells is a reflection of the difference between human and mouse ES cells, with hES cells being in fact the human counterpart of mouse EpiSCs [389]. In agreement with this, mouse EpiSCs and hES cells share the ability to differentiate *in vitro* into extra-embryonic tissues [390], whereas mouse ES cells can only differentiate into cells of the three germ layers. It has been shown that EpiSCs can be differentiated from mouse ES cells in culture, which indicates that EpiSCs are a more restricted derivative from ES cells [391]. Also reprogramming of EpiSCs to ES cells by over-expression of the pluripotency factor *Klf4* [391] or *Nanog* [367], or by extended culture in LIF [392], is accompanied by reactivation of the inactive X chromosome.

How can human ES cells be the human equivalent of a more differentiated cell type, despite the fact that human ES cells are also derived from the ICM, like mouse ES cells? It is possible that the culture conditions used for the derivation of hES cells may allow the differentiation of ground state hES cells to hES cells with EpiSCs characteristics, and prevent *in vitro* stabilization of the pluripotent state of the human ICM [393]. Also, there are clear differences in early development between rodents and humans, such as the presence of an egg cylinder stage or a temporary arrest in embryonic development (diapause), present in the mouse but absent in human. This might explain why for human

cells a shorter time window may exist to derive ground state ES cells, comparable to mouse cells [394]. As a result, during human ES cell derivation, in fact only more differentiated cells might be derived, which would explain XCI in these cells.

The presence of an inactive X in undifferentiated hES cells could also be explained by a selective pressure against two active X chromosomes. In fact, only a short time window exists in which cells in the early mammalian embryo have two active X chromosomes. Since these cells are not programmed for an infinitive state in the ICM, the human cells might adapt to culture conditions during ES cell derivation by initiating XCI, which might confer XaXi cells with a growth or survival advantage. Selection against two active X chromosomes is also seen in some mouse ES cell lines, and analysis of female mouse ES cells indicated genome wide hypomethylation [395], possibly resulting in genome instability. This may explain why many inbred mouse ES cells loose one of the two X chromosomes during expansion, and only ES cells from hybrid crosses stably propagate two X chromosomes. Since hES cells are not characterized by a tendency of X chromosome loss, cells which have successfully initiated XCI under culture conditions may be the cells which are selectively maintained. Could the recent emergence of human iPS cells provide us with a better model to study XCI? For mouse iPS cells, reactivation of the silent X chromosome of somatic cells during reprogramming has been shown [67-68], and these cells initiate XCI upon differentiation. At the start of this thesis research, no studies had addressed the activity state of the X chromosome in female human iPS cells.

Taken together, the finding that XCI is initiated in undifferentiated hES cells, before the onset of differentiation, could have many different reasons. Searching for an explanation, we will most likely encounter a combination of mechanisms regarding epigenetic variation observed for ES cells from different species. Future studies are needed to determine the mechanistic origin of this finding, since uncertainties about the epigenetic stability of hES cells and the differentiation potential of these cells should be addressed before the introduction of hES cells for any clinical application can be considered [361, 396-398].

Chapter 1

Part 2: The X chromosome, X chromosome inactivation and its implications for human disease

Differences between females and males in human disease

In human, the sex of an individual is determined by the presence or absence of the Y chromosome. Genetically speaking, an embryo has an equal chance of obtaining the X or the Y from the father, resulting in a female or a male, respectively. Indeed, although earlier studies have hypothesized that sperm cells containing a Y chromosome might have an advantage in swimming velocity due to the smaller size of this chromosome compared to the X, such a difference has not been found in more recent studies [399-400], and therefore it seems likely that at the moment of fertilization there is indeed a 50% chance for the zygote to become either XX or XY. However, if we look at the male to female ratio at birth, it seems that more males are born. Taking a look at the birth rates in The Netherlands during the first decade of this century, the average male to female ratio is around 1.05 (**Figure 11A**). Paradoxically, however, amongst the stillborn children, there is a higher percentage of males, indicating that gestation might be a critical period in particular for male fetuses (**Figure 11B**). This would indicate that in fact, the male to female ratio obtained upon birth is an underestimation of reality, with an even higher number of male embryos compared to female embryos during the course of the pregnancy. But how does this relate to an equal chance of becoming a male or a female at the moment of fertilization? Are more females dying *in utero* compared to males? Surprisingly, studies on miscarriages of recognizable pregnancies during the first trimester seem to show the opposite. In chromosomally normal fetuses, the rate of spontaneous abortion is 1.3 times higher for male fetuses compared to female fetuses [401]. Also for the chromosomally abnormal fetuses, with trisomies of chromosomes 13 or 18, (Patau and Edwards syndrome, respectively) were the sex has no influence on the cause of these trisomy syndromes, it seems that female embryos have a better chance to be maintained throughout pregnancy [402-404]. Thus apparently, although at birth more males are found, during the course of pregnancy males are more prone to die? At least during the course of recognizable pregnancies this seems to be the case. However, studies have shown that the majority of spontaneous abortions occur prior to the recognition of the pregnancy [405-407], before or during implantation of the embryo [399, 406]. Since monosomies are not found in later stage miscarriages (except the monosomy of the X chromosome resulting in Turner syndrome), but should occur as frequent as trisomies, it seems likely that many monosomy embryos or embryos with even more detrimental chromosomal aneuploidies are lost at this time of the pregnancy [408]. However, also here it seems unlikely that a sex difference in occurrence of these anomalies would result in female specific lethality. How can the loss of female embryos during pre-implantation development be explained? A possible and intriguing hypothesis is that many female embryos are lost due to failure of the X chromosome inactivation process.

It has been shown that among differentiating mouse ES and ICM cells, cells can be found with an aberrant number of inactivated X chromosomes [162, 179, 188]. Proposing that initiation of X chromosome inactivation is explained by a stochastic mechanism [179] implies that a percentage of female embryos might fail to proper establish one inactive X

A

	total	males	females	Male/Female Ratio
2004	194892	99707	95185	**1,047507**
2005	188281	96535	91746	**1,052198**
2006	185568	95279	90289	**1,055267**
2007	181700	92768	88932	**1,043134**
2008	185017	95051	89966	**1,056521**

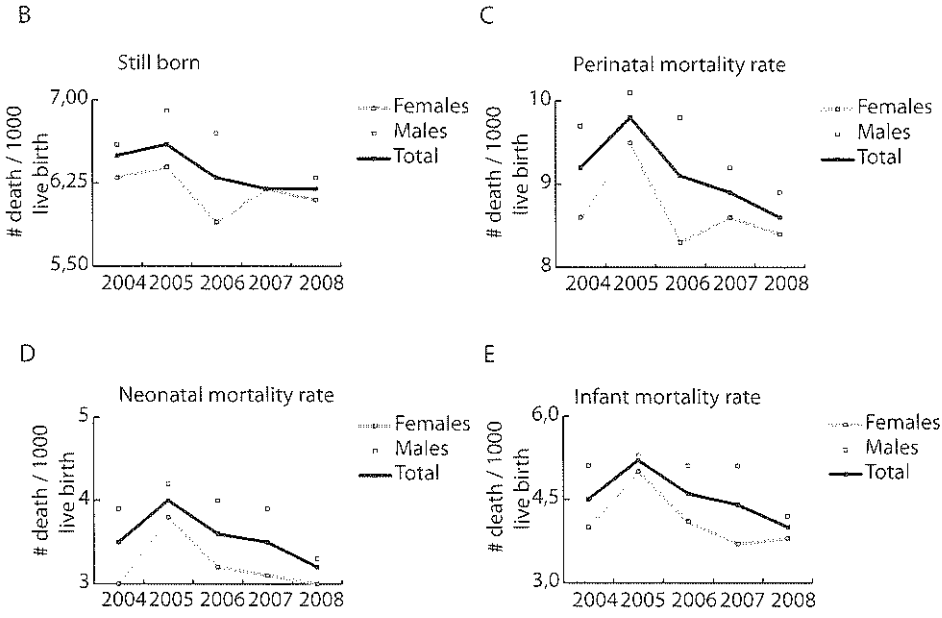

Figure 11:
Birth and child death for males and females in the Netherlands from 2004 to 2008
Source: Centraal Bureau voor de Statistiek (www.CBS.nl), retrieved 19 april 2012

A) Table showing the total number of birth, the number of females and males and the relative ratio between both sexes born in the Netherlands during the period 2004-2008
B) Number of still born children, without any sign of life, after a pregnancy of 22 weeks or longer, per 1000 live birth.
C) Perinatal mortality rate, defined as the number of still born children, without any sign of life, or children who died in their first 7 days of life, after a pregnancy of 22 weeks or longer, per 1000 live birth.
D) Neonatal mortality rate, defined as the number of children who died between day 1 and day 28 after birth, after a pregnancy of 22 weeks or longer, per 1000 live birth.
E) Infant mortality rate, defined as the number of children who died prior to their first 1 years birthday, after a pregnancy of 22 weeks or longer, per 1000 live birth.

chromosome. If none of the X chromosomes is inactivated, cells can try again later but might still fail to obtain an Xi and an Xa, and if two X chromosomes are inactivated, that will lead to immediate cell death. In some female embryos, too many cells might be lost by some failure in XCI initiation. We suggest that this might explain female- biased lethality prior to and around the time of implantation, resulting in a sex bias towards the birth of males, despite an equal chance of becoming a male or female at the moment of fertilization and a higher loss of male fetuses at later steps of gestation.

In the year 2010, 8 391 956 females lived in The Netherlands, compared to 8 223 344 males [409], and in most Western civilizations females are overrepresented in the elderly. This longevity advantage of females could be related not only to genetic and hormonal differences, but also to differences in occupation and lifestyle. However, it might be relevant to note that in all age categories, also at very young age, males have a higher mortality rate compared to females, as illustrated by the mortality rate during the first 7 days (**Figure 11C**), the first 28 days (**Figure 11D**) or the first year of life (**Figure 11E**) of children born in The Netherlands. From the moment of birth on, males seems to encounter more serious diseases more often, including birth defects, infectious diseases, intellectual disability and delayed development, and even malignancies [410-416]. Apparently, males are more vulnerable to lethal disease compared to females. Although many of the differences in disease susceptibility between males and females will most likely be explained by hormonal differences, and the other factors mentioned above, the presence of only one X chromosome in males might play an additional and not unimportant role. Since males have only one X chromosome, every mutation in a gene located on this chromosome may result in the presence of a non-functional or absent protein produced by the mutated gene, possibly resulting in a disease phenotype. In contrast, females will have the chance of compensating an X-linked mutation due to the presence of their two X chromosomes and the random XCI process, resulting in protection from so-called male-only diseases. Hence, although the presence of two X chromosomes and the obligatory dosage compensation mechanism might result in a higher lethality during peri-implantation development, the presence of both of these female specific characteristics seem to make females less vulnerable to lethal disease compared to males.

Mendelian inheritance of X-linked traits

Many decades and even centuries ago, prior to the discovery of chromosomes and genes, it was noticed that several diseases, including color-blindness and hemophilia, were occurring almost only in males [417-419] (reviewed in [420]). It was noticed that these diseases were not transmitted from affected males to their sons, but that their healthy daughters could give birth to sons who were again affected. Although at that time no explanation existed for this way of inheritance, it is now clear that this pattern of inheritance is typical for X-linked traits. The first X-linked trait, the white-eye characteristic, was discovered more than a century ago in *Drosophila* [421]. It was found that when a white-eye male fly was bred to a red-eye female, all offspring had red eyes. When this offspring was inbred with each other, a quarter of all offspring had again white eyes, and these white-eyed flies were all males. From this it was concluded that the trait for eye color in flies must be sex-linked, and that

the red eyes trait in flies is dominant, whereas the white-eye characteristic is recessive [421]. This and other work in flies was extended to the X and Y system in human, leading to the first rules on X-linked inheritance [422-423]. These rules can still be found in nowadays textbooks of genetics [424], and state the following: a character is dominant when it is expressed in a heterozygote, and recessive when not. X-linked recessive diseases almost exclusively affect males (since they are hemizygous for the X chromosome), and rarely affect homozygous recessive females. Affected males cannot transmit their trait to their male sons, rendering male-to-male transmission impossible. Transmission however can occur through their daughters, since all daughters will be obligate carriers, but since they are most likely heterozygous, they will not express the trait. These female carriers however can transmit the trait to their offspring, resulting in 50% of the daughters being a carrier, and 50% of the sons being affected. Therefore, affected males can transmit an X-linked recessive disease to 50% of their grandsons through their obligate carrier daughters. In X-linked dominant diseases, an excess of affected females exists in pedigrees of the disease, and again male-to-male transmission is impossible. However, all daughters of an affected male will have the disease, since the dominant trait will be expressed in the heterozygous females. Since both sexes in the offspring of these females have an equal chance of obtaining the X chromosome carrying the mutant allele, half off the offspring of both sexes will be affected.

Although these rules seem strait, and are in concordance with the inheritance of sex-linked traits in *Drosophila*, several important exceptions seem to apply in humans. As discussed above, dosage compensation in *Drosophila* is achieved by up-regulation of gene expression from the single X chromosome in males [46]. In human, however, one of the two X chromosomes in females is silenced, and since this inactivation is basically random in every cell, females are a mosaic of cells in which either the maternal or paternal X chromosome is inactivated [30]. In *Drosophila*, a recessive trait on the X chromosome is really behaving recessively, since both X chromosomes in a cell of the female fly are active and thus being expressed. However, in women, this is not the case. If both X chromosomes have an equal chance of being inactivated, in half of the cells the recessive allele will be inactivated and hence not expressed, whereas in the other half of the cells the recessive allele will be present on the active X chromosome. Thus even a recessive trait will be uniquely expressed in half of the cells of women, therefore making it dominant at the cellular level, and should thus result in a phenotype similar to that in hemizygous males. Indeed, far more female carriers of an X-linked disease present with clinical symptoms [425-427], which cannot be explained by the simplified rules of dominant and recessive X-linked inheritance as obtained in the *Drosophila* model, deduced in a time that knowledge on differences between human and *Drosophila* dosage compensation was lacking [428]. In agreement with this, a systematic review of 32 X-linked diseases has shown that, as expected based on the X-linked pattern of inheritance, the severity and penetrance, which is the frequency with which a genotype manifest itself in a given phenotype, are higher in males then in females carrying an X-linked disease mutation, whereas the severity and penetrance are highly variable in heterozygous females, varying from high, to intermediate and low between different disorders, but also in females being affected with the same disease [428]. Thus apparently, for X-linked diseases, classifications as recessive and dominant are misleading, and can better be described as X-linked [428].

X chromosome inactivation mosaicism and skewing as modifiers of X-linked human disease in females

In complex organisms like humans, many different cell types have to work together to obtain a normal physiology. As a consequence of XCI, and the clonal propagation of the inactivated state of the inactive X chromosome, women are a mosaic of two cell populations, with either the maternally or the paternally inherited X chromosome being inactivated [33]. Both populations of cells make up all organs, and despite the mixing of both different cell populations, a proper interaction is required for development and physiology. Different forms of communication are present between cells, whether it is through direct cell-cell contacts or secreted factors, which most of the time result in a metabolic cooperation between cells [427]. In the light of X-linked disease, these interactions can have crucial consequences for the outcome of the disease severity for a female carrier of a heterozygous mutation [429]. If an X-linked mutation results in the absence of a certain protein, a cell which has inactivated the wild type, non mutated, X chromosome will experience problems from the absence of the protein, possibly resulting in a growth disadvantage of that cell, or even cell death, which will result in selection against the mutant cells. However, if the protein or signal can be acquired from cells in the surrounding of the mutant cells, for example by uptake through endocytosis or gap junctions, the deficiency of the mutant cell can be hidden, and function might be restored. This form of metabolic cooperation between cells seems to be true for a variety of X-linked metabolic diseases, including Lesch-Nyhan syndrome, Fabry disease and Hunter syndrome which manifest themselves with a severe phenotype in affected males, but only present mild symptoms in heterozygous females. In iduronate sulfatase deficiency (Hunter syndrome, OMIM: 309900), large amounts of mucopolysaccharides accumulate in mutant cells, resulting in bone abnormalities, deafness and enlarged organs in affected males. In female heterozygote carriers of the same mutation, iduronate sulfatase is transferred from wild type cells to the mutant ones, and hence the accumulation of harmful products does not occur in these women, resulting in a minimal presentation or absence of disease symptoms [430]. In Fabry disease (OMIM: 301500), another lysosomal storage disease which results in accumulation of glycosphingolipids in blood and lysosomes of most cells, causing clotting of blood vessels and tissue damage, females also have milder symptoms, since the α-galactosidase A enzyme can transfer from unaffected cells to the mutant cells, although at a lower efficiency compared to iduronate sulfatase. In Lesch-Nyhan syndrome (OMIM: 300322), males have hypoxanthine phosphoribosyltransferase (HPRT) deficiency, causing a defect in recycling of purine bases, resulting in mental retardation, cerebral palsy, self-destructive biting behavior and accumulation of uric acid in joints. Heterozygous female carriers of the disease are not affected, because inosinate, a product of the HPRT metabolic reaction, is transferred through gap junctions. This transport is possible in fibroblasts, resulting in a fibroblast population of both wild type cells and surviving mutant cells, but in circulating blood cells, where gap- junctions are not present, this form of rescue cannot occur, resulting in the selection against cells which do express the mutant allele [425]. Most likely, these cells are gradually outcompeted by the wild type cells, which will have a proliferative advantage over the mutant cells [429, 431-432].

Most of the time, the presence of an X-linked mutation results in a growth disadvantage of cells expressing the mutated allele [433], but this is not always the case. In adrenoleukodystrophy (OMIM: 300100), were mutations in the *ABCD1* gene result in a non-functional ALDP protein, cells expressing the mutated form of the protein proliferate faster [434-435]. ALDP is involved in the transport of fatty acids into the peroxisomes, were fatty acids are being oxidized in the beta-oxidation pathway, as a means of energy production. When the function of ALDP is ablated in males, fatty acid accumulation in cells cause a loss of function of the adrenal glands, and progressive destruction of myelin in the central nervous system. Several variations of the disease exist, which affect only the adrenal glands, or show a phenotype also in the central nervous system or even the spinal cord (adrenomyeloneuropathy). Heterozygous females are often symptom free at the beginning of their life, but during aging they can develop spinal cord symptoms, which indicates that the mutant cells gradually take over, due to a growth advantage which is currently not explained.

Interestingly, not always does cell communication result in an amelioration of an X-linked disease, and in some cases it might even worsen the phenotype in heterozygous females. This is the case for mutations in the *EFNB1* gene which cause craniofrontonasal syndrome (OMIM: 304110) [436-437]. The absence of functional ephrin B1 protein, a signaling molecule involved in many developmental processes, results in premature closure of the coronal suture (craniosynostosis), and thus aberrant skull development, only in females. Males with mutations in EFNB1 do not develop these skull deformations, because other redundant signaling molecules are able to replace the function of ephrin B1. In the case of heterozygous females, where XCI has resulted in a mixture of cells which are either positive or negative for ephrin B1, such a redundant signaling pathway is disrupted by a mechanism called cellular interference [438-439].

Although XCI in principal results in two different populations of cells, and this can have a profound effect on the manifestation of X-linked diseases in heterozygous females, another layer of complexity is added by the fact that the ratio of the two cell lines, with either the maternal or paternal X chromosome being inactivated, is not always 50:50. In fact, studies have shown that in large populations of healthy women, the ratio between both cell types follows a bell-shaped distribution, with a mean of 50:50 and extremes approaching 100:0 or 0:100 [440-441]. Just by chance, a proportion of women will have a deviation from the 50:50 ratio and this deviation is called skewing of XCI (**Figure 12**). How can this skewing be explained? Several factors might contribute, and most likely one of the most important factors will be the presence of a limited amount of cells at the moment that XCI is initiated. Even when every cell has a 50% chance of inactivating the one or the other X chromosome, when the starting pool of cells is small, just by chance the majority of cells might choose to inactivate for example the X derived from father. Although it is not exactly known how many cells are present at the moment that XCI is initiated in the human embryo, it is estimated that there are most likely between 10-20 cells which commence to initiate XCI [442-444]. Hence, with such a small pool of progenitor cells, it seems likely that the stochastic nature of the process plays an important role in determining the XCI fate of the X chromosomes present.

Skewing of XCI likely is also genetically determined. In mice, distortions from random XCI are observed when several inbred mouse strains are intercrossed, and since

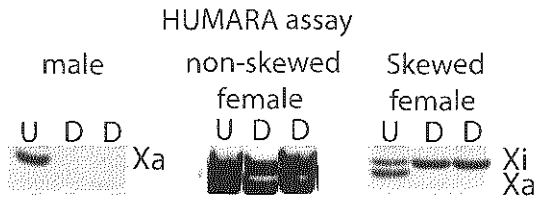

Figure 12: XCI skewing analysis in females using the HUMARA assay
To determine the degree of XCI skewing, a frequently used method is the Human Androgen Receptor assay, which makes use of the presence of a polymorphic repeat in the *androgen receptor* and methylation of the inactive X chromosome. Prior to digestion with a methylation-sensitive enzyme (undigested, U) PCR analysis will show a single allele in males (left panel), and two alleles in females (when polymorphism is present). Upon digestion with a methylation sensitive enzyme (digestion, D), only the allele which is inactivated, and hence methylated, will be amplified. Therefore in males upon digestion, no band is detectable. When XCI is random in females, 50% of cells will methylate the one allele, whereas 50% of cells will methylate the second allele. Therefore, in a non-skewed female, the same bands will be seen upon digestion as in the undigested sample (middle panel). Upon complete skewing (right panel), only a single allele will be detected.

these deviations are not caused by cell selection, they are referred to as primary non-random XCI. This has resulted in the classification of mouse strains according to differences in the strength of the X controlling element (Xce), a genetically defined locus which affects skewing [445-447]. Although the identity of this locus is still unknown, genetic mapping studies have indicated that it lies downstream of *Xist* [448-450]. Alternatively the amount of skewing might correlate with the presence of SNPs in XCI regulatory elements, including the *Xist* promoter or the gene itself, or other regulators, like XCI-activators and -inhibitors, or their binding places. In agreement with this, SNPs have been found in the human *XIST* promoter, which seem to correlate with skewing [451-453]. In both cases, a CTCF binding site seems to be affected, by a nucleotide change located at -43 bp of the transcriptional start site of *XIST*. Whether an XCE exists in human is unclear at the moment [454-455]. Several families have been identified in which extreme skewing of XCI is inherited, but this extreme skewing could also be caused by the presence of an unidentified X-linked disease allele which is being selected against [456-461] when affected cells have a proliferative disadvantage, or die, as discussed above. Therefore, skewing could also be caused by X-linked mutations affecting the viability of the cell, followed by negative selection, or sometimes even positive selection, as in the case of adrenoleukodystrophy. An even more extreme form of this secondary non-random XCI, is found in so-called trisomic zygote rescue, and might also be causative in the development of skewing. Some cases have been described, in which the placental tissues consist of a high proportion of trisomic cells, whereas the resulting fetus consist of diploid cells, which have a severely skewed XCI phenotype [462]. It has been hypothesized that such fetuses may survive, since the initial zygote, which must have been trisomic as well, lost the supernumerary chromosomes. Since such a lucky event will only occur in a minority of cells in such an otherwise lethal embryo, even more cells might have been lost from the

already small pool of cells which initiate XCI, resulting in the extreme skewing observed in the girl born. Such a reduction in progenitor pool size might also underlay the observed more extreme skewing in monozygotic twins compared to singlets [373, 463-475], although not all studies agree on this [443, 476-479].

The selection pressure for or against a cell carrying an X-linked mutation does not seem to be the same in all tissues or at all developmental time points. For example, it has been found that several X-linked diseases only result in skewing in particular tissues. In X-linked agammaglobulinemia (Bruton's agammaglobulinemia, OMIM: 300300), caused by mutations in the *BTK* gene, mutant B cells are unable to mature, and mutant B cells are thus absent in the peripheral blood system of heterozygous females, where wild type B cells are selected for [480-483]. The mutant B cell progenitors however can be found in the bone marrow, indicating that different stringencies of selective pressure are maintained in different tissues. Also other cell types, where *BTK* is not expressed, will most likely be confronted with an absence of a selection pressure against mutant cells. The same tissue-specific skewing can be found in other hematological X-linked diseases, including X-linked severe combined immunodeficiency (X-SCID, OMIM: 300400) [442, 481, 484-485] and Wiskott-Aldrich syndrome (OMIM: 301000) [486-490], and extreme skewing has even been used to identify carriers of the disease mutations prior to genetic testing of the disease genes [491-495].

Skewing is not only influenced by tissue specificity, but also by aging. Interestingly, a large number of studies have found that skewing is more prevalent in elderly women [441, 454, 461, 479, 496-501]. Certain X-linked diseases only develop in elderly women due to age-related skewing. Examples include sideroblastic anemia (OMIM: 300751) [502-503] and X-linked hemolytic anemia (OMIM: 305900) caused by G6PD deficiency [504-506]. The reason for this is not clear, but might involve stochastic clonal loss [507], or genetic selection, maybe due to subtle, hidden mutations or SNPs affecting gene function or expression of X-linked genes, which manifest themselves gradually in a growth advantage or disadvantage [497, 508-510].

What is clear from the issues discussed above is that the variability of symptoms in heterozygous female carriers of an X-linked disease can be influenced by many factors. Genetic and stochastic factors will determine in the first place the mosaic distribution of cells in embryonic tissues having inactivated the X derived from father or from mother. This immediately results in a mosaic distribution of mutant and wild type cells, through the growing tissues. The effect of the mutation itself on the cell viability and growth of the mutant cells will further result in a complicated interplay between wild type and mutant cells, either favoring wild type cells when the mutation results in a negative outcome for the affected cells, or favoring the mutant cells when the mutation is advantageous. When mutations affect cell-autonomous proteins and pathways, a different outcome can be expected compared to the situation in which mutant cells can be rescued by wild type proteins obtained from neighboring cells. Thus not only does skewing influence the outcome of genetic disease, also the opposite is true; namely, due to X-linked disease the ratios between cells having inactivated the wild type or the mutant X chromosome will differ, dependent on the effect of the mutation. However, since females have two X chromosomes, favorable skewing of XCI, either primary or secondary due to selection, can thus often result in a better outcome of X-linked diseases compared to males, which suffer

from their higher vulnerability for X-linked diseases due to the presence of the hemizygous X chromosome, lacking a backup allele for X-linked loci. **Table 2** summarizes several diseases in which favorable skewing has been found in heterozygous carriers of X-linked disease, presenting themselves with minimum symptoms compared to males.

When mosaicism causes a disadvantage: emergence of manifesting heterozygotes

Not always does the mosaic expression or a totally skewed XCI result in a benefit for a woman. This can occur when extreme skewing results in inactivation of one X chromosome, maybe because of selection against a mutant allele, but unfortunately also the active X chromosome harbors a genetic defect. This disease allele, which would otherwise maybe be selected against, or the disease outcome would benefit from a mosaicism, will now be active in all cells, causing disease which is otherwise not seen in heterozygous female carriers. Such a case has been described in which a female inherited a mutation in the incontinentia pigmenti gene *NEMO* (OMIM: 308300) from her mother, and a mutation in the *F8* gene causing haemophilia A (OMIM: 3067000) from her father [511]. The *NEMO* mutation is detrimental for cells, and thus strongly selected against, rendering all cells with the wild type incontinentia pigmenti gene active. Unfortunately for this patient, the X chromosome containing the wild type *NEMO* gene also contains the mutant *F8* gene, therefore resulting in a bleeding disorder in the affected female.

Many cases of these so-called manifesting heterozygotes have been described in the literature [513, 520-522], and some of these have even been crucial for the discovery of the disease alleles involved. The reason for the extreme skewing which results in the manifestation of the X-linked disease can be variable, ranging from chance to genetic causes, as discussed above. In the case of a girl presenting with Wiskott-Aldrich syndrome (OMIM: 301000) [523-524], the affected girl, and her mother and grandmother showed extreme skewing, pointing to a genetic cause. The mutant Wiskott-Aldrich syndrome was located on the active X chromosome, causing the disease, which is normally not seen in females due to XCI of the X carrying the disease allele. Other women with Wiskott-Aldrich syndrome have been described, where skewing of XCI resulted in 100% of cells with the mutated allele on Xa [525-526], or absence of skewing against the mutant allele was observed [527-529]. Other similar examples includes affected females with haemophilia B (OMIM: 306900) [530-531], myotubular myopathy (OMIM: 310400) [532-534], X-linked hemolytic anemia (OMIM: 305900) [535], ATRX syndrome (OMIM: 301040) [536] and Fabry disease (OMIM: 301500) [537], where also extreme skewing of XCI towards inactivation of the wild type X chromosome was found.

Another frequent cause of manifesting heterozygotes are chromosome translocations involving the X chromosome [538]. In translocations, two breaks occur, one in the X chromosome, and another one on an autosome, after which the broken parts can be rejoined together. Generally, two types of X-to-autosome translocations can be distinguished, a balanced or an unbalanced translocation. In unbalanced X translocations, an additional part of the X chromosome is present, linked to a piece of autosome, representing a partial trisomy of that autosome. In general trisomies of autosomes are not at

Table 2: X-linked disorders associated with favorable skewing and minimal disease in females

Disease	Gene	Gene location	OMIM	Phenotype in males	Reference skewing in females
Agammaglobulinemia	*BTK*	Xq21.33-q22	300300	Decreased number of peripheral B-cells, decreased antibody levels and recurrent infections	Allen et al 1994 [480] Li et al 1998 [481] Moschese et al 2000[482]
Alpha-thalassemia / mental retardation syndrome	*ATRX*	Xq21.1	301040	Dysmorphic features, mental retardation, hemoglobin H disease, epilepsy	Gibbons et al 1992 [512] Wada et al 2005 [513]
Barth syndrome	*TAZ*	Xq28	302060	Cardiomyopathy, neutropenia, skeletal myopathy and growth delay	Orstavik et al 1998 [514]
Dyskeratosis congenita	*DKC1*	Xq28	305000	Premature aging, abnormal skin pigmentation, nail dystrophy, leukoplakia, progressive bone marrow failure	Ferraris et al 1997 [515] Devriendt et al 1997 [516] Vulliamy et al 1997 [517]
Dystonia-deafness-optic neuronopathy syndrome	*DDP*	Xq22.1	304700	Progressive form of deafness, visual disability leading to cortical blindness, dystonia, fractures, mental deficiency	Orstavik et al 1996 [460]
Hypohidrotic ectodermal dysplasia with immunodeficiency	*NEMO*	Xq28	300291	Hypomorphic mutations resulting in skin lesions and recurrent infections	Orstavik et al 2006 [518]
MECP2 duplication syndrome	*MECP2*	Xq28	300260	Intellectual deficits, autism, muscular hypotonia, frequent recurrent infections and mild dismorphic features	Van Esch et al 2005 [519]
Severe combined immunodeficiency syndrome	*IL2RG*	Xq13	300400	Increased susceptibility to infections, low antibody levels, thymus atrophy	Hendriks et al 1992 [485] Hendriks et al 1993 [484] Puck et al 1992 [442] Li et al 1998 [481]
Wiskott-Aldrich syndrome	*WASP*	Xp11.23-p11.22	301000	Thrombocytopenia with small-sized platelets, eczema, recurrent infections	Gealy et al 1980 [487] Prchal et al 1980 [488] Fearon et al 1988 [490] Goodship et al 1991 [489]

all tolerated, except for partly viable trisomies of chromosome 13, 18, 21 (Patau, Edwards, and Down syndromes, respectively) or 22, which nevertheless result in severe health problems. An unbalanced X-autosome translocation will only be viable if the translocated piece of X chromosome is able to undergo inactivation and to silence the attached piece of autosome by the spreading of XCI. Therefore the translocated piece of X chromosome must at least contain the XIC, located at Xq13. If this is not the case, this will most likely result in a non-viable situation, since the cells will be confronted with a higher dosage of autosomal genes. If, in the case of an unbalanced translocation, there is no duplicated, extra part of an autosome present, silencing of the translocated X chromosome might result also in silencing of the attached autosomal segment, resulting in a monosomy of autosomal genes, which is also likely to be lethal. In case of balanced translocations, the situation is different [539]. In a balanced translocation, the total amount of chromosome parts is the same as in a normal genome, but now a piece of X chromosome is translocated to a piece of autosome, and also the other two broken parts are joined together. Since these cells still have together two X chromosomes, one of them has to undergo XCI. However, if the X containing the autosomal part would start inactivation, it would also silence autosomal genes, leading to a monosomy of the autosomal part of the attached chromosome. Since autosomal monosomies are not compatible with life, cells having inactivated the translocation chromosome will be selected against. Therefore, in a balanced translocation, the wild type X chromosome is always inactivated, leaving the translocation products active, and resulting in the best genetic balance. Hence, most of the carriers of balanced translocations have a normal phenotype, although they might be sterile [539]. However, in the process of translocation break and repair, parts of the X chromosome might get lost, or the breakage can disrupt a gene coding sequence. Since the wild type X chromosome in these balanced X-to-autosome translocations is always inactivated, the disrupted gene will be on the active (parts of the) X chromosome(s), and therefore can result in a manifesting disease in a female. Examples of this include girls with hypohidrotic ectodermal dysplasia (OMIM: 305100) [540], Lowe oculocerebrorenal syndrome (OMIM: 309000) [541], Simpson-Golabi-Behmel syndrome (OMIM: 312870) [542] and hyper IgM immunodeficiency syndrome (OMIM: 308230) [543]. Such X-to-autosome translocations have also been helpful in the mapping of several X-linked disease genes, including genes underlying Duchenne muscular dystrophy (OMIM: 310200) [544-548], oligophrenin-1 syndrome (OMIM: 300486) [549-550], Aarskog-Scott syndrome (OMIM: 305400) [551], incontinentia pigmenti (OMIM: 308300) [552] and chronic granulomatous disease (OMIM: 306400) [553-554].

Diseases where females likely benefit from their mosaicism: male lethal diseases and diseases with reduced viability of males

A severely detrimental mutation on the single X chromosome will result in male lethality, so that no males are born carrying such a disease allele. Indeed, several X-linked disorders have been described which result in male lethality, or highly reduced male viability, and therefore these diseases are only found in females (**Table 3**) [555-557]. This group of diseases is characterized by symptoms in heterozygous females, and they were originally classified as being X-linked dominant. However, symptoms amongst affected females are variable, with some patients presenting full blown disease phenotypes, whereas others present as asymptomatic carriers. In most instances, XCI skewing and mosaicism are responsible for the different phenotypes observed, and explain that many affected females are alive despite carrying a disease allel which is lethal in males. Indeed, in the majority of these diseases, favorable skewing is associated with reduced symptoms [558-569]. In case of Rett syndrome (OMIM: 312750), where mutations in the MECP2 gene cause autism, ataxia, tremors, loss of purposeful hand use and dementia [570], XCI is often random amongst affected females [571]. However, some sporadic, unaffected female carriers of the mutation, show preferential inactivation of the disease allele [572], and favorable skewing has been observed also amongst milder affected females [573]. Also in another male lethal neurodevelopmental disorder, called microphthalmia with linear skin defects syndrome (OMIM: 309801) caused by mutations in the *HCCS* gene, skewed XCI has been observed in the majority of cases [574-576]. Here it seems that the presence of severe skewing is the only reason that female patients are alive, as skewing has been reported in all heterozygous females [556]. Apparently, HCCS mutant cells have such a pronounced growth disadvantage that in the majority of tissues massive selection has occurred against cells with the mutant allele on the active X chromosome. The efficiency with which this process occurrs in different tissues might explain the variable phenotypes observed between different affected females harboring the same mutations. Besides favorable skewing, another advantage for females might be the possibility of genes escaping XCI. For both incontinentia pigmenti (OMIM: 308300) and oral-facial-digital syndrome type I (OMIM: 311200) it has been found that these genes escape XCI in humans [240, 577-578]. For the latter syndrome, this might explain why human females carrying an *OFD1* mutation are alive, whereas mice with a heterozygous *Ofd1* knockout allele die, because *Ofd1* is not escaping XCI in mouse [557, 579-580]. Escape most often is not complete and might be tissue specific, and this might explain why skewing of XCI is still observed in some cases of these syndromes [559, 564].

X-linked disease in females not related to X chromosome inactivation or skewing

As is clear from the discussion above, X chromosome inactivation can have a great influence on the phenotype and severity of X-linked diseases in females. However, not all female diseases due to X-linked mutations are necessarily influenced by X chromosome inactivation. Besides what is seen in manifesting heterozygotes due to unfavorable skewing, females might also experience symptoms of an X-linked disease just due to the fact that they inherited two mutant alleles for the same disease. Examples of homozygotes for X-linked diseases include females with hemophilia [581-584], congenital X-linked nystagmus (OMIM: 310700) [585], X-linked recessive ichthyosis (OMIM: 308100) [586], hypophosphatemic rickets (OMIM: 307800) [587] and Becker muscular dystrophy (OMIM: 300376) [588], amongst others. The chance of inheriting two X-linked recessive alleles is low, except for genetically homogenous families or families where X-linked diseases are known to occur on both parental sides [589-590]. In addition, homozygous mutations for X-linked genes can also be caused by *de novo* mutations [582], or in rare causes of uniparental disomy, where both X chromosomes present are derived from the same parent [591]. Also, manifestations of X-linked diseases in females sometimes discover a hidden, or not yet diagnosed form of Turner syndrome, in which a female has only one X chromosome, thus rendering a Turner female prone to the same risk of developing an X-linked disease as a hemizygous male [592-598]. Even more rarely, the presence of an X-linked disease has discovered cases of dysregulated sex-determination, where affected females turned out to have a male karyotype [599-603].

The benefits or disadvantages of mosaicism related to X-linked gene expression may not always be related to X chromosome inactivation. For example, rare cases of mosaicism may be caused by fusion of two distinct zygotes, or due to placental transport of cells between twins [604-605]. Such chimaeras might display mosaicism, in which one population of cells harbors an X-linked mutation, whereas the other carries a wild type allele. Also mutations occurring in the postzygotic stages of an embryo will result in the fact that not all cells of the body will harbor a mutation. The later in embryonic development the mutation occurs, the fewer cells will be affected [614]. In such cases, it is also possible that the mutation does not affect the germ line, which is important for counseling issues and the risk of transmitting the disorder to the offspring [615-617].

Table 3: X-linked Disorders with reduced viability in males

Disease	Gene	Gene location	OMIM	Clinical phenotype	XCI	Reference
Aicardi syndrome	Not found	Xp22	304050	Abnormal brain development, mental retardation, rib and vertebral defects	Random Skewed	Wieacker et al 1985 [606] Neidich et al 1990 [607] Hoag et al 1997 [608] Eble et al 2009 [609]
Angioma serpiginosum	*PORCN*	Xp11.3-q12	300652	Nonpurpuric red punctate lesions, hyperkeratosis, dysplastic nails	Skewed	Blinkenberg et al 2008 [569]
Chrondodysplasia punctata type 2	*EBP*	Xp11.23	302960	Skin, skelet and craniofacial defects, cataracts	Random Skewed	Shirahama et al 2003 [562] Canucto et al 2011 [610]
Congenital hemidysplasia with ichthyosiform erythroderma and limb defects (CHILD)	*NSDHL*	Xq28	308050	Ichthyosiform nevi; limb, kidney and cardiac defects; brain malformations	Random	König et al 2002 [611]
Focal dermal hypoplasia (Goltz syndrome)	*PORCN*	Xp11.23	305600	Skin atrophy and other abnormalities, mental retardation, digital, ocular and oral anomalies	Random	Leoyklang et al 2008 [568]
Frontometaphyseal dysplasia (OPD spectrum disorder)	*FLNA*	Xq28	305620	Generalized skeletal dysplasia, deafness, urogenital defects	Skewed	Robertson et al 2006 [567]
Incontinentia pigmenti	*NEMO*	Xq28	308300	Malfomations of brain, heart, eyes, teeth and skeleton, abnormal skin pigmentation	Skewed	Parrish et al 1996 [561] Fusco et al 2004 [564]
Melnick-Needles syndrome (OPD spectrum disorder)	*FLNA*	Xq28	309350	Skeletal dysplasia, Ureteral obstruction	Skewed	Kristiansen et al 2002 [565]
Microphthalmia with linear skin defects (MIDAS) syndrome	*HCCS*	Xp22	309801	Microphthalmia and dermal aplasia, brain and eye abnormalities, mental retardation, congenital heart defects	Skewed	Lindsay et al 1994 [575] Ogata et al 1998 Franco et al 2006 [556] Schluth et al 2007 [612]
Oculo-facio-cardio-dental syndrome	*BCOR*	Xp11.4	300166	Facial, eye and teeth abnormalities, cardiac septal defects	Skewed	Hedera et al 2003 [563]

Table 3: Continued

Oral facial digital syndrome type 1	*OFD1*	Xp22	311200	Facial and limb abnormalities, brain malformations, mental retardation and polycystic kidney disease	Random Skewed	Thauvin-Robinet et al 2006 [559]
Otopalatodigital syndrome (OPD spectrum disorder)	*FLN1*	Xq28	311300	Palate and mild skeletal anomalies, conductive deafness caused by ossicular anomalies	Skewed	Robertson et al 2003 [560]
Rett syndrome	*MECP2*	Xq28	312750	Autisme, dementia, ataxia and loss of purposeful hand use	Random Skewed	Huppke et al 2006 [573] Chahrour et al 2007 [571] Dayer et al 2007 [572]
Rett-like syndrome	*CDKL5*	Xp22.13	300203	Developmental delay, autistic features, tactile hypersensitivity, Rett-like features	Random	Bahi-Buisson et al 2008 [558]
Terminal osseous dysplasia and pigmentary defects syndrome	*FLNA*	Xq27.3-q28	300244	Bone and limb abnormalities, skin lesions and dysmophic features	Skewed	Baroncini et al [613]

Overview of X-linked diseases

The following discussion summarizes a selection of the most important X-linked diseases organized by organ systems, which are being discussed, where possible, in the context of their relationship to X chromosome inactivation. A more detailed discussion on the clinical symptoms, characteristics and treatments of these diseases is beyond the scope of this thesis, and the interested reader is referred to a selection of reviews as indicated in the text, or to online resources (Online Mendelian Inheritance in Man (OMIM) database, http://www.ncbi.nlm.nih.gov/omim) for further information. Since several diseases manifest their selves with symptoms in different organ systems, they might be discussed at multiple places.

X-linked disorders of the hematopoietic system

One of the most classical examples of an X-linked disease is certainly the bleeding disorder hemophilia, with one of its most prominent patients being the Russian Tsar crown prince Alexei [618] amongst other European Royals [619]. Two different X-linked genes, *F8* (hemophilia A) and *F9* (hemophilia B), encode blood clotting factors, which are essential for hemostasis after injury. When these proteins are deficient, affected patients, mainly males, will suffer from hemorrhages upon mild trauma, which can result in lethal conditions. Women are most often not affected, with the exception of manifesting heterozygotes, discussed above. Interestingly, female asymptomatic carriers do not show signs of XCI skewing [620], indicating that 50% of the cells retaining normal levels of clotting factor are sufficient to prevent major bleedings. Only when skewing adversely affects the percentage of cells carrying a wild type clotting factor allele, manifestation of the disease may occur [530, 621].

Several X-linked disorders affect the red blood cell fraction, which can result in lethal anemias. X-linked hemolytic anemia (OMIM: 305900) is caused by mutations in the *G6PD* gene, which is essential for the pentose phosphate pathway (generation of NADPH) of red blood cells. Males suffer from chronic anemia, as well as drug induced acute anemias, whereas females are only mildly affected, due to favorable skewing caused by cell selection [433, 622]. Certain *G6PD* mutations are more common in areas which are endemic for malaria, as G6PD deficiency protects against this intracellular parasite [623-624].

Other anemias include Fanconi anemia [625], X-linked sideroblastic anemia [626] and GATA1-related anemia [627]. Fanconi anemia (complementation group B, OMIM: 300514) is a heterogenous disorder affecting multiple organ systems due to genomic instability caused by mutations in the *FAAP95* gene affecting DNA repair. Clinical characteristics include multiple congenital abnormalities in different organs, a predisposition to develop cancer, and early onset bone marrow failure. Females are in general less affected, and in the majority of female carriers of the disease gene favorable skewing has been found [628-629]. The same is observed in X-linked sideroblastic anemia (OMIM: 300751), where mutations in the *ALAS2* gene result in hypochromic microcytic anemia and iron overload due to chronic ineffective erythropoiesis. Interestingly, for this

disease a clear correlation between the amount of skewing and the symptoms has been observed in several cases [630-632]. Also in GATA1 related macrothrombocytopenia and anemia (OMIM: 300367) extreme skewing has been found in female carriers of the gene mutation [633].

Influence of the X chromosome and X chromosome inactivation on the immune system

Complex organisms continuously face the threat of pathogens, toxic substances and other environmental hazards. To survive, a complex immune system has evolved in mammals, which consists of different layers of defense, including physical barriers, the complement system, different cell populations, and a complex antibody system, which is able to conquer most of the envisioned challenges. Many of the genes directly or indirectly involved in these processes are located on the X chromosome, including genes involved in the Toll-like receptor-nuclear factor κB signaling machinery (*IRAK1*, *NEMO* and *BTK*), genes involved in the apoptosis cascade (*XIAP* and *PDCD8*), and genes functioning in the oxidative burst of phagocytes (*CYBB* and *G6PD*), amongst approximately 50 others [634]. Interestingly, many sex-specific differences in the immune response exist, and women, in general, seem to have evolved a better immune system. This is illustrated by the fact that males are more susceptible to infectious diseases [635-636], and females have better antibody responsiveness to stimuli [637-638], which might contribute to the fact that in many species, including human, females have a higher life expectancy compared to males [639]. This better equipped immune system in females is likely the consequence of the presence of two cell populations with different parental active X chromosomes, thereby resulting in more diversity when facing immunological challenges, and also preventing the risks of deleterious gene mutations in a heterozygous genetic background [640-642]. Indeed, several X-linked primary immune deficiencies exist, which mainly affect males, and result in skewed XCI in female carriers, with minimal disease symptoms (**Table 4**).

A pitfall of this better female adaptive immune response is the higher incidence of autoimmune diseases in females. Almost 80% of all patients with autoimmune diseases, including rheumatoid arthritis, systemic lupus erythematosus, autoimmune thyroid diseases, amongst many others, are women [643-644]. Many factors have been proposed to explain this sex bias, including differences in sex hormones, pregnancy related risk factors, sex-specific environmental factors, fetal microchimerism, sex chromosome defects and extremely skewed XCI or failure of XCI [643]. The so-called loss of mosaicism hypothesis for the onset of autoimmune diseases states that in a female with random XCI, two

Table 4: X-linked primary immunodeficiencies

Disease	Gene	location	OMIM	Clinical phenotype	XCI	Reference
Agammaglobulinemia	*BTK*	Xq21.3-q22	300300	Decreased number of peripheral B-cells, decreased antibody levels and recurrent infections	Skewed	Allen et al 1994 [480] Li et al 1998 [481] Moschese et al 2000 [482]
Chronic granulomatous disease	*CYBB*	Xp21.1	306400	Severe bacterial and fungal infections, colitis, granulomata	Skewed	Koker et al 2006 [645]
Hyper-IgM syndrome type 1	*CD40L*	Xq26	308230	Recurrent infections, biliary tract disease, gastro-intestinal tumors	Skewed Random	Notarangelo et al 1991 [646] Hendriks et al 1990 [647]
Hypohidrotic ectodermal dysplasia with immunodeficiency	*NEMO*	Xq28	300291	Hypomorphic mutations resulting in skin lesions and recurrent infections; elevated IgM levels	Skewed	Orstavik et al 2006 [518]
Immune dysregulation-polyendocrinopathy-enteropathy-X-linked (IPEX)	*FOXP3*	Xp11.23	304790	Severe enteropathy, diabetes mellitus, dermatitis, nephropathy, recurrent infections	Random	Tommasini et al 2002 [648]
Properdin deficiency	*PFC*	Xp11.4-p11.23	312060	Fulminant Meningococcal infections	Random	Van den Bogaard et al 2000 [649]
Severe combined immunodeficiency syndrome	*IL2RG*	Xq13	300400	Increased susceptibility to infections, low antibody levels, thymus atrophy	Skewed	Hendriks et al 1992 [485] Hendriks et al 1993 [484] Puck et al 1992 [442] Li et al 1998 [481]
Wiskott-Aldrich syndrome	*WASP*	Xp11.23-p11.22	301000	Thrombocytopenia with small-sized platelets, eczema, recurrent infections	Skewed	Gealy et al 1980 [487] Prchal et al 1980 [488] Fearon et al 1988 [490] Goodship et al 1991 [489]
X-linked lymphoproliferative disease type 1	*SH2D1A*	Xq25	308240	Severe EBV infections, fulminant infectious mononucleosis	Random	Woon et al 2008 [650]
X-linked lymphoproliferative disease type 2	*XIAP*	Xq25	300635	Splenomegaly, bone marrow failure, hepatic necrosis, lymphoproliferation, lymphomas, hypo-agammaglobulenemia	Skewed	Marsh et al 2009 [651]

populations of dentritic cells will exist, which will express either the X-chromosomal maternal or paternal self-antigens for negative selection in the thymus, thereby preventing that potentially autoreactive lymphocytes will be released in the immune system. When a female displays an extreme form of skewed XCI, in which for example the maternal X is always inactivated, only paternal self-antigens located on the X chromosome will be expressed. Therefore, autoreactive T cells against the maternal self-antigens will escape the negative selection, making it possible that B cells will become activated and produce antibodies against the maternal self-antigens, thereby causing an autoimmune disease [652-654]. In line with this, extreme skewing is found in many patients with an autoimmune disease, including juvenile idiopathic arthritis [655], autoimmune thyroiditis, and systemic sclerosis [656-660]. Males with Klinefelter's syndrome (47,XXY), which also display more often severe skewing, have an increased risk of developing systemic lupus erythematosus compared to 46,XY males [661]. In contrast, extreme skewing is not seen in other autoimmune diseases, like Sjögren's syndrome, primary biliary cirrhosis, multiple sclerosis, and rheumatoid arthritis [662-663]. Another hypothesis states that reactivation of the inactive X chromosome might contribute to an increased risk of developing autoimmune disease in females [664-665]. Indeed, reactivation of the silenced X-linked gene *CD40L* has been observed in T cells, and has been implicated to play a role in the pathogenesis of systemic lupus erythematosus female patients [664, 666]. However, whether this mechanism is playing a more general role in the emergence of autoimmune diseases needs to be addressed in future studies. Interestingly, loss of dosage compensation has also been proposed to explain the high levels of expression of polyamines in autoimmune diseases. Two X-linked genes involved in polyamine synthesis and recycling, *SMS* and *SAT1*, might be responsible for such a high polyamine level, and have also been implicated in disturbance of intracellular methylation [667]. Finally, it has been hypothesized that haploinsufficiency plays an important role in the development of autoimmune diseases. Females with Turner's syndrome (45,X) show a higher prevalence of autoimmune diseases [668-670], which has been correlated to haploinsufficiency of genes located in the pseudoautosomal region of the X chromosome. A high rate of X chromosome monosomy has also been observed in lymphocytes of patients with primary biliary cirrhosis, autoimmune thyroiditis and systemic sclerosis, arguing for an important role of haploinsufficiency in the development of these diseases [671-672]. In contrast, systemic lupus erythematosus patients are not characterized by a higher incidence of X chromosome monosomy [673]. However, the precise mechanism of a potential role for X chromosome monosomy and genes involved in the pathogenesis of autoimmune diseases needs to be identified.

X-linked mental retardation

The human X chromosome is enriched in particular in genes expressed in brain [14]. It is therefore not surprising that many genes involved in the pathogenesis of mental retardation and mental disability are found on the X chromosome. Mental retardation, defined as suboptimal functioning of the central nervous system resulting in significant limitations both in intellectual performance and adaptive behavior as expressed in conceptual, social

and practical adaptive skills, affects 1 to 3% of the general population [674]. Around 50% of these cases are caused by genetic causes, amongst which X-linked mental retardation is the most common cause of monogenic intellectual disability [674]. More than 215 X-linked mental retardation disorders and syndromes have been described, and more than 80 genes have been mapped to the X chromosome causing these disorders [674], with more genes still being identified [675-676]. X-linked mental retardation genes are found along the whole X chromosome, but two areas of higher enrichment are found in Xp11.2 and Xq28 [674]. In the majority of cases, males are affected, whereas females show no or only mild symptoms. Indeed, a study investigating the X inactivation pattern in 155 female subjects from 24 families in which males were affected by X-linked mental retardation showed that 50% of the X-linked mental retardation female carriers showed extreme skewed inactivation of the mutated allele in blood cells [677]. Of note, in several of the disorders studied, including X-linked mental retardation with short stature and tremor syndrome (OMIM: 300354), all female carriers showed extreme skewing, which argues for a selection mechanism against cells expressing the mutant proteins involved [677]. In other syndromes more variable skewing has been found. The latter category includes Allan-Herndon Dudley syndrome (OMIM: 300523), caused by mutations in the thyroid hormone transporter *SLC16A2* (also known as *XPCT* or *MCT8*) gene, where only several female carriers were found with extreme skewing [677]. This might be caused by tissue specific skewing, which might be different between the brain and the blood cells [678]. In our own studies on manifesting heterozygotes of *SLC16A2* mutations, we detected preferential X chromosome inactivation of the mutated allele in blood samples of affected females (Barakat T.S. and Friezema E., unpublished observations, **Figure 13**), which also argues that the skewing ratios might differ in between tissues. The same is observed in patients with mutations in the creatine transporter *SLC6A8*, causing mental retardation and constipation, where also different skewing ratios in different tissues have been found [679].

The most frequent X-linked mental retardation syndrome is fragile X syndrome (OMIM: 300624), affecting 1 in 4000 males and 1 in 6000 females. Fragile X syndrome is characterized by mental retardation, autistic behavior, macroorchidism, a characteristic facial appearance and hyperextensible joints, and is caused by expansion of a CGG repeat in the 5'untranslated region of the *FMR1* gene, which causes the transcriptional silencing of the gene and thus the absence of the FMRP protein [680]. In normal individuals, the repeat size of the CGG repeat consists of 5-50 repeats, whereas the repeat size is expanded to more than 200 repeats in case of a full mutation. This repeat expansion results in methylation of the *FMR1* promoter and the transcriptional shut-down of the gene. The *FMR1* gene is subject to X chromosome inactivation [681], and skewed X inactivation has explained the variable symptoms in affected females [682-686]. Interestingly, some males harboring the full mutation have a better phenotype, which correlates with the presence of cells with non-methylated *FMR1* alleles [687-688]. Therefore in females carrying the full mutation, the presence of unmethylated alleles and favorable X chromosome inactivation skewing will result in a milder phenotype [689]. A repeat size between 50 and 200, the so-called premutation allele, is not only associated with the risk of expansion towards the full mutation when transmitted through the female germ line, but does also cause the fragile X associated tremor/ataxia syndrome (OMIM: 300623), which is characterized by adult-onset progressive intention tremor and ataxia in up to a third of all premutation carriers. In

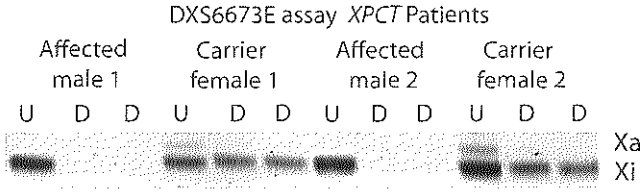

Figure 13: Female carriers for a *XPCT* mutation show preferential inactivation of the X chromosome harboring the mutation
Skewing of XCI was analysed using the methylation status of the X-linked DXS6673E locus, for a family of two males affected for Allan-Herndon Dudley syndrome and their respective mothers. Upon PCR on undigested DNA (U), a single allele is detected in the male patient (X chromosome harboring the mutation), whereas two alleles are detected in the female carriers. Upon digestion (D) with a methylation sensitive enzyme followed by PCR, only the methylated allele can be amplified, which is derived from the inactivated X chromosome. For the carrier females, this is always the smaller allele, which is the same allele present in the affected males.

contrast to the full mutation, the premutation results in a higher expression of *FMR* RNA, compared to a wild type level, which results in cytotoxicity. Also here, X inactivation skewing is related to phenotypic differences in the disease onset and severity [690].

Mutations in the *MECP2* gene cause Rett syndrome (OMIM: 312750), which is one of the most severe X-linked disease, resulting in autism, ataxia, loss of purposeful hand use and dementia in affected females, and are not compatible with male viability [570]. XCI is often random among affected females [571], but some sporadic, unaffected female carriers of the mutation show preferential inactivation of the disease allele [572], and also among milder affected woman favorable skewing has been observed [573]. Not only the absence of a functional *MECP2* allele results in a neurodevelopmental disorder, but also its duplication. The *MECP2* duplication syndrome is characterized by intellectual deficits, absence of speech, muscular hypotonia, frequent recurrent infections and mild dismorphic features [519, 691-694]. Furthermore, an association between autism and *MECP2* duplication exist. MECP2 seems to interact with ATRX *in vitro*, and both proteins work together with cohesin to silence a set of imprinted genes in the postnatal mouse brain [695]. This might explain why male patients having both a duplication of *MECP2* and *ATRX* have an even more severe phenotype with cerebellar atrophy [696], which is normally not a feature of the *MECP2* duplication syndrome. Mutations in the *ATRX* gene result in a neurodevelopmental condition with various degrees of gonadal dysgenesis [697]. Unaffected female carriers of both the *MECP2* duplication syndrome and *ATRX* mutations, and also women in the family of the concomitant duplication of *MECP2* and *ATRX*, show complete XCI skewing, resulting in preferential inactivation of the duplicated or mutated allele [519, 696]. In contrast, random X inactivation is observed in manifesting heterozygotes [698-699].

X-linked myopathies

Several disorders affecting the muscle compartment are caused by gene mutations on the X chromosome. Among the most well-known genes on the X chromosome is the dystrophin locus (*Duchenne muscular dystrophy* gene, *DMD*), the longest gene locus in the human genome spanning more than 2 Mb of Xp21. Mutations at different locations in the *DMD* gene lead to a spectrum of muscle diseases called the dystrophinopathies, which consist of Duchenne muscular dystrophy (OMIM: 310200) and Becker muscular dystrophy (OMIM: 300376). Duchenne muscular dystrophy is more common (affecting 1 in 3500 boys), and results in a severe phenotype, due to complete absence of dystrophin protein, causing early onset muscle weakness, wheelchair dependence and early death due to cardiac and respiratory failure [700]. Becker muscular dystrophy is less common and leads to a milder form of the disease, in which patients remain ambulant and can have a normal life span. In both cases, most often males are affected, whereas female carriers are often asymptomatic, with the exception of manifesting heterozygotes which can have full blown disease due to X-to-autosome translocations [545, 547] or extreme skewing of inactivation of the wild type X chromosome [521-522, 701]. Female carriers are typically symptom free, but if they present symptoms these are most often correlated to unfavorable skewing, and a later disease onset, with an increased risk for cardiomyopathy [702-705]. A recent study also indicated that many unspecified myopathies in young females might be caused by *DMD* mutations, which manifest themselves aspecifically, probably due to X inactivation skewing [706].

Also for several other X-linked muscle diseases, the relation between disease phenotype and X chromosome inactivation has been explored. The majority of carriers of Barth syndrome (OMIM: 302060), a rare X-linked disorder characterized by a short stature, cardiac and skeletal myopathy and neutropenia [707], show skewed X inactivation, thereby rendering the mutant X chromosome inactive [514]. In X-linked myotubular myopathy (OMIM: 310400), mutations in the *MTM1* gene cause severe myopathy in males, which most often die in the postnatal period. Most female carriers are asymptomatic, but can manifest symptoms of unilateral muscle weakness and progressive myopathy later during life. The severity of these symptoms seems to be often, but not always, correlated to the degree of X chromosome inactivation skewing [708-711]. In spinal and bulbar muscular atrophy (Kennedy's disease, OMIM: 313200), an expansion of a transcribed and translated CAG repeat (encoding a stretch of glutamine residues) in the *androgen receptor* gene causes an X-linked adult-onset neuromuscular disease, which is characterized by proximal muscle weakness, contraction fasciculation, bulbar palsy, postural tremor and gynecomastia [712]. Females are usually unaffected, but several carriers manifesting the disease have been described [713-716]. The variation in disease symptoms is often explained by different levels of X chromosome inactivation skewing. Of note, one study observed no symptoms in carriers which show a totally skewed X inactivation pattern inactivating the wild type X chromosome, suggesting that other factors might contribute as well to the phenotypical variations observed in female carriers [717]. However, since skewing was only analyzed in peripheral blood cells, a more likely explanation might be that the skewing ratio was different in the affected spinal motor neurons. The same may hold true for X-linked Danon disease (OMIM: 300257) [718-719], caused by mutations in the *LAMP2* gene and characterized by hypertrophic cardiomyopathy, skeletal myopathy and mental

retardation, where also random X chromosome inactivation has been found in blood cells [720]. A direct investigation of affected heart tissue obtained after heart transplantation has indeed shown an unfavorable skewing of XCI in an affected female patient [719]. A similar mechanism might apply in X-linked Charcot-Marie-Tooth disease (OMIM: 302800), which is a neuromuscular disorder in which mutations in the *GJB1* gene result in aberrant Schwann cell function, leading to neuropathy with difficulty of walking, distal muscle weakness and sensory loss [721]. Whereas some studies show preferential inactivation of the mutated allele explaining the asymptomatic or variable phenotype in females [722], others did not observe a correlation between X inactivation pattern in blood and the phenotype of the affected females [723-724]. Since affected females show a more variable phenotype compared to males, it seems likely that the skewing of XCI does affect the phenotype, and that skewing found in peripheral blood is not always representative for Schwann cells. Indeed, several studies have shown that skewing ratios between different tissues do not always correlate well, thereby adding another layer of complexity to investigations aiming to unravel mechanisms of X-linked diseases in females [678, 725-726].

X-linked metabolic disorders

Many metabolic disorders are caused by mutations on the X chromosome. In many of these disorders, cells are able to share metabolic products, which often results in a less severe phenotype in the females. Among others, these include Lesch-Nyhan syndrome (OMIM: 300322) and a group of lysosomal storage diseases. The latter group consists of Hunter syndrome (mucopolysaccharidosis type II, OMIM: 309900), Danon disease (OMIM: 300257) and Fabry disease. Whereas in case of Hunter disease, symptoms in affected females are minimal, due to the fact that iduronate sulfatase can be efficiently transferred between wild type and mutant cells [430], symptoms in Fabry disease are more severe [727-728]. This is likely caused by the fact that alpha-galactosidase A, encoded by the X-linked *GLA* gene, can only be inefficiently transferred between cells. The accumulation of glycosphingolipids in blood and lysosomes of most cells due to the absence of functional alpha-galactosidase A, results in clotting of blood vessels and tissue damage, which leads to progressive renal disease, cardiac hypertrophy, vascular abnormalities, and early stroke due to ischemia. Whereas in males diagnosis of Fabry disease can be facilitated with a reliable enzyme test, this is more difficult in heterozygous females due to random XCI [729], which results in cells expressing the functional protein. Affected females can have significant symptoms [730], and it has been speculated that several female cases are caused by a non-random XCI in females favoring inactivation of the wild type allele [456, 731]. Studies on XCI skewing in woman with Fabry disease have given different outcomes, in which one study showed a clear correlation between the degree of skewing favoring inactivation of the wild type allele and disease symptoms [732], whereas two other studies did not show such a correlation [733-734].

A rare X-linked disorder of copper metabolism is Menkes disease (OMIM: 309400) [735]. Mutations in the *ATP7A* gene lead to a disturbed intracellular transport of copper, and as a consequence a diminished activity of copper-dependent enzymes [736-

738]. This results in neurological degeneration and mental retardation, arterial and bone lesions and a characteristic hair depigmentation. Affected males usually die around the age of 5 years, whereas female carriers are unaffected thanks to favorable skewing [739]. A female patient has been described which suffered from Menkes disease due to a balanced translocation between chromosome 16 and the X chromosome, which disrupted the *ATP7A* locus. Since the wild type X chromosome was being inactivated, the active X chromosome harbored the genetic defect causing the disease [740]. A milder form of the disease, which is most likely also influenced by skewing, has been described as occipital horn syndrome (OMIM: 304150) [741], which is caused by splicing mutations of the *ATP7A* gene [742].

Another example of an X-linked metabolic disorder is ornithine transcarbamylase (OTC) deficiency (OMIM: 311250) [743]. The *OTC* gene is located on the short arm of the X-chromosome and encodes a mitochondrial-matrix enzyme that catalyzes conversion of ornithine and carbamyl phosphate to citrulline during the second step in the urea cycle. The urea cycle is the most important pathway for detoxification of ammonia in humans, and deficiency of OTC results in an X-linked disorder that can cause fatal hyperammonemia in male newborns. Heterozygous girls may be asymptomatic or may have episodes of hyperammonemic encephalopathy and hence present with a decline in cognitive function. These episodes can be evoked even later during life, and might be caused by events as infections, pregnancy or other situations which compromises normal physiology [744-748]. The variation of symptoms observed in females has been linked to variation in XCI skewing, and a study has shown that skewing levels in liver tissues correlate well with the measured enzyme activity [725]. In contrast, XCI skewing analysis in peripheral blood did not find such a correlation [725].

X-linked renal disorders

Renal function is crucial for the physiology of the body, by regulating the water and waste homeostasis. The kidneys consist of a complicated architecture of nephrons and glomeruli, which function to excrete waste products, and regulate the water balance. Although the clonal basis of kidney development has not been elucidated, and it is not clear what the extent of mosaicism is in this organ, it also seems clear that the presence of mosaic expression of X-linked genes in kidney result in a benefit for women, as in general men have a worse prognosis regarding renal disease [749]. Several disorders affecting renal function are caused by genes located on the X chromosome (**Table 5**). For most of the diseases, males suffer from serious renal disease, often ending in end stage renal failure, whereas females are generally less severe affected, varying from minimal symptoms in carriers to more severe renal disease in manifesting heterozygotes.

A classical renal X-linked disorder is Alport syndrome (OMIM: 301050), which is caused by mutations in the *COL4A5* gene, encoding a collagen protein. Besides affecting the kidney, Alport syndrome causes hearing loss and ocular lesions. Due to mutations in *COL4A5*, defects in the basement membrane of the tubules and glomeruli of the kidney arise, which result in hematuria and proteinuria, finally leading to end stage renal disease (ESRD). Males almost always suffer from this end stage renal failure, whereas in females, the symptoms are more viable, with only 25% of the carriers developing severe renal disease. In mice, it has been shown that XCI skewing is able to modify the disease [750], which is also likely to be the case in humans, although studies in human carriers have failed to show a direct correlation [751]. However, severe renal disease has been observed in a female patient where the wild type X chromosome was preferentially inactivated [752-753]. The same manifesting heterozygosity has been observed in a family suffering from Lowe syndrome (Dent 2 disease, OMIM: 309000) [754], a renal tubular dysfunction with involvement of multiple tissues and organs, caused by mutations in the *OCRL1* gene.

Nephrogenic diabetes insipidus is a disorder in which the kidney is not able to concentrate urine, leading to excessive water loss. Some 90% of the cases are caused by mutations in the X-linked arginine vasopressin receptor 2 (*AVPR2*), whereas the remainder is caused by mutations of the autosomally encoded aquaporin-2 water channel. Since nephrogenic diabetes insipidus mainly affects males, female cases were in the past believed to be caused by the autosomal mutations. However, it is now clear that also in women this disease can be caused by the X-linked mutation, due to unfavorable skewing inactivating the wild type X chromosome [755-757]. In addition, female heterozygous carriers without symptoms seem to benefit from favorable skewing [758].

Also systemic metabolic disorders, like Fabry disease (OMIM: 301500), or Lesch-Nyhan syndrome (OMIM: 300322) can affect the kidneys. Since in both these cases the mutant proteins can be obtained from wild type neighboring cells, the phenotype in females is mild, but can be more severe in case of unfavorable skewing [469, 764-765].

Table 5: X-linked disorders affecting the kidney						
Disease	**Gene**	**Gene location**	**OMIM**	**Renal phenotype, mainly affecting males**	**XCI**	**reference**
Alport syndrome	*COL4A5*	Xq22.3	301050	Nephritis, glomerulitis, hematuria and ESRD	Likely skewed	Rheault et al 2010 [750]
Leiomyomatosis with nephropathology	*COL4A5* and *COL4A6*	Xq22.3	308940	Nephritis, glomerulitis, hematuria and ESRD	Skewed in leiomyoma, not studied in somatic tissues	Oohashi et al 2011 [759]
Dent disease type 1	*CLCN5*	Xp11.22	300009	Progressive proximal tubular disease, ESRD, hypercalciuria, nephrolithiasis, proteinuria, hypophosphatemic rickets	Not studied in female carriers	--
Dent disease type 2	*OCRL*	Xq26.1	300555	Proteinuira, aminoaciduria, phospateuria	Skewed in one family	Cau et al 2006 [754]
Fabry disease	*GLA*	Xq22	301500	Cytoplasmic inclusions, proteinuria, ESRD	Skewed Random	Dobrovolny et al 2005 [732] Maier et al 2006 [733] Elstein et al 2012 [734]
Hypophosphatemic rickets	*PHEX*	Xp22.1-2	307800	Hypophosphatemia, nephrocalcinosis	Random	Orstavik et al 2006 [760] Owen et al 2009 [761]
Lesch-Nyhan syndrome	*HPRT*	Xq26-27.2	300322	Uric acid stones, nephropathy and renal obstruction	Random or skewed, dependent on cell type	Migeon et al 1971 [432] Marcus et al 1992 [458]
Nephrogenic diabetes insipidus	*AVPR2*	Xq28	304800	Extensive diuresis	Skewed in carriers with manifesting disease	Nomura et al 1997 [756] Faerch et al 2010 [762] Satoh et al 2008 [758]
Syndrome of inappropriate antidiuresis	*AVPR2* (gain of function)	Xq28	300539	Hyponatremia, systolic hypertension	Skewed	Decaux et al 2007 [763]
Oral facial digital syndrome type 1	*OFD1*	Xp22.2	311200	Fetal death in males, polycystic kidney disease, ESRD in females	Random Skewed	Thauvin-Robinet et al 2006 [559]

X-linked dermatological disorders

Close examination of properties of the skin and coat color of mice have been crucial for Mary Lyon's hypothesis on dosage compensation by X chromosome inactivation in females [30]. Likewise, also the human skin is characterized by a patchy mosaicism in females, which can be seen in a large group of X-linked skin disorders (**Table 6**). Many skin abnormalities in these disorders follow the lines of Blaschko [766], which represent the patterns of embryonic cell migration during the development of the skin, and which are distinct from the dermatomes that follow nervous innervation. Alfred Blaschko noted an archetypal pattern with characteristic linear appearance on the extremities, a V-shaped pattern on the back, and S-shaped curves on the trunk, in his studies on epidermal and sebaceous nevi [766]. Since in females with X-linked dermatological disorders some lines were affected, whereas other were not, he hypothesized that these variability between lines correspond to early embryonic events. Only many years later, it became clear that this embryonic event can be affected by XCI with lines being affected or unaffected representing cells which have inactivated the wild type or mutant X chromosome in the progenitor cells, respectively [767-768]. An example of a skin disorder in which the lines of Blaschko are visible is X-linked anhidrotic ectodermal dysplasia (OMIM: 305100), where mutations in the X-linked ectodysplasin A (*EDA*) gene cause absence of sweat glands in skin patches [769]. Analog to the lines of Blaschko, embryonic migration of cells might also be visible in other organs, and might contribute to our understanding of the benefits of mosaicism in females. For example, in X-linked amelogenesis imperfecta (OMIM: 301200) and focal dermal hypoplasia (OMIM: 305600), teeth show a linear arrangement of enamel dyplasia [770-771]. Likewise, in X-linked oculocutaneous albinism (OMIM: 300500), a radial pattern of hypomelanosis is found on the retina of female carriers [772], and also cataracts show a sectorial arrangement in chrondodysplasia punctata type 2 (OMIM: 302960). Similar migration patterns might apply to other organ systems, as it has been found that intestinal villi consist of a heterogenous mix of cells having inactivated the maternal of paternal X chromosome, whereas intestinal crypts are monoclonal in origin [678, 773]. Even in the brain, where extensive intermingle of cells is expected, a columnar pattern of cell clones has been described [774].

Not all X-linked skin disorders follow the lines of Blaschko. Two other patterns have been observed, the lateralization and the checkerboard pattern. The former is seen in CHILD syndrome (OMIM: 308050), caused by mutations in *NSDHL*, which might interfere with sonic hedgehog signaling involved in conferring a left-right asymmetry to the embryo [775]. The checkerboard pattern is found in X-linked congenital generalized hypertrichosis (OMIM: 307150), were heterozygous carriers show a checkerboard-like pattern of hypertrichosis. Some other skin disorders do not display a particular pattern in affected females, or might even result in symptom free females. This can be the case when the gene involved escapes X chromosome inactivation, and is thus being expressed in female cells,

like for X-linked ichthyosis (OMIM: 308100) [782-783], or in diseases were the protein involved can be shared among cells, as in Fabry disease (OMIM: 301500).

X-linked ocular diseases

A classical textbook example of an X-linked disease affecting the eyes is X-linked color blindness, which usually affects only males [784]. Females are much less affected, because a non-mutant allele resists on the second X chromosome. Most X-linked eye disorders are characterized by the same sex distribution, in which males are affected and females have either an absence of the disease, or minimal disease presentation. Examples include X-linked ocular albinism (Nettleship-Falls) (OMIM: 300500) [785], and choroideremia (OMIM: 303100). Also in Norrie disease (OMIM 310600), a rare X-linked disorder characterized by congenital blindness, usually only males are affected. Approximately 40 to 50% of the affected males additionally develop deafness and mental retardation. In the few described female cases, no clear skewing difference was reported between affected and non-affected individuals [786].

Another disease which usually affects only males is X-linked retinoschisis (OMIM: 312700), which is the leading cause of macular degeneration and is caused by mutations in the *RS1* gene. The visual deterioration in this disease is caused by splitting within the inner retinal layers. Rare cases of affected females have been described, in which females were found to have Turner syndrome [787], or had homozygous mutations in the *RS1* gene [788-789].

Finally, idiopathic infantile nystagmus (OMIM: 310700) [790], caused by mutations in the *FRMD7* gene located at Xq26-27, is characterized by the presence of early onset abnormal eye movements. Although affected females report slightly better visual acuity than affected males, the influence of XCI skewing is unclear at the moment, as some studies reported skewed XCI in affected females [791-792] whereas another study did not find a clear relationship [793].

Besides these typical eye disorders, many systemic X-linked disorders cause ocular symptoms. Among others, these include Fabry disease (OMIM: 301500), incontinentia pigmenti (OMIM: 308300), Alport syndrome (OMIM: 301050) [794], chronic granulomatous disease (OMIM: 306400), and chondrodysplasia punctata type 2 (OMIM: 302960). Several diseases with mainly skin related symptoms are also characterized by eye involvement, and include X-linked hypohidrotic ectodermal dysplasia (OMIM: 305100) [795], microphthalmia with linear skin defects syndrome (OMIM: 309801), and keratosis follicularis spinulosa decalvans (OMIM: 308800), among others. In these disorders, influence of XCI skewing is variable, as already discussed before for several of the disorders mentioned.

Table 6: X-linked disorders affecting the skin

Disease	Gene	location	OMIM	Phenotype	XCI	Reference
Anhidrotic ectodermal dysplasia	*EDI*	Xq12-q13.1	305100	Variable defects in morphogenesis of ectodermal structures, including hair, skin, nails, and teeth	Random, skewed in manifesting carriers	Lexner et al 2008 [769]
Angioma serpiginosum	*PORCN*	Xp11.3-q12	300652	Nonpurpuric red punctate lesions, hyperkeratosis, dysplastic nails	Skewed	Blinkenberg et al 2008 [569]
Bazex syndrome	Not found	Xq24-q27	301845	Triad of congenital hypotrichosis, follicular atrophoderma,development of basal cell neoplasms	Not studied	--
Congenital hemidysplasia with ichthyosiform erythroderma and limb defects (CHILD)	*NSDHL*	Xq28	308050	Ichthyosiform nevi; limb, kidney and cardiac defects; brain malformations	Random	König et al 2002 [611]
Chrondodysplasia punctata type 1	*ARSE*	Xp22.3	302950	Skin, skelet and craniofacial defects, cataracts	Not studied	--
Chrondodysplasia punctata type 2	*EBP*	Xp11.23	302960	Skin, skelet and craniofacial defects, cataracts	Random Skewed	Shirahama et al 2003 [562] Canueto et al 2012 [610]
Chronic granulomatous disease	*CYBB*	Xp21.1	306400	Severe bacterial and fungal infections, colitis, granulomata	Skewed	Koker et al 2006 [645]
Coffin-Lowry syndrome	*RPS6KA3*	Xp22.12	303600	X-linked mental retardation, skeletal malformations, growth retardation, hearing deficit, paroxysmal movement disorders, cognitive impairment	Random, skewed towards normal allele in manifesting carriers	Jurkiewicz et al 2010 [776] Wang et al 2006 [777] Simensen et al 2002 [778]
Craniofronto-nasal syndrome	*EFNB1*	Xq12	304110	Frontonasal dysplasia, craniofacial asymmetry, craniosynostosis; males: hypertelorism	Random	Twigg et al 2004 [437]
Cutis laxa X-linked (Occipital Horn syndrome)	*ATP7A*	Xq21.1	304150	Hyperelastic, bruisable skin, hernias, bladder diverticula, hyperextensible joints, multiple skeletal abnormalities.	Skewed	Desai et al 2011 [739]

Table 6: Continued

Dyskeratosis congenital	*DKC1*	Xq28	305000	Ectodermal dysplasia characterized by dermatologic manifestations and nail dystrophy, bone marrow failure	Skewed	Ferraris et al 1997 [515] Devriendt et al 1997
Ehlers-Danlos variant, heterotopia, periventricular	*FLNA*	Xq28	300537	Focal seizures, irregular collagen fibrils, and brain malformations	Skewed	Robertson et al 2003 [560]
Epidermolysis bullosa, macular type	Not found	Xq27.3-qter	302000	Atraumatic bullae , absence hair, hyperpigmentation, depigmentation, acrocyanosis, dwarfism, microcephaly, mental inferiority, short tapering fingers	Not studied	--
Fanconi pancytopaenia B	*FAAP95*	Xp22.31	300514	Developmental abnormalities in major organ systems, early-onset bone marrow failure, high predisposition to cancer	Skewed	Holden et al 2006 [628]
Focal dermal hypoplasia (Goltz syndrome)	*PORCN*	Xp11.23	305600	Skin atrophy and other abnormalities, mental retardation, digital, ocular and oral anomalies	Random	Leoyklang et al 2008 [568]
Hypohidrotic ectodermal dysplasia with immune deficiency	*IKBKG/ NEMO*	Xq28	300291	Congenital disorder of teeth, hair, and eccrine sweat glands	Skewed	Orstavik et al 2006 [518]
Ichthyosis follicularis, atrichia and photophobia syndrome	*MBTPS2*	Xp22.12-p22.11	308205	Ichthyosis follicularis, atrichia, and photophobia, mental retardation	Skewed in manifesting carriers	Aten et al 2010 [779]
Immune dysregulation-polyendocrinopathy-enteropathy-X-linked (IPEX) syndrome	*FOXP3*	Xp11.23-q13.3	304790	Severe enteropathy, diabetes mellitus, dermatitis, nephropathy, recurrent infections	Random	Tommasini et al 2002 [648]
Incontinentia pigmenti	*NEMO*	Xq28	308300	Malfomations of brain, heart, eyes, teeth and skeleton, abnormal skin pigmentation	Skewed	Parrish et al 1996 [561]
Keratosis follicularis spinulosa decalvans	*MBTPS2*	Xp22.12-p22.11	308800	Hyperkeratotic follicular papules, scalp alopecia, photophobia, corneal dystrophy	Skewed	Aten et al 2010 [779]
Lowe oculocerebro-renal syndrome	*OCRL*	Xq25-q26	309000	Hydrophthalmia, cataract, mental retardation, vitamin D-resistant rickets, amino aciduria, and reduced ammonia production by the kidney	Skewed in one family manifesting disease	Cau et al 2006 [754]

Table 6: Continued

Menkes syndrome	*ATP7A*	Xq21.1	309400	Generalized copper deficiency	Skewed	Desai et al 2011 [739]
Microphthalmia with linear skin defects (MIDAS) syndrome	*HCCS*	Xp22.2	309801	Microphthalmia and dermal aplasia, brain and eye abnormalities, mental retardation, congenital heart defects	Skewed	Lindsay et al 1994 [575] Ogata et al 1998 Franco et al 2006 [556] Schluth et al 2007 [612]
Opitz-Kaveggia syndrome	*OKS*	Xq13	305450	Mental retardation syndrome, dysmorphic features, sensorineural hearing loss, joint laxity	Skewed	Graham et al 2008 [780]
Orofaciodigital syndrome type 1	*OFD1*	Xp22	311200	Facial and limb abnormalities, brain malformations, mental retardation and polycystic kidney disease	Random Skewed	Thauvin-Robinet et al 2006 [559]
Simpson-Golabi-Behmel syndrome type 1	*SGBS1*	Xq26	312870	Pre-and postnatal overgrowth, developmental delay, macrocephaly, macroglossia, skin lesions, and multiple congenital anomalies	Random (mildly Skewed)	Yano et al 2011 [781]
Simpson-Golabi-Behmel syndrome type 2	*OFD1*	Xp22.3-p22.2	300209	Multiple congenital anomalies, hypotonic and neurological impairment	Not studied	--
Terminal osseous dysplasia and pigmentary defects	*FLNA*	Xq28	300244	Bone and limb abnormalities, skin lesions and dysmophic features	Skewed	Baroncini et al [613]
Torticollis, keloids, cryptochidism and renal dysplasia	Not found	Xq28	314300	Torticollis, cryptorchidism, varicose veins, oligospermia	Not studied	--
X-linked ichthyosis	*STS*	Xpp22.32	308100	Palmar hyperlinearity, keratosis pilaris, fine scale	Random (escaping gene)	Shapiro et al 1979 [34]
X-linked oculocutaneous albinism	*GPR143*	Xp22.2	300500	Nystagmus, impaired visual acuity, iris hypopigmentation , albinotic fundus, macular hypoplasia, normally pigmented skin and hair	Not studied	--
X-linked congenital generalized hypertrichosis	Not found	Xq24-q27.1	307150	Hypertrichosis, dental anomalies, deafness	Not studied	--

Influence of the X chromosome on recurrent pregnancy loss and female fertility

Recurrent spontaneous abortion has been defined as two ore more consecutive pregnancy losses before 20 weeks of gestation, and affects 1-3% of all couples [796]. Several studies have shown that the incidence of extreme XCI skewing is higher amongst females suffering from recurrent pregnancy loss, compared to controls [797-803]. Although several other studies have not shown such an association [804-805], or only found a non-significant correlation [806], the extreme skewing in these females might be caused by selection against a mutated X-linked gene, in female carriers of undiagnosed X-linked lethal disorders. Transmission of such a gene to the offspring could result in male lethality of the fetuses, in particular, thereby explaining the higher incidence of spontaneous abortions. Some studies also noticed a higher incidence of trisomic pregnancy losses amongst females with extreme skewing, and this might be related to a decreased size of the follicular pool caused by X chromosomal abnormalities, hence explaining the skewing [807-808]. Such an association is however disputed by others [809].

The X chromosome itself is also implicated in premature ovarian failure (OMIM: 311360), a condition characterized by hypergonadotropic ovarian failure and thus infertility before the age of 40 years [810]. Monosomy of the X chromosome and haploinsufficiency of several regions of the X chromosome are associated with the disease, and based on the breakpoints of truncated X chromosomes several candidate genes for this condition have been identified [810-812]. Although the majority of these candidates need to be verified, at least two X-linked genes seem to be implicated in the pathogenesis of premature ovarian failure, namely *BMP15* [813-814] and the *FMR1* premutation [815]. Initial reports found evidence for a correlation between X chromosome inactivation skewing and the presence of premature ovarian failure, which might be explained by selection against activity of X chromosomes bearing large deletions or mutations, which are themselves causative for the premature ovarian failure [816-817]. More recent studies however did not find such a correlation [818-822].

Influence of the X chromosome on cancer

Several mechanisms involve a functional and specific link between the X chromosome and the development of cancer. First, several genes located on the X chromosome are involved in tumor growth and progression [14], including for example the *androgen receptor* gene, which plays an important role in prostate cancer in males. A special group of these X-linked cancer genes consists of X-linked tumor suppressors [823-825], which include the X-linked *WTX* gene involved in Wilms tumor [826] and the *FOXP3* gene involved in breast cancer [827-828]. Being present in only a single copy in males, these genes do not fit the general rule stating that the inactivation of a tumor suppressor requires bi-allelic inactivation, the so-called two-hit theory [829]. In females, due to X chromosome inactivation, only one of the two copies of these genes will be active in every cell. Therefore, also in females a single hit might be enough to result in a gene mutation on the active X chromosome, which might then result in cancer initiation.

Secondly, amplification of the X chromosome has been found in several tumors [830], including germ cell tumors [355, 831-832], breast cancer [223, 833], ovarian cancer [834], cervical cancer [835] and malignant lymphomas [836]. The mechanisms behind this supernumerary X chromosomes are not completely understood, but often involve a gain of the active and a loss of the inactive X chromosome, which is likely to be a consequence of the genomic instability of cancer cells [837-838]. The gain of an active X chromosome might provide the tumor cells with a growth advantage, and might therefore be selected for. The loss of the Xi likely explains the reduced levels of *XIST* expression which have been often found in tumors, and which have even been used as a marker for disease progression for some female tumors [834-835].

Finally, genes directly involved in the XCI process have also been implicated in cancer. These include several genes encoding components of PcG complexes [839-840], the nuclear proteins *SatB1* and *SatB2* [274-275], genes involved in DNA methylation [841-842] and the *BRCA1* gene, although for the latter its precise role in X chromosome inactivation is being debated [221-224, 843].

Numerical and structural abnormalities of the X chromosome

Whereas aberrations of autosome number is almost always lethal, or results in severe health problems, like seen in Down syndrome, a varying number of sex chromosomes is rather well tolerated, with frequently reported karyotypes like 45,X, 47,XXX, 48,XXXX, 47,XXY or 48,XXYY. About 1 in 1000 males has an additional X chromosome (47,XXY), a condition known as Klinefelter syndrome, first described by Harry Klinefelter in 1942 [844] and later linked to the presence of an additional X chromosome in males [845]. Klinefelter males usually suffer from hypergonadotropic hypogonadism and infertility, and are characterized by a tall stature, sparse body hair, gynecomastia, small testes and sometimes a decreased verbal intelligence [846]. The prevalence of Klinefelter males seems to rise in recent years [847], although many males are only diagnosed because of their infertility, due to a wide variation in presenting symptoms. Klinefelter patients have an equal chance of obtaining the additional X chromosome from their mother or father, and studies of severity of the syndrome have failed to find a correlation between symptoms and parent of origin of the extra X chromosome [846]. The supernumerary X chromosome seems to be faithfully inactivated, although several studies showed some evidence for excessive skewing in Klinefelter patients [848-849], and it has been implicated that the length of the polymorphic androgen receptor CAG repeat might correlate with disease severity [846, 849-850]. Most of the symptoms can be explained by a higher dosage of X-linked genes from the pseudo-autosomal region (PAR), and other genes escaping X chromosome inactivation, as these are present in a higher copy number compared to normal 46,XY males. Indeed, over-expression of SHOX, located at PAR1, has been implicated in a tall stature [851]. Since Klinefelter males undergo XCI, they benefit from the same mosaic advantages like normal females regarding X-linked diseases. This mosaicism does also explain why, sometimes, male-lethal X-linked disorders like incontinentia pigmenti

(OMIM: 308300) can be found in Klinefelter individuals [852-856]. It also might explain the higher incidence of autoimmune disorders among these men [661].

One of the most frequent numerical aberration of sex chromosomes in females is Turner syndrome, which is found in 1 to 2500 females and is caused by a monosomy of the X chromosome (45,X), the presence of an isochromosome X in which the Xq is duplicated and Xp missing, or by deletions of Xp. All of these abnormalities might be present in a mosaic, with some cells still displaying a normal 46,XX karyotype. Henry Turner first described this syndrome in 1938 [857], in females showing an infantile development of genitalia and prepubertal appearance, streak gonads, a short stature and varying degrees of dysmorphologies, including a webbed neck, cubitus valgus, lymphedema, amongst more severe kidney and aorta malformations [668, 670]. In 1959, this syndrome was linked to the presence of only one X chromosome in the absence of a Y chromosome [858]. As discussed above, due to this X chromosome monosomy Turner patients are at increased risk to manifest X-linked diseases otherwise not seen in females [593-598], and might suffer from an increased risk for autoimmune disease [669]. The latter might be caused by haploinsufficiency of genes located in the PAR, which has been hypothesized to be involved in the pathogenesis of certain autoimmune diseases. Although the majority of Turner embryos die during gestation, the presence of a single X chromosome itself does thus only lead to a mild range of symptoms in survivors, which are likely caused by the lower dosage of gene products of genes either escaping XCI, or located on the PAR (the PAR from a second X, or the PAR from the Y is missing), as these genes are normally not being inactivated, and hence expressed from two X chromosomes (or an X and a Y) [859]. Indeed, the short stature again seems to be explained mainly by the *SHOX* gene, as haploinsufficiency for SHOX results in a short stature [860] (also known as Leri-Weill dyschondrosteosis, OMIM: 127300 [861]). The streak gonads are caused by the absence of follicles, due to the fact that oocytes need two active X chromosomes. Although female Turner foetuses have the same number of oocytes at three months of gestation, an accelerated loss results in the premature absence of germ cells, and the subsequent fibrosis resulting in the characteristic streak gonads [810, 862].

A subgroup of Turner patients has a mosaic karyotype, consisting of cells with a 45,X karyotype, and cells with an additional tiny ring X chromosome (46,X, r(X)). These ring X chromosomes are remnants of an X chromosome that underwent two simultaneous breaks distal to the centromere, resulting in rejoining of the ends, and formation of a ring structure, which thus misses telomeric sequences, and can be visualized in standard chromosome metaphase spreads as a small ring [863]. Peculiarly, this subgroup of patients shows a more severe phenotype displaying severe mental retardation, developmental delay and severe congenital anomalies, including facial dysmorphism, soft tissue syndactyly of upper and lower limbs and cardiovascular defects [864-870]. It has been shown that the severe phenotype correlates with the inability of the ring X chromosome to be inactivated, resulting in a partial functional X chromosome disomy [871-873]. Indeed, the majority of ring X chromosomes has been shown to miss the *XIST* locus, thereby explaining the inability to inactivate [873-877]. However, several ring X chromosomes have been described in the literature in which the *XIST* locus is present, but in which still no inactivation is observed. These ring X chromosomes may therefore miss the regulatory sequences necessary for adequate expression of *XIST*, and thus for XCI to occur, and might

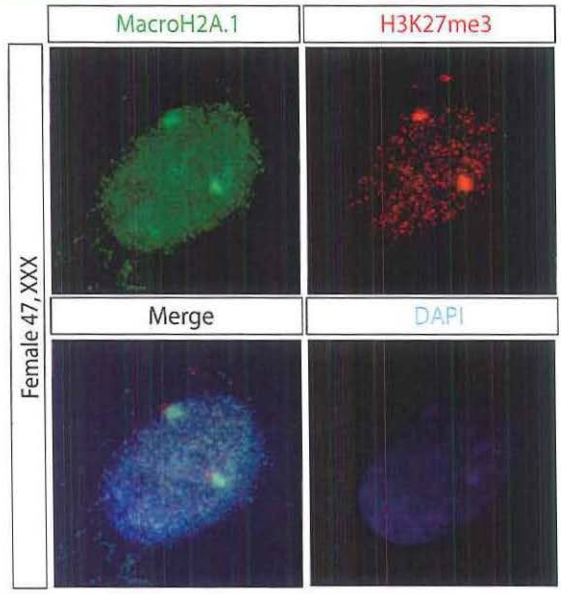

Figure 14: Two inactive X chromosomes in 47, XXX fibroblasts
Fibroblasts from a patient with triple X syndrome were stained for MacroH2A1 (green) and H3K27me3 (red), two heterochromatin markers enriched on the inactive X chromosome. DNA is counterstained with DAPI (blue). 47, XXX fibroblasts inactivate two X chromosomes, which are visible as local areas of enrichment for heterochromatin marks, which is co-localizing with a Barr-body.

therefore be relevant for investigations to determine the regulatory network of X chromosome inactivation.

Besides Klinefelter and Turner syndromes, more X chromosome aneuplodies are occurring. Among the most common ones is the triple X syndrome (47,XXX) in females [158]. These females are diagnosed in chromosomal surveys, because they most often lack any symptoms, since the additional X chromosome is properly silenced [878-879] (**Figure 14**). Only escaping genes and genes located in the PAR will be expressed at a higher level, which might explain for example the average higher length of triple X females, due to higher levels of SHOX [880], or their thicker tooth enamel due to higher expression of the X-linked AMELX gene [881]. Besides three X chromosomes, even more sex chromosomes might be present, resulting in rare karyotypes as 48,XXXX, 48,XXXY, 48,XXYY, 49,XXXXX or 49,XXXXY. Generally speaking, any of these sex chromosomal aneuplodies will result in variants of Klinefelter syndrome, when the Y chromosome is present. The presence of several additional X chromosomes is fairly well tolerated, but will result in more symptoms, including mental retardation, the more additional chromosomes are present, due to the higher dose of PAR genes and genes escaping X chromosome inactivation [882]. In case of the pentasomy X (49,XXXXX), symptoms (as severe as mental retardation, delayed speech development, facial dysmorphologies, skeletal and limb

abnormalities [883-884]) might also be explained by a failure of XCI to inactivate four out of five X chromosomes in all cells, hence leading to symptoms due to the presence of more than one active X chromosome [885-888]. Also karyotypes with additional Y chromosomes have been described. Of note, it has been proposed that males with 47,XYY might have a higher risk of violent behavior [889-890] or other behavioral difficulties [891].

Scope of this thesis

In this thesis work, we have investigated mechanisms involved in regulation of the initiation of X chromosome inactivation (XCI). Starting point was our earlier hypothesis that the initiation of XCI is a stochastic process, controlled in *trans* by autosomally-encoded XCI-inhibitors and X-encoded XCI-activators. The XCI-inhibitors prevent initiation of XCI in undifferentiated cells or early embryos. Upon differentiation of these cells during development, XCI is initiated in females only, by the activity of X-linked XCI-activators, which reach a higher concentration in female cells compared to male cells, due to the location of the encoding genes on the X chromosome. As described in Chapter 2, we found that the E3 ubiquitin ligase RNF12 acts as an important X-encoded activator of X chromosome inactivation. When extra copies of *Rnf12* are transgenically expressed in male ES cells, the encoded higher level of RNF12 is able to induce XCI on the single X chromosome, whereas such over-expression in female ES cells leads to ectopic XCI on both X chromosomes in a significant portion of the cells. *Rnf12* becomes up-regulated in female ES cells during the developmental time window when XCI is normally occurring, and genetic ablation of one copy of *Rnf12* in female ES cells results in a significant delay in the XCI process. Chapter 4 discusses this discovery in the context of the stochastic model for XCI initiation, controlled by XCI-activators and XCI-inhibitors, and further provides evidence that all features of XCI initiation can indeed be explained by this model. A novel BAC targeting strategy described in Chapter 3 enabled efficient, fast and reliable genetic modifications of mouse ES cells, and this strategy was used throughout this thesis work. Among others, it allowed us to generate the *Rnf12* homozygous knockout ES cells, described in Chapter 5. Using these cells, we provide evidence that RNF12 is essential for XCI to occur, and mediates its effect mainly through activation of the *Xist* gene. In Chapter 6, we show that this is an indirect mechanism, in which RNF12 targets the XCI-inhibitor REX1 for proteasomal degradation. The *Rnf12* gene is located in the vicinity of *Xist*, which ensures rapid silencing of *Rnf12* transcription in *cis* shortly after initiation of XCI. Chapter 7 addresses the question whether other genes located near *Xist* and *Rnf12* are also functional in the regulation of the XCI process. We found that *Jpx*, *Ftx* and the *Xpr* region have a *cis* regulatory role, in which these regions likely create an open chromatin domain, which is needed to enable activation of *Xist* by the *trans* action of RNF12. We also provide data which suggest that direct interaction between the two X chromosomes in a female nucleus, X-pairing, is not functionally required for XCI to occur. Rather, more evidence was obtained supporting an indispensible role for the *trans* action of RNF12, during all stages of XCI initiation. In Chapter 8, we describe an *Rnf12* knockout mouse, which we have generated from the *Rnf12* mutant ES cells studied in this thesis work. As expected from the observations showing loss of XCI in *Rnf12* homozygous knockout ES cells, homozygous *Rnf12* knockout females are not born, suggesting that RNF12 has an important role in XCI initiation also during *in vivo* development. The ongoing analysis of these mice indicated that females heterozygous for the *Rnf12* mutation also have an XCI phenotype, with transcriptional activity from two X chromosomes in some cells from adult tissues

representing loss of XCI. This surprising and remarkable phenotype awaits detailed investigation. Finally, in Chapter 9, we proceeded to translate the newly obtained knowledge on the regulation of XCI initiation from mouse to human. We studied XCI in female human induced pluripotent stem cells, and provide evidence that the one X chromosome that is inactivated in a founder human fibroblast becomes reactivated upon somatic reprogramming. The General Discussion, Chapter 10, aims to integrate our current views on the initiation of XCI with previously published observations, and provides an outlook for future investigations.

Chapter 2

Rnf12 is an X-encoded dose dependent activator of X chromosome inactivation

This chapter has been published in

Iris Jonkers*, Tahsin Stefan Barakat*, Eskeatnaf Mulugeta Achame, Kim Monkhorst, Annegien Kenter, Eveline Rentmeester, Frank Grosveld, J. Anton Grootegoed and Joost Gribnau (2009)
"RNF12 is an X-Encoded dose-dependent activator of X chromosome inactivation"
Cell 139:999-1011

* both authors contributed equally

RNF12 is an X-encoded dose-dependent activator of X chromosome inactivation

Iris Jonkers[1,2#], Tahsin Stefan Barakat[1#], Eskeatnaf Mulugeta Achame[1], Kim Monkhorst[3], Annegien Kenter[1], Eveline Rentmeester[1], Frank Grosveld[2], J. Anton Grootegoed[1] and Joost Gribnau[1,4]

[1]Department of Reproduction and Development, [2]Department of Cell Biology, and [3] Department of Experimental Pathology, Erasmus MC, University Medical Center, Rotterdam, The Netherlands.
[#]these authors contributed equally
[4]corresponding author

Contact details:
Joost Gribnau
Department of Reproduction and Development
Erasmus MC
Room Ee 09-71
PO Box 2040
3000 CA Rotterdam
The Netherlands
Phone +31-10-7043069
Fax +31-10-7044736
Email: j.gribnau@erasmusmc.nl

Abstract

In somatic cells of female placental mammals, one X chromosome is inactivated to minimize sex-related dosage differences of X-encoded genes. Random X chromosome inactivation (XCI) in the embryo is a stochastic process, in which each X has an independent probability to initiate XCI, triggered by the nuclear concentration of one or more X-encoded XCI-activators. Here, we identify the E3 ubiquitin ligase RNF12 as an important XCI-activator. Additional copies of mouse *Rnf12* or human *RNF12* result in initiation of XCI in male mouse ES cells and on both X chromosomes in a substantial percentage of female mouse ES cells. This activity is dependent on an intact open reading frame of *Rnf12* and correlates with the transgenic expression level of RNF12. Initiation of XCI is markedly reduced in differentiating female heterozygous *Rnf12*+/- ES cells. These findings provide evidence for a dose-dependent role of RNF12 in the XCI counting and initiation process.

Introduction

In the mouse embryo proper, XCI is random with respect to the parental origin of the inactivated X chromosome, and is initiated around 5 days *post coitum*, or upon ES cell differentiation *in vitro* [892]. Initiation of XCI is marked by transcriptional up-regulation of the X-encoded *Xist* gene on the future inactive X chromosome (Xi). *Xist* is a non-coding, spliced and poly-adenylated RNA, which spreads over the Xi while attracting protein complexes required for the silencing process [86-87, 99]. *Tsix* and *Xite* gene sequences overlap with the *Xist* gene, but are transcribed in anti-sense direction and play an important role in suppression of *Xist* transcription during the XCI process [119, 136].

XCI starts with counting of the number of X chromosomes and selection of the future active X (Xa) and Xi. This process is stochastic, and every X chromosome has an independent probability to initiate XCI [179]. The probability for any X chromosome to be inactivated increases with an increased X to autosome ratio, suggesting involvement of an X-encoded activator in the XCI counting process [179, 189]. Studies with cell lines and mice carrying *Xist* and *Tsix* over-expression and knockout alleles have indicated that these genes play a crucial role in determining the probability to initiate XCI [104, 119, 123, 177]. *Tsix* takes part in setting up a threshold that has to be overcome by *Xist* in order to initiate XCI. In counteracting *Tsix*, X-encoded XCI-activators are responsible for dose-dependent activation of *Xist* expression, and autosomally-encoded XCI-inhibitors act as dose-dependent suppressors of *Xist*. XCI-activators might act either through activation of *Xist* directly, or by suppression of *Tsix*, thereby lowering the threshold for initiation of XCI. Similarly, XCI-inhibitors can be involved in direct suppression of *Xist* activation, or exert their activity through an indirect mechanism such as activation of *Tsix* expression.

During early embryonic development, or upon ES cell differentiation, the concentration of the XCI-activators will be sufficient, in female cells but not in male cells, to initiate XCI with a specific probability per time frame. In this working hypothesis, inactivation of both X chromosomes in female cells is prevented by *cis* inactivation of the genes encoding the XCI-activators and the stochastic nature of XCI initiation. Nonetheless,

the second X chromosome will keep a probability to initiate XCI until the XCI-activator concentration has dropped below the threshold required to initiate XCI, after silencing of the XCI-activator gene(s) in *cis*.

Recent findings indicate that CTCF, YY1, NANOG, SOX2, and OCT4 exert activities as XCI-inhibitors, by taking part in suppression of *Xist* expression [186, 191, 193], and appears to involve *Tsix*-dependent and -independent pathways. So far, X-linked genes encoding XCI-activators have not been identified. Candidate regions on the X chromosome involved in activation of XCI are delineated by different transgenes, several of them containing *Xist* and flanking sequences which have been shown to induce ectopic XCI in male cells [166-167, 169]. However, this effect was only obtained with multi-copy transgenes [175]. In addition, our finding that XCI is initiated in heterozygous ΔXTX female cells [179] indicates that *Xist*, *Tsix* and *Xite* play redundant or marginal roles in the XCI counting and initiation process, and suggest that important sequences regulating X chromosome counting and initiation of XCI are located outside the deleted region. To identify genes encoding XCI-activators we have performed a screen with male and female BAC transgenic ES cell lines. From this, we have obtained evidence that the X-encoded E3 ubiquitin ligase RNF12 is a dose-dependent factor involved in counting the number of active X chromosomes present per mammalian cell nucleus, which triggers initiation of random X chromosome inactivation.

Results

A screen to identify XCI-activator genes

Previous studies have indicated that genes encoding the putative XCI-activators are most likely located within a region of 10 megabases (Mb) surrounding the *Xist* locus [72-73]. To identify the XCI-activator genes, we generated transgenic male and female ES cell lines with stably integrated BAC transgenes covering part of this 10 Mb region. Our working hypothesis predicts that initiation of XCI upon differentiation in transgenic male ES cells on the single X, or initiation of XCI on both X chromosomes in a substantial percentage of transgenic female ES cells, signifies the presence of additional copies of a gene encoding an XCI-activator on the respective BAC.

Studies with mouse or human *Xist/XIST* transgenes in mouse ES cells indicated that autosomal integration of these transgenes results in activation of the endogenous *Xist* gene [167, 169, 171]. This suggests that these transgenes include sequences encoding an XCI-activator. We therefore started our screen with a BAC covering mouse *Xist*, excluding the transcription start sites of *Tsix* and *Xite*. BAC RP24-180B23 was stably transfected into male ES cells. Clones were expanded under neomycin selection and differentiated for 3 days before analysis. Besides wild type ES cells, we also made use of a male ES cell line 1.3 which contains 16 copies of an ms2 repeat integrated in exon 7 of *Xist* (**Figure 1A**). This ms2 tag does not interfere with XCI, and allows discrimination between endogenous *Xist*-ms2 and transgenic *Xist* [92]. BAC integration and copy number were determined by DNA-FISH and/or qPCR. The percentage of cells with accumulated *Xist* covering the Xi (*Xist* cloud) was determined by RNA-FISH using an *Xist* cDNA probe, which detects *Xist* and *Tsix* (in all FISH panels DNA is stained with DAPI). The pinpoint signal detected with this *Xist* cDNA probe is similar to the pinpoint signal obtained with a *Tsix* specific probe, and represents basal *Tsix/Xist* transcription which is clearly distinguishable from an *Xist*-covered Xi (**Figure 1B**). In most cell lines with an autosomal integration of the transgene, we found male cells with single *Xist* clouds (**Figure 1C**, **Supplemental Table 2A**). RNA-FISH using *Xist* (FITC) and ms2 (rhodamine red) probes performed on five different BAC transgenic 1.3 ES cell lines which were differentiated for 3 days revealed no ms2 positive clouds (**Figure 1D**), indicating that the endogenous *Xist* gene was never up-regulated (which would lead to conversion of the pinpoint signal to a cloud). This result was confirmed using a RP23-338B22 BAC sequence covering all of *Xist, Tsix,* and *Xite* (**Supplemental Table 2A**). Autosomal *Xist* spreading in differentiating male ES cells can be attributed to the absence of autosomal *Tsix* sequences (RP24-180B23), or loss of autosomal *Tsix* expression in *cis* due to truncation of one of the transgene copies or position effects (RP23-338B22, **Supplemental Figure 1A**). As a consequence of the absence of *Tsix* expression in *cis*, a relatively low XCI-activator concentration will be sufficient to induce autosomal *Xist* expression and spreading in male cells, similar to findings with male *Tsix* knockout ES cells [123, 127, 178]. Male and female mouse ES cell lines transgenic for BAC sequences CTD-2200N19 and CTD-2183M22 covering both human *XIST* and *TSIX*, or *XIST* alone (**Figure 1F**) also did not show significant induction of endogenous *Xist* in male cells (**Figure 1E**, and **Supplemental Table 2A**) or endogenous *Xist* accumulation on both X chromosomes in female cells (**Figure 1G**, and **Supplemental Figure1B** and **C**). These results indicate that the tested regions do not induce ectopic XCI in transgenic male and female cells under the conditions that we used. Our findings contrast previous claims

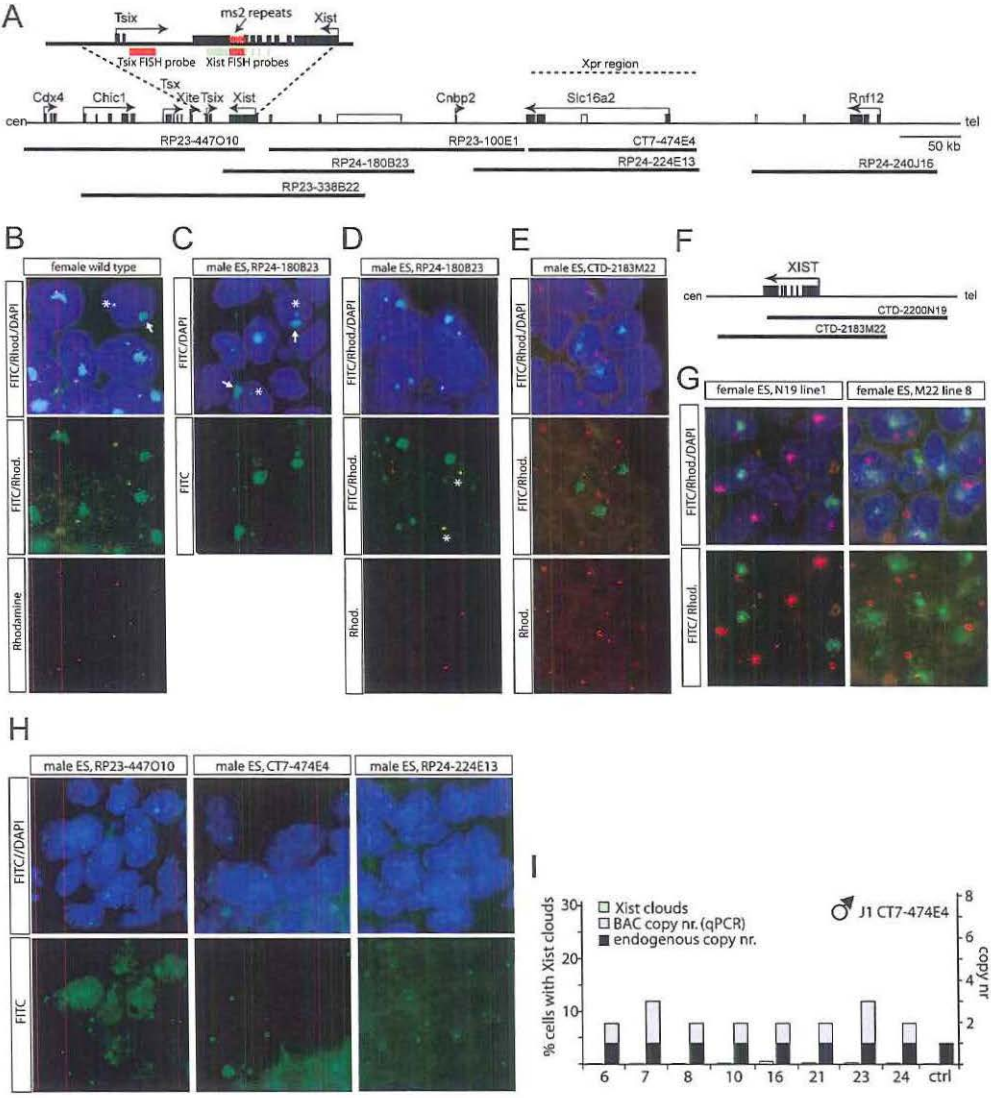

Figure 1: BAC contig covering the X inactivation center

A) Map showing part of the mouse X chromosome, the location of the BAC sequences used in this study, and the position of ms2 repeats within *Xist*. RNA-FISH probes are indicated in green and red, and non-annotated genes in grey. **B)** RNA-FISH with *Xist* (FITC) and *Tsix* probes (rhodamine red) on day 3 differentiated wild type ES cells, showing cells with *Xist* clouds only detected with the *Xist* probe (one marked with an arrow), and pinpoint signals detected with both *Xist* and *Tsix* probes (one marked with a star). **C)** RNA-FISH with an *Xist* probe (FITC) on day 3 differentiated male ES cells with an integration of BAC RP24-180B23, showing cells with *Xist* clouds (some marked with arrows), and pinpoint signals (some marked with a star). **D)** RNA-FISH with *Xist* (FITC) and ms2 (rhodamine red) probes on day 3 differentiated 1.3 male ES cells with an integration of BAC RP24-180B23, showing that *Xist* clouds are associated with autosomes, at a different location then the ms2 positive *Tsix/Xist*

that the *Xist* and *Tsix* regions are involved in the XCI counting process [166-167, 169, 171], but may be explained by a difference in transgene copy number or the number of clones that we analyzed.

We continued our search for an XCI-activator gene by generating transgenic male ES lines with BACs covering *Tsix* including a region 100 kb centromeric to *Tsix* (RP23-447O10), and BACs covering a region 300 kb telomeric to *Xist* (CT7-474E4, RP24-224E13, and RP23-100E1), including two BACs (CT7-474E4 and RP23-224E13) covering the *Xpr* region, which was recently implicated in pairing and activation of *Xist* [187]. RNA-FISH analysis only revealed pinpoint *Tsix/Xist* signals at day 3 of differentiation, indicating the absence of XCI initiation on the wild type X chromosome (**Figure 1G**, and **Supplemental Table 2B**). We also found no significant induction of XCI on both X chromosomes in female BAC RP23-100E1, CT7-474E4 and RP23-224E13 transgenic ES cells analyzed at day 3 of differentiation (**Supplemental Table 2C**). These results show that, despite involvement of the *Xpr* region in X chromosome pairing [187], additional transgenic copies of the *Xpr* region do not interfere with the XCI counting and initiation process.

A region on the X chromosome involved in activation of XCI

We continued our search for an XCI-activator gene and analyzed transgenic cells with an integration of BAC RP24-240J16, which covers an area from 410 kb to 570 kb telomeric to *Xist* (**Figure 1A**). Transgenic male ES cell lines were established using three independent ES cell lines (F1 2-3, J1, and 1.3), and the BAC integration was confirmed by qPCR and/or DNA-FISH (**Figure 2B**, **2C**, and **Supplemental Figure 2A**, **2B**). Interestingly, RNA-FISH analysis of day 3 differentiated BAC transgenic ES cell lines showed several lines with a significant number of cells with *Xist* clouds, which we never observed in control male cell lines (95% confidence interval, **Figure 2A**, **2B**, **Supplemental Table 1** and **Supplemental Figure 2A**). DNA/RNA-FISH analysis detecting both the X chromosome and *Xist* RNA confirmed that these male ES cells initiated XCI on the single X chromosome (**Figure 2D**). In transgenic female cell lines we also obtained an increased percentage of cells with two *Xist* clouds (**Figure 2A** and **2C**). RNA-FISH analysis on two independent day-3-differentiated RP24-240J16 transgenic female lines, heterozygous for the ms2 tag, showed that female cells with two *Xist* clouds only had one ms2 positive cloud (**Figure 2E**). Because aneuploidy would have resulted in a significant proportion of cells with either two ms2 positive or two negative clouds, this finding confirms that the transgenic female cells contained two X chromosomes. Our results therefore suggest that BAC RP24-240J16 harbors a gene encoding an XCI-activator.

Figure 1: continued
pinpoint signals (star). **E)** RNA-FISH detecting mouse *Xist* (rhodamine red) and human *XIST* (FITC) on day 3 differentiated male cells transgenic for human CTD-2183M22 (**Figure 1F**). **F)** Map of human *XIST* and the location of the BAC sequences used to generate transgenic ES cell lines. **G)** RNA-FISH detecting murine *Xist* (rhodamine red) and human *XIST* (FITC) on day 3 differentiated transgenic female ES cells. **H)** Similar to C), but with BACs RP23-447O10, CT7-474E4, and RP24-224E13. **I)** Percentage of CT7-474E4 male transgenic cell lines (6-24) with *Xist* clouds (green, BAC copies in grey, endogenous copies in black, n>100 per cell line).

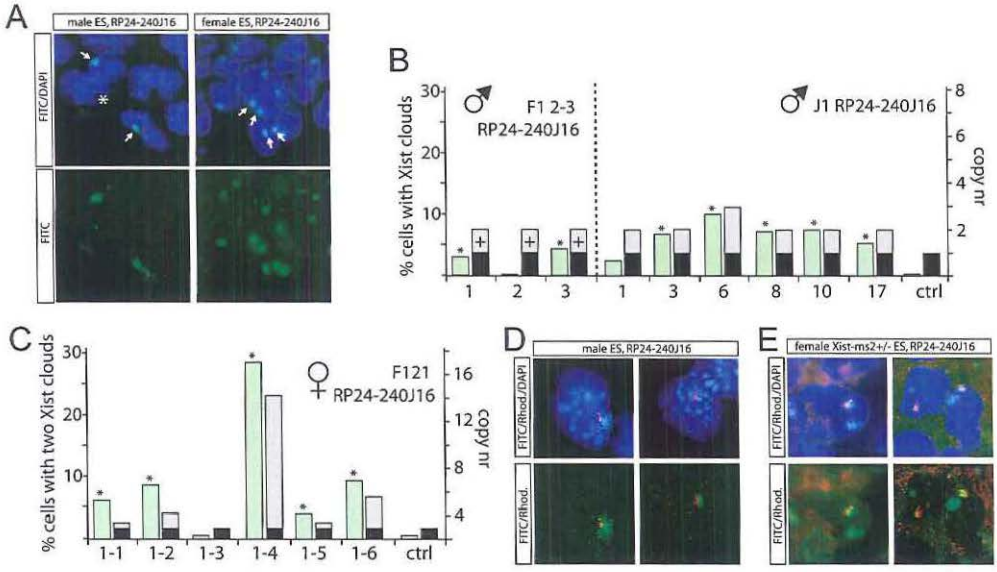

Figure 2: Ectopic XCI in transgenic male and female ES cells
A) RNA-FISH with an *Xist* probe (FITC) on day 3 differentiated ES cells with an integration of BAC RP24-240J16, showing male cells with *Xist* clouds (arrows) or pinpoint signals (star), and female cells with two *Xist* clouds (arrows). **B,C)** Percentage of male cells with single *Xist* clouds B) and female cells with two *Xist* clouds at day 3 of differentiation C), and BAC copy nr determined by qPCR (BAC copies in grey, endogenous copies of *Rnf12* in black, + indicates integration confirmed by DNA-FISH only, n>100 per cell line). Female line 1-3 has no BAC integration. ES cell lines that show a significant percentage of cells with *Xist* clouds compared to wild type control lines are indicated with an asterisk (non-overlapping 95% confidence interval, $p<0.05$). **D)** RNA/DNA-FISH detecting *Xist* (FITC) and an X chromosome specific probe (rhodamine red), on day 3 differentiated 1.3 male ES cells. **E)** RNA-FISH detecting *Xist* (FITC) and ms2 (rhodamine red) on day 3 differentiated female ES cells heterozygous for the *Xist*-ms2 tag, showing cells with two *Xist* clouds, one marked by ms2. Cells with two *Xist* clouds only showed one *Xist* and one *Xist*-ms2 cloud (Line 8 n=46, line 9 n=55).

Rnf12 is an XCI-activator

BAC RP24-240J16 encompasses *Rnf12* which is ubiquitously expressed in early mouse development, and two predicted genes for which no expression data is available (**Figure 1A**). To identify the sequences required for induction of XCI in male cells, we fine-mapped the area using mouse BAC sequences covering part of BAC RP24-240J16, thereby reducing the minimal region required for ectopic XCI to 10 kb (**Figure 3A**, and **Supplemental Table 3**). Expression analysis using total RNA of day 3 differentiated female ES cells hybridized to a tiling array covering BAC RP24-240J16 provided unequivocal data that *Rnf12*, which encodes an E3 ubiquitin ligase, is the only transcribed sequence within this region, and that the 10 kb region overlaps with the promoter and exon 1 and 2 of *Rnf12* (**Figure 3B**).

To establish a direct role of RNF12 in XCI, we disrupted the open reading frame of *Rnf12* by insertion of a neomycin/kanamycin resistance cassette in two orientations into exon 5 of *Rnf12*. This mutation disrupts most of the open reading frame, but leaves the 10

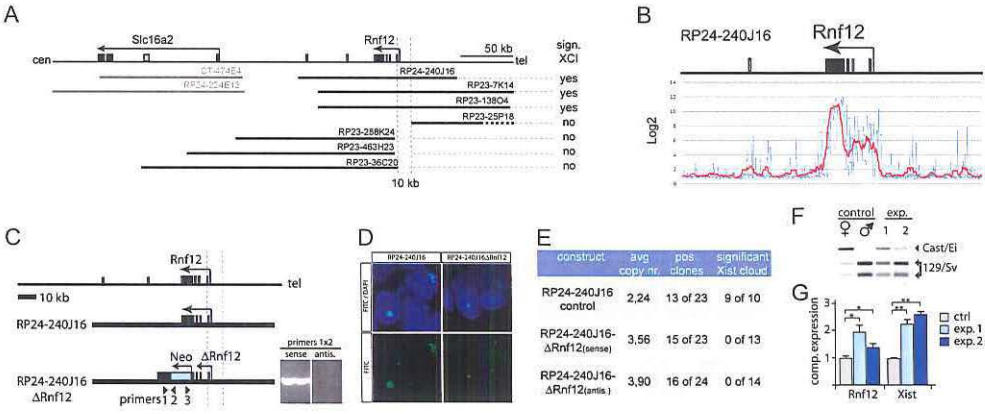

Figure 3: *Rnf12* encodes an XCI-activator
A) Position of BACs used for the fine-mapping, and their potential to stimulate XCI. BAC RP23-25P18, covering part of BAC RP24-240J16, was truncated (the part shown as a solid line was found to be present using PCR analysis; not shown). The minimal region required for ectopic XCI is marked in blue. **B)** Tiling array expression analysis with total RNA of day 3 differentiated female ES cells (top panel, moving average in red, raw data in blue, y-axis expression in log2). **C)** Map of part of the X chromosome covered by BAC RP24-240J16, and the modified BAC RP24-240J16ΔRnf12 with a neomycin resistance cassette inserted in two orientations (only the sense orientation is shown). Right panel shows confirmation of homologous recombination by PCR using the primer combination as indicated. **D)** RNA-FISH detecting *Xist* (FITC) on day 3 differentiated BAC RP24-240J16 (left panels) and RP24-240J16ΔRnf12 (right panels). **E)** Summary of the results obtained with all RP24-240J16 and RP24-240J16ΔRnf12 cell lines. Avg copy nr. is average of copynumber determined by qPCR of all clones with extra BAC integrations. Pos. clones indicates the number of clones with extra BAC integrations versus all picked clones. A 95% non-overlapping confidence interval was used for scoring ES cell lines with a significant percentage of *Xist* clouds ($p<0.05$), as determined by RNA-FISH of *Xist*. Not all positive clones with BAC integrations could be analyzed. **F)** RT-PCR analysis with RNA isolated from day 3 differentiated male (129/Sv) and female (Cast/Ei 129/Sv) control cells and male cells transiently transfected with an *Rnf12* expression construct (exp.). Analysis of NheI digested PCR products after gel electrophoresis indicates expression of transgenic *Rnf12* (Cast/Ei). **G)** RT-qPCR analysis of *Rnf12* and *Xist* expression in day 3 differentiated male cells transiently transfected with an *Rnf12* expression construct (exp. 1 and 2). Expression was compared to the expression level set at 1 in control cells (ctrl, T-test: * $p<0.05$, ** $p<0.01$).

kb minimal region required for ectopic XCI intact. This allowed us to test whether the induction of XCI is evoked by either *Rnf12*-encoded protein or by a DNA element within the 10 kb region (**Figure 3C**). Analysis of day-3-differentiated male ES cell lines with randomly integrated BAC RP24-240J16ΔRnf12 (sense and anti-sense) transgenes containing the mutated *Rnf12* gene, revealed no significant induction of XCI, in contrast to control transgenic male ES lines which showed significant induction of XCI in most cell lines (**Figure 3D**, **3E**, and **Supplemental Table 4A**). This result was confirmed with transgenic 30Δ1 female ES cells, where only random integration of the unmodified BAC RP24-240J16 resulted in an increased percentage of cells with two Xi's (**Supplemental Table 4B**),

Transient expression of the *Rnf12* cDNA might be sufficient to induce XCI in male cells. To investigate this, we transiently transfected male 1.3 ES cells with a *Rnf12* expression vector at day one of differentiation, and *Rnf12* and *Xist* expression was

determined after two more days of differentiation. *Xist* RNA-FISH experiments to test whether this transient expression of *Rnf12* resulted in activation of XCI were inconclusive, most likely due to a low transfection efficiency (<10%; measured by co-transfection of a GFP expression vector). Using RT-PCR amplification of *Rnf12* mRNA, followed by digestion with NheI, which digests an RFLP present in the endogenous *Rnf12* (129/Sv origin) PCR product but not in the transgenic *Rnf12* (Cast/Ei origin) PCR product, we could show that the transgenic *Rnf12* gene is transcribed (**Figure 3F**). In agreement with this, RT-qPCR analysis indicated an increase in transgenic *Rnf12* expression, and this correlated with increased *Xist* expression, which was up-regulated more than two-fold in *Rnf12* transfected samples (**Figure 3G**). These results support the view that *Rnf12* is involved in *Xist* up-regulation. The observed up-regulation of *Xist* was less pronounced than what would be expected from the studies with BACs containing *Rnf12*, but this is most likely due to the low transfection efficiency and cell death of male 1.3 ES cells after initiation of XCI. In addition, in the cells that have been transfected, the increased concentration of RNF12 may be lethal due to other functions of RNF12 which may be compromised when there is an overdose of the protein. Interestingly, *Rnf12* BAC transgenic ES cells did not survive freeze thawing. We think that extensive cell death may be initiated through activation of RNF12 by the thawing procedure, possibly resulting in ectopic XCI or mis-regulation of other processes.

In summary, fine mapping and expression studies revealed a 10 kb region on BAC RP24-240J16 to be required for ectopic XCI. This region overlaps with exon 1 and 2 of *Rnf12*, which is the only transcriptionally active gene covered by BAC RP24-240J16. In addition, transgenes with a disrupted *Rnf12* open reading frame do not induce ectopic XCI, whereas over-expression of *Rnf12* results in induction of *Xist* expression. These results provide strong evidence that *Rnf12* encodes an XCI-activator.

Conservation of RNF12 and dose-dependent activation of XCI by RNF12

Xist-mediated XCI is present in all eutherians, and previous studies have indicated that *Rnf12* is highly conserved among mammals and other species [893]. We wanted to test whether human RNF12 can induce XCI in transgenic male and female mouse ES cells. To this end, transgenic mouse ES cells were generated containing human BAC CTD-2530H13 (**Figure 4A**), which covers an area that is homologous to the region covered by mouse RP24-240J16 (**Figure 1A**) and shows high sequence homology in the promoter and coding regions of *Rnf12/RNF12* (**Figure 4B**). Upon differentiation of several of these CTD-2530H13 transgenic cells, XCI is induced in a significant proportion of the male cells, and on both X chromosomes in an increased percentage of the female cells, suggesting that the function of RNF12 in XCI in mouse and human is conserved (**Figure 4C**, **4D** and **4E**).

To further test whether RNF12 acts as a dose-dependent activator of XCI, we EB-differentiated transgenic BAC CTD-2530H13 ES cell lines for 3 days, and determined the expression of mouse endogenous *Rnf12* and *Xist*, and human transgenic *RNF12* by RT-qPCR. Comparison of *Xist* RNA-FISH and RT-qPCR expression analysis showed a correlation between transgenic *RNF12* expression, *Xist* up-regulation, and activation of XCI on the single X in male cells (Pearson 0.77, $p<0.001$ and Pearson 0.67, $p<0.01$, respectively, **Figure 5A** and **5B**). The effect of transgenic *RNF12* on *Xist* expression,

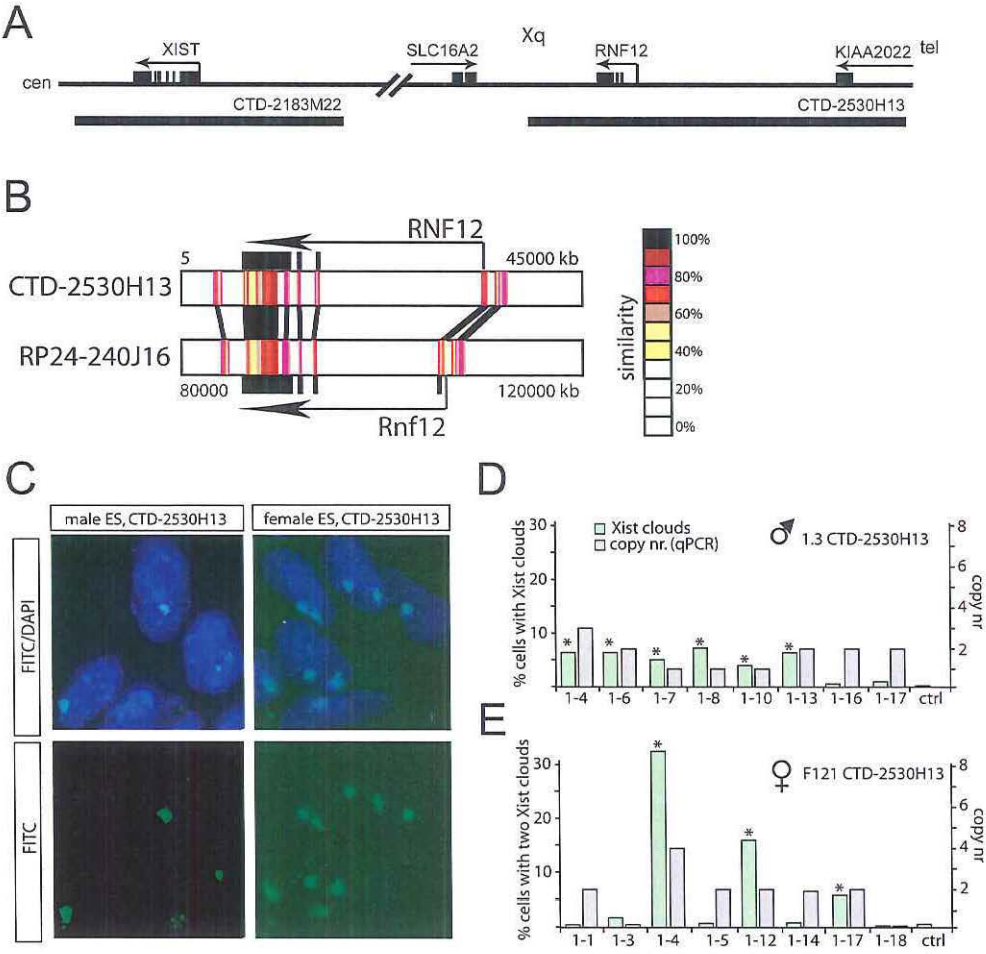

Figure 4: The action of human RNF12 is conserved in mouse
A) Schematic map of part of the human X chromosome and location of the BACs used for the analysis. **B)** Alignment of mouse (RP24-240J16) and human (CTD-2530H13) BAC sequences (bottom panel). Shown is the region containing the *Rnf12 / RNF12* gene. **C)** RNA-FISH detecting *Xist* (FITC) on day 3 differentiated CTD-2530H13 transgenic male ES cells (left panels) and female ES cells (right panels). **D, E)** Quantification of RNA-FISH presented in C), for BAC transgenic male D) and female E) cell lines, and BAC copy number determined by qPCR (grey, n>100 per cell line). Day 3 differentiated ES cell lines with a significant percentage of cells with *Xist* clouds compared to wild type control lines are indicated with an asterisk (non-overlapping 95% confidence interval, $p<0.05$).

determined by RT-qPCR, is more pronounced in male than female cell lines, because *Xist* is normalized to the level present in male and female control cell lines, respectively (**Supplemental Figure 4A** and **4B**). Some lines did not show ectopic XCI despite expression of transgenic *RNF12* (clone nrs: ♂ 2-6, 2-21 (**Figure 5B**) and ♀ 2-22 (**Supplemental Figure 4B**)), which may be attributed to truncated transgenes giving rise to

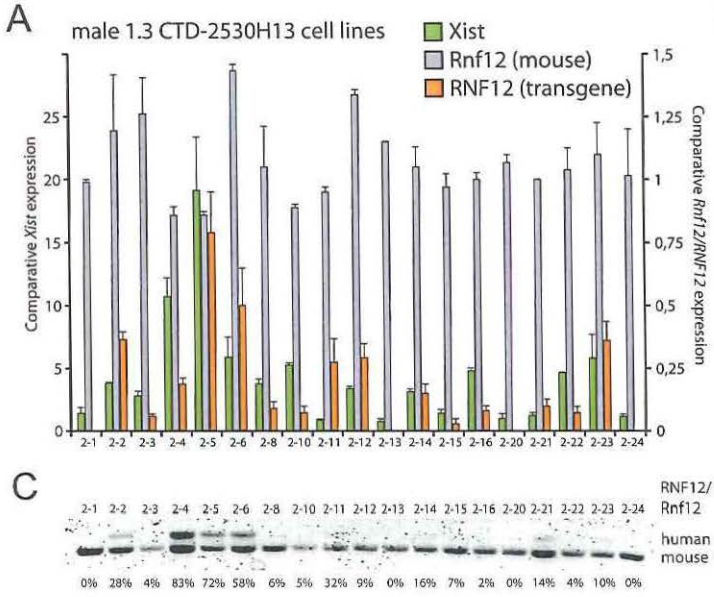

B

Male 1.3 CTD-2530H13 line	qPCR copy nr	RNA-FISH 1xXist	n
2-1	-	0%	103
2-2	++	3%*	136
2-3	+	4%*	152
2-4	++	12%*	198
2-5	+++	36%*	106
2-6	++	0%	75
2-8	+	no cells	-
2-10	+	7%*	152
2-11	+	5%*	115
2-12	+	no cells	-
2-13	-	N.D.	-
2-14	+	5%*	114
2-15	+	no cells	-
2-16	+	7%*	114
2-20	-	0%	108
2-21	+	0%	133
2-22	+	9%*	117
2-23	++	6%*	108
2-24	-	0%	142

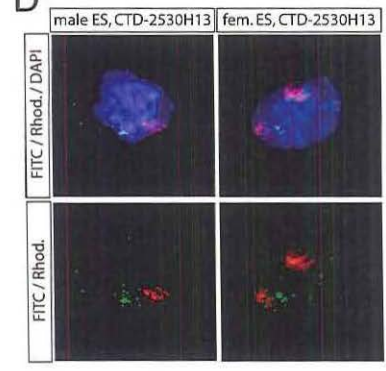

E

male 1.3 construct	RNF12	1xXist	1xXist and RNF12	n
CTD-2530H13 line 2-4	45%	14%	95%	604
CTD-2530H13 line 2-5	50%	12%	96%	711

female F1 2-1 construct	RNF12	1xXist	2xXist	2xXist and RNF12	n
CTD-2530H13 line 2-3	30%	42%	11%	100%	276
CTD-2530H13 line 2-5	21%	46%	7%	90%	268

Figure 5: RNF12 is a dose-dependent activator of XCI
A) Expression analysis of male 1.3 cell lines targeted with the human CTD-2530H13 BAC containing *RNF12*. RT-q-PCR was performed with primer sets for *Xist* (green), *Rnf12* (grey), and *RNF12* (orange). All samples were normalized to beta-*actin*, and expression was compared to the average of wild type cell lines 1.3 H13 1/13/20/24. Expression of human *RNF12* was compared to expression of mouse *Rnf12* of the control cell lines. **B)** Table of male 1.3 cell lines targeted with the human CTD-2530H13 BAC containing *RNF12*. The relative copy number of the BAC integration, ranging from – (no integration) to +++ (several copies). The RNA-FISH column represents percentage of cells with one *Xist* cloud (1x*Xist*, * $p<0.05$ based on a 95% confidence interval, n is number of cells counted). **C)** RT-PCR analysis detecting a length polymorphism distinguishing *Rnf12* and *RNF12*. The relative expression of *RNF12* compared to endogenous *Rnf12* is depicted below each lane. **D)** *Xist-RNF12* RNA-FISH with day 3 differentiated BAC CTD-2530H13 transgenic male and female ES cell lines, detecting *Xist* clouds (rhodamine red) and *RNF12* transcription foci (FITC). **E)** Quantification of *RNF12* transcription foci (*RNF12*), single (1x *Xist*) or double (2x *Xist*) *Xist* clouds, and the percentage of cells with a single *Xist*

a non-functional RNA, or to variegated expression through position effects resulting in only a few cells expressing the transgene at a relative high level. To compare the expression level of *RNF12* versus *Rnf12,* we amplified a length polymorphism distinguishing *RNF12* from *Rnf12* by RT-PCR (**Figure 5C**). Quantification of the relative intensity of *RNF12* and *Rnf12* confirmed a correlation between expression of transgenic *RNF12, Xist* up-regulation, and XCI (Pearson 0.67, $p<0.01$ and Pearson 0.58, $p<0.05$ respectively). Our results also indicate that transgenic expression is moderate, not reaching the endogenous level, suggesting selection against cells that express *RNF12/Rnf12* at higher levels. We further investigated whether expression of *RNF12* correlated with *Xist* cloud formation, by combined RNA-FISH detecting *Xist* and *RNF12.* Analysis of two transgenic male and female cell lines indicated that a single *Xist* cloud in male cells and two *Xist* clouds in female cells were almost exclusively present in cells which showed an *RNF12* RNA-FISH signal ($P<0.0001$, Z-test for proportion, **Figure 5D** and **5E**).

Although the function in XCI appears to be conserved, we do not know whether the specific activities of mouse and human RNF12 are equal. We therefore repeated the experiment shown in **Figure 5**, but generated 1.3 male transgenic ES cells harboring a BAC sequence covering the *Mus. musculus mollosinus Rnf12* gene, which allowed us to use a RFLP (NheI) that discriminates between endogenous and transgenic *Rnf12* cDNA. *Xist* RNA-FISH with day 3 differentiated transgenic ES cell lines containing at least one transgene copy showed induction of XCI in a significant proportion of cells for most ES cell lines (**Supplemental Figure 4D** and **4E**). RT-PCR expression analysis confirmed that *Mus. musculus mollosinus Rnf12* is expressed in the undifferentiated transgenic male cell lines that induce XCI, at 0.4- to 2.0-fold levels compared to the expression level of one endogenous *Rnf12* copy (**Supplemental Figure 4E**). In addition, Western blot analysis with anti-RNF12, and anti-ACTIN as a control, confirmed elevated expression of RNF12 in day one differentiated transgenic male ES cell lines compared to a wild type control cells (not all cell lines were analyzed, **Supplemental Figure 4F**). Expression of *Rnf12* correlated with cells that initiated XCI at day 3 of differentiation (Pearson 0.67, $p<0.01$). Similar to our findings with CTD-2530H13 transgenic ES cell lines, we only observed ES cell lines that showed moderate expression of transgenic *Rnf12*.

The results obtained with transgenic ES cell lines harboring human *RNF12* and *Mus. musculus mollosinus Rnf12* transgenes indicate that the function of RNF12 is most likely conserved from human to mouse. Furthermore, expression of ectopic *RNF12* positively correlates with expression of *Xist* and subsequent initiation of XCI.

Figure 5: continued
cloud together with an *RNF12* signal in BAC CTD-2530H13 transgenic male ES cell lines (1x*Xist* and *RNF12*), or two *Xist* clouds together with an *RNF12* signal in BAC CTD-2530H13 transgenic female ES cell lines (2x*Xist* and *RNF12*), at day 3 of differentiation (n=number of cells analyzed).

Endogenous RNF12 expression correlates with XCI

Rnf12 encodes an E3 ubiquitin ligase involved in the regulation of LIM-homeodomain containing factors, by targeting LIM interacting proteins LDB1 and LDB2 for degradation [893]. In addition, RNF12 also appears to be involved in gene activation, and telomere length homeostasis, indicating that this multifaceted protein is involved in many important processes besides XCI [894-895]. To play a dose-dependent role in XCI, it is to be expected that, prior to XCI, the RNF12 concentration is two-fold higher in female cells compared to male cells, and that expression of RNF12 is correlated with the developmental time period were XCI is initiated. In addition, to properly regulate XCI *Rnf12* expression should be subject to XCI to ensure down-regulation of RNF12 preventing initiation of XCI on the second X chromosome.

The endogenous RNF12 expression was estimated in nuclear extracts of male and female ES cells at different time points of differentiation, using Western blot analysis with an antibody detecting RNF12, and anti-ACTIN as a loading control. This analysis revealed that RNF12 is up-regulated in female and male cells around the time XCI is initiated in female cells, after which expression decreases in time (**Figure 6A**, and data not shown). Comparison of RNF12 expression in nuclear and cytoplasmic extracts indicated that RNF12 is almost exclusively present in the nucleus (data not shown). Immuno-cytochemistry also revealed nuclear localization of RNF12 at day 3 of differentiation (**Figure 6C**), and indicated that RNF12 did not localize to the Xi. Comparison of RNF12 expression in Cast/Ei/129/Sv male and female ES cell lines prior to XCI, and around the time XCI is initiated, confirms that RNF12 is higher expressed in female compared to male cells (**Figure 6B**). This difference in RNF12 expression was absent in male and female mouse embryonic fibroblasts (MEF), suggesting that one copy of *Rnf12* is inactivated in female MEFs. Allele specific RT-PCR analysis with RNA of undifferentiated and day-7-differentiated heterozygous *Tsix* mutant ES cells, which exclusively inactivate the mutant 129/Sv X [123], indeed confirmed that *Rnf12* expression is subject to XCI (**Figure 6D**). The above Western blot analysis indicated that RNF12 is already expressed prior to XCI, from which it can be suggested that additional copies of *Rnf12* may lead to XCI in undifferentiated ES cells. We targeted F1 2-1 female cells with BAC RP24-240J16 and picked and expanded neomycin positive clones. Undifferentiated ES cell lines with additional transgenic copies of *Rnf12*, determined by qPCR, appeared indistinguishable from wild type undifferentiated ES cells. Undifferentiated and day three differentiated ES cells were fixed and subjected to *Xist* RNA-FISH analysis. We found that all the undifferentiated cell lines with transgenic copies of *Rnf12* showed *Xist* clouds, which were not present in undifferentiated female control cells (**Figure 6E** and **6F**). Interestingly, several of the cell lines with the highest percentages of Xi's in undifferentiated ES cells, showed extensive cell loss upon differentiation, with no or a few cells left to analyze at day 3 of differentiation. The relative expression of *Rnf12* was estimated by RT-PCR amplifying an RFLP (NheI). This analysis indicated increased expression of transgenic *Rnf12* in almost all undifferentiated transgenic ES cell lines tested (**Figure 6F**), which correlated with *Xist* cloud formation (Pearson 0.86, $p<0.01$). Also the RNF12 protein levels in nuclear extracts from cells at day 3 of differentiation were increased in most transgenic ES cell lines

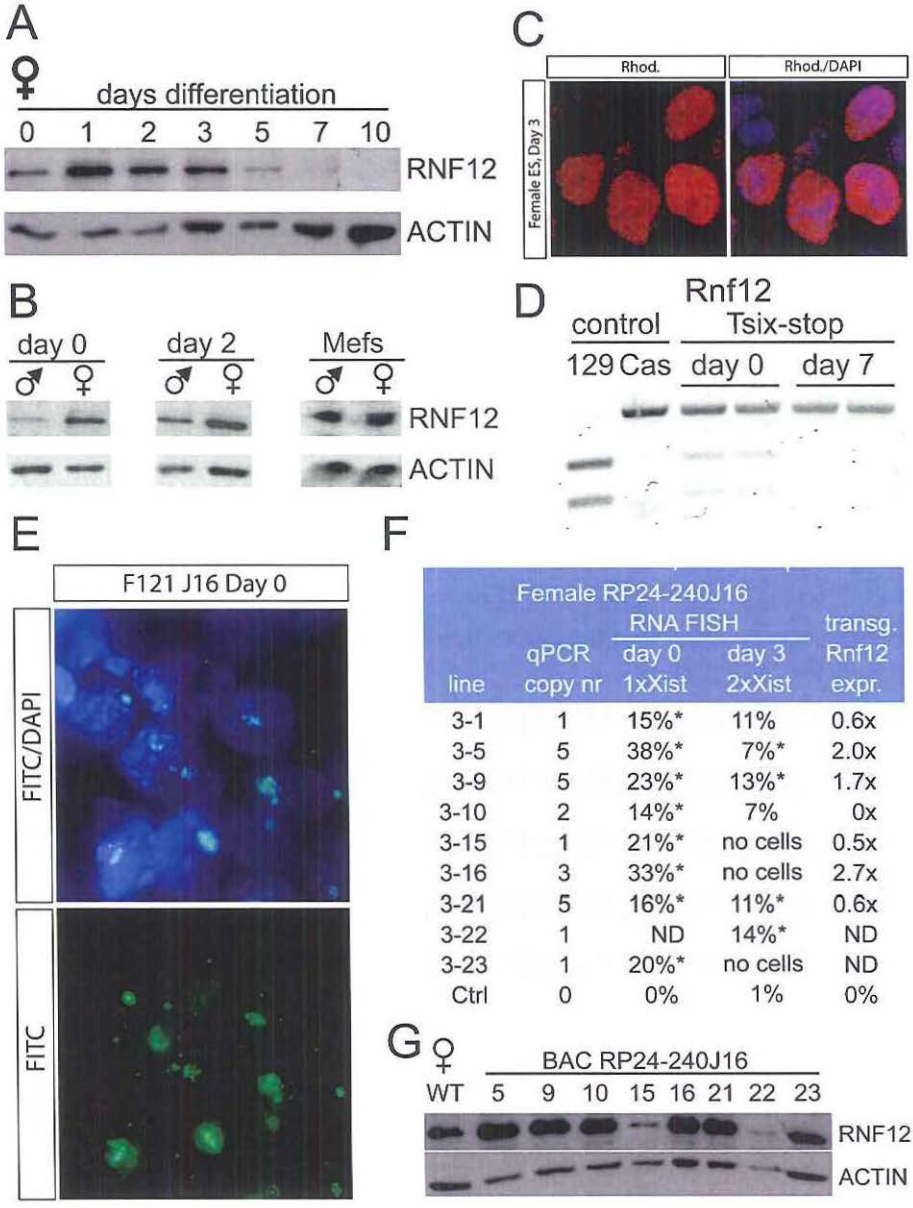

Female RP24-240J16		RNA FISH		transg.
line	qPCR copy nr	day 0 1xXist	day 3 2xXist	Rnf12 expr.
3-1	1	15%*	11%	0.6x
3-5	5	38%*	7%*	2.0x
3-9	5	23%*	13%*	1.7x
3-10	2	14%*	7%	0x
3-15	1	21%*	no cells	0.5x
3-16	3	33%*	no cells	2.7x
3-21	5	16%*	11%*	0.6x
3-22	1	ND	14%*	ND
3-23	1	20%*	no cells	ND
Ctrl	0	0%	1%	0%

Figure 6: Expression analysis of RNF12
A) Western blot analysis detecting RNF12 (top panel) and ACTIN (bottom panel) in female ES cells at different time points in differentiation. **B)** Western blot analysis detecting RNF12 (top panel) and ACTIN (bottom panel), comparing RNF12 expression in male and female undifferentiated (left panel), day 2 differentiated ES cells (middle panel), and in MEFs (right panel). **C)** Immunocytochemistry on day 3 differentiated female ES cells using an antibody detecting RNF12 (rhodamine red). **D)** RT-PCR

compared to wild type female cells (**Figure 6G**), although lines 3-15 and 3-22 did not show an increase in RNF12 expression, possibly due to cell loss of cells over-expressing RNF12.

Taken together, these findings indicate that RNF12 is expressed in the time window of ES cell differentiation were XCI is initiated, with a nuclear concentration of RNF12 that is higher in female compared to male cells. Our results suggest that the RNF12 concentration is well titrated to ensure a dose-dependent role for RNF12 in activation of XCI. In agreement with this, additional copies of *Rnf12* can induce XCI in undifferentiated female ES cells, indicating that an increase in the RNF12 concentration is sufficient to trigger XCI.

Figure 6: continued
expression analysis of *Rnf12* with RNA isolated from undifferentiated and day 7 differentiated 129/Sv Cast/Ei *Tsix*-stop ES cells, which exhibit non-random XCI of the mutated 129/Sv X chromosome, using a NheI cleavage of the PCR product at an RFLP present in the 129/Sv allele. The left two lanes show control 129/Sv and Cast/Ei samples. **E)** RNA-FISH detecting *Xist* (FITC) on undifferentiated BAC RP24-240J16 (left panels) transgenic female ES cells. **F)** Table of female F1 2-1 cell lines targeted with BAC RP24-240J16. The copy number of the BAC integration, and the percentage of undifferentiated cells containing one *Xist* cloud (1x*Xist*) and day 3 differentiated cells with two *Xist* clouds (2x*Xist*) are depicted. The column on the right shows the level of transgene expression, determined by RFLP RT-PCR, relative to one endogenous copy of *Rnf12* in undifferentiated ES cell lines. ES cell lines that show a significant percentage of cells with *Xist* clouds compared to wild type control lines are indicated with an asterisk (confidence interval 95%, $p<0.05$). **G)** Western blot analysis detecting RNF12 (top panel) and ACTIN (bottom panel) with nuclear extracts of day 3 differentiated ES cell lines described in F).

Figure 7

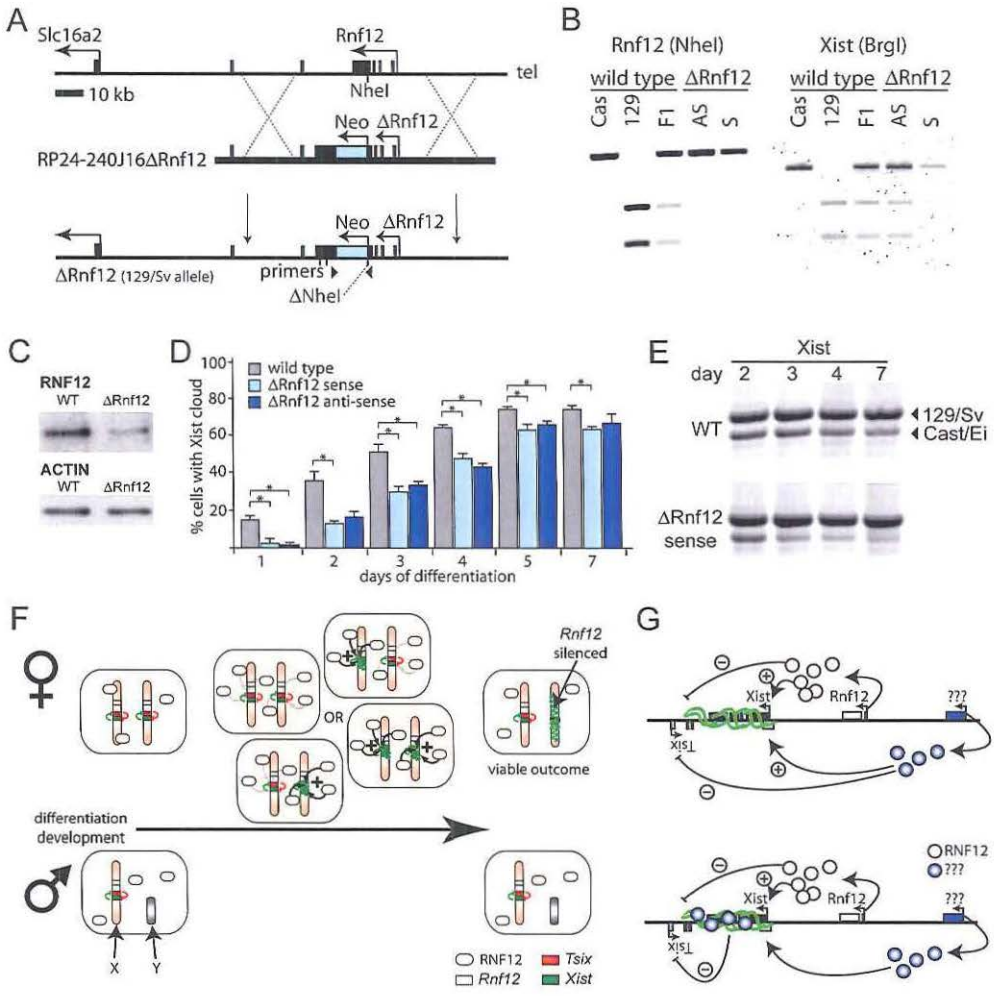

Figure 7: Generation and analysis of *Rnf12+/-* female ES cells
A) A map of part of the X chromosome and the BAC RP24-240J16ΔRnf12 targeting construct with a neomycin resistance cassette inserted in two orientations (only sense orientation is shown), and the targeted 129/Sv allele, and location of PCR primers used for genotyping. **B)** Left panel, RT-PCR with primers amplifying a RFLP (NheI) in the 129/Sv *Rnf12* allele. Right panel, RT-PCR with a primer set amplifying a RFLP (BrgI) in the 129/Sv *Xist* allele. **C)** Western blot analysis detecting RNF12 (top panel) and ACTIN (bottom panel) in nuclear extracts from a wild type female and Δ*Rnf12+/-* ES cell line. **D)** Bar graph showing the percentage of wild type and Δ*Rnf12+/-* (sense and anti sense) ES cells that initiated XCI, detected by *Xist* RNA-FISH, at different time points of EB differentiation. Significant differences are marked with an asterisk (T-test, * $p<0.05$) **E)** RT-PCR expression analysis of *Xist* originating from the 129/Sv allele (top band) and the Cast/Ei allele (bottom band) with RNA isolated from day 2, 3, 4 and

XCI is reduced in Rnf12+/- female cells

RNF12 appears to be an important activator of X chromosome counting and initiation of XCI, but it may not act as a single factor, and the existence of one or more additional XCI-activators or cofactors with some RNF12-independent activity cannot be excluded. To study this, we deleted *Rnf12* from one X chromosome (129/Sv) by targeting BAC RP24-240J16ΔRnf12 (sense and antisense) to a polymorphic F1 2-1 female (Cast/Ei-129/SV) ES cell line (**Figure 7A**). Correct targeting was confirmed by PCR amplification of a sequence containing a RFLP (NheI) which was removed from the targeted allele (**Figure 7B**). Some 129/Sv product is still detectable due to feeder cell (129/Sv) contamination. X chromosome copy number and origin were confirmed by DNA-FISH (**Supplemental Figure 5**), qPCR (not shown) and PCR amplification of a sequence containing a RFLP (BrgI) in *Xist* (**Figure 7B**). Western blot analysis with nuclear extracts from undifferentiated wild type and Δ*Rnf12*+/- (sense) ES cells confirms that RNF12 expression is reduced in the heterozygous knockout ES cells (**Figure 7C**). Two heterozygous Δ*Rnf12*+/- (sense and anti-sense) ES cell lines were EB-differentiated, fixed at different time points, and subjected to *Xist* RNA-FISH. We found that initiation of XCI in both Δ*Rnf12*+/- ES cell lines was severely reduced, by more than 80%, at the start of differentiation (day 1-3) but recovered later in the differentiation process (**Figure 7D**). EBs generated with Δ*Rnf12*+/- ES cells appeared smaller (data not shown), indicating cell selection against cells that retain two active X chromosomes and selection against cells that inactivated the wild type endogenous *Rnf12,* which would result in a RNF12 null cell. Analysis of *Xist* expression using a length polymorphism to distinguish cDNA originating from the 129/Sv or Cast/Ei allele revealed that *Xist* is expressed from both alleles in the beginning of the XCI process (**Figure 7E**), indicating that the probability to initiate XCI is reduced for both X chromosomes in Δ*Rnf12*+/- cells and is not caused by a *cis* effect of the *Rnf12* mutation. The F1 2-1 ES cells used in our studies show skewed XCI, with a preference for *Xist* expression from, and inactivation of, the 129/Sv X chromosome, caused by the presence of two different Xce's with different allelic properties. In Δ*Rnf12*+/- cells, from day 3 of differentiation onwards, *Xist* is almost exclusively expressed from the 129/Sv allele, suggesting cell selection in favor of cells that inactivated the mutant *Rnf12* allele. The presence of female Δ*Rnf12*+/- cells that do initiate XCI indicates that one or more additional X-encoded XCI-activators are involved in initiation of XCI. Nonetheless, the severe reduction in cells that initiate XCI in the Δ*Rnf12*+/- cells, and our studies with *Rnf12/RNF12* transgenic ES cells, both emphasize an important role for RNF12 in XCI counting and initiation.

Figure 7: continued
7 differentiated wild type and Δ*Rnf12*+/- (sense) ES cells. **F)** Upon differentiation of the ES cells, the concentration of RNF12 and/or an unknown target or modifier of RNF12 increases, which potentiates the action of RNF12. This leads to stochastic up-regulation of *Xist* transcription (grey arrows, up-regulation low, black arrows, up-regulation high), resulting in a probability to initiate XCI, and accumulate along the X (+). Spreading of *Xist* RNA leads to silencing of *Rnf12* transcription in *cis*, resulting in a drop of the nuclear RNF12 concentration, prohibiting inactivation of the second X. In male cells, the RNF12 concentration does not reach the threshold required to start this sequence of events. **G)** *Rnf12* mediated activation of XCI, could involve activation of *Xist*, or suppression of *Tsix* through direct or indirect mechanisms (RNF12 in yellow). The action of other putative XCI-activators (blue) could involve a similar mechanism as hypothesized for RNF12 (left panel), or could involve silencing of *Tsix* by *Xist* RNA mediated recruitment (right panel).

Discussion

Herein, we have identified RNF12 as an X-encoded activator of X chromosome inactivation (XCI) in mouse embryonic stem (ES) cells. Additional copies of mouse or human *Rnf12/RNF12* result in an increased probability to initiate XCI, resulting in XCI on the single X chromosome in male cells and on both X chromosomes in female cells. The action of RNF12 is dose-dependent, and analysis of heterozygous *ΔRnf12*+/- ES cells confirms a role for *Rnf12* in XCI. At the same time, our findings indicate that one or more additional XCI-activators are involved in counting and initiation of XCI. Still, it is evident that RNF12 plays a key role in control of X-chromosomal gene dosage between male and female cells, and is therefore the first X-linked dose-dependent activator of XCI.

RNF12 is a potent activator of XCI

Previous studies have indicated that ectopic XCI is initiated in transgenic male cells containing additional copies of *Xist/XIST* and flanking sequences [166-167, 169, 171]. In the present analysis, these same regions did not evoke ectopic XCI in transgenic male and female cells. To try to explain this discrepancy, one could argue that transgene copy number was different in the various studies, and that the integration site and variegated transgene expression might be implicated. In addition, analysis of XCI at later time points of the differentiation process might reveal induction of XCI. The absence of initiation of ectopic XCI in our *Xist/Tsix* transgenic cell lines indicates that additional sequences are required for proper Xic function, which is supported by our previous finding that ΔXTX heterozygous ES cells still initiate XCI [179], and the finding that single copy *Xist/Tsix* transgenes do not induce XCI on the endogenous X chromosome [175]. The *Xpr* region located ~200 kb telomeric to *Xist* has been implicated in proposed pairing of two X chromosomes [187], and activation of *Xist*. However, our findings indicate that extra transgenic copies of the *Xpr* region are not sufficient for initiation of ectopic XCI, although this does not preclude a role for this region in the XCI process. Regarding the present studies it should be noted that almost all the male and female cell lines that we generated with a BAC transgene containing *Rnf12* resulted in XCI on the single X chromosome in male cells (32 out of 38 cell lines), and on both X chromosomes in female cells (17 out of 20 cell lines). For most cell lines activation of XCI also correlated with expression of transgenic RNF12. From this, we feel that we can safely conclude that RNF12 is a very potent activator of XCI.

The observation that the RP24-240J16 transgenic cells did not initiate XCI on all X chromosomes, can be explained by our finding that RNF12 is not the only XCI-activator. Also, cells that inactivate too many X chromosomes will be counter-selected, possibly masking the effect of *Rnf12* on XCI, and expression of the transgenes may have been variegated. More importantly, extra copies of *Rnf12/RNF12* will lead to an increased probability to initiate XCI in transgenic cells, which may never reach 100% in the time interval required for one cell division, so that always some cells can retain at least one Xa. Our expression analysis also indicates that the expression level of transgenic *Rnf12* is modest. This suggests that higher expression levels are not tolerated, because this most likely results in extensive induction of XCI already in undifferentiated ES cells, and subsequent loss of the transgenic cells. Higher RNF12 concentrations may also compromise cell viability due to mis-regulation of other pathways in which RNF12 takes part. We think

this may also explain why the effect of transient expression of RNF12 on *Xist* induction is smaller than what is obtained in low copy transgenic ES cell lines, because the effect of transient expression of RNF12 on XCI may be masked through extensive counter-selection against transfected cells.

We found that XCI can be induced in undifferentiated female transgenic ES cells expressing exogenous RNF12. This finding could suggest that RNF12 over-expression induces ES cell differentiation. However, undifferentiated wild type and transgenic ES cells appeared morphologically similar, and female ES cells with two copies of *Rnf12* have not been reported to be more differentiated than male cells with one copy of *Rnf12* [38]. Also, activation of XCI in *Rnf12* transgenic male ES cells cannot be explained by an effect of RNF12 on differentiation. It is therefore more likely that *Rnf12* transgenic ES cells remain undifferentiated, which implies that all other factors required for initiation of XCI are already present in undifferentiated ES cells, although the level of these other factors may increase upon differentiation. Our results also suggest that repression of *Xist* can be overcome by increased expression of RNF12, even in undifferentiated ES cells.

Stochastic initiation of XCI

A stochastic model for XCI predicts that every X chromosome has an independent probability to be inactivated [179]. This contrasts with all other models that explain counting and initiation of XCI through mutually exclusive mechanisms [892]. Our present findings support a stochastic model for XCI and indicate that the probability to initiate XCI is directed by a chance process which is dependent on the nuclear concentration of different factors that promote or suppress XCI.

As described and referenced in the introduction, *Xist* and *Tsix* knockout and over-expression studies have indicated that the probability to initiate XCI is determined by the balance between *Xist* and *Tsix* transcription, which is regulated by X-encoded XCI-activators and autosomally encoded XCI-inhibitors. XCI-activators are involved in dose-dependent up-regulation of *Xist* expression, whereas XCI-inhibitors are involved in suppression of *Xist*. Protein expression analysis of differentiating female ES cells indicates that RNF12 is expressed and up-regulated around the time XCI is initiated. The nuclear concentration of RNF12 will reach a threshold, in female and not in male cells, that is sufficient to up-regulate *Xist* expression, either directly or indirectly, to a point where it initiates XCI (**Figure 7F**). Other XCI activators may be present at a constant concentration or reach a threshold in a similar fashion. The observed initiation of XCI in undifferentiated female ES cells upon transgenic RNF12 expression indicates that up-regulation of RNF12 may be required and sufficient to trigger XCI in female cells. However, the predicted E3 ubiquitin ligase activity of RNF12 suggests that expression or activity of additional factors, acting as substrate or modifier of RNF12 action, are likely to be involved in XCI.

RNF12 or its downstream target(s) may act through activation of *Xist* directly, or indirectly by suppression of *Tsix* (**Figure 7G**). Another possibility is that RNF12 is recruited by *Xist* RNA in order to silence *Tsix*, but RNF12 immuno-staining did not show specific accumulation of RNF12 anywhere in the nucleus suggesting that this is the least likely option. The evolutionary conservation of RNF12 and activation of XCI in mouse ES cells by human RNF12, taken together with the absence of an established role for *TSIX* in human X inactivation, makes it likely that RNF12 is involved in activation of *Xist/XIST*

transcription. This is also supported by studies with *Xist* promoter transgenes, which showed higher expression in female cells compared to male cells [89].

After initiation of XCI, the XCI-activator genes will be silenced in *cis*, providing a simple mechanism to decrease the concentration of the XCI-activators. Such a feedback mechanism will prevent inactivation of the second X chromosome in female cells, although the other X chromosome(s) still have a probability to initiate XCI, in the time window in between initiation of XCI and down-regulation of the XCI-activator concentration at the protein level. Previous studies have indicated that genes which are in close proximity to *Xist* are more likely to be inactivated at an earlier time point of development or ES cell differentiation than genes located further away. Close proximity of *Rnf12* to *Xist* may therefore facilitate a quick down-regulation of RNF12 [38]. Re-evaluation of the data used for this study indicates that *Rnf12* indeed belongs to the category of genes that is silenced early during ES cell differentiation (**Supplemental Figure 6**). Interestingly, *Rnf12* is also among the first genes to be down-regulated in imprinted XCI, which commences around the four- to eight-cell stage of embryonic development [311], and silencing of *Rnf12* is strictly dependent on *Xist* [896]. Also, the stability of RNF12 has been reported to be much lower than other nuclear proteins [897], which would facilitate a rapid feed-back mechanism to prevent inactivation of the second X chromosome.

Whether RNF12 is required for *Xist* expression after the Xi is established, remains to be determined. The observation that *Xist* remains expressed on the Xi can be explained by silencing of its negative regulator *Tsix*. On the Xi a lower XCI-activator concentration would then be sufficient for sustained expression of *Xist*. Following XCI, the reduced concentration of XCI-activators will be too low to induce XCI of the Xa, and its *Xist* gene is silenced in a *Tsix* dependent process involving *Xist* promoter specific DNA methylation and repressive histone modifications [89, 112, 898].

More XCI-activators involved

Rnf12 is ubiquitously expressed in embryos around the onset of XCI [893]. One known target of RNF12 is LDB1, which interacts with LIM-homeodomain transcription factors. RNF12 is also involved in activation of estrogen receptor α [895] and degradation of a telomere associating protein TRF1 with an effect on telomere length homeostasis [894]. Hence, RNF12 likely acts as a regulator, activator or repressor, also outside the context of XCI, but none of the known RNF12 partners from other pathways have been implicated in XCI.

Analysis of Δ*Rnf12*+/- cell lines indicates that *Rnf12* is not the only X-encoded XCI-activator regulating initiation of XCI. Similar to *Rnf12*, these activators may be involved in activation of *Xist* transcription or repression of *Tsix* through a direct mechanism or by *Xist* RNA mediated recruitment (**Figure 7G**). Studies on other organisms provide clear examples of how dosage compensation processes can be triggered by single master switch genes: *Sxl* in *Drosophila* and *Xol-1* in *C. elegans*. In both species, these master switch genes are regulated by several X-encoded numerator genes and autosomally encoded denominator genes, suggesting that more than one numerator and denominator gene is required to suppress the noise in the system [899]. For eutherians, a similar mechanism may apply, with the *Xist/Tsix* locus representing the master switch locus that is regulated by several XCI-activators and inhibitors to count the number of X chromosomes and activate

initiation of XCI. Previous studies suggest that NANOG, SOX2, OCT4, CTCF and YY1 act as XCI-inhibitors. Depletion of these factors results in increased *Xist* transcription indicating an involvement in determining the threshold that has to be overcome for initiation of XCI, either by direct repression of *Xist* or activation of *Tsix* [186, 191, 193]. However, the genes encoding the three pluripotency factors factors NANOG, SOX2, and OCT4, and also the genes encoding CTCF and YY1, are all located on autosomes, and are most likely not differentially expressed between male and female cells. Therefore, despite a clear involvement in XCI, these genes are not likely candidates to direct the XCI counting process. In contrast, the X-chromosomal *Rnf12* gene can be readily envisaged to encode a protein that acts as a numerator, to discriminate between chromosomally male and female cells in relation to XCI. RNF12 represents the first identified XCI-activator, involved in determining the probability to initiate XCI. Identification and characterization of the direct target or modifier of RNF12, and other genes encoding XCI-activators, will be the next step to further elucidate the control of counting and initiation in X chromosome inactivation.

Acknowledgements

We would like to thank Nilhan Gunhanlar, Cristina Gontan Pardo, Akiko Inagaki, Bas de Hoon, and Maureen Eijpe for help with experiments. We also thank all department members for helpful discussions. This work was supported by HFSP CDA, NWO-VIDI and TOP grants to J.G., and a grant from the Dutch government (BSIK programme 03038, SCDD).

Supplemental Data

The Supplemental Information contains BAC engineering procedures, procedures for BAC copy number determination and expression analysis, statistical procedures, six figures and four tables.

Methods

Cell lines

Transgenic ES cell lines were generated using wild type male J1 (129/Sv), F1 2-3 (129/Sv-Cast/Ei) ES lines or a wild type female line F1 2-1 (129/Sv-Cast/Ei). For determination of the origin of *Xist* a male line 1.3 and female line 30Δ1 were used, which both contain one *Xist* allele with 16 ms2 repeats integrated in exon 7 [92]. ES cells were grown and differentiated as described [179]. *Rnf12* transgenic ES cells did not survive freeze thawing and were made fresh prior to analysis. All wild type cell lines and modified BACs will be made available on request.

Transient expression of Rnf12

Cast/Ei *Rnf12* cDNA was PCR amplified and cloned into pEGFP-N1 (Clontech), replacing the EGFP coding sequence. Male 1.3 ES cells were EB differentiated for one day, and then transfected with or without the *Rnf12* expression construct using lipofectamine (Invitrogen). The cells were co-transfected with a GFP expression construct for determining the transfection efficiency. The cells were harvested at day three of differentiation.

RNA and RNA/DNA-FISH

RNA-FISH and RNA/DNA-FISH were performed as described [92, 179]. For detection of the region surrounding *Xist* (Xic probe) a cocktail of biotin labeled BAC sequences was used (CT7-474E4, CT7-45N16, CT7-155J2 and CT7-211B4). The *Tsix* RNA-FISH probe was a 5 kb SacII-SalI fragment (134071-139156 in AJ421479)

Supplemental Figures

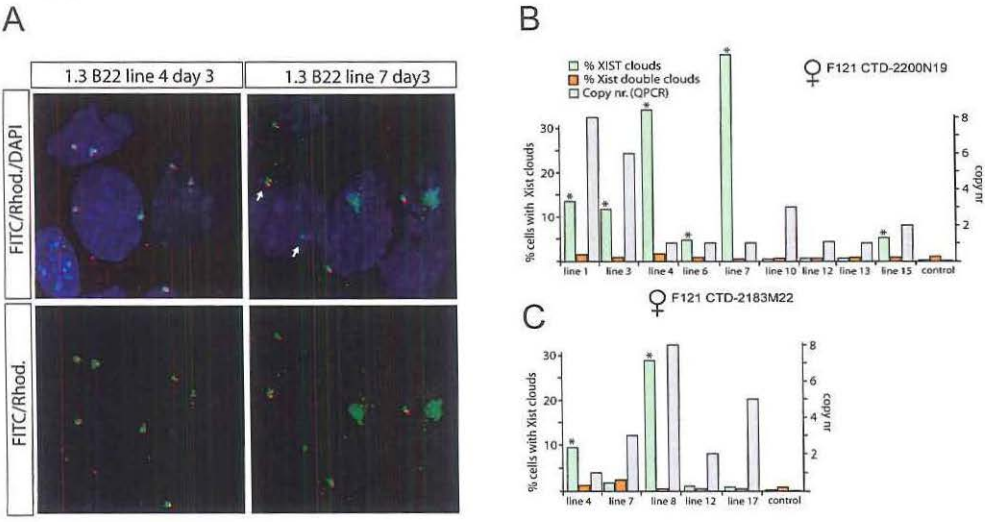

Supplemental Figure 1: XCI in ES cell lines with a mouse and human *Xist/XIST* transgenes
A) RNA-FISH with *Xist* (FITC) and *Tsix* probes (rhodamine red) on two day three differentiated ES cell lines with different integrations of a single copy BAC RP23-338B22 transgene. In line 1.3 RP23-338B22-7 that harbors one copy of the transgene and shows autosomal *Xist* accumulation, combined *Xist-Tsix* RNA-FISH revealed that a substantial proportion of cells displayed two *Xist* pinpoint signals, at day 1 of differentiation, of which only one colocalized with a *Tsix* specific pinpoint signal. We never observed that RP23-338B22-7 cells contained two *Tsix* pinpoint signals, in contrast to line 1.3 RP23-338B22-4 that did not show autosomal *Xist* accumulation. This indicates that, in the RP23-338B22-7 cells that showed autosomal spreading of *Xist*, the autosomal *Tsix* gene was already silent. **B,C)** Percentage of CTD-2200N19 (B) and CTD-2183M22 (C) female transgenic cells with two murine *Xist* clouds (orange) and a single human *XIST* cloud (green), and BAC copy number as determined by qPCR (BAC copies in grey, n>100 per cell line, * $p<0.05$, confidence interval 95%).

A ♂

RP24-240J16, male ES 1.3			
line	copy nr	% Xist	n
15	3	4%*	204
17	4	9%*	156

B

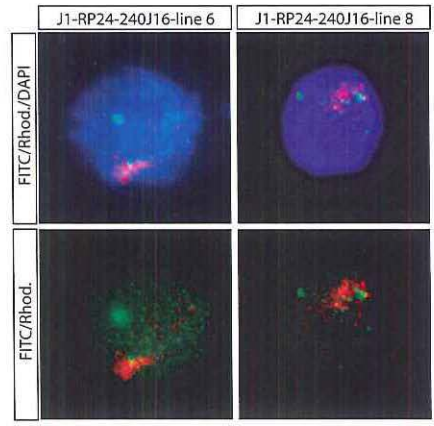

Supplemental Figure 2: XCI in RP24-240J16 transgenic male ES cell lines
A) Copy number determination and quantification of the percentage of cells that initiated XCI at day 3 of differentiation in 1.3 male ES cell lines transgenic for RP24-240J16 (* $P<0.05$, confidence interval 95%). **B)** DNA-FISH analysis with a RP24-240J16 BAC probe (FITC) and an X chromosome paint probe (Cy3), showing the autosomal integration of the BAC in J1 transgenic lines 6 and 8. Note that the intensity of the FITC signal correlates with the copy number determined by qPCR (**Figure 2B**).

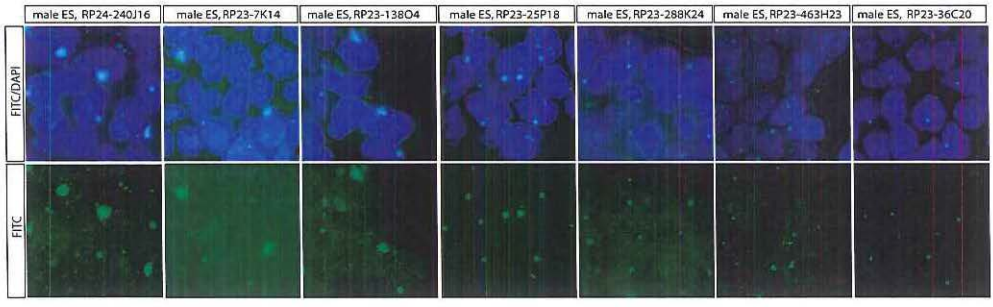

Supplemental Figure 3: A 10 kb region from BAC contig RP24-240J16 activates XCI in male cells
RNA-FISH detecting *Xist* (FITC) on day 3 differentiated male ES cells with different BAC transgenes (**Figure 3A**), showing that the 10 kb region depicted in **Figure 3A** is required for initiation of XCI in male cells.

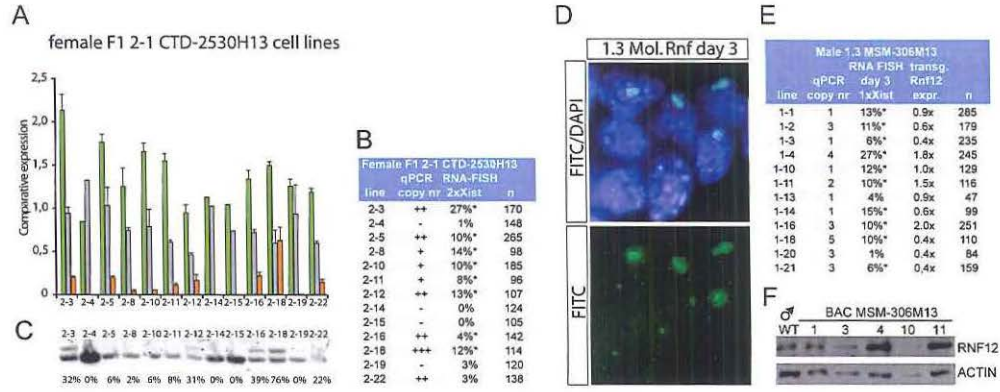

Supplemental Figure 4: Expression of transgenic RNF12 and *Rnf12* correlates with XCI
A) Expression analysis of female F1 2-1 cell lines targeted with the human CTD-2530H13 BAC containing *RNF12*. RT-qPCR was performed as in **Figure 5A**. Expression was compared to the average of wild type cell lines F1 2-1 H13 4/14/15, which did not display ectopic expression of *RNF12*. **B)** Table of female F1 2-1 cell lines targeted with the human CTD-2530H13 BAC containing *RNF12* as in **Figure 5B** (* P<0.05, confidence interval 95%). **C)** RT-PCR analysis detecting a length polymorphism distinguishing *Rnf12* from *RNF12* expression. The relative expression *RNF12/Rnf12* is depicted below each lane. **D)** RNA-FISH with an *Xist* probe (FITC) on day 3 differentiated BAC MSM-306M13 transgenic 1.3 male ES cell lines. **E)** Copy number determination and quantification of the percentage of cells that initiated XCI at day 3 of differentiation in 1.3 male ES cell lines transgenic for BAC MSM-306M13. The right two columns show the level of transgene expression of *Rnf12* relative to the endogenous copy of *Rnf12*, determined by RT-PCR followed by RFLP digestion, and the number of cells analyzed for determining the percentage of *Xist* clouds (* P<0.05, confidence interval 95%). **F)** Western blot analysis detecting RNF12 (top panel) and ACTIN (bottom panel) with nuclear extracts of wild type male cells and MSM-306M13 transgenic ES cell lines at day 1 of differentiation.

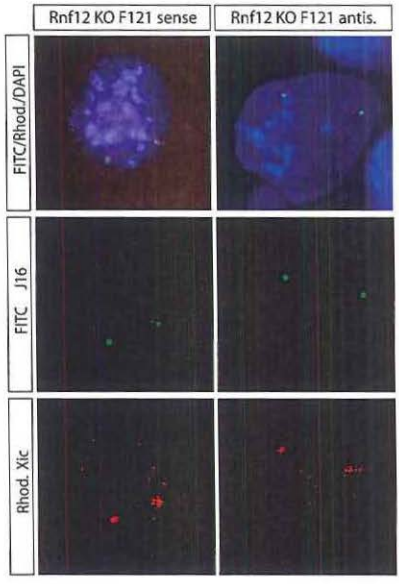

Supplemental Figure 5: Establishment of *ΔRnf12+/-* ES cell lines
DNA-FISH on two different *Rnf12* knockout cell lines (sense and antisense) with a BAC RP24-240J16 probe (FITC) and a probe detecting the Xic (rhodamine red), confirming the correct integration of the targeting construct.

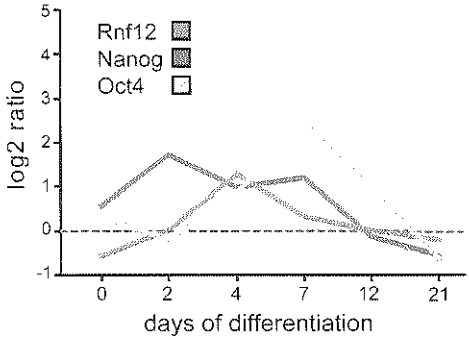

Supplemental Figure 6: RNA expression analysis of *Rnf12*, *Nanog* and *Oct4* in differentiating female ES cells
Expression data for *Rnf12*, *Nanog* and *Oct4* in differentiating female ES cells by Lin et al. [38], were retrieved and the log2 expression ratio was plotted in time.

F121-9	0%	0	235	F121-9	50%	± 5.1	0.27%	±0,53	370
F123	0%	--	773	F123	0%		--		862
J1	0%	--	704	J1	0.14%	±0.27	--		720
1.3	0%	--	653	1.3	0%		--		526

Supplemental Table 1: XCI in control cell lines
XCI was determined by *Xist* RNA-FISH in undifferentiated (left table) and day 3 differentiated (right table) male and female control cell lines.

A ♂

1	+	8%	90	4	1	0%	1%	142	± 1.6	1	2	0%	0%	125		10	1	0%	0%	118
3	-	10%	455	6	2	7%	0%	165		3	2	0%	1%	101	± 1.9	11	4	50%	0%	224
18	+	3%	77	7	1	24%	1%	144	± 1.6	5	2	40%	0%	152		14	1	0%	0%	122
21	+	12%	112	9	5	66%	1%	140	± 1.6	6	2	14%	0%	116		15	1	49%	0%	212
25	+	16%	272	10	1	1%	1%	110	± 1.9	7	3	0%	2%	124	± 2.5	16	2	0%	0%	140
				12	3	31%	0%	100		8	1	38%	0%	240						
										9	1	37%	0%	189						

B ♂

10	2	0%	73	2	2	0%	>100			2	2	0%	>100			4	3	0%	>100
14	5	0%	46	3	2	0%	>100			3	2	0%	>100			7	2	0%	>100
				4	2	0%	>100			11	2	0%	94			14	2	0%	>100
				14	3	0%	112			13	4	0%	85			15	2	0%	>100
				15	3	0%	143												

C ♀

9	3	0%	110		2	+	1%	117	± 1.8	1	+	2%	49	± 3.9
8	12	0%	61		3	+	2%	70	± 3.3	2	+	4%	49	± 5.0
10	2	1%	177	± 1.5	4	+	0%	90		3	+	2%	43	± 4.2
					5	+	1%	72	± 2.3	4	+	0%	40	
					6	+	1%	133	± 1.7	13	+	0%	38	
										14	+	0%	40	

Supplemental Table 2: XCI in BAC transgenic male and female ES cell lines
A) Copy number determination by qPCR and quantification of the percentage of cells that show accumulated *XIST* and/or *Xist* at day 3 of differentiation in male ES cell lines transgenic for RP24-180B23, RP23-338B22 and CTD-2183M22. (+), Integration confirmed by DNA-FISH only. For BAC RP23-338B22 and CTD-2183M22 transgenic ES cell lines the 95% confidence interval of endogenous mouse *Xist* accumulation is shown. **B)** Copy number determination by qPCR and quantification of the percentage of cells that initiated XCI at day 3 of differentiation in male ES cell lines transgenic for RP23-447O10, RP23-100E1, CT7-474E4, and RP24-224E13 as determined by presence of an *Xist* cloud. **C)** Copy number determination by qPCR and quantification of the percentage of cells that initiated XCI on two X chromosomes at day 3 of differentiation in female ES cell lines transgenic for RP23-447O10, CT7-474E4, and RP24-224E13 as determined by presence of two *Xist* clouds. (+), Integration confirmed by DNA-FISH only. The 95% confidence interval of endogenous mouse *Xist* accumulation is shown in the right column.

♂

17	2	9%*	142 ± 4.7	6	5	5%*	377 ± 2.2	1	2	0%	>100
18	2	2%	205 ± 1.9	9	2	5%*	320 ± 2.4	2	2	0%	>100
				13	4	6%*	228 ± 3.1	3	2	0%	>100
								4	2	0%	>100
								10	2	0%	>100
								13	8	0%	>100
								16	12	0%	>100
								23	5	0%	>100

2	3	0%	140	2	2	0%	140	1	6	0%	133
3	3	0%	106	3	3	0%	106	2	3	0%	111
5	3	0%	102	5	2	0%	102	3	3	0%	92
13	15	0%	122	13	15	0%	122	15	3	0%	75
16	1	0%	109	16	2	0%	109				

Supplemental Table 3: XCI in BAC transgenic male ES cell lines covering part of BAC RP24-240J16

Copy number determination by qPCR and quantification of the percentage of cells that initiated XCI at day 3 of differentiation as determined by presence of an *Xist* cloud in J1 male transgenic RP23-7K14, RP23-138O4, RP23-25P18, RP23-288K24, RP23-463H23 and RP23-36C20 ES cell lines. For BAC RP23-7K14 and RP23-138O4 transgenic ES cell lines the 95% confidence interval of endogenous mouse *Xist* accumulation is shown (* $P<0.05$).

A

♂

2-4	2	6%*	68	± 5.6	1	2	0%	101		1	5	0%	119	
2-5	2	11%*	122	± 5.5	5	3	0%	121		3	2	0%	130	
2-9	3	10%*	144	± 4.9	6	4	0%	114		5	7	0%	110	
2-11	2	11%*	68	± 7.4	9	6	0%	136		6	2	0%	102	
2-14	3	21%*	105	± 7.8	11	3	0%	133		9	3	0%	112	
2-15	2	7%*	145	± 4.2	12	6	1%	113	± 1.8	11	8	1%	161	± 1.5
2-16	2	0%	105		13	2	0%	114		14	3	0%	134	
2-21	2	9%*	58	± 7.4	14	2	0%	107		15	2	0%	113	
2-23	3	9%*	58	± 7.4	15	2	0%	108		16	2	0%	121	
2-24	2	13%*	174	± 5.0	16	5	0%	108		19	2	0%	116	
					17	2	0%	147		20	13	0%	150	
					19	5	1%	139	± 1.7	21	2	0%	136	
					22	3	1%	105	± 1.9	23	4	1%	156	± 1.6
										24	3	0%	162	

B

2-2	3	2%*	232	± 1.8	1	3	0%	63		1	5	1%	134	± 1.6
2-3	3	8%*	79	± 5.9	3	3	0%	127		3	3	0%	114	
2-5	3	4%*	117	± 3.6	6	3	0%	134		7	6	0%	121	
2-6	5	7%*	105	± 4.9										

Supplemental Table 4: XCI in BAC transgenic RP24-240J16 and RP24-240J16ΔRnf12 male ES cell lines

A) Copy number determination and quantification by qPCR of the percentage of cells that initiated XCI at day 3 of differentiation in 1.3 male transgenic RP24-240J16, RP24-240J16ΔRnf12(sense), and RP24-240J16ΔRnf12(anti-sense) ES cell lines as determined by presence of an *Xist* cloud. The 95% confidence interval of endogenous mouse *Xist* accumulation is shown in the right column (* $p<0.05$).

B) Copy number determination by qPCR and quantification of the percentage of cells that initiated XCI on both X chromosomes at day 3 of differentiation in 30Δ1 female transgenic RP24-240J16, RP24-240J16ΔRnf12(sense), and RP24-240J16ΔRnf12(anti-sense) ES cell lines as determined by presence of two *Xist* clouds. The 95% confidence interval of endogenous mouse *Xist* accumulation is shown in the right column (* $P<0.05$).

Supplemental Methods

Modification of BACs

BACs were acquired from BACPAC (C57/B6 libraries), Resgen (129/Sv library) or Riken (*Mus musculus mollosinus*), and a kanamycin/neomycin resistance cassette was introduced by *in vitro* lox recombination. This cassette was generated by introduction of a lox sequence and SceI site BglII-NotI into pEGFP-N1 (Clontech). RP24-240J16ΔRnf12 was generated by homologous recombination in bacteria [900]. The targeting cassette was PCR amplified using primers (GCCTTCGAACATCTCTGAGC, GAGCCGGACTAATCCAAACA), cloned into pCR-BluntII-TOPO (Invitrogen), and linearized with NheI to introduce a kanamycin/neomycin cassette AflII-EcoO109I excised from EGFP-N1. Homologous recombination in bacteria was confirmed by PCR with primers 1, GGCAGAGAGCCACTTTCATC, 2, CTGGCACTCTGTCGATACCC, 3, TTCCACAGCTGGTTCTTTCC, and gel electrophoresis. BACs were SceI linearized and electroporated into female F1 2-1 ES cells. Homologous recombination in ES cells was confirmed with primers GCCTTCGAACATCTCTGAGC, GAGCCGGACTAATCCAAACA, amplifying a NheI polymorphism present in the wild type 129/Sv allele. The presence of two polymorphic X chromosomes was confirmed by amplification of a sequence located in *Xist*, with the primers CAGTGGTAGCTCGAGCCTTT and CCAGAAGAGGGAGTCAGACG, and subsequent digestion with BrgI which digests a RFLP present in the 129SV allele.

Expression analysis

For allele specific *Rnf12* RT-PCR analysis, RNA was reverse transcribed (Invitrogen Superscript III) and amplified with primers TAAAGAGGGTCCACCACCAC and GGCAGAGAGCCACTTTCATC. PCR products were purified and digested with NheI, which digests the 129/Sv but not the Cast/Ei PCR product. For RT-qPCR expression studies, *Xist* was amplified with GCCTCAAGAAGAAGGATTGC and GGGATTGTTTGTCCCTTTGG; *Rnf12* with CCCCAGGTGAAAGTACTGAGG and CTCTCCAGCTCTATTTTCATCG; *RNF12* with TGAGAGATAACAATTTGCTAGGC and GTGGGCCTTCTTTAATTTGC; and *Actin* with ACTATTGGCAACGAGCGGTTC and AGAGGTCTTTACGGATGTCAACG. Co-amplifycation of *Rnf12/RNF12* was performed with AAGAAGAGTTCGTCCTGGAGAATA and CGAAGTTTGTTGCCTTCTGT.

RNF12 protein was detected with a mouse anti RNF12 antibody (Abnova), ACTIN was detected with a mouse anti ACTIN antibody (Sigma). For expression analysis of the region covered by RP24-240J16 total RNA was isolated from two day 3 differentiated wild type female ES lines, labeled and hybridized to Niblegene tiling arrays, covering the X chromosome with 30 bp intervals, excluding repetitive and non annotated sequences.

BAC copy number determination

BAC copy number was determined with qPCR using primers;
GTTCTTACCACCAATTGAAAACG, CAAAACAGACTCCAAATTCATCC, for RP24-180B23 and RP23-338B22,
ACCATGACCAAAGCAACTCC, CTCCTCCAGTACCATGTCTGC, for RP23-447O10
CCGCTGAAGATAGCTCTTGG, GCCACAACCAAACAGAATCC for RP24-224E13 and CT7-474E4,
ATCTCACCGTACCCATGAGC, CCTCTGGTACGACCTCTTGC, for RP23-100E1,
AGCCCCGATGAAAATAGAGG, GGCATTTCTGGATAATCTTTGG for RP24-240J16, RP23-7K14, RP23-138O4, RP23-288K24, RP23-463H23 and RP23-36C20,
AGTCATTGGCTGGTCACTCC, ATCAACCCAGACACCAAACC, for RP23-25P18,
GATAGCAGGTCAGGCAGAGG, ACGCAAAGCTCCTAACAAGC, for CTD-2183M22 and CTD-2200N19,
CTCATTTTGAGCCCTTCTGC, ACCACATTTGCCTCAGATCC, for CTD-2530H13 and GCACCCATATCCGCATCCAC, GCATTTCTTCCCGGCCTTTG, for Zfp-42 as an autosomal normalization control.

Statistics

The 95% confidence intervals for the proportion were calculated by:

$$p-\left[1.96\times\sqrt{\frac{p(1-p)}{n}}\right] \text{ to } p+\left[1.96\times\sqrt{\frac{p(1-p)}{n}}\right]$$, with n for the number of cells analyzed, and p representing the percentage of *Xist* clouds measured. Non overlapping intervals between transgenic and non transgenic control cells were scored as significant ($p<0.05$).

The Z-test for proportion was calculated by:

$$z=\frac{|p-\pi|-\frac{1}{2n}}{\sqrt{px\frac{(1-p)}{n}}}$$, with n for the number of cells analyzed, and p and π representing the proportion and average proportion.

The correlation coefficient, Pearsons r was determined by:

$$r=\frac{\sum(xi-\bar{x})(yi-\bar{y})}{\sqrt{\sum(xi-\bar{x})^2\sum(yi-\bar{y})^2}}$$, where xi and yi are the values of X and Y for the i^{th} measurement, followed by $r\sqrt{\frac{n-2}{1-r^2}}$, to determine the p value, with n representing the degrees of freedom.

Chapter 3

Precise BAC targeting of genetically polymorphic mouse ES cells

This chapter has been published in

Tahsin Stefan Barakat, Eveline Rentmeester, Frank Sleutels, J. Anton Grootegoed and Joost Gribnau (2011)
"Precise BAC targeting of genetically polymorphic mouse ES cells"
Nucleic Acids Res 39:e121
&
Tahsin Stefan Barakat and Joost Gribnau
"A Restriction Fragment Length Polymorphism based Bacterial Artificial Chromosome targeting strategy for efficient and fast generation of knockout alleles in polymorphic mouse Embryonic Stem cells"
(*Manuscript in preparation*)

Precise BAC targeting of genetically polymorphic mouse ES cells

Tahsin Stefan Barakat, Eveline Rentmeester, Frank Sleutels*, J. Anton Grootegoed and Joost Gribnau[#]

Department of Reproduction and Development, * and department of Cell Biology, Erasmus MC, University Medical Center, Rotterdam, The Netherlands.
[#] corresponding author

Contact details:
Joost Gribnau
Department of Reproduction and Development
Erasmus MC
Room Ee 09-71
PO Box 2040
3000 CA Rotterdam
The Netherlands
Phone +31-10-7043069
Fax +31-10-7044736
Email: j.gribnau@erasmusmc.nl

Abstract

The use of bacterial artificial chromosomes (BACs) provides a consistent and high targeting efficiency of homologous recombination in ES cells, facilitated by long stretches of sequence homology. Here, we introduce a BAC targeting method which employs restriction fragment length polymorphisms (RFLP) in targeted polymorphic C57Bl/6 / Cast/Ei F1 mouse ES cell lines to identify properly targeted ES cell clones. We demonstrate that knockout alleles can be generated either by targeting of an RFLP located in the open reading frame thereby disrupting the RFLP and ablating gene function, or by introduction of a transcription stop cassette that prematurely stops transcription of an RFLP located downstream of the stop cassette. With both methods we have generated *Rnf12* heterozygous knockout ES cells, which were identified by allele specific PCR using genomic DNA or cDNA as a template. Our results indicate that this novel strategy is efficient and precise, by combining a high targeting efficiency with a convenient PCR based readout and reliable detection of correct targeting events.

Introduction

The discovery of mouse embryonic stem (ES) cells and the possibility to manipulate the ES cell genome through homologous recombination has provided a powerful methodology to study gene function *in vitro* and *in vivo* [55-56, 901]. Initial studies indicated that key factors important for efficient gene targeting include the length of the targeting arms, which positively correlates with the targeting efficiency [902-903], and the use of isogenic DNA for the generation of targeting constructs, as the presence of SNPs in a targeting vector would reduce the targeting efficiency [902, 904]. Increased targeting efficiency was obtained by targeting of mouse ES cells with a BAC (bacterial artificial chromosomes) strategy. Several annotated BAC libraries are now available for different mouse laboratory strains, to target a variety of different ES cell lines with isogenic targeting vectors (http://www.ncbi.nlm.nih.gov/clone/). Correct targeting with BAC targeting vectors is generally verified by quantitative real time PCR (qPCR) amplifying a fragment spanning the projected deletion/insertion, together with a qPCR amplifying a fragment located in one of the arms [905]. Also DNA-FISH has been applied to determine a correct genetic modification [906]. However, because conventional Southern blotting techniques cannot be applied, these techniques are prone to detect false positive and negative clones. To avoid this problem, BAC targeting vectors are used that have both short and long targeting arms, allowing detection and/or confirmation of positive clones by Southern blotting using an external probe [907]. This requires a BAC that is properly positioned around the insertion site, or is modified by trimming one of the arms through homologous recombination in bacteria. Together, the current strategy still is associated with several problems. In view of this, we have developed a new BAC targeting strategy which makes use of RFLPs present in genetically polymorphic ES hybrid cell lines, generated by crossing C57Bl/6 female mice with Cast/Ei male mice, providing a convenient readout for proper gene targeting. In the present study, the proof of principle target gene was *Rnf12*, which encodes a nuclear

factor involved in X chromosome inactivation (XCI) [174]. For this gene, our results indicate that the new strategy can be used to efficiently introduce genetic modifications in ES cells using BAC targeting cassettes combined with a reliable readout based on allele specific PCR.

Methods

ES cell derivation and cell culture

Female C57Bl/6 mice were crossed to male Cast/Ei mice, and blastocysts were seeded onto irradiated mouse embryonic fibroblasts (MEFs) in DMEM, 15% v/v knockout serum replacement (Invitrogen), 100 U ml^{-1} penicillin, 100 mg ml^{-1} streptomycin, non-essential amino acids, 0.1mM ß-mercaptoethanol, 5000 U ml^{-1} leukaemia inhibitory factor (LIF) and 50 µM MEK1 inhibitor (New England Biolabs). The dissociated inner cell mass outgrowth was seeded on new feeders and after one passage grown in standard ES medium containing DMEM, 15% v/v foetal calf serum, 100 U ml^{-1} penicillin, 100 mg ml^{-1} streptomycin, non-essential amino acids, 0.1mM ß-mercaptoethanol, and 1000 U ml^{-1} LIF. To induce differentiation, ES cells were split, and pre-plated on non-gelatinised cell culture dishes for 60 minutes. ES cells were then seeded in non-gelatinised bacterial culture dishes containing differentiation medium to induce embryoid body (EB) formation. EB-medium consisted of IMDM-glutamax, 15% v/v foetal calf serum, 100 U ml^{-1} penicillin, 100 mg ml^{-1} streptomycin, non-essential amino acids, 37.8 µl l^{-1} monothioglycerol and 50 µg/ml ascorbic acid. To generate chimaeras, C57Bl/6 mice where superovulated and mated, and day 3,5 blastocysts were isolated. ES cells were injected, and the embryos were transfered to pseudopregnant foster mothers. Chimeras were crossed to C57Bl/6 mice, and germ line transmission was judged by coat color. All animal experiments were in accordance with the regulations of the Erasmus MC Animal Experimental commission.

RFLP analysis and genotyping

To confirm the parental origin of the derived C57Bl/6 / Cast/Ei hybrid mouse ES cells, RFLP analysis on genomic DNA was performed by PCR followed by restriction digestion using the following primers and enzymes: *Xist* CAGTGGTAGCTCGAGCCTTT and CCAGAAGAGGGAGTCAGACG, BsrGI; *Cdyl*: ACAGGCAGAAGGAGCTGTGT, and CCCAGCTGTAAAGGCTTCAG, ZraI. *Sry* was amplified using ATTTATGGTGTGGTCCCGTGGT and TATGTGATGGCATGTGGGTTCC.

Karyotyping, RNA-FISH and DNA-FISH

For karyotyping, cells were blocked in metaphase using colcemid, and metaphase spreads were prepared by hypotonic treatment, followed by fixation in methanol acetic acid (3:1 v/v), according to standard procedures. *Xist* RNA-FISH and DNA-FISH were performed as described [174]. For DNA-FISH, a mouse BAC probe (RP24-240J16) containing the *Rnf12* gene was digoxigenin-labelled and used to determine the number of integration sites of the *Rnf12* targeting constructs. A cocktail containing biotin-labelled BAC sequences containing *Xist* (CT7-474E4, CT7-45N16, CT7-155J2 and CT7-211B4) was used as a probe to determine the number of X chromosomes.

RT-PCR

RNA was isolated from undifferentiated ES cells using Trizol reagent (Invitrogen), according to manufacturer's instructions, and cDNA was prepared using the SuperScript TM III First-Strand Synthesis System (Invitrogen). RT-PCR for pluripotency markers was performed using the following gene specific primers: *Oct4*: CCCCAATGCCGTGAAGTTG, TCAGCAGCTTGGCAAACTGTT; *Nanog*: AGGATGAAGTGCAAGCGGTG, TGCTGAGCCCTTCTGAATCAG; *Sox2*: CACAGATGCAACCGATGCA, GGTGCCCTGCTGCGAGTA; *β-Actin*: CAACGAGCGGTTCCGATG, GCCACAGGATTCCATACCCA.

Construction of targeting constructs

The *Rnf12* targeting construct has been described [174]. To generate the SA-tpA stop constructs, a cassette containing a floxed splice acceptor and polyadenylation sequence and a Frt site flanked neomycin/kanamycin fusion gene was generated, starting with a pEGFP-NI vector (Clontech). A linker containing a Lox66 and EcoRV, BglII and BamHI sites together with a linker containing a Lox71 and Frt sites flanking a ScaI site were cloned BglII-NotI into pEGFP-N1, releasing EGFP (complete sequence: GATCTAATATAACTTCGTATAGCATACATTATACGAACGGTAGATATC AGATCTGGATCCTATTGAAGCATATTACATACGATATGCTTGCCATTTAATTCC GGAGAATCCGGGAAGTTCCTATTCTCTAGAAAGTATAGGAACTTCAGTACTGA AGTTCCTATTCTCTAGAAAGTATAGGAACTTCTAGG). The ScaI site was used to insert a DraIII-AseI kanamycin/neomycin fragment. The SA-tpA sequence was a BamHI fragment from pSStpA [123], inserted in the BamHI site of the linker. Three unique restriction sites in introns 2, 3 and 4 of *Rnf12* were PCR amplified, with 500 bp of flanking region, and cloned into pPCR-Topo-bluntII, using the following primers and unique restriction sites: intron 2 BglII GGGCTACACAGAGAAAGAAACC, AGCCATGCATGCTTGTGTTA; intron 3 NheI GAAACAGCTTGTTTTATAATGTTTCTT, TTGAACATGTGTTGCAAAATTAC; intron 4 AvrII ACATTTTGTTTGGGGAGGTG, GAATTGTGCAACTCGGAACA. The SA-tpA kanamycin/neomycin cassette was NheI-AflII released and inserted into the unique restriction sites of the intronic targeting constructs. The final constructs were used for homologous recombination in bacteria of a C57Bl/6 BAC RP24-240J16 [900]. Positive clones were screened by PCR for the correct recombination event using primers spanning the homologous recombination arms of the targeting constructs and insert specific primers: *Rnf12* intron 2 AAAGGTTTTGGCTGGATGGT, rev TGTGCCATAATGCTTGGCTA, *Rnf12* intron 3 CCCAGGTAAGCTGCATGTAA, rev TGTAGTCTTCTGAGCAACTCTTCC, *Rnf12* intron 4 ACAGAGCCCCGATGAAAAT, rev ACACGATTAGGACACTCATGG.

Targeting of ES cells

Targeting constructs were linearized by PI-SceI digestion. For each electroporation, approximately 40 µg of DNA and 1.0 x 10^6 ES cells were used. Cells were seeded on drug resistant male feeder cells (MEFs), and selection with neomycin (270 µg ml^{-1}, active) was started 24 hours post-transfection and continued for 7-12 days. Drug resistant clones were picked and expanded.

RFLP analysis of targeted ES clones

Genomic DNA (gDNA) of ES clones was isolated, and RFLP analysis was performed using the following primers and enzymes: *Rnf12* GCCTTCGAACATCTCTGAGC, GAGCCGGACTAATCCAAACA, NheI; *Xist* CAGTGGTAGCTCGAGCCTTT and CCAGAAGAGGGAGTCAGACG, BsrGI. For analysis of cell lines targeted with the stop constructs, RNA was isolated, cDNA prepared and expression of *Rnf12* was analyzed by RFLP analysis using primers TAAAGAGGGTCCACCACCAC and GGCAGAGAGCCACTTTCATC followed by NheI restriction digestion.

qPCR copy number analysis

Copy number of genomic sequences was determined by real time qPCR with genomic DNA using the following primers: *Rnf12* (NheI site): GTTCGTCCTGGAGAATACCG, GGAAAAGGTACGCCTAAAACC; *Rnf12*: AGCCCCGATGAAAATAGAGG, GGCATTTCTGGATAATCTTTGG ; *Zfp42*: GCACCCATATCCGCATCCAC, GCATTTCTTCCCGGCCTTTG.

Southern blotting

Five to 10 µg of genomic DNA was digested overnight with NheI, and separated on a 0,7% agarose gel. DNA was blotted to Hybond membranes using standard procedures, and the blot was hybridized with a PCR amplified probe (primers: GGCAGAGAGCCACTTTCATC, GCCAAAGACCTCCAACCATA)

Results

Existing methodology for screening positive clones after homologous recombination with BAC targeting cassettes involves qPCR or DNA-FISH. These methods are prone to detect false positive and negative clones, and we therefore set out to develop a method to screen targeting events by using RFLPs in F1 hybrid cell lines. In the first approach the BAC targeting vector destroys the RFLP and inserts a kanamycin/neomycin resistance cassette in the open reading frame of the gene of interest, thereby ablating gene function (**Figure 1A-I**). Removal of the RFLP can be screened by PCR using genomic DNA as a template and subsequent digestion of the PCR product with the restriction enzyme recognizing the targeted RFLP. In another approach, we introduce a splice acceptor poly-adenylation transcription stop cassette (SA-tpA) in an intron of the gene of interest, prematurely abrogating gene transcription resulting in a non-functional protein. For this second approach, positive clones are identified by RT-PCR amplification of a cDNA sequence, which contains an RFLP that is located downstream of the transcription stop cassette (**Figure 1A-II**).

Generation and targeting of F1 ES hybrid cell lines

To obtain genetically polymorphic ES cell lines with a high number of RFLPs that could be used for gene targeting, we generated F1 hybrid ES cell lines by crossing C57Bl/6 female mice with Cast/Ei male mice. The C57Bl/6 classical inbred *Mus musculus* mouse strain is among the most widely used and best characterized mouse strains. The C57Bl/6 mouse genome has been sequenced, and several well-annotated BAC libraries have been generated [908]. The Cast/Ei inbred strain has been derived from a wild population of the subspecies *Mus musculus castaneus*, is more difficult to breed, but offers advantages related to its variant genetic background [909]. Intercrosses between Cast/Ei and other strains have been extensively used for SNP based distinction of the maternal and paternal genome, for instance to study genomic imprinting and XCI. The C57Bl/6 and Cast/Ei mouse strains are highly polymorphic, with an estimate of one SNP per 311 base pairs, providing a sufficient number of RFLPs to allow targeting of almost every gene [909]. The Cast/Ei *Mus m.* subspecies is currently being sequenced, a BAC library is available, and a SNP database is publically accessible (www.perlegen.com).

We generated five different F1 ES cell lines, with the proper karyotype and ES cell morphology, which were successfully differentiated into embryoid bodies (EB) (**Figure 1B**). RT-PCR expression analysis confirmed expression of the pluripotency markers *Oct4*, *Sox2* and *Nanog* (**Figure 1C**). Karyotyping and PCR analysis of genomic DNA with a primer set specific for *Sry* showed that three ES cell lines were male and two female (**Figure 1D**). We confirmed the C57Bl/6 / Cast/Ei F1 genotype by PCR amplification of the autosomal gene *Cdyl* and the X-linked gene *Xist*, and digestion with restriction enzymes specific for RFLPs that discriminate between a C57Bl/6 or Cast/Ei PCR product (ZraI for *Cdyl*, and BsrGI for *Xist*). Digestion of the *Xist* PCR products from genomic DNA (gDNA) of the male ES cell lines revealed only a C57Bl/6 product, as expected, because the single X chromosome in male cells is inherited from the C57Bl/6 mother. Two male ES cell lines, E3 and E14, were injected in C57Bl/6 blastocysts and several founders (5 for E3, 2 for E14) were retrieved, all showing high coat color contribution (representative animals are shown in **Supplementary Figure 1**). Different founders were crossed with C57Bl/6 females and all tested animals showed germline transmission (**Figure 1E**). Taken together, we generated three male and two female C57Bl/6 / Cast/Ei F1 ES cell lines. Because of our interest in the female specific X chromosome inactivation process female ES line E15 was used for further targeting studies.

Targeted disruption of the Rnf12 open reading frame

For BAC mediated targeting of an RFLP we selected the X-chromosomal *Rnf12* gene as a target (**Figure 2A**). We have recently shown that the encoded RNF12 acts as a dose-dependent activator of X chromosome inactivation (XCI) in female ES cells [174, 910-911]. RNF12 is an E3 ubiquitin ligase that regulates XCI through activation of the X-linked gene *Xist* [911]. The transcribed *Xist* RNA coats the inactive X chromosome in *cis* (**Figure 1B**), thereby attracting chromatin modifying enzymes involved in establishing inactive chromatin [892].

Rnf12 consists of five exons, spanning 24 kb. In the SNP database we identified NheI as an RFLP located in exon 5 of the C57Bl/6 *Rnf12* allele, and confirmed the RFLP

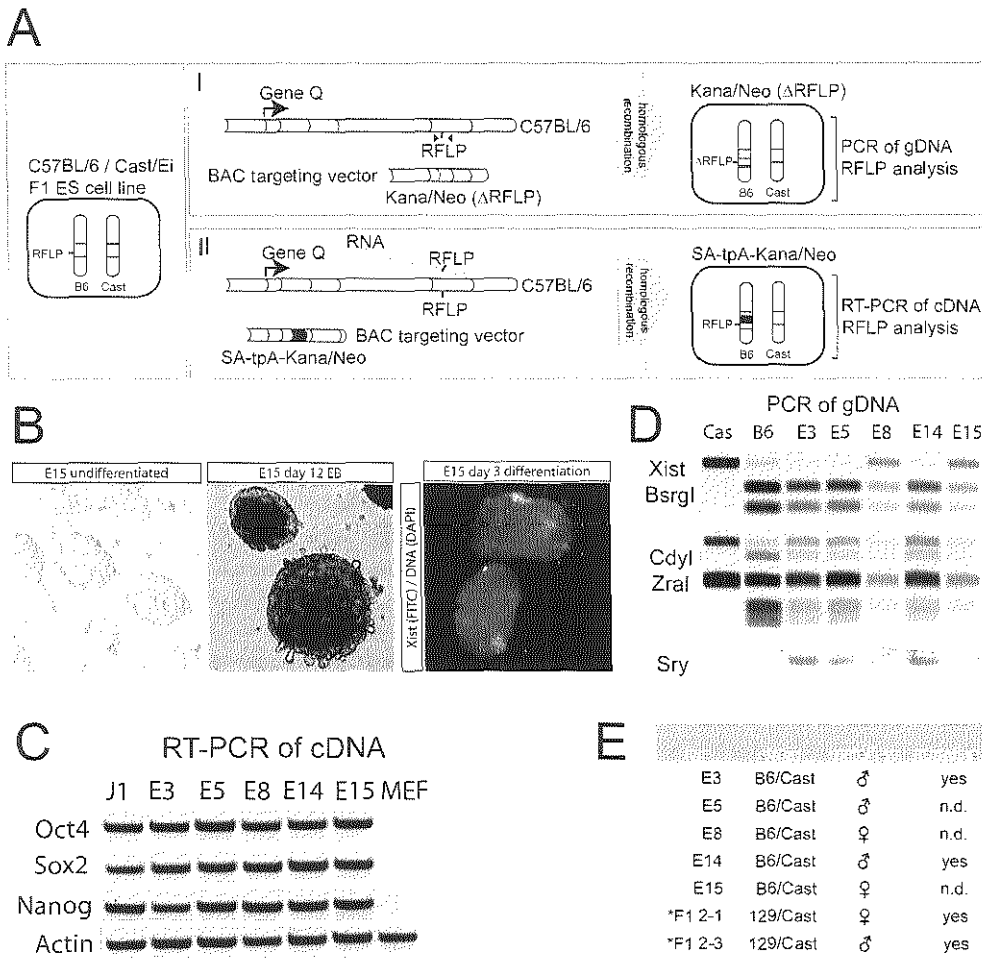

Figure 1: Two approaches of a new strategy for manipulation of hybrid mouse ES cell lines
A) Schematic overview of RFLP mediated BAC targeting of hybrid C57Bl/6 / Cast/Ei ES cells. Chromosomes from C57Bl/6 are indicated with B6 and from Cast/Ei with Cast. Exons of the gene of interest are indicated in green, the kanamycin/neomycin resistance cassette in white, and the transcription stop cassette in black. **B)** C57Bl/6 / Cast/Ei hybrid ES cells show proper ES cell morphology (left panel), are able to differentiate *in vitro* in embryoid bodies (middle panel), and female lines can initiate X chromosome inactivation upon differentiation (right panel, showing *Xist* RNA labelled in FITC, and DNA stained with DAPI). **C)** RT-PCR of pluripotency genes. The generated C57Bl/6 / Cast/Ei ES cells (E3-E15) express the pluripotency factors *Oct4*, *Sox2* and *Nanog*. J1 is a male control ES cell line, MEFs were used as negative control, and *Actin* is a control mRNA. **D)** PCR amplification of gDNA of different C57Bl/6 / Cast/Ei ES cell lines (E3-E15) and control gDNA (Cas and B6), and digestion with restriction enzymes identifying allele specific products for *Xist* (X-encoded, BsrGI, top panel), *Cdyl* (autosomal, ZraI, middle panel) and PCR amplification of *Sry* (Y-encoded, bottom panel).
E) Table summarizing the characteristics of the C57Bl/6 / Cast/Ei ES cell lines analyzed in this study, and two other polymorphic 129/Sv / Cast/Ei cell lines (*) that have been used in other gene targeting studies [174].

by sequencing analysis of gDNA isolated from C57Bl/6 and Cast/Ei mice. Disruption of RNF12 activity by insertion of a neomycin/kanamycin resistance cassette in this NheI RFLP would lead to a premature translation stop of RNF12, resulting in a 331 aa protein lacking the RING finger that is crucial for RNF12 activity. Based on this, we generated a targeting construct to disrupt *Rnf12*, by PCR amplification of the NheI RFLP and 500 bp of flanking sequence, and subsequent insertion of a kanamycin/neomycin resistance cassette in the NheI site. The C57Bl/6 BAC RP24-240J16, covering the *Rnf12* gene, was targeted through homologous recombination in bacteria [900], and correct targeting was confirmed by PCR amplification using primers inside the resistance cassette and outside the targeting arms (data not shown). The targeting efficiency in bacteria was >80%. The modified BAC sequence was linearized with SceI and targeted to female ES cell line E15, and subsequent to neomycin selection clones were picked and expanded for further analysis. Genomic DNA of these clones was subjected to PCR using primers spanning the targeted NheI site, and the PCR product was digested with NheI. Correctly targeted clones are expected to have an undigested Cast/Ei product only, although contamination by feeder cells (C57Bl/6) might result in the presence of some digested material (**Figure 2B**). We therefore also grew the targeted clones without feeders, which indicated that 12% of the picked clones showed a loss of the C57Bl/6 specific PCR product (**Figure 2C**, and **Figure 3C**).

Our results were confirmed by qPCR analysis with primers spanning the NheI site, which indicated a reduction in copy number from two to one, and primers amplifying a region proximal to the NheI site, indicating no change in the copy number (**Figure 2E**). The loss of one NheI site could be attributed to a correct targeting event, or loss of an X chromosome. Although the qPCR results indicated that both X chromosomes were present, we also performed a PCR amplification of a BsrGI polymorphism in the *Xist* gene. Digestion of the PCR products with BsrGI, which only digests the C57Bl/6 PCR product, indicated that both X chromosomes were present in all clones that showed a loss of the C57Bl/6 *Rnf12* PCR product (**Figure 2D**). We confirmed this finding by DNA-FISH with two different probes, one covering the BAC used for targeting the ES cells, and the other covering *Xist* and flanking sequences. We found that clones that lost the RFLP had retained the expected 40,XX karyotype, providing evidence for a correct targeting event, and precluding the presence of randomly integrated BACs (**Figure 2F**). Finally, genomic DNA of targeted clones was subjected to Southern blotting analysis, which indicated the correct targeting event; loss of the C57Bl/6 specific 5.4 kb band in knockout clones that were selected based on the RFLP PCR assay and no loss in control clones (**Figure 2G**).

Analysis of all our targeted clones indicated that targeting with a C57Bl/6 construct, was specific for the C57Bl/6 allele. However, our previous studies also indicated that the same construct can be used to target the 129/Sv allele in F1 2-1 129/Sv / Cast/Ei female ES cells [174]. The targeting efficiency for this experiment was lower, probably due to the presence of SNPs in the targeting construct (**Figure 3C**). Using a Cast/Ei targeting construct in which kanamycin/neomycin was replaced by a ampicillin/puromycin resistance cassette, we were also able to target the Cast/Ei allele, resulting in a homozygous *Rnf12*-/- ES cell line [911]. In this experiment the efficiency was lower (3%) than found for the C57Bl/6 construct targeting the C57Bl/6 allele, possibly due to selection against cells deficient for *Rnf12* (**Figure 3C**).

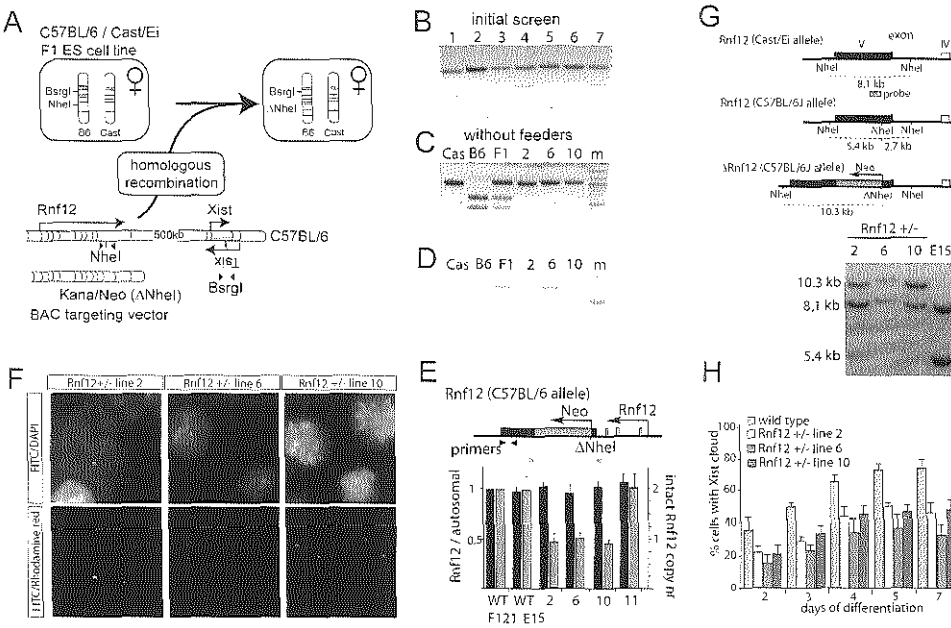

Figure 2: Generation of *Rnf12* knockout ES cell lines by disruption of the *Rnf12* open reading frame

A) Targeting of *Rnf12* by insertion of a kanamycin/neomycin resistance cassette into the exon containing a NheI RFLP destroys the RFLP (present in the C57Bl/6 allele). **B)** PCR analysis with primers indicated in **Figure 2A** amplifying the NheI RFLP located in *Rnf12* using genomic DNA of targeted clones 1-7. PCR fragments were digested with NheI. **C)** Same as in **Figure 2B**, but with gDNA isolated from clones 2, 6 and 10, grown without feeder cells. Cast/Ei (Cas), C57Bl/6 (B6) and Cast/Ei / C57Bl/6 (F1) DNA was used as a control (m=marker). **D)** Same as in Figure 2C, but PCR analysis amplifying the BsrGI RFLP located in *Xist* using gDNA of the targeted clones. PCR fragments were digested with BsrGI. **E)** qPCR analysis with primers indicated using gDNA of different targeted clones. Values were normalized to values obtained with a primer set amplifying the autosomal *Zfp42* gene. **F)** DNA-FISH analysis with a BAC probe covering the targeting cassette (FITC), and a mix of BAC probes detecting *Xist* and flanking regions (Rhodamine red) (DNA stained with DAPI). **G)** Southern blotting analysis, using a probe that distinguishes between the Cast/Ei (8.1 kb) and C57Bl/6 (5.4 kb) alleles. A neo insertion event destroying the NheI RFLP present on the C57Bl/6 allele results in a 10.3 kb fragment (clones 2, 6 and 10). **H)** Three different *Rnf12*+/- ES cell lines and a wild type female ES cell line were differentiated, and subjected to *Xist* RNA-FISH. The relative number of cells showing an *Xist* cloud, indicative for initiation of XCI, is shown at different time points of differentiation (N>100 per time point, error bars represent 95% confidence intervals).

To demonstrate the value of the strategy described herein for studying a specific cellular process, we tested the effect of the heterozygous *Rnf12* deletion on XCI. We analyzed the percentage of cells that initiated XCI, by *Xist* RNA-FISH at different time points of EB differentiation, for three *Rnf12*+/- clones. Previously, we found that a heterozygous deletion of *Rnf12* in female cells results in a significant reduction of XCI, as part of the evidence that RNF12 is an important activator of XCI [174]. In agreement with this, analysis of the present C57Bl/6 / Cast/Ei *Rnf12* +/- female ES lines also showed a reduction in the number of cells that initiated XCI (**Figure 2H**). These results indicate that

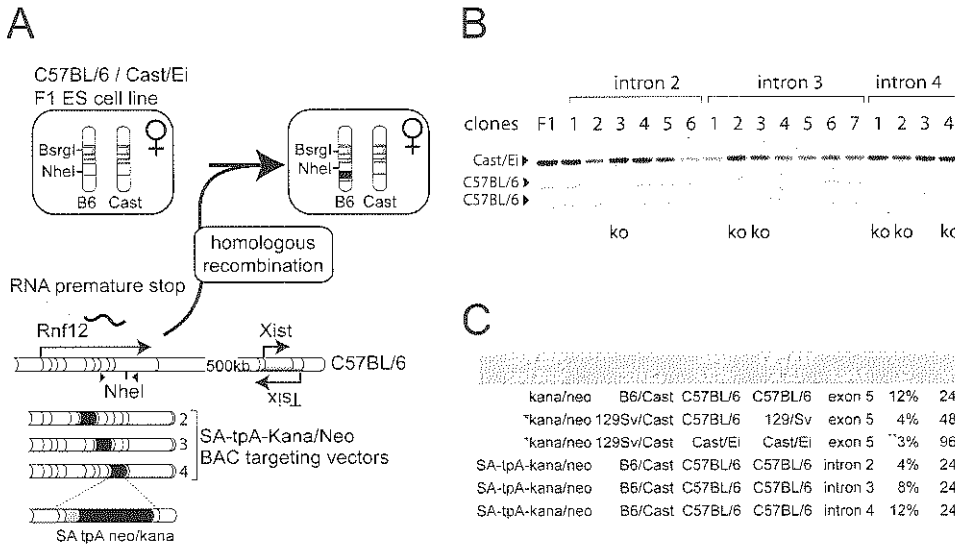

kana/neo	B6/Cast	C57BL/6	C57BL/6	exon 5	12%	24
*kana/neo	129Sv/Cast	C57BL/6	129/Sv	exon 5	4%	48
*kana/neo	129Sv/Cast	Cast/Ei	Cast/Ei	exon 5	**3%	96
SA-tpA-kana/neo	B6/Cast	C57BL/6	C57BL/6	intron 2	4%	24
SA-tpA-kana/neo	B6/Cast	C57BL/6	C57BL/6	intron 3	8%	24
SA-tpA-kana/neo	B6/Cast	C57BL/6	C57BL/6	intron 4	12%	24

Figure 3: Generation of *Rnf12* knockout ES cell lines by insertion of a transcription stop cassette
A) Generation of *Rnf12* knockout ES cell lines by integration of a splice acceptor triple poly-adenylation sequence (SA-tpA) together with a kanamycin/neomycin resistance cassette. Different targeting constructs were generated to target the stop cassette to one of the introns 2, 3 or 4. **B)** RT-PCR analysis with cDNA form clones targeted with cassettes targeting different introns, using primers amplifying the NheI RFLP located in exon 5. RT-PCR products were digested with NheI to reveal allele specific PCR products. Correctly targeted clones are indicated (ko). **C)** Table summarizing the targeting efficiency of the constructs described for targeting the C57Bl/6 allele (n=number of clones picked). (*) Targeting efficiencies of previously described experiments involving C57Bl/6, and Cast/Ei exon 5 targeting constructs used to target the 129/Sv and Cast/Ei alleles in F1 2-1 129/Sv / Cast/Ei female ES cells [174, 911]. (**) The Cast/Ei allele was targeted in *Rnf12*+/- (129/Sv / Cast/Ei) ES cells creating a *Rnf12* null ES cell, which may affect the targeting efficiency.

homologous recombination of RFLPs with BAC targeting constructs provides an efficient and precise method to generate knockout ES cell lines.

Premature abrogation of Rnf12 transcription

Even in the highly polymorphic ES cells used for the present study, a relatively small percentage of all genes will not contain suitable RFLPs to allow targeting of a resistance cassette abolishing expression of a functional transcript. For such genes, a splice acceptor triple poly-adenylation (SA-tpA) cassette could be used to insert into an intronic RFLP, thereby leading to a premature stop of transcription. Alternatively, a SA-tpA cassette could be inserted into an intron of the gene of interest, using a transcribed RFLP located downstream of the insertion site to screen for proper integration. Both modifications of the present method provide many more possible targeting sequences. As proof of principle, we generated targeting vectors aimed to prematurely stop transcription in one of the introns 2, 3 or 4 of *Rnf12* (**Figure 3A**). BAC targeting cassettes were generated through homologous recombination of a SA-tpA cassette flanked by a kanamycin/neomycin resistance cassette

in different introns of *Rnf12* in C57Bl/6 BAC RP24-240J16. Proper integration of the SA-tpA cassette was verified by PCR (not shown), and the targeting vectors were electroporated into female E15 C57Bl/6 / Cast/Ei ES cells. Neomycin resistant clones were expanded without feeder cells for RNA isolation. To determine the clones with a proper integration of the SA-tpA cassette abolishing *Rnf12* expression from the targeted C57Bl/6 allele, we generated cDNA and performed RT-PCR amplifying the exon 4-5 junction of *Rnf12* including the previously described NheI RFLP. Allele specific expression was determined by digestion of the RT-PCR product with NheI, which only digests the C57Bl/6 PCR product. For each targeting vector we obtained positive clones which showed expression of the Cast/Ei allele only, indicating proper integration of the transcription stop cassette (**Figure 3B**). Loss of an X chromosome was ruled out by PCR amplification of a BsrGI RFLP located in the *Xist* gene, using gDNA and subsequent digestion with BsrGI (data not shown). The targeting efficiencies were 4%, 8%, and 12%, for targeting of introns 2, 3, and 4, respectively, which is in the range of previously reported targeting efficiencies of BAC targeting constructs [906]. These results indicate that different targeting methods, either removing an RFLP or ablating expression of an RFLP combined with an allele specific PCR to detect a correct targeting event, can be applied to introduce genetic modifications in ES cells.

Discussion

Previous attempts to generate genetically modified ES cell lines by homologous recombination of BAC targeting vectors have been challenging, mainly because a clear readout for proper integration of the targeting cassette was missing. Here, we have generated and targeted F1 C57Bl/6 / Cast/Ei hybrid ES cell lines, which are genetically polymorphic, carrying a high density of RFLPs.

We have opted for two different approaches for BAC mediated gene targeting, both using RFLPs as a readout for properly targeted clones. In one strategy a resistance cassette is integrated into the open reading frame of a gene, ablating gene function and disrupting the RFLP. In another approach, a splice acceptor transcription stop cassette is inserted in a transcribed RFLP, or in a genomic location upstream of an RFLP, and subsequently the RFLP is used to detect loss of expression of the targeted allele. The last strategy can even be used to generate conditional knockout or rescue alleles, by using inverted asymmetric lox sites. The combination of these approaches provides an opportunity to disrupt a wide selection of candidate target genes. Nonetheless, even in the F1 C57Bl/6 / Cast/Ei ES cell lines for some genes no RFLPs will be available. Especially, single exon genes or genes covering a relative small genomic region may not entail enough SNPs for the design of a proper targeting approach. Also, the targeting strategy based on screening of expressed RLFPs requires the targeted gene to be expressed in ES cells. Fortunately, this is true for many genes, and even genes which only play a role in embryonic development and differentiation processes appear to be expressed at a base level in ES cells, sufficient to allow application of the second approach.

The targeted F1 C57Bl/6 / Cast/Ei ES cell lines can directly be used to study the effect of the mutation introduced *in vitro*, or can be used for the generation of mice, either

through the generation of chimaeric mice by injection of ES cells in a diploid blastocyst or by the tetraploid complementation technology [912]. For several studies, the analysis of mutant mice generated with these hybrid ES cell lines requires extensive back crossing. However, mice generated by tetraploid complementation could avoid this problem. Also, the effect of many mutations can be studied in hybrid mice, and for studies involving genomic imprinting and X inactivation a hybrid back ground is even the preferred back ground for studying the consequence of an introduced mutation.

Regarding efficiency of the new strategy, for targeting of the *Rnf12* locus, we find that analysis of less than a hundred clones results in a sufficient number of properly targeted cell lines (**Figure 3C**), in agreement with previous findings using homologous recombination with BAC targeting vectors [906]. Although there is neither a gain or loss in efficiency, the use of RFLPs to perform an allele specific PCR profoundly facilitates the detection of positive clones, and omits less reliable and more laborious techniques such as DNA-FISH and qPCR. Therefore, our new strategy for gene targeting combines the high efficiency of BAC targeting technology with a convenient readout to screen for positive targeting events. The highly polymorphic C57Bl/6 / Cast/Ei ES cell lines we generated, in combination with the different approaches described here, for targeting a gene of interest, provides many options for efficient and precise BAC targeting of almost every gene in the mouse genome.

Acknowledgements

We would like to thank all laboratory members for helpful discussions. This work was supported by grants from the Dutch Research Council (NWO-TOP, and -VICI) to J.G.

Supplemental data

Supplemental data contains one supplementary figure.

Supplementary Figure

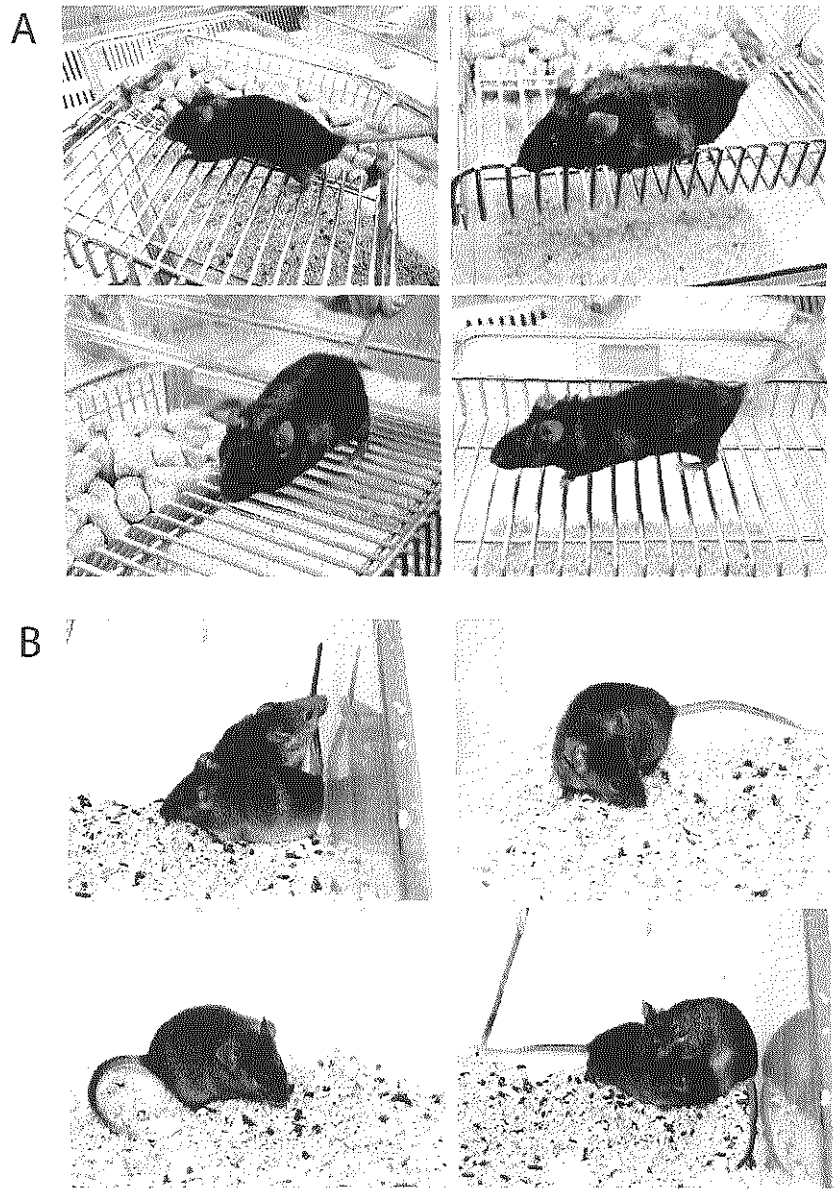

Supplementary Figure 1: Germ line transmission of C57Bl/6 / Cast/Ei ES cell lines
A) Founders generated by injection of E3 (top two panels), and E14 (bottom two panels), show high coat color contribution. **B)** Offspring of founders shown in **A**, indicating germ line transmission.

A Restriction Fragment Length Polymorphism based Bacterial Artificial Chromosome targeting strategy for efficient and fast generation of knockout alleles in polymorphic mouse Embryonic Stem cells

Tahsin Stefan Barakat and Joost Gribnau[#]

Department of Reproduction and Development, Erasmus MC, University Medical Center, Rotterdam, The Netherlands.
[#] corresponding author

Contact details:
Joost Gribnau
Department of Reproduction and Development
Erasmus MC
Room Ee 09-71
PO Box 2040
3000 CA Rotterdam
The Netherlands
Phone +31-10-7043069
Fax +31-10-7044736
Email: j.gribnau@erasmusmc.nl

Abstract

The isolation of germ line competent mouse Embryonic Stem (ES) cells and the ability to modify the genome by homologous recombination has revolutionized life science research. Since its initial discovery, several approaches have been introduced to increase the efficiency of homologous recombination, including the use of isogenic DNA for the generation of targeting constructs, and the use of Bacterial Artificial Chromosomes (BACs). BACs have the advantage of combining long stretches of homologous DNA, thereby increasing targeting efficiencies, with the possibilities delivered by BAC recombineering approaches, which provide the researcher with almost unlimited possibilities to efficiently edit the genome in a controlled fashion. Despite these advantages of BAC targeting approaches, a widespread use has been hampered, mainly because of the difficulties in identifying BAC-targeted knockout alleles by conventional methods like Southern Blotting. Recently, we introduced a novel BAC targeting strategy, in which Restriction Fragment Length Polymorphisms (RFLPs) are targeted in polymorphic mouse ES cells, enabling an efficient and easy PCR-based readout to identify properly targeted alleles. Here we provide a detailed protocol for the generation of targeting constructs, targeting of ES cells and convenient PCR-based analysis of targeted clones, which enable the user to generate knockout ES cells of almost every gene in the mouse genome within a two month period.

Introduction

Mouse ES cells are characterized by their ability to self-renew and differentiate into all cell types of all the three germ layers, both *in vitro* and *in vivo* [55-56, 913]. One crucial finding was that mouse ES cells are permissive for homologous recombination, allowing gene targeting approaches to alter the mouse genome, allowing the creation of loss-of-function (knockout) and gain-of-function (knock-in) mouse models to study gene function [901, 914-918]. More than two decades after its initial description, gene targeting approaches have resulted in thousands of knockout mouse models, and large scale, high-throughput projects aiming to disrupt every single gene in the mouse are underway [919-923]. In addition to generating knockout alleles, gene targeting approaches can also be used to generate fusions between the gene of interest and a reporter gene (e.g. EGFP, mCherry, LacZ and others), to facilitate *in vivo* tracing of gene expression, or to generate tagged versions of genes (Flag-tag, His-tag, FTAB-tag and others), which can be used in affinity purification and proteomic studies to characterize protein interaction partners [924-925]. Besides the advantages for generating animal models, ES cell and homologous recombination techniques also provide valuable tools for *in vitro* studies, in which modified ES cells can be used to study the outcome of gene ablation or modification on a wide range of processes, including DNA damage repair, signaling pathways, epigenetics and X chromosome inactivation amongst many others.

Conventional studies on homologous recombination in ES cells make use of plasmid constructs containing a positive selection cassette, rendering targeted cells resistant to a particular antibiotic, flanked by homology arms, together with a negative selection

cassette eliminating cells with a randomly integrated transgene. The size of the homologous DNA sequence was found to be crucial for the efficiency of a successful targeting event, with longer stretches of homologous arms facilitating more recombination events [902-903]. The degree of homology between the targeting construct and the genome of the ES cell is also important, as the presence of SNPs differing between the sequence of the targeting vector and the endogenous DNA sequence can significantly affect the targeting efficiency [902]. Therefore, it is advisable to use isogenic DNA of the construction of the targeting vector [904]. The need for long, isogenic homology arms to construct successful targeting vectors can be challenging and time-consuming as conventional methods like restriction enzyme-based cloning will be difficult when large vectors (>20kb) are being generated. To circumvent these problems, BACs have been introduced as targeting constructs for homologous recombination [905-907, 926-929].

BAC constructs were originally developed to allow cloning of large pieces of genomic DNA (up to >200 kb) which could be used for physical mapping and sequencing approaches, and are characterized by a high-clonal stability and low level chimaerism, compared to YAC based vectors, which are prone to spontaneous rearrangements [908, 930-938]. BAC plasmids are based on the *Escherichia coli* F-factor plasmid, which is maintained in low copy number in bacteria [930, 939-940]. The large insert size of genomic fragments make BAC constructs popular in transgenesis approaches, as complete genes including all regulatory sequences can be included [174, 941-942]. Several well annotated BAC libraries exist from different species, including a large variety of mouse strains, which can be easily accessed through public available genome databases like the UCSF (http://genome.ucsc.edu/) or Ensemble genome browsers (http://www.ensembl.org/), and the NCBI Clone Registry (http://www.ncbi.nlm.nih.gov/clone/). After choosing the BAC clone of interest, these can be easily ordered through non-commercial sources and commercial companies, including the BACPAC resource center at CHORI (http://www.chori.org), the RIKEN Biosource Center (http://www.brc.riken.jp/inf/en/index.shtml) or Invitrogen (http://www.invitrogen.com).
A main advantage of the use of BACs is that they can be easily modified through BAC recombineering techniques, which allow insertions of selectable markers into the BAC, deletions of unwanted genomic areas, and substitutions of complete regions, thereby enabling the creation of isogenic targeting constructs for subsequent homologous recombination in ES cells, since BACs from the desired mouse strain can be used [900, 905-906, 927-928, 943-953]. Most of the BAC recombineering techniques rely on the RecA protein, and inducible induction of the recombination machinery in bacteria, which enables recombination of the BAC with a recombination substrate transformed into the bacteria (**Figure 1**). Excellent reviews and protocols on all the details of BAC recombination have been published, and we refer the reader to those sources for a more in depth overview of these techniques [952-957] (http://recombineering.ncifcrf.gov/). By combining the easiness of BAC recombineering, and the use of isogenic, long homology arms, high targeting efficiencies for many different loci have been obtained in BAC targeting approaches, ranging from 7-28% of clones being properly targeted [906].

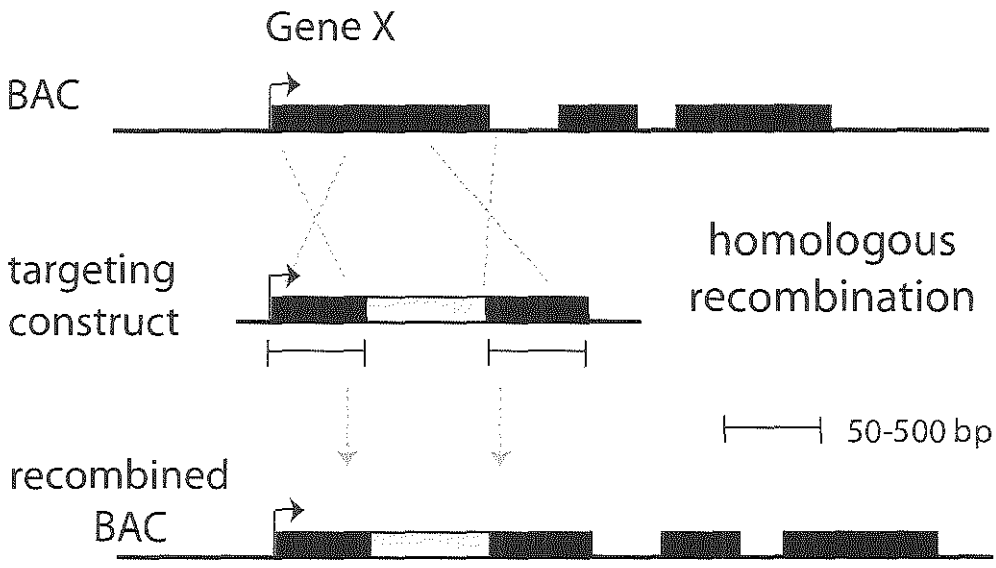

Figure 1: Principle of BAC recombination
Using homologous recombination in bacteria, a selection cassette (depicted in grey), cloned between homologous arms, is integrated in the coding sequence of gene X (exons in black) located on a schematic BAC (black line).

Beside the above mentioned advantages of BACs as targeting constructs, their wide-spread use in the scientific community is currently hampered by the difficulties in identifying correct targeted clones after BAC based targeting approaches. Conventional Southern Blotting techniques are difficult to employ, since the presence of large homology arms impedes the use of external probes [905]. Therefore, to identify correct targeted clones, quantitative real time PCR (qPCR) and DNA-FISH techniques have been applied [905-906]. In the qPCR approach, primers are chosen which amplify a fragment spanning the projected deletion/insertion, together with a qPCR amplifying a fragment located in one of the arms. A change in copy number detected by the first and not the second primer set is indicative for a correct targeting event. In the DNA-FISH approach, two probes are applied, one spanning the targeting construct, the other spanning the genomic location flanking the gene of interest. When both probe signals co-localize, it is likely that homologous recombination has occurred, and the targeting construct is not randomly integrated elsewhere in the genome. However, all of these techniques allow a high percentage of false positive and negative clones. qPCR is prone to false positive results, and its use depends on the design of sensitive primer pairs, which might not always be possible for every genomic location. DNA-FISH is a laborious technique, especially if many clones have to be screened, and small fragmentized pieces of randomly integrated targeting constructs may not be detected. To circumvent these problems, and fully benefit from the advantages of the BAC targeting approach, we have recently introduced a novel strategy which relies on the

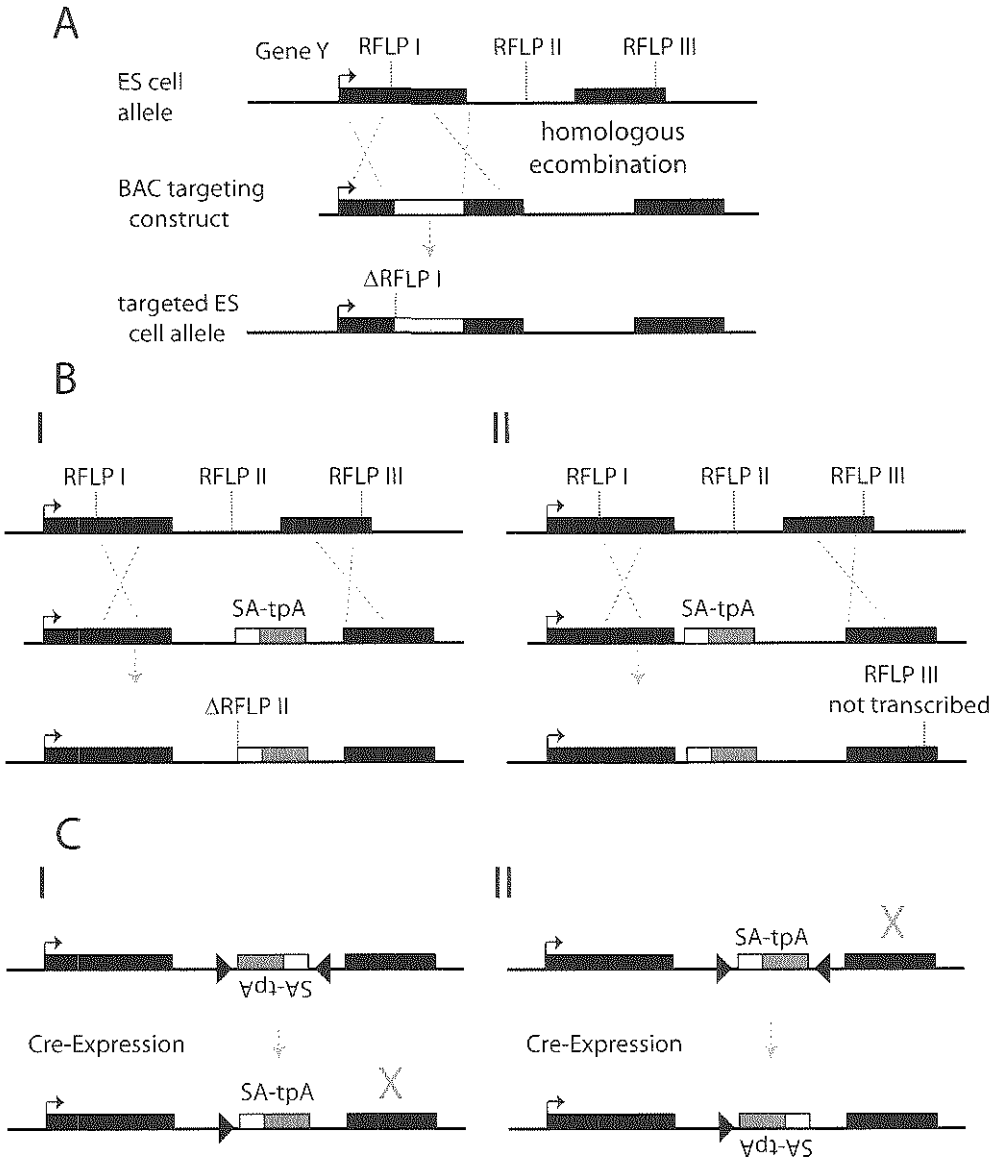

Figure 2: RFLP based targeting strategy
A) Insertional mutagenesis: a selection cassette (grey) is integrated in an exon (black) of gene Y, thereby disrupting RFLP I. Deletion of RFLP I can be detected using PCR. **B)** SA-tpA in an intron: the SA-tpA cassette consists of a splice acceptor (SA, white), a transcriptional stop (tpA, grey) and a resistance cassette (not shown for simplicity), which is flanked by either Lox or Frt sites (not shown). The SA-tpA cassette can be targeted to an intron, thereby disrupting the intronic RFLP II (option I), which can be used to detect the correct targeting. Alternatively, proper targeting of the SA-tpA cassette can be detected by screening for expression of the downstream RFLP III (option II), which will not be

presence of RFLPs [958], and have applied this strategy to generate genetically modified ES cells used in different studies on X chromosome inactivation [174, 911].

For our strategy, we make use of highly polymorphic ES cells derived from crosses between C57Bl/6 females and male Cast/Ei mice. The classical inbred *Mus musculus domesticus* mouse strain C57Bl/6, is among the most widely used and best characterized mouse strains [959]. The C57Bl/6 genome has been completely sequenced, functions as the reference genome for the mouse species and several well characterized BAC libraries are available [908]. The Cast/Ei inbred strain has been derived from a wild population of the subspecies *Mus musculus castaneus*, has been sequenced, and a BAC library is available. Cast/Ei mice are more difficult to breed, but offer the advantage of a distinct genetic background. Therefore, Cast/Ei mice have been extensively used in crosses to other strains in studies which needed the possibility to distinguish the maternal and paternal genome by means of SNPs, as for example to study genomic imprinting and X inactivation. The Cast/Ei and C57Bl/6 strains are highly polymorphic, with one estimated SNP per 311 bp [909]. Therefore, RFLPs which can distinguish between both strains will be present in virtually every gene. In our BAC targeting strategy, we make use of this fact, by designing BAC targeting vectors in such a way, that after proper targeting an RFLP is distroyed, or transcription through an RFLP is abrogated (**Figure 2**). By combining PCR analysis with restriction digestion of the PCR product, an easy and straightforward readout is obtained, which permits the reliable identification of properly targeted clones.

Figure 2: continued
expressed from the targeted allele in case of a correct targeting event. **C)** When the SA-tpA construct is flanked by asymmetrical lox sites (black arrow heads), the construct can be used to generate inducible knockout (option I) or rescue alleles (option II). In the inducible knockout approach (option I), the SA-tpA construct is targeted to an intron as shown in **B**, but in the antisense orientation. In this orientation, the SA-tpA does not inhibit transcription. After targeting, the resistance cassette, flanked by Frt sites (not shown) is looped out using transient expression of Flpase. Upon Cre expression, the SA-tpA cassette is inverted, and transcription is disrupted. Since asymmetrical Lox sites are used, inversion leads to the loss of one Lox site, thereby locking in the inversion event. To generate an inducible rescue allele (option II), the SA-tpA is targeted in the sense orientation, thereby enforcing a preliminary stop of transcription. After FLPase-mediated loop out of the selection cassette (not shown), the SA-tpA can be inverted, thereby restoring transcription of gene Y.

I targeting plasmid

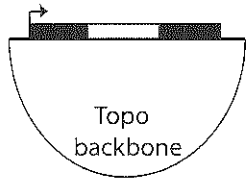

II BAC recombination

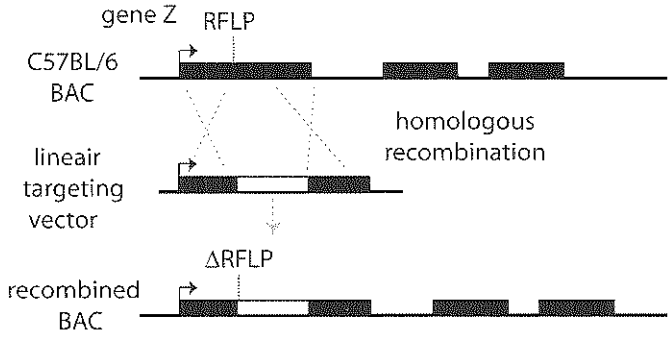

III targeting of ES cells

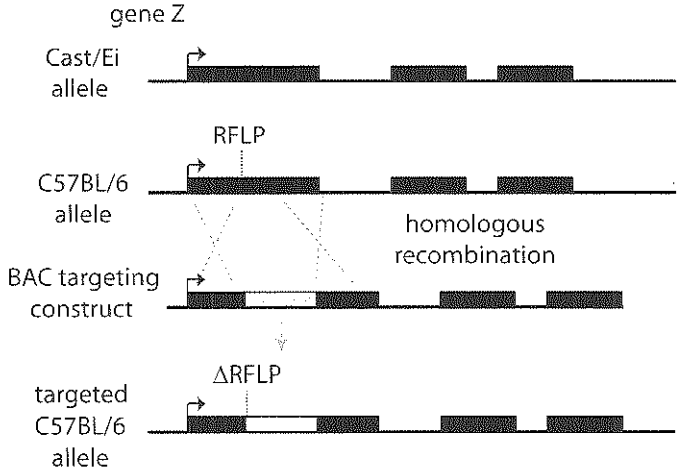

Figure 3: The targeting strategy in three basic steps
In the first step (I), a targeting plasmid is developed, which can be used to modify a BAC. An 800-1000 bp fragment surrounding the selected RFLP is PCR amplified, subcloned, and the RFLP is used to insert a selection cassette (grey). In the plasmid, the selection cassette is thus flanked by two

Our strategy involves the design of different variants to generate knockout alleles by insertional mutagenesis, introduction of a premature transcriptional stop, and even the generation of inducible knockout and rescue alleles using a single targeting event. In the first approach (**Figure 2A**), the BAC targeting vector disrupts an RFLP located within the coding region of a gene, and inserts a selection cassette in to the open reading frame of the gene of interest, thereby ablating gene function. This approach is especially helpful when an RFLP located in the proximal region of the gene can be found, and when important domains for the encoding protein are located downstream of the RFLP. In another approach, a splice acceptor poly-adenylation stop cassette (SA-tpA) together with a selection cassette is introduced into a proximal intron of the gene of interest, thereby prematurely stopping gene transcription (**Figure 2B**). The SA-tpA –selection cassette can be either introduced into an RFLP located in the intron, thereby allowing efficient screening for properly targeted clones as in the first approach (**Figure 2B I**), or an RFLP downstream of the insertion site can be used to screen for absence of transcription accross the RFLP in candidate clones (**Figure 2B II**). The introduction of an intronic SA-tpA cassette also allows the generation of inducible knockout or rescue alleles (**Figure 2C**). The SA-tpA cassette can be flanked by asymmetrical Lox sites resulting in a locked inversion of the cassette upon expression of the Cre recombinase protein [960-963]. To generate an inducible knockout allele, the SA-tpA cassette, flanked by the Lox sites, is introduced in the antisense orientation into an early intron located 5' in the gene. In this orientation, the SA is not recognized, and gene transcription is not inhibited. Upon expression of Cre, the SA-tpA cassette is inverted, and gene transcription will be abrogated (**Figure 2C I**). To generate an allele in which expression of the gene can be inducible rescued, the SA-tpA cassette is first introduced in the sense orientation, and Cre expression is used to disable the premature stop of transcription (**Figure 2C II**).

The generation of targeted ES cells using our strategy consists of a three step process (**Figure 3**). In the first step, a targeting plasmid for recombining a BAC containing the gene of interest is developed. In the second step, the BAC is recombined using BAC recombineering techniques in bacteria, and in the final step, the modified BAC is used for gene targeting in ES cells. As a first step, RFLPs present in the gene of interest are identified. Several SNP databases exist (http://www.perlegen.com, http://www.informatics.jax.org/), in which SNPs and RFLPs between the C57Bl/6 and Cast/Ei mice can be identified. A decision on the approach must then be taken: A conventional knockout allele based on insertional mutagenesis, introduction of a SA-tpA cassette, or generation of an inducible allele? After identification of a suitable RFLP and

Figure 3: continued
homologous arms (black boxes). In the BAC recombination step (II), the linearized plasmid from step I is used for homologous recombination of, in this case, a BAC of C57Bl/6 origin. The selection cassette is thus integrated in the BAC, thereby disrupting the RFLP which was used for cloning. In the final step (III), the BAC targeting construct, is used for homologous recombination in ES cells. Since a C57Bl/6 BAC was used to generate the targeting construct, targeting will preferentially occur at the isogenic C57Bl/6 allele, thereby disrupting the RFLP restriction site, which is only present at the C57Bl/6 allele, but not at the Cast/Ei allele. Loss of the RFLP at the C57Bl/6 allele can be detected by PCR analysis, thereby enabling a straightforward readout of proper targeting.

the desired approach, a BAC must be chosen which contains the RFLP and flanking regions. Location of BACs can be found in the UCSF or Ensemble genome browsers, or Mapviewer (http://www.ncbi.nlm.nih.gov/mapview/), from which also the sequences can be retrieved. In general, it appears best to choose a BAC with a length between 150-200 kb, which is centrally located around the RFLP, allowing an equal length of homology arms on both flanking sites. To generate the targeting plasmid, an 800-1000 bp fragment surrounding the selected RFLP is PCR amplified using a proof-reading high fidelity polymerase, and cloned into a vector suitable for subcloning of PCR products (e.g. pCR-BluntII-Topo, Invitrogen). It is important that in the selected region the target RFLP represents an unique restriction site, which does not digest elsewhere in the amplified fragment, or in the vector backbone, enabling single step insertion of the selection cassette into the RFLP. To allow the fast generation of knockout BAC constructs, we have generated a couple of vectors (overview **Table 1**, available upon request), from which the selection cassette with or without the SA-tpA and Lox sites can be easily released by restriction digestion. These fragments, which contain all necessary elements to express resistance genes for both antibiotic selection in pro- and eukaryotes, can then be cloned into the unique RFLP restriction site, thereby finishing the targeting plasmid, in which the selection cassette is now flanked by two homologous arms of around 500 bp. Although BAC recombination can be accomplished with homology arms of only 50 bp, increasing the length can in general increase the efficiency. In the subsequent step, the generated plasmid is used for BAC recombineering. Proper modification of the BAC is verified by colony PCR and restriction digestion, and ones established, the modified BAC can be used to target ES cells. After selection with the desired antibiotic, emerging colonies are picked, and screened for the correct recombination event using an RFLP-based allele-specific PCR.

The many RFLPs present in the hybrid C57Bl/6-Cast/Ei ES cells, combined with the different approaches presented above make it possible to modify virtually every gene using this BAC targeting strategy, benefitting from the high targeting efficiency of BAC targeting vectors. In this protocol, we provide detailed steps for the generation of a BAC targeting construct, the transfection of ES cells with the modified BAC constructs, and the identification of properly targeted clones. Several excellent protocols on BAC recombineering [952], BAC transgenesis [955] and design of targeting constructs in general [954] already exist. In this protocol we introduce crucial new steps related to BAC recombineering including time-saving shortcuts in regard to previously published methods. Combined with our novel RFLP-based strategy this protocol permits the generation of knockout ES cells in a very short time span (**Figure 4**), to be used for *in vitro* studies, or can be used to generate mouse models, by generation of chimaeras or through tetraploid embryo complementation [912, 964-967].

Lox-Kana/Neo-Frt	1995 bp	EcoRI
Lox-Kana/Neo-Lox	1978 bp	EcoRI
Lox-Frt-Kana/Neo-Frt	2369 bp	NheI-AflII
Amp/puro	2733 bp	SfiI-NotI
Lox66-SA-tpA-Lox71	3287 bp	DraIII-AseI

Table 1: Overview of targeting cassettes
Table summarizing the available selection cassettes, fragment sizes in base pairs, and the restriction digest which is used to release the cassette from its vector. Lox: Lox-site for Cre-recombination. Frt: Frt-site for Flpase-recombination. Kana/Neo: cassette with a dual prokaryotic/eukaryotic promoter driving a gene encoding a protein rendering bacteria resistant to kanamycin, and ES cells resistant to neomycin (Geneticin, G418). Amp/Puro: cassette with an ampicilline resistance gene allowing selection in bacteria, and a puromycin resistance gene for use in ES cells. Lox66 and Lox71: asymmetrical Lox sites. SA-tpA: cassette encoding a splice acceptor (SA) and a triple transcriptional stop signal (tpA).

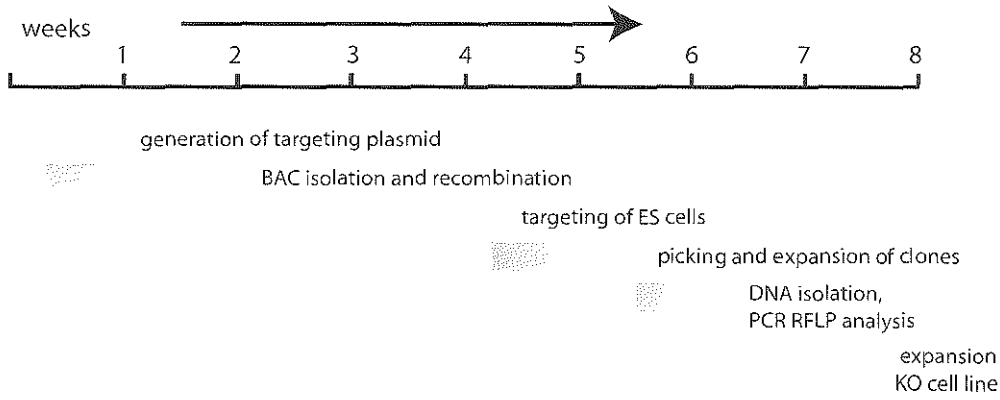

Figure 4: Time line
The time line for the RFLP-based targeting strategy, following the different steps described in this protocol. See text for details.

Materials

Reagents

- Plasmids containing selection cassettes and/or SA-tpA sequences (are available upon request).
- Bacterial artificial chromosomes (BACs in DH10ß host bacteria; BACPAC Resources at CHORI, Invitrogen, or Riken BioResource Center)
- C57Bl/6-Cast/Ei ES cell lines (available upon request)
- Recombination proficient bacteria, EL250 [900]
- Ampicillin (Sigma-Aldrich, A-9518)
- Kanamycin (Sigma-Aldrich, K0254)
- Chloramphenicol (Sigma-Aldrich, C7795)
- Distilled H_2O (dH_2O) (Baxter, TKF7114)
- Agarose (Sigma-Aldrich, A9539-500g)
- NucleoSpin gel extraction kit Extract II (Bioke, 740609250)
- NucleoBond Maxi kit Xtra Maxi (Macherey-Nagel, 740414100)
- Ethidium bromide solution (10 mg ml^{-1}; Sigma-Aldrich, E1510) **CAUTION** EtBr has mutagenic properties, wear gloves at all times
- dNTP mixture, 10 mM each, PCR grade (Invitrogen, 10297-018)
- Restriction enzymes (New England Biolabs or Roche diagnostics)
- PI-SceI restriction enzyme (New England Biolabs, R0696S)
- T4 DNA ligase (Roche, 11000321)
- Phusion high fidelity polymerase (New England Biolabs, MO530L)
- Taq-polymerase (homemade, or for example Invitrogen, 11342-020)
- $MgCl_2$ 50mM (Invitrogen, PNY02016)
- Klenow enzyme (Roche, 14267420), T4 DNA-polymerase (11004786001)
- Calf intestinal Alkaline phosphatase (Promega, M182A)
- Glycerol (Fisher Scientific, BP229-1)
- BSA, purified, 100x (New England Biolabs, B9001S)
- molecular weight marker (New England Biolabs, N3232L)
- DH5α chemical competent bacteria, Max Efficiency (Invitrogen, 18258-012)
- DMSO (Sigma, D2650) **CAUTION** Toxic substance. Avoid skin contact.
- Geneticin, 270 µg/ml, active (G418, Gibco, 11811-031)
- Puromycin, 1µg/ml (Invitrogen, A11138-02)
- LIF (home made, or for example Chemicon, ESG1107)
- Gelatin (Sigma, G1890-100G)
- DPBS, Dulbecco's Phosphate Buffered Saline (Sigma-Aldrich, D8537)
- DMEM (Invitrogen, 11960085)
- FCS, Fetal Calvine Serum (Invitrogen, 10099141)
- Penicillin–streptomycin (100×) (Invitrogen, 15140-122)

- Non-essential aminoacids (Invitrogen, 11140-050)
- ß-mercaptoethanol (Sigma, M7522) **CAUTION** Avoid inhalation. Flammable; harmful if swallowed; toxic when in contact with skin and eye; use protective gloves and safety glasses when handling.
- Trypsin-EDTA 0.25% (v/v) trypsin/0.2% (w/v) EDTA in PBS (GIBCO, 25200-056)
- Mouse Embryonic Fibroblast (MEFs) commercial (for instance Millipore (http://www.millipore.com) or self prepared from E13.5 embryos **CAUTION** All experiments requiring animal handling should be conducted in accordance with international animal protection guidelines and local animal protection laws.
- Proteinase K, Prot.K (Roche 03115852001)
- SDS (Roche, 11667262001) **CAUTION** Do not inhale dust. Keep away from sources of ignition. Avoid contact with skin and eyes.
- pCR-BluntII-Topo, Zero Blunt Topo PCR Cloning-Kit (Invitrogen, 45-0245)
- PCR primers (Invitrogen)
- Ethanol, absolute (Sigma-Aldrich, 32221-2.5L) **CAUTION** Ethanol is flammable and may be harmful by inhalation or ingestion.
- Isopropanol (Sigma-Aldrich, 59300) **CAUTION** Isopropanol is flammable and may be harmful by inhalation or ingestion.
- LB agar, Miller (BD, 244510)
- Bacto-tryptone (Difco)
- yeast extract (Difco)
- NaCl (Sigma-Aldrich, 71380-5kg)
- Trizma base, Tris (Sigma-Aldrich, T6066-5kg)
- NaOH pellets (Riedel-de Haën, 06203) **CAUTION** It is corrosive and causes burns to any area of contact.
- KAc (Sigma-Aldrich, 25059)
- EDTA (Sigma-Aldrich, E1644-1kg)
- HCL, 37% solution (Fluka, 84422) **CAUTION** It is corrosive, and both the liquid and fuming vapour can cause severe burns.
- Acetic acid (Fluka, 45730-1l) **CAUTION** It is corrosive, and both the liquid and fuming vapour can cause severe burns.
- NaAc (Sigma-Aldrich, S7670)
- tRNA, yeast (10 mg/ml, Invitrogen, 15401-029)
- RNAse A (10 mg/ml, Invitrogen, 12091-039),
- Trizol (Invitrogen, 10296010)
- DNAse I (Invitrogen, 18068-015)
- Super script III cDNA synthesis kit (Invitrogen, 11904-018)

Equipment

- 1,5 ml Eppendorf tubes (Eppendorf, 0030120086)
- 15 ml sterile Falcon tubes (Falcon, 352196)
- 50 ml sterile Falcon tubes (Falcon, 352070)

- cryo-vial (Nunc, 375353)
- Sterile 1-20 µl filter tips (Rainin Bio Clean, GP-L10F)
- Sterile 20-200 µl filter tips (Rainin Bio Clean, GP-L200F)
- Sterile 20-1000 µl filter tips (Rainin Bio Clean, RT-1000F)
- Gilson pipettes P20, P200, P1000, multi-channel P200
- 25 cm^2 cell culture flasks (Greiner Bio-one, 690160)
- 10 cm^2 cell culture dishes (Greiner Bio-one, 664160)
- 96-well cell culture plates, flat-bottom (Greiner Bio-one, 655180)
- 96-well cell culture plates, U-shaped (Greiner Bio-one, 650160)
- 24-well cell culture plates, (Greiner Bio-one, 662160)
- 96-well micro titer plate (BD-Falcon, Flexible plate, U-bottom, without lid, 353911)
- Bottle-top cell culture filter, 0.22 µm (Corning, 430758)
- PCR disposable adhesive (EU opti-seal, 157300)
- Tubes for bacterial culture (Greiner Bio-one, 201150)
- Erlenmeyer 200 ml
- Erlenmeyer 2000 ml
- Eppendorf Refrigerated Microcentrifuge Model 5417R (Eppendorf)
- Eppendorf Refrigerated Centrifuge Model 5810R (Eppendorf)
- Beckman J6-MC centrifuge (Beckman)
- Inverted tissue culture microscope with phase contrast microscope (4x, 10x, 20x, 40x objectives)
- Electroporation system for bacteria (Gene Pulser System, Bio-Rad)
- Electroporation system for ES cells (Gene Pulser Xcell, Bio-Rad)
- Cuvettes for bacteria electroporation (Biorad)
- Cuvettes for ES cell electroporation (BTX Cuvettes Plus, 2 mm, 45-0125)
- Nanodrop photospectrometer
- OD spectrometer Genesys20 Spectro Photometer (Thermo Spectronic)
- UV-transilluminator
- Thermocycler (Biorad, S1000 thermal Cycler)
- Bacterial incubator (New Brunswick Scientific, Inova43)
- Heat-block incubator (Eppendorf, Thermomixer compact)
- plate shaker (MO-BIO, 11996)
- Cell culture incubator
- Biosafety cabinet with aspirator for tissue culture
- Water bath
- Refrigerator
- -20°C freezer
- -80°C freezer
- Liquid nitrogen tank **CAUTION**: wear eye protection and thermo gloves when handling liquid nitrogen. Liquid nitrogen can cause severe burnings.
- Diaper
- Petri dishes for bacterial plates

Reagent Setup

- 1M Tris: Mix 121 g of Tris base and 1000 ml of dH_2O. Adjust the pH to 7.4 with HCl. Store at RT.
- 10mM Tris pH 7.4: dilute 1M Tris pH 7.4 100x, and store at RT.
- 0.5 M EDTA Mix 186.1 g of EDTA and 800 ml of dH_2O. Adjust the pH to 8 with ~20 g of NaOH pellets. Store at room temperature.
- P1 buffer: mix together 50 ml 1M Tris pH 8, 20 ml 0.5 M EDTA pH 8, 10 ml RNAse A (10mg/ml), 920 ml dH_2O. Store at 4°C.
- P2 lysis buffer: mix together 930 ml dH_2O, 50 ml 20% SDS, 20 ml 10 M NaOH. Store at RT.
- P3 buffer: 2.8 M KAc, pH 5.1. Add 274.8 g KAc to 400 ml dH_2O, set pH to 5.1 by adding HCL, and add dH_2O to 1L). Store at 4°C.
- 70% ethanol
- 50x TAE for gel electrophoresis: Mix together 1210 g Tris base, in 500 ml 0.5M EDTA pH 8, 285.5 ml Acetic Acid and add dH_2O to 5L. Autoclave and store at RT.
- 0.2% gelatin solution: add 2g gelatin to 1L dH_2O. Autoclave and store at 4°C.
- 2x Freezing solution: add together 60 ml DMEM, 20 ml FCS, 20 ml DMSO. Mix and filter sterilize. Store at 4°C for up to a month.
- Mouse Embryonic Stem Cell Medium: DMEM, 15% foetal calf serum, 100 U ml^{-1} penicillin, 100 mg ml^{-1} streptomycin, non-essential amino acids, 0.1 mM ß-mercaptoethanol, and 1000 U ml^{-1} LIF. Filter sterilize and store at 4°C for maximal 2 weeks.
- Low SDS lysis solution: mix together 40 ml Tris 0.5M, 2 ml EDTA 0.5M, 2 ml 20% SDS and 8 ml NaCl 5M, and add dH_2O to a total volume of 200 ml. Store at RT. Add 50 µl Prot.K (10 µg/ml) / ml lysis solution before use. **CAUTION** contains SDS. Protect eyes.
- 3M NaAc, pH5.6
- LB: mix 10 g of Bacto-tryptone, 5 g of yeast extract, 5 g NaCl and 1 liter dH_2O, pH 7.2. Autoclave and store at RT.
- LB-agar bacteria plates: add 10 g of LB-agar to a 500 ml LB medium bottle, and autoclave. Cool down, until bottle can be touched, then add appropriate antibiotic, and pour plates. Store plates at 4°C for up to a month.
- Ampicilline stock solution: 50 mg/ml in dH_2O, aliquot and store at -20°C. Use at a final concentration of 25 µg/ml for plasmids, and 8 µg/ml for BACs.
- Kanamycin stock solution: 50 mg/ml in dH_2O, aliquot and store at -20°C. Use at a final concentration of 50 µg/ml for plasmids, and 15 µg/ml for BACs
- Chloramphenicol stock solution: 34 mg/ml in ethanol, aliquot and store at -20°C. Use at a final concentration of 12.5 µg /ml for BACs.

Procedure

In silico design of strategy Timing: 1 day

1. Identify suitable RFLP in the gene of interest, and choose BAC clone. Several computer-based databases exist, in which SNPs and RFLPs can be selected (for instance http://www.informatics.jax.org/). Retrieve genome sequences (http://www.ncbi.nlm.nih.gov/mapview/), and select the targeting cassette and approach. It is good practice to generate sequence files in which the modified, recombinant sequence is assembled. This can be done in several software programs (e.g. DNAMAN, Lynnon Biosoft, or Clonemanager, Scientific & Educational software), and will save valuable time later on, when primers or restriction digestions to verify cloning steps are chosen.
2. Order selected BAC clone. Take care that a BAC is chosen from an isogenic library, which is derived from the same mouse strain as the genotype of the allele being targeted.
3. Design primers to amplify an 800-1000 bp fragment surrounding the selected RFLP. Primers can be designed in different software programs (DNAMAN, Clonemanger etc), or online applications such as Primer 3 (http://frodo.wi.mit.edu/). We usually design primers with an annealing temperature around 58 °C. Critical Step: the RFLP restriction site should be unique and absent from the cloning vector which is used to clone in the PCR product later on. This will facilitate the insertion of the selection cassette into the targeting plasmid in a single cloning step.

Generation of targeting plasmid for BAC recombineering Timing: 5-6 days

4. PCR amplify homologous fragments surrounding the RFLP using the primers designed in step 3. Dilute primers to a 100 pM stock in 10mM Tris pH 7.4. Use a high-fidelity Taq-polymerase with proofreading activity (e.g. Phusion, NEB), to prevent mutations. Use either genomic DNA from the mouse strain of the allele being targeted, or use BAC DNA (50 ng of DNA as PCR template). Isogenic DNA can also be ordered from the Jackson's laboratory (http://www.jax.org). It is advisable to verify the presence of the RFLP in PCR products amplified from genomic DNA of the ES cells which will be used for targeting, by restriction digestion or sequencing.

Component	Amount
5x High-Fidelity Buffer	10 µl
dNTP (1 mM)	1 µl
Forward primer (100 pM)	0.5 µl
Reverse primer (100 pM)	0.5 µl
Phusion polymerase	0.2 µl
DNA template (50 ng/µl)	1 µl
Sterile dH_2O	36.8 µl
Total Volume	50 µl

5. Run the PCR on a thermocycler, using the following parameters:

Cycle	Denature	Anneal	Extend
1	98 °C, 2 min		
2-31	98 °C, 15 s	58 °C, 30 s	72 °C, 1 min
32			72 °C, 10 min
33			Hold at 12 °C

6. Run the PCR product on a 1% agarose gel using standard molecular methods [968] together with a molecular weight marker. Visualize with a UV-transilluminator set at low UV intensity. Isolate the PCR band running at the expected size. Critical Step: do not too long expose the DNA to UV-light, as this can introduce mutations. Always use an UV-transilluminator set at low UV intensity when visualizing DNA which is subsequently used for cloning. See Troubleshooting.
7. Clean up the DNA fragment using a commercial gel extraction kit (e.g. NucleoSpin, Macherey-Nagel), following manufactures instructions. Elute DNA in a total of 20 µl elution buffer. Pause point: DNA can be stored at -20°C for several years.
8. Clone the PCR product in pCR-BluntII-Topo using the pCR-BluntII-Topo-kit (Invitrogen) (or an alternative vector suitable for subcloning of blunt PCR products). Mix in an Eppendorf tube: 2 µl PCR product, 0.5 µl Salt solution and 0.5 µl vector (Topo-vector). Vortex and spin down shortly. Incubate for 30 minutes at RT.
9. Transform the Topo-reaction product from step 8 in chemically competent DH5α bacteria by heat-shock. Chemically competent bacteria are commercially available, or can be prepared following published protocols [968].
    (I) Thaw a vial of DH5α bacteria on ice, and mix with the Topo-reaction product. Incubate on ice for 15 minutes.
    (II) Heat-shock bacteria at 42°C for 45 s, and put on ice immediately.
    (III) Add 1 ml LB-medium (no selection) and incubate bacteria for 60 min at 37°C, shacking at 700 rpm in a Theromixer.
    (IV) Spin bacteria down (1 min, 6000 rpm, microcentrifuge), and remove LB medium by flicking tube up-side-down. Some fluid will remain in the tube.
    (V) Resuspend bacteria in the remaining LB present in the tube, and plate bacteria on LB-agarose plates with kanamycin selection (10 µg/ml). Incubate at 37°C O/N.
10. The next day, visible colonies should be present on the bacteria plates. Pick single colonies (between 12 and 24,) with a pipette tip and innoculate in 3 ml of LB medium with kanamycin. Incubate these mini-cultures at 37°C O/N in a shaker at 200 rpm. See Troubleshooting.
11. Isolate the plasmid DNA from the mini-cultures ("mini-prep"):
    (I) Take 1.5 ml of bacterial culture, transfer to Eppendorf tube, and centrifuge 13200 rpm, 1 min in a microcentrifuge.
    (II) Remove supernatant, and resuspend pellet in 300 µl buffer P1. Let shake for approximately 5 min at 1400 rpm, 37°C until all cells are in suspension.

(III) Add 300 µl lysis buffer P2, invert five times, and wait 20 sec.
(IV) Add 300 µl ice cold buffer P3. Invert tube 5 times, and incubate on ice for 5 min to precipitate bacterial protein and DNA. Critical point: do not shake vigorously at this step, since this will result in contamination of the mini-prep with bacterial genomic DNA.
(V) Centrifuge at 13200 rpm for 8 min in a microcentrifuge.
(VI) Pour supernatant in a new Eppendorf tube, filled with 700 µl isopropanol, and shake vigorously to precipitate the plasmid DNA.
(VII) Centrifuge at 13200 rpm for 8 min in a microcentrifuge.
(VIII) Remove supernatant, and wash DNA pellet with 500 µl 70% ethanol. Centrifuge at 13200 rpm for 5 min in a microcentrifuge.
(IX) Remove supernatant, air dry and resuspend pellet in 100 µl 10mM Tris pH 7.4.

12. Check obtained plasmid DNA by restriction digestion, to verify the presence of a correct fragment inserted in Topo-vector. The choice of the restriction digest is determined by sequence of amplified fragment. In general, it is helpful to choose one enzyme located at the beginning or end of sequence, together with an enzyme which digests only once in the Topo-vector. This will enable you to check both the presence of the proper fragment, and also determine the orientation of insertion in to the Topo-vector. The amplified RFLP can also be used for digestions. For digestion with multiple enzymes, use the NEB Double Digest finder (http://www.neb.com/nebecomm/DoubleDigestCalculator.asp), or other sources, to determine the appropriate buffer and incubation conditions. Digest 10 µl of mini-prep DNA, with 5 µl of 10x buffer, 0.5 µl 100x BSA (if required), 1 µl of each enzyme, in a total volume of 50 µl, and incubate at appropriate temperature (37°C for most enzymes) for 2h. For multiple digestions, this can be easily done in 96-well micro titer plates, sealed with tape, and placed in an incubator. Separate restriction products on a 1% agarose gel, and continue with a clone showing the expected restriction fragments. See Troubleshooting. Pause point: Mini-DNA can be stored at -20 °C for several years.
13. In the next step, the selection cassette of choice, with or without the SA-tpA cassette (**Table I**), or any other preferred selection cassette is cloned into the RFLP restriction site in the amplified fragment. First, release the cassette from its vector, by digestion with the appropriate enzyme (**Table I**) and generate blunt ends (except when generated overhangs are compatible with RFLP-site). Digest 2-5 µg of plasmid, together with 10 µl 10x Buffer, 1 µl 100x BSA (if required), 2 µl of each enzyme, in a total volume of 100 µl, at 37°C for 2 h. To generate blunt ends, use Klenow enzyme to fill in 5' overhangs, or T4 polymerase to fill in 5' overhangs or remove 3' overhangs. For a Klenow reaction, add 2 µl of 10x Buffer, 3 µl dH_2O, 12 µl 330 µM dNTP and 3 µl Klenow enzyme to the digestion mix after incubation, mix and incubate 15 min at RT. Immediately run reaction product on a 1% agarose gel. For T4 DNA polymerase, add 2 µl of 10x Buffer, 2.8 µl dH_2O, 0.2 µl 100x BSA, 12 µl 100 µM dNTP and 3 µl T4 DNA polymerase, mix and incubate 15 min at 12°C. Immediately run reaction product on a 1% agarose gel. Isolate the correct sized fragment, and clean up, as described in step 7. Critical

point: because of endonuclease activity of Klenow enzyme and T4 DNA polymerase, do not incubate for more than 15 min.

14. Open the amplified fragment (targeting arms) cloned in Topo from step 12 with the RFLP enzyme. Digest 20 µl of plasmid with 10 µl 10x Buffer, 1 µl 100x BSA (if required), 2 µl of enzyme, 1 µl of Calf intestinal phosphatase (CIP) in a total volume of 100 µl, at 37°C for 2 h. Dephosphorylation of the 5' termini will prevent self-closure of the plasmid upon ligation. Remove the 5' or 3' overhangs of the plasmid if necessary and clean up the DNA as described in step 13.
15. Ligate the selection cassette from step 13 to the linearized plasmid from step 14. Add in an Eppendorf tube the linearized plasmid, and selection cassette, in a 1:3 ratio (60 ng end concentration), together with 1 µl 10x Ligation buffer and 0.5 µl T4 DNA Ligase in a total reaction of 10 µl, mix and incubate for 2h at RT, or O/N at 16 °C.
16. Mix the ligation product with competent DH5α bacteria and heat shock transform the bacteria as described in step 9. If an ampiciline resistance gene is included in the selection cassette, include ampiciline in the LB-agarose plates (25 µg/ml). If colonies are emerging the next day, start mini-cultures (step 10), isolate mini-DNA (step 11), and check final targeting plasmid by restriction digestions, to verify proper insertion in correct orientation (step 12). See Troubleshooting. Pause point: Plasmids can be stored at -20 °C for several years.
17. Digest the final targeting plasmid from step 16 to isolate the homology arms and selection cassette from the Topo-vector. This will increase the efficiency of BAC recombineering, as the targeting cassette will not be able to replicate independently in bacteria. Digest 30 µl of plasmid, in a 50 µl reaction, run on an agarose gel, isolate the correct fragment and clean up the DNA (step 7). Meassure concentration by Nanodrop. Pauze point: A linearized targeting fragment can be stored at -20 °C for at least one year.

BAC isolation and recombination Timing: 12 days

18. Upon arrival of the BAC clone ordered in step 2, plate the BAC clone (delivered in DH10ß cells) on LB-agar plates with chloramphenicol selection (12.5 µg/ml), and incubate at 37°C O/N
19. Pick single colonies with a pipette tip, and inoculate 3 ml LB (with chloramphenicol (12.5 µg/ml), and incubate at 37°C O/N, shaking at 200 rpm. Although for the first steps of BAC recombineering only limited amounts of BAC DNA are required, which could be obtained from a mini-prep (step 11), we prefer to grow a maxi-culture from every new arriving BAC. This offers the advantage that cleaner DNA and larger quantities are obtained, which is convenient for subsequent control experiments, and long term storage. See Troubleshooting.
20. Add complete content of the O/N cultures to a 2 L Erlenmeyer flask filled with 500 ml of LB with chloramphenicol (12.5 µg/ml). Incubate at 37°C O/N, shaking at 200 rpm.
21. Prepare a glycerol freeze-stock of every new BAC clone: transfer 850 µl of BAC culture to a cryo-vial, and add 150 µl 97% Glycerol, mix, and immediately snap-

freeze bacteria in liquid nitrogen. Store bacteria at -80°C. Pauze point: Glycerol stocks of bacteria can be maintained at -80°C for several years.

22. Isolate Maxi-BAC-culture:
    - (I) Transfer the 500 ml of culture to a bucket, and centrifuge 10 min at 4000 rpm, 4°C in a Beckmann J16-MC centrifuge.
    - (II) Remove the supernatant, and add 100 ml of buffer P1. Vortex the bucket for approximately 30 sec, until all bacteria are resuspended.
    - (III) Add 100 ml of lysis buffer P2. Invert bucket 6 times. Incubate 1 min at RT. Critical point: do not shake vigorously at this point, since this will result in contamination with bacterial genomic DNA.
    - (IV) Add 100 ml of ice cold buffer P3. Invert bucket 6 times, and put on ice for 20 min. Proteins and bacterial genomic DNA will precipitate. Critical point: do not shake vigorously at this point, since this will result in contamination of bacterial DNA in the BAC preparation.
    - (V) Centrifuge 30 min at 4000 rpm, 4°C in a Beckmann J16-MC centrifuge.
    - (VI) Equibrilate a NucleoBond (Macherey-Nagel) maxi-prep column, by adding 25 ml of Equibrilation buffer, carefully wetting the complete filter insert.
    - (VII) Add the supernatant from step (V) to the column, and let pass through by gravity. This will require several loading steps.
    - (VIII) When all fluid has passed through, add 15 ml of Equibrilation buffer to the column, carefully wetting the complete filter insert.
    - (IX) Remove Filter, and add 25 ml of Wash buffer. Allow to empty by gravity.
    - (X) Place a 50 ml Falcon tube under the column, and add 15 ml of Elution buffer (pre-heated at 65°C) to the column. The BAC DNA will now be eluted into the tube. Pauze point: eluted BAC DNA can be stored O/N at 4°C
    - (XI) Precipitate the BAC DNA by adding 10.5 ml Isopropanol to the tube, and shake vigorously. Centrifuge 30 min at 4000 rpm, 4°C.
    - (XII) Remove supernatant, and wash DNA pellet with 70% ethanol, centrifuge 15 min at 4000 rpm, 4°C.
    - (XIII) Remove supernatant, air dry pellet and dissolve in 200 µl 10mM Tris, pH 7.4. To facilitate dissolving, incubate at 50°C for 1h, or 4°C O/N. Collect content by short centrifugation. Pauze point: BAC DNA can be stored at 4°C for several months. Critical point: do not freeze BAC DNA, as this will result in fragmentation of the BAC DNA. Also prevent vigorous pipetting, as this might result in breaks through shearing of DNA.
23. Check obtained BAC DNA by restriction digestion, or PCR analysis, to verify that correct clone was obtained. A standard restriction enzyme such as EcoRI or BamHI, will result in a "finger-print" pattern of the respective BAC, which can easily be recognized. Use 2 µl of BAC DNA per digestion (approximately 1 µg/µl), 5 µl of 10 x restriction buffer, 0.5 µl 100x BSA (if required) and 2 µl of

enzyme, in a 50 µl digest. Incubate for 2h at the appropriate temperature, and run on 1% agarose gel. To check the BAC by PCR analysis, dilute an aliquot of BAC DNA 10x, and take 1 µl as template. Use any primer combination available, for example primers located in the gene of interest, or primers used to amplify the region surrounding the RFLP (step 4). There is no need to use a high fidelity polymerase, every Taq-polymerase and conditions used in your lab should work. See Troubleshooting.

Transformation of BAC clone into recombination proficient bacteria

24. Streak recombination proficient bacteria [900] from a frozen glycerol stock onto LB-agar plates with no selection, and incubate at 30°C O/N. Critical point: recombination proficient bacteria must be grown at 30 °C, to prevent activation of the recombination machinery at higher temperatures.
25. Pick a single colony, and inoculate a 5 ml LB-culture (no antibiotics), and grow O/N at 30°C, shaking at 200 rpm.
26. Take 0.5 ml of the bacteria culture, and inoculate a 50 ml LB-culture (no antibiotics), and grow for 4-5h at 30°C, shaking at 200 rpm, until an OD600 of 0.6-0.8 is reached.
27. Collect bacteria in a 50 ml Eppendorf tube, and centrifuge 10 min, 3000 rpm at 4°C.
28. Recombination proficient bacteria will now be rendered electrocompetent, by washing steps in ice cold dH_2O. Remove the supernatant from step 27, and resuspend the pellet in 10 ml ice cold dH_2O. Centrifuge 10 min 3000 rpm at 4°C.
29. Remove the supernatant, and repeat the washing steps with ice cold dH_2O three times (4x 10 min in total).
30. Remove the supernatant, and resuspend the pellet in 250 µl ice cold dH_2O, and store on ice. The bacteria are now electrocompetent, and the amount of bacteria is enough for 5 transformations.
31. Divide the bacteria over 5 Eppendorf tubes, and add different concentrations of BAC DNA: 0.2 µl, 0.5 µl, 1 µl, 2 µl and 4 µl. Incubate 15 min on ice. Add the bacteria-DNA mixture to a bacterial electroporation curvette (Biorad), pre-chilled on ice, and electroporate at 1.8 kV, 25 mF, 200 Ω, using a Biorad pulser. Add 1 ml LB medium, transfer to an Eppendorf tube and let recover for 60 min at 30°C, shaking at 200 rpm. Critical point: Although in principal one electroporation can be enough to transform the BAC into the recombination proficient bacteria, we found that for several BACs it is rather difficult to be transformed into bacteria. The use of different concentrations of BAC DNA will increase the chance that one of the electroporations results in positive colonies, thereby saving valuable time. See Troubleshooting.
32. Spin down the bacteria at 6000 rpm, 30 sec, and flick the tube upside-down to remove the supernatant. Resuspend pellet in remaining fluid, and plate to LB-agar plates containing chloramphenicol (12.5 µg/ml). Incubate O/N at 30 °C.
33. If colonies are appearing after 24h, pick single colonies using a pipette tip, and inoculate 3 ml LB cultures (12-24 per BAC), with chloramphenicol selection (12.5 µg/ml). Incubate O/N at 30 °C.

34. Isolate BAC mini DNA the next morning, following the mini isolation protocol (step 11), with the exception of the last step, where DNA is dissolved in 50 µl 10mM Tris pH 7.4. Check the DNA by restriction digestion, using 25 µl of BAC DNA, using the same enzyme which was chosen to obtain a "finger-print" pattern of the BAC (step 23). If the same pattern is observed compared to the original BAC clone, it can be concluded that transformation was successful. See Troubleshooting.
35. Select a clone from step 34 which shows the expected restriction digestion pattern, and make a glycerol stock (step 21), since future applications of the BAC in recombination proficient bacteria might be required.

BAC recombination

36. Add 0.5 ml of the fresh bacteria culture from step 35 to a 200 ml Erlenmeyer flask containing 50 ml of LB-medium with chloramphenicol (12.5 µg/ml), and incubate at 30 °C for 4-5h, shaking at 200 rpm, until OD600 = 0.6-0.8.
37. Place Erlenmeyer with bacteria culture in a 42 °C shaking water bath for 20 minutes. At 42 °C, the recombination machinery will be activated.
38. Collect the bacteria by centrifugation 10 min, 3000 rpm at 4 °C, and make cells electrocompetent (step 28-30). Take 50 µl of electrocompetent bacteria in an Eppendorf tube, and add 100 ng of linearized targeting fragment (step 17). Electroporate as in step 31, and let bacteria recover for 60 min at 30 °C, shaking at 200 rpm. Electroporation of the small targeting fragment is very efficient; therefore it is not necessary to try different concentrations.
39. Spin down the bacteria at 6000 rpm, 30 sec, and flick the tube upside-down to remove the supernatant. Resuspend pellet in remaining fluid, and plate to LB-agar plates containing chloramphenicol (12.5 µg/ml) and dependent on the targeting cassette used, kanamycin (3 µg/ml) or ampiciline (8 µg/ml). It might be helpful to plate $1/10^{th}$ of the bacteria to a separate plate, to prevent overgrowing of the plate when recombination turns out to be highly efficient. Incubate O/N at 30 °C.

Colony PCR to check proper recombination.

40. After 24h, small colonies are appearing. For some BACs, it can take more time until colonies are emerging (up to 40h). Check emerging colonies by colony PCR, to verify that the correct recombination event has occurred. Use primers which are located outside the homologous arms used for recombination, combined with primers located in the inserted selection cassette (**Figure 5**) Primers used originally to amplify the homologous arms (step 4) can be used as a negative control, since after recombination PCR amplification with these primers should no longer give the expected product (either a longer band is obtained, including the selection cassette, or no band at all if fragment becomes too large to be amplified efficiently). In general, we use two primer combinations, and choose a clone which is positive both on the 5' and 3' site. See Troubleshooting.
    (I) Pick 48 colonies (less can be enough to find correct clone), and mark and number them on the bacteria plate. Touch with a pipette tip the colony, and drop the tip in an Eppendorf tube filled with 20 µl dH_2O. If plate is too crowded to mark isolated colonies, touch complete colony with pipette tip, streak bacteria to a new plate with

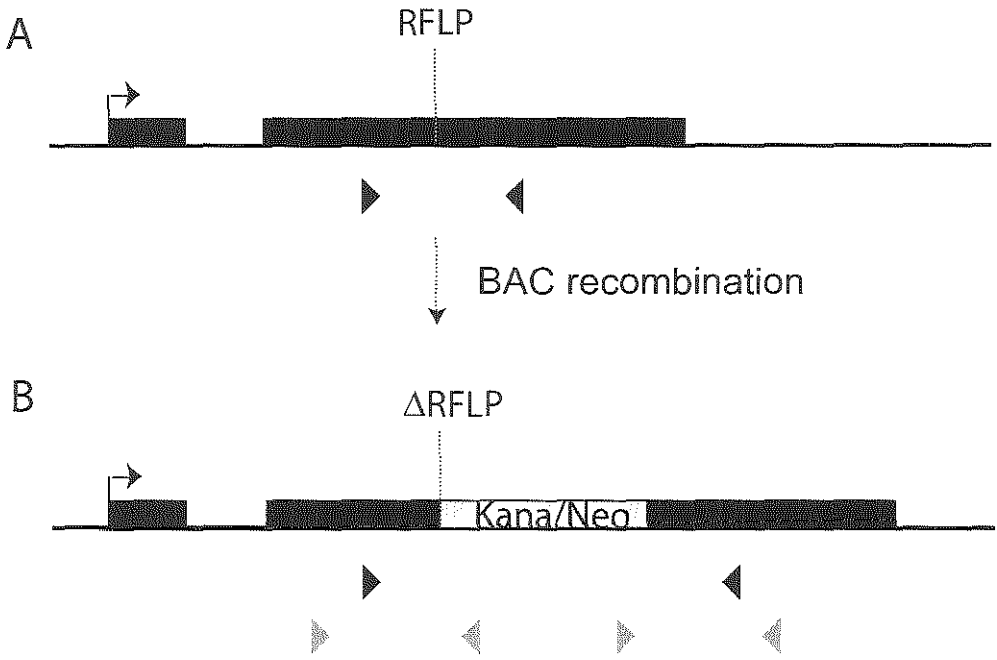

Figure 5: Primer location for colony PCR screen
A) Primers used to amplify the homologous arms surrounding the selected RFLP used for BAC recombination are indicated with the black arrow heads. **B)** After BAC recombination, the Kana/Neo cassette disrupts the RFLP. The primers used in **A)** will no longer amplify the genomic fragment, since insertion of the Kana/Neo cassette results in a fragment which is too long to be amplified using the same extension time. To check the colonies obtained after BAC recombination, the primer combinations shown in grey are used. These consist of primers located within the Kana/Neo cassette, and primers located outside the homologous arms. Therefore these primers do not amplify the targeting plasmid, but will only result in a band when recombination has occurred.

proper antibiotics, on a marked location, and then drop the pipette tip in dH_2O. Incubate the replica plate at 30°C for later use.

(II) Prepare a master mix for PCR, using a Taq polymerase of your choice. Take 1 µl of template, directly pipetting 1 µl from the Eppendorf tubes from (I) using the same pipette tip used to touch the colony, into the PCR plate.

Component	**Amount for 1 reaction**	**Amount for 50 reactions**
10x PCR buffer	2.5 µl	125 µl
$MgCl_2$ (50mM)	0.9 µl	45 µl
dNTP 1mM	1 µl	50 µl
Forward primer (100 pM)	1.25 µl	62.5 µl
Reverse primer (100 pM)	1.25 µl	62.5 µl
Taq-polymerase	0.4 µl	20 µl
dH_2O	16.7 µl	835 µl
Template	1 µl	
Total volume	25 µl	Divide 24 µl per well and add 1 µl template

41. Run PCR on a thermocycler, using the following parameters, where annealing temperature and extension time are dependent on the primer and fragment size, respectively:

Cycle	**Denature**	**Anneal**	**Extend**
1	98 °C, 2 min		
2-31	98 °C, 15 s	58 °C, 30 s	72 °C, 1 min
32			72 °C, 10 min
33			Hold at 12 °C

42. Separate the PCR amplified fragments on a 1% agarose gel, and choose several colonies which are positive for all primer combinations tested. Grow a mini-culture of these colonies at 30°C, shaking 200 rpm, starting from the marked bacterial plate or the replica plate, and isolate DNA through a BAC-mini protocol (step 34). Check by restriction digestion, whether BAC "finger-print" is still detectable. The "finger-print" might be modified by the recombination event, although the amount of DNA obtained with the BAC mini-prep protocol might be too low to definitively judge this. Critical point: any abnormal, especially high intensity bands, at this stage indicate that something went wrong with the recombination, or that the targeting fragment is still independently proliferating in the bacteria, thereby rendering the bacteria resistant to selection. See Troubleshooting.
43. Grow a maxi-culture (with the appropriate antibiotics) of two candidate clones containing the recombinant, modified BAC, and isolate BAC DNA as in step 22. Also make glycerol stocks (step 21). Check the isolated BAC DNA by different

restriction digestion reactions, to verify correct insertion of the targeting fragment. If all digests confirm the expected pattern based on the predicted, modified, sequence (step 1), the final BAC targeting vector for targeting of ES cells has been obtained. Pause Point: The BAC targeting vector can be stored for several months at 4°C, if required. A fresh preparation will however increase the targeting efficiency.

44. For targeting of ES cells, the final BAC targeting vector needs to be linearized, using digestion with PI-SceI (this restriction site is present in most available BAC-backbones). For one targeting, we use between 60-80 µg of DNA, which will be approximately 60-80 µl of BAC DNA derived from the BAC-maxi isolation. The amount of DNA obtained following the BAC isolation protocol is more or less constant (we estimate the concentration by restriction analysis of 1µl on an agarose gel), therefore digest BAC DNA as follows: 83 µl BAC DNA, 10 µl 10x PI-SceI buffer, 1 µl 100x BSA, 6 µl PI-SceI enzyme. Incubate at 37°C O/N, and inactivate enzyme at 65°C for 20 min. Store at 4°C until use. Critical point: BAC DNA can be very viscous, especially when freshly prepared. Use scissors to cut of the pipette tip. Linearized BAC DNA should be used soon after linearization.

Targeting of mouse Embryonic Stem cells Timing: 17 days

45. Detailed protocols on mouse ES cell culture have been described elsewhere [969-971]. Here we assume that the reader is familiar with the basics of ES cell culture, which are required to maintain ES cells in a pluripotent, undifferentiated state. Sterile culture techniques should always be applied. Both female and male hybrid C57Bl/6-Cast/Ei ES cell lines, have been described [958], are germ line competent, and will be made available upon request (**Table 2**).
46. Coat a 25 cm^2 cell culture flask with 0.2% Gelatin solution, and incubate for minimal 5 min at RT.
47. Thaw a vial of Mouse Embryonic Fibroblasts (MEFs, $2x10^4/ cm^2$), which function as feeder cells for ES cells. For long term storage both MEFs and ES cells are stored at -180 °C. Also defreeze a vial of ES cells. Put both vials in a 37°C water bath, until thawed. Clean vials with 70% ethanol, and transfer to cell culture hood. Transfer the content of both vials drop-wise to a 15 ml Falcon tube filled with 5 ml pre-warmed (37°C) ES cell medium, and centrifuge 5 min, 1000 rpm to remove the DMSO used for freezing. Critical point: MEFs can be prepared from day E13.5 mouse embryos [969], or can be purchased commercially.
48. Remove the gelatin from the cell culture flask. Resuspend the cell pellet from step 47 in 5 ml ES medium, and transfer to cell culture flask. Rock plate to homogenously spread the cells, and incubate in a cell culture incubator at 37°C, 5% CO_2.
49. Change medium daily. Small, sharp edged, doom-shaped colonies should appear on top of the feeder layer (**Figure 6**). Cells should become confluent after 3-4 days. If only a few colonies appear, cells must be split 1:1 (see below). See Troubleshooting.

line	strain	male/female	germline
E3	B6/Cast	♂	yes
E5	B6/Cast	♂	n.d.
E8	B6/Cast	♀	n.d.
E14	B6/Cast	♂	yes
E15	B6/Cast	♀	n.d.

Table 2: overview of available ES cell lines
Table summarizing the available C57Bl/6-Cast/Ei mouse ES cell lines. E3, E5 and E14 are male, whereas E8 and E15 are female. Several cell lines have been shown to be germ line competent. N.D.: not determined.

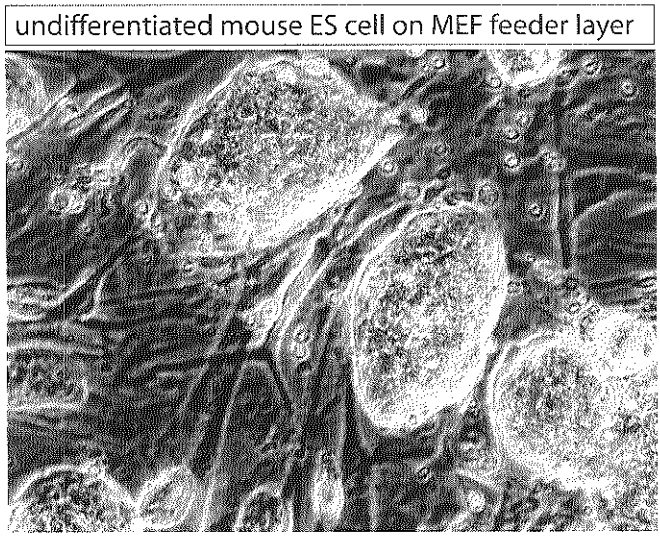

Figure 6: ES cell morphology
Morphology of mouse ES cell colonies grown on MEF feeders. Note the shiny edge and dome-like colony shape of the ES cells.

50. Split cells as follows:
    (I) Aspirate medium, and wash 2 times with cell culture PBS.
    (II) Remove PBS, and add 1.5 ml Trypsin-EDTA (pre-warmed at 37°C). Incubate at 37°C for 7 min. After 3.5 min, gently shake the plate to break up colonies.
    (III) After incubation, add 4 ml of ES cell medium to inactivate the Trypsin-EDTA. Pipette cells up- and down to obtain a single cell solution, and transfer cells to a 15 ml Falcon tube. Spin 5 min at 1000 rpm. See Troubleshooting.
    (IV) If cells will be passaged, resuspend cells in ES medium, and transfer to a new culture flask, already gelatinized, and coated with MEFs. If cells are used for targeting, proceed with the next step.
    (V) Wash cells with pre-warmed (37°C) DMEM, 5 min, 1000 rpm, to wash out the serum.
    (VI) Resuspend cells in 320 µl DMEM, and transfer to a 2 mm electroporation curvette (BTX). Add 80 µl of linearized BAC DNA (step 44) using a cut pipette tip, and carefully pipet up-and down a few times to mix cells and DNA. Critical point: precipitation of DNA after PI-SceI digestion, as found in many protocols is not needed, and does not increase targeting efficiency (our unpublished observations), and will lead to introduction of more DNA breaks in the BAC DNA.
    (VII) Electroporate cells at 118 kV, 1200 µF, ∞ Ω, using a Biorad Xcell pulser. Critical point: different settings might be optimal when using a different pulser. Optimization might be required.
    (VIII) Resuspend ES cells in 1 ml ES medium and plate to a 50 cm^2 dish, already gelatinized and coated with MEFs, in a total volume of 10 ml ES medium. Rock the plate, and place in cell culture incubator. Critical point: MEFs used for the targeting plate, and subsequent selection must be resistant against the antibiotic used.
51. After 24h, some death cells will be visible, but the majority of cells will have attached. Remove medium, and add ES cell medium with selection, depending on which resistant cassette was chosen for the generation of the BAC targeting construct (neomycin (Geneticin, G418), 270 µg/ml, active; puromycin, 1 µg/ml). See Troubleshooting.
52. Day 2 till day 14: change medium daily. After the first few days, cell death will be increasing, as selection starts. This will be more rapid for puromycin selection, whereas neomycin selection starts more gently. At the end of the first week, small resistant ES cell colonies should be emerging, which will grow larger over the next days. Critical point: if MEFs do not resist selection well (e.g. death cells, holes in the feeder layer), plate out additional MEFs on the selection plate, as these are crucial to keep ES cell colonies undifferentiated. See Troubleshooting.

Picking clones in 96-well plates for freezing and DNA isolation. Timing: 7 days

53. Expect to obtain between 50 and 200 clones, which can be picked approximately two weeks after electroporation. Emerging clones can to be picked and expanded when visible with the naked eye. To pick clones, proceed through the following steps:
    (I) Gelatinize two flat-bottom 96-well plates, by adding 50 µl 0.2% gelatin with a multi-channel pipette, and incubate minimal 5 min at RT
    (II) Defreeze a vial of MEFs, enough for a 50 cm^2 plate, as described in step 47. Resuspend the cells in 10 ml of ES medium (no selection).
    (III) Remove gelatin from 96-well plates. Label one plate with "DNA" and the other with "Freezing". Add 10 ml of ES medium to a disposable cell culture reservoir (reservoir), and pipette using the multi-channel pipette 100 µl of medium in every well of the "DNA" plate. Add 100 µl of MEF dilution (step II) to every well of the "Freezing" plate. Rock the plate to homogenously spread the cells, and put in cell culture incubator until use.
    (IV) Take a U-shaped bottom 96-well plate, and add 10 µl of cell culture PBS to every well using a reservoir and multi-channel pipette.
    (V) Place a microscope in the cell culture hood, and clean with ethanol.
    (VI) Place the plate with targeted ES cells under the microscope, and start picking colonies. Do not remove medium from this plate, as ES cells will stay better in ES medium. To pick a colony, use a P20 pipette and filter-tips to take up a single colonies in 2 µl, and transfer this to a well of the U-bottom shaped 96-well plate covered with PBS. It is convenient to pick 96 colonies (if available), as this amount, together with the high targeting efficiency of BAC targeting will almost certainly guarantee you at least one correctly targeted clone.
    (VII) When all 96 colonies have been picked, add 25 µl Trypsin-EDTA (pre-warmed at 37°C) using a reservoir and multi-channel pipette, and incubate at 37°C for 7 min. Shake the plate at half-time, to break-up the colonies.
    (VIII) Immediately add 165 µl ES medium to every well using a reservoir and the multi-channel pipette to inactivate the Trypsin-EDTA. Set the pipette at 100 µl and pipette a few times up- and down, to break up the colonies into single cells. Divide the 200 µl in every well over the "DNA" and "Freezing" plate prepared in step (III). Rock the plates, and place in incubator. Critical point: it is crucial to label both replica plates identically at this point, as later on one plate will be frozen, and the other one will be used to analyze the DNA. Mixing up at this point will ruin your complete targeting experiment, as you might defreeze the wrong clone later on.
54. The next few days, check clones daily, and change medium when turning yellowish. Usually, the "Freezing" plate will grow slightly faster, as in the "DNA"

plate cells grow without the feeder support. Also differentiation will occur in the "DNA" plates, but that will not affect the quality of DNA. See Troubleshooting.

55. When the "Freezing" plate becomes confluent (clones will have the same, normal ES cell morphology), the plate can be frozen as follows:
    (I) Aspirate medium, and wash two times with cell culture PBS.
    (II) Add 35 µl of Trypsin-EDTA (pre-warmed to 37°C), and incubate 7 min at 37°C. Shake the plate at half-time.
    (III) Add 80 µl ES cell medium to each well (using a reservoir and multi-channel pipet), and pipette cells up-and down a few times, to obtain a single cell solution.
    (IV) Add 115 µl 2x Freezing solution, and carefully pipette up-and down a few times using the multi-channel pipette.
    (V) Close lid of the plate, and wrap plate with a diaper. Immediately store at -80°C. Critical point: it is important not to freeze cells instantly, since this will result in cell death. By wrapping in the isolating diaper, the temperature of the plate will decrease more slowly. ES cells can be stored for a few months at -80°C, but for long term storage they should be placed at -180°C.

DNA purification in 96-well plates and PCR RFLP analysis to identify correct targeted clones Timing: 2 days.

56. The "DNA" plate should only be harvested when wells are really confluent. In general, this will be 3-4 days later than the "Freezing" plate. Depending on the strategy chosen, at this point it might be required to isolate RNA, to ascertain the loss of transcription of a downstream RFLP (SA-tpA strategy, option II, **Figure 2B**). To isolate RNA use Trizol reagent, isolate RNA, treat with DNAse, and prepare cDNA using Superscript III, according to manufacturer's instructions, and proceed to step 57. To obtain the DNA:
    (I) Remove the medium, by turning plate up-side down above the sink, and blot on a paper-tissue.
    (II) Add 100 µl of Low SDS lysis solution [972] supplemented with prot.K. Seal the plate using tape or a disposable adhesive and place at 37°C for minimal 4h.
    (III) Precipitate the DNA, by adding 100 µl isopropanol, seal the plate and shake, or incubate for 10 min on a plate shaker.
    (IV) Centrifuge plate 30 min, 4000 rpm at 4°C.
    (V) Remove supernatant by turning plate upside down, and blotting on a paper-tissue. Small DNA precipitations will be visible on the bottom of the wells.
    (VI) Wash with 100 µl 70% ethanol, and centrifuge plate 15 min, 4000 rpm at 4°C.
    (VII) Remove supernatant by turning plate upside down on a paper-tissue. Let plate dry until most ethanol has evaporated. Dissolve DNA in 20 µl 10mM Tris pH 7.4. To facilitate dissolving, seal plate, and put at 37°C for 2h. Spin plate down, and store at 4°C.

57. To analyze whether the expected targeting event has occurred, perform a PCR using primers spanning the RFLP. These can be the same primers used to amplify the homologous arms for BAC recombination in bacteria (step 4). Digest PCR product with the RFLP enzyme.
    (I) Perform a PCR using the same conditions as in step 4, and run the program from step 5. Take 1 µl of clone DNA or cDNA as template. Critical step: Since amount of DNA obtained might be low, using a high fidelity Taq polymerase can improve the results.
    (II) Precipitate the PCR products, by adding the following components to the PCR reaction: 50 µl PCR product, 4 µl tRNA (10 mg/ml), 6 µl 3M NaAc, pH 5.6. Mix, and add 150 µl ice cold 100% ethanol. Seal plate and shake vigorously.
    (III) Incubate plate at -20°C for 20 min, and centrifuge 30 min, 4000 rpm at 4°C.
    (IV) Remove supernatant by turning the plate upside down on a paper-towel. Precipitated DNA and tRNA will be visible at the bottom of the PCR plate.
    (V) Add 100 µl 70% ethanol, and wash 15 min, 4000 rpm at 4°C.
    (VI) Remove supernatant by turning the plate upside down on a paper-towel. Dry plate completely, until all ethanol has evaporated. Critical point: To facilitate removal of all ethanol traces, the plate can be placed at 37°C for a couple of hours.
    (VII) Prepare a master mix for the restriction digestion: for each sample, prepare 5 µl 10x buffer, 0.5 µl 100x BSA (if required), 0.25 µl RNAse (10 mg/ml), 1 µl of enzyme, in a total volume of 50 µl. Add 50 µl of the master mix to every well of the PCR plate. Seal plate, and incubate at 37°C for 2h.
    (VIII) Run digest on an agarose gel, and verify whether targeted RFLP is lost in several clones. Critical point: In non-targeted clones, PCR amplification of the RFLP fragment followed by restriction digestion will result in 3 bands: one higher molecular weight band corresponding to the allele which does not contain the RFLP restriction site, and two lower molecular weight bands, which represent the allele with the RFLP. If a correct targeting event has occurred, the RFLP will be destroyed by the insertion of the selection cassette. Therefore, PCR amplification followed by restriction digestion will only reveal the higher molecular weight band, which is undigested because of the absence of a restriction site. See Troubleshooting.
58. Select the candidate targeted clones based on the allele-specific PCR from step 57, and repeat the PCR analysis one more time, or with a different set of primers, to exclude the possibility that the non-digested pattern was obtained due to failure of restriction digestion. If pattern is confirmed, this indicates that clones were correctly targeted.

59. To defreeze the targeted clones, prepare a 24-well plate, coated with gelatin and plated with MEFs in ES medium (0.5 ml per well). Put the "Freezing" plate (step 55) from the -80°C at 37°C in a cell culture incubator, and wait until wells start to thaw. Pipette the 230 µl content of the well corresponding to the targeted clones into the 24-well plate. Take another 200 µl of ES medium, and pipette up-and down in the well of the "Freezing" plate, to collect all remaining cells, and add this to the 24-well plate. Incubate in a cell culture incubator.
60. Change medium the next day. It will take 4-5 days for the clones to recover. When confluent, split to a 6-well plate, and subsequently expand further and freeze stocks. Isolate new DNA, and confirm PCR results. See Troubleshooting.

Timing

Step 1-3, *In silico* design of strategy: 1 day
Step 4-17, Generation of targeting plasmid for BAC recombineering: 5-6 days
Step 18-44, BAC isolation and recombination: 12 days
Step 45-52, Targeting of mouse Embryonic Stem cells: 17 days
Step 53-55, Picking of clones in 96-well plates for Freezing and DNA: 7 days
Step 56-60, DNA purification in 96-well plates and PCR RFLP analysis to identify correct targeted clones: 2 days.

Troubleshooting

Step	Problem	Possible Reason	Solution
6	correct PCR fragment not obtained	- PCR did not work, pipetting error - primers are not working	- repeat PCR - try temperature gradient, to find better annealing temperature - order new primers
10	no colonies obtained	- wrong kanamycin concentration used -clean up of DNA prior to Topo reaction failed - Topo reaction or heat shocking went wrong	- ensure correct concentration is used - check concentration of DNA by Nanodrop, and put an aliquot on gel. - repeat Topo reaction. Transform a circular control plasmid. Hundreds of colonies should emerge if bacteria are competent.
12	-no DNA obtained -expected digestion fragments not present	-mini-prep went wrong -digest did not work -hidden restriction site present -wrong PCR fragment cloned	-check buffers. Did precipitation of proteins occur? -try new enzyme, repeat digest - check sequence and fragment size of different bands. Is total length as expected? - try new primers
16	-no colonies obtained -digestion gives unexpected bands	-wrong antibiotic, too high concentration -ligation did not work, concentration of DNA used too low -ligation did not work, CIP used for both vector and insert -ligation did not work, no blunt ends generated -CIP forgotten, self-closure of plasmid - wrong cassette fragment used -unexpected orientation	-ensure correct concentration is used, make new plates -check DNA concentration, and try again with higher concentration -isolate new fragments, and ligate again -try with new Klenow enzyme, new digestions. Are all overhangs suitable for Klenow enzyme? Try T4 polymerase as alternative -repeat digestions, blunting and ligation -check total size of plasmid. Try new ligations -check sequence. Can wrong orientation be used as alternative? Try new ligations. Sometimes inverted repeats are generated that will be selected against by the bacteria, therefore a certain orientation might always be obtained.
19	-no colonies obtained	-wrong antibiotic, concentration too high -BAC got degenerated while in traffic	-ensure correct concentration is used, make new plates -order new BAC clone

23	-no DNA obtained or only high molecular weight bands visible	- BAC has recombined, or only bacterial DNA has been isolated -digestion did not work -concentration of isolated DNA too low -BAC clone is wrong/recombined	-repeat isolation of a new, fresh culture. Follow protocol carefully. If failed again, try growing BAC at 30°C. Check buffers (pH?) - repeat digestion - add more DNA to digestion -order new BAC clone
31	-bacteria explode during electroporation	-salt concentration in DNA too high -wrong settings of pulser -bacteria not electrocompetent	- try less DNA. Try new BAC preparation -adjust correct settings -make new bacteria, try again
34	-BAC not transformed, or recombined	-bacteria grown at wrong temperature -BAC difficult to transform	-adjust temperature to 30°C - try again! Use fresh DNA
40	-no colonies obtained -plate is overgrown, too many colonies	-wrong concentration of antibiotic -recombination machinery not induced -problem with electroporation? - antibiotic for introduced resistance cassette forgotten? -targeting fragment is replicating and co-transfected in bacteria	-Ensure correct concentration is used -be sure that bacteria were put at 42°C for 20 min -see step 31 - check plates, and prepare new ones -ensure that Ori is deleted. Try other restriction digest to isolate the fragment
42	-PCR did not show expected bands	- pipetting error -primers are not optimal -extension time too short? -recombination did not work -wrong BAC?	-make new master mix, and try again -try different annealing temperature. -check PCR program -try new recombination. Check more colonies -verify that correct BAC is present, and no mix-up has occurred
49	-ES cells are not growing properly	- wrong medium? -FCS is not ES cell supportive -feeders do not support ES cells -few cells had been frozen -badly frozen vial? -mycoplasm infection?	-check medium composition. Make new medium if any doubts -try different batch of FCS -try different batch of feeders -give cells some time. Split 1:1. -defreeze another vial -test for mycoplasm. Treat if necessary, or try different, non-infected cell line, or earlier passage.
50	-no single cell suspension obtained	-medium not completely removed -Trypsin-EDTA too cold	-wash two times with PBS -pre-warm Trypsin-EDTA
51	-no viable ES cells left	-electroporation killed all cells -cells were plated in medium with selection -infection?	-try to optimize conditions for your pulser -only start selection after 24h -check for visible signs of infection: yellow medium, bacteria or yeast visible? Remove culture and start over again. Always use sterile culture techniques.

52	-too many or too less cells dying during selection	-wrong concentration of antibiotics used? -wrong concentration for cell line used?	-check concentration and adjust -perform a kill curve to find optimal range for your cells.
54	-clones are not growing	-see step 49	-see step 49
57	-expected PCR and digestion product not obtained	-isolation of DNA went wrong, concentration too low or too much ethanol left -PCR did not work -precipitation did not work -no correct targeted clone obtained	-check concentration of DNA and quality by nanodrop. If too low, maybe time point too harvest DNA was too early? Defreeze "Freezing" plate, and at next split, split new DNA plate. -repeat PCR with new master mix -repeat PCR, and test some samples on gel prior to precipitation. -bad luck, start again. Consider changing construct, as particular genomic region might be difficult to recombine?
60	-thawed clones do not have the correct PCR bands after repeat of analysis to confirm generation of targeted cell line	-PCR did not work -a mix-up has occurred, wrong clone thawed	-repeat again -take a week off, and start new targeting experiment!

Anticipated results

Using our strategy, we have recently generated targeted alleles for the X-linked genes *Rnf12* and *Xist* [174, 911]. RNF12 is an X-linked, dose dependent activator of X chromosome inactivation, which is an important epigenetic process resulting in the transcriptional shut down of one X chromosome in all mammalian female cells. By generating heterozygous *Rnf12*+/- ES cells, we could show *in vitro* that RNF12 acts as a crucial, dose dependent activator of *Xist* which is the master regulator of X chromosome inactivation. By targeting the second allele, generating a homozygous *Rnf12*-/- ES cell line, we obtained evidence that RNF12 is crucial for the initiation of X chromosome inactivation. Furthermore, by generating a targeted deletion of the *Xist* intron 1 region using the same RFLP-based strategy, we could show that pluripotency factor binding to the *Xist* intron 1 region is not essential for *Xist* repression in undifferentiated ES cells. In the latter targeting, we designed homologous arms for BAC recombineering in such a way, that a 2.1 kb region of the BAC was replaced by the insert selection cassette, thereby showing that our strategy can also be used to generate deletions. Although this approach requires an additional cloning step during the generation of the targeting plasmid, it offers an interesting possibility when insertional mutagenesis is not favored.

In our BAC recombineering step, we found that between 70-100% of bacteria colonies are positive for the correct integration of the selection cassette. This high efficiency, combined with the ease of the protocol, allows the generation of multiple constructs for different genes at the same time, within a short time frame. Using the BAC targeting approach, we have obtained higher targeting efficiencies compared to our

previous experience with conventional targeting constructs [179]. By targeting 4 different loci within the *Rnf12* gene, we found that between 3 and 12% of our obtained ES cell clones are correctly targeted [958]. We are currently applying a similar strategy to a type of human iPS cells (hLR5 cells [973]), where we have found similar targeting efficiencies (our unpublished observations). The generated targeted ES cell lines can be used for *in vitro* experiments, or can be used for blastocyst injections or for tetraploid embryo complementation to generate mouse models [912, 964-967]. If required, the second allele can subsequently be targeted *in vitro*, or can be intercrossed in the obtained mice. When *in vitro* targeting is required, a BAC construct is generated using a BAC library isogenic for the second allele. The same targeting arms can be used, but need to be ligated to a different selection cassette (e.g targeting one allele with neomycin, and the second one with puromycin). The RFLP screen in targeted ES cell clones then consist of detection of complete absence of the PCR product spanning the original RFLP used, since both the first and second targeted allele will be modified by insertion of the targeting cassette.

The use of hybrid C57Bl/6-Cast/Ei ES cells allows the use of a plethora of available RFLPs for targeting, but might offer disadvantages for certain studies where the genetic background of knockout mouse models is important. Therefore some backcrossing might be required for certain studies. We have currently developed other hybrid ES cells from several other strains, which might circumvent this problem in the future. In other fields, it might even be beneficial to use hybrid ES cells or mice, since polymorphisms can be used to trace parental gene expression. Combined with the many possibilities offered by BAC recombineering, the high efficiency of BAC targeting approaches and our straightforward readout, BAC targeting to generate knockout alleles has become our method of choice to manipulate the mouse genome.

Acknowledgments

We would like to thank all past and present laboratory members for helpful suggestions and fruitful discussions. Work in the Gribnau lab is supported by funding from the Dutch Research Council (NWO-TOP and –VICI and an ERC-starting grant to J.G.)

Chapter 4

X-changing information on X inactivation

This chapter has been published in

Tahsin Stefan Barakat, Iris Jonkers, Kim Monkhorst and Joost Gribnau (2010)
"X-changing information on X inactivation"
Experimental Cell Research 316:679-687

X-changing information on X inactivation

Tahsin Stefan Barakat[1], Iris Jonkers[1,2], Kim Monkhorst[1,3] and Joost Gribnau[1,4]

[1]Department of Reproduction and Development, Erasmus MC, University Medical Center, Rotterdam, the Netherlands, [2]Current address: Department of Molecular Biology and Genetics, Cornell University, Ithaca, USA, [3]Current address: Department of Pathology, Erasmus MC, University Medical Center, Rotterdam, the Netherlands, [4]corresponding author

Contact details:
Joost Gribnau
Department of Reproduction and Development, Room Ee 09-71
Erasmus MC
PO Box 2040, 3000 CA Rotterdam
The Netherlands
Phone +31-10-7043069
Fax +31-10-7044736
Email: j.gribnau@erasmusmc.nl

Abstract

In female somatic cells of mammalian species one X chromosome is inactivated to ensure dosage equality of X-encoded genes between females and males, during development and adulthood. X chromosome inactivation (XCI) involves various epigenetic mechanisms, including RNA mediated gene silencing in *cis*, DNA methylation, and changes in chromatin modifications and composition. XCI therefore provides an attractive paradigm to study epigenetic gene regulation in a more general context. The XCI process starts with counting of the number of X chromosomes present in a nucleus, and initiation of XCI follows if this number exceeds one per diploid genome. Recently, X-encoded RNF12 has been identified as a dose-dependent activator of XCI. In addition, other factors, including the pluripotency factors OCT4, SOX2 and NANOG, have been implicated to play a role in suppression of initiation of XCI. In this review, we highlight and explain these new and old findings in the context of a stochastic model for X chromosome counting and XCI initiation.

Introduction

In mammalian species the dosage of X-linked genes is equalized between XX females and XY males by inactivation of one of the two X chromosomes in every female cell [30]. In mouse, X chromosome inactivation (XCI) is present in two forms. In the extra-embryonic tissues XCI is imprinted, with the paternal X chromosome (Xp) being inactivated in all cells [53]. This process is initiated very early during development, around the two- to eight-cell stage [51-52], and is maintained in the developing extra-embryonic tissues of the embryo, including the fetal placenta. In contrast, the Xp is reactivated in the inner cell mass (ICM), which gives rise to the embryo proper, after which random X inactivation is initiated around day 5.5 of development. After the inactive X chromosome (Xi) is established by random XCI of either Xp or Xm, this inactive state is propagated clonally. Also in the human embryo proper, XCI is random and initiated early during development [368]. Whether the imprinted form of XCI is present in the early human embryo is not clear, and conflicting reports claim either the presence or absence of imprinted XCI in human extra-embryonic tissues [369-370, 373-374, 376].

In mouse, two X-linked genes, *Xist* and *Tsix*, have been identified to play an important role in XCI [84-86, 93-94, 119]. Both genes were mapped to the X inactivation center (Xic, **Figure 1**), that was determined by genetic studies revealing a maximum region of 10 megabases on the X chromosome required for XCI [72, 974]. Although *Xist* is a non-coding gene, the *Xist* transcript is spliced and poly-adenylated. Accumulation of processed *Xist* RNA on the Xi in *cis* is a decisive factor leading to inactivation. *Tsix* is transcribed anti-sense to *Xist* and overlaps completely with *Xist* [118]. *Tsix* transcripts are also spliced and poly-adenylated, and *Tsix* transcription is initiated at different promoters. *Tsix* and *Xite*, the latter acting as an enhancer of *Tsix* [136], are both transcribed from the active X chromosome (Xa) before and at the onset of XCI, and are involved in down-regulation of *Xist*, counteracting X inactivation. The XCI process involves different phases, starting with a counting and choice process which includes determination of the number of X

chromosomes and the choice which X will be inactivated. Subsequently, the Xi is established through recruitment of different chromatin modification complexes, and the silent state is then maintained through an almost unlimited number of cell divisions, throughout development and adult life [33]. In this review, we will focus on the mechanisms directing the XCI counting and choice process. For a detailed description of mechanisms involved in the establishment and maintenance we refer to a complementary recent review [975].

Counting and initiation of X inactivation

XCI is initiated if the number of X chromosomes exceeds one per diploid genome set. In the female embryo proper, and also in differentiating female ES cells in culture, the choice is random with respect to the parental origin of the X to be inactivated. Several genes and chromosomal regions have been attributed to be involved in the counting process. Removal or addition of regions involved in counting can lead to complete or partial loss of initiation of XCI in female cells, or an opposite effect, leading to XCI on both X chromosomes in female cells, or even initiation of XCI in male cells. Transgenic male ES cell lines with autosomal insertions of small transgenes (30-80kb) covering *Xist* and *Tsix*, or *Xist* alone revealed, besides autosomal spreading of transgenic *Xist* in *cis*, ectopic XCI of the single X chromosome in a significant proportion of cells [167, 169]. This indicated that gene(s) or elements(s) involved in determining the number of X chromosomes may be located within the region covered by these transgenes. Different male *Tsix* mutant ES cell lines indeed displayed initiation of XCI on the single X chromosome, which suggested a direct role for *Tsix* in the XCI counting process (**Figure 1**) [123, 127, 178]. Interestingly, the same mutations did not affect counting in heterozygous female cells, which almost exclusively inactivate the mutated *Tsix* allele [119-120].

Studies with female cell lines and mice with deletions of parts of *Xist* showed that *Xist* is required for XCI to occur in *cis* [93-95]. However, *Xist* transcription and the deleted part of the *Xist* gene are not involved in the counting process because initiation of XCI in heterozygous female *Xist* mutant cells still occurred on the wild type X chromosome [104, 176-177]. We recently deleted a region spanning more than 60 kb including *Xist*, *Tsix* and *Xite* (ΔXTX) from one X chromosome in female cells [179]. As for the studies which involved *Xist* sequences alone, female cells with a heterozygous deletion of this region still initiate XCI on the wild type X chromosome. These findings indicate that *Xist*, *Tsix* and *Xite* affect the choice process by playing an important role in 'in *cis*' inactivation, but are not required for 'in *trans*' communication regulating the counting process. This is also supported by our findings that BAC transgenes covering *Xist* or *Tsix* alone or both *Xist* and *Tsix* do not induce XCI on the endogenous X, which contrasts previous reports,and suggest that *Xist* and *Tsix* may only play a marginal role in the counting process. The results obtained with the heterozygous ΔXTX ES cells and studies with BAC and YAC transgenes also indicated that factors involved in the counting process are located outside the region covering *Xist*, *Tsix* and *Xite* [166, 175, 187].

Models for XCI counting and choice

The initial step in the XCI process has always been viewed to be the result of a mutual exclusive choice process leading to inactivation of only one X chromosome in every female

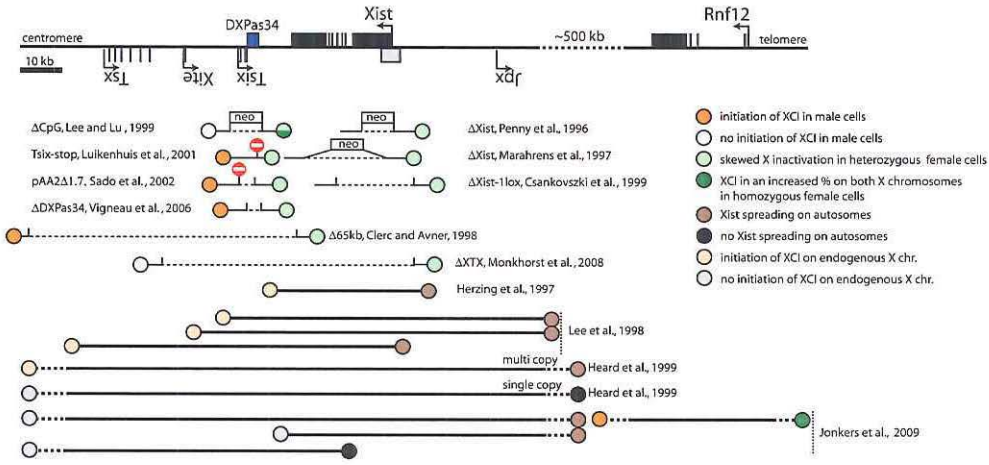

Figure 1: *Xist* and *Tsix* mutations and transgenes
Schematic representation of part of the Xic, including the location and size of the different *Xist* deletions, and *Tsix* deletions and stop cassettes described in this article (thin dashed line represents the sequence removed). The colored circles indicate the results obtained. The relative size and location and experimental findings of the cosmid and BAC sequences covering *Rnf12*, *Xist* or *Tsix* alone, or *Xist* and *Tsix* used in transgenic studies are shown below (thick dashed line represents sequences not shown on the map).

cell. Several models have been postulated that explain the XCI process based on this assumption. The blocking factor (BF) model states that a limiting factor blocks XCI on one X chromosome in a diploid cell; either one of the two X chromosomes in female cells or the single X chromosome in male cells [72]. The cell is able to count, because the BF is encoded by an autosomal gene, and thus the excess of autosomes over X chromosomes determines whether enough BF is present in order to inhibit XCI on one X chromosome in a diploid background. The putative BF binds an element in the Xic that prevents *Xist* to accumulate on that X chromosome in *cis*. However, if this allele is impaired for XCI, because *Xist* is deleted for example, then the cell should not be able to inactivate, which would result in death of half the cell population. In contrast, cells with a heterozygous *Xist* deletion all make the right choice and initiate XCI on the wild type X chromosome, resulting in primary non-random XCI [176-177]. Therefore, a positive XCI factor was hypothesized, named the competence factor (CF). One model comprising the combined action of a BF and CF postulates that the abundantly present CF inactivates all X chromosomes but not the one to which BF is bound [177]. Another hypothesis states that also the X-encoded CF is limiting and is titrated away by one 'copy' of the autosomally-encoded BF, which corresponds to a single X chromosome. When more than one X chromosome is present in a diploid background, the extra copies of CF will not be titrated by the BF, and will inactivate the remaining unprotected X chromosome(s) [119, 976].

The main problem of the BF model is that a single entity, acting as a single 'copy' or molecule, is present in a diploid cell, which binds only one X chromosome. Cell-to-cell variegation is likely to make such a system unstable. A model in which not one entity, but many factors bind only one of two X chromosomes in a female diploid cell would

overcome this problem [164-165]. The so-called symmetry-breaking model that follows from this, states that blocking complex, composed of many autosomally encoded molecules that will bind to the DNA and itself through self-assembly, will form on one X chromosome at the onset of XCI. Computational analysis shows that self-assembly is energetically more favorable on only one X chromosome in a nucleus, rather than on two. Unfortunately, evidence of formation of such a complex, on the active X and at the onset of XCI, has not been presented yet.

Unlike the blocking factor models, the alternate state model postulates that the choice of an X chromosome to be inactivated is intrinsically determined by the chromatin state of the X prior to XCI [181]. The nature of this chromatin state is unknown, but can be determined by allelic cohesion differences present after DNA replication. An X chromosome with sister chromatids in more close proximity is more prone to XCI than an X with sister chromatids farther apart [181]. Differences in sister chromatid cohesion may reflect local *Xist* spreading in *cis*, which could be transient but is locked in at the onset of XCI, thereby ensuring random XCI. However, the reported correlation is not absolute, and also in cells that show primary non-random X inactivation, due to *Xist* or *Tsix* deletions, the ratio between cells with either more separated or more closely associated sister chromatids changes marginally, arguing against a direct involvement of sister chromatid cohesion in XCI choice.

A different model is based on the observation that co-localization, or pairing, of the Xics of the two X chromosomes in XX ES cells precedes XCI. This get-together of the X chromosomes is very transient and can only be observed in a subset of cells, but does occur more frequently than what would be expected from random co-localization of the Xics [182-183]. Several regions within the Xic are involved in pairing. A *Tsix* or *Xite* deletion in female ES cell lines results in loss of pairing and loss of random XCI [182-183, 185]. However, single copy *Xist/Tsix/Xite* transgenes cannot induce X-autosome pairing [182], indicating that another pairing region is crucial for initiation of XCI. Indeed, a BAC sequence located ~400 kb upstream of *Xist* was found to pair with other copies of the same region, and to induce *Xist* transcription in male ES cells when randomly integrated [187]. This region was named the X-pairing, *Xpr*, region, and it was suggested that the *Xpr* region is essential for sensing the presence of more than one X chromosomal allele and subsequent initiation of XCI. In this model, pairing of the *Tsix* and *Xite* region between two X chromosomes provides a feedback loop to prevent inactivation of the second X chromosome [187]. *Trans*-acting factors suggested to be involved in the proposed pairing are CTCF and OCT4. Knock-down of both CTCF and OCT4 was reported to counteract the pairing, but whereas knock-down of CTCF in female cells results in reduced initiation of XCI, knockdown of OCT4 results in inactivation of both X's in an increased number of female cells [185-186]. This indicates that the pairing model might not be the best model to explain random XCI. Interestingly, it was observed that transcriptional activity of *Tsix* and *Xist* is another requirement for pairing [185]. When DNA polymerase II transcription is inhibited, pairing of the *Tsix* and *Xist* regions is lost [977]. This result might indicate that the pairing events observed are not the cause of XCI, but a consequence of transcriptional activation of *Xist* and flanking genes at the onset of XCI, which may result in relocation of the Xic in the nucleus.

A stochastic model for initiation of XCI

All the above mentioned models predict a mutual exclusive and deterministic XCI process, in which a single X is inactivated in every female cell. Interestingly, *in vivo* and *in vitro* studies indicate that this is not the case. *In vivo* studies with diploid and tetraploid XX and XXXX embryos indicated the presence of a substantial population of cells with too many Xa's [162]. *In vitro* studies performed by us and others with diploid and tetraploid ES and ICM cells confirmed this finding, and also revealed a significant percentage of cells with too many Xi's [179, 188]. Cells with too many Xi's have to a lesser extent also been reported in embryos, but selection against these cell types is most likely more stringent than cells with too many Xa's. The fact that XCI is almost never initiated in diploid XY and tetraploid XXYY cells, indicates that initiation of XCI on too many X chromosomes in diploid XX and tetraploid XXXY and XXXX cells cannot be attributed to noise in the counting and initiation mechanism. Based on these findings we have proposed a stochastic mechanism directing the XCI process, in which every X chromosome has an independent probability to initiate XCI, eliminating the requirement for a choice process [179]. Comparison of the relative number of cells that initiated XCI between different diploid, triploid and tetraploid ES cells indicates that the X to autosome ratio determines the probability for an X chromosome to be inactivated [189]. The probability is most likely the resultant of one or more X-encoded XCI-activators and autosomally encoded XCI-inhibitors that promote or repress *Xist* accumulation, respectively. Upon development or differentiation, the concentration of the XCI-activator will rise and/or the concentration of the XCI-inhibitor will drop, and in female cells this will be sufficient to generate a specific probability in time for enough *Xist* to accumulate and start to spread in *cis* (**Figure 2A**). The XCI-inhibitor is involved in setting up a threshold that has to be overcome by *Xist* to accumulate. Because the XCI-activator gene is X-linked, spreading of *Xist* will down regulate the XCI-activator gene(s) in *cis* to a level below the threshold, thereby preventing the second X chromosome from inactivation. In this model, initiation of spreading is a stochastic event, so that the chance for silencing of the XCI-activator gene(s) on either X is equal, if not influenced by differential allelic properties of the individual X chromosomes. In male cells the concentration of the XCI-activator will not be sufficient to break the threshold and initiate XCI. Studies with female cell lines and mice that harbor *Xist* or *Tsix* mutations that affect the expression of one of the genes indicate that *Xist* and *Tsix* are the major players in setting up the probability, and that the XCI-activators and XCI-inhibitors are likely to act through these genes. Recently, we and others have identified several genes encoding one XCI-activator and several XCI-inhibitors.

XCI-activators and -inhibitors

In a stochastic model for XCI, preferential and timely initiation of XCI in female cells is obtained through a sex-dependent dosage difference in one or more X-encoded XCI-activators that promote *Xist* accumulation. An XCI-activator can act directly on transcription initiation of *Xist*, and/or in an indirect manner, by suppression of *Tsix* expression (**Figure 2B**). Several findings supported the presence of one or more XCI activators. Luciferase transgenes linked to an *Xist* promoter are higher expressed in female compared to male cells [89]. Also, female cells with a heterozygous deletion of the region encompassing *Xist*, *Tsix* and *Xite* still initiate XCI, indicating that an additional X-encoded

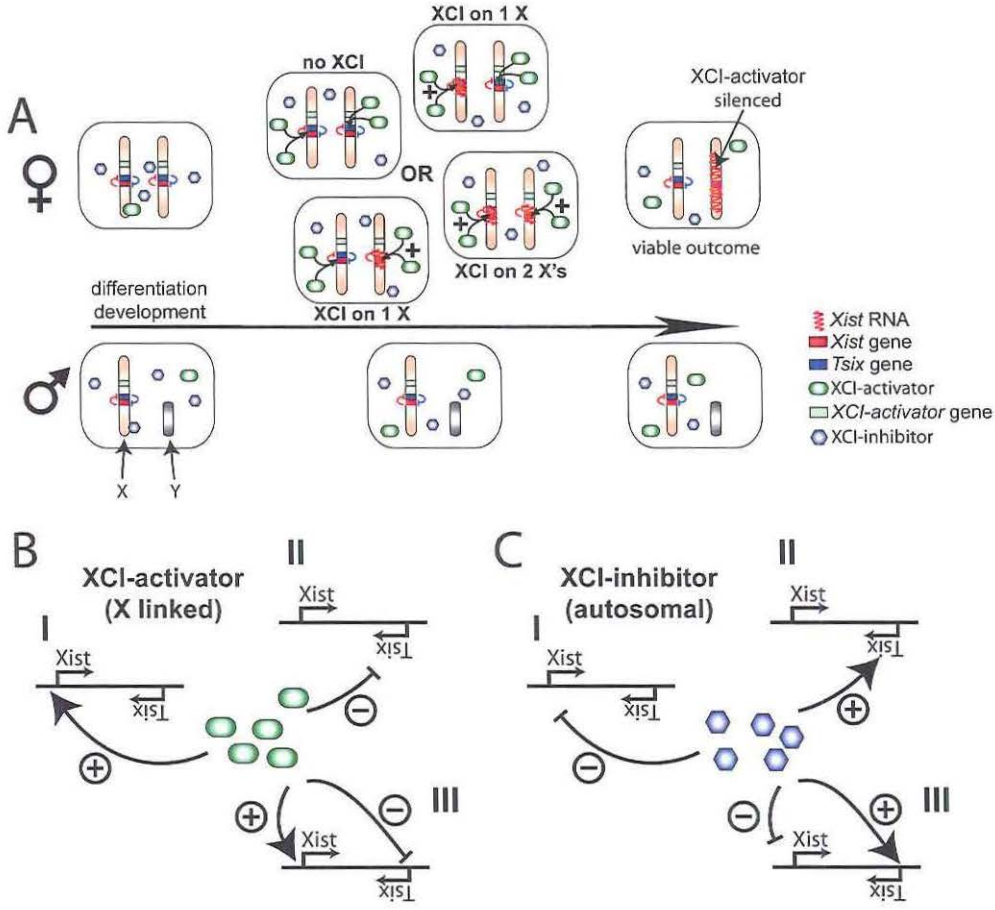

Figure 2: A stochastic model for XCI
A) Upon differentiation or development the concentration of the XCI-activator increases (green), or the concentration of the XCI-inhibitor drops (blue), or a combination of these changes occurs (both options are shown). As a result, in female cells and not in male cells, accumulation of *Xist* in *cis* (+) is initiated with a specific probability (arrows, all four possible outcomes are shown). *Xist* mediated silencing of the XCI-activator gene in *cis* and a subsequent drop in the XCI-activator concentration prevents initiation of XCI on the second X. **B)** XCI-activators can act by activation of *Xist* (I), by suppression of *Tsix* (II), or through both mechanisms (III). **C)** XCI-inhibitors can act by suppression of *Xist* (I), by activation of *Tsix* (II), or through both mechanisms (III).

protein or X-linked element is involved in XCI [179]. Furthermore, XCI initiation in cells with different X-to-autosome ratios displays a correlation between the rate of initiation and the X:A ratio, also supporting the presence of an X-encoded activator of XCI [189].

We recently identified X-encoded RNF12 as a dose-dependent XCI-activator [174]. Transgenic expression of additional copies of the *Rnf12* gene result in ectopic initiation of XCI on the single X in male cells and on both X's in an increased percentage

of female cells. *Rnf12* expression and over-expression correlates with initiation of XCI, and heterozygous *Rnf12*+/- female ES cells displayed reduced initiation of XCI upon differentiation. *Rnf12* encodes the E3 ubiquitin ligase RNF12 (RLIM), involved in the regulation of LIM-homeodomain transcription factors, telomere length homeostasis, and estrogen receptor alpha (ERα signaling; however, none of the known targets or partners of RNF12 have been implicated in XCI. These findings indicate a versatile role for *Rnf12* in embryonic development, and suggest that the regulation of XCI piggybacks onto existing developmental mechanisms. Although our findings indicate that RNF12 is an important XCI-activator, they also indicate that more XCI-activators are involved. X-chromosomal regions potentially harboring XCI-activator genes are the recently identified *Xpr* region, and regions including *Xist* and *Tsix*. However, in the same study we could not detect any effect of transgenes covering the *Xpr* and *Xist/Tsix* regions on initiation of XCI on the endogenous X chromosome(s), and we suggest that additional genes encoding XCI-activators will be located more distal to *Rnf12* or proximal to *Tsix*.

An inhibitor of XCI is most likely autosomally encoded, and will be involved in activation of *Tsix* expression and/or direct repression of *Xist* (**Figure 2C**). Among the proteins involved in *Tsix* regulation are the insulator protein CTCF and the transcription factor yin yang 1 (YY1), for which several tandemly organized binding sites have been identified both in the *DXpas34* region, which is involved in *Tsix* regulation, and the *Xite* promoter. Knockout studies involving *Yy1*, or partial ablation of *Yy1* and *Ctcf* through RNAi mediated repression, revealed down-regulation of *Tsix* expression and concomitant up-regulation of *Xist* expression, supporting a role for YY1 and CTCF in *Tsix* expression [193]. Proteins initially implicated to act directly on *Xist*, bypassing *Tsix* mediated repression, are the pluripotency factors SOX2, NANOG and OCT4. ChIP experiments have identified binding sites for these factors in intron 1 of *Xist*, and *Nanog* deficient ES cells showed up-regulation of *Xist* [191]. Up-regulation of *Xist* precedes down-regulation of *Tsix*, suggesting a *Tsix* independent mechanism for these three pluripotency factors in suppression of *Xist*. Interestingly, a different study indicates that OCT4 also binds the *DXPas34* element and the *Xite* promoter, and interacts with CTCF suggesting that OCT4 also acts in a *Tsix* dependent pathway [186].

Determining the probability to initiate XCI

XCI-inhibitors are expected to set up the threshold that has to be overcome by *Xist* to allow accumulation and silencing in *cis*. *Tsix* knockout studies have indicated that *Tsix* is an important player in setting up the in *cis* threshold for *Xist* accumulation. *Tsix* is involved in accumulation of chromatin modifications at the *Xist* promoter [89, 111], and anti-sense transcription through the *Xist* promoter is required for proper *Xist* suppression [112]. Whether the action of *Tsix* and accumulation of histone modifications at the *Xist* promoter involves a small regulatory RNA pathway, in which factors such as Dicer are involved, remains speculative and is still a matter of debate [132-134]. OCT4, SOX2 and NANOG-mediated silencing of *Xist* appears to act both in *Tsix*-dependent and -independent pathways, indicating that different mechanisms are involved in setting up the threshold. Sex-specific initiation of XCI, however, can never be accomplished only by autosomally encoded factors such as SOX2, OCT4 and NANOG, because the concentration of these factors is most likely the same in male and female cells (unless their concentration would

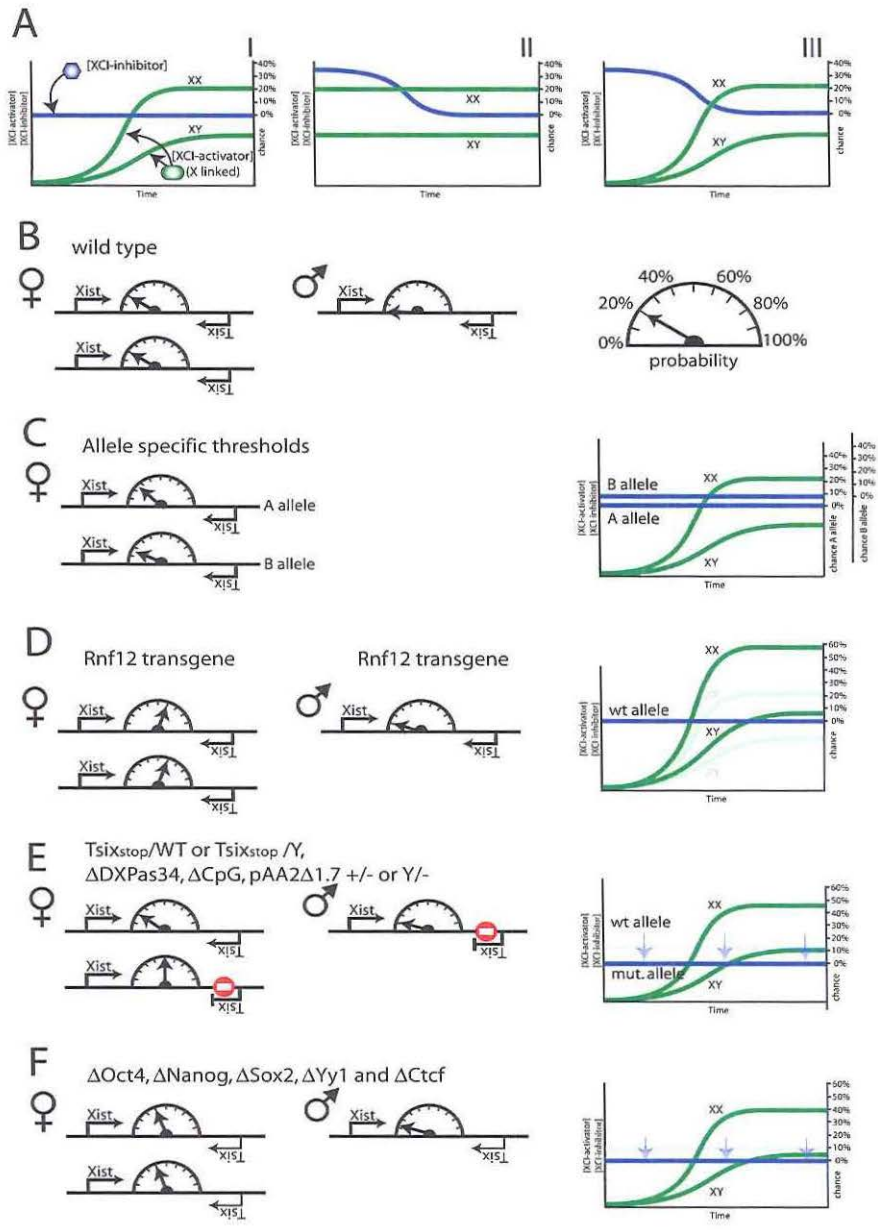

Figure 3: Determining the probability

A) Three possible mechanisms to determine the probability to initiate XCI. I) The concentration of the X-encoded XCI-activator increases in time upon onset of ES cell differentiation or in development (green line), and only in female cells the concentration is sufficient to break a stable threshold (blue line) required to generate a probability to initiate XCI. The probability shown on the Y-axis is an estimated

be regulated by an X-encoded factor). Key to the counting and initiation process is therefore the presence of X-encoded activators such as RNF12 that are differentially expressed between male and female cells. We have found that upon differentiation of ES cells, the concentration of RNF12 increases, and the concentration of other XCI-activators may increase as well. In contrast, the concentration of XCI-inhibitors will decrease during differentiation, as indeed was found for OCT4, SOX2 and NANOG, or might stay the same, as observed for YY1 and CTCF. Most likely, different combinations of changes are involved (**Figure 3A**, [978]). The combined changes will lead to increased *Xist* expression, either because XCI-activators activate *Xist* or suppress *Tsix*, or exert an effect through both mechanisms (**Figure 2B**). Currently, we do not know whether RNF12 acts through *Xist*, *Tsix* or both.

In one model, *Tsix* suppression is *Xist* independent, and stochastic inactivation of *Tsix* through the action of RNF12 and/or other XCI-activators allows accumulation of *Xist* and subsequent silencing in *cis*. Autonomous silencing of *Tsix* in male cells during ES cell differentiation indeed supports a mechanism in which *Tsix* is down-regulated independent of *Xist*. On the contrary, a mechanism by which *Tsix* is silenced though the action of *Xist* is supported by the finding that increased expression of *Xist*, effectuated by insertion of a neo cassette upstream of the *Xist* promoter, increases the probability for the mutated X chromosome to be inactivated [104]. In a model where *Xist* silences *Tsix*, *Xist* gene transcription activation depends on the concentration of RNF12 and other XCI-activators and is stochastic, thus resulting in increased bursts of RNA polymerase II activity initiated in one time frame. On the contrary, transcription initiation of *Tsix* is constant or decreases in time. In the battle between *Xist* and *Tsix*, *Xist* transcripts are more likely to reach the poly-adenylation sequence, resulting in a stabilized transcript, which will aid *Xist* mediated silencing of *Tsix*. Either mechanism or a combination of the two may be applicable to explain the XCI counting and initiation process. So far there is no clear evidence whether *Tsix* silencing at the onset of XCI is mediated by *Xist* or not, and further experimental evidence needs to be obtained to answer this question.

Figure 3: continued
cumulative probability of one day. II) The XCI-inhibitor concentration drops in time, lowering the threshold. The XCI-activator concentration is constant but is twice as high in female compared to male cells, which is sufficient to generate a probability to initiate XCI only in female cells. III) A combination of mechanisms I and II. **B)** In wild type female cells the concentration of the XCI-activator is sufficient to generate a probability to initiate XCI on both X chromosomes (left). In male cells the XCI-activator concentration is too low for XCI to be initiated (middle). The probability scale is shown on the right. **C)** In cells with two different alleles for instance due to SNPs, the alleles show differential *Xist* or *Tsix* expression and allele specific thresholds (blue lines) determine the probability to initiate XCI. **D)** In male (left) and female cells (middle) with a transgene covering *Rnf12* or another XCI-activator gene, the concentration of RNF12 and the other XCI-activator(s) is increased leading to an increased probability to initiate XCI in male and female cells. The graph to the right shows the threshold level and the XCI-activator concentration in transgenic (green line) and wild type (light green line) male and female cells, according to mechanism I from A (graphs for the other mechanisms are not shown). **E)** In heterozygous and hemizygous *Tsix*-stop, ΔDXPas34, ΔCpG and pAA2Δ1.7 cells the allele specific threshold of the mutated allele is lowered (blue line), resulting in an increased probability for this allele to initiate XCI. Note that the probability for the mutated allele to initiate XCI is higher in female compared to male cells. **F)** In cells with a reduced concentration of OCT4, NANOG, SOX2, YY1 and CTCF, the threshold is lowered (blue lines), resulting in an increased probability to initiate XCI for both X chromosomes in female cells, and for the single X in male cells. Also here the probability in female cells is higher compared to male cells.

In female cells, and not in male cells, the concentration of RNF12 and other XCI-activators is expected to be sufficient to generate a probability to initiate XCI on each X chromosome. This probability is expected to be modest, but in the time window where XCI can be initiated, it will be continuously present until XCI is initiated on one or more X chromosomes, resulting in silencing of the XCI-activator genes in *cis* and a drop in the concentration of RNF12 and other XCI-activators and the probability to initiate XCI. This feedback mechanism prevents XCI on the second X in female cells, and the *Xist* promoter on this Xa will be silenced through persistent expression of *Tsix* (similar to *Xist* in male cells). Silencing is most likely consolidated by chromatin modifiers and the action of DNA methyl transferases DNMT1, DNMT3a, and DNMT3b [89, 113-114, 298]. On the Xi, *Tsix* is silenced, and it is expected that a lower concentration of RNF12 and other XCI-activators is sufficient to maintain *Xist* expression on this X chromosome.

Predictions of a stochastic model

A stochastic model for XCI predicts that every X chromosome in a nucleus has a probability to initiate XCI [179]. Using a computer simulation model we have been able to match experimentally obtained data with differentiating female XX ES cells using a probability that plateaus at a ~20% per day probability to initiate XCI for each X chromosome in a female diploid cell [189]. Applying a lower or higher probability results in too many cells with two Xa's or Xi's, respectively. Nevertheless, also with a probability of 20% a significant percentage of cells in our simulations end up with two Xa's or Xi's, resulting in a reduced number of female cells compared to male cells (12% reduction). Studies of early mouse embryos indeed indicate that female embryos are significantly smaller than male embryos between 6.5 and 10.5 dpc [979]. This effect is also present in a comparison between XO and XX female mice, suggesting a role for XCI related cell death in the reported size difference.

Besides the balance between the XCI-activator and -inhibitor concentrations that determine the probability of XCI in *trans*, allele specific thresholds will be involved in setting up the probability for each X chromosome in *cis* (**Figure 3B** and **C**). Promoter SNP's or mutations affecting transcription initiation of *Xist*, *Tsix* or *Xite*, will have an effect on the probability to initiate XCI. Indeed, a SNP in a domain of the human *XIST* promoter implicated in CTCF binding results in complete skewing of XCI in favor or against inactivation of the polymorphic allele depending on the nucleotide change [452]. Similarly, mouse *Xist* and *Xite* promoter SNPs have been reported to co-segregate with skewing of XCI [452, 980].

We recently identified RNF12 as the first transacting factor involved in activation of XCI [174]. Additional copies of *Rnf12* result in an increased probability to initiate XCI in transgenic female cells resulting in a high percentage of cells with two Xi's (**Figure 3D**). Also in *Rnf12* transgenic male cells XCI is initiated in a significant percentage of cells. Over-expression of RNF12 even results in XCI in undifferentiated *Rnf12* transgenic female cells, supporting a dose dependent role for RNF12 in activation of XCI. This also indicates that the other unidentified XCI-activators are expressed in undifferentiated ES cells. The mechanism by which RNF12 activates XCI is unclear, but ectopic induction of XCI in human RNF12 transgenic mouse cells suggests that RNF12 acts through *XIST/Xist*, as evidence for a role of human *TSIX* in XCI is missing.

In recent years, several *cis* and *trans* acting factors have been identified which are good candidates for setting up the threshold required for XCI to be initiated with a specific probability. A stochastic model predicts that a change in the threshold level will have a different effect in male *versus* female cells, because the XCI-activator level is sex dependent (**Figure 3B**, **E** and **F**). Indeed, female cells with mutations that down-regulate or completely abolish *Tsix* expression, thereby lowering the threshold, show a much higher percentage of inactivation of the mutated allele than male cells containing the same mutations (**Figure 3E**) [127, 179]. This effect could explain the reported sex-ratio distortion in hemi/homozygous *Tsix* mutant mice, in favor of male mice, which may not or only occasionally initiate XCI on the single X chromosome while female cells initiate XCI on both X chromosomes much more frequently [180]. In contrast to the ΔCpG mutation used for this study, other reported *Tsix* deletions and *Tsix* stop alleles did result in a substantial percentage of male cells showing ectopic initiation of XCI, indicating that the ΔCpG mutation represents a hypomorphic allele with a threshold that is higher than other reported *Tsix* mutations. Depletion of *Oct4* also has a more profound effect on XCI in female compared to male cells (**Figure 3F**) [186]. These findings support a role for *Tsix* and OCT4 in determining the threshold for XCI to be initiated, and show that XCI counting and initiation is regulated through an intricate balance between these factors and other inhibitors and activators of XCI. So far RNF12 is the only identified XCI-activator, which acts in concert with the XCI-inhibitors, OCT4, SOX2, NANOG, CTCF and YY1, but more XCI-activators and XCI-inhibitors are likely to be involved. Identification of all XCI-activators and -inhibitors and unraveling of the interplay between these factors will be crucial for a further understanding of the XCI process.

Acknowledgements

We would like to thank all members of the laboratory for helpful discussions, and J. Anton Grootegoed and Hikke van Doorninck for critically reading the manuscript.

Chapter 5

RNF12 activates Xist and is essential for X chromosome inactivation

This chapter has been published in

Tahsin Stefan Barakat, Nilhan Gunhanlar, Cristina Gontan Pardo, Eskeatnaf Mulugeta Achame, Mehrnaz Ghazvini, Ruben Boers, Annegien Kenter, Eveline Rentmeester, J.Anton Grootegoed and Joost Gribnau (2011)
"RNF12 activates *Xist* and is essential for X chromosome inactivation"
PLoS Genetics 2011;7(1):e1002001

Addendum:
Tahsin Stefan Barakat, Nilhan Gunhanlar and Joost Gribnau
"Mice deleted for *Xist* intron 1 mice do not show an X chromosome inactivation phenotype"
(Work in progress)

RNF12 activates *Xist* and is essential for X chromosome inactivation

Tahsin Stefan Barakat[1], Nilhan Gunhanlar[1], Cristina Gontan Pardo[1], Eskeatnaf Mulugeta Achame[1], Mehrnaz Ghazvini[1,2], Ruben Boers[1], Annegien Kenter[1], Eveline Rentmeester[1], J. Anton Grootegoed[1] and Joost Gribnau[1,3]

[1]Department of Reproduction and Development, Erasmus MC, University Medical Center, Rotterdam, The Netherlands.
[2]Erasmus Stem Cell Institute, Erasmus MC, University Medical Center, Rotterdam, The Netherlands.
[3]corresponding author

Contact details:
Joost Gribnau
Department of Reproduction and Development
Erasmus MC
Room Ee 09-71
PO Box 2040
3000 CA Rotterdam
The Netherlands
Phone +31-10-7043069
Fax +31-10-7044736
Email: j.gribnau@erasmusmc.nl

Abstract

In somatic cells of female placental mammals, one of the two X chromosomes is transcriptionally silenced to accomplish an equal dose of X-encoded gene products in males and females. Initiation of random X chromosome inactivation (XCI) is thought to be regulated by X-encoded activators and autosomally encoded suppressors, controlling *Xist*. Spreading of *Xist* RNA leads to silencing of the X chromosome in *cis*. Here, we demonstrate that the dose dependent X-encoded XCI activator RNF12/RLIM acts in *trans*, and activates *Xist*. We did not find evidence for RNF12-mediated regulation of XCI through *Tsix* or the *Xist* intron 1 region, which are both known to be involved in inhibition of *Xist*. In addition, we found that *Xist* intron 1, which contains a pluripotency factor binding site, is not required for suppression of *Xist* in undifferentiated ES cells. Analysis of female *Rnf12*$^{-/-}$ knockout ES cells showed that RNF12 is essential for initiation of XCI, and is mainly involved in the regulation of *Xist*. We conclude that RNF12 is an indispensable factor in up-regulation of *Xist* transcription, thereby leading to initiation of random XCI.

Author Summary

In all placental mammals, the males have only one X chromosome per diploid genome, as compared to the females having two copies of this relatively large chromosome, carrying more than 1000 genes. Hence, the evolution of the heterologous XY sex chromosome pair has resulted in an inevitable need for gene dosage compensation between males and females. This is achieved at the whole chromosome level, by transcriptional silencing of one of the two X chromosomes in female somatic cells. Initiation of X chromosome inactivation (XCI) is regulated by X-encoded activators and autosomally encoded suppressors, controlling *Xist* gene transcription. Spreading of *Xist* RNA in *cis* leads to silencing of one of the X chromosomes. Previously, we obtained evidence that the X-encoded E3 ubiquitin ligase RNF12 (RLIM) is a dose-dependent XCI activator. Here, we demonstrate that RNF12 exerts its action in *trans*, and find that RNF12 regulates XCI through activation of transcription from the *Xist* promoter. Furthermore, analysis of female *Rnf12*$^{-/-}$ knockout ES cells shows that RNF12 is essential for initiation of XCI and that loss of RNF12 resulted in pronounced and exclusive down-regulation of *Xist*. It is concluded that RNF12 is an indispensable factor in *Xist* transcription and activation of XCI.

Introduction

X chromosome inactivation (XCI) in placental mammals is random with respect to the parental origin of the X chromosome that undergoes inactivation, during early embryonic development [30]. In contrast, in marsupials and mouse extra-embryonic tissues XCI is imprinted. Imprinted XCI always targets the paternally inherited X chromosome (Xp), and is initiated during the early cleavage divisions [51-53]. In the inner cell mass (ICM) of the mouse blastocyst, the paternally inherited inactive X chromosome is reactivated, after which random XCI is initiated around 5.5 days of embryonic development.

In mouse, two non-coding X-linked genes, *Xist* and *Tsix*, play a central role in the random XCI mechanism. Upon initiation of XCI, *Xist* is up-regulated on the future inactive X chromosome (Xi), and the transcribed RNA spreads along the X in *cis*, directly and indirectly recruiting chromatin modifying enzymes acting to establish the Xi [74, 85-86]. *Tsix* is a negative regulator of *Xist*; the *Tsix* gene overlaps with *Xist* but is transcribed in the anti-sense direction [118-119].

Random XCI is a stochastic process in which each X chromosome has an independent probability to become inactivated [179, 189]. Initiation of XCI is thought to be regulated by X-encoded activators and autosomally encoded inhibitors [179, 910]. With two active X chromosomes, female cells will have a concentration of XCI activators two-fold higher than male cells, sufficiently different to drive XCI in female cells only. Rapid down-regulation of XCI activator genes in *cis*, after initiation of XCI on either one of the X chromosomes, prevents initiation of XCI on the second X chromosome.

XCI inhibitors are involved in maintaining a threshold for XCI to occur. So far, several XCI inhibitors have been identified, acting through different mechanisms, in mouse. YY1 and CTCF act as positive regulators of *Tsix*, by binding the DXpas34 *Tsix* regulatory element [193]. The pluripotency factors OCT4, SOX2 and NANOG were proposed to regulate XCI by binding to intron 1 of *Xist* and suppressing *Xist* expression directly [191]. OCT4 and SOX2 have also been implicated in the positive regulation of *Tsix* and *Xite*, the latter being an enhancer of *Tsix* [186]. These findings indicate that several proteins and pathways act in concert to suppress *Xist* transcription and to block *Xist* RNA spreading in *cis*.

XCI activators could act by activation of *Xist*, but also by suppression of negative regulators of *Xist* such as *Tsix* and the *Xist* intron 1 region. Recently, we identified RNF12 (RLIM) as the first X-linked activator of XCI [174]. This E3 ubiquitin ligase is involved in regulation of LIM-homeodomain transcription factors and telomere length homeostasis, through degradation of LDB1 and TRF1, respectively [893-894]. Previously, we found that additional transgenic copies of the *Rnf12* gene encoding this protein resulted in induction of XCI on the single X in transgenic male cells, and on both X chromosomes in a high percentage of female cells. XCI was also affected in *Rnf12*$^{-/-}$ ES cells supporting a dose-dependent role for RNF12 in activation of XCI. In the present study, we aimed to dissect the role of RNF12 in XCI, and we obtained evidence that RNF12 regulates XCI in *trans*, by activation of the *Xist* promoter. In addition, the generation and analysis of *Rnf12*$^{-/-}$ ES cells indicated that RNF12 is required for the XCI process and appears to be involved in XCI mainly by activation of *Xist*. The results reinforce that RNF12 is a key player in regulation of the XCI process.

Results

RNF12 acts in trans to activate XCI

XCI is regulated by several *cis* elements, and *Rnf12* is located in close proximity to *Xist* (~500kb). Therefore, we aimed to test whether all the activity of RNF12 is mediated in *trans*. Our previous studies showed that *Rnf12*$^{+/-}$ female ES cells induce XCI in a reduced number of ES cells. Here, we rescued 129/Sv / Cast/Ei (129/Cas) polymorphic *Rnf12*$^{+/-}$ female ES cells by introducing a 129 BAC (RP24-240J16) construct covering *Rnf12*. RT-PCR analysis followed by RFLP detection confirmed expression of the transgenic copies of *Rnf12* (**Figure 1A**). *Xist* RNA-FISH analysis, to detect the *Xist* coated inactive X chromosome (Xi) in day 3 differentiated transgenic ES cell lines with one additional copy of *Rnf12*, shows that XCI was restored to wild type level (**Figure 1B**). In line 20, with 5 transgenic copies of *Rnf12* the percentage of cells with one or two Xi's is even more pronounced, supporting a dose dependent role of RNF12 in XCI (**Figure 1B, 1C**). XCI is skewed in wild type 129/Cas female ES cells towards inactivation of the 129 X. This is due to the presence of different X-linked *cis* elements (Xce) that affect random choice [446]. RT-PCR detecting a length polymorphism was used to distinguish *Xist* emanating from either the 129 or the Cas alleles. We observed that skewed XCI is more pronounced in the *Rnf12*$^{+/-}$ cells, as compared to XCI in wild type cells at day 3 of differentiation (**Figure 1D**). This could be caused by selection against cells inactivating the wild type X chromosome, which would result in complete loss of RNF12 from these cells. However, RNF12 possibly is not essential for cell survival, also of differentiated cells, so that selection against cells inactivating the wild type X chromosome might point to a role for RNF12 in maintaining *Xist* expression. In the rescued cell lines, *Xist* was up-regulated from both alleles at day 3 of differentiation (**Figure 1D**). This result demonstrates that RNF12 activates XCI in *trans*.

Counteracting roles for RNF12 and NANOG

One possible mechanism for regulation of XCI by RNF12 might be a direct interaction with *Xist* RNA to target chromatin components. However, examination of day 3 differentiated female cells by immunocytochemistry detecting RNF12, together with the Polycomb protein SUZ12 which accumulates on the Xi [97-98], excludes this possibility (**Figure 2A**). Interestingly, we noticed that the RNF12 staining intensity was much more dynamic in female compared to male cells (**Figure 2B**, **Figure S1**). Also, in female cells, a SUZ12 coated Xi appeared mainly in cells with low RNF12 staining (**Figure 2A**, **Figure S2**, and data not shown). Immunostaining of differentiating female ES cells indicated a negative correlation between expression of RNF12 and NANOG, although expression was not completely mutually exclusive (**Figure 2C**). To analyze this in more detail, we targeted an *Rnf12* promoter-mCherry construct into ES cells, also harboring a knock-in GFP transgene in the *Nanog* and *Oct4* loci. We analyzed expanded individual clones and pooled clones and obtained similar results. FACS analysis, prior to differentiation and at different time points after differentiation of these double transgenic ES cell lines, showed a negative correlation between RNF12-mCherry and NANOG-GFP expression, but not for RNF12-mCherry and OCT4-GFP (**Figure 2D**, **E**, **Figure S3**). Our findings therefore suggest specific counteracting regulatory roles for RNF12 and NANOG in XCI, which might include an inhibitory effect of NANOG on *Rnf12* transcription. Interestingly, NANOG has been

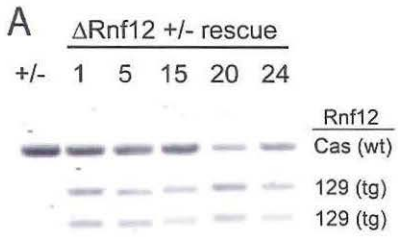

B

line	qPCR copy nr	RNA FISH day 3 1xXist	RNA FISH day 3 2xXist
ΔRnf12+/-	1	33%	0%
wild type	2	51%	1%
1	2	42%	0%
5	2	65%	5%
15	2	58%	2%
20	6	78%	17%
24	2	64%	4%

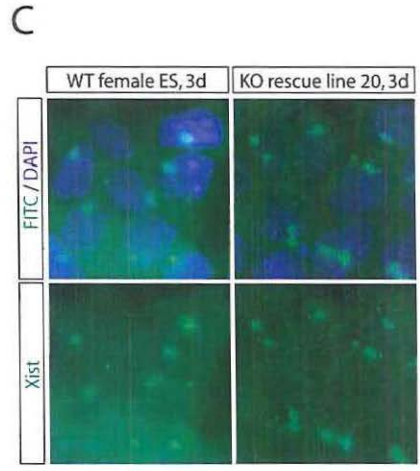

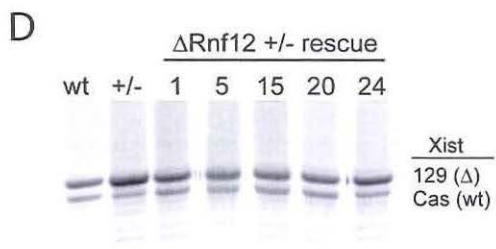

Figure 1: RNF12 activates X chromosome inactivation in *trans*
A) Allele specific RT-PCR analysis of *Rnf12* expression with RNA isolated from day 3 differentiated female *Rnf12*$^{+/-}$ ES cells (Cas/129, 129 *Rnf12* targeted), and rescued cell lines obtained after stable integration of an 129 *Rnf12* transgene. NheI digested 129 products were separated from undigested Cas products. **B)** Overview of RNA-FISH experiments detecting *Xist* expression in female wild type, *Rnf12*$^{+/-}$ and *Rnf12*$^{+/-}$ rescued cell lines. qPCR copynumber analysis was performed on genomic DNA. RNA-FISH analysis was performed on day 3 differentiated ES cells, and the percentage of cells harboring one *Xist* coated X chromosome (*Xist* cloud (=Xi), 1x *Xist*) or two *Xist* coated X chromosomes (2x *Xist*) was determined. **C)** Representative pictures of RNA-FISH analysis, detecting *Xist* (FITC) in day 3 differentiated female wild type and *Rnf12*$^{+/-}$ rescued ES cells (line 20, *Rnf12* over-expression). DNA is counterstained with DAPI in all RNA-FISH slides. **D)** Allele specific RT-PCR analysis of day 3 differentiated wild type, *Rnf12*$^{+/-}$ and *Rnf12*$^{+/-}$ rescued cell lines, detecting an *Xist* length polymorphism that discriminates 129 and Cas *Xist*.

implicated in the regulation XCI by direct suppression of *Xist* in ES cells, and *Xist* suppression in the ICM of the developing blastocyst corresponds with up-regulation of NANOG expression [367]. Therefore, mutual exclusive expression of RNF12 and NANOG may be required for initiation of XCI.

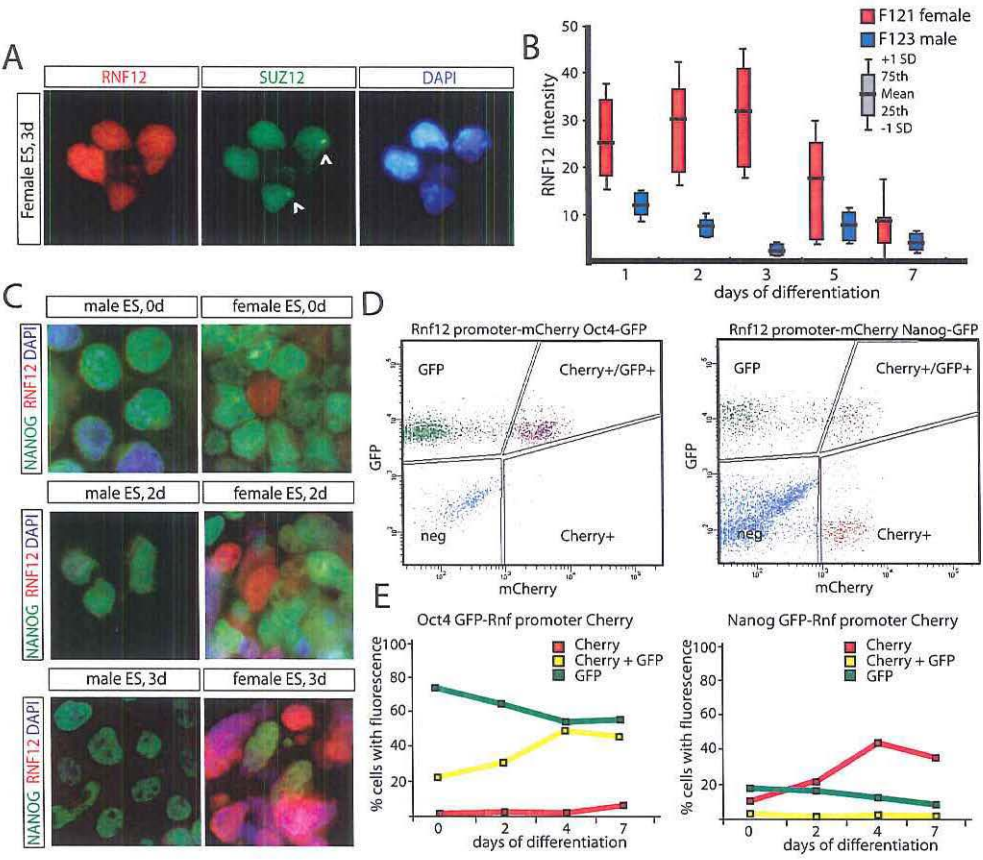

Figure 2: Counteracting roles for RNF12 and NANOG in XCI

A) Immunocytochemistry detecting RNF12 (Alexa 546) and SUZ12 (Alexa 488) in day 3 differentiated female ES cells. Cells showing accumulation of SUZ12 on the X chromosome (Xi) show low levels of nuclear RNF12, suggesting that RNF12 is downregulated upon XCI. RNF12 does not accumulate on the SUZ12 coated Xi. **B)** Quantification of RNF12 staining intensities in female and male ES cells at different timepoints of differentiation. Red and blue box plots show results for female and male cells, respectively. Mean, interquartil range and standard deviation are indicated. N > 100 cells per timepoint. Female cells show higher staining intensities and more fluctuation of RNF12 expression compared to male cells. **C)** Immunocytochemistry detecting RNF12 (rhodamine) and NANOG (FITC) in undifferentiated and day 2 and 3 differentiated male and female ES cells. **D)** FACS analysis of NANOG-GFP (right panel) and OCT4-GFP (left panel) ES cells transgenic for an *Rnf12*-mCherry promoter construct. FACS plots show results of undifferentiated ES cells. Cells are gated for GFP+, Cherry+, GFP+Cherry+ or negative. Results of a representative experiment are shown. **E)** Quantification of FACS analysis of NANOG-GFP (right panel) and OCT4-GFP (left panel) ES cells transgenic for an *Rnf12* mCherry promoter construct. Cells were differentiated for up to 7 days, and the percentage of positive cells was determined (Cherry+, red line; GFP+, green line; Cherry+GFP+, yellow line).

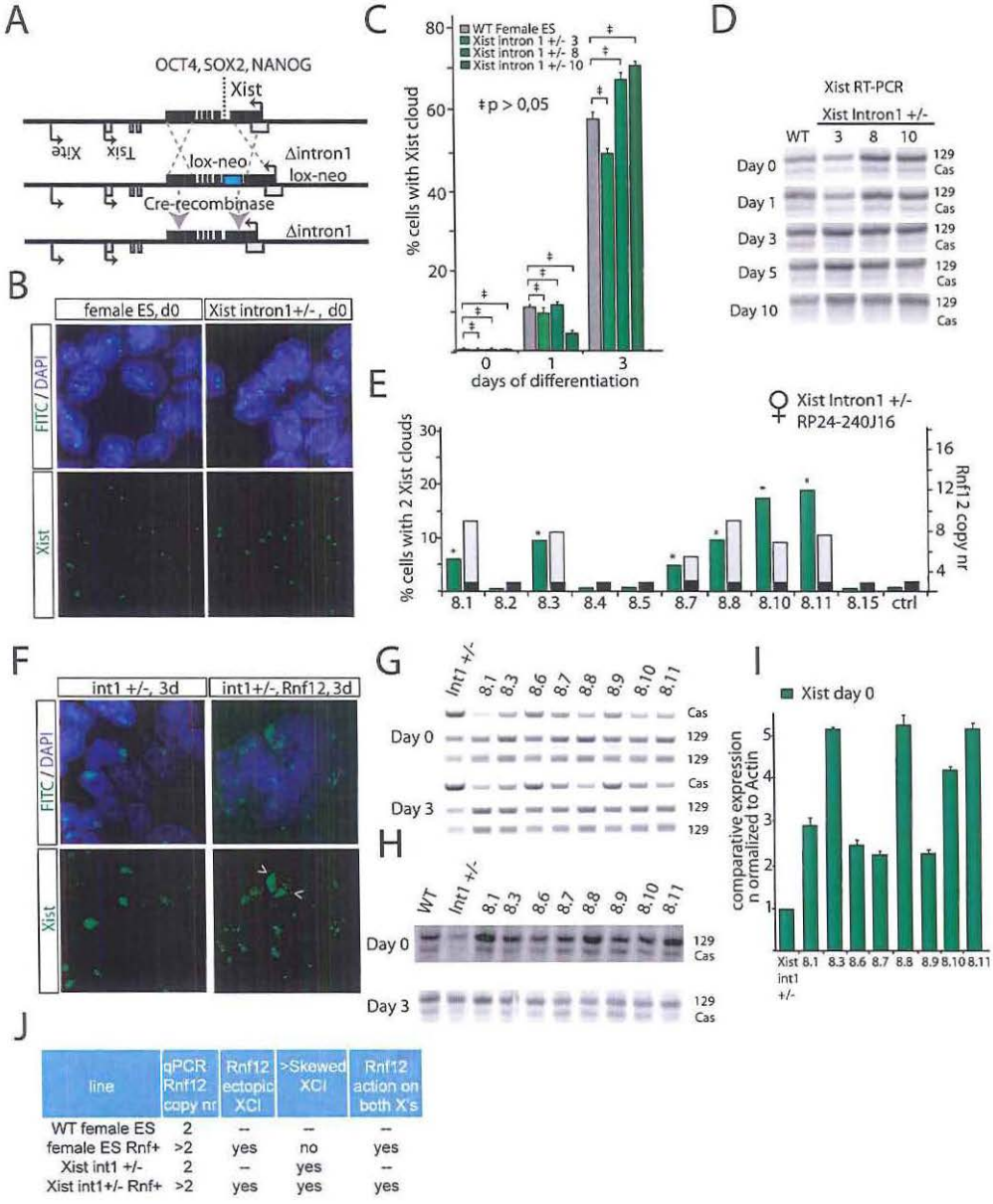

J

line	qPCR Rnf12 copy nr	Rnf12 ectopic XCI	>Skewed XCI	Rnf12 action on both X's
WT female ES	2	–	–	–
female ES Rnf+	>2	yes	no	yes
Xist int1 +/-	2	–	yes	–
Xist int1+/- Rnf+	>2	yes	yes	yes

Figure 3: RNF12 initiates XCI independent of pluripotency factor binding to *Xist* intron 1
A) Schematic representation of part of the X chromosome and the strategy to target the *Xist* intron 1 pluripotency factor binding sites. A BAC targeting construct replacing *Xist* intron 1 by a floxed neomycin resistance cassette (Neo) was used to target specifically the 129 allele in Cas/129 female ES cells. The Neo cassette was looped out after transient expression of Cre recombinase. **B)** RNA-FISH analysis detecting *Xist* (FITC) in undifferentiated female wild type and *Xist* $^{\text{intron 1+/-}}$ ES cells. In both wild type and *Xist* intron 1 deleted cells, only pinpoint signals are visible, representing basal *Xist* and *Tsix* expression.

RNF12 does not regulate XCI through Xist intron 1

Recently, the first intron of *Xist* has been identified as a region involved in recruitment of three pluripotency factors, OCT4, NANOG and SOX2 [191]. It was shown that down-regulation of *Nanog* and *Oct4*, through gene ablation, resulted in an increase in *Xist* expression, and initiation of XCI in male cells. Interestingly, the intron 1-mediated suppression of XCI was suggested to directly act on *Xist*, without involvement of *Tsix*. To study if RNF12 might regulate XCI by interfering with binding of pluripotency factors to the intron 1 region of mouse *Xist*, we removed 1.2 kb of *Xist* intron 1 including all reported NANOG, OCT4 and SOX2 binding sites by homologous recombination with a BAC targeting construct, without disturbing the integrity of the *Xist* transcript. Targeted clones were screened by PCR amplification of a targeted RFLP (BsrgI) in female F1 2-1, 129/Cas polymorphic ES cells, which was confirmed by Southern blotting, followed by Cre mediated loop-out of the kanamycin/neomycin resistance cassette (**Figure 3A**, **Figure S4**). *Xist* RNA-FISH at different time points of differentiation of several *Xist*$^{\text{intron 1}-/-}$ ES cell lines indicated that XCI is initiated with the same kinetics as in wild type cells, and showed that the intron 1 region is not required for repression of *Xist* in undifferentiated ES cells or early during initiation of XCI (**Figure 3B**, **3C**, and **Figure S4G**). Nevertheless, *Xist* specific RT-PCR, detecting a length polymorphism distinguishing 129 and Cas *Xist*, showed enhanced skewing at day 3 of differentiation towards 129 *Xist* expression, suggesting a role for the intron 1 region in suppressing *Xist* at later stages of differentiation, when NANOG, OCT4 and SOX2 are expressed at a lower level (**Figure 3D**). To test an involvement of the intron 1 region in RNF12-mediated activation of XCI, we introduced an *Rnf12* BAC transgene into the *Xist*$^{\text{intron 1}+/-}$ ES cell lines. Additional copies of *Rnf12* resulted in induction of *Xist*, even in undifferentiated ES cells (**Figure 3E**, **3F**, **3I**), confirming our previous findings [174]. However, allele specific RT-PCR did not point to an increased preference for expression of the mutated or wild type allele, in undifferentiated ES cells (**Figure 3G**, **3H**), indicating that RNF12-mediated action on XCI does not require the *Xist* intron 1 region (**Figure 3J**). At day 3 of differentiation, in several cell lines, we found higher expression of Cas *Xist* in *Rnf12* transgenic *Xist*$^{\text{intron 1}+/-}$ cells compared to *Xist*$^{\text{intron 1}+/-}$ only cells. We attribute this finding to an increase in the percentage of cells with two *Xist* clouds.

Figure 3: continued
C) Bar graph showing the percentage of wild type and *Xist* $^{\text{intron 1}+/-}$ ES cells that initiated XCI, detected by *Xist* RNA-FISH, at different time points of EB differentiation. No statistical significant differences were noticed between the wild type control and the cell lines harboring a deletion of *Xist* intron 1 (95% confidence interval, N>100 cells per time point ‡ p>0.05). **D)** Allele specific RT-PCR analysis detecting *Xist* expression in female wild type and *Xist* $^{\text{intron 1}+/-}$ cell lines (clone 3, 8 and 10) during differentiation. **E)** qPCR analysis to determine the *Rnf12* copy number in *Xist* $^{\text{intron 1}+/-}$ ES cells transgenic ES cell lines (transgenic, grey, and endogenous, black, copy number), and percentage of cells with two *Xist* clouds at day 3 of differentiation. **F)** RNA-FISH analysis detecting *Xist* (FITC) in day 3 differentiated *Xist* $^{\text{intron 1}+/-}$ ES cells, without (left panels) and with (right panels) an *Rnf12* transgene. The *Xist* clusters in one cell with two *Xist* clusters are indicated with arrowheads. **G)** RFLP RT-PCR amplifying a NheI RFLP present on the endogenous129 *Rnf12* allele, and the *Rnf12* transgene. Relative expression analysis was performed with RNA isolated from undifferentiated and day 3 differentiated ES cell lines. **H)** RT-PCR amplifying a length polymorphism distinguishing *Xist* emanating from the mutated 129 allele and the wild type Cas allele, with RNA isolated from undifferentiated and day 3 differentiated ES cell lines. **I)** *Xist* expression in undifferentiated *Rnf12* transgenic *Xist* $^{\text{intron 1}+/-}$ ES cells, and an *Xist* $^{\text{intron 1}+/-}$ control cell line was quantified qPCR. **J)** Table summarizing the results obtained with female wild type, *Rnf12* transgenic, *Xist* $^{\text{intron 1}+/-}$ and *Xist* $^{\text{intron 1}+/-}$ *Rnf12* transgenic ES cell lines.

We conclude that the *Xist* intron 1 region is not essential for suppression of XCI in undifferentiated ES cells, but may play a role later during differentiation. Furthermore, RNF12-mediated activation of XCI is independent from the *Xist* intron 1 region.

RNF12 regulates Xist

RNF12 could regulate XCI through activation of *Xist* or suppression of *Tsix*, or both. Previously, we analyzed *Xist* transgenic male ES cell lines with a BAC RP24-180B23 integration covering *Xist* only [174], or a BAC RP23-338B22 sequence containing both *Xist* and *Tsix* (**Figure 4A**). These male transgenic ES cell lines also contained 16 copies of an ms2 bacteriophage repeat sequence located in exon 7 of the endogenous *Xist* gene, allowing separate detection by RNA-FISH of autosomal versus endogenous *Xist* spreading [92]. Differentiation of transgenic male ES lines containing the *Xist-Tsix* transgene resulted in expression of *Xist* from the autosomal integration site in cell lines containing multicopy integrations. Autosomal spreading of *Xist* in these cell lines is most likely due to accumulation of enough *Xist* RNA to silence at least one copy of *Tsix*, allowing spreading of *Xist* in *cis*. Integration of truncated transgenes that lack *Tsix* would facilitate this process [174]. This also explained autosomal *Xist* spreading in BAC RP-24-180B23 single copy male transgenic ES cell lines upon differentiation, because *Tsix* is not covered by this BAC [174]. We used two of these, *Xist* only, BAC RP-24-180B23 ES cell lines to introduce 129 BAC RP24-240J16 transgenes covering *Rnf12*, and found *Xist* spreading on the single endogenous X (**Figure 4B** and **C**), confirming previous results. We also found a significant increase in the number of cells with autosomal *Xist* spreading, indicating that RNF12 activates XCI through *Xist*. Next, we introduced an *Rnf12* transgene (BAC RP24-240J16) in a single copy *Tsix* male transgenic ES cell line that lacks transgenic *Xist* (BAC RP23-447O10). These double transgenic ES cell lines contain a Cas X chromosome which allowed RFLP mediated discrimination of endogenous (Cas) and transgenic (129) *Tsix*. Analysis of these cell lines indicated that transgenic over-expression of RNF12 does not lead to down-regulation of *Tsix*, as measured by qPCR and by RNA-FISH examining the relative number of *Tsix* pinpoint signals (**Figure 4D**, **E** and **G**). Interestingly, allele specific RT-PCR indicated that endogenous *Tsix* (Cas) is even down-regulated in samples with higher *Xist* expression, indicating *Xist*-mediated silencing of *Tsix* in *cis* (**Figure 4F**). Taken together, these results indicate that *Xist* and not *Tsix* is the functionally most important downstream target of RNF12.

RNF12 is required for XCI

We previously found that the rate of initiation of XCI is reduced in differentiating female $Rnf12^{+/-}$ ES cells, compared to wild type ES cells [174]. The RNF12 protein level in these $Rnf12^{+/-}$ female cells is equal to that in male cells [174], but XCI is still occurring at a higher rate than in male cells. This indicated the presence of additional X-encoded XCI activators, but did not exclude the possibility that RNF12 is essential for XCI. To address this point, we generated $Rnf12^{-/-}$ female ES cells by targeting the wild type Cas *Rnf12* allele in $Rnf12^{+/-}$ ES cells (**Figure 5A**). Correct targeting was confirmed by RT-PCR, showing loss of a targeted RFLP located in exon 5 of *Rnf12* (**Figure 5B**). The presence of two X chromosomes in these $Rnf12^{-/-}$ female ES cells was ascertained by X chromosome DNA-FISH analysis and amplification of an RFLP in the *Xist* gene (**Figure 5C**, and data not

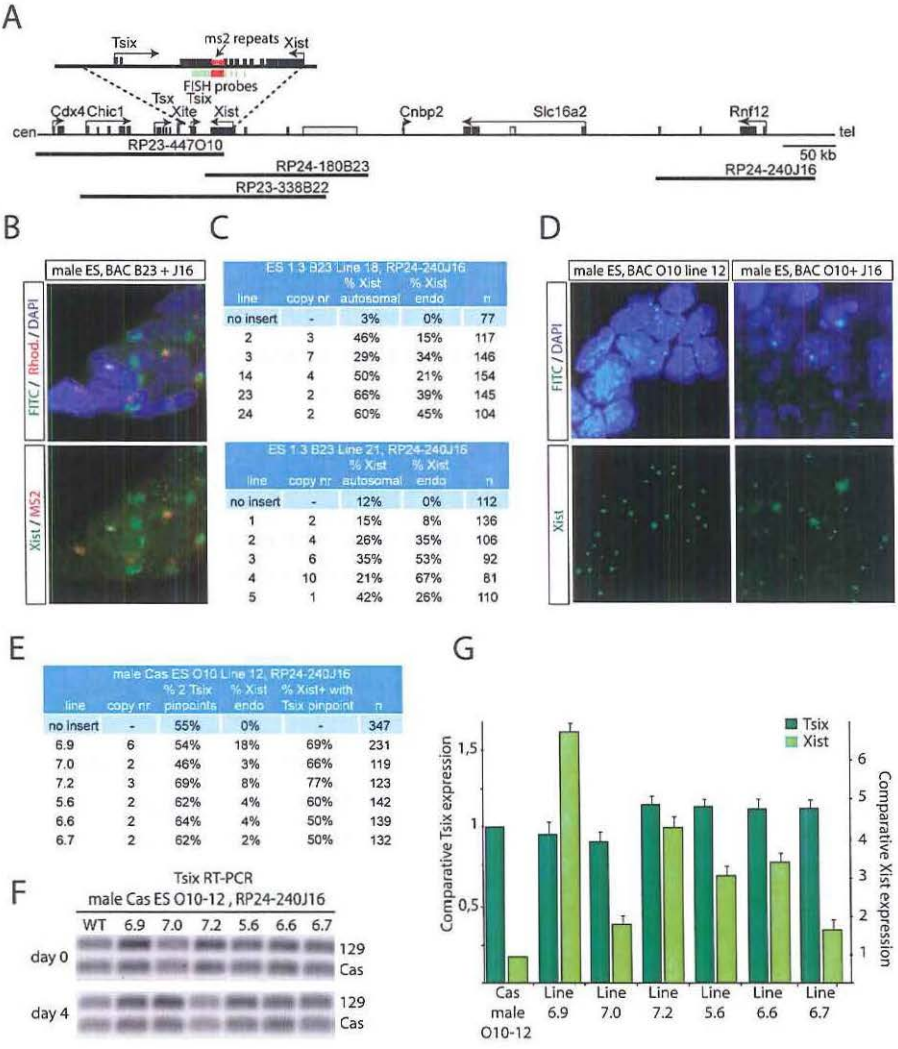

Figure 4: RNF12 activates *Xist* directly, but does not inhibit *Tsix*
A) Map showing part of the mouse X chromosome, the location of the BAC sequences used, and the position of ms2 repeats within *Xist*. RNA-FISH probes are indicated in green and red, and non-annotated genes in grey. **B)** RNA-FISH analysis detecting endogenous *Xist* (ms2, rhodamine and FITC positive) and exogenous *Xist* (FITC) from the autosomally integrated *Xist*-only BAC RP24-180B23 in day 3 differentiated male ES cells transgenic for *Rnf12* (BAC RP24-240J16). **C)** Table summarizing RNA-FISH results from B). Copy number of the *Rnf12* transgene was determined by gDNA qPCR. Shown are the percentage of autosomal and endogenous *Xist* clouds; N, number of cells analyzed. **D)** RNA-FISH analysis detecting endogenous and transgenic *Tsix* (FITC, pinpoint signals) and endogenous *Xist* (FITC, clouds) in day 3 differentiated *Tsix* transgenic male cells (left panels) and day 4 differentiated *Tsix* transgenic male cells with additional copies of an *Rnf12* transgene (right panels).**E)** Table summarizing results obtained with single copy *Tsix* transgenic male ES cell lines with a *Rnf12*

shown). Western blotting analysis confirmed the absence of RNF12 protein in the knockout cells (**Figure 5D**). RT-PCR and qRT-PCR of pluripotency associated genes and differentiation markers gave information that differentiation of the *Rnf12*$^{-/-}$ ES cells was not different from that of wild type ES cells (**Figure 5E, 5F** and **Figure S5**). However, *Xist* RNA-FISH analysis showed that differentiating *Rnf12*$^{-/-}$ ES cells only sporadically initiate XCI (**Figure 5G, H** and **I**). qPCR analysis confirmed that *Xist* is not detectably up-regulated when measured for a population of *Rnf12-/-* cells upon differentiation. Moreover, DNA-FISH detecting a whole chromosome X paint probe at day 7 and 10 of differentiation excluded X chromosome loss (**Figure S5**). The few *Rnf12*$^{-/-}$ cells that initiated XCI appeared in clusters, suggesting clonal expansion of a few cells that initiated XCI (**Figure S5**). We therefore conclude that RNF12 is an essential factor in XCI.

RNF12 activates the Xist promoter

Evidently, the *Rnf12*$^{-/-}$ knockout cells present the possibility to study control of gene expression by RNF12. Therefore, we next performed micro-array expression analysis comparing day 3 differentiated *Rnf12*$^{-/-}$ and wild type cells. We found that *Xist* was the only gene that was subject to differential regulation, showing pronounced down-regulation (**Figure 5J**). Interestingly, none of the known downstream targets of RNF12 appeared affected in our analysis. This may be due to our ES cell differentiation system resulting in a mixed population of cells at different stages of differentiation. In addition, the 3-day-time span allowed in our studies for cell differentiation may have prevented detection of effects on downstream targets which are expressed at later stages of differentiation. Nevertheless, our results indicate that the main function of RNF12 at this early stage of differentiation concerns the regulation of XCI. The observed dependency of *Xist* transcription on RNF12 might be effectuated by RNF12 acting through the *Xist* promoter. To test this, we expressed *Xist* promoter luciferase reporter constructs, both transiently and stably, in wild type female and *Rnf12*$^{-/-}$ ES cell lines and differentiated these cells for 3 days. The results revealed an unequivocal correlation between RNF12 expression and luciferase expression (**Figure 5K**). Our results therefore demonstrate that RNF12 activates the *Xist* promoter, although this does not exclude a role for other *cis* regulatory sequences, further away from the *Xist* promoter, in RNF12-mediated activation of XCI.

Figure 4: continued
transgene, 4 days after differentiation. Shown are copy number of the *Rnf12* transgene, percentage of cells with two *Tsix* signals, cells with an *Xist* cloud, and the percentage of cells with an *Xist* cloud and *Tsix* pinpoint signal (n is number of cells analyzed). **F)** Allele specific RT-PCR detecting transgenic (129) and endogenous (Cas) *Tsix* in undifferentiated and day 4 differentiated *Tsix /Rnf12* double transgenic ES cells. **G)** qPCR analysis to quantify *Xist* and *Tsix* expression in day 4 differentiated *Tsix /Rnf12* double transgenic ES cells, and a control cell line without an *Rnf12* transgene.

Discussion

In ES cells, RNF12 exerts its main function in XCI

Here, we present evidence that RNF12 is an essential activator of random XCI. RNF12 acts in *trans* on the *Xist* promoter, in differentiating mouse ES cells, to activate *Xist* transcription, leading to *Xist* RNA cloud formation and spreading of the silencing complex over the future inactive X chromosome in *cis*. Although our results show that RNF12 acts in *trans*, it is to be expected that the close proximity of the *Rnf12* gene to the *Xist* locus, taken together with the dose-dependent action of RNF12, is quite crucial for well-tuned regulation of XCI. Such proximity most likely facilitates rapid down-regulation of *Rnf12* in *cis* upon initiation of XCI, leading to a lower nuclear RNF12 content, thereby preventing inactivation of the second X chromosome.

Whole genome expression analysis suggests that the major function of RNF12 in ES cells is its regulation of *Xist* RNA expression, hence XCI. This is a very surprising finding, as RNF12 has been implicated in many other biological pathways. Apparently, in the present cell differentiation system, loss of expression of RNF12 does not cause a deviation from the wild type differentiation process to such an extent that it affects gene expression other than that of *Xist*. However, also based on our studies we do not exclude a function for RNF12 at later stages of cell differentiation, or in mouse development. In addition, redundant pathways or proteins such as RNF6, a close homologue of RNF12, may prevent full phenotypic expression of loss of RNF12. However, RNF12 exerts a predominant role in targeting *Xist*, as evidenced by our observation that *Xist* is largely silenced in the RNF12 deficient cells.

While our manuscript was under review, Shin et al. (2010) published a paper suggesting that RNF12 might be required in particular for imprinted XCI in mice [981]. Remarkably, that study included the observation that RNF12 depletion did not prevent initiation of random XCI in a significant percentage of *Rnf12-/-* ES cells derived from mouse blastocysts. This discrepancy with our findings might be explained by experimental differences, such as differences concerning the design of the knockout, the genetic background of the ES cells, or the cell derivation and culture procedures. Differences in cell differentiation protocols have been shown to have a pronounced impact on the XCI process [982]. Also, ES cells derived from embryos with a different genetic background could express XCI activators and XCI inhibitors at different levels, allowing XCI in either a lower or a higher percentage of *Rnf12-/-* cells. Future studies comparing the two independently generated *Rnf12-/-* ES cell lines will yield useful information about these points.

Other XCI activators

Although our observations provide evidence that RNF12 is an essential factor for the XCI process to occur in differentiating ES cells, we anticipate that other XCI activators act in parallel, and might independently regulate *Xist* or *Tsix*, or both. Dosage compensation mechanisms in species such as *D. melanogaster* and *C. elegans* also involve multiple factors and pathways, possibly leading to increased fidelity of these mechanisms [899]. In such a mechanism involving multiple factors, RNF12 would be the dose-dependent factor that is required to exceed the cumulative threshold limit to proceed towards initiation of XCI. It is feasible that female *Rnf12*$^{-/-}$ cells sometimes do initiate XCI (**Figure 6A**), as a consequence of the stochasticity of the process. This would be compatible with a

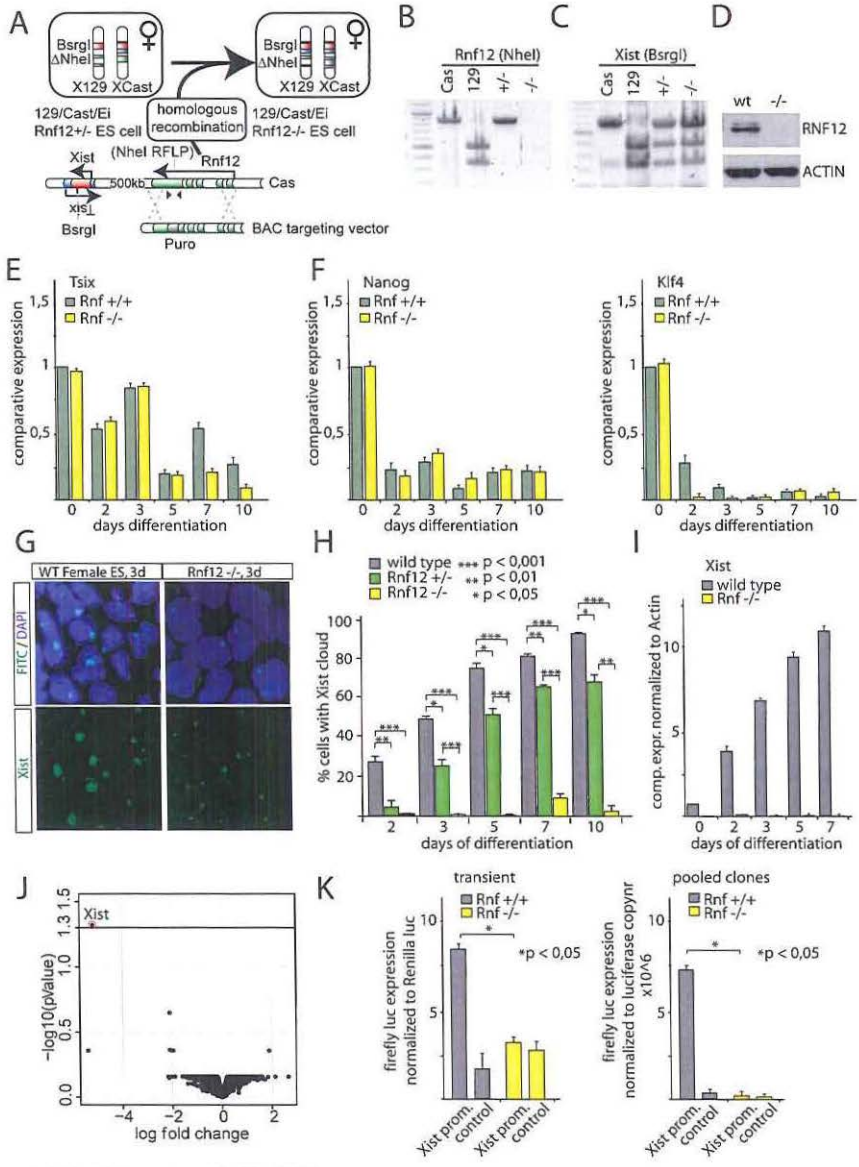

Figure 5: RNF12 is essential for XCI

A) Targeting strategy to generate *Rnf12*$^{-/-}$ ES cells. The Cas *Rnf12* allele of the previously generated heterozygous *Rnf12*$^{+/-}$ ES cells (Cas/129) was targeted with a BAC construct containing a puromycin selection cassette disrupting the open reading frame of *Rnf12*. **B)** PCR RFLP analysis with primers spanning a NheI RFLP descriminating the Cas (no NheI site) and the 129 (NheI site present) alleles, which was used to insert the targeting cassette. **C)** PCR RFLP analysis confirming the presence of two X chromosomes in *Rnf12*$^{-/-}$ ES cells. PCR primers span a BsrgI RFLP located in *Xist*. **D)** Western

mechanism, in which the combined total activity of all putative XCI activators exclusive of RNF12 is just below or around the threshold to initiate XCI. Interestingly, *Xist* cloud formation is also sporadically found in male cells, but in contrast to female *Rnf12*$^{-/-}$ cells, this represents a lethal condition and will be selected against.

Our studies indicate that RNF12 participates in *Xist* promoter activation, through an action which requires the presence of the minimal promoter. Although the direct protein target(s) of RNF12 remain elusive, its reported E3 ubiquitin ligase activity [893] would be compatible with RNF12 targeting an inhibitor of *Xist* transcription through proteasome-mediated degradation. This does not exclude that RNF12 might be involved, in addition or alternatively, in activation of a transcription factor driving *Xist* expression through positive regulation of transcription. Furthermore, RNF12 could be involved in regulation of *cis*-regulatory sequences other than the *Xist* promoter, yet to be identified and further away from the *Xist* locus.

A function for RNF12 in maintaining Xist expression

Selection against cells inactivating the X chromosome containing the wild type allele of *Rnf12* in the heterozygous *Rnf12*+/- ES cells could point to a continued requirement for *Rnf12* in maintaining *Xist* expression, following the early stages of differentiation. From the fact that male *Rnf12*-/*Y* knockout male mice are viable [981], it can be concluded that RNF12 deficiency is compatible with survival of differentiated cells in which XCI does not play any role. Hence, it would be difficult to explain the observed selection against cells inactivating the wild type X chromosome in the heterozygous *Rnf12*+/- ES cells by loss of any possible function of RNF12 independent of XCI. If RNF12 would be required for maintaining *Xist* expression and XCI, the cells inactivating the wild type allele and becoming deficient in RNF12 can be expected to lose *Xist* expression and to reactivate the Xi. In contrast, cells inactivating the X chromosome containing the mutated allele, keeping one functional allele of *Rnf12*, will be able to maintain *Xist* expression and XCI. In a population of cells this will lead in skewed XCI of the mutated allele. In fact, such a mechanism might also be relevant to explain the reported defect in imprinted XCI resulting from an *Rnf12* mutation [981].

Figure 5: continued
analysis of RNF12 protein and ACTIN in wild type and *Rnf12*$^{-/-}$ ES cells. **E)** qRT-PCR analysis detecting *Tsix* expression in female wild type and *Rnf12*$^{-/-}$ ES cells differentiated for up to 10 days. Results were normalized to Actin. **F)** qRT-PCR analysis as in (H), but now detecting Nanog (left graph) and Klf4 (right graph) expression. **G)** RNA-FISH analysis detecting *Xist* (FITC) in day 3 differentiated female wild type and *Rnf12*$^{-/-}$ ES cells. **H)** Bar graph showing the percentage of female wild type, *Rnf12*$^{+/-}$ and *Rnf12*$^{-/-}$ ES cells that initiated XCI, as determined by *Xist* RNA-FISH, at different time points of differentiation. *** $p<0.001$; ** $p<0.01$; * $p<0.05$, Student's T-test. **I)** qRT-PCR detecting *Xist* in female wild type and *Rnf12*$^{-/-}$ ES cells differentiated for up to 7 days. Results were normalized to *Actin*. **J)** Genome wide expression analysis comparing day 3 differentiated *Rnf12*$^{-/-}$ and wild type ES cells. Shown are the Log fold expression change and the adjusted P value. **K)** Luciferase assay detecting expression of an *Xist*-promoter-luciferase construct in female wild type and *Rnf12*$^{-/-}$ ES cells differentiated for 3 days. For transient experiments, cells were co-transfected at day 0 with the *Xist*-promoter-luciferase or control vector (empty luciferase vector) and a Renilla plasmid. Results were normalized to Renilla expression. For stable pooled clones, the promoter constructs were transfected, clones were pooled after selection and differentiated 3 days prior to analysis.

Imprinted XCI involves activation of *Xist* on the Xp, and the observed phenotype concerns lack of this imprinted XCI of the Xp when the mutant *Rnf12* allele is inherited from the mother. It was observed that no female embryos were born, inheriting a mutated *Rnf12* allele from either a $Rnf12^{-/-}$ or a $Rnf12^{+/-}$ mother in crosses with wild type males. In contrast, the mutated allele was transmitted to male offspring. Maternal storage of RNF12 in the oocyte was proposed to play a crucial role in imprinted silencing of the Xp in the early embryo [981]. *Rnf12* is at a 46cM distance of the centromere, so that it can be expected that many haploid oocytes generated by the first meiotic division (the reduction division) of $Rnf12^{+/-}$ oocytes, which occurs at the time of ovulation, will contain both wild type and *Rnf12* mutated alleles, as a consequence of meiotic recombination. Hence, we anticipate that there will be ongoing expression of *Rnf12* in a high percentage of oocytes transmitting the mutated *Rnf12* allele, until fertilization triggers meiotic division II. The recombined wild type and mutant alleles which are present within one haploid oocyte, will be exposed to the same maternal storage of RNF12. Taken together with the observation that $Rnf12^{+/-}$ oocytes did not give rise to female offspring carrying the mutant allele, whereas female offspring carrying the wild type allele were obtained at the expected mendelian ratio from these oocytes [981], this argues against a predominant role for maternal storage in imprinted XCI. Rather, we favor the hypothesis that continued transcription of *Rnf12* throughout ovulation and after fertilization is required for sustained expression of RNF12, activation of *Xist* from the Xp, and maintenance of the inactive Xp. Future research will be required to address this hypothesis.

The link to pluripotency

Our results indicate a negative correlation between NANOG and RNF12 expression. NANOG and the other pluripotency factors OCT4 and SOX2 have been shown to be recruited to the *Xist* intron 1 region in undifferentiated ES cells, and were proposed to play a role in *Tsix* independent suppression of *Xist* [191]. In this regulatory mechanism, ablation of *Tsix* did not result in up-regulation of *Xist* in undifferentiated ES cells, and *Tsix* was not required for repression of *Xist* located on the inactivated paternal X chromosome in the inner cell mass. This pointed to an important role for recruitment of NANOG, OCT4 and SOX2 to *Xist* intron 1 in suppression of *Xist* in ES and ICM cells [191]. However, the present findings show that the intron 1 region is dispensable, in silencing the XCI process in undifferentiated ES cells. Deletion of *Xist* intron 1 caused an effect, but only in the form of skewing of XCI, which was notable at later stages of differentiation. Interestingly, a previous study analyzing an *Xist* mutant allele that lacks the intron 1 region but leaves the *Xist* promoter intact, also did not show up-regulation of the mutated allele in undifferentiated ES cells [94]. Although these latter results support our findings, they should be interpreted with caution because the selection cassette was still present in the cells analyzed by Marahrens et al. [94].

Like for the role of RNF12, this points to the presence of additional mechanisms, involved in suppression of XCI. *Tsix* and *Xite* are the most likely candidate genes taking part, and the combined action of these repressive mechanisms may be sufficient to suppress *Xist*. However, even with all the repressive elements in place RNF12 can induce *Xist* expression and XCI in undifferentiated ES cells [174]. This points towards another

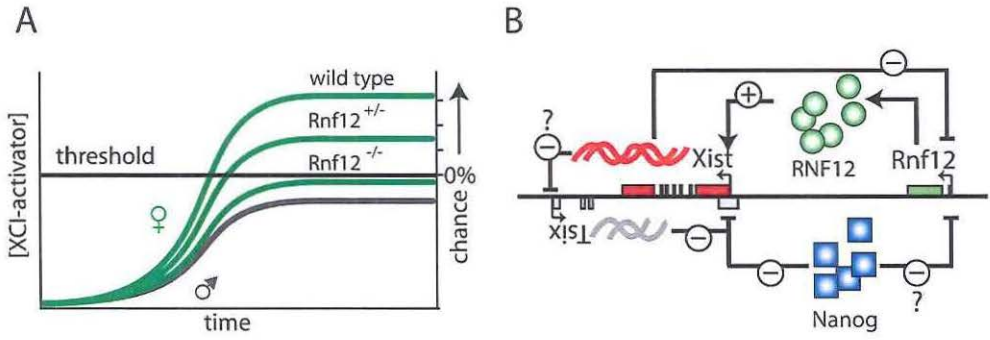

Figure 6: RNF12 and its role in the XCI regulatory network
A) In wild type and *Rnf12*$^{+/-}$ cells the XCI activator concentration is above the threshold required to generate a probability to initiate XCI. In contrast, in most *Rnf12*$^{-/-}$ cells the XCI activator concentration is not sufficient to reach the threshold required to initiate XCI. **B)** The regulatory network of XCI. *Xist* is repressed in *Tsix* dependent and independent pathways (NANOG binding in intron 1). Activation of XCI is accomplished by RNF12 through activation of the *Xist* promoter, and possibly *Xist* mediated silencing of *Tsix*. Finally, *Rnf12* is repressed by *Xist* and possibly NANOG.

mechanism involved in *Xist* suppression, in which the nuclear concentration of the XCI activator may be too low in undifferentiated ES cells and ICM cells to allow *Xist* expression and initiation of XCI, even in the absence of repressive elements such as the intron 1 region. Future research should clarify whether these mechanisms indeed act synergistically in silencing the XCI process.

The negative correlation of RNF12 and NANOG expression that we report could reflect the differentiation state of the ES cells, and does not necessarily entail a cross-regulatory role for these proteins. Nevertheless, NANOG and other pluripotency factors are also recruited to the *Rnf12* promoter in ES cells, where it might be involved in down-regulation of *Rnf12* (**Figure 6B**) [983], which opens the intriguing possibility that NANOG might also be implicated in regulation of the initiation of XCI through suppression of *Rnf12*. This highlights the complexity of the overall mechanism and the interconnection of the different players involved in XCI, but also reinforces the predominant role of RNF12 in this process.

Methods

ES cell culture

ES cells were grown in standard ES medium containing DMEM, 15% foetal calf serum, 100 U ml^{-1} penicillin, 100 mg ml^{-1} streptomycin, non-essential amino acids, 0.1mM ß-mercaptoethanol, and 1000 U ml^{-1} LIF. To induce differentiation, ES cells were split, and pre-plated on non-gelatinised cell culture dishes for 60 minutes. ES cells were then seeded in non-gelatinised bacterial culture dishes containing differentiation medium to induce embryoid body (EB) formation. EB-medium consisted of IMDM-glutamax, 15% foetal calf serum, 100 U ml^{-1} penicillin, 100 mg ml^{-1} streptomycin, non-essential amino acids, 37.8 µl l^{-1} monothioglycerol and 50 µg/ml ascorbic acid. EBs were plated on coverslips 1 day prior to harvesting, and allowed to grow out.

Transgenesis and generation of Knockout ES cell lines

For the *Rnf12* rescue experiments, an ampicillin-puromycin resistance cassette was inserted in the backbone of BAC RP24-240J16 by homologous recombination in bacteria. The modified BAC was electroporated in to female heterozygous *Rnf12+/-* cells [174], and colonies were picked after 8-10 days of puromycin selection, expanded and differentiated. BAC copynumber was determined by qPCR, and transgene specific expression was determined by allele specific RT-PCR, as described previously [174].

To generate the female homozygous *Rnf12 -/-* ES cell line, the previously generated *Rnf12+/-* ES cell line was targeted with an *Rnf12* BAC targeting construct containing an ampicillin-puromycin cassette disrupting the open reading frame of *Rnf12*. To generate this targeting construct, targeting arms were PCR amplified using primers GCCTTCGAACATCTCTGAGC, GAGCCGGACTAATCCAAACA, cloned into pCR-BluntII-TOPO (Invitrogen), and linearized with NheI to introduce an ampicillin-puromycin cassette from pBluescript. The targeting cassette was inserted in a Cast/Ei *Rnf12* BAC RP26-81P4 by homologous recombination in bacteria, and the resulting construct was used to target specifically the Cast/Ei X chromosome of the *Rnf12 +/-* ES cell line. Colonies were selected under neomycin and puromycin selection, and the absence of *Rnf12* expression was confirmed by Western analysis.

To generate the *Xist* intron 1 deletion, a BAC targeting construct was generated by homologous recombination, replacing intron 1 by a floxed neomycin cassette. Targetting arms were PCR amplified using primers 5'Forw: CATCAGGCTTGGCAGCAAGT, 5'R: CCTTGTTGGTCCAGACGACTATT and 3'Forw: CCAGACCAGGTCTTTGTATGCA, 3'Rev: GTGCTCCTGCCTCAAGAAGAA. Correctly targeted clones were identified by allele specific RFLP analysis using primers CAGTGGTAGCTCGAGCCTTT and CCAGAAGAGGGAGTCAGACG, followed by BsrGI digestion. The neomycin cassette was removed by transient transfection with a CrePAC vector and selection with puromycin. The final cell lines were verified by Southern blotting.

Rnf12 and Xist reporter constructs

To generate the *Rnf12* promoter cherry reporter cell lines, the *Rnf12* promoter was PCR amplified using previous described primers [984], and cloned into pCR-BluntII-TOPO and sequence verified. The *Rnf12* promoter was then released from pCR-BluntII-TOPO by digestion with SacI and KpnI, and blunt cloned into an AseI-BamHI fragment from pmCherry-N1 (Clonetech), thereby replacing the pCMV promoter of pmCherry-N1 with the *Rnf12* promoter. The resulting construct was used to electroporate in Oct-GFP and Nanog-GFP ES cell lines. Both pooled cell lines and single colonies were expanded, and cherry expression was analysed by FACS analysis using a BD FACSAria apparatus.

The *Xist* promoter was amplified using primers: TCCCAAGGTATGGAGTCACC, and GGAGAGAAACCACGGAAGAA, and cloned into pGL3-basic vector. As a control, the promoter less pGL3-basic vector was transfected.

Stable pooled cell lines of wild type or *Rnf12* -/- ES cells were generated by co-transfection with a puromycin or hygromycin selection vector. Expression of Luciferase was determined using the Bright-Glo luciferase assay system (Promega) and measured using a Promega luminometer. Results were normalized to the amount of protein present in the cell lysate measured by nanodrop, and copynumber of *Xist* promoter integration determined by qPCR. qRT-PCR using primers detecting luciferase (TCTAAGGAAGTCGGGGAAGC and CCCTCGGGTGTAATCAGAAT) confirmed the results obtained. For transient luciferase experiments, cells were co-transfected using the *Xist* reporter constructs and a control Renilla construct, using Lipofectamine 2000. Luciferase activity was measured using the Dual Glo luciferase system (Promega)

Xist RNA-FISH, immunofluorescence and Western analysis

Xist RNA-FISH was performed as described [174, 179]. Immunofluorescence was performed using standard procedures. RNF12 and NANOG were detected using a mouse anti- RNF12 antibody (1:250, Abnova), and a rabbit anti-NANOG antibody (1:100, SC1000, Calbiochem). ImageJ software was used to measure staining intensities; at least 100 cells were measured for each indicated time point, and background correction was performed. Western blotting was performed as previously described [174].

Expression analysis

RNA was isolated using Trizol reagent (Invitrogen) using manufacturer's instructions. DNAse treatment was performed, and cDNA was prepared using SuperScriptII (Invitrogen), using random hexamers. qRT-PCR was performed using a Biorad thermocycler, using primers described in **Table S1**. Results were normalized to *Actin*, using the ΔCT method.

Whole genome wide expression analysis of female wild type and *Rnf12*-/- ES cells differentiated for 3 days was performed with Affymetrix Mouse Genome 430 2.0 Arrays. Differentially expressed genes were identified using Limma (Bioconductor package) in R software.

Acknowledgements

We would like to thank Cathérine Dupont for helpful comments and help with experiments. Rudolf Jaenisch for supplying Nanog-GFP and Oct4-GFP ES cell lines. Elvira Myronova, Selma van Staveren and Reinier van der Linden are acknowledged for their help with experiments. We also thank all department members for helpful discussions.

Supplemental Data

Supplemental Data contains five figures and one table.

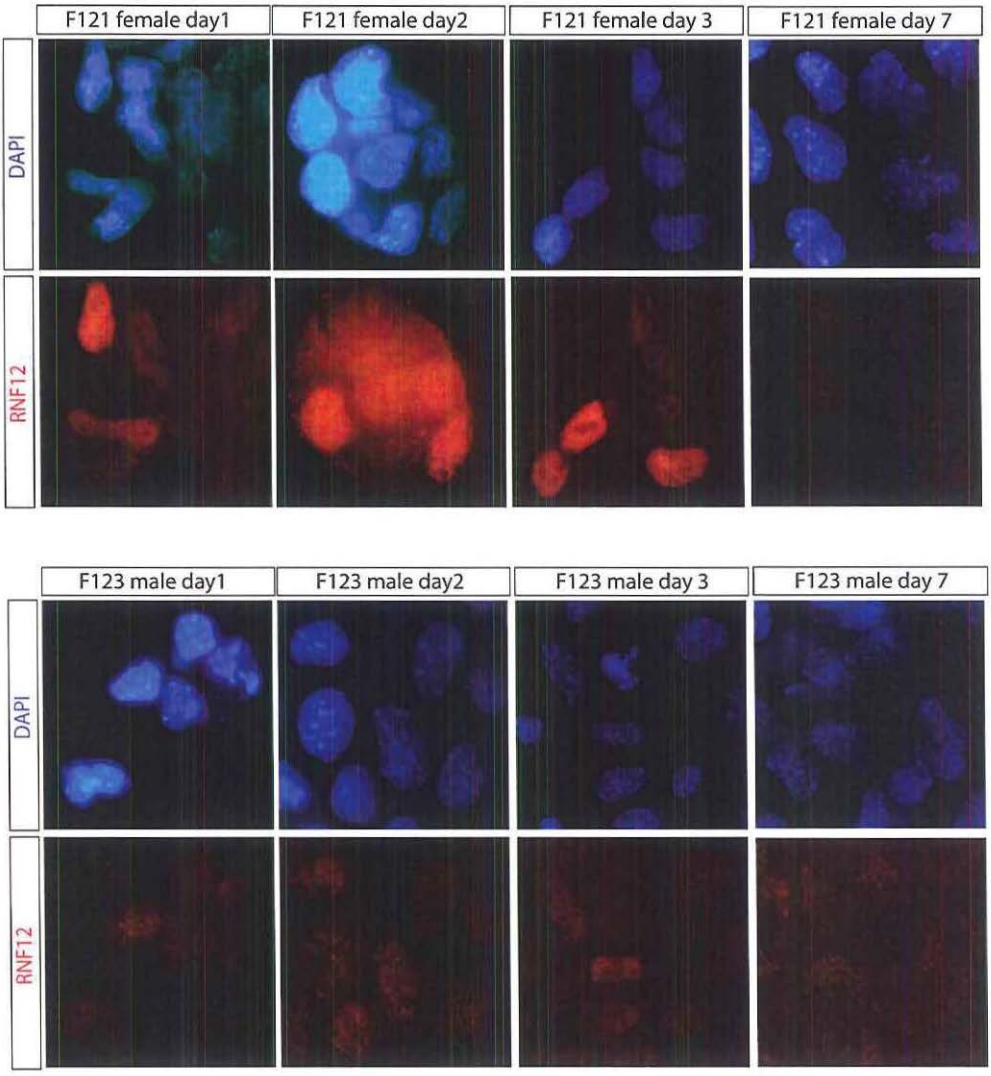

Figure S1
Immunocytochemistry detecting *RNF12* (rhodamine) at different stages of differentiation of female and male ES cells.

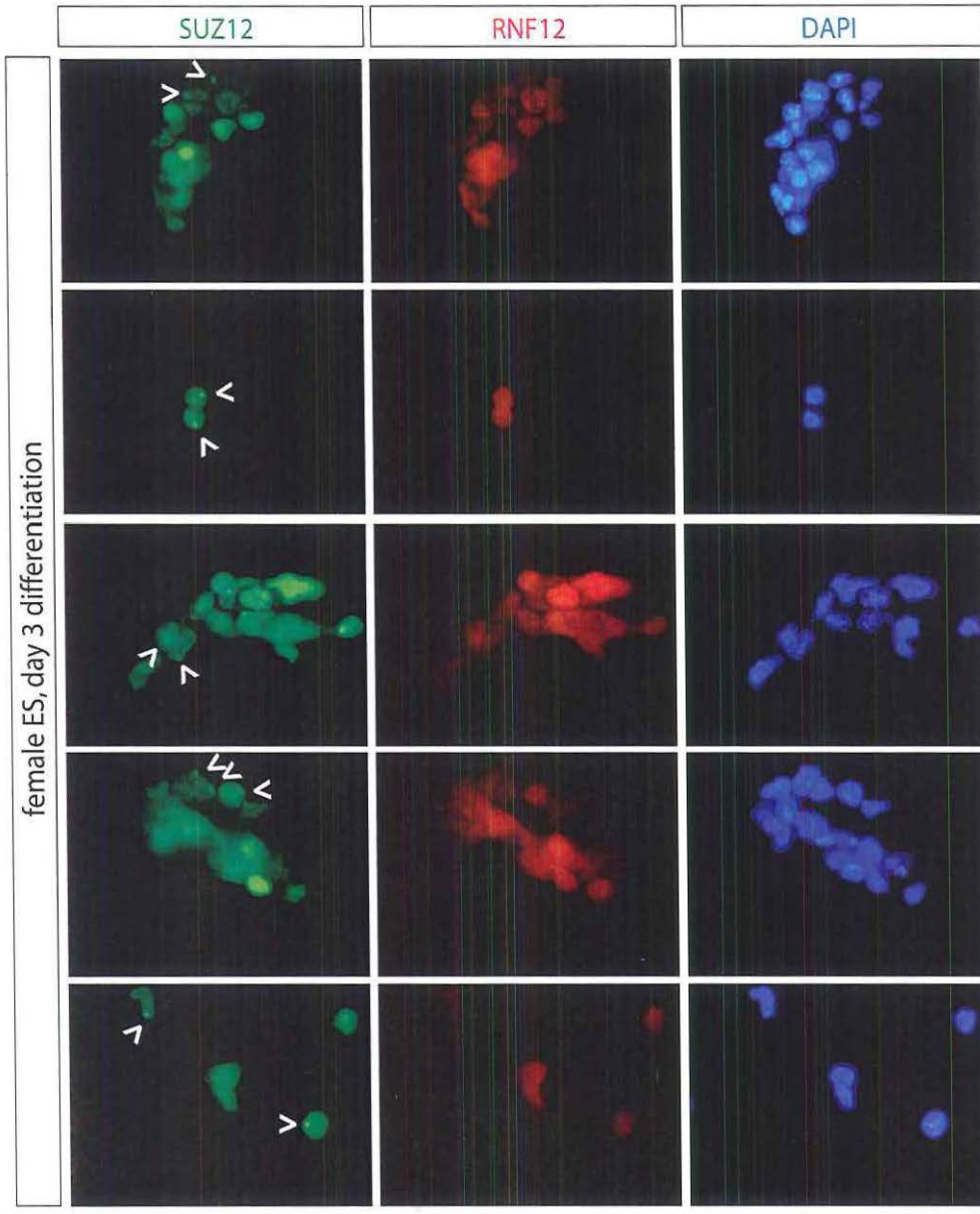

Figure S2
Immunocytochemistry detecting *RNF12* (rhodamine) and *SUZ12* (FITC) in day 3 differentiated female ES cells. *SUZ12* accumulations on the Xi are indicated with arrowheads.

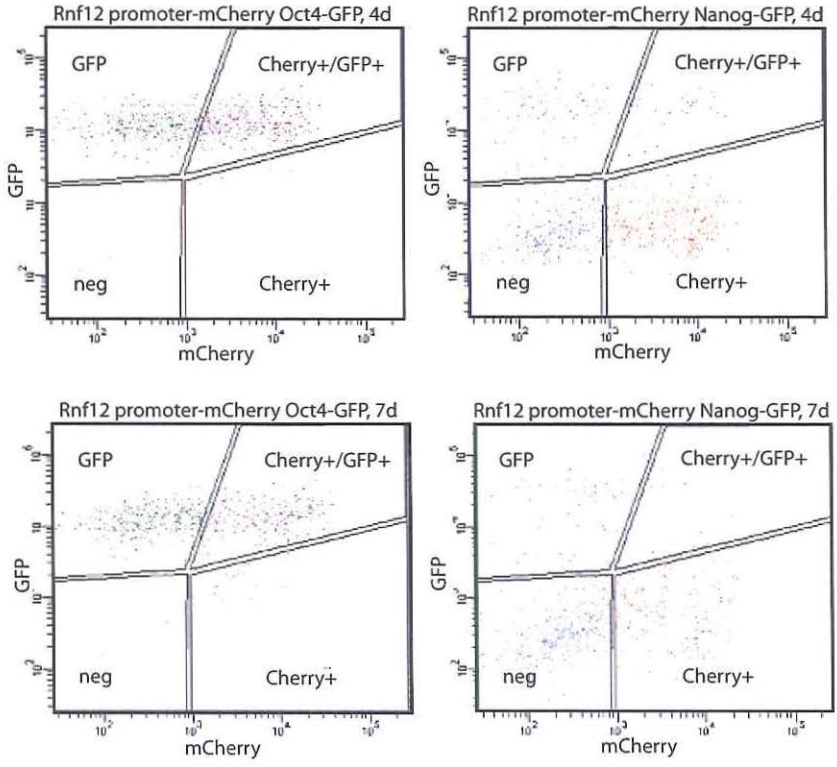

Figure S3
FACS analysis of NANOG-GFP (right panel) and OCT4-GFP (left panel) ES cells transgenic for an *Rnf12*-mCherry promoter construct. FACS plots show results of day 4 (upper panel) and day 7 (lower panel). Cells are gated for GFP+, Cherry+, GFP+Cherry+ or negative. 10.000 cells analyzed per time point.

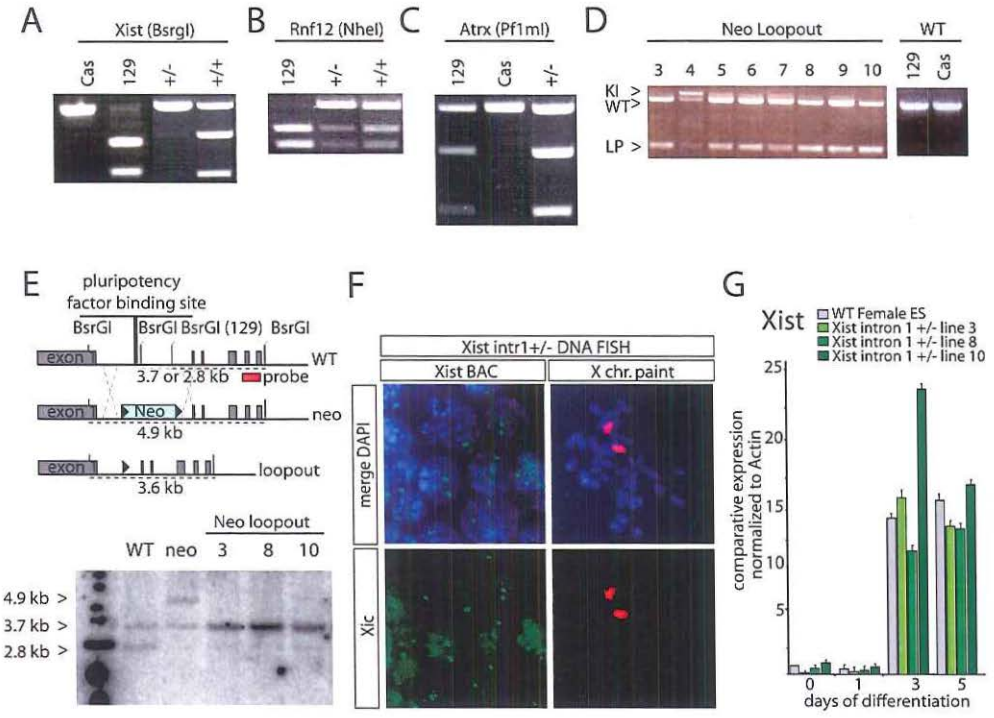

Figure S4

A) RFLP-PCR amplifying a BsrgI RFLP located in *Xist* intron 1. The BsrgI site is present on the targeted 129 allele, and is disrupted by the targeting event. **B,C)** Analysis of RFLPs in *Rnf12* (B) and *Atrx* (C) confirmed the presence of 2 X chromosomes in *Xist* intron 1 targeted ES cells. **D)** Confirmation of loop out of the neomycin resistance cassette. Primers amplify a region across the neomycin cassette. **E)** Map and targeting strategy for the intron 1 deletion. The map shows expected allele specific fragment sizes prior to, and after targeting and Cre mediated loopout. Bottom panel shows Southern analysis of female wild type, *Xist* $^{intron\ 1+/-}$ neo clone (neo) and neo loop out clones 3, 8 and 10. **F)** DNA-FISH detecting the *Xist* locus in *Xist* $^{intron\ 1+/-}$ cells (left panels), and X-paint DNA-FISH analysis (Rhodamine red, right panels). **G)** qRT-PCR analyzing *Xist* expression in female wild type and *Xist* $^{intron\ 1+/-}$ ES cells during a differentiation assay for up to 5 days. Results were normalized to *Actin*.

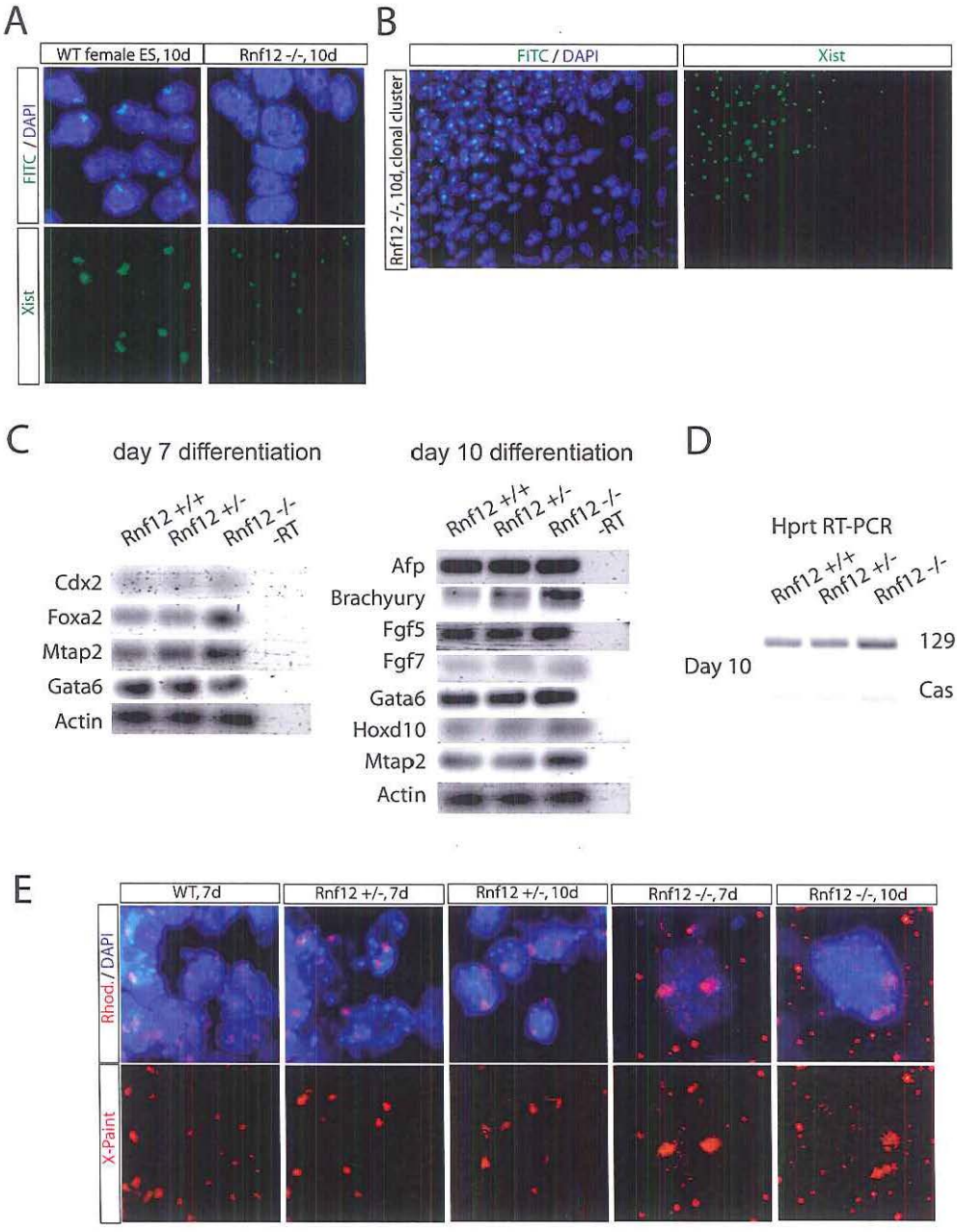

Figure S5
A) RNA-FISH analysis detecting *Xist* (FITC) in day 10 differentiated female wild type and *Rnf12*$^{-/-}$ ES cells. **B)** Example of clonal cluster of cells which have initiated XCI in *Rnf12*$^{-/-}$ ES cells differentiated for

Figure S5: continued
10 days as detected by *Xist* RNA-FISH. **C)** RT-PCR examining expression of several differentiation markers with RNA of day 7 (left panel) and day 10 (right panel) differentiated female wild type, *Rnf12*$^{+/-}$ and *Rnf12*$^{-/-}$ ES cells. **D)** Allele specific RT-PCR determining *Hprt* with a 129 and Cas origin, indicating the presence of both X chromosomes in all cell lines tested. **E)** DNA-FISH detecting a whole chromosome X paint probe in wild type, *Rnf12*$^{+/-}$ and *Rnf12*$^{-/-}$ ES cells differentiated for 7 or 10 days. Slides were first used for RNA-FISH, and subsequently denatured and hybridized to the DNA probe. Virtually all cells in the *Rnf12*$^{-/-}$ ES cells which did not show *Xist* clouds stained positive for the presence of two X chromosomes.

Table S1: Primers used in this study:

Primer	Forward	Purpose	Digest	Ref
Kpn1-RLIM Prom	TTGGTACCCTAGTTAGAGCCTCGAGG AGGCCTT	*Rnf12* promoter		984
PlusProm-Sac1	CCTAGGAGCTCGCCAGCTCGGAGAC GTAGCTCA	*Rnf12* promoter		984
mXistI 1-3L	CAGTGGTAGCTCGAGCCTTT	*Xist* RFLP	BsrgI	
mXistI 1-3R	CCAGAAGAGGGAGTCAGACG	*Xist* RFLP	BsrgI	
Atrx RFLP FW	TCCCCAATTA AAGGTGTTGA	*Atrx* RFLP	PflmI	
Atrx RFLP RV	AATTCACGTTCTCCTCTTTCACT	*Atrx* RFLP	PflmI	
Nhe GenA F	GCCTTCGAACATCTCTGAGC	*Rnf12* RFLP	NheI	174
Nhe GenA R	GAGCCGGACTAATCCAAACA	*Rnf12* RFLP	NheI	174
Rnf12 arm F	GCCTTCGAACATCTCTGAGC	Targeting arms		174
Rnf12 arm R	GAGCCGGACTAATCCAAACA	Targeting arms		174
Luc qPCR 1 F	TCTAAGGAAGTCGGGGAAGC	Luciferase qPCR		
Luc qPCR 1 R	CCCTCGGGTGTAATCAGAAT	Luciferase qPCR		
b-actin for	ACTATTGGCAACGAGCGGTTC	qPCR		174
b-actin rev	AGAGGTCTTTACGGATGTCAACG	qPCR		174
Nanog for	AGGATGAAGTGCAAGCGGTG	qPCR		191
Nanog Rev	TGCTGAGCCCTTCTGAATCAG	qPCR		191
Oct3/4 for	CCCCAATGCCGTGAAGTTG	qPCR		191
Oct3/4 rev	TCAGCAGCTTGGCAAACTGTT	qPCR		191
Sox2 for	CACAGATGCAACCGATGCA	qPCR		191
Sox2 rev	GGTGCCCTGCTGCGAGTA	qPCR		191
Klf4 for	GTGCCCCGACTAACCGTTG	qPCR		134
Klf4 rev	GTCGTTGAACTCCTCGGTCT	qPCR		134
Xist for	GCCTCAAGAAGAAGGATTGC	qPCR		174
Xist rev	GGGATTGTTTGTCCCTTTGG	qPCR		174
Rnf12 ex4-5 for	GGTCCACCACCACAGAGC	qPCR		
Rnf12 ex4-5 rev	TGACCACTTCTTGTTGTATTTCC	qPCR		
AFP for	CCTATGCCCCTCCCCCATTC	qPCR		
AFP rev	CTCACACCAAAGCGTCAACACATT	qPCR		
T-S764	ATGCCAAAGAAAGAAACGAC	qPCR		61
T-AS1579	AGAGGCTGTAGAACATGATT	qPCR		61
Gata6-S917	ACCTTATGGCGTAGAAATGCTGAGG GTG	qPCR		61
Gata6-AS1250	CTGAATACTTGAGGTCACTGTTCTCG GG	qPCR		61
Mtap2-S629	CATCGCCAGCCTCGGAACAAACAG	qPCR		61
Mtap2-AS867	TGCGCAAATGGAACTGGAGGCAAC	qPCR		61
Cdx2-2 for	TCCAGGCTGAGCCATGA	qPCR		61
Cdx2-2 rev	CGTGGGTAGGAGGAGAGGAAT	qPCR		61
Hoxd10 for	CTGAGGTTTCCGTGTCCAGT	qPCR		67
Hoxd10 rev	TTCTGCCACTCTTTGCAGTG	qPCR		67
Fgf7 for	CCATGAACAAGGAAGGGAAA	qPCR		67
Fgf7 rev	TCCGCTGTGTGTCCATTTAG	qPCR		67
Foxa2 for	ACACGCCAAACCTCCCTACT	qPCR		
Foxa2 rev	GGCACCTTGAGAAAGCAGTC	qPCR		
Fgf5 for	GCTGTGTCTCAGGGGATTGT	qPCR		
Fgf5 rev	TCTTGGCTTTCCCTCTCTTG	qPCR		
Gapdh ex-intr3 for	CCTGGGGCTCACTACAGACC	qPCR		
Gapdh ex-intr 3 rev	AATCTCCACTTTGCCACTGC	qPCR		

Tsix X9 for	TGACCAGTACCTCGCAAGTTC	qPCR		191
Tsix X9 rev	CTAAGAGCACCTGGCTCCAC	qPCR		191
NS18	GGTAACAATTTTCCCGCCATGTG	*Tsix* RFLP	MnlI	137
NS19	GGAAATAAACGGAACGCAGTACC	*Tsix* RFLP	MnlI	137
Tsix1 for	ACCATGACCAAAGCAACTCC	Copy-number		174
Tsix1 rev	CTCCTCCAGTACCATGTCTGC	Copy-number		174
Rnf4-5 for	AGCCCCGATGAAAATAGAGG	Copy-number		174
Rnf4-5 rev	GGCATTTCTGGATAATCTTTGG	Copy-number		174
Zfp42 for	GCACCCATATCCGCATCCAC	Copy-number		174
Zfp42 rev	GCATTTCTTCCCGGCCTTTG	Copy-number		174
Xist LP 1445	ACTGGGTCTTCAGCGTGA	RT-PCR LP		
Xist LP 1446	GCAACAACGAATTAGACAACAC	RT-PCR LP		
Xist LP2 1447	GGGAATAGGTAAGACACACTG	RT-PCR LP		
Rnf12 cDNA for	TAAAGAGGGTCCACCACCAC	RT-PCR RFLP	NheI	174
Rnf12 cDNA rev	GGCAGAGAGCCACTTTCATC	RT-PCR RFLP	NheI	174
Hprt SfaNI cas for	ATGCCCAGCGTCGTGATTAG	RT-PCR RFLP	SfaNI	
Hprt SfaNI cas REV	TGGCAACATCAACAGGACTC	RT-PCR RFLP	SfaNI	

Addendum: Mice deleted for Xist intron 1 do not show an X chromosome inactivation phenotype

Tahsin Stefan Barakat, Nilhan Gunhanlar and Joost Gribnau
(work in progress)

Abstract

Inactivation of one of the two X chromosomes in placental mammals is essential for survival of females, and is initiated during embryonic development. This X chromosome inactivation (XCI) process is coupled to mouse development, and is suppressed or reversed in undifferentiated pluripotent cells, including female mouse embryonic stem (ES) cells, cells in the inner cell mass (ICM) of the female embryo, and female primordial germ cells (PGCs). The molecular coupling between the pluripotent state and lack of XCI has been proposed to involve direct suppression of *Xist*, the master *cis* regulator of the inactivation process, by recruitment of the pluripotency factors OCT4, SOX2, and NANOG to a region in *Xist* intron 1. Here, we have generated a mouse model with a genetic ablation of all pluripotency factor binding sites in *Xist* intron 1. The female $Xist^{\Delta intron1/+}$ and $Xist^{\Delta intron1/\Delta intron1}$ mice were found to be healthy and gave birth to offspring with a Mendelian distribution of the mutation. This indicates the absence of a role for the deleted region in imprinted XCI. In addition, from analysis of adult tissues, we conclude that random XCI was not affected. We conclude that the *Xist* intron 1 pluripotency factor recruitment site is not essential for *Xist* repression *in vivo*.

Introduction

Eutherian females inactivate one of their two X chromosomes in a process called X chromosome inactivation (XCI), to achieve a balanced dosage of X-linked and autosomal genes, compared to males [30]. In the female mouse embryo, XCI is initiated at the 2-4 cell stage, and is imprinted resulting in the exclusive inactivation of the paternal X chromosome [53, 985-986]. This form of imprinted XCI is maintained in the extra-embryonic tissues, but is reversed in the cells of the inner cell mass (ICM) of the blastocyst, where during a short window in development two active X chromosomes are tolerated [54]. Upon further differentiation, random XCI is initiated in the post-implantation epiblast, which will give rise to all embryonic cell lineages. Female embryonic stem (ES) cells, derived from the ICM harbor two active X chromosomes, and undergo random XCI upon *in vitro* differentiation, whereas female epiblast stem cells (EpiSCs), derived from the post-implantation embryo, represent a post-XCI state, in which one of the X chromosomes is transcriptionally silenced (for review, see [987]).

The non-coding RNA *Xist* is essential for XCI to occur. Expression of this X-transcribed RNA is up-regulated, and subsequent spreading of *Xist* in *cis* results in heterochromatinization and transcriptional shut-down of the X chromosome [74, 84-85, 93]. Recent years have highlighted progression in the understanding of *Xist* regulation in ES cells, their differentiated progeny and embryos. We have shown that an increased concentration of the X-encoded XCI-activator RNF12 upon differentiation results in XCI initiation [174], and *Xist* up-regulation does not occur in the absence of this crucial activator [911]. Suppression of *Xist* in undifferentiated cells might be a result of absence of *Xist* activation, as over-expression of *Rnf12* can result in *Xist* upregulation in undifferentiated ES cells [174]. *Xist* is also negatively regulated by its antisense partner gene *Tsix*, which is highly expressed in undifferentiated ES cells [118-119, 180, 988]. As *Xist* up-regulation is coupled to differentiation [190], and *Xist* is suppressed in undifferentiated cells, the pluripotency factor network has been implicated in direct and indirect suppression of *Xist* [192]. Indirect mechanisms might include activation of *Tsix* in undifferentiated cells by pluripotency factors [186, 989], and suppression of XCI activators [990]. A direct interaction between *Xist* suppression and the pluripotency factor network has been proposed to involve a region within *Xist* intron 1 [191].

Chromatin immunoprecipitation experiments have shown that the key pluripotency factors NANOG, OCT4 and SOX2 bind *Xist* intron 1 in both male and female undifferentiated ES cells, but not in differentiated cells, mouse embryonic fibroblast [191] and EpiSCs [991]. Genetic ablation of *Nanog* in male ES cells, which does not result in a loss of recruitment of OCT4 and SOX2 to the *Xist* intron 1 region, resulted in a modest up-regulation of *Xist* expression, whereas forced down-regulation of *Oct4* resulted in loss of binding of all pluripotency factors to the intron 1 region and a drastic increase of *Xist* expression suggested to be independent of *Tsix* regulation [191]. These correlative data have been proposed to support the hypothesis that the key pluripotency factors NANOG, OCT4 and SOX2 are crucial for a *Tsix*-independent repression *Xist* in undifferentiated ES and ICM cells. In support of this, it has been found that only NANOG expressing ICM cells undergo reactivation of the paternal inactivated X chromosome [367], which further supports a crucial role for NANOG in *Xist* repression. Furthermore, the intron 1 region contains a developmentally regulated DNAse hypersensitivity site [992], and recruitment of two other transcription factors *Prdm14* and *Tcf3* to *Xist* intron 1 [194-195], support a role for this region in *Xist* suppression.

We recently addressed the question whether the *Xist* intron 1 region is required for *Xist* suppression in undifferentiated ES cells, by generating a targeted deletion of all reported pluripotency factor binding sites in a female ES cell line [911]. Surprisingly, deleting *Xist* intron 1 did not affect XCI initiation, as $Xist^{\Delta intron1/+}$ ES cell lines initiated random XCI with normal kinetics without preferential inactivation of the Δintron1 allele, and undifferentiated $Xist^{\Delta intron1/+}$ ES cells did not show aberrant *Xist* expression. We reported only mild skewing towards inactivation of the mutant allele during later stages of differentiation, which argues against an important role for the *Xist* intron 1 region in the regulation of XCI. Here we study the role of the *Xist* intron 1 region in XCI *in vivo*. *Xist* intron 1 knockout mice appear to be fertile, give birth to normal offspring, and show random XCI in all tissues analyzed. We conclude that the *Xist* intron 1 region is not required for XCI regulation *in vivo*.

Results

To generate a mouse model in which all reported pluripotency factor binding sites in *Xist* intron 1 were deleted, a polymorphic 129/Sv-Cast/Ei *Xist* $^{intron\ 1(2lox)/+}$ ES cell line 29 [911], in which a 1,2 kb region of *Xist* intron 1 is replaced by a floxed neomycin cassette, was used to generate chimaeric mice. Germ line transmission was verified by genotyping for the presence of the neomycin cassette integrated in *Xist* (data not shown). *Xist* $^{intron\ 1(2lox)/+}$ females were bred to males expressing pCAGGS-Cre, to loop out the selection cassette. Loopout of the selection cassette was verified by PCR on genomic tail-tip derived DNA. The resulting *Xist* $^{\Delta intron\ 1/+}$ mice were bred to wild type mice, and showed transmission of the deletion to both male and female offspring, in a Mendelian distribution (**Figure 1** and **Table 1A**). Crosses of *Xist* $^{\Delta intron\ 1/Y}$ males with heterozygous *Xist* $^{\Delta intron\ 1/+}$ females resulted in homozygous offspring (**Figure 1**), which were successfully used to breed with *Xist* $^{\Delta intron\ 1/Y}$ males. The *Xist* $^{\Delta intron\ 1/Y}$ male and *Xist* $^{\Delta intron\ 1/\Delta intron\ 1}$ female offspring followed a Mendelian distribution and resulted in a normal litter size.

To analyze the level of skewing in adult mice, female heterozygous *Xist* $^{\Delta intron\ 1/+}$ mice were bred to Cast/Ei males. The resulting F1 hybrid female mice, carrying a Cast/Ei derived X chromosome with the wild type *Xist* intron 1 region, and one *Xist* intron 1 deleted allele on a mixed C57Bl/6 and 129/Sv X chromosome was used to assess skewing of random XCI. Randomness was determined by amplification of a length polymorphism in *Xist* used to determine allele specific expression analysis with cDNA obtained from different organs of wild type and *Xist* $^{\Delta intron\ 1/-}$ littermates. In the wild type mice we found the expected 60:40 ratio favoring *Xist* expression from the C57Bl/6 (**Figure 2**), indicating skewed XCI in favour of the C57Bl/6 X chromosome due to differences in XCE strength between the C57Bl/6 and Cast/Ei X chromosomes [445]. Subsequent analysis X-linked gene expression examing *Mecp2*, *G6pdx* and *Atp7a* using RFLPs and length polymorphisms that distinguish between C57Bl/6 and Cast/Ei expression showed a reciprocal expression of these genes favoring Cast/Ei expression. In *Xist* $^{\Delta intron\ 1/+}$ female mice (N=2) allele specific *Xist* and X-linked gene expression was indifferent from to wild type litter mates, which indicates that *Xist* intron 1 heterozygous females undergo normal random XCI (**Figure 2**). Random XCI was also found in informative female offspring obtained from matings between *Xist* intron 1 mutant males with wild type F1 hybrid females carrying a C57Bl/6 and a Cast/Ei X chromosome (N=2, data not shown).

Discussion

Here we have generated a mouse model in which the pluripotency factor binding site in *Xist* intron 1 region, proposed to be important for *Xist* suppression in undifferentiated cells, is deleted. Surprisingly, *Xist* intron 1 deleted mice are healthy, fertile and undergo random X chromosome inactivation. These results indicate that the *Xist* intron 1 region is not essential for *Xist* suppression *in vivo*.

It was previously suggested that recruitment of pluripotency factors to the *Xist* intron 1 region is required for *Xist* repression in undifferentiated cells [191]. However, we found that genetic ablation of this region did not result in aberrant *Xist* expression in ES

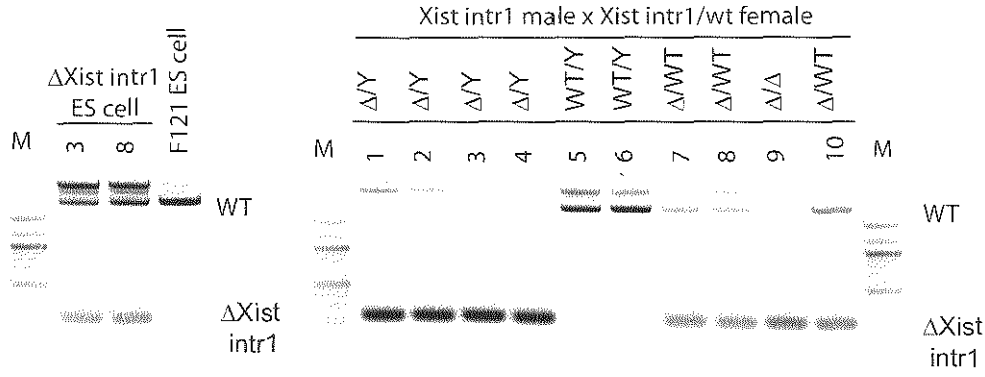

Figure 1: **Genotyping of *Xist* intron 1 mutant mice**
Left panel: genotyping of wild type and *Xist*$^{intron\ 1\ +/-}$ ES cells.
Right panel: example of a litter of mice obtained after mating of an *Xist* intron 1 mutant male with a heterozygous *Xist* intron 1 deleted female, genotyped by PCR on genomic DNA. Animal 1 till 6 are males (data not shown), of which 4 show the presence of a band diagnostic for the *Xist* intron 1 deletion (*ΔXist* intron 1). Animal 7 till 10 are females, with animal 9 showing loss of the wild type allele, diagnostic of a homozygous deleted female.

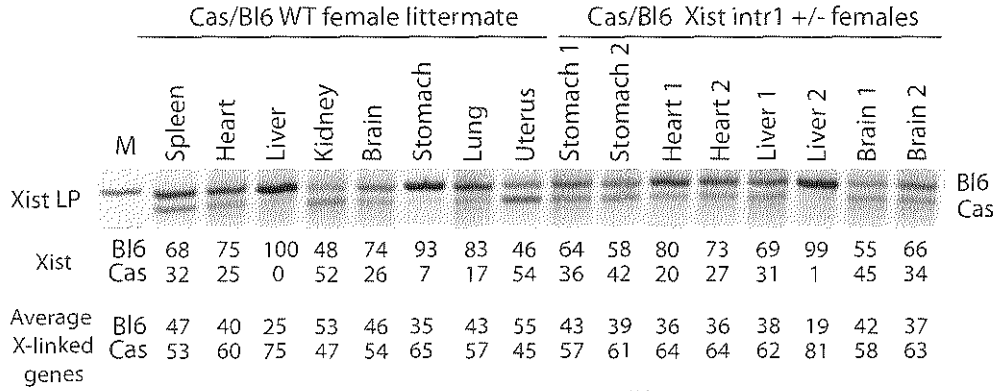

	Average all tissues	Cas/Bl6 WT female	Cas/Bl6 Xist intr1 +/- females 1	2
Xist	Bl6	73	67	74
	Cas	27	33	36
Average X-linked genes	Bl6	43	40	33
	Cas	57	60	67

Figure 2: ***Xist* intron 1 deleted females show random X chromosome inactivation in adult tissues**
Upper panel shows RT-PCR for a length polymorphism differentiating between *Xist* expression from Cast/Ei and C57Bl/6 in a wild type hybrid mice, and two hybrid *Xist* intron 1 mutant females. Allele specific ratios are plotted under the gel. Average X-linked gene expression, as determined for *Mecp2*, *G6pdx* and *Atp7a* is plotted as well.

cells, but this does not exclude a role for this region *in vivo* [12]. Two of the pluripotency factors recruited to this region, OCT4 and SOX2, are already expressed from the morula stage onwards in pre-implantation embryos were imprinted XCI occurs. However, the inactivated paternal X chromosome of imprinted XCI only becomes reactivated at a later stage in epiblast cells that express *Nanog* [367]. It was therefore hypothesized that NANOG binding to the *Xist* intron 1 region is required for proper reactivation of the inactive X chromosome [993]. The same reactivation function of NANOG might be required in PGCs and in mouse iPS cells, which both show reactivation of the inactive X chromosome [68-69]. Alternatively, it was hypothesized that the paternal *Xist* intron 1 region might carry an imprint, which would prevent specific recruitment of OCT4 and SOX2 to the paternal X chromosome, thereby preventing suppression of *Xist* in *cis* [993]. Binding of NANOG to both alleles during later stages of development would then allow erasure of the imprint, and repression of both *Xist* alleles in cells of the ICM, followed by random XCI in the post-implantation epiblast. The present data argue against both models. In the heterozygous mice analyzed, random XCI was observed, both when the *Xist* intron 1 deletion was transmitted through the mother or the father, indicating proper reactivation of the X chromosome. Although imprinted XCI was not investigated directly, the normal Mendelian distribution of offspring obtained in all crosses with *Xist* intron 1 mutant mice argues against a failure of imprinted XCI, as such a failure would result in female embryonic lethality during post-implantation stages [93-94].

In previous *in vitro* studies [911], we did not find compelling evidence for an important role of the *Xist* intron 1 region in *Xist* suppression, as *Xist* $^{\Delta intron\ 1/+}$ ES cells underwent XCI with normal kinetics, and no aberrant *Xist* activation was detected in undifferentiated cells. Although these results indicate that pluripotency factor binding to the *Xist* intron 1 region might not be crucial for *Xist* suppression *in vitro*, it cannot be ruled out that redundant mechanisms work together to prevent up-regulation of *Xist* in undifferentiated cells. Indeed, as antisense *Tsix* transcription is important for *Xist* suppression, it might be that a more subtle effect of the *Xist* intron 1 region can only be revealed when *Tsix* is inhibited in *cis*. In agreement with this, a recent study has reported that the combined removal of the *Xist* intron 1 region and the *Tsix* transcriptional start site results in loss of repression of *Xist* from autosomally integrated transgenes [994]. However, in that study, only transgenes were investigated, and therefore the results might have been affected by differences in transgene copy number and position effect variegation. A definitive answer can only be obtained when both the *Xist* intron 1 region and *Tsix* are removed in *cis* from the endogenous loci.

An alternative mechanism explaining the coupling of differentiation to *Xist* up-regulation might involve the developmentally regulated activity of *Xist* activators. Under such a scenario, pluripotency factor mediated *Tsix* activation [186, 989] and lack of *Xist* activation will result in the absence of *Xist* accumulation in undifferentiated cells. In agreement with this, *Rnf12*, the only identified XCI-activator to date, becomes up-regulated upon differentiation of female ES cells [174]. A negative correlation between RNF12 and NANOG expression has been observed in differentiating ES cells [911], and *Rnf12* expression seems to be negatively regulated by pluripotency factors [911, 983, 990]. Similar mechanisms might apply *in vivo*, where up-regulation of RNF12 might result in *Xist* activation in imprinted and random XCI, and reactivation of the imprinted paternal X

Xist intr1-/Y x WT female	4	26	11 (42%)	15 (58%)	0 (0%)	15 (100%)		
WT male x Xist intr1+/- female	3	20	8 (40%)	12 (60%)	6 (75%)	9 (75%)		
Xist intr1-/Y Xist intr1+/- female	4	32	14 (44%)	18 (56%)	4 (29%)	10 (71%)	7 (39%)	11 (61%)
Xist intr1-/Y x Xist intr1-/- female	3	15	9 (60%)	6 (40%)	0 (0%)	9 (100%)	0 (0%)	6 (100%)

Table 1: *Xist* intron 1 mice give birth to viable offspring in Mendelian distribution
The different types of crossings, number of pups obtained and their genotype is indicated.

chromosome in the ICM might occur by down-regulation of *Rnf12* expression and other XCI-activators by pluripotency factors. Therefore, an important area of future research involves the unravelling of the molecular interplay between pluripotency factors and XCI activators both *in vitro* and *in vivo*.

Methods

All animal experiments were in accordance with the legislation of the Erasmus MC Animal Experimental Commission. Generation of *Xist* $^{\Delta intron\ 1/+}$ ES cells has been described [911]. Tail-tip derived DNA was isolated according to standard procedures, and genotyping of the *Xist* intron 1 deletion was performed by PCR using primers 9,999 XIn1b (ccttgttggtccagacgactatt)
and 11,82 XIn1e (cactggactgggagagaggg). To assess XCI skewing, hybrid female mice were sacrificed by cervical dislocation, parts of organs were collected, snap-frozen and triturated using micro-pestils in 1 ml of Trizol reagent (Invitrogen). After an additional centrifugation to clear debris, 700 µl was added to 300 µl fresh Trizol, and RNA was purified following manufacturer's instructions. RNA was reverse-transcribed with SuperScript II (Invitrogen), using random hexamers. Allele specific *Xist* expression was analyzed by RT-PCR amplifying a length polymorphism using primers *Xist* LP 1445 (actgggtcttcagcgtga) and *Xist* LP 1446 (gcaacaacgaattagacaacac). To determine allele specific X-linked gene expression of *Atp7a*, *Mecp2* and *G6pdx*, primers 335 moF3930 (agggcaaacgtgtagcaatggtag) and 336 moF4812 (agagcttgttctaactcactgttct) were used for *Atp7a* amplifying a length polymorphism, [995], primers (catggtagctgggatgttagg) and (gcaatcaattctactttagagcg), for *Mecp2* amplifying a DdeI RFLP in *MeCP2*, and primers (ggagtgatgaactcagggaagc) and (atgtagctgggtttactggtgg) to amplify a ScrFI RFLP in *G6PD*. PCR products were gel purified and digested with the indicated restriction enzymes and analyzed on a 2% agarose gel stained with ethidium bromide. Allele specific expression was determined by measuring relative band intensities using a Typhone image scanner and ImageQuant software.

Chapter 6

RNF12 initiates X chromosome inactivation by targeting REX1 for degradation

This chapter has been published in

Cristina Gontan, Eskeatnaf Mulugeta Achame, Jeroen Demmers, Tahsin Stefan Barakat, Eveline Rentmeester, Wilfred van IJcken, J. Anton Grootegoed and Joost Gribnau (2012)
"RNF12 initiates X chromosome inactivation by targeting REX1 for degradation"
Nature 485: 386-390

RNF12 initiates X chromosome inactivation by targeting REX1 for degradation

Cristina Gontan[1], Eskeatnaf Mulugeta Achame[1], Jeroen Demmers[2], Tahsin Stefan Barakat[1], Eveline Rentmeester[1], Wilfred van IJcken[3], J. Anton Grootegoed[1] and Joost Gribnau[1,4]

[1]Department of Reproduction and Development, [2]Proteomics Center, and [3]Biomics Department, Erasmus MC, University Medical Center, Rotterdam, The Netherlands
[4]corresponding author

Contact details:
Joost Gribnau
Department of Reproduction and Development
Erasmus MC
Room Ee 09-71
PO Box 2040
3000 CA Rotterdam
The Netherlands
Phone +31-10-7043069
Fax +31-10-7044736
Email: j.gribnau@erasmusmc.nl

Evolution of the mammalian sex chromosomes has resulted in a heterologous X and Y pair, where the Y chromosome has lost most of its genes. Hence, there is a need for X-linked gene dosage compensation between XY males and XX females. In placental mammals, this is achieved by random inactivation of one X chromosome (XCI) in all female somatic cells [30]. Up-regulation of *Xist* transcription on the future inactive X chromosome (Xi) acts against *Tsix* antisense transcription, and spreading of *Xist* RNA in *cis* triggers epigenetic changes leading to XCI. Previously, we have shown that the X-encoded E3 ubiquitin ligase RNF12 is up-regulated in differentiating mouse embryonic stem cells (ESCs) and activates *Xist* transcription and XCI [174]. Here, we have identified the pluripotency factor REX1 as a key target of RNF12 in the XCI mechanism. RNF12 causes ubiquitination and proteasomal degradation of REX1, and *Rnf12* knockout mouse ESCs show an increased level of REX1. Using ChIP-seq, REX1 binding sites were detected in *Xist* and *Tsix* regulatory regions. Over-expression of REX1 in female ESCs was found to inhibit *Xist* transcription and XCI, whereas male *Rex1*+/- ESCs showed ectopic XCI. From this, we propose that RNF12 causes REX1 breakdown through dose-dependent catalysis, thereby representing an important pathway to initiate XCI. *Rex1* and *Xist* are present only in placental mammals, which points to co-evolution of these two genes and XCI.

The initiation of XCI in female cells implies a need for X-linked XCI activators which act in a dose-dependent manner to sense the number of X chromosomes present per diploid genome [179, 189]. We recently identified X-encoded RNF12 as a dose-dependent activator of XCI in mouse ESCs [174]. Additional transgenic copies of *Rnf12* resulted in initiation of XCI in male cells, and on both X chromosomes in a high percentage of female cells [174]. Random XCI was found to be markedly reduced in differentiating *Rnf12*+/- and *Rnf12*-/- female ESCs, which indicated an important role for RNF12 in the regulation of XCI, although the mechanism by which this E3 ubiquitin ligase initiates XCI remained elusive[911, 981].

To address this question, we generated FLAG-*Rnf12* transgenic female *Rnf12*+/- ESCs to identify interaction partners of RNF12 by FLAG-affinity purification. RNF12 is very unstable and the addition of the proteasome inhibitor MG132 facilitates its detection (**Figure 1a**). FLAG-RNF12 was purified from nuclear extracts of two FLAG-RNF12 ESC lines (**Supplementary Figure 1A**). Purified RNF12 samples and control samples were separated on SDS polyacrylamide gels (**Supplementary Figure 1B**) and analyzed by mass spectrometry (**Supplementary Table 1**). The only transcription factor consistently co-purifying with RNF12 was REX1 (**Figure 1B** and **Supplementary Table 1**). Previous studies have demonstrated that *Rex1* expression strictly correlates with the pluripotent state of ESCs [996], and REX1 has been implicated in suppression of genes involved in ESC differentiation [997]. We performed the reverse experiment, using two transgenic female ESC lines expressing a FLAG-V5-tagged REX1 fusion protein (**Supplementary Figure 1C**). In both REX1 purifications (**Supplementary Figure 1D, E**), performed with nuclear extracts of undifferentiated transgenic ESCs, RNF12 was present as a prominent interacting partner (**Figure 1B**). Co-purified RNF12 was non-ubiquitinated, but mass spectometry analysis and phosphatase treatment indicated that a significant fraction of RNF12 is phosphorylated (**Supplementary Figure 1F**). We confirmed the REX1-RNF12 interaction by co-immunoprecipitation of endogenous RNF12 and REX1 from undifferentiated female

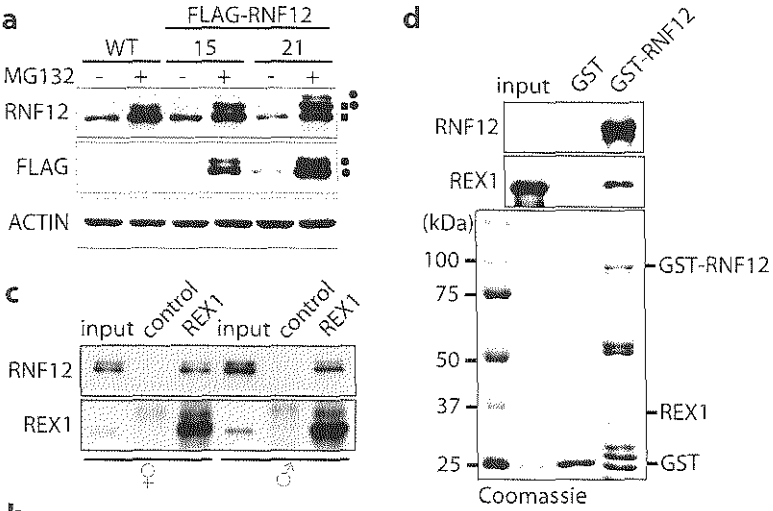

b

FLAG purifications

Protein	Mascot	Peptides	Mascot	Peptides	Mascot	Peptides	Mascot	Peptides
RNF12	1308	21(40)	1490	23(48)	1214	18(95)	1535	22(132)
REX1	124	2(5)	61	1(4)	558	11(71)	603	11(89)

Figure 1: RNF12 interacts with REX1 in mouse ESCs
A) Nuclear extracts of wild-type (WT) and transgenic FLAG-RNF12 ESC clones 15 and 21 were immunoblotted with RNF12 and FLAG antibodies (running positions of WT RNF12 and FLAG-RNF12 is indicated with ▪ and •). Where indicated, cells were treated with proteasome inhibitor (MG132). ACTIN was used as a loading control. **B)** Mass spectrometry analysis of FLAG-affinity purifications from FLAG-RNF12-expressing ESC clones 15 and 21, and FLAG-REX1-expressing clones 3 and 11. Mascot score, number of unique peptides and total number of peptides identified (between brackets) are shown for RNF12 and REX1 proteins in each of the purifications. **C)** REX1-RNF12 co-immunoprecipitation from nuclear extracts of female (left) and male (right) ESCs. Immunoprecipitations with REX1 antibody or control rabbit IgG were immunoblotted with RNF12 and REX1 antibodies. **D)** Direct binding of recombinant GST-RNF12 to recombinant REX1. RNF12 and REX1 are detected by immunoblotting (upper panels) and by Coomassie staining of a SDS-PAGE gel (lower panel). GST alone was used a negative control.

and male ESCs nuclear extracts (**Figure 1C**), and co-immunoprecipitation of recombinant GST-RNF12 and REX1 (**Figure 1D**). Mapping of the RNF12 region(s) involved in the interaction with REX1 indicated that both the N-terminal and C-terminal halfs of RNF12 contribute to the interaction (**Supplementary Figure 2A, B**).

We generated two catalytically inactive RNF12 mutants (**Figure 2A**). Transient expression in ESCs showed a increased stability of the RNF12 mutants (**Supplementary Figure 2C**), indicating that auto-ubiquitination contributes to the high turn-over of RNF12. To test whether REX1 is a bona fide substrate of RNF12, we transfected combinations of expression vectors encoding wild-type or mutant RNF12-GFP, with REX1-Cherry fusion proteins into HEK293 cells (**Figure 2B** and **Supplementary Figure 3A, B**). FACS analysis of REX1-Cherry transfected HEK 293 cells showed a more than ten-fold decrease in

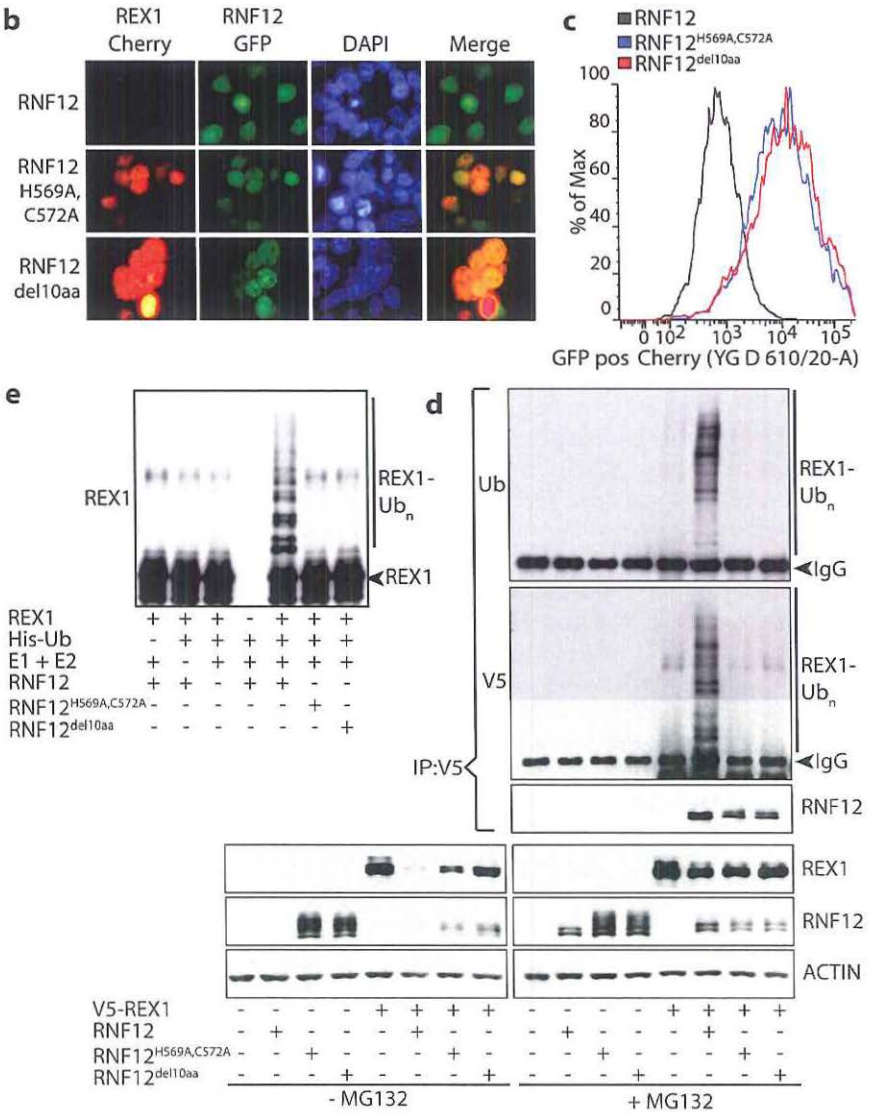

Figure 2: RNF12 polyubiquitinates and targets REX1 for proteasomal degradation
A) Sequence alignment of the RING finger domain corresponding to the WT and two catalytically inactive RNF12 mutants (two arginine substitutions are shown in red). **B)** Analysis of the fluorescence in HEK293 cells, 24 h after transfection with REX1-Cherry fusion expression vector alone or in combination with wild-type or catalytically inactive RNF12-GFP expression constructs. **C)** Quantification

Cherry intensity when cells were cotransfected with wild-type RNF12 compared to co-transfection with the RNF12 mutants (**Figure 2C** and **Supplementary Figure 3C, D**). This result suggests a strict correlation between RNF12 expression and REX1 degradation.

To provide evidence that REX1 is indeed ubiquitinated by RNF12, HEK293 cells were transfected with V5-REX1, and either RNF12 wild-type or the two inactive RNF12 mutants. REX1 was degraded in the presence of wild-type RNF12 but not in the presence of the RNF12 mutants (**Figure 2D**), and degradation was blocked by the proteasome inhibitors MG132 or epoxomicin (**Figure 2D** and **Supplementary Figure 4**). We subjected the nuclear extracts to immunoprecipitation with anti-V5 agarose beads, and probed with V5 and ubiquitin antibodies to visualize poly-ubiquitinated REX1 (**Figure 2D**, and **Supplementary Figure 4**). Mass spectrometric analysis detected five putative lysine acceptor sites for ubiquitin linkage (**Supplementary Figure 5**). In addition, an ubiquitination assay performed with recombinant proteins revealed poly-ubiquitination of REX1 only in the presence of wild-type RNF12, but not in the presence of either of the two RNF12 mutants (**Figure 2E**). These results indicate a direct role for RNF12 in targeting REX1 for degradation by the proteasome in an ubiquitin-dependent manner.

Our results predict that RNF12 and REX1 protein levels show a reciprocal correlation. Indeed, we found a pronounced increase of the REX1 protein level in *Rnf12-/-* ESCs (**Figure 3A**). Western blot analysis of RNF12 and REX1 protein levels in female wild-type ESCs indicated that REX1 is quickly down-regulated upon differentiation, coinciding with an initial increase in RNF12 (**Figure 3B**). In *Rnf12-/-* ESCs, the REX1 protein level is also down-regulated but the starting level is much higher. Comparison of the REX1 protein level in wild-type, *Rnf12+/-* and *Rnf12-/-* female ESCs, and in wild-type male cells, by immunoblotting, indicates that the REX1 level is very low in wild-type female ESCs (**Supplementary Figure 6B**), in agreement with a high ubiquitination-dependent turnover of REX1. Female *Rnf12+/-* cells and wild-type male cells display a lower RNF12 expression level and an increased REX1 protein level, although this relationship was not strictly two-fold which may be related to the pluripotent state of the ESC lines and enzyme kinetics (**Supplementary Figure 6A** and **Figure 3C**). *Rnf12* gene dosage did not affect other known factors involved in XCI, including YY1, NANOG and SUZ12 (**Figure 3B** and **Supplementary Figure 6A**). *Rex1* gene transcription, analyzed by qPCR, was not affected in *Rnf12-/-* cells (**Supplementary Figure 6B**), indicating that the down-regulation of REX1 by RNF12 is post-transcriptional.

Figure 2: continued
of **B** by FACS analysis. **D)** Left bottom panels show nuclear protein extracts of HEK293 cells co-transfected with the indicated expression constructs for V5-REX1, WT RNF12, or the catalytically inactive RNF12 mutants. Immunoblots were probed with the indicated antibodies. Right bottom panels show the same transfections, but in the presence of MG132. Upper panels: V5-tagged REX1 was immunoprecipitated with anti-V5 agarose beads and analysed by immunoblotting to detect the poly-ubiquitinated REX1 (REX1-Ub_n) with V5 and ubiquitin (Ub) antibodies. RNF12 co-immunoprecipitated with REX1 was detected with RNF12 antibody. **E)** REX1 ubiquitination assay with recombinant proteins. Recombinant REX1, His-ubiquitin, UBE1 (E1), UbcH5a (E2), recombinant RNF12 and RNF12 mutants were added in the indicated combinations. Ubiquitinated forms of REX1 were detected by immunoblotting with REX1 antibody.

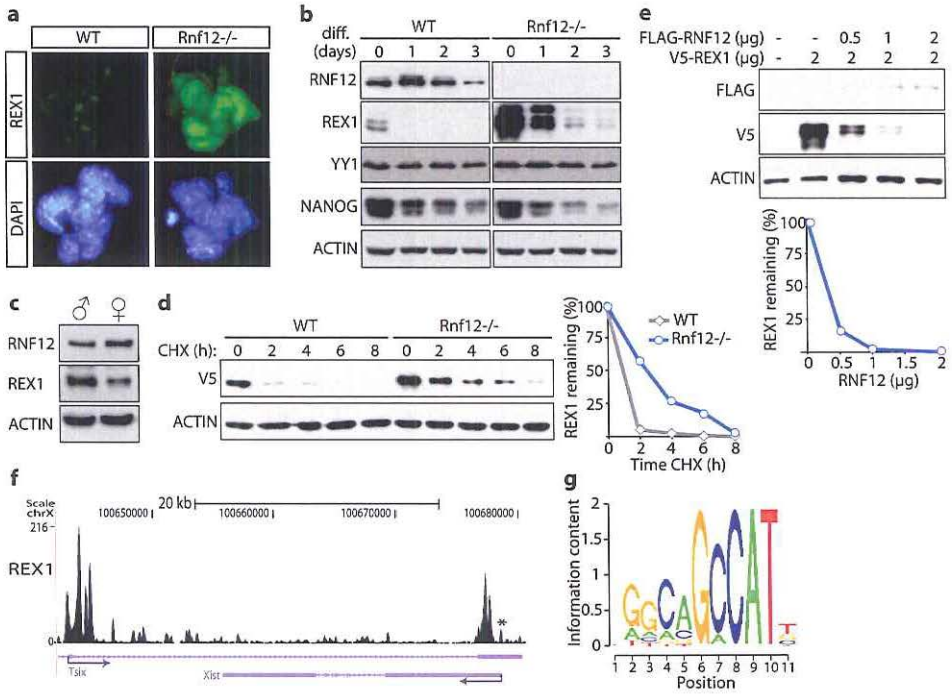

Figure 3: RNF12 is a dose-dependent regulator of REX1 expression
A) REX1 immunostaining (green) on WT and *Rnf12-/-* ESCs. **B)** Immunoblots of WT and *Rnf12-/-* ESCs at day 0, 1, 2 and 3 of differentiation, probed with antibodies against RNF12, REX1, YY1 and NANOG. **C)** RNF12 and REX1 protein levels were detected in female and male ESC nuclear extracts by immunoblotting. **D)** REX1 half-life measurements in WT and *Rnf12-/-* ESCs. ESCs were transiently transfected with V5-REX1 and treated 24 h post-transfection with 100 µg/ml cycloheximide (CHX) for the indicated times. Left panel: nuclear protein extracts were immunoblotted for V5-REX1 with V5 antibody. Right panel: quantitation of the REX1 level, using ImageJ software, at different time points compared to t=0 h (100%) in WT or *Rnf12-/-* ESCs. **E)** REX1 degradation by RNF12 is dose-dependent. FLAG-RNF12 or V5-REX1 constructs were co-transfected into HEK293 cells. Upper panel: levels of V5-REX1 and FLAG-RNF12 visualized by immunoblotting with V5 or FLAG antibodies. Bottom panel: quantification of the V5-REX1 level in cells co-transfected with RNF12, compared to the 100% level in cells transfected only with V5-REX1 plasmid. ACTIN was used as a loading control in **B-E.** **F)** REX1 binding pattern in the *Xist/Tsix* genomic region in female ESCs, as determined by V5-REX1 ChIP-sequencing. Identified sequence reads were plotted relative to genomic location and visualized using UCSC Genome Browser. Location and transcription start sites (arrows) of the *Tsix* and *Xist* loci are indicated. The asterisk marks a REX1 binding site in the *Xist* promoter. **G)** The REX1 consensus motif highly enriched in the genome-wide REX1 ChIP-seq peaks.

The marked increase of REX1 protein level in *Rnf12-/-* cells, points to an increase in REX1 protein stability in the absence of RNF12. Indeed, half life experiments, after cycloheximide treatment of V5-Rex1 transfected wild type and *Rnf12-/-* ESCs, indicate a strong increase in the half life (t½) of REX1 in *Rnf12-/-* ESCs (t½ >2hrs) compared to wild-type cells (t½ < 0.5hrs) (**Figure 3D**). Also, the REX1 protein level is down-regulated more effectively with an increasing dose of RNF12, as detected in HEK293 cells co-transfected

with a fixed concentration of V5-*Rex1* and an increasing concentration of FLAG-*Rnf12* expression vectors (**Figure 3E**). We previously found that male (as well as female) ESC lines stably over-expressing *Rnf12* show ectopic XCI [174]. To determine if over-expression of *Rnf12* would also affect the REX1 level, we stably introduced a BAC covering *Rnf12* into male ESCs, resulting in ectopic XCI at day 3 of differentiation (**Supplementary Figure 6C**). When undifferentiated, these clones show a lower level of REX1, which confirms that over-expression of RNF12 in male cells lowers REX1 stability (**Supplementary Figure 6C**). qPCR analysis showed that *Xist* is up-regulated in ESCs transiently over-expressing wild type RNF12, which is not observed using mutant RNF12, demonstrating that an intact RING-finger is required for initiation of XCI (**Supplementary Figure 6D**).

For RNF12 to function as an XCI-activator through degradation of REX1, REX1 could either repress *Xist* or activate *Tsix*. Indeed, a recent ChIP-qPCR study identified REX1 recruitment to the *Tsix* regulatory element *DXPas34*, which was found to be important for effective elongation of RNA polymerase II [989]. To identify all binding sites of REX1 in the region encompassing *Xist* and *Tsix*, we performed ChIP-seq analysis on undifferentiated FLAG-V5-*Rex1* female ESCs. This analysis confirmed enrichment for previously published REX1 binding sequences in *Tsix* [989], and showed specific REX1 binding sites in the *Xist* promoter and promoter distal region (**Figure 3F**), although REX1 recruitment to the *Xist* promoter was detected only in the presence of MG132. The observed genome-wide REX1 peaks revealed a highly enriched consensus binding motif (**Figure 3G**). Recruitment of REX1 to *Xist* and *Tsix* was also detectable, but less prominent in the absence of MG132 (**Supplementary Figure 7**). This result may explain why REX1 recruitment to *Xist* was not detected in a previous study [989] which did not include the use of proteasome inhibitors. Our results indicate that REX1 may perform a dual function, in the repression of *Xist* and the activation of *Tsix*.

To elucidate the role of REX1 in XCI, we analyzed XCI in day-3-differentiated *Rex1+/-* male ESCs [998] and control male ESCs. As expected, we found a small percentage of male control cells that contained *Xist* clouds (1%), detected with *Xist* RNA-FISH. In contrast, as many as 7.5% of the *Rex1+/-* male cells showed *Xist* clouds, hence initiation of XCI, supporting a dose-dependent role for REX1 in repression of XCI (**Figure 4A, B**). We next analyzed the female ESC lines over-expressing FLAG-V5-tagged REX1 and determined the percentage of cells that initiated XCI after 3 days of differentiation, by *Xist* RNA-FISH. For both REX1 over-expressing lines (Rex1_3 and Rex1_11) we detected a severely reduced number of cells with an *Xist* coated Xi, compared to wild-type female cells (**Figure 4C, D**), indicating a strong inhibition of XCI. *Rnf12-/-* cells showed no *Xist* clouds, consistent with our previous studies [911]. To test whether the XCI phenotype in *Rnf12-/-* ESCs was directly related to the resulting increased REX1 level we performed *Rex1* knock-down experiments in *Rnf12-/-* ESCs. A reduction in *Rex1* expression by more than 50%, 3 days after transient transfection of a *Rex1* shRNA vector, resulted in a more than 5-fold induction of *Xist*, in agreement with a mechanism in which REX1 acts downstream of RNF12 to activate XCI (**Figure 4E**). Next we analyzed the RNA expression level of *Rex1*, *Xist* and *Tsix* by qPCR in undifferentiated and day-3-differentiated wild-type and *Rex1* over-expressing ESC lines. In the latter cells, *Rex1* mRNA expression was 2.8-4.5-fold up-regulated before differentiation, followed by partial down-regulation at day 3 of

Figure 4: REX1 dependent regulation of XCI

differentiation due to silencing of endogenous *Rex1* and reduced expression of the transgene (**Figure 4F**). qPCR analysis of differentiation and pluripotency markers provided evidence that the *Rex1* over-expressing ESC lines undergo proper differentiation, which implies that the XCI phenotype is not a consequence of a differentiation defect (**Supplementary Figure 8**). Our analysis also indicated that *Tsix* expression was slightly up-regulated in undifferentiated REX1 over-expressing compared to wild type cells. Expression of *Tsix* was down-regulated at day 3 of differentiation, but was still higher than in wild type cells, consistent with our combined *Xist/Tsix* RNA-FISH analysis and supporting a role for REX1 in activation of *Tsix* (**Figure 4F** and **Supplementary Figure 9**). In contrast, up-regulation of *Xist* expression during differentiation was markedly reduced in the cells over-expressing REX1 (**Figure 4F** and **Supplementary Figure 9**). Our ChIP-seq data showing REX1 binding in the *Xist* regulatory regions, and genetic studies also indicated that *Xist* is under direct control of RNF12 [911]. To test a direct action on *Xist* independent of *Tsix* in more detail, we transiently transfected male ESCs harboring a non-functional *Tsix* stop allele with a *Rex1* expression vector. This *Rex1* over-expression resulted in suppression of *Xist*, providing further evidence for a *Tsix* independent pathway in the repression of *Xist* by REX1 (**Figure 4G**). We next performed luciferase assays with a luciferase reporter gene linked to the *Xist* promoter alone (*Xist*-luc), or including the distal region covering the REX1 recruitment sites in *Xist* exon1 (*Xist*-2p-luc). The constructs were transiently transfected into female wild-type cells, two *Rex1* over-expression ESC lines, and *Rnf12-/-* ESCs, and luciferase activity was measured at day 3 of differentiation. We found that both reporter constructs were down-regulated in the female *Rnf12-/-* and *Rex1* over-expression cell lines compared to a wild-type control female cell line (**Figure 4H**).

Figure 4: continued
A) *Xist* RNA-FISH (FITC) on day-3-differentiated WT and *Rex1+/-* male ESCs. **B)** Quantification of *Xist* clouds in **A** (n>100, error bars represent 95% Wilson confidence interval). **C)** *Xist* RNA-FISH (FITC) on day-3-differentiated female WT, *Rex1* over-expressing clones 1_3 and 1_11, and *Rnf12-/-* ESCs. **D)** Top panel: nuclear extracts of WT, transgenic FLAG-V5-REX1 lines 3 and 11 and *Rnf12-/-* ESCs were immunoblotted with REX1 antibody (open triangle: endogenous REX1, closed triangle: FLAG-V5-REX1). ACTIN was used as a loading control. Bottom panel: quantification of *Xist* clouds in **C** (n>200). Average percentage of cells with *Xist* clouds is shown. **E)** *Xist* and *Rex1* qPCR analysis of *Rnf12-/-* ESCs 72h after transfection with a *Rex1* shRNA construct or a control vector. **F)** qPCR analysis of *Rex1*, *Xist* and *Tsix* expression in undifferentiated and day-3-differentiated WT and the Rex1_3 and Rex1_11 clones. **G)** qPCR analysis of *Rex1* and *Xist* expression in day-3-differentiated male *Tsix*-stop ESCs, after transient transfection with a *Rex1* or control (mock) expression vector. **H)** Upper panel, schematic representation of constructs used in the luciferase reporter assay: empty vector, *Xist* promoter (*Xist*-luc) and *Xist* promoter + proximal part of exon 1 (*Xist*-2p-luc) constructs. Lower panel: luciferase activity of the different constructs in WT, Rex1_3 and Rex1_11 clones, and *Rnf12-/-* female ESCs, tranfected with the corresponding reporter constructs and differentiated for 3 days. All data in (**D**,**E**,**F**,**G** and **H**) represent the average ± s.d (n = 3). **I)** The XCI regulatory network. Prior to differentiation of ESCs *Xist* is repressed by *Tsix* dependent and independent mechanisms, regulated by different factors. The RNF12 protein level is low leading to repression of *Xist* and activation of *Tsix*, respectively. Upon differentiation, the RNF12 nuclear protein concentration increases, resulting in an enhanced rate of degradation of REX1 and subsequent activation of *Xist*. **J)** Phylogenetic tree, showing the presence or absence of XCI, *Xist*, *Rnf12*, *Yy1* and *Rex1* in different species (n.d., not determined, n.a. not applicable).

Down-regulation was more prominent for the *Xist*-2p-luc construct in all cell lines, suggesting that REX1 represses *Xist* through the *Xist* promoter and its downstream region. Taken together with the previous findings [989], we suggest that REX1 inhibits XCI by repression of *Xist*, and by activation of *Tsix*. This leads to a model in which, upon ESC differentiation or during development, an increased RNF12 concentration results in a decrease in the nuclear REX1 concentration. Because RNF12 is X-encoded, this effect will be more pronounced in differentiating female cells compared to male cells, allowing de-repression of *Xist* in female cells only (**Figure 4I**).

Recently, *Rex1* homozygous knockout ESCs and mice have been generated [997, 999]. Although no effect on XCI has been reported, *Rex1-/-* embryos were born at a sub-Mendelian ratio [999]. From the present study, we would expect that the threshold for initiation of XCI might be lower, in both male and female *Rex1-/-* embryos compared to wild-type embryos, resulting in aberrant initiation of XCI. The fact that some live *Rex1-/-* offspring was generated, indicates that additional factors, possibly acting downstream or independent of RNF12, exert control over the XCI process. Interestingly, *Rex1* is present only in placental mammals, representing a retro-transposed copy of *Yy1*, a gene also implicated in the regulation of XCI [1000] (**Figure 4J**). *Rex1* is not present in marsupials, which also lack *Xist* mediated XCI. This suggests co-evolution of *Xist* and *Rex1* in conjunction with the appearance of an XCI mechanism which requires *Xist*. In contrast to REX1, we found that YY1 expression is not up-regulated in *Rnf12-/-* cells (**Figure 3B**). Co-immunoprecipitation experiments using HEK293 cells indicate that YY1 and RNF12 interact (**Supplementary Figure 10**), but YY1 is not ubiquitinated by RNF12. Although our findings do not preclude a role for RNF12 mediated control of YY1 they clearly emphasize that the RNF12-mediated control of REX1 concerns a specific interplay, which does not occur between RNF12 and YY1, which evolved after a retro-transposition event generated the *Rex1* retrogene. We propose that the origin of *Rex1* has played a key role in the evolution of random XCI in placental mammals.

Methods Summary

REX1 was identified as an RNF12 interaction partner by mass spectrometry analysis on FLAG affinity purified FLAG-RNF12, isolated from nuclear extracts of day 3 differentiated FLAG-*Rnf12* transgenic ESC lines treated with the proteasome inhibitor (MG132). Protein purification and mass spectrometry analysis were done as described in [1001]. For the ubiquitination assay in HEK293 cells, the cells were transiently transfected with polyethylenimine (PEI) (Polysciences Inc.) with the indicated expression vectors. The REX1 ChIP and ChIP-sequencing (ChIP-seq) experiments were performed as described in [1002] with minor modifications. RNA-FISH was performed as described in [179]. For the luciferase reporter assay, ESCs were transfected with the indicated vectors, using lipofectamine 2000 (Invitrogen). Firefly and Renilla luciferase activity were measured using a Dual-Luciferase reporter assay system (Promega). A full description of the methods can be found in the Supplementary Information.

Acknowledgements

We would like to thank Reinier Van der Linden and Cheryl Maduro for their help with some of the experiments, Akiko Inagaki, Charlotte Andrieu-Soler, Daniel Warmerdam, Long Zhang and Adone Mohd-Sarip for experimental advice, and Claire Rougeulle and Rudolf Jaenisch for providing the *Tsix*-stop cells. This work was supported by grants from the Netherlands Organisation for Scientific Research (NWO-TOP and NWO-VICI) and the ERC to J.G.

Author Contributions

C.G. and J.G. designed the experiments. C.G. performed most experiments assisted by E.R.. T.S.B., C.G. and J.G. generated the *Rnf12*-/- ES cells. C.G., J.D., W.IJ. and E.M.A. performed the mass spectrometry and sequencing analysis. J.G., J.A.G. and C.G. wrote the manuscript.

Supplementary Information

Methods

Plasmids and antibodies

The coding sequences of *Rnf12*, *Rex1* and *Yy1* were amplified from mouse ESC cDNA and cloned into a TOPO blunt vector (Invitrogen). RNF12^{H569A,C572A} and RNF12^{del10aa} amino acid mutants were generated by PCR site-directed mutagenesis. For mammalian expression, the wild-type and two mutant *Rnf12* coding sequences were subcloned into pCAG-FLAG, a CAG-driven expression vector containing a FLAG-tag (a kind gift from D. van den Berg) and pEGFP-N3 (Clontech) vectors; *Rex1* and *Yy1* were subcloned into pCAG-FLAG-V5 and *Rex1* also into a modified pCherry-C1 vector (kind gifts from H. Lans). *Rex1* cDNA and *Rnf12* cDNA and truncated forms were subcloned into pGEX-6P-1 (GE Healthcare) vector for expression in bacteria. For the *Rex1* knock down experiments, a mouse Rex1 shRNA sequence ACGGAGAGCTCGAAACTAA [989] was cloned into pSuper-GFP-Neo (Oligoengine) and a pSuper-GFP-Neo-control-shRNA was used as a control.
For the luciferase reporter constructs, DNA fragments containing the REX1 binding sites within the *Xist* promoter alone (*Xist*-luc, nt -548 to +47) or including the *Xist* promoter distal region (*Xist*-luc-2p, nt -548 to +2161) were amplified by PCR and cloned into the promoterless pGL4.10 [luc2] vector (Promega). All constructs were checked by DNA sequencing. Antibodies used were against V5 (Invitrogen), Flag-M2 (Sigma), NANOG (Calbiochem), OCT4 (Santa Cruz), SOX2 (R&D systems), REX1 (Abcam and Santa Cruz), SUZ12 (Upstate), RNF12 (Abnova), YY1 (Santa Cruz), Ubiquitin (Enzo) and β-ACTIN (Sigma).

Cell culture and DNA transfection

Mouse ESCs were grown and differentiated as previously described [179]. FLAG-*Rnf12* and FLAG-V5-*Rex1* transgenic ESC lines were generated by electroporation of *Rnf12*+/- [174] and wild-type female ESC lines F1 2-1 (129/Sv-Cast/Ei), with pCAG-FLAG-*Rnf12* or pCAG-FLAG-V5 vectors followed by puromycin selection. F1 2-1, F1 2-3 (129/Sv-Cast/Ei), 1.3 (16xms2), *Rnf12*+/-, and *Rnf12*-/- ESC lines have been described [174, 911]. Male 1.3 *Rnf12* over-expressing ESC lines were generated as described in Jonkers et al. [174]. The E14tg2a control and *Rex1*+/- male ESC line with a gene trap insertion in intron 3 of *Rex1* has been previously characterized [998], and was obtained from BayGenomics (gene trap clone no. XB238). ESCs were transfected using lipofectamine 2000 (Invitrogen), according to the manufacturer's instructions. For the *Rex1* knock-down experiments, *Rnf12*-/- ESCs were transfected with pSuper-GFP-Neo Rex1 shRNA or control vectors and after 24 h GFP positive cells were sorted by FACS and 48 h later cells were harvested for RNA isolation. HEK293 cells were cultured under standard conditions in DMEM (Dulbecco's modified Eagle's medium) supplemented with 10% (v/v) FCS (fetal calf serum) and penicillin-streptomycin, and transfected with polyethylenimine (PEI) (Polysciences Inc.).

Nuclear extract preparation

Unless otherwise indicated, cells were treated with proteasome inhibitor (15 μm MG132, Sigma) for 3 h before harvesting. We also tested the effect of the proteasome inhibitor epoxomicin (1 μM). ESCs and HEK293 cells were scraped from the culture dishes in ice cold PBS plus protease inhibitor (Roche). Embryoid bodies (EBs) grown in suspension, were collected by centrifugation, and washed twice in ice-cold PBS plus protease inhibitor. Nuclear extracts were prepared as described in [1003] but instead of dialysed, were diluted 1:1 with buffer 0 (20 mM Hepes pH 7.6, 20% glycerol, 1.5 mM MgCl2, 0.2 mM EDTA, 0.5 mM DTT, 15 μM MG132 and protease inhibitors). To confirm phosphorylation of RNF12, female ESCs nuclear extracts were incubated for 30 min at 30°C in the presence or absence of lambda protein phosphatase (New England Biolabs).

Protein purification and mass spectrometry

Protein purification and mass spectrometry analysis were done essentially as described in [1001]. Briefly, nuclear extract from Flag-*Rnf12* ESCs at day 3 of differentiation or FLAG-V5-*Rex1* undifferentiated ESCs were incubated with Flag M2 antibody-agarose beads (Sigma) for 3 hours at 4°C, in the presence of Benzonase (Novagen). Bound proteins were eluted with Flag-tripeptide (Sigma). Elutions were pooled by TCA precipitation, proteins were separated by SDS-PAGE and the gel was stained with the colloidal blue staining kit (Invitrogen). Mass spectrometry analysis was performed on a capillary liquid chromatography system (Nanoflow LC-MS/MS 1100 series; Agilent Technologies) coupled to a mass spectrometer (LTQ-Orbitrap; Thermo Fisher Scientific).

GST pull-down assays

Recombinant GST-*Rex1*, GST-*Rnf12* full-length cDNA and the truncated forms were expressed at 20°C overnight in *E. coli* BL21 (Invitrogen). Cells were harvested and flash-frozen. 50 mL lysis buffer (25 mM Hepes pH 7.6, 10% glycerol, 0.5 M NaCl, 0.01% NP-40mM, 4 mM DTT, 2.5 mM MgCl2, 50 μM ZnCl2, 0.15 mg/ml lysozyme and protease inhibitors) was added per litre of culture. After sonication, soluble GST fusion proteins were bound to glutathione-sepharose beads (GE Healthcare) and analyzed by Coomassie staining. For *in vitro* binding assays, the GST tag was removed from the GST-REX1 fusion protein though enzymatic digestion with PreScission Protease (GE Healthcare).
RNF12-bound beads were equilibrated in buffer 100 (20 mM Hepes pH 7.6, 10% glycerol, 100 mM KCl, 1.5 mM MgCl2, 0.2 mM EDTA, 0.02% NP40, 0.5 mM DTT, protease inhibitors) and incubated for 2 hours at 4°C in the presence of Benzonase (Novagene) with nuclear extracts of HEK293 cells transiently expressing V5-tagged Rex1 protein, or with 0.5 ug recombinant REX1 protein. Nuclease Benzonase was added to the extract to show DNA-independence of the REX1-RNF12 interaction. Bound proteins were eluted with sample buffer and analyzed by immunoblotting.

Immunoprecipitation

Undifferentiated female and male ESC nuclear extracts were incubated for 2 h with REX1 antibody or control rabbit IgG (Santa Cruz), followed by addition of protein A Sepharose (Amersham) for 1 h. After washing, bound proteins were eluted with SDS sample buffer and analysed by immunoblotting with RNF12 and REX1 antibodies.

Ubiquitination assays

For the ubiquitination assay in HEK293 cells, the cells grown in 10-cm dishes were transiently transfected for 48 h with 2 μg wild-type or mutant *Rnf12* expression vectors, in the absence or presence of 2 μg V5-tagged *Rex1 or Yy1* expression vectors. Where indicated, cells were treated with proteasome inhibitor MG132 (15 μM for 3 h, Sigma) or epoxomicin (1 μM for 6h, Sigma) before harvesting. Cells were collected by scraping in ice cold PBS and nuclear extracts were prepared as described above. To detect protein expression, 10% of the nuclear extracts were used for immunoblotting with antibodies against REX1, YY1 or RNF12, and ACTIN was used as a loading control. To recover V5-tagged REX1 and YY1, 15 μl of V5 antibody-agarose beads (Sigma) were added to the nuclear extracts and the mixture was rotated for 1.5 h at 4 °C. The beads were washed with buffer 150 (20 mM Hepes pH 7.6, 10% glycerol, 150 mM KCl, 1.5 mM MgCl2, 0.2 mM EDTA, 0.02% NP40, 0.5 mM DTT, protease inhibitors). Bound proteins were eluted with sample buffer and visualized by immunoblotting. Co-immunoprecipitated RNF12 was detected with RNF12 antibody and poly-ubiquitinated REX1 with V5 and Ub antibodies.
The *in vitro* ubiquitination assay was carried out by adding recombinant REX1 (1 μg), GST-*Rnf12* wild-type or mutant (0.5 μg), E1 (55 ng UBE1, Boston Biochem), E2 (300 ng UbcH5a, Boston Biochem) and His-Ub (2 ug, Sigma) to ubiquitination buffer (50 mM Tris pH 7.5, 150 mM NaCl, 5 mM $MgCl_2$, 2 mM ATP, 1 mM DTT and protease inhibitors) to a final volume of 30 μl. The reactions were incubated at 30 °C for 1 h, terminated by boiling for 5 min with sample buffer, and resolved by SDS-PAGE gel followed by immunobloting with anti-Rex1 antibody.

Quantitative real-time PCR

Total RNA was extracted by using Trizol (Invitrogen) and then reverse transcribed by with Superscript II reverse transcriptase (Invitrogen) according to the manufacturer's instructions. Real-time PCR was performed using SYBR Green (Sigma) in a CFX384 real-time PCR machine (Bio-Rad). Actin was used as a normalization control. All qPCR data represents the mean ± s.d. of triplicate samples performed on cDNA isolated from three independent experiments. The primer sequences used for qPCR are listed in the **Supplementary Table 3**, and **Supplementary Table 2** list the primers used for ChIP-qPCR.

Immunofluorescence staining

ESCs were grown on coverslips without feeders and fixed with 4% paraformaldehyde for 10 min at room temperature. Subsequently, cells were permeabilized with 0.4% Triton X-100 in PBS for 10 min at RT and blocked with 10% goat serum in PBST (PBS with 0.05% Tween 20) for 30 min at RT. The coverslips were incubated with REX1 antibody overnight at 4°C. After washing with PBST, cells were incubated with the secondary antibody, Alexa Fluor 488 goat anti-rabbit IgG (Molecular Probes) for 1 hour at RT. After a final wash with PBS, coverslips were mounted with Vectashield Plus DAPI (Vector Laboratories). Images were acquired using a fluorescence microscope (Axioplan2; Carl Zeiss).

RNA-FISH

RNA-FISH was performed as described in [179] with minor modifications. Pre-plated female ESCs were seeded on gelatin-coated coverslips without feeders in EB differentiation media (IMDM + Glutamax (GIBCO), 15% FCS, 50 μg/μl ascorbic acid, NEAA, penicillin-streptomycin, 37.8 μl/l monothioglycerol (97%)). At day three of differentiation, cells were fixed and subjected to RNA-FISH. *Xist* clouds were counted for three different coverslips per cell line analyzed. The *Xist* probe was a 5.5kb BglII cDNA fragment covering *Xist* exon 3-7. The *Tsix* probe was a 5.1 kb SalI-SacII fragment of *Tsix* intron 3.

ChIP and ChIP-sequencing

The ChIP and ChIP-sequencing (ChIP-seq) experiments were performed as described [1002] with minor modifications. Briefly, female ESCs expressing V5-tagged REX1 and control wild-type ESCs were grown without feeders to 80% confluence ($3 \cdot 10^7$ cells per ChIP or $1 \cdot 10^8$ cells per ChIP-seq). For ChIP-seq and ChIP (where indicated), the cells were treated for 3 h with proteasome inhibitor (15 μm MG132, Sigma) before chromatin was cross-linked for 10 min at RT with 1% formaldehyde. The cross-linking reaction was stopped by addition of 0.125 M glycine. Sonicated chromatin was immunoprecipitated with 60 μl of pre-blocked V5 antibody-agarose beads (Sigma) for each ChIP-seq. Purified ChIP-DNA was prepared for sequencing on a HiSeq 2000 sequencer (Illumina).
The data was analyzed using a combination of bioconductor packages (Shortread, ChIP-Seq, and MACS). Illumina reads (36bp) were aligned against the mouse genome (*M. musculus* NCBI build 37) using Solexa Genome Analyzer ELAND Software. Aligned reads were imported, filtered, normalized and coverage was calculated using Shortread and ChIP-Seq packages. The resulting coverage graph was visualized using the USCS Genome Browser. The significance of peaks was calculated using MACS package. Peaks with a fold change of >=4 and fdr<=0.001 were taken as significant.

Luciferase reporter assay

ESCs were seeded into 24-well plates in differentiation medium and after 24 h transfected with 0.8 μg of the indicated vectors, using lipofectamine 2000 (Invitrogen). To normalize for transfection efficiency, a GL4.74 (hluc/TK) vector (Promega) expressing *Renilla* luciferase was co-transfected. Firefly and *Renilla* luciferase activity were measured 48 h post-transfection using a Dual-Luciferase reporter assay system (Promega) according to manufacturer's instructions. Three independent experiments were performed in triplicate, and the data are shown as the mean ± s.d.

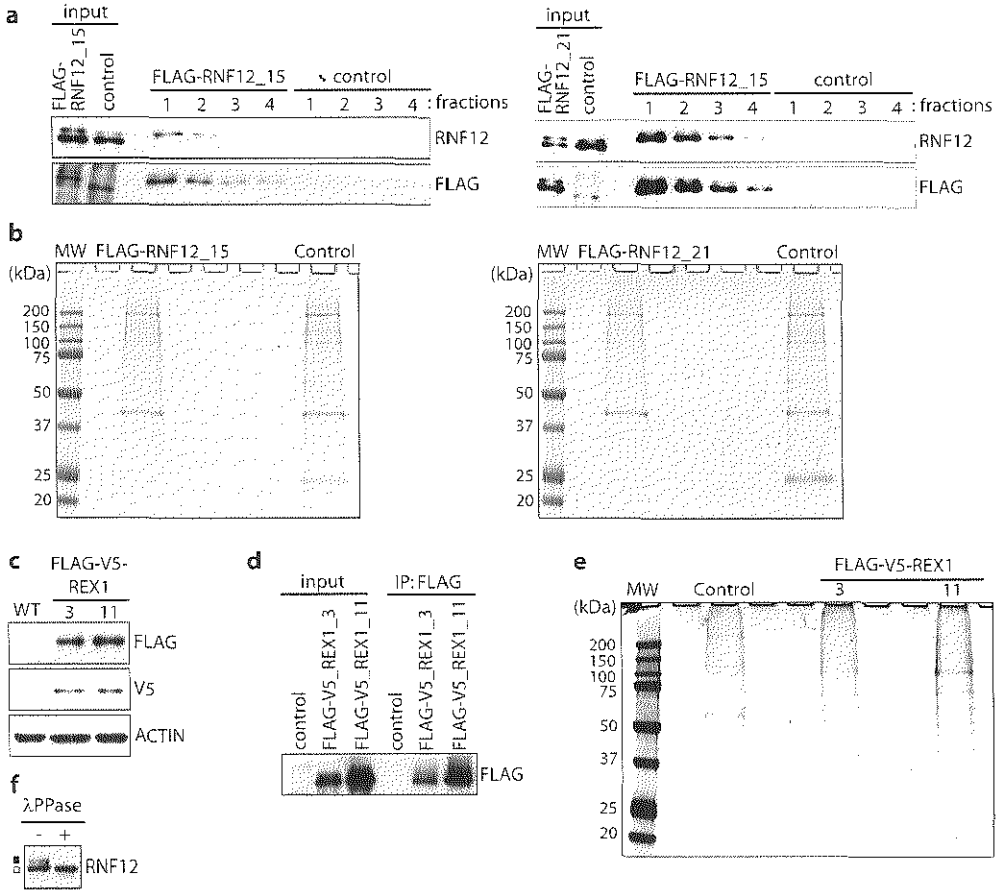

Supplementary Figure 1: Purification of FLAG-tagged proteins
A) Purification of FLAG-RNF12 by FLAG-affinity from nuclear extracts of wild-type (WT) and two FLAG-RNF12 transgenic ESC lines were immunoblotted with RNF12 and FLAG antibodies. Inputs and elution fractions from the FLAG-RNF12 and control cell lines are shown. **B)** Proteins from **A** were resolved by SDS-PAGE and stained with Coomassie. **C)** Nuclear extracts of WT and two FLAG-V5-REX1 transgenic ESC lines were immunoblotted with FLAG and V5 antibodies. ACTIN was used as a loading control. **D)** Purification of FLAG-V5-Rex1 by FLAG-affinity from nuclear extracts of WT and two FLAG-V5-REX1 transgenic ESC lines were immunoblotted with FLAG antibody. Inputs and elution fractions from the FLAG-V5-REX1 and control cell lines are shown. **E)** Proteins from **D** were resolved by SDS-PAGE and stained with Coomassie. **F)** Nuclear extracts of undifferentiated WT ESC were incubated in the presence (+) or absence (-) of λPPase and immunoblotted with RNF12 antibody (running positions of the unphosphorylated and phosphorylated forms of WT RNF12 are indicated with □ and ■).

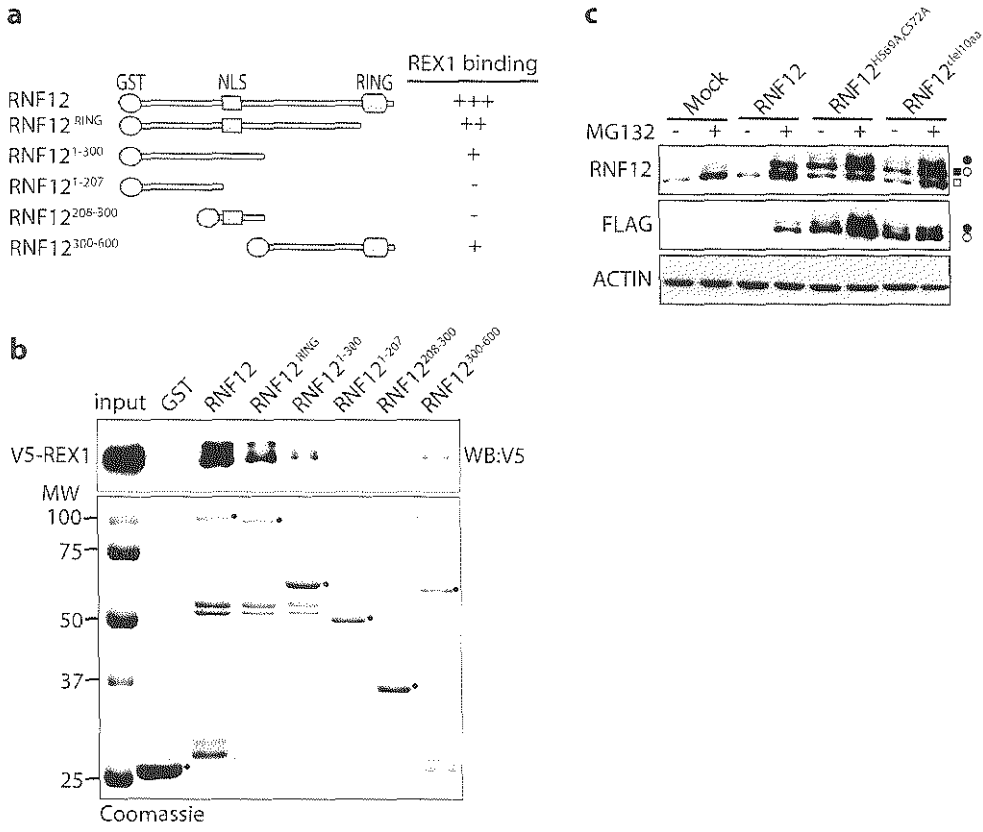

Supplementary Figure 2: Mapping of RNF12-interacting domains with REX1
A) Schematic representation of GST-RNF12 recombinant protein and the different truncation mutants used in **B**. NLS: nuclear localization signal; RING: RING finger domain. Relative level of binding of the different GST-RNF12 mutants to REX1, from the experiment in **B**, is indicated. **B)** GST pull-down with immobilized WT GST-RNF12 or the indicated truncated recombinant GST-RNF12 proteins from nuclear extract of HEK293 cells transfected with a V5-Rex1 expression construct. Upper panel: input and bound fractions were analysed by immunoblotting with V5 antibody to detect REX1 binding to recombinant RNF12. Bottom panel: eluted control GST and the different GST-RNF12 truncated recombinant proteins were detected by SDS-PAGE and Coomassie staining. The black dots point to GST and the various GST-RNF12 proteins. **C)** ESCs were transiently transfected with WT RNF12 and the two catalytically inactive RNF12 mutants in the presence or absence of the proteasome inhibitor (MG132). "Mock" refers to the empty plasmid. Nuclear extracts were prepared and analysed by immunoblotting with RNF12 and FLAG antibodies (running position of WT RNF12 and FLAG-RNF12 is indicated with □,○, the phosphorylated forms with ■,●). ACTIN was used as a loading control.

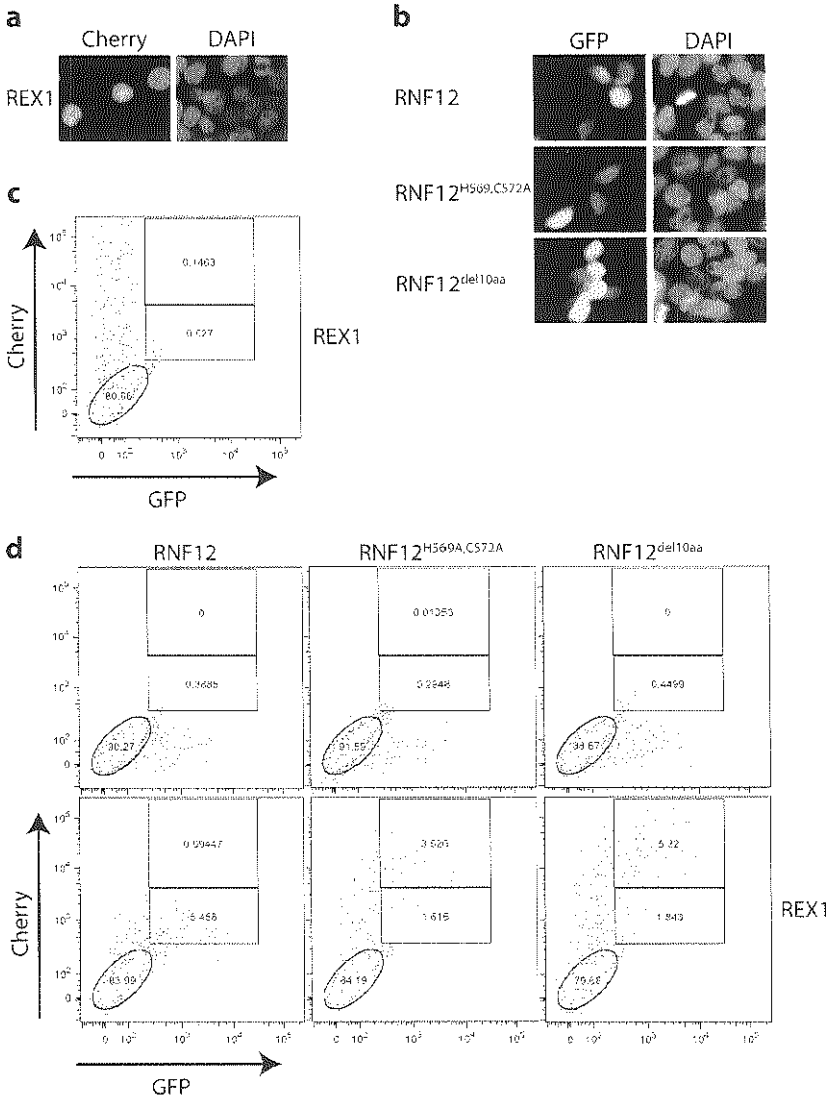

Supplementary Figure 3: Expression analysis of RNF12-GFP and REX1-Cherry in transgenic HEK293 cells

A), B), HEK293 cells seeded in a 12 well plate were transfected to test the expression constructs, with 0.6 µg of REX1-Cherry fusion expression vector **A** or 1.8 µg of WT or catalytically inactive mutant RNF12-GFP expression vectors, **B. C)** FACS analysis of HEK293 cells transfected with REX1-Cherry only. **D)** Upper panels show FACS analysis of HEK293 cells transfected with a RNF12-GFP vector, or two mutant RNF12-GFP fusion constructs. Bottom panels show the FACS profile of HEK293 cells co-transfected with REX1-Cherry in combination with either WT RNF12-GFP, or two different mutants RNF12-GFP. Shown in **C** and **D** is Cherry expression on the Y-axis, and GFP expression on the X-axis. The gated fractions represent the GFP positive, Cherry-high and Cherry-low cell populations.

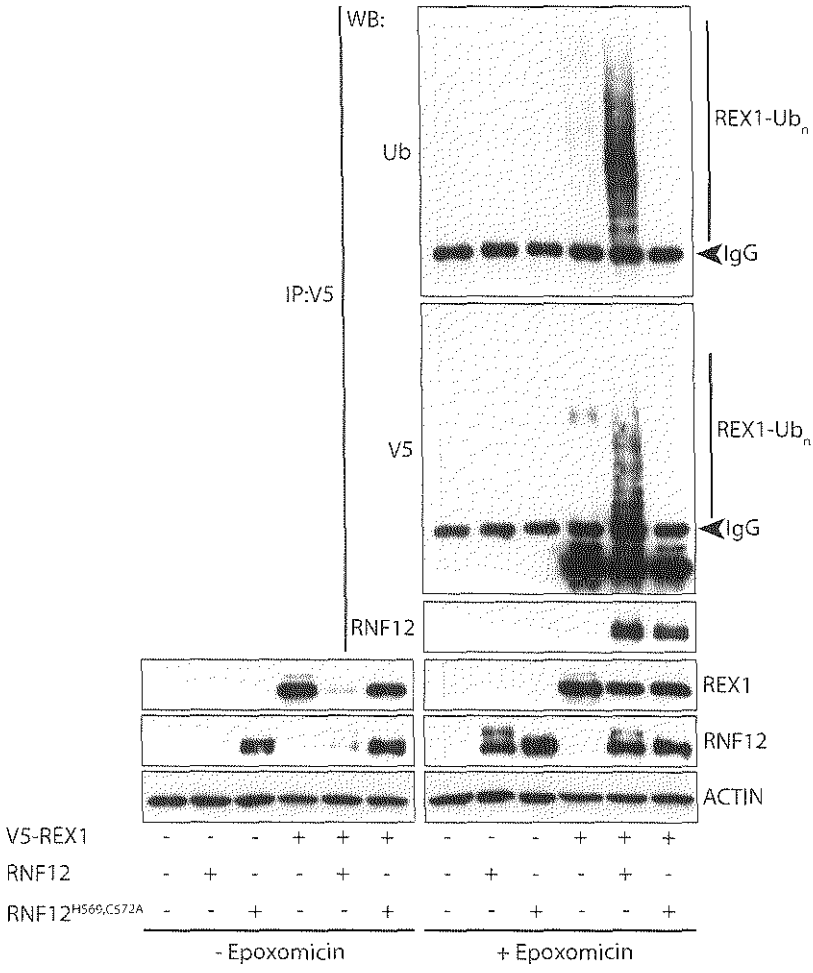

Supplementary Figure 4: REX1 ubiquitination assay in HEK293 cells
Left bottom panels show nuclear protein extracts of HEK293 cells co-transfected with the indicated expression constructs for V5-REX1, WT RNF12, or the catalytically inactive RNF12^{H569A,C572A} mutant. Immunoblots were probed with the indicated antibodies. Right bottom panels show the same transfections, but cells were treated with 1 μM epoxomicin for 6 hours before protein harvest. Upper panels, V5-tagged REX1 was immunoprecipitated with anti-V5 agarose beads and analysed by immunoblotting to detect the poly-ubiquitinated REX1 with V5 and ubiquitin antibodies. RNF12 co-immunoprecipitated with REX1 was detected with RNF12 antibody.

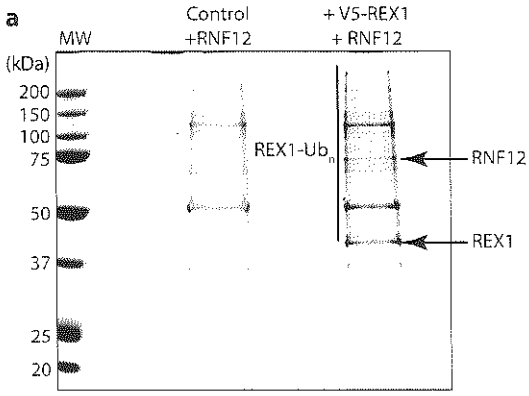

b

REX1
Peptides
LTLKQDEARPVQNTR
GTKQEKTEVTQETPPLR
QEKTEVTQETPPLR
AFTESSKLK
AFTESSKLKR

c

REX1
[1-288] mass = 32397.9
Cleavege at KR
Zinc finger domains

MNEQK...K...TSGQK...ALDR...QDEARPVQNTR...VTYTIR...
...GEFSEPILEEDFLFK...QVLEASSLLESSLEYMTK...QE...VGASS
LLAGGPAEKPEGGVYCGVLSMLECPQAGCK...K...DK...K...R...AFTESS...R...
...R...THIR...R...SFIQSNNQK...AGK...C

d

Ubiquitin sequence
MQIFV...TLTG...TITLEVEPSDTIENV...AK...IQD...EGIPPDQQRLIFAG...QKEDGRTLSDYNIQ...ESTKHLVLRLRGG

Ubiquitin linkages			
Lys	Peptides	Counts	Functions
K11	TLTGKTITLEVEPSDTIENVK	multiple	proteasomal degradation, misfolded proteins, ERAD
K48	LIFAGKQIEDGR	multiple	proteasomal degradation
K63	TLSDYNIQKESTIHLVLR	weak hit with low score	signalling, trafficking, DNA damage response

Supplementary Figure 5: REX1 is polyubiquitinated by RNF12
A) V5-affinity purification from nuclear extracts of HEK293 cells co-transfected with *Rnf12* and V5-*Rex1* expression constructs or *Rnf12* only in the control. 48 hours after transfection, cells were treated with MG132 for 3 hours before protein harvest. Purified proteins were resolved on a SDS-PAGE gel and stained with Coomassie. Putative bands representing RNF12, REX1 and poly-ubiquitinated REX1 are indicated. **B)** Sequences of the REX1-ubiquitinated peptides, identified by mass spectrometry, with the diglycine-modified lysine highlighted in red. Mass spectrometry analysis was done as described in the Methods section, with the modification that D2-iodoacetamide was used as alkylating agent to block cysteine residues. **C)** Amino acid sequence of mouse REX1. Highlighted in alternating black and grey are the peptides theoretically obtainable after trypsin digestion. Underlined are the peptides actually detected by mass spectrometry. Putative target lysines for ubiquitination are indicated in red. Green-shaded regions mark the four zinc finger domains and (*) marks the residues known to bind DNA. **D)** Table shows the ubiquitin sequence with the seven lysine residues highlighted in red and the polyubiquitin linkages that were present in the V5-REX1-RNF12 sample.

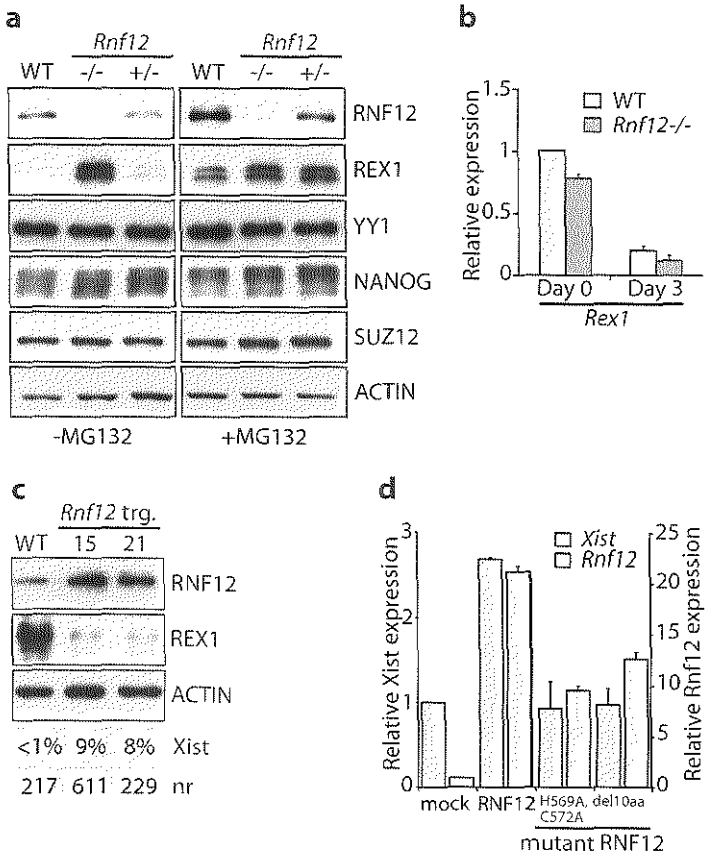

Supplementary Figure 6: RNF12 and REX1 protein levels show a reciprocal correlation
A) RNF12, REX1, YY1, NANOG and SUZ12 protein levels were compared by immunoblotting of nuclear extracts from undifferentiated WT, *Rnf12-/-* and *Rnf12+/-* female ESCs in the absence or presence of MG132. ACTIN was used as a loading control. **B)** WT and *Rnf12-/-* female ESCs have a similar *Rex1* mRNA level. *Rex1* expression was analysed by qPCR in WT and *Rnf12-/-* undifferentiated ESCs and at day 3 of differentiation. **C)** Nuclear extracts of wild-type and *Rnf12* transgenic male ESC lines 15 and 21 were immunoblotted with REX1 and RNF12 antibodies. ACTIN served as a loading control. Bottom panels show the percentage of cells with *Xist* clouds at day 3 of differentiation, and the total number of cells counted for each cell line. **D)** Male ESCs transiently transfected with an empty vector, or vectors expressing WT or two mutant forms of RNF12 were differentiated for 3 days. *Xist* RNA and *Rnf12* expression was determined by qPCR. All data represent the average expression ± s.d. ($n = 3$)

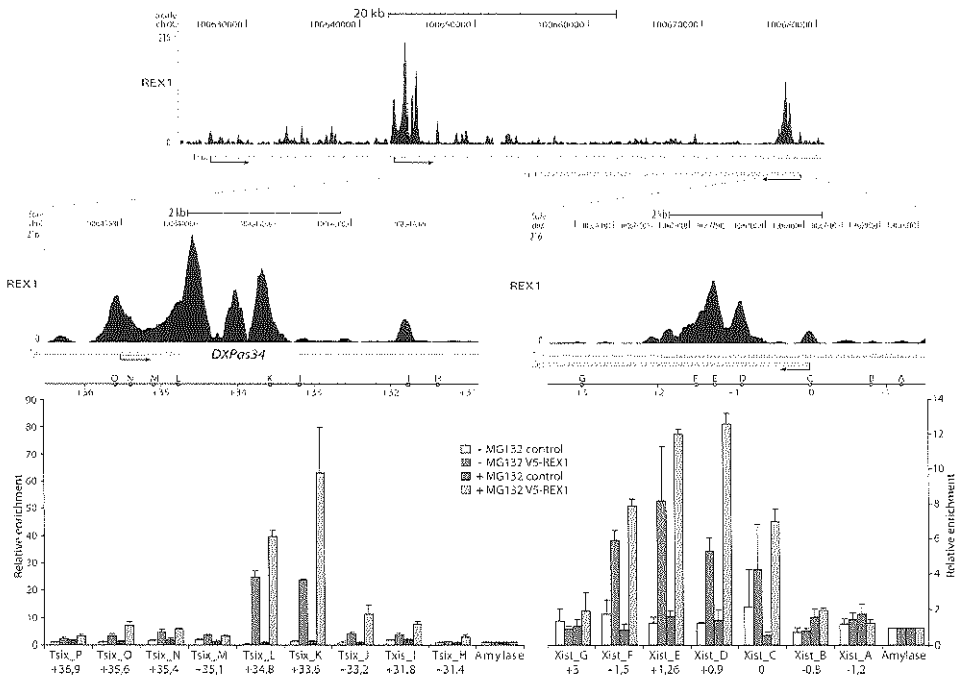

Supplementary Figure 7: Detailed view and confirmation of REX1 binding sites in the *Xist-Tsix* region

Upper panel: REX1 binding pattern in the *Xist/Tsix* genomic region in female ESCs, as determined by V5-REX1 ChIP-sequencing. Identified sequence reads were plotted relative to genomic location and visualized using UCSC Genome Browser. Location and transcription start sites (arrows) of the *Tsix* and *Xist* loci are indicated. **Middle panels**: higher magnification of the REX1 binding profile around the *DXPas34* region and the *Tsix* start site (left) or the *Xist* start site (right). Distance from the *Xist* transcriptional start site is indicated in kbs and genomic areas amplified in the V5-REX1 ChIP experiments (**lower panels**) are indicated by a red dot and the letters A to O. **Lower panels**: V5-REX1 ChIP using V5-REX1 expressing ESCs or control ESCs in the presence or absence of MG132. Relative enrichment over the *Amylase* negative control genomic region is indicated. Amplified regions are indicated in the **middle panels**, and the distance (in kbs) of the amplified regions from the *Xist* start site is indicated. All data represent the average expression ± s.d. (n = 3).

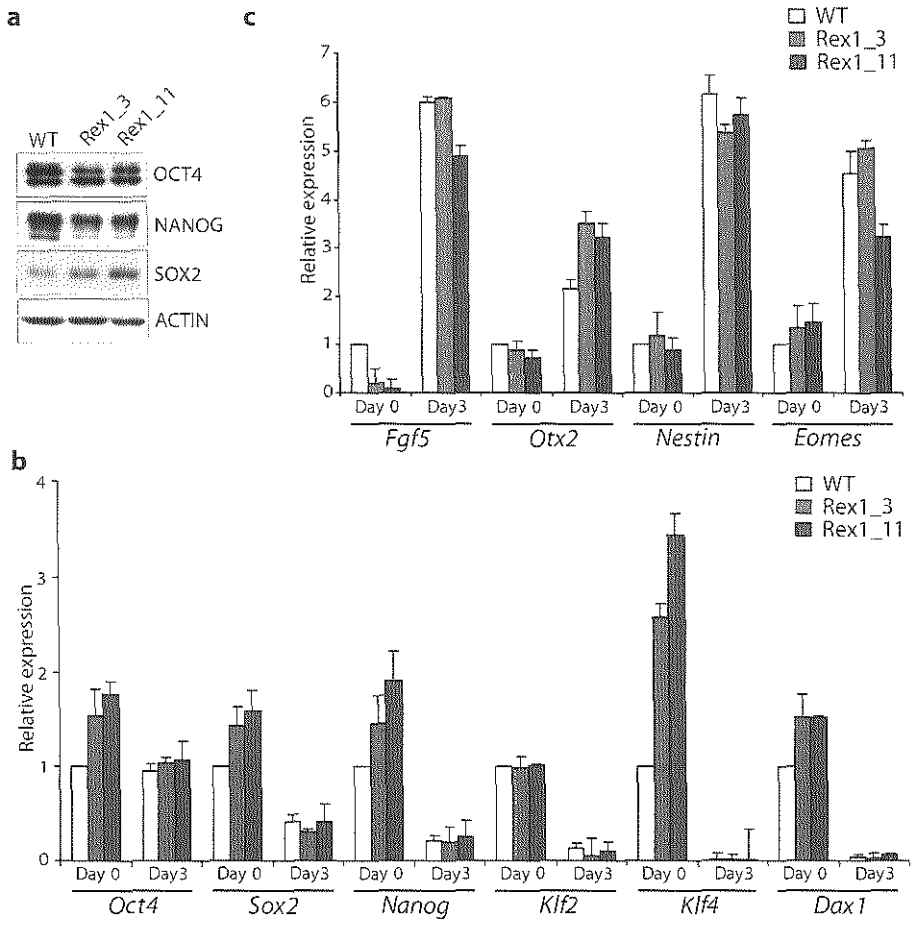

Supplementary Figure 8: Expression analysis of Rex1 over-expression ESC lines
A) Immunoblots with nuclear extracts of undifferentiated WT and Rex1 over-expression cell lines 3 and 11 detecting OCT4, NANOG, and SOX2. ACTIN was used as a loading control. **B), C)** Quantitative-PCR analysis of pluripotency markers *Oct4, Sox2, Nanog, Klf2, Klf4* and *Dax1*, and differentiation markers, *Fgf5, Otx2, Nestin* and *Eomes* in undifferentiated and day-3-differentiated WT and the Rex1_3 and Rex1_11 clones. Shown is the average expression ± s.d. (n = 3).

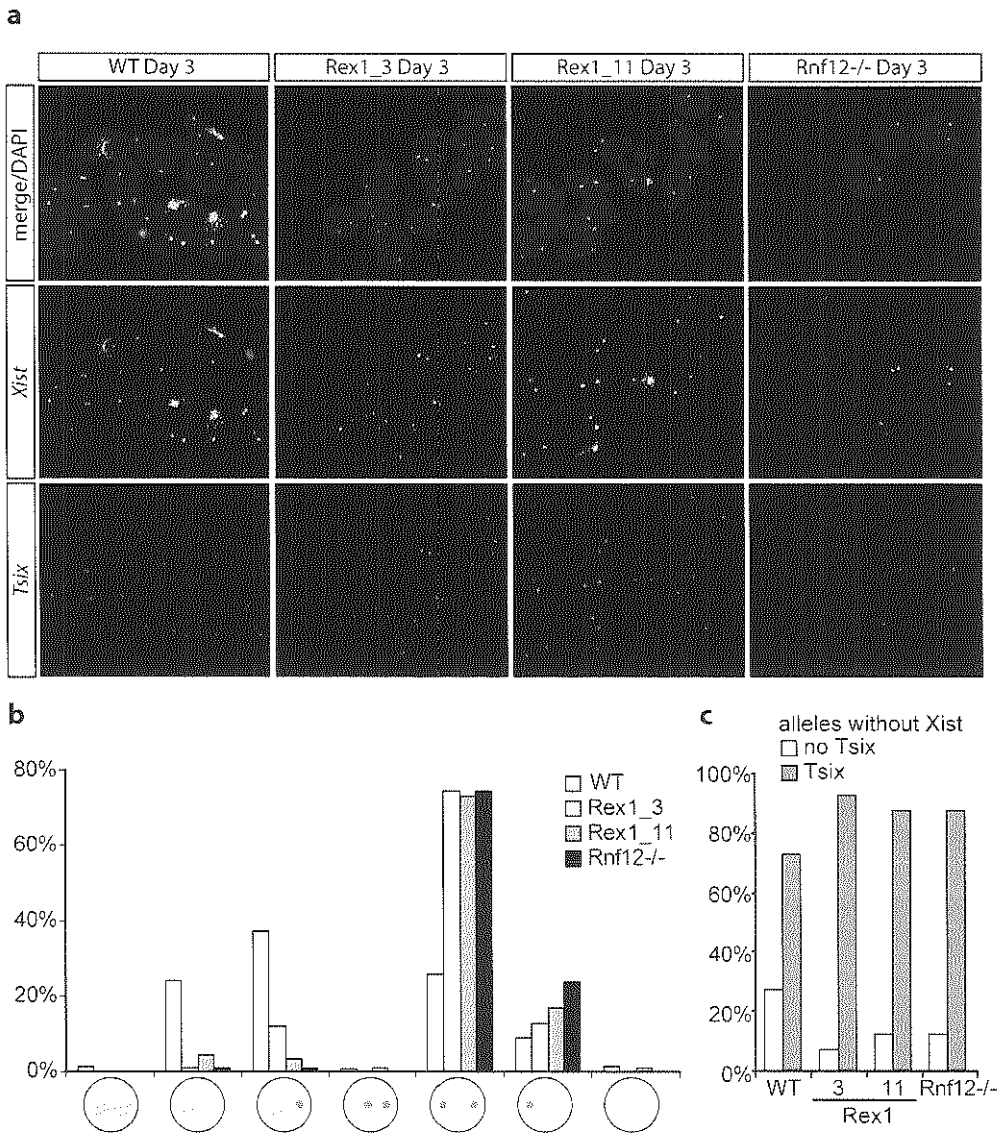

Supplementary Figure 9: *Xist* and *Tsix* expression in wild type and REX1-over-expression cell lines

A) *Xist* and *Tsix* RNA-FISH (bottom panel: *Tsix* in rhodamine; middle panel: *Xist* in FITC; top panel: merged *Xist-Tsix* signals and DNA stained with DAPI) on day-3-differentiated female WT, two *Rex1* over-expressing transgenic ESC lines and *Rnf12-/-* ESCs. **B)** Quantification of the *Xist* and *Tsix* RNA-FISH experiment described in **A**. **C)** The percentage of *Tsix* positive and negative alleles within the fraction of *Xist* negative alleles described in **A**. Shown is relative percentage of all observed combinations of *Xist* and *Tsix* expression ($n > 100$ per cell line).

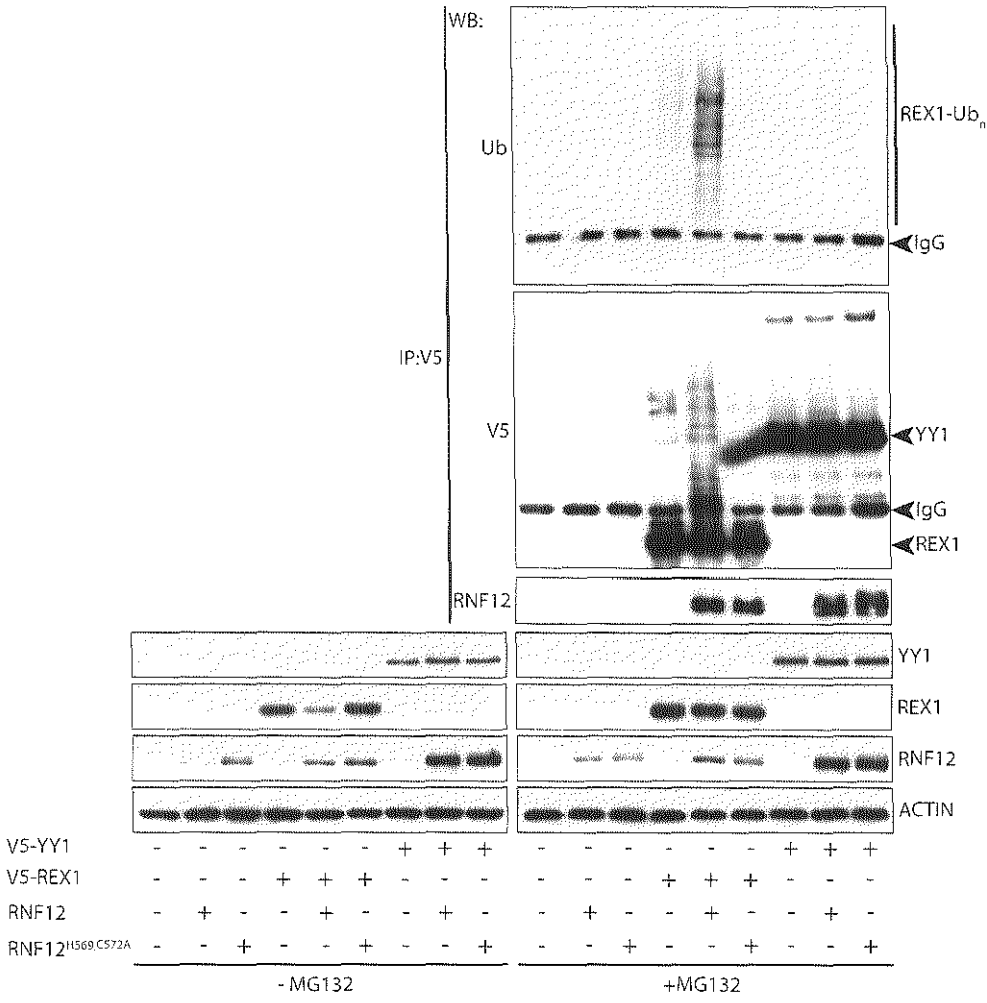

Supplementary Figure 10: RNF12 binds but does not ubiquitinate YY1
Ubiquitination assay in HEK293 cells, left bottom panels show nuclear protein extracts of HEK293 cells co-transfected with the indicated expression constructs encoding V5-YY1, V5-REX1, WT RNF12, or a catalytically inactive RNF12 mutant. Immunoblots were probed with the indicated antibodies. Right bottom panels show the same transfections, but in the presence of MG132. Upper panels, V5-tagged REX1 or V5-YY1 were immunoprecipitated with anti-V5 agarose beads and analysed by immunoblotting to detect the poly-ubiquitinated forms, if present, with V5 and ubiquitin antibodies. RNF12 co-immunoprecipitated with REX1 or YY1 was detected with RNF12 antibody.

Chapter 7

Initiation of X inactivation is regulated by trans-acting activators and cis-acting elements: no evidence for a functional involvement of X-pairing

Tahsin Stefan Barakat, Selma van Staveren, Friedemann Loos, Elvira Myronova, Mehrnaz Ghazvini, J. Anton Grootegoed and Joost Gribnau

(Submitted)

Initiation of X inactivation is regulated by *trans*-acting activators and *cis*-acting elements: no evidence for a functional involvement of X-pairing

Tahsin Stefan Barakat[1], Selma van Staveren[1], Friedemann Loos[1], Elvira Myronova[1], Mehrnaz Ghazvini[1,2], J. Anton Grootegoed[1] and Joost Gribnau[1,3]

[1]Department of Reproduction and Development, Erasmus MC, University Medical Center, Rotterdam, The Netherlands.
[2]Erasmus Stem Cell Institute, Erasmus MC, University Medical Center, Rotterdam, The Netherlands.
[3]corresponding author

Contact details:
Joost Gribnau
Department of Reproduction and Development
Erasmus MC
Room Ee 09-71
PO Box 2040
3000 CA Rotterdam
The Netherlands
Phone +31-10-7043069
Fax +31-10-7044736
Email: j.gribnau@erasmusmc.nl

Abstract

Dosage compensation of X-linked genes in placental mammals is accomplished by random inactivation of one X chromosome in female XX cells. X chromosome inactivation (XCI) is initiated by up-regulation and *cis*-spreading of X-encoded *Xist* RNA along the inactive X chromosome (Xi). The X-encoded XCI-activator RNF12 directs dose-dependent *trans*-activation of *Xist*, possibly assisted by direct interaction of the X chromosomes in the form of X-pairing. Here we show that XCI is initiated without all known X-linked elements required for X-pairing, and in male nuclei of XX-XY heterokaryons, indicating that XCI is regulated by *trans*-acting diffusible factors. The continuous presence of RNF12 is found to be required for establishment of the Xi, and the *cis*-acting elements *Jpx, Ftx* and *Xpr* lower the RNF12 threshold for *Xist* activation. Our results support the presence of a *cis*-X inactivation center (*cis*-XIC) encompassing all the elements regulating *Xist* in *cis*, and a *trans*-XIC covering all *trans*-acting activators of XCI.

Introduction

Evolution of the heterologous X and Y sex chromosomes has confronted mammalian species with a need for dosage compensation of X-encoded genes in female XX cells, which is achieved by inactivation of one of the two X chromosomes. In mouse, two forms of X chromosome inactivation (XCI) are found. Early cleavage stage female mouse embryos display an imprinted form of inactivation of the paternally inherited X chromosome. This is maintained in the extra-embryonic tissues, but the paternal X is reactivated in the inner cell mass of the blastocyst, after which random inactivation of either the paternal or maternal X chromosome is initiated around day 5.5 of female embryonic development. The inactive state of the Xi is stable and clonally propagated. Two overlapping X-linked, non-coding and *cis*-acting genes, *Xist* and *Tsix*, play key roles in initiation of XCI in the mouse. *Xist* is up-regulated on the future inactive X chromosome (Xi), and the transcribed *Xist* RNA coats the Xi in *cis*, thereby attracting chromatin modifying complexes involved in silencing [84-85]. *Tsix* is a negative regulator of *Xist*, generating transcripts in antisense direction and in conflict with *Xist* transcription, which prevents XCI of the future active X chromosome (Xa) early during development [118, 136].

Xist and *Tsix* represent the master switch locus regulated by *cis*- and *trans*-acting regulatory elements and genes involved in the repression or activation of XCI. Chromatin conformation capture studies indicated that *Xist* and *Tsix* are embedded in two distinct topological associated domains (TADs) of 500 and 200 kb respectively [1004]. Interestingly, *Xist* and *Tsix* positive regulatory genes and elements reside within the TAD that harbors the gene they regulate. Two non-coding genes *Xite* and *Tsx* are located within the *Tsix* TAD, and gene ablation experiments indicated that these genes promote *Tsix* expression in *cis* [136, 1005]. Mutation of two other non-coding genes *Jpx* and *Ftx*, residing within the *Xist* TAD, revealed these genes to be involved in the activation of *Xist* [1006-1007]. The *Xist* and *Tsix* TADs are separated by a boundary element, involved in CTCF recruitment, and removal of this boundary results in partial merging of both interaction domains and dysregulation of XCI [1004, 1008]. These studies underscore the important

roles of the higher order chromatin structure as well as *cis*-interactions of elements and genes in the activation of *Xist* or *Tsix*. However, it is important to note that the *cis*-interacting landscape cannot distinguish between male XY and female XX cells. In contrast, *trans*-acting factors are instrumental in the determination of the number of X chromosomes present in a nucleus, and subsequent initiation of XCI if more than one X is present per diploid genome [179, 910]. *Trans*-acting factors can be separated in two classes, inhibitors and activators of XCI. In models described before [910, 987], XCI-inhibitors are autosomally encoded and repress *Xist*, whereas activators of XCI are X-linked and promote *Xist* expression. In addition to exerting control over *Xist*, the actions of some of these inhibitors and activators include reciprocal actions on *Tsix*.

XCI is closely linked to loss of pluripotency towards cell differentiation. The pluripotency-associated factors NANOG, OCT4, REX1, SOX2 and KLF4 have been identified as XCI-inhibitors in mouse ES cells, involved in repression of *Xist* [191], or activation of *Tsix* [186, 989]. In addition, the ubiquitously expressed transcriptional regulators YY1 and CTCF were reported to suppress XCI by activation of *Tsix*, through binding to the *cis*-acting positive element *DXPas34* [193]. It is likely that XCI is blocked in undifferentiated ES cells and in the peri-implantation mouse embryo through different pathways acting in parallel, but converging to suppress *Xist* RNA production and accumulation. Autosomally-encoded gene products will be expressed at equal levels in female and male cells, and hence will not be sufficient to accomplish initiation of XCI exclusively in female cells. Rather, this requires X-encoded activators which can reach a higher expression level in undifferentiated female cells with two active X chromosomes, compared to XY male cells. Recently, we identified X-encoded RNF12 as an XCI-activator [174, 911]. The *Rnf12* gene is located just 500 kb upstream of *Xist*, which is relevant because this location may ensure rapid silencing of *Rnf12* on the future Xi soon after initiation of XCI. RNF12 is an E3 ubiquitin ligase, catalyzing dose dependent breakdown of REX1 by targeting REX1 for proteasomal degradation in differentiating ES cells [1009]. In undifferentiated ES cells, REX1 inhibits *Xist* and stimulates *Tsix* transcription, thereby blocking initiation of XCI. One single transgenic copy of *Rnf12* is sufficient to lower the REX1 protein level, leading to initiation of XCI in a high percentage of transgenic male ES cells. Reciprocally, the REX1 protein level is up-regulated in $Rnf12^{+/-}$ and $Rnf12^{-/-}$ female ES cells, resulting in a significant reduction in initiation of XCI. In developing wild type mouse embryos or upon ES cell differentiation in culture, RNF12 expression is up-regulated resulting in breakdown of REX1. This breakdown of REX1 is more prominent in differentiating female cells, which have two active copies of *Rnf12*. This RNF12/REX1 mechanism is in full agreement with the proposed stochastic nature of the initiation of XCI [179], and also explains that bi-allelic initiation of XCI in most cells is prevented by spreading of *Xist* and silencing of XCI-activator genes on the future Xi in *cis*.

It is anticipated that full control of the initiation of XCI involves a high level of complexity, where new factors and interactions await identification. The presence of XCI-activators acting independent of RNF12 is indicated by the observation that XCI is initiated in some $Rnf12^{+/-}$ female ES cells [174, 958]. Several non-coding genes and elements, located in close proximity to *Xist*, have been implicated to exert XCI-activator activity. These include the non-coding genes *Jpx* and *Ftx*, which are up-regulated upon ES cell differentiation and partially escape XCI. Deletion of *Jpx* has been reported to result in a

severe loss of XCI, leading to massive cell death [1006]. This phenotype was rescued by introduction of a *Jpx* transgene, but also by mutating *Tsix* which interacts with endogenous *Jpx* in *cis*, supporting a role for *Jpx* in *trans*- and in *cis*-activation of *Xist*. A deletion of *Ftx* negatively affects expression of both *Xist* and *Jpx*, but this has only been analyzed in male cells, which impedes making a distinction between *cis* and *trans* effects [1007]. Finally, an intriguing mechanism was indicated by the identification of the *Xpr* region and its postulated suggested role in pairing of the two X chromosomes at the onset of XCI [187]. The available evidence indicates that X-pairing might play a role in counting or sensing the number of X chromosomes present in a nucleus, but the molecular mechanisms for pairing remain elusive. It can be questioned whether pairing is a cause or consequence of XCI.

In this study, we have addressed the role of X-pairing in XCI. We find that XCI is initiated also in the absence of all elements known to be required for pairing. Moreover, in the absence of direct physical interaction of wild type X chromosomes, XCI was still initiated, indicating that XCI is regulated by diffusible *trans*-acting factors. Our studies also reveal that *Jpx*, *Ftx* and *Xpr* activate *Xist* exclusively in *cis*. This precludes a role for *Jpx* and *Ftx* as XCI-activators able to distinguish between male and female cells, in contrast to X-encoded and *trans*-acting RNF12. The present results provide evidence for a functional division of the X inactivation center in two parts: a *cis*-acting Xic, involved in *cis*-regulation of *Xist*, and a *trans*-acting Xic, which regulates the XCI initiation process.

Results

Cis elements required for activation of Xist

In previous studies, we have demonstrated that RNF12 activates the initiation of XCI by dose-dependent breakdown of REX1, a transcription factor which takes part in repression of *Xist* and activation of *Tsix* [174, 911, 1009]. In other words, *trans*-acting RNF12 eliminates REX1, leading to activation of *Xist*. In male cells, the concentration of X-encoded RNF12 (in combination with other *trans*-acting factors) is insufficient to activate *Xist*. In agreement with this, a single copy of an autosomally-integrated *Xist/Tsix* BAC RP23-338B22 transgene did not initiate autosomal spreading of *Xist* upon male ES cell differentiation (**Figure 1A, B, C**). Enforced expression of RNF12 is sufficient to allow activation of *Xist* and initiation of XCI in male ES cells [174]. To test this for the autosomal transgene, we introduced an additional BAC RP24-240J16 transgene covering *Rnf12* into the *Xist/Tsix* BAC RP23-338B22 transgenic male cells (**Figure 1A**). Integration and *Rnf12* over-expression was verified by qPCR analysis, and we differentiated the ES cells for 3 days to analyze *Xist* expression by RNA-FISH (**Figure 1D**). The *Xist/Tsix* transgenic ES cell line harbors 16 copies of a bacteriophage ms2 repeat sequence allowing distinction between the endogenous ms2+ and autosomal *Xist* (ms2-) RNA sequences. As expected, the *Rnf12* transgenic *Xist/Tsix* ES cell lines showed robust *Xist* accumulation in 3-9% (single-copy *Rnf12*) or 15-42% (multi-copy *Rnf12*) of the cells, emanating from the endogenous *Xist* locus. In contrast, we did not observe *Xist* spreading from the autosomal *Xist/Tsix* BAC transgene (**Figure 1C** and **1D**). We conclude that the *Xist/Tsix* BAC RP23-

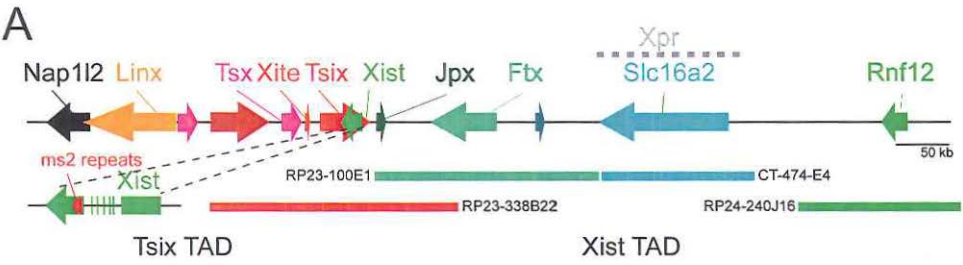

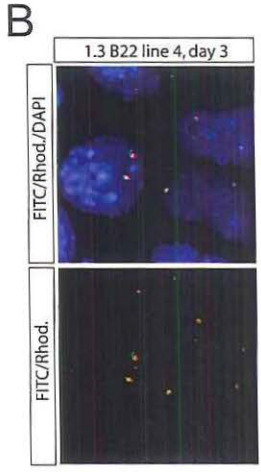

C

ES 1.3 B22 line 4, RP24-240J16

line	copy nr	% Xist autosomal	% Xist X chr.	n
4	0	0%	0%	142
4-4	1	0%	3%	79
4-5	1	0%	9%	35
4-10	1	0%	3%	37
4-14	1	0%	6%	32
4-17	1	0%	6%	69
4-20	2	0%	15%	52
4-12	3	0%	21%	90
4-22	4	0%	22%	61
4-13	5	0%	42%	64

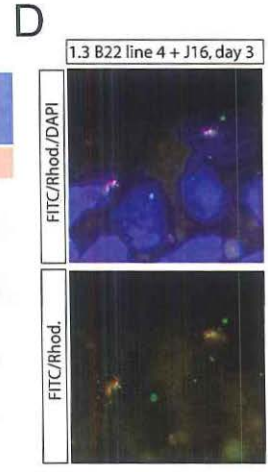

Figure 1: XCI in male *Xist/Tsix* transgenic ES cells
A) Schematic representation of the region encompassing the known regulators of XCI. The location of the *Xist* and *Tsix* TADS, the ms2 repeat sequences in *Xist*, and the BACs used for targeting and transgenesis experiments are shown below. **B)** Combined *Xist* (FITC) and ms2 (Rhodamine Red) RNA-FISH on day 3 differentiated male single copy *Xist/Tsix* transgenic ES cell line nr 4 (DAPI is blue). **C)** Quantification of autosomal and X chromosomal spreading of *Xist* in day 3 differentiated *Xist/Tsix* only transgenic ES cell lines and quantification of XCI in day 3 differentiated double transgenic *Rnf12 Xist/Tsix* ES cell lines generated by *Rnf12* transgenesis of *Xist/Tsix* transgenic ES cell line nr 4. **D)** Combined *Xist* (FITC) and ms2 (Rhodamine Red) RNA-FISH on day 3 differentiated male *Rnf12-Xist/Tsix* double transgenic ES cell line nr 12 (DAPI is blue).

338B22 transgene lacks important sequences required for the proper activation of *Xist*. BAC RP23-338B22 covers *Jpx*, but other putative XCI-activator sequences including *Ftx* and *Xpr*, and also most of the *Xist* TAD, are missing (**Figure 1A**), which may explain the lack of transgene activation. However, there also could be an important role for the genomic environment, in the activation of *Xist*, as is indicated by YAC transgene studies using female ES cells, which have shown that multi-copy but not single-copy *Xist/Tsix* transgenes initiate autosomal *Xist* spreading [175].

Deletion of the Xist chromatin interaction domain

Chromatin conformation capture studies indicate that *Xist* is located within a 500 kb interaction domain spanning from *Xist* through to *Rnf12* [1004]. To analyze the role of this

domain in *Xist* activation, we generated female ES cell lines lacking the complete *Xist* interaction domain but leaving *Xist* and a 5 kb upstream region intact. Polymorphic F1 Cast/Ei / C57Bl/6 female ES cells were generated containing a conditional C57Bl/6 $Xist^{2lox/+}$ allele (**Figure 2A** and **2B**). These $Xist^{2lox/+}$ ES cells were targeted with an *Rnf12* BAC vector, targeting a NheI RFLP located in exon 5 of *Rnf12*, and introducing a lox sequence (**Supplementary Figure 2A**). All sequences from in between *Xist* and *Jpx* up to and including *Rnf12* (*Jpx, Ftx*, the *Xpr* region, and *Rnf12*) were removed by transient expression of Cre recombinase, yielding Δ(Jpx-Rnf12) in which *Xist* was still present (**Figure 2C** and **Supplementary Figure 1**).

To test whether the Δ(Jpx-Rnf12) deletion resulted in an XCI phenotype we analyzed undifferentiated and embryonic body (EB) differentiated +/Δ(Jpx-Rnf12) ES cells. We did not see a morphological difference or a difference in cell viability and proliferation between wild type and +/Δ(Jpx-Rnf12) undifferentiated and differentiated ES cells analyzed at different time points after the start of differentiation, although we found some variation between sub-clones (**Figure 2D** and **Supplementary Figure 2B**, **2C** and **2D**). Previously, we have shown that XCI is reduced in $Rnf12^{+/-}$ female ES cells [174, 911]. *Xist* RNA-FISH expression analysis confirms this finding and indicates an even further reduction in XCI in +/Δ(Jpx-Rnf12) ES cells at all time points analyzed (**Figure 2E** and **2F**). Blastocyst injection of the heterozygous Δ(Jpx-Rnf12) female ES cells resulted in +/Δ(Jpx-Rnf12)/male chimaeric mice which expressed *Xist* (**Supplementary Figure 3A** and **3B**). Expression of *Xist*, measured by qPCR analysis with RNA isolated from different organs, was lower than in wild type female control samples but corresponded with ES cell contribution to the chimaeric animals (data not shown). These results contrast with findings presented in a previous study indicating loss of XCI in $Jpx^{+/-}$ female cells, resulting in massive cell death [1006]. This $Jpx^{+/-}$ phenotype could be rescued by introduction of a *Jpx* transgene, suggesting a role of *Jpx* in *trans* in the activation of *Xist*. To test whether the effect of the heterozygous Δ(Jpx-Rnf12) mutation was *cis* or *trans*, we performed allele specific RT-PCR analysis on *Xist* RNA isolated from day 3 differentiated +/Δ(Jpx-Rnf12) and wild type female ES cells. In wild type female F1 Cast/Ei / C57Bl/6 ES cells, XCI is skewed with a preferential inactivation of the C57Bl/6 X chromosome, visible as a 70%-30% expression ratio of C57Bl/6-Cast/Ei *Xist* RNA (**Figure 2G**). In accordance with our previous studies [174, 958], $Rnf12^{+/-}$ female ES cells have completely skewed XCI, at the present level of detection, in favour of inactivation of the C57Bl/6 X chromosome carrying a Δ*Rnf12* deletion (**Figure 2G**). In these cells inactivation of the wild type Cast/Ei X chromosome would lead to a *Rnf12* null cell, which may be selected against, or which may not be able to maintain *Xist* expression due to the absence of RNF12. However, in the present +/Δ(Jpx-Rnf12) cells, we find severe skewing in favour of *Xist* expression from the mutant C57/Bl/6 X chromosome, but we also detected some expression of *Xist* from the wild type Cast/Ei X chromosome, at day 3 of differentiation (**Figure 2G**). At different time points after initiation of ES cell differentiation of wild type cells and +/Δ(Jpx-Rnf12) cells, this partial loss of complete skewing towards *Xist* expression from the mutant allele is detectable during initiation of XCI, at days 3-10 of ES cell differentiation (**Figure 2G**). This finding might point to a repressive role for *Jpx*, *Ftx* and *Xpr* in *trans*. Alternatively, there could be a role for the region encompassing these genes in the activation of *Xist* in *cis*.

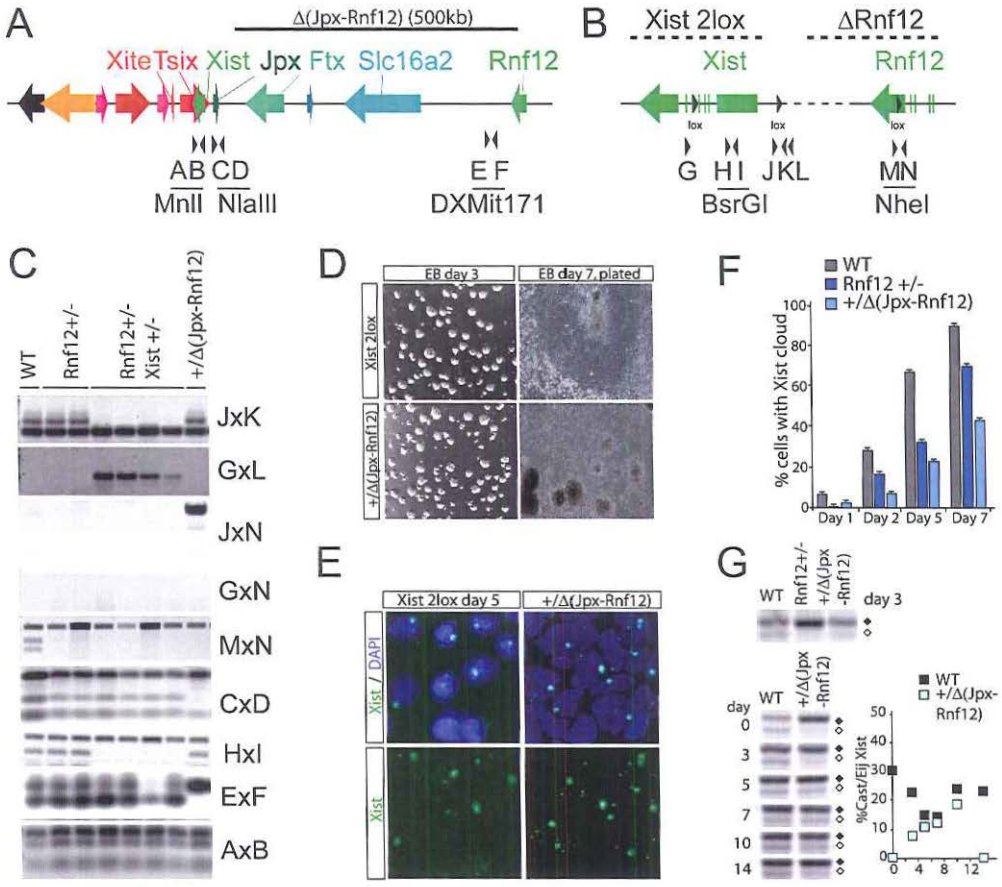

Figure 2: Generation of the +/Δ(Jpx-Rnf12) ES cell line

A), B) Map showing the location of the primers used to genotype the ES cell clones. **C)** PCR analysis on genomic DNA of *Xist*$^{2lox/+}$ *Rnf12*$^{-/+}$ ES cell clones after transient Cre expression using primer combinations indicated in **A** and **B**. **D)** Pictures of day 3 and day 7 differentiated +/Δ(Jpx-Rnf12) and *Xist*$^{2lox/+}$ control ES cells. **E)** *Xist* RNA-FISH (FITC) on day 5 differentiated +/Δ(Jpx-Rnf12) and *Xist*$^{2lox/+}$ ES cells (DAPI is blue). **F)** Quantification of relative number of *Xist* clouds in +/Δ(Jpx-Rnf12), *Rnf12*$^{+/-}$ and wild type ES cells at different time points of differentiation. **G)** Allele specific expression analysis of *Xist* by amplification of an *Xist* length polymorphism comparing day 3 differentiated wild type, *Rnf12*$^{+/-}$ and +/Δ(Jpx-Rnf12) ES cells (top panel, C57/Bl/6 is black rectangle, Cast/Ei is open rectangle). The bottom panel and graph show the relative expression and quantification of *Xist* emanating from the targeted Δ(Jpx-Rnf12) C57/Bl/6 allele and wild type Cast/Ei allele analyzed at different time points after differentiation.

Jpx, Ftx and Xpr act in cis to activate Xist

To investigate if *Jpx*, *Ftx* and *Xpr* act in *cis* or in *trans* to either activate or repress *Xist*, respectively, we introduced BAC transgenes in +/Δ(Jpx-Rnf12) ES cells covering *Rnf12* (RP24-240J16), *Xpr* (CT-474E4), or both *Jpx* and *Ftx* (RP23-100E1) (**Figure 1A**). Positive clones with a transgene insertion were identified by qPCR on genomic DNA of expanded clones (data not shown), followed by RT-qPCR analysis to verify transgenic expression of *Ftx*, *Jpx* and *Rnf12* on RNA isolated from day 5 differentiated ES cell clones. We also performed RFLP RT-PCR analysis, discriminating between endogenous and transgenic *Jpx*, *Ftx*, and *Rnf12* expression (**Figure 3A**, **3B** and **3C**). *Slc16A2*, which overlaps with the *Xpr*, is not expressed in ES cells, precluding verification of these clones by expression analysis, but DNA-FISH was performed to confirm the presence of this and the other transgenes (**Supplementary Figure 4**). RT-qPCR analysis of *Xist* expression in +/Δ(Jpx-Rnf12) day 5 differentiated ES cell clones expressing transgenic *Xpr*, *Jpx–Ftx*, or *Rnf12* transgenes, showed up-regulation of *Xist* expression only in clones with an *Rnf12* transgene integration (**Figure 3D** and **Supplementary Figure 5A-D**). Introduction of the *Rnf12* transgene, as a second transgene, into the Δ(Jpx-Rnf12) ES cells transgenic for *Xpr* or *Jpx–Ftx* resulted in up-regulation of *Xist* in most of these double transgenic ES cell lines (**Supplementary Figure 6A** and **6B**), providing a control excluding negative *trans* action of *Xpr* or *Jpx–Ftx*. These results clearly show that *Xpr*, *Jpx* and *Ftx* play a role only in *cis*, in contrast to *Rnf12*, which encodes a true activator of XCI which activates *Xist* in *trans*.

Next, we determined the origin of *Xist* RNA in +/Δ(Jpx-Rnf12) ES cells harboring different *Rnf12* integrations, by RFLP RT-PCR analysis on day 5 of differentiation. Clearly, the *Rnf12* transgenes induced preferential up-regulation of *Xist* expression from the Cast/Ei wild type X chromosome (**Figure 3E**). Such an effect was not observed in *Xpr* and *Jpx-Ftx* transgenic +/Δ(Jpx-Rnf12) ES cell lines (**Supplementary Figure 6C** and **6D**). This result provides a strong indication that *trans*-activation by RNF12 of *Xist* located on the mutant X is severely compromised. This is confirmed using the *Jpx–Ftx* and *Xpr* transgenic Δ(Jpx-Rnf12) ES cells recued with a *Rnf12*, where allele specific RT-PCR detecting *Rnf12* and *Xist* showed preferential up-regulation of *Xist* emanating from the wild type Cast/Ei X chromosome (**Supplementary Figure 6E** and **6F**).

Next to *Xist*, we looked at expression of *Tsix*, compared to other flanking genes. RT-qPCR analysis at different time points of differentiation of +/Δ(Jpx-Rnf12) female ES cells showed a clear up-regulation of *Tsix* expression (**Figure 3F**). In contrast, expression of *Nap1L2*, a gene which is located centromeric to *Xist*, within the *Tsix* TAD, was not affected (**Figure 3F**). Down-regulation of *Ftx* expression in these +/Δ(Jpx-Rnf12) ES cells (**Figure 3F**) is explained by loss of one allele. To test whether removal of *Tsix* transcription in *cis* would restore initiation of XCI on the Δ(Jpx-Rnf12) allele, we replaced the transcriptional start site of *Tsix* by a mCherry gene and a stop cassette by insertion and subsequent loopout of a neo targeting cassette. Proper targeting was verified by RFLP mediated gDNA PCR to detect the neo insertion and subsequent loopout (**Supplementary Figure 7**). With RT-qPCR analysis, we found a reduction of *Tsix* expression in +/Δ(Jpx-Rnf12)-ΔTsix ES cell lines carrying this deletion (data not shown). *Xist* RNA-FISH studies on two different +/Δ(Jpx-Rnf12)-ΔTsix ES cell lines at different time points of differentiation showed an almost complete rescue of the XCI phenotype of the +/Δ(Jpx-Rnf12) cells (**Figure 3G**). Taken together, the results indicate that activation of *Xist* and

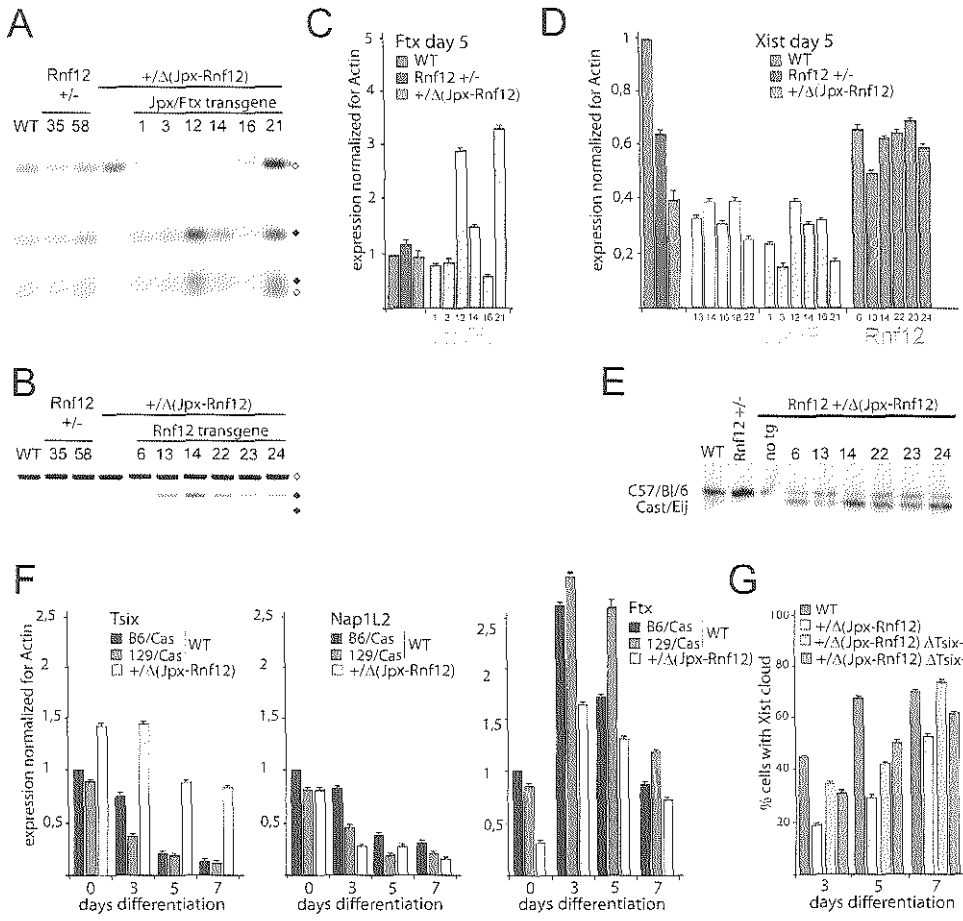

Figure 3: *Rnf12*, and not *Xpr* and *Jpx/Ftx* activate XCI in *trans*.
A), B) Allele specific expression analysis of *Jpx* (**A**) and *Rnf12* (**B**) (129/Sv / C57/Bl/6 is black rectangle, Cast/Ei is open rectangle), indicating expression of transgenic *Jpx* (129/Sv) and *Rnf12* (129/Sv) in *Jpx/Ftx* and *Rnf12* transgenic +/Δ(Jpx-Rnf12) ES cells. **C)** qPCR analysis of *Ftx* expression, normalized to *Actin* expression, in day 5 differentiated *Jpx/Ftx* transgenic ES cell clones. **D)** *Xist* expression normalized to *Actin*, on *Xpr*, *Jpx/Ftx*, and *Rnf12* transgenic ES cell clones differentiated for 5 days. **E)** Allele specific expression analysis of *Xist* in day 5 differentiated *Rnf12* transgenic +/Δ(Jpx-Rnf12) clones. **F)** qPCR expression analysis of *Tsix* (left panel), *Nap1L2* (middle panel), and *Ftx* (right panel), normalized to *Actin*, at different time points after initiation of differentiation of C57/Bl/6 / Cast/Ei and 129/Sv / Cast/Ei wild type and +/Δ(Jpx-Rnf12) ES cells. **G)** Quantification of relative number of *Xist* clouds in wild type, +/Δ(Jpx-Rnf12), and two +/Δ(Jpx-Rnf12) ΔTsix ES cell lines, at different time points after start of differentiation.

initiation of XCI on the X chromosome carrying the Δ(Jpx-Rnf12) allele is counteracted by upregulation of *Tsix* neighboring the deletion, meaning that the *Jpx*, *Ftx* and *Xpr* region play an important role in setting up a *cis*-environment to overcome *Tsix* mediated repression of *Xist* activation.

Initiation of XCI does not require previously identified pairing elements

One mechanism that has been advocated to explain mutual exclusive initiation of XCI on either one of the two X chromosomes in female cells involves transient co-localization and pairing of the X chromosomes upon ES cell differentiation [182-183]. This X-pairing process is guided by different genetic elements on the X chromosome, including *Tsix*, *Xite* and the *Xpr* region [182-183, 187]. In view of our above findings, providing evidence for a role for *Jpx, Ftx* and *Xpr* in *cis*, we have reinvestigated the importance of X-pairing in a novel experimental set-up.

First, to test whether XCI is eliminated in the absence of all elements known to be implicated in X-pairing, we introduced a *Xite* targeting cassette to obtain Cre mediated deletion of the region from *Xite* through to and including part of *Rnf12*, which is identical to the present *Jpx-Rnf12* deletion but includes an extra 70 kb sequence to incorporate *Xist*, *Tsix*, and *Xite* into the deletion (**Figure 4A**). Proper targeting of this cassette was verified by Southern blotting (**Figure 4B**). Different Xite-neo (ΔJpx-Rnf12) positive clones were expanded, followed by Cre mediated loopout of the intervening sequences yielding +/Δ(Xite-Rnf12) ES cell lines (**Figure 4C**). Two different +/Δ(Xite-Rnf12) ES cell lines were EB differentiated and fixed at several time points to analyze XCI. As would be expected based on the X-pairing model, *Xist* RNA-FISH analysis indicated that *Xist* cloud formation in differentiating ES cell lines was severely compromised by the heterozygous deletion Δ(Xite-Rnf12) (**Figure 4D** and **4E**). In addition, the *Xist* clouds looked more dispersed, as if *Xist* targeting to the Xi was disturbed. This is not explained by loss of one *Rnf12* allele, because the XCI phenotype is more pronounced than what we observed in the +/Δ(Jpx-Rnf12) cells (**Figure 2E**).

The above findings show that loss of all elements known to be involved in X-pairing leads to an XCI phenotype, but loss of X-pairing might not be the only possible explanation for this phenotype, as XCI in these +/Δ(Xite-Rnf12) ES cell can only occur on the wild type X chromosome, which might lead to *Rnf12* silencing in *cis*, and hence a failure of XCI maintenance. Since pairing cannot be directly experimentally addressed in the +/Δ(Xite-Rnf12) ES cells, as all regions known to pair are deleted and can thus not be followed by DNA-FISH to observe their movements in the nucleus, we proceeded as follows. We generated male/female ES cell heterokaryons and we monitored XCI upon differentiation (**Figure 5A**). Our previous studies with XXYY and XXXY tetraploid synkaryons indicated that XXYY ES cells never initiate XCI upon differentiation, whereas XXXY ES cells initiate XCI on one of the X chromosomes [179], in agreement with cells always maintaining one X active per diploid genome. We aimed to investigate if XCI in XX-XY heterokaryons with two diploid nuclei would proceed as observed for XXXY tetraploid synkaryons, with one X being inactivated. To generate the XX-XY and XY-XY heterokaryons, the plasma membranes of male and female ES cells were labelled with the viable dyes DiD and DiO. Cells were allowed to recover for two days and then fused with polyethylene glycol followed by FACS analysis to sort the double positive heterokaryons, which were plated out in EB medium (**Figure 5B**). Heterokaryons were differentiated for 2.5 and 5 days and fixed for immuno-RNA-FISH analysis. We made use of a male ES cell line that harbors a ms2 tagged *Xist* gene, allowing discrimination between *Xist* expression in the male (ms2+) and female (ms2-) nucleus. Immuno-RNA-FISH was performed

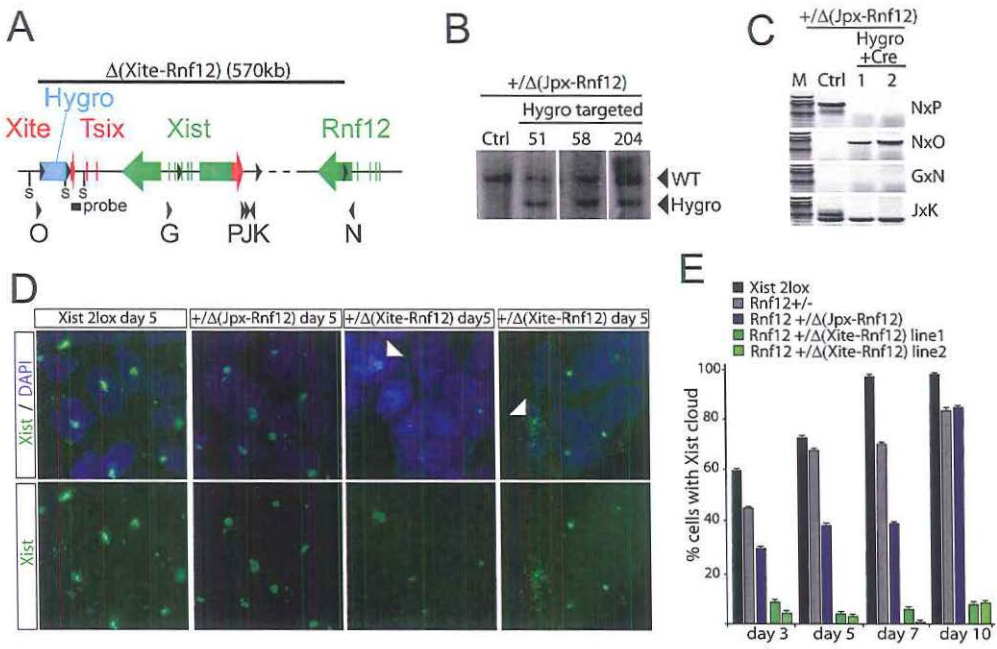

Figure 4: Loss of XCI in +/Δ(Xite-Rnf12) ES cells.
A) Map and location of targeting cassette, the lox sites for Cre mediated recombination, and primers used for genotyping analysis. Also shown in **A** are the SpeI restriction sites and probe used for Southern analysis to identify 5' *Xite* targeted ES cell clones **(B)**. **C)** Cre mediated loopout was confirmed by PCR analysis using primer sets depicted in **A**. **D)** *Xist* RNA-FISH (FITC) on day 5 differentiated $Xist^{+/2lox}$, +/Δ(Jpx-Rnf12) and two +/Δ(Xite-Rnf12) ES cell lines (DAPI is blue). **E)** Quantification of relative number of *Xist* clouds in cells shown in **D** and in $Rnf12^{+/-}$ cells.

detecting ACTIN, to discriminate between synkaryons and heterokaryons, and *Xist*-ms2 to identify male nuclei that initiated XCI. The number of heterokaryons found was 7.9% and 1.5% for day 2.5 and day 5 differentiated heterokaryons, respectively. The decrease in heterokaryons during the differentiation process is most likely the result of cell death and fusion of nuclei, forming synkaryons. Examination of the remaining XX-XY heterokaryons showed male nuclei with *Xist*-ms2 clouds, which we never observed in XY-XY heterokaryons (**Figure 5C**, and **Table 1A** and **1B**). By quantification of the ms2+ nuclei, we counted that 6.6% and 25% of the male nuclei in the available heterokaryons had initiated XCI at day 3 and day 5 of differentiation, respectively (**Table 1A** and **1B**). These percentages are expected based on random XCI with an equal probability for each one of the three X chromosomes to initiate XCI. In XXXY tetraploid synkaryons, 18% and 76% of the cells have been found to initiate XCI on one X chromosome, at days 3 and 5 of differentiation, respectively [179], meaning that the chance to be randomly inactivated at these time points is 6% and 25.3% for each one of three X chromosomes per two diploid genomes, as is the situation in the present XX-XY heterokaryons. This result indicates that in the present XX-XY heterokaryons, initiation of XCI and counting happen normally, even in male nuclei where physical contact between the X chromosomes is absent.

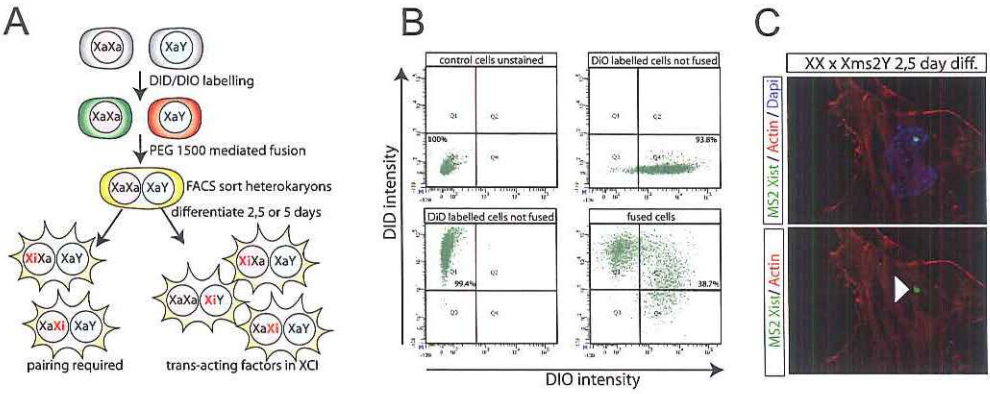

Figure 5: X-pairing not required for XCI
A) Male and female ES cells were DiD and DiO labelled and fused to form XY-XX heterokaryons, which were FACS sorted prior to differentiation. Initiation of XCI in the male nucleus of XY-XX heterokaryons indicates that pairing is not required for XCI initiation. **B)** FACS analysis after fusion of DiD and DiO labelled XX and XY cells. **C)** Immuno-RNA-FISH analysis detecting ms2 tagged *Xist* (FITC) and ACTIN (Rhodamine Red), in the XY nucleus of a XY-XX heterokaryon.

The above-described initiation of random XCI in the male nucleus of XX-XY heterokaryons excludes a role for X-pairing in counting and initiation of XCI. Rather, the results are explained by regulation of random XCI in *trans* through diffusible factors which can pass across nuclear membranes. Therefore the XCI phenotype in differentiating +/Δ(Xite-Rnf12) ES cells cannot be attributed to an X-pairing defect.

Rnf12 expression is required for maintained Xist expression

As described above, dysregulation of XCI in +/Δ(Xite-Rnf12) ES cell lines is more pronounced than what we observed in the +/Δ(Jpx-Rnf12) cells. This is not explained by total loss of the possibility for the X chromosomes to engage in pairing in the +/Δ(Xite-Rnf12) cells, and requires a different explanation. A continuous requirement for RNF12 throughout the early phases of the XCI process may explain skewing towards inactivation of the X chromosome carrying an *Rnf12* mutation, such as observed in the heterozygous $Rnf12^{+/-129/Sv}$ cell line, on a mixed Cast/Ei / 129/Sv background. This predicts that reciprocal targeting of the Cast/Ei allele to obtain $Rnf12^{+/-Cast/Ei}$ ES cells would lead to preferential inactivation of the X carrying the Cast/Ei allele. To test this, we targeted female F1 2-1 Cast/Ei /129/Sv with a Cast/Ei specific targeting vector for *Rnf12*, and PCR screened for properly targeted clones making use of a RFLP which is destroyed upon targeting (**Supplementary Figure 8A**). In addition, we targeted the remaining functional Cast/Ei *Rnf12* allele in +/Δ(Jpx-Rnf12) ES cells to determine whether *Rnf12* is required to initiate XCI in +/Δ(Jpx-Rnf12) cells (**Supplementary Figure 8C**). Analysis of the latter ΔRnf12/Δ(Jpx-Rnf12) ES cells indicated a severe down-regulation of XCI at all time points during ES cell differentiation, reinforcing that RNF12 plays a crucial role in the XCI initiation process (**Supplementary Figure 8D** and **E**). Examination of XCI by *Xist* RNA-FISH for the differentiated $Rnf12^{+/-Cast/Ei}$ ES cells did not reveal a difference compared to $Rnf12^{+/-129/Sv}$ ES cells, showing reduced initiation of XCI at all time points tested for both

A

cell lines day 2.5 heterokaryons	N	X_{ms2}-X_{ms2} XistClouds	%
male Xms2Y x female XX	151	10	6,6 %
maleXms2Y x male Xms2Y	112	0	0 %

B

cell lines day 5 heterokaryons	N	X_{ms2}-X_{ms2} XistClouds	%
male Xms2Y x female XX	12	3	25 %
maleXms2Y x male Xms2Y	14	0	0 %

Table 1
Number of heterokaryons analyzed, and the number and percentage of X_{ms2}Y-XX and X_{ms2}Y-XY heterokaryons with an ms2 coated X chromosome at day 2.5 **(A)** and day 5 **(B)** of differentiation.

type of cells (**Figure 6A** and **Supplementary Figure 8B**). Allele specific expression analysis indicated that, as expected, Cast/Ei *Xist* is preferentially up-regulated in $Rnf12^{+/-Cast/Ei}$ cells (**Figure 6B**). However, skewing of XCI in the $Rnf12^{+/-Cast/Ei}$ cells was found to be less pronounced compared to $Rnf12^{+/-129/Sv}$ and +/Δ(Jpx-Rnf12) cells. We think this reflects the different allele specific thresholds to initiate XCI, which is higher for the Cast/Ei allele [910].

In the present +/Δ(Xite-Rnf12) ES cells, *Rnf12* is expressed from the wild type Cast/Ei X chromosome prior to and during the early stages of XCI, but this expression will be lost when XCI is initiated on that wild type chromosome, which is the only option available, since the mutant X chromosome lacks *Xist*. This loss of RNF12 is expected to lead to a higher concentration of REX1 resulting in repression of *Xist* on the wild type X chromosome. To test this hypothesis, we generated a $Xist^{1lox/+}Rnf12^{+/-}$ *cis* compound knockout ES cell line with both mutations located on the same X chromosome. These ES cells can only induce XCI on the wild type Cast/Ei X chromosome rendering the cells RNF12 null upon XCI. If continued expression of RNF12 is required for proper initiation of XCI, then $Xist^{1lox/+}Rnf12^{+/-}$ ES cells should also show a block in XCI. $Xist^{1lox/+}Rnf12^{+/-}$ ES cells were generated by targeting the *Xist*-2lox C57Bl/6 allele with an *Rnf12* targeting cassette using $Xist^{2lox/+}$ ES cells. Targeting was verified by RFLP PCR analysis detecting loss of an NheI RFLP located in exon 5 of *Rnf12*. Cre mediated loopout of *Xist* was performed by transient transfection of a Cre expression cassette and proper recombination was verified PCR using genomic DNA (**Figure 2B**). Several $Xist^{1lox/+}Rnf12^{+/-}$ ES cell lines were EB differentiated and analyzed at different time points by *Xist* RNA-FISH. We found a severely reduced percentage of $Xist^{1lox/+}Rnf12^{+/-}$ cells, compared to wild type control cells and $Xist^{1lox/+}Rnf12^{+/+}$ ES cell lines (**Figure 6C**). In addition, as in the Δ(Xite-Rnf12) cells, *Xist* clouds in $Xist^{1lox/+}Rnf12^{+/-}$ cells were dispersed, as if *Xist* could not properly accumulate, or representing cells which accumulated *Xist* followed by a shut-down of the *Xist* promoter. Our results indicate that $Xist^{1lox/+}Rnf12^{+/-}$ cells initiate XCI on the Cast/Ei X chromosome harboring the intact *Xist* allele, but that initiation leads to silencing of *Rnf12* in *cis* resulting in a block in XCI. The same block in XCI is likely to explain the XCI phenotype of +/Δ(Xite-Rnf12) ES cells. To test whether this phenotype could be rescued we introduced an *Rnf12* transgene into our +/Δ(Xite-Rnf12) ES cells. Transgene copy number was determined by qPCR, and transgene expression by RFLP RT-PCR (**Figure 6D**). Indeed analysis of EB differentiated *Rnf12* rescued Δ(Xite-Rnf12) ES cells showed robust up-regulation of *Xist*. *Xist* clouds looked robust and localized at the Xi, indicating that *Rnf12* is the limiting factor.

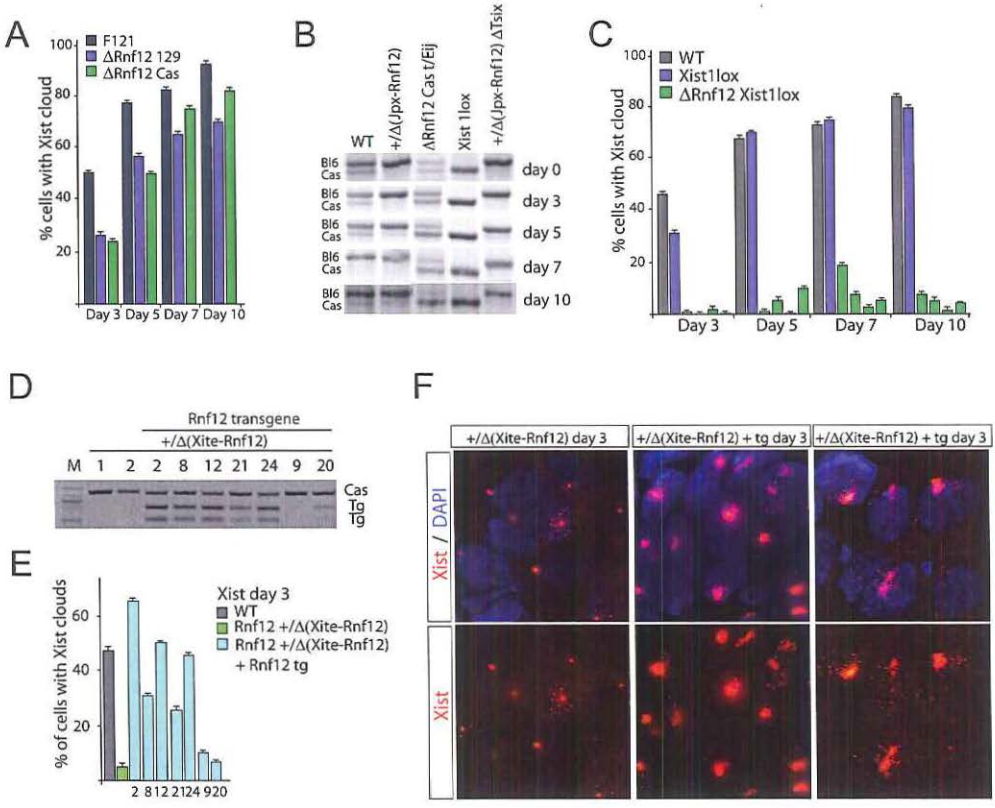

Figure 6: RNF12 required for proper establishment of the Xi
A) Quantification of the percentage of cells with *Xist* clouds at different time points of differentiation, in wild type and *Rnf12*$^{+/-}$ cells with a targeted 129/Sv or Cast/Ei allele. **B)** Allele specific expression analysis of *Xist* detecting a length polymorphism, comparing wild type, +/Δ(Xite-Rnf12), *Rnf12*$^{+/-\ (Cast/Ei)}$, *Xist*$^{1lox/+}$, +/Δ(Jpx-Rnf12)-ΔTsix ES cell lines at different time points of differentiation. **C)** Quantification of percentage of wild type, *Xist*$^{1lox/+}$, and four different *Xist*$^{1lox/+}$ *Rnf12*$^{-/+}$ ES cell lines at day 3, 5, 7 and 10 of differentiation. **D)** Allele specific expression analysis of *Rnf12* transgenic +/Δ(Xite-Rnf12) ES cells shows expression of transgenic *Rnf12* (129/Sv) in most clones. **E), F)** *Xist* RNA-FISH (FITC, **F**) and quantification of percentage of cells with *Xist* clouds **(E)** on wild type, +/Δ(Xite-Rnf12), and *Rnf12* rescued +/Δ(Xite-Rnf12) ES cell lines.

These findings indicate that *Rnf12* is crucial for the XCI process to be initiated and is continuously required to allow spreading of *Xist* and establish the inactive state of the Xi.

Discussion

Co-activation of Xist, Jpx and Ftx

Knowledge about *cis-* or *trans*-activating activity of regulators of XCI is crucial to understand the XCI counting and initiation process. *Cis*-acting elements and genes are important regulators of *Xist* activity by regulating *Xist* directly or indirectly through *Tsix*. However, *cis*-acting information will not allow the cell to discriminate between male and female, which is determined by the dose dependent action of *trans*-acting XCI-activators and -inhibitors. The recent decade, several *cis*-acting sequences have been identified to regulate *Xist* or *Tsix*, and 3C and 5C studies indicated that *Xist* and *Tsix* reside in different neighboring chromatin interaction domains [992, 1004]. *Jpx*, *Ftx* and *Xpr* reside in the *Xist* TAD, and previous experimental data confirmed a positive regulatory role for these elements in activation of *Xist* [187, 1006-1007]. Our study indicates that this same region acts in *cis* to regulate *Xist*. Transgene studies do not reveal any *trans*-acting activity of this region, which contrasts a recent study suggesting a role for *Jpx* in the regulation of XCI in *trans* [1006]. Although we cannot exclude the possibility that our deletion masks the effect of the mutation of a single gene, the lack of detectable *trans*-acting activity in our transgene assays indicates that the predominant function of *Jpx*, *Ftx* and *Xpr* is the *cis*-activation of *Xist*.

One key question is how *Jpx*, *Ftx* and *Xpr* regulate *Xist*. In our study we find that *Xist* expression is severely compromised on the X chromosome with a Δ(Jpx-Rnf12) deletion. Introduction of an autosomally integrated *Rnf12* transgene shows preferential up-regulation of *Xist* from the wild type X chromosome, indicating that the threshold to initiate XCI on the Δ(Jpx-Rnf12) X chromosome is very high (**Figure 7A**). By removing *Tsix* in *cis* we were able to reduce the threshold allowing increased initiation of XCI. These results indicate that *Jpx*, *Ftx* and *Xpr* counteract the repressive action of *Tsix* by activating *Xist* but only when the concentration of *trans*-acting activators is sufficient.

To facilitate initiation of XCI *Xist*, *Jpx*, *Ftx* and *Xpr* may act synergistically by co-activation. Indeed, chromatin conformation capture studies indicate that these genes form an interaction hub together with *Xist* and not *Tsix*, which may lead to co-activation through a mass action model [1010]. In support of such a model, the disruption of *Ftx* results in down-regulation of both *Jpx* and *Xist* [1007]. This would mean that the additive activity of promoters and regulatory elements within the *Xist* TAD is crucial in the regulation of *Xist*, suggesting that the individual role of the *Xpr* region may be small, because *Slc16A2* is not transcribed in our differentiation assays. In addition, co-activation through promoter contacts may indicate that there is no function for the *Jpx* and *Ftx* RNA in activation of *Xist*, supported by the absence of *trans*-activation activity of *Jpx-Ftx* transgenes. This may also explain the poor conservation of the exon-intron structure of these genes throughout the mammalian class; however our current knowledge does not preclude a function for the RNAs in the activation of *Xist*. Insertion of premature stop cassettes in the first exons of both genes will be instrumental to answer this question.

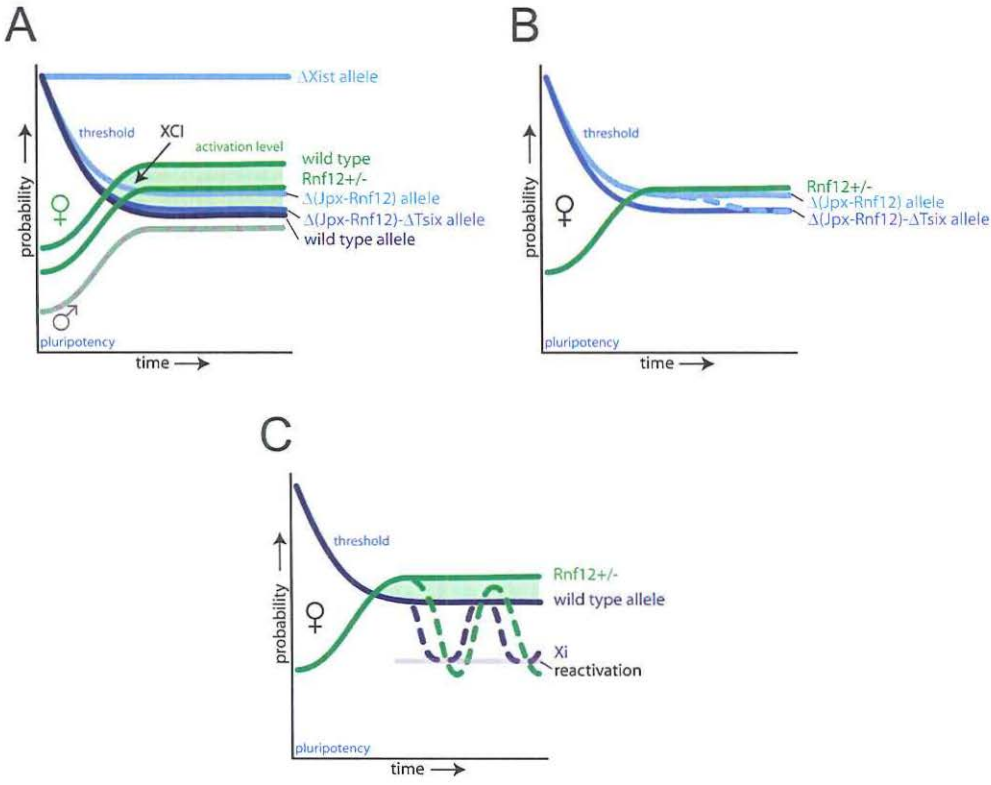

Figure 7: *Cis* and *trans*-activating properties of the X inactivation center
A) Upon differentiation or development the concentration of XCI-activators exceeds the threshold allowing initiation of XCI. In *Rnf12*$^{+/-}$ ES cells the activation level is lower compared to wild type cells. For the Δ(Jpx-Rnf12) allele the threshold for XCI to be initiated is higher than for the wild type allele, but deletion of *Tsix* in *cis* results in a drop of the threshold for *Xist* activation on the resulting Δ(Jpx-Rnf12)-ΔTsix allele. **B)** In +/Δ(Jpx-Rnf12) cells initiation of XCI on the mutated allele results in a silencing of *Tsix* in *cis* lowering the threshold (dashed line) for maintained *Xist* expression similar to the threshold for the Δ(Jpx-Rnf12)-ΔTsix allele. **C)** Initiation of XCI on the wild type X will also results in silencing of *Tsix* in *cis* and a drop in the threshold (dashed blue line), but silencing of the single functional *Rnf12* allele will result in down-regulation of *Rnf12* reaching a level insufficient to maintain XCI, and subsequent loss of the Xi. This circle may repeat itself several times.

A role for pairing in XCI?

Several studies have indicated that both X chromosomes come in close proximity prior to the initiation of XCI [182-183]. Initial reports showed a significant percentage of cells with both XIC's located within a 2 μm distance at the onset of XCI. More recently, time lapse imaging studies even revealed a short complete overlap of both XICs prior to *Xist* spreading [184]. Several elements, including *Xite*, *Tsix* and *Xpr* have been implicated in regulating this pairing process, which also requires active transcription and CTCF [182-183, 186-187]. In this study we addressed the question whether pairing is required for XCI to be initiated. Initiation of XCI in male nuclei in XX-XY heterokaryons, and initiation of XCI in cells that lack all *cis*-elements identified to be crucial for the pairing process, indicate that pairing is not required for XCI initiation. Pairing may therefore reflect changes in transcriptional activity of genes located within the *Xist* and *Tsix* TADs, and may be the consequence of the XCI process. This is supported by the finding that transcription is required for pairing to occur, and the absence of pairing after CTCF knockdown could reflect the disturbed activation of the XCI process. Active genes are preferentially located in the nuclear interior whereas silent gene loci reside in the nuclear periphery, and transient activation of *Xist*, and other genes within the *Xist* TAD, on both X's may lead to relocation of the loci. In addition, association of co-regulated genes has been reported for the globin and other erythroid specific genes that are preferentially recruited to a limited number of transcription factories enriched for shared transcription factors [1010]. Similarly *Xist* and possibly *Jpx*, *Ftx* and *Xpr* could transiently share the same, in number restricted, transcriptional interactomes. These inter X chromosomal associations will happen by chance and could likely explain the pairing process reported for XCI.

RNF12 expression crucial for maintained Xist expression

The near absence of XCI in *Rnf12*$^{-/-}$ ES cells indicates a crucial role for *Rnf12* in the initiation of XCI. In this study we find that also after *Xist* up-regulation *Rnf12* is required to maintain *Xist* expression and establish the Xi. In +/Δ(Xite-Rnf12) and *Xist*$^{+/1lox}$*Rnf12*$^{+/-}$ cells accumulation of *Xist* on the wild type X chromosome will shut down the single functional *Rnf12* gene in *cis*. Rapid down-regulation of the RNF12 protein level due to auto-ubiquitination will result in up-regulation of REX1 which in turn leads to repression of *Xist* and activation of *Tsix*. Within the early window of XCI initiation, XCI is reversible and loss of *Xist* coating, visible in our +/Δ(Xite-Rnf12) and *Xist*$^{+/1lox}$*Rnf12*$^{+/-}$ cells as dispersed signals after *Xist* RNA-FISH, probably results in reactivation of the Xi, allowing RNF12 to increase and start XCI again (**Figure 7C**). In +/Δ(Xite-Rnf12) and *Xist*$^{+/1lox}$*Rnf12*$^{+/-}$ cells this vicious circle never allows spreading of *Xist* in most cells. The low amount of cells that do show dispersed spreading of *Xist* could be explained by the presence of other activators of XCI, or represent cells that have not silenced *Rnf12* yet.

Our findings indicate that the loss of *Rnf12*$^{+/-}$ embryos with a maternally inherited Δ*Rnf12* allele may not be attributed to a defect in maternal storage [981], but may be related to a loss of *Xist* expression from the paternal X chromosome due to silencing of the functional *Rnf12* allele. Similarly, in *Rnf12*$^{+/-}$ ES cells initiation of XCI on the wild type X will therefore lead to reactivation of the X, explaining completely skewed XCI towards inactivation of the mutated X chromosome (**Figure 7B**). Only when the threshold to initiate XCI on the mutated allele is raised by deletion of the *cis*-regulatory region in the +/Δ(Jpx-

Rnf12) cells we were able to detect some cells that initiate XCI on the wild type X. However, this effect was only transiently present, probably because only cells that initiate XCI on the Δ(Jpx-Rnf12) allele continue to maintain XCI. Previously we have shown that a small percentage of female XX cells initiate XCI on both X chromosomes and stop dividing [179]. The present results indicate that these cells are not lost from the population, but reactivate one or both X chromosomes to result in cells with only one single Xi. The fact that only few +/Δ(Xite-Rnf12) and $Xist^{+/Hox}Rnf12^{+/-}$ cells show *Xist* spreading underscore the robust feedback mechanism involving close proximity of *Rnf12* to *Xist*, but also the high turn over of both RNF12 and its target REX1. The high percentage of cells with two *XIST* clouds in rabbit and human female pre-implantation embryos [379] could represent a stage where feedback is absent, but can quickly be resolved by activation of the missing component such as REX1 or other proteins involved in the feedback mechanism.

A cis- and trans-X inactivation center

The X inactivation center was determined by genetic studies involving X-autosome translocation products or trunctated X chromosomes in mouse and human cells that either indicated the presence or absence of XCI. These studies delineated a 10 Mb region in mouse and a 700 kb region in human to be required for XCI [1011]. Both the mouse and human XIC encompass the *Xist* and *Tsix* TADs, which are remarkably conserved in both species [1004, 1012]. Most of the gene interactions are restricted within the TADs and are much more abundant than inter TAD interactions, suggesting that the *Xist* and *Tsix* TADs most likely represent the *cis*-regulatory region required for XCI and represent the *cis*-XIC. Our findings support this and indicate that all important *Xist* regulatory elements reside within the *Xist* TAD. However, in order to regulate *Xist* and *Tsix* in a sex specific manner *trans*-acting cues are crucial. Activators of XCI can be located anywhere on the X chromosome, although close proximity to *Xist* would facilitate a rapid feed back mechanism preventing XCI on both X chromosomes. The *trans*-XIC therefore could encompass multiple regions on the X chromosome involved in activation of the XCI process. Our studies indicate that RNF12 is an important activator of XCI in random XCI, but initiation of XCI in $Rnf12^{+/-}$ cells indicates that more activators might be present. Further studies need to address how many other activators are involved in initiation of XCI.

Acknowledgements

We would like to thank Dr. Edith Heard for helpful comments on the manuscript. We also thank all department members for helpful discussions.

Supplemental data

Supplemental data contains 8 figures and one table.

Methods :

ES cell culture, generation of knockout cell lines and transgenesis

Wild type ES cells and culture media for ES cell culture and differentiation have been described [911]. To generate the deletion cell lines, a female *Xist* 2lox ES cell line, containing a wild type Cast/Ei X chromosome and a C57Bl/6 X chromosome with a floxed *Xist* allele [95] was used. *Rnf12* was targetted using the previously described BAC targetting vectors and methods [174, 911], thereby introducing an additional lox site on the C57Bl/6 X chromosome. Correct targetting was verified using an RFLP based screening method and Southern blotting [958]. Transient expression of Cre was used to delete either only *Xist* or the *Jpx/Ftx/Xpr* region. Correct deletion was verified using PCR using the primers described in Table 1, and confirmed by DNA-FISH. To target *Tsix*, a BAC targetting vector was created which replaced the transcriptional start site of *Tsix* by mCherry, thereby abolishing *Tsix* transcription. Correct targetting was verified by PCR. To remove *Xite* and *Tsix* sequences, a pXite DTA Hygro TK vector was used to insert a lox site upstream of *Xite* [179] in the cell line already deleted for *Jpx*, *Ftx*, *Xpr* and mutated for *Rnf12*. After verification of correct targetting by Southern blotting [179], transient Cre expression was used to loopout *Xite*, *Tsix* and *Xist*, which was detected by PCR analysis. For rescue experiments, the previously modified BAC transgenes covering *Rnf12*, *Jpx/Ftx* or the *Xpr* [174], with either neomycin or puromycin selection were used. Copy number of transgenes was estimated using qPCR on genomic DNA, as previously described [174, 911].

Expression analysis

Expression analysis was performed by qPCR, as previously described [911], using the primers listed in Supplementary Table 1.

Generation of experimental heterokaryons

Male (1.3) [92] and female (F121) mouse ESCs were labelled with Vibrant 1,1'-dioctadecyl-3, 3, 3', 3' tetramethylindodicarbocyanine (DiD) and 3,3'-dioctadecyloxacarbocyanine perchlorate (DiO) cell labelling solutions (Molecular Probes, Invitrogen), respectively. Cells were resuspended at $1{\cdot}10^6$ cells/ml in DMEM and labelled with 5 µl/ml of dye at 37°C for 15 min. After washing, cells were allowed to recover for two days in ES cell medium on MEFs. ES cells were then preplated and mixed in a 1:1 ratio, washed, and fused with 50% polyethylene glycol (pH 7.4) (PEG 1500; Roche Diagnostics) at 37°C over 1 min before dilution. Cells were washed and cultured in ES-media overnight in gelatinised culture dishes. Differentiation was started after 12 hours, by washing and addition of EB-medium. After 12 hours of differentiation, DiD+DiO+ cells were FACS sorted using a FACSAria cell sorter (BD Bioscience). The DiO+DiD+ sorted cells were plated out on chamber slides in EB-medium and differentiated for additional 48 hours (day 2.5) or 108 hours (day 5) prior to fixation.

Fluorescent in situ hybridization and immunofluorescence

Procedures, probe labelling and probes for RNA-FISH have been described [174, 911]. For DNA-FISH, BAC CT7-474E4 and RP23-100E1 were used to detect the *Xpr* and *Ftx/Jpx* region, respectively. For immuno-FISH, cells were fixed for 10 minutes using 4% PFA/PBS, permeabilized using 0,1% Triton-X100 for 5 minutes, and post-fixed for 5 minutes with 4% PFA/PBS. Detection of MS2 *Xist* in male nuclei occured with a Digoxygenin-labelled MS2 probe [92]. ACTIN was detected using a mouse-anti- β-ACTIN antibody (Sigma).

Cell proliferation assays

For cell proliferation analysis, equal amounts of cells were allowed to differentiate on gelatinised culture dishes. Cells were washed, trypsinized, and viable cells were counted at the different time points indicated. For EB differentiation, cells were collected at different time points, and DNA was isolated and concentration meassured. All meassurements and countings were performed in triplicate, on three independent differentiations.

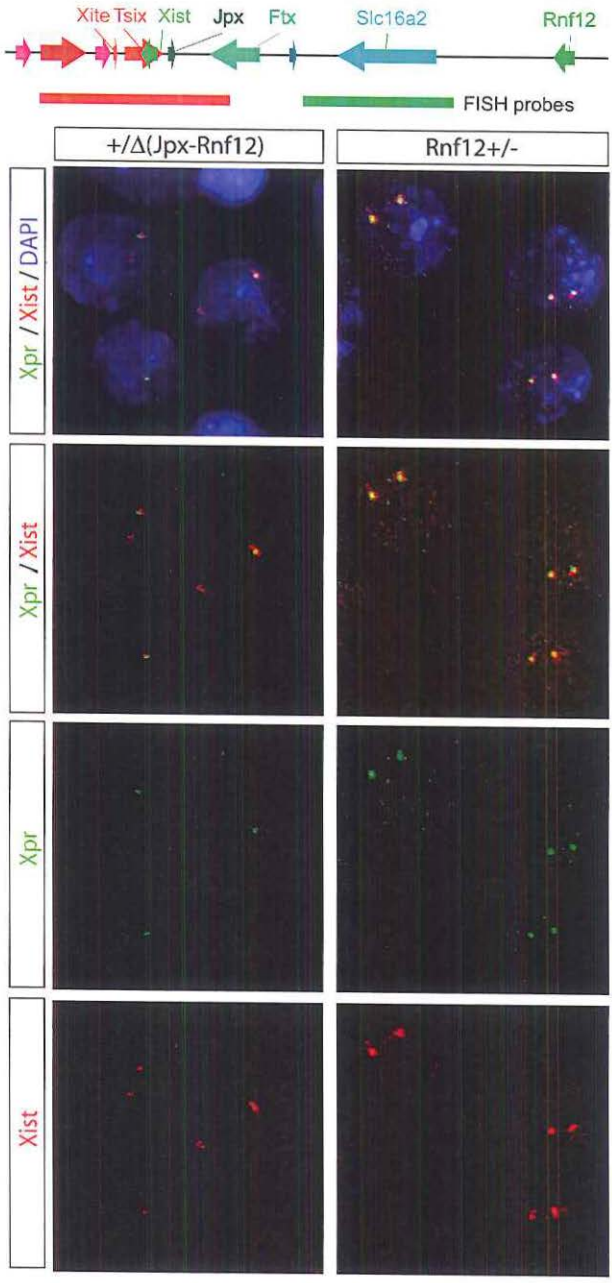

Supplementary Figure 1
Map of part of the Xic showing the location of the FISH probes used in the panels below to detect the deletion of the *Xpr* region in undifferentiated +/Δ(Jpx-Rnf12) ES cells (*Xpr* in FITC, *Xist* in Rhodamine Red, DAPI is blue).

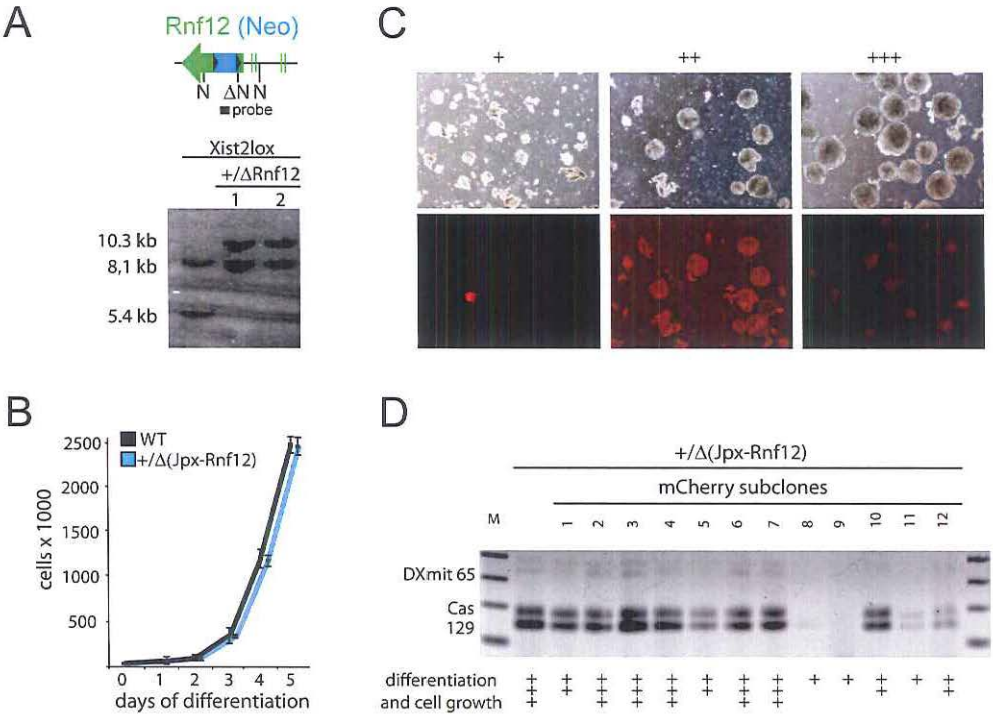

Supplementary Figure 2
A) Map showing the *Rnf12* locus and restriction sites used for Southern blotting analysis to identify clones with the proper integration of the neo targeting cassette. **B)** Cell proliferation analysis during ES cell differentiation of wild type and +/Δ(Jpx-Rnf12) ES cells. **C)** Clonal variegation in cell differentiation was found in wild type and +/Δ(Jpx-Rnf12) ES cell clones, with clones that differentiated poorly (+), and others differentiating very well (+++). A pmCherry expression construct was used for selection of targeted clones. **D)** Amplification of a microsatellite marker (DXmit 65) indicating the presence of both X chromosomes after differentiation of +/Δ(Jpx-Rnf12) ES cell clones. Shown below are the differentiation characteristics per clone.

A

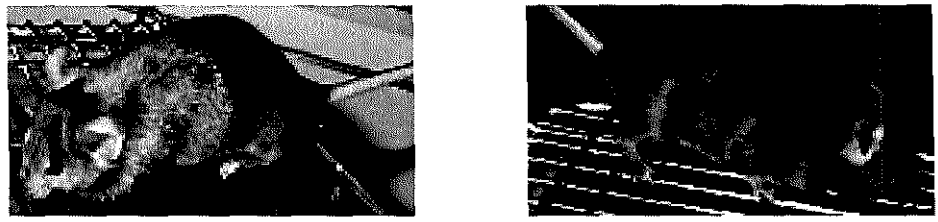

B

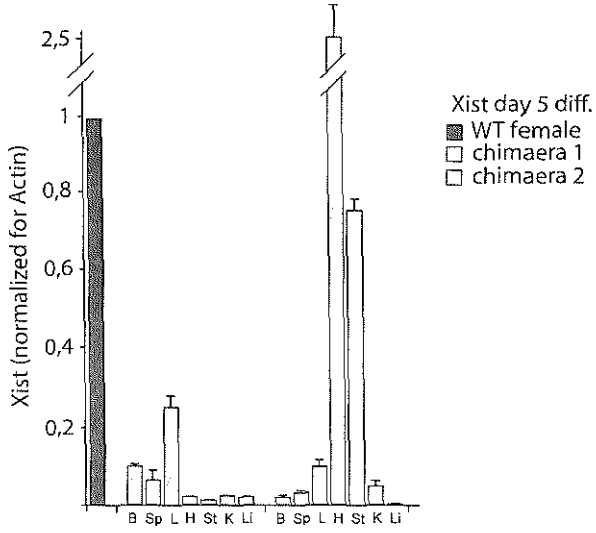

Supplementary Figure 3
A) Wild type / +/Δ(Jpx-Rnf12) chimaeric male mice, showing a high percentage of coat colour contribution. **B)** *Xist* expression analysis normalized to *Actin*, determined by qPCR analysis with RNA isolated from different organs of two different male mice chimaeric for the female +/Δ(Jpx-Rnf12) ES cells (B=brain, Sp=spleen, L=liver, H=heart, St=stomach, K=kidney, Li=liver).

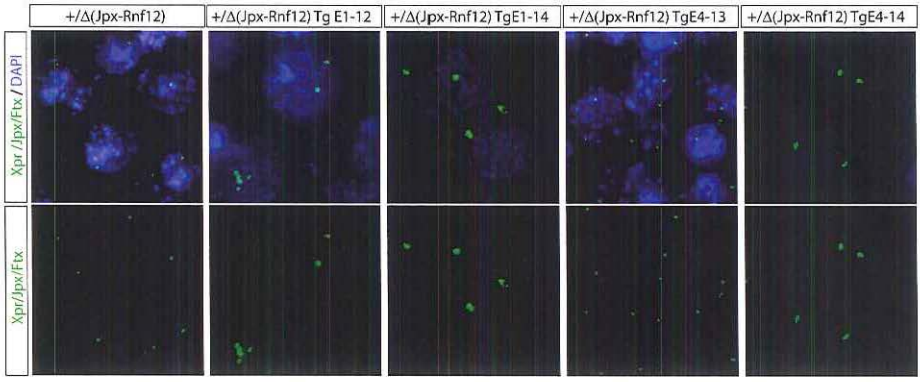

Supplementary Figure 4
DNA-FISH analysis on +/Δ(Jpx-Rnf12) and *Jpx/Ftx* and *Xpr* transgenic +/Δ(Jpx-Rnf12) ES cell lines, using BAC probes detecting the *Jpx/Ftx* (E1, BAC RP23-100E1) or *Xpr* transgene (E4, BAC CT-474E4) and endogenous sequences.

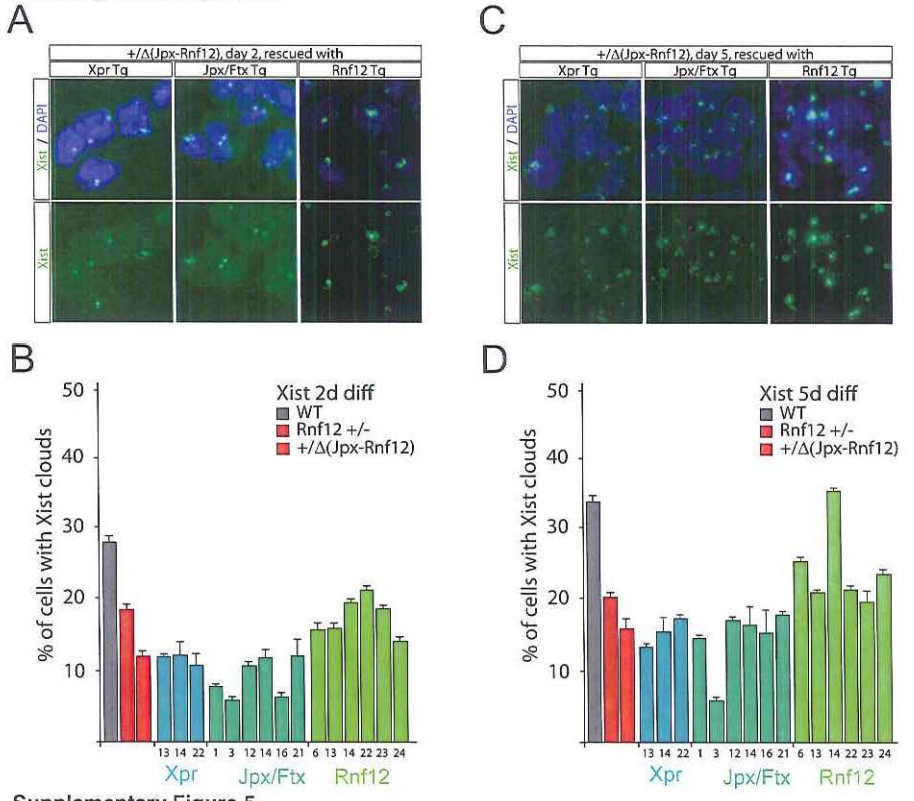

Supplementary Figure 5
Xist RNA-FISH (FITC) on *Xpr*, *Jpx/Ftx* and *Rnf12* transgenic +/Δ(Jpx-Rnf12) ES cell lines fixed at day 2 **(A)** and 5 **(C)** of differentiation (DAPI is blue). **(B,D)** Quantification of the percentage of *Xist* clouds in **(A)** and **(C)**, comparing transgenic ES cell lines with wild type, *Rnf12*$^{+/-}$ and +/Δ(Jpx-Rnf12) ES cell lines.

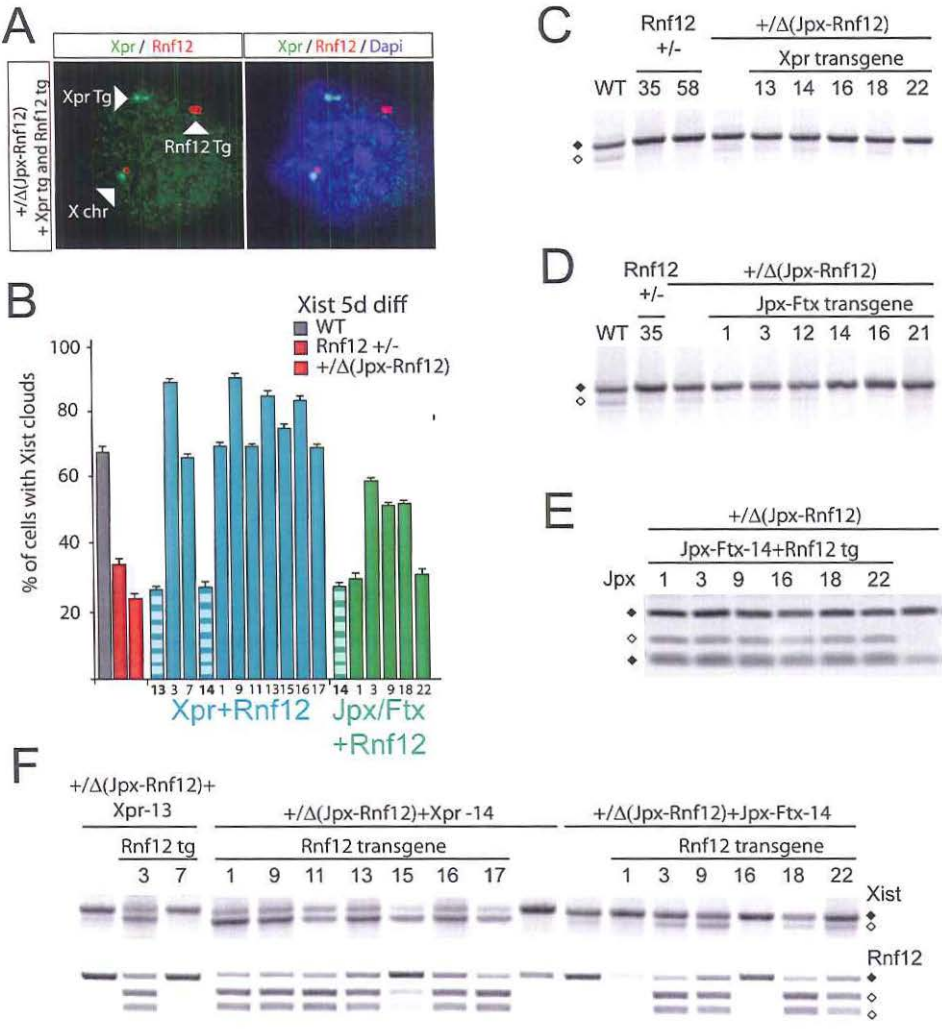

Supplementary Figure 6

A) DNA-FISH analysis on Δ(Jpx-Rnf12), *Xpr* and *Rnf12* double transgenic undifferentiated ES cells, with *Xpr* (FITC) and *Rnf12* (Rhodamine Red) probes (FISH signals are indicated with triangles). **B)** Quantification of percentage of *Xpr+Rnf12* and *Jpx/Ftx+Rnf12* double transgenic ES cells with an *Xist* cloud at day 5 of differentiation. Also shown are the percentage of *Xist* clouds in the founder cell lines with the *Xpr* and *Jpx/Ftx* transgenes alone (dashed bars), and wild type, *Rnf12*$^{+/-}$ and +/Δ(Jpx-Rnf12) ES cell lines. **C), D)** Allele specific *Xist* expression analysis with RNA from *Xpr* **(C)** and *Jpx/Ftx* **(D)** transgenic ES cells differentiated for 5 days (targeted Δ(Jpx-Rnf12) C57/Bl/6 allele is black rectangle, wild type Cast/Ei is open rectangle). **E)** Endogenous (black rectangles) and transgenic (open rectangle) *Jpx* expression in day 5 differentiated *Jpx/Ftx+Rnf12* double transgenic ES cells. **F)** Allele specific RT-PCR analysis detecting an *Xist* length polymorphism (top panel, black rectangle: targeted Δ(Jpx-Rnf12) C57/Bl/6 allele, open rectangle: wild type Cast/Ei), and an NheI RFLP located in *Rnf12* (bottom panel, endogenous *Rnf12* black rectangle, transgenic *Rnf12* open rectangles).

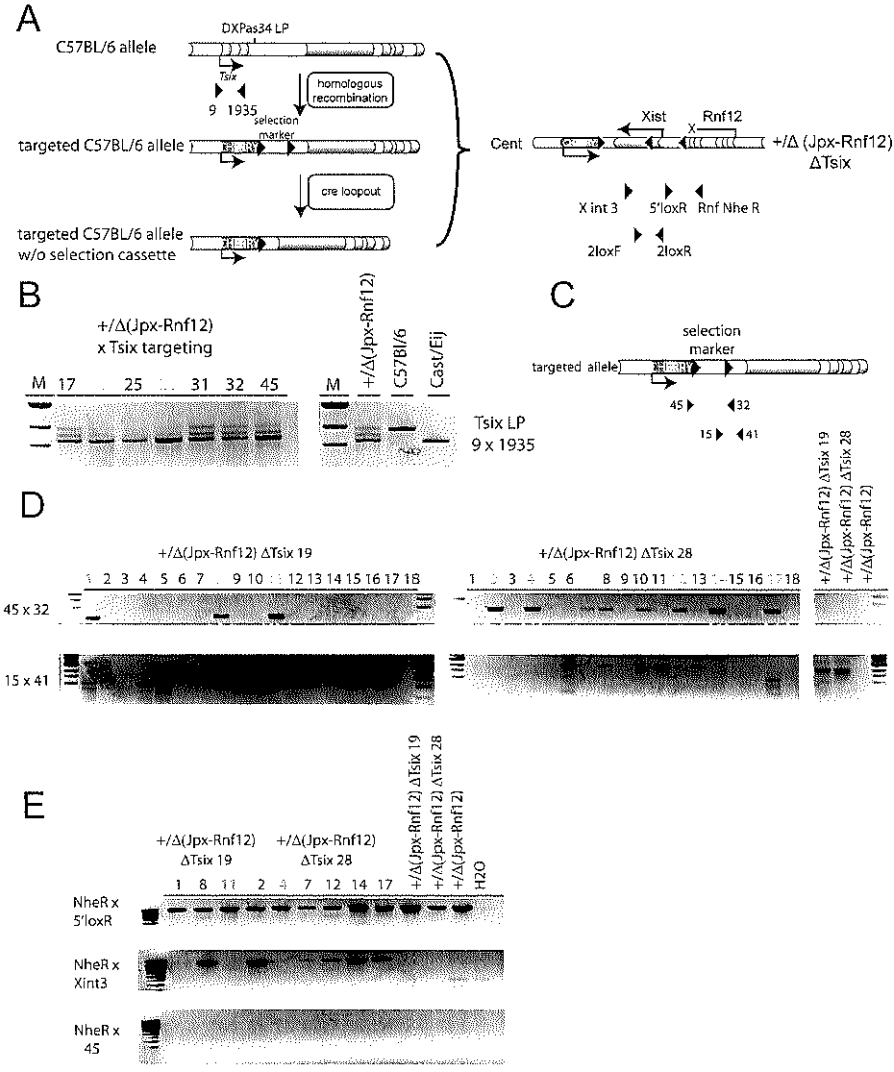

Supplementary Figure 7

A) Scheme showing the strategy for targeting of *Tsix* in the Δ(Jpx-Rnf12) ES cell line. The first exon of *Tsix* is replaced by a Cherry sequence, stop cassette and a floxed neomycin selection marker. The selection marker is then looped out by transient expression of Cre. Location of primers is indicated. **B)** PCR amplification of a length polymorphism in *Tsix*. Targeting of the C57Bl/6 *Tsix* allele results in loss of the high molecular weight band, as found for clone 19 and 28. **C)** Cartoon showing location of primers used to verify correct loopout of the selection cassette after transient Cre expression. **D)** PCR amplification of different fragments using primers shown in **C** on genomic DNA extracted from +/Δ (Jpx-Rnf12) ΔTsix clones after transient Cre expression, confirming loopout of the selection cassette in several clones indicated in red. **E)** PCR analysis on a selected group of clones from **D** using primers confirming the presence of *Xist* in the looped-out clones. Clone 11 and 4 were used for further analysis.

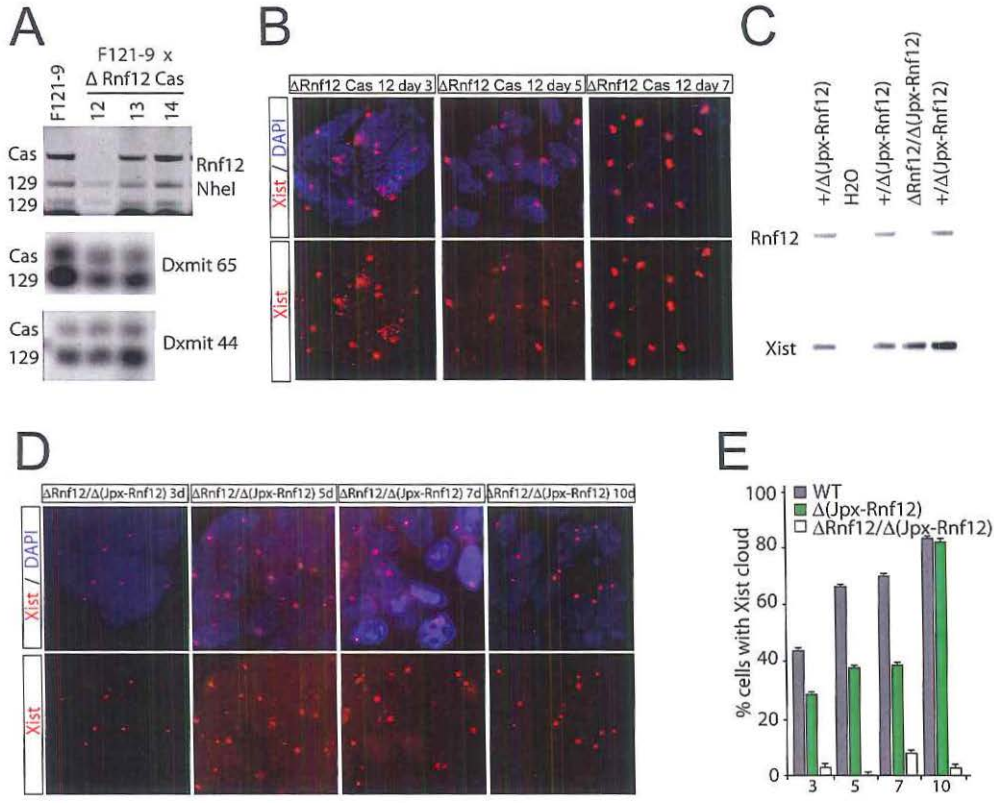

Supplementary Figure 8

A) PCR amplification of a genomic fragment in *Rnf12*. Targeting of an NheI RFLP present on the Cast/Ei allele, results in a loss of the high molecular weight band. DXmit65 and DXmit44 primers amplifying X-linked micro-satellite repeat sequences indicate the presence of both the 129/Sv and Cast/Ei X chromosomes. **B)** *Xist* RNA-FISH (Rhodamine Red) on day 3, 5 and 7 differentiated $Rnf12^{+/-}_{Cast/Ei}$ ES cells (DAPI is blue). **C)** PCR amplification across the targeting cassette integration site in *Rnf12*, shows loss of both alleles in ΔRnf12/Δ(Jpx-Rnf12). **D)** *Xist* RNA-FISH (Rhodamine Red) on day 3, 5, 7 and 10 differentiated ΔRnf12/Δ(Jpx-Rnf12) ES cells (DAPI is blue). **E)** Quantification of relative number of wild type, Δ(Jpx-Rnf12), and ΔRnf12/Δ(Jpx-Rnf12) ES cells with *Xist* clouds during differentiation.

Supplementary Tabel 1: Primers used in this study:

Primer	Forward	Purpose	Digest	Ref
2Lox R (K)	CATGAGAATTGCTCCATCCA	PCR loopout analysis		
2Lox F (J)	GGCCAGTTTCTGACACCCTA	PCR loopout analysis		
X prom L (L)	TTCTGGTCTTTGAGGGCAC	PCR loopout analysis		
X intr 3R (G)	CACTGGCAAGGTGAATAGCA	PCR loopout analysis		
5'LOX R (P)	ACCCTTGCCTTTTCCATTTT	PCR loopout analysis		
Nhe GenA F (M)	GCCTTCGAACATCTCTGAGC	*Rnf12* RFLP	NheI	174
Nhe GenA R (N)	GAGCCGGACTAATCCAAACA	*Rnf12* RFLP	NheI	174
mXistI 1-3L (H)	CAGTGGTAGCTCGAGCCTTT	*Xist* RFLP	BsrgI	911
mXistI 1-3R (I)	CCAGAAGAGGGAGTCAGACG	*Xist* RFLP	BsrgI	911
JpxUp (C)	CGGCGTCCACATGTATACGTCC	*Jpx* RFLP	NlaIII	1006
JpxLo (D)	TAGGAATGAGCCTCCCCAGCCT	*Jpx* RFLP	NlaIII	1006
DXMit171 for (E)	TAGAATTTTCAGGTGTTTGTTTGC	LP differing Cas/Bl6		
DXMit171 rev (F)	TGAGTATGCATGGGCACATT	LP differing Cas/Bl6		
NS18 (A)	GGTAACAATTTTCCCGCCATGTG	*Tsix* RFLP	MnlI	137
NS19 (B)	GGAAATAAACGGAACGCAGTACC	*Tsix* RFLP	MnlI	137
Xite C (O)	GGACATTTTGTCCTGGCAGT	detection loopout *Xite-Xist*		179
DXMit55 for	CTGCTTCCAGAATATTATCACTACTCC	LP differing Cas/Bl6		
DXMit55 rev	AAAACATCCATTTATGTTAACACACA	LP differing Cas/Bl6		
DXMit44 for	TCTAAAAGCATGCCAAATTGG	LP differing Cas/Bl6		
DXMit44 rev	TTCCTATCGCTCAGGTTTTTG	LP differing Cas/Bl6		
b-actin for	ACTATTGGCAACGAGCGGTTC	qPCR		174
b-actin rev	AGAGGTCTTTACGGATGTCAACG	qPCR		174
Xist for	GCCTCAAGAAGAAGGATTGC	qPCR		174
Xist rev	GGGATTGTTTGTCCCTTTGG	qPCR		174
Tsix X9 for	TGACCAGTACCTCGCAAGTTC	qPCR		191
Tsix X9 rev	CTAAGAGCACCTGGCTCCAC	qPCR		191
Jpx e1-F	GCACCACCAGGCTTCTGTAAC	qPCR		1006
Jpx e1-R	GGGCATGTTCATTAATTGGCCAG	qPCR		1006
FtxE8.9Up	CTTGATTCAGCAACACATGAGGA	qPCR		1007
FtxE10.9Lo	TCCAGGCAAGAGGGACCAG	qPCR		1007
Nap1L2 for	CAGACCGTCCAAAAGGACTTA	qPCR		1007
Nap1L2 rev	AGTAAGGGTTGGTACATTTCAG	qPCR		1007
q-copy 0474e4 forw	CCGCTGAAGATAGCTCTTGG	Copy-Number *Xpr*		174
q-copy 0474e4 rev	GCCACAACCAAACAGAATCC	Copy-Number *Xpr*		174
q-copy E1 forw	ATCTCACCGTACCCATGAGC	Copy-Number *Jpx/Ftx*		174
q-copy E1 rev	CCTCTGGTACGACCTCTTGC	Copy-Number *Jpx/Ftx*		174
Tsix1 for	ACCATGACCAAAGCAACTCC	Copy-number		174
Tsix1 rev	CTCCTCCAGTACCATGTCTGC	Copy-number		174
Rnf4-5 for	AGCCCCGATGAAAATAGAGG	Copy-number		174
Rnf4-5 rev	GGCATTTCTGGATAATCTTTGG	Copy-number		174
Zfp42 for	GCACCCATATCCGCATCCAC	Copy-number		174
Zfp42 rev	GCATTTCTTCCCGGCCTTTG	Copy-number		174
Xist LP 1445	ACTGGGTCTTCAGCGTGA	RT-PCR LP		911

Xist LP 1446	GCAACAACGAATTAGACAACAC	RT-PCR LP		911
Rnf12 cDNA for	TAAAGAGGGTCCACCACCAC	RT-PCR RFLP	NheI	174
Rnf12 cDNA rev	GGCAGAGAGCCACTTTCATC	RT-PCR RFLP	NheI	174
Tsix LP 9 FWD	AGTGCAGCGCTTGTGTCA	RT-PCR LP		
Tsix LP 1935 REV	TATTACCCACGCCAGGCTTA	RT-PCR LP		
Xite probe For	AAGCTTGGGTCCTCCTCTGT	Southern probe		179
Xite probe Rev	CCACTCAGACATCCCCAGAT	Southern probe		179
Rnf12 probe for	GGCAGAGAGCCACTTTCATC	Southern probe		958
Rnf12 probe rev	GCCAAAGACCTCCAACCATA	Southern probe		958
mTsix_5arm_FWD1	CTTTGGTCTCTGGGTTTCCA	Arms for BAC recombination		
mTsix_5arm-PinAI_REV1	TACCGGTAGCTGGCTATCACGCTCTTC	Arms for BAC recombination		
mTsix_3arm_FWD	GAGGGCAGATGCCTAAAGTG	Arms for BAC recombination		
mTsix_3arm_REV	CGCAGGCATTTTACCTTCAT	Arms for BAC recombination		
15 HSVTK_pA FWD1	GGGAGGCTAACTGAAACACG	*Tsix* loopout		
32 mTsix_3arm_REV2	AAGTACTGACTACGCAGGCATTTTACCT	*Tsix* loopout		
41 mTsix_+1935 REV	TATTACCCACGCCAGGCTTA	*Tsix* loopout		
45 EGFPpA FWD2	CTCCCCCTGAACCTGAAAC	*Tsix* loopout		

Chapter 8

Loss of random and imprinted XCI in Rnf12 mutant mice

Tahsin Stefan Barakat, Cathérine Dupont, J. Anton Grootegoed and Joost Gribnau

(Work in progress)

Loss of random and imprinted XCI in *Rnf12* mutant mice

Tahsin Stefan Barakat, Cathérine Dupont, J. Anton Grootegoed and Joost Gribnau[1]

Department of Reproduction and Development, Erasmus MC, University Medical Center, Rotterdam, The Netherlands.
[1]corresponding author

Contact details:
Joost Gribnau
Department of Reproduction and Development
Erasmus MC
Room Ee 09-71
PO Box 2040
3000 CA Rotterdam
The Netherlands
Phone +31-10-7043069
Fax +31-10-7044736
Email: j.gribnau@erasmusmc.nl

Abstract

In mammals the dosage of X-linked genes is equalized in male and female cells by inactivation of one X chromosome in every female somatic cell. In mouse imprinted X chromosome inactivation (XCI) leads to inactivation of the paternal X chromosome in all extra-embryonic tissues, and precedes random XCI which is initiated in the embryo proper just after implantation. X-encoded *Xist* is up-regulated on the inactive X chromosome (Xi), and *Xist* RNA spreads in *cis*, thereby silencing the X chromosome by recruitment of chromatin remodeling complexes. *Rnf12* is an X-linked regulator of *Xist*, and *Rnf12* knockout studies in mice have indicated that *Rnf12* is required for imprinted XCI. Here we study the role of *Rnf12* in imprinted and random XCI in the mouse. By analysis of pre-implantation *Rnf12* knockout embryos we found that *Rnf12* regulates imprinted XCI by activation of *Xist*, and not through repression of its negative regulator *Tsix*. Examination of XCI in *Rnf12*$^{+/-}$ adult mice indicates that random XCI is initiated in a very small pool of cells. In addition, for several X-linked genes we found a partial loss of XCI, suggesting that *Rnf12*$^{+/-}$ mice are chimaeric animals with cells subject to normal XCI, and cells that partially or completely lost XCI. Loss of XCI is the consequence of inactivation of the wild type X chromosome in *Rnf*12$^{+/-}$ mice leading to *Rnf12* null cells which cannot properly establish the Xi. The loss of XCI phenotype in *Rnf*12$^{+/-}$ mice is age related, and in time cell selection processes result in an increase of cells which normally inactivated one X chromosome. Our findings indicate that, in a chimaeric context, female mice can life with a partially inactivated X chromosome, without clear phenotypic consequences.

Introduction

The gene expression dosage and changes in these expression levels are instrumental in cell fate decisions and development. This is illustrated by the restricted development of most aneuploid mammalian embryos, and even the presence of one extra relatively small chromosome 21 leads to Down syndrome in human. The evolution of the mammalian sex chromosomes, and the concomitant loss of more than thousand genes from the Y chromosome forced the up-regulation of dose sensitive genes on the remaining X chromosomal copy. This form of dosage compensation would lead to over-expression of X-linked genes in female cells, which is prevented by inactivation of one X chromosome in every female somatic cell [30]. In mammals X chromosome inactivation (XCI) is present in two forms. Imprinted XCI is found in all extra-embryonic tissues of the mouse and leads to inactivation of the paternal X chromosome (Xp) [53]. Imprinted inactivation of the Xp in the mouse is reversed in the inner cell mass (ICM) [52, 54], followed by a round of random XCI which is initiated at around 5.5 days post coitum (E5.5). So far, no evidence has been presented indicating imprinted XCI in other eutherian species, suggesting that the imprinted form of XCI may have evolved specifically in the mouse.

XCI is very robust involving several layers of epigenetic modifications that maintain the inactive state through a near infinite number of cell divisions. In human more than 15% of the genes located on the X escape or partially XCI, although this pattern is very variable [240]. Escape of XCI correlates with the evolutionary history of the sex

chromosomes, with genes added later to the X more often escaping XCI. In mouse only a small number of genes escape XCI suggesting that evolution of XCI may be more advanced in this species.

The XCI process is directed by *cis*-acting genes located within the X-linked *cis*-X inactivation center (XIC), regulated by *trans*-acting activators and inhibitors of XCI [987]. The *cis*-XIC encompasses several non-coding genes, most of them conserved in all eutherian species. *Xist* encodes a 17kb long functional RNA transcribed from the inactive X chromosome (Xi), which coats the Xi in *cis* thereby recruiting factors involved in the establishment of the Xi [74, 84-85]. In mouse, another non-coding gene *Tsix* acts as a negative regulator of *Xist* [118-119]. *Tsix* fully overlaps with *Xist* and is transcribed in anti-sense direction and both the act of transcription and the resulting RNA have been implicated in *Xist* repression, either by transcriptional interference or recruitment of chromatin remodelers to the *Xist* promoter. Female specific activation of *Xist* is accomplished by the dose dependent action of X-encoded activators of XCI involved in the activation of *Xist* and repression of *Tsix* [179, 189, 910]. Inhibitors of XCI counteract the XCI-activator activity by activation of *Tsix* and repression of *Xist*.

Rnf12 encodes the single identified XCI-activator so far [174, 911]. RNF12 is a ring finger protein directing the dose-dependent breakdown of the pluripotency factor REX1 [1009], which is a repressor of *Xist* and activator of *Tsix* [989, 1009]. Upon differentiation of ES cells or in the epiblast of the developing embryo the concentration of RNF12 is higher in female compared to male cells, resulting in sufficient REX1 degradation to allow activation of *Xist* in female cells only. Stochastic initiation of XCI is followed by spreading of *Xist* in *cis* and silencing of one copy of *Rnf12*. Robust feed back through the fast turn-over of RNF12 and REX1 prevents initiation of XCI on both X chromosomes in most cells. Homozygous *Rnf12* knockout ES cells show a loss in XCI [911], whereas heterozygous *Rnf12* ES cells show skewed XCI in favor of inactivation of the mutated X chromosome [174]. These studies indicated that *Rnf12* is continuously required during the early stages of XCI. Initiation of XCI on both X chromosomes will lead to a loss of RNF12 expression, followed by REX1 stabilization and reactivation of the Xi's in the time window where XCI is reversible. In heterozygous $Rnf12^{+/-}$ ES cells differentiation therefore results in completely skewed XCI towards inactivation of the *Rnf12* mutant X chromosome. Similar results have been obtained in the mouse which shows non-random expression of RNF12 in all tissues suggesting completely skewed XCI [981]. These studies also indicated that female mice were only born when the mutated *Rnf12* allele was inherited through the paternal germ line. Inheritance of a mutated *Rnf12* allele through the maternal germ line leads to loss of imprinted XCI and embryos die shortly after implantation due to defects in development of extra-embryonic tissues. Loss of imprinted XCI has been attributed to a lack of maternal RNF12 storage, but could possibly be attributed to a lack in maintained expression of RNF12 in the pre- and peri-implantation embryo.

Here we study the role of *Rnf12* in imprinted and random XCI. Imprinted XCI results in exclusive inactivation of the paternal X chromosome (Xp). Nevertheless, in female embryos with two maternal X chromosomes, delayed initiation of XCI on the maternal X has been reported [1013]. In $Rnf12^{+/-}$ pre-implantation embryos we never detected initiation of *Xist* from the maternal X (Xm). In addition, maternal inheritance of

the *Rnf12* mutation leads to down regulation of *Xist* and not *Tsix* expression. These findings suggest a dose dependent role for *Rnf12* in activation of *Xist* in imprinted XCI. We also investigated random XCI in the adult $Rnf12^{+/-}$ mouse, and our findings suggest that XCI is initiated in a small pool of cells that make up the embryo and adult mouse. Interestingly, $Rnf12^{+/-}$ mice show a loss of XCI which varies per tissue and per mouse. Loss of XCI decreases with age suggesting selection against cells with two active X chromosomes or cells with a partially inactivated X chromosome. Our findings suggest that cells with two active X chromosomes, or cells with a partially inactivated X chromosome can survive in a chimaeric environment together with cells that properly initiated XCI.

Results

Generation of the Rnf12 knockout mouse

To study the role of *Rnf12* in XCI *in vivo* we generated *Rnf12* knockout mice by blastocyst injection of $Rnf12^{+/-}$ and $Rnf12^{-/-}$ ES cells. These polymorphic Cast/Ei / 129/Sv ES cell lines were generated by BAC targeting of the 129/Sv allele to generate $Rnf12^{+/-(neo)}$ ES cells [174], and targeting of the second Cast/Ei *Rnf12* allele resulting in $Rnf12^{-(puro)/-(neo)}$ ES cells [911]. Our previous studies indicated that XCI is severely down-regulated in differentiating $Rnf12^{-/-}$ ES cells, with clonal expansion of a few cells which properly up-regulated *Xist* [911]. To our surprise we obtained male and female founders with a high coat color contribution of $Rnf12^{-/-}$ ES cells. Allele specific PCR amplification of a BsrGI RFLP in *Xist* was performed with genomic DNA isolated from different organs of a $Rnf12^{-/-}$ chimaeric male. BsrGI digests the Cast/Ei allele, not present in wild type cells, and our analysis indicated that the contribution of $Rnf12^{-/-}$ ES cells varied per tissue (**Figure 1A**). *Xist* expression analysis by qPCR on RNA isolated from different organs of one male $Rnf12^{-/-}$ chimaeric mice showed that *Xist* was activated, suggesting that *in vivo* initiation of XCI is more robust than in differentiating $Rnf12^{-/-}$ ES cells (**Figure 1B**).

$Rnf12^{-/-}$ chimaeric female mice were bred with wild type males, and 1 out of 5 female founders gave $Rnf12^{Y/-(neo)}$ and $Rnf12^{Y/-(puro)}$ offspring. No female offspring was observed with a heterozygous *Rnf12* mutation (n=17 litters, 103 pups, 6 male knockouts, 97 wild type animals). Interbreeding of different genotypes confirmed previous findings which showed that male *Rnf12* knockout mice are born at a Mendelian ratio, whereas transmission of the *Rnf12* mutation through the female germ line is lethal (**Figure 1C**, maternal genotype is always shown first). Interestingly we observed one female animal with a maternally inherited *Rnf12* knockout allele indicating that some embryos do survive. This may be explained by a small number of extra-embryonic $Rnf12^{-/-}$ cells reported to initiate XCI [981] which may be sufficient to support embryo survival. In this embryo imprinted XCI may have been reversed leading to *Xist* activation on the Xm, as is found in embryos with two uniparental maternally inherited X chromosomes [1013]. We decided to study this finding in more detail.

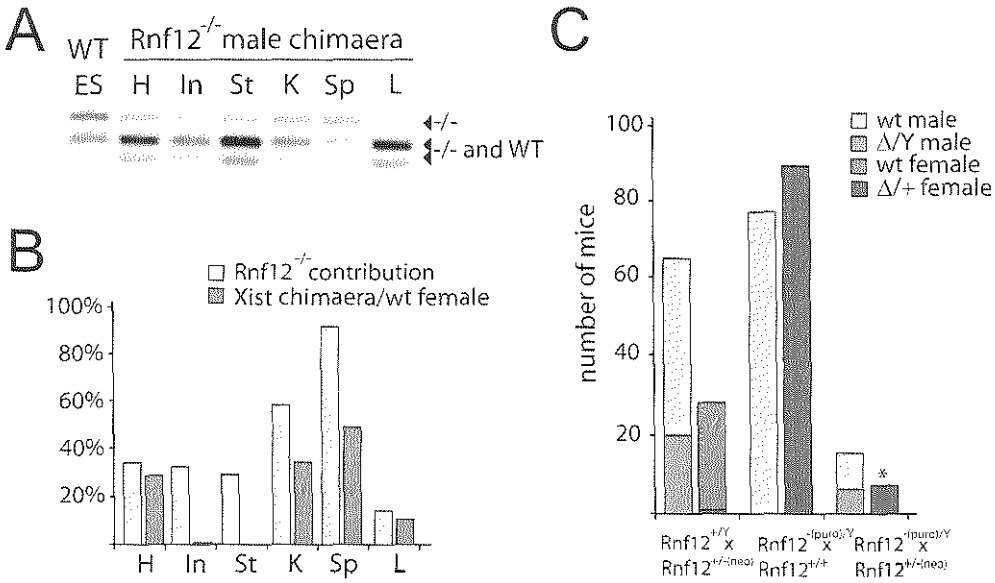

Figure 1: Analysis of *Rnf12* knockout mice
A) Contribution of *Rnf12*$^{-/-}$ cells to a male chimaeric animal was determined by allele specific amplification of a BsrGI RFLP in *Xist*. The top band is *Rnf12*$^{-/-}$ specific, the bottom two bands represent a mix of digestion products from one wild type and one *Rnf12*$^{-/-}$ X chromosome. **B)** Quantification of the relative contribution of *Rnf12*$^{-/-}$ cells to a male chimaeric animal shown in **A**, and qPCR expression analysis of *Xist* per organ. Shown is the relative *Xist* expression compared to wild type females. **C)** Offspring observed in different crosses of wild type, *Rnf12*$^{+/-(neo)}$ and *Rnf12*$^{-(puro)/Y}$ mice (* all Δ/+ female mice inherited the Δ*Rnf12* (puro) allele from father)

Rnf12 is required for pre-implantation development

Inheritance of a mutated *Rnf12* allele through the maternal germ line was reported to be embryonic lethal due to a loss of imprinted XCI leading to a defect in the development of extra-embryonic tissues [981]. In that study *Rnf12*$^{-/+}$ mice were generated by crossing wild type males with *Rnf12*$^{2lox/2lox}$ females harboring an oocyte specific Cre expression cassette [981]. Cre mediated knockout of *Rnf12*$^{2lox/2lox}$ in the developing oocyte leads to complete depletion of RNF12 during oocyte maturation, and the loss of XCI phenotype was therefore attributed to a lack of the maternal storage of RNF12. Interestingly, maternal inheritance of a Δ*Rnf12* allele and not the wild type allele in oocytes from *Rnf12*$^{-/+}$ females leads to embryonic lethality. The first and second meiotic divisions happen very late during oocyte maturation. Therefore in oocytes of *Rnf12*$^{+/-}$ female mice maternal storage of RNF12 will be similar in oocytes carrying the Δ*Rnf12* and wild type allele, and cannot explain the *Rnf12* phenotype. To better understand the loss of *Rnf12*$^{-/+}$ animals with a maternally inherited Δ*Rnf12* allele, we crossed *Rnf12*$^{Y/-(puro)}$ and wild type male mice with *Rnf12*$^{+/-(neo)}$ female mice and studied imprinted XCI in the resulting pre-implantation embryos. Fertilized oocytes were isolated and allowed to develop *in vitro* until E3.5 and 4.5 and both RNA and DNA was isolated from single embryos. All possible genotypes were observed in normal Mendelian ratio's indicating no loss of *Rnf12*$^{-(neo)/-(puro)}$ and *Rnf12*$^{-/-(puro)}$ embryos at

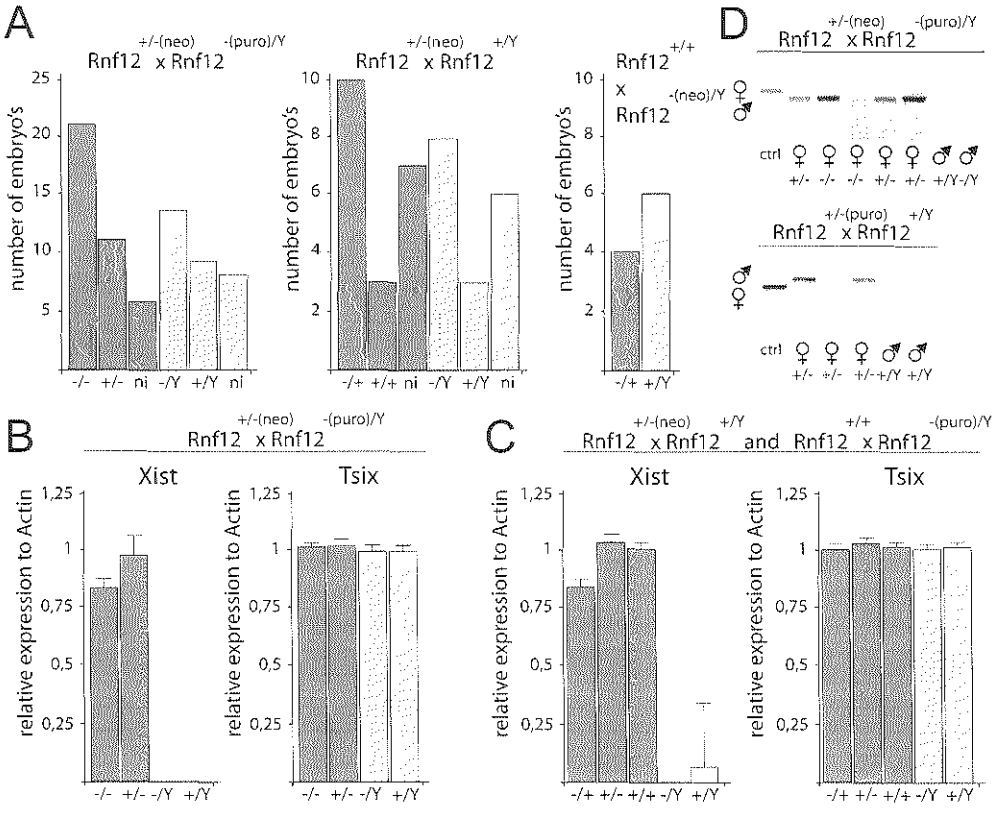

Figure 2: *Xist* but not *Tsix* expression affected in the *Rnf12*$^{-/+}$ and *Rnf12*$^{-/-}$ embryo
A) The number of day E3.5 and E4.5 pre-implantation embryos with different genotypes obtained in different crosses involving wild type, *Rnf12*$^{+/-\,(neo)}$ and *Rnf12*$^{-\,(puro)/Y}$ mice is shown. No difference between day E3.5 and E4.5 pre-implantation embryos was found and therefore the data were pooled (for all genotypes the maternally inherited allele is shown first) **B)** *Xist* and *Tsix* qPCR expression analysis on pre-implantation embryos obtained after mating *Rnf12*$^{+/-\,(neo)}$ and *Rnf12*$^{-(puro)/Y}$ mice. The values shown represent the average per genotype with standard deviation. **C)** As in **B** but with pre-implantation embryos obtained by mating *Rnf12*$^{+/-\,(neo)}$ and *Rnf12*$^{+/Y}$ and by mating *Rnf12*$^{+/+}$ and *Rnf12*$^{-(puro)\,/Y}$ mice. **D)** Allele specific expression analysis detecting a length polymorphism in *Xist* does not reveal maternal *Xist* expression in *Rnf12*$^{+/-\,(neo)}$ and *Rnf12*$^{-(neo)\,/-\,(puro)}$ pre-implantation embryos (♀,♂ *Xist* expression from the maternal and paternal allele, respectively).

this stage of development (**Figure 2A**). qPCR analysis indicated down regulation of *Xist* in *Rnf12*$^{-(neo)/-(puro)}$ and *Rnf12*$^{-(neo)/+}$ embryos compared to wild type embryos (**Figure 2B** and **2C**). No down regulation was observed in *Rnf12*$^{+/+}$ and *Rnf12*$^{+/-(puro)}$ embryos, indicating that the reduced expression of *Xist* cannot be attributed to differences in maternal storage as all embryos were derived from *Rnf12*$^{+/-(neo)}$ oocytes. Analysis of *Tsix* expression by qPCR did not reveal a difference between all obtained genotypes, suggesting that the main role of *Rnf12* in imprinted XCI is the regulation of *Xist*. Although imprinted XCI results in exclusive inactivation of the Xp, female embryos with two uniparental maternal X

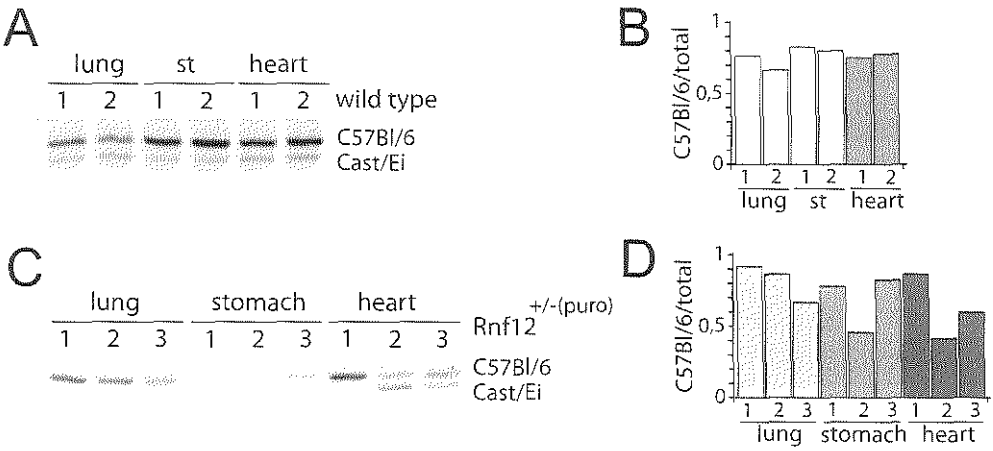

Figure 3: XCI is initiated in a small pool of cells in *Rnf12*$^{+/-}$ mice
A) Allele specific *Xist* expression in F1 C57Bl/6 / Cast/Ei in different organs of two wild type mice. St, stomach. **B)** Quantification of allele specific *Xist* expression wild type mice shown in **A**. st, stomach **C), D)** As in (**A**,**B**) but performed with different organs of three *Rnf12*$^{+/-}$ mice, the Δ*Rnf12* allele(puro) is located on the paternally inherited Cast/Ei X chromosome

chromosomes show delayed initiation of XCI around the blastocyst stage. Reversal of XCI could explain the reported initiation of XCI in a small number of cells of *Rnf12*$^{-/-}$ embryos. We therefore performed allele specific RT-PCR analysis of *Xist* and found exclusive expression of *Xist* from the paternal X chromosome in our *Rnf12*$^{(neo)/+}$ and *Rnf12*$^{(neo)/(puro)}$ embryos, indicating that XCI is never initiated on the Xm (**Figure 2D**). This suggests that the RNF12 expression level, which is twice as high in embryos with an uniparental maternal X chromosome, may be limiting factor for the activation of *Xist* on the Xm.

Non-random expression of Xist in adult mouse

Our previous work involving *Rnf12*$^{-/-}$ ES cells has indicated that besides a role for *Rnf12* in imprinted XCI, *Rnf12* is also required for random XCI [911]. Also heterozygous *Rnf12*$^{-/-}$ ES cells showed delayed and less robust initiation XCI compared to female control ES cell lines [174]. These findings predict that XCI may be initiated in a smaller pool of cells in *Rnf12*$^{+/-}$ and *Rnf12*$^{-/-}$ chimaeric animals. *Xist* up-regulation in *Rnf12*$^{+/-}$ and chimaeric *Rnf12*$^{-/-}$ mice may be explained by clonal expansion of cells which initiated XCI and cell selection against cells with two Xa's may mask the effects of *Rnf12* on random XCI. To test whether XCI is indeed initiated in a smaller pool of cells in *Rnf12*$^{+/-}$ mice we isolated RNA from different mouse organs of *Rnf12*$^{+/-}$ and control mice. The Δ*Rnf12* (puro) allele in the mice we studied was located on the paternally inherited Cast/Ei chromosome allowing allele specific amplification of an *Xist* length polymorphism by RT-PCR. Although XCI is random, several inter strain mouse crosses result in skewed XCI in favor of one of the X chromosomes due to differences in the strength of the Xce [445]. This Xce has been genetically pinpointed to a 1.8 Mb region on the X chromosome partially overlapping with *Tsix* but not *Xist* [448-449]. In wild type female mice we consistently found skewing of *Xist* expression towards expression from the C57Bl/6 allele, with an expected skewing ratio of

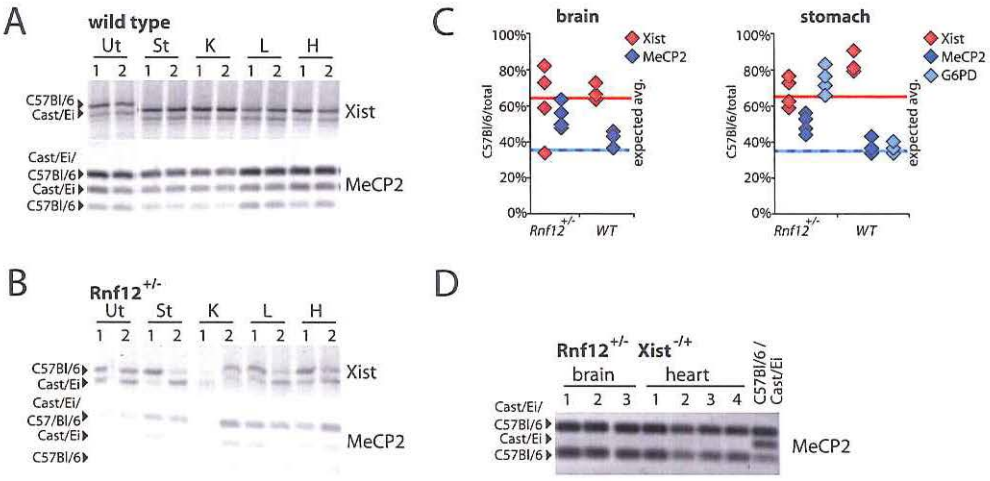

Figure 4: Loss of XCI in *Rnf12*$^{+/-}$ mice
A) Analysis of allele specific *Xist* and *MeCP2* expression in different organs of two wild type F1 C57Bl/6 / Cast/Ei mice, shows preferential expression of C57/Bl/6 *Xist* and reciprocal expression of *MeCP2*. This reciprocal expression pattern is absent in *Rnf12*$^{+/-}$ mice **(B)**. **C)** Quantification of allele specific *Xist*, *MeCP2* and *G6PD* expression in brain and stomach of several wild type and *Rnf12*$^{+/-}$ animals. **D)** Allele specific expression analysis of *MeCP2*, in *Rnf12*$^{+/-}$ *Xist*$^{-/+}$ *trans*-compound mice, shows completely skewed XCI of the Δ*Rnf12* harboring Cast/Ei X chromosome.

65%/35% (**Figure 3A** and **3B**). In different tissues of three different heterozygous *Rnf12*$^{+/-\,(puro)}$ knockout mice, obtained through crosses of *Rnf12*$^{-(puro)/Y}$ males with wild type females, we found significant deviation of the expected 65%/35% skewing ratio (**Figure 3C** and **3D**). This finding suggests that in our *Rnf12*$^{+/-}$ knockout mice random XCI was initiated in a smaller cell population leading to a larger patch size detectable in our analysis.

Loss of XCI in adult mice

The high contribution of *Rnf12*$^{-/-}$ cells in our chimaeric mice, and *Xist* up-regulation in *Rnf12*$^{-/-}$ cells was unexpected based on ES cell differentiation studies and suggest that additional cues, not present in our ES differentiation protocols, are directing the XCI process. However, when comparing the relative contribution of *Rnf12*$^{-/-}$ cells in different organs and the level of *Xist* expression, we noticed that *Xist* expression is less robust compared to female cells, suggesting an XCI phenotype (**Figure 1B**). Also, our previous studies indicated that continuous expression of *Rnf12* is required for persistent *Xist* expression and proper establishment of the Xi. Therefore in differentiated *Rnf12*$^{+/-}$ ES cells *Xist* expression is completely skewed towards expression from the mutated allele. In contrast, in our *Rnf12*$^{+/-}$ mice we did not find severe skewing of *Xist* expression towards expression from the mutated X chromosome.

To test whether random XCI was properly initiated in *Rnf12*$^{+/-\,(puro)}$ mice we isolated RNA of different organs and performed allele specific RT-PCR analysis. In the tested *Rnf12*$^{+/-\,(puro)}$ mice the mutated Δ*Rnf12* (puro) allele was located on a Cast/Ei X chromosome, whereas the wild type X chromosome was C57Bl/6 derived,

providing sufficient RFLPs for allele specific expression analysis. In all organs of wild type animals we found preferential expression of C57Bl/6 *Xist*, and the expected reciprocal expression pattern for the X-linked genes *Hprt*, *MeCP2*, *Atp7a* and *G6PD* (**Figure 4A** and data not shown). In *Rnf12*$^{+/-\ (puro)}$ mice expression of *Xist* fluctuated with in some organs preferential expression from the C57Bl/6 and in other organs from the Cast/Ei X chromosome. Expression analysis of the X-linked genes, *Hprt*, *MeCP2*, *Atp7a* and *G6PD*, indicated that the expected reciprocal expression pattern, compared to *Xist*, was almost absent (**Figure 4B** and data not shown). Quantification of allele specific expression confirmed loss of XCI in *Rnf12*$^{+/-(puro)}$ mice, showing a clear deviation of the expected 65%/35% ratio in most organs of different animals. In contrast to wild type animals in most organs of *Rnf12*$^{+/-\ (puro)}$, for most X-linked genes, expression was in favor of the C57Bl/6 allele. Our studies do not reveal whether loss of XCI is chromosome wide or only affects a subset of X-linked genes. However, the differences we found in deviation from the expected 65%/35 ratio in between X-linked genes in the same organ suggest that loss of XCI is variable and may not be a chromosome wide phenomenon.

To better understand the XCI phenotype in *Rnf12*$^{+/-\ (puro)}$ mice we crossed *Rnf12*$^{-\ (puro)/Y}$ males with female mice carrying a heterozygous *Xist*$^{1lox/+}$ mutation. In the resulting *Rnf12*$^{+/-\ (puro)}$ *Xist*$^{1lox/+}$ *trans*-compound mice *Xist* can only be activated on the Δ*Rnf12* Cast/Ei X chromosome. If the *Rnf12*$^{+/-\ (puro)}$ mutation affects silencing of the Δ*Rnf12* Cast/Ei X chromosome this should have resulted in expression of X-linked genes located on the Cast/Ei X chromosome. Allele specific expression analysis of *MeCP2*, *Atp7a* and *G6PD* showed complete and exclusive inactivation of the Δ*Rnf12* Cast/Ei X chromosome, suggesting that the loss of XCI in our *Rnf12*$^{+/-\ (puro)}$ mice must be attributed to the a lack of XCI initiation on the wild type C57Bl/6 X chromosome (**Figure 4D** and data not shown).

Survival of cells with 2 active X chromosomes, or 1 active and 1 partially active X chromosome may be supported by the presence of cells in the near vicinity that properly initiated XCI in a chimaeric context. However, in time cells with two Xa's may be selected against. We tested this hypothesis by analysis of X-linked gene expression in different organs of mice sacrificed 6 weeks after birth and of mice sacrificed at 11 weeks or later. We found that in older mice *Xist* expression was more biased towards the Cast/Ei X chromosome harboring the Δ*Rnf12* allele (**Figure 5A-E**). In addition, comparison of *Hprt*, *MeCP2* and *G6PD* expression between these age groups indicated a better correlation between *Xist* expression and reciprocal X-linked gene expression. This effect was found in all tested organs, suggesting selection against cells which lost or partially lost XCI. In addition, a shift in *Xist* expression towards expression from the Δ*Rnf12* harboring X chromosome suggests that cells which initiated XCI on the wild type C57Bl/6 X chromosome are lost from the population (**Figure 5D** and **5E**). This is consistent with *in vitro* studies which indicate that *Xist* spreading is only obtained on the Δ*Rnf12* X chromosome in *Rnf12*$^{+/-}$ ES cells.

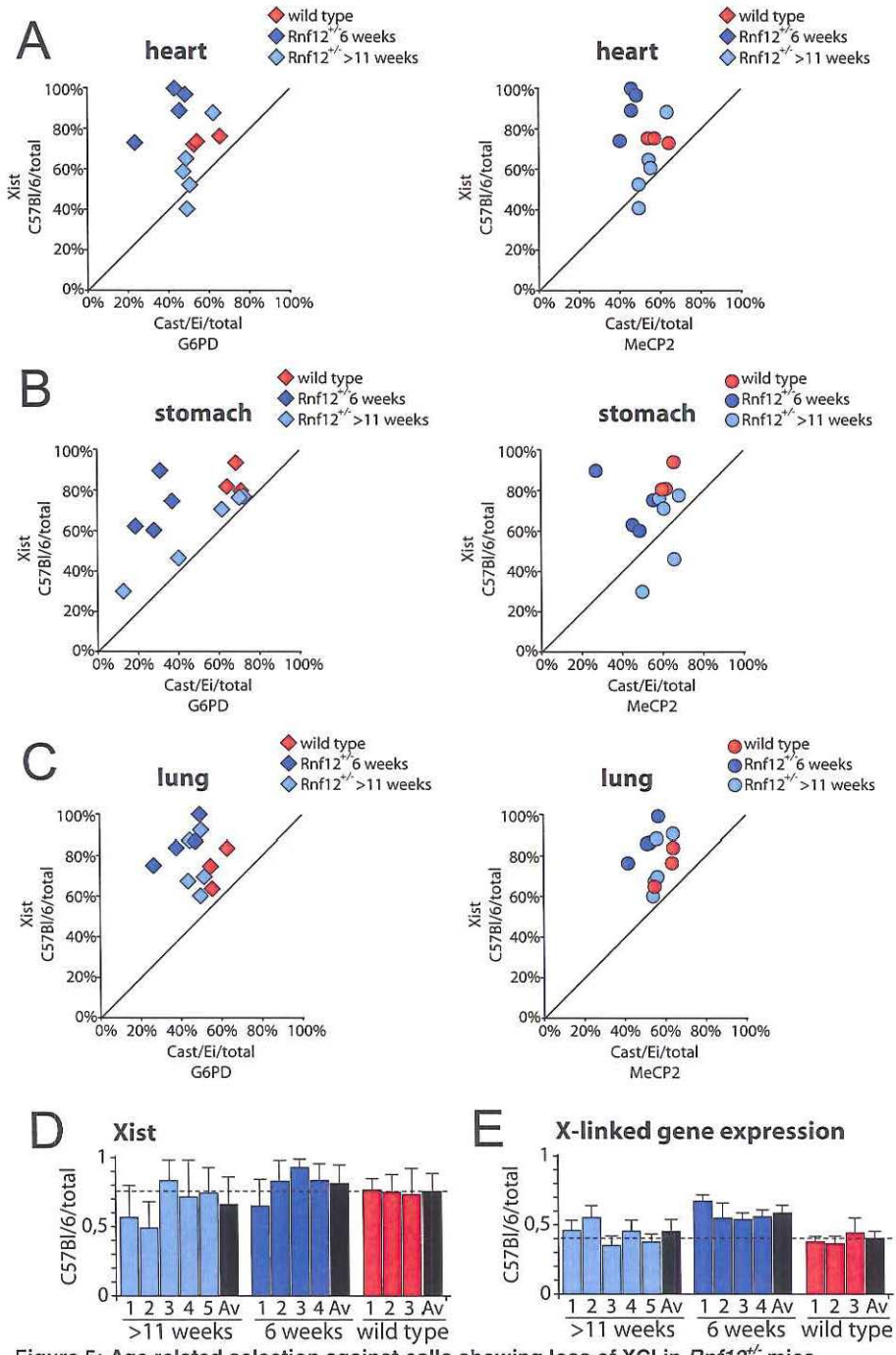

Figure 5: Age related selection against cells showing loss of XCI in *Rnf12*$^{+/-}$ mice

Discussion

Female specific activation of *Xist* is directed by the dose dependent action of X-encoded activators of XCI. *Rnf12* encodes an important activator of XCI, involved in imprinted XCI in mouse and in random XCI in ES cells [174, 911, 981, 1009]. In this study we investigated the role of *Rnf12 in vivo*, by studying pre-implantation and adult *Rnf12* mutant mice. Our studies support previous findings that *Rnf12* is required for imprinted XCI. Interestingly, one *Rnf12*$^{-/+}$ female mouse was born with a Δ*Rnf12* allele inherited from the mother. Allele specific *Xist* expression indicated that the survival of this embryo cannot be attributed to a switch in *Xist* expression leading to XCI of the maternal X chromosome, as is found in embryos with two maternal X chromosomes [1013]. In a published study, in *Rnf12*$^{-/+}$ mice obtained through cre mediated knockout of *Rnf12* in *Rnf12*$^{2lox/2lox}$ oocytes only a few cells were reported to initiate imprinted XCI [981]. Our analysis on single embryos indicated that *Xist* expression in *Rnf12*$^{-/+}$ embryos is down-regulated, but only by 20%. This finding might be explained by dispersed *Xist* expression, not located to the X chromosome. Our previous work indicated that in *Rnf12*$^{+/-}$ *Xist*$^{+/-}$ *cis*-knockout ES cells, cells only initiate XCI on the wild type X chromosome leading to silencing of the single functional *Rnf12* allele, which in turn leads to repression of *Xist*. In these cells *Xist* is visible as dispersed clouds, and *Xist* therefore might be stable and detectable in our expression analysis even when detached from the X. Alternatively, the mild effect of the maternal *Rnf12* mutation on *Xist* expression in our *Rnf12*$^{-/+}$ mice may indicate a role for the maternal storage of RNF12 in imprinted XCI, as oocytes in our study are only 50% depleted for RNF12 in contrast to the previous studies that involved oocytes that were devoid of RNF12. However, as most of our *Rnf12*$^{-/+}$ embryos and not the *Rnf12*$^{+/+}$ littermates are lost during development this indicates that the maternal storage cannot explain the *Rnf12* knockout phenotype. Nevertheless, maternal storage of RNF12 may explain the survival of one *Rnf12*$^{-/+}$ mouse with a maternally inherited Δ*Rnf12* allele. In this embryo maternally inherited RNF12 may have supported initiation of imprinted XCI, in sufficient cells to successfully support embryonic growth. Further analysis of pre-implantation embryos by *Xist* RNA-FISH should reveal which of these non-mutual exclusive options is most likely.

Figure 5: continued
A) The ratio of allele specific *Xist* expression in the heart plotted against the reverse ratio of allele specific expression of *G6PD* (left panel) or *MeCP2* (right panel). Shown are wild type animals (red), 6 week old *Rnf12*$^{+/-}$ mice (dark blue), and *Rnf12*$^{+/-}$ mice older than 11 weeks (light blue). **B), C)** As in (**A**) but performed with RNA isolated from stomach (**B**), and lung (**C**). **D)** The average ratio of allele specific *Xist* expression per animal, and per investigated group (>11weeks *Rnf12*$^{+/-}$ mice, 6 weeks *Rnf12*$^{+/-}$ mice, and wild type mice). As in (**D**) with the average of the ratios obtained for the *G6PD*, *MeCP2* and *Atp7a*.

XCI in the embryo proper is random with respect to the parental origin of the X chromosome. However, several mouse crosses result in skewed XCI due to differences in the strength of the genetically determined Xce, located distal to *Xist*. In the mouse crosses analyzed in this study the C57Bl/6 X chromosome is more likely to be inactivated than the Cast/Ei X chromosome. This skewing of XCI is detectable in all tissues, suggesting that initiation of XCI happens in a relative large pool of cells. Interestingly, in our *Rnf12*$^{+/-}$ mice allele specific *Xist* expression fluctuates between the tissues of the same mouse but also between the same tissues of different mice. This finding suggests that in the *Rnf12*$^{+/-}$ mice XCI is initiated in a relative small pool of cells that make up the embryo. Studies involving ES cell injections of a limited number of cells in tetraploid blastocysts have indicated that injection of one ES cell is sufficient to support the development of a viable animal [1014]. Also in these animals the pool of cells contributing to the peri-implantation embryo where XCI is initiated is small, but this situation is compatible with life. Whether cells that activate *Xist* are the only cells that contribute to the developing embryo or if a mosaic of *Xist* positive and negative cells is present in *Rnf12*$^{+/-}$ mice needs to be determined by *Xist* RNA-FISH on post-implantation embryos and adult mice.

Our finding that XCI is partially lost at the loci we tested is very surprising. So far it is unclear whether our *Rnf12*$^{-/-}$ mice are chimaeric animals with XaXi cells and cells with two Xa's and/or with cells with one Xa and one partially activated X chromosome. RNA-FISH and allele specific RNA-sequencing experiments need to be performed to answer this question. Although cells without a late replicating X chromosome have been described in the early developing embryo, previous studies involving *Xist*$^{+/-}$ mice and our analysis of *Xist*$^{-/+}$ *Rnf12*$^{-/-}$ *trans*-compound mice, indicated that XCI was fully skewed towards inactivation of the wild type X chromosome without detectable escape of XCI. The loss of *Xist*$^{+/-}$ embryos which inherited the mutated *Xist* allele through the male germline also indicates a requirement of imprinted XCI for the proper development of extra-embryonic tissues. These findings suggested a strict requirement for dosage compensation. However, the observation in human that a high percentage of genes partially escapes XCI suggests that the dependence on XCI may be less strict than anticipated. Interestingly, requirement of XCI for embryonic development, for instance through an ICM specific knockout of *Xist*, has never been tested. Although this embryonic *Xist* knockout will most likely not be viable, homozygous *Xist* knockout cells may contribute to a wild type embryo in a chimaeric context, and this possibility should be addressed experimentally.

Analysis of XCI in *Rnf12*$^{+/-}$ ES cells indicated the preferential initiation of XCI on the mutated *Rnf12* allele. In these cells activation of XCI on the wild type allele results in RNF12 null cells, leading to repression of *Xist* and subsequent reactivation of the Xi. Within the time window where the Xi can be established repeated initiation of XCI will eventually lead to, almost exclusive XCI of the Δ*Rnf12* harboring X chromosome. In our *Rnf12*$^{+/-}$ knockout mice we do not find preferential XCI of the Δ*Rnf12* allele, and XCI even seems to be more skewed towards inactivation of the wild type C57Bl/6 X chromosome. This effect may be explained by differences in allele specific thresholds for XCI to be initiated *in vitro* and *in vivo* favoring initiation of XCI on the C57Bl/6 chromosome *in vivo*. Also the time window in which XCI can be initiated and the silencing mediated feedback of RNF12 action may be different in the developing embryo compared to differentiating ES cells. Nevertheless, our data do support the preferential loss of XCI in cells that initiated

XCI on the wild type X chromosome. First, *Xist*$^{-/-}$ *Rnf12*$^{+/-}$ compound mice show completely skewed XCI of the mutated X chromosome, indicating that the RNF12 expression level is sufficient for proper silencing of the mutated X chromosome. Second, comparison of young and old mice showed increased silencing of all tested loci in older mice, and a concomitant loss of cells with *Xist* expression emanating from the wild type X chromosome. The reported expression of RNF12 in all cells in *Rnf12*$^{+/-}$ knockout female mice, even suggests that XCI is incomplete on nearly all wild type X chromosomes [981]. Although we cannot exclude a possible selection against RNF12 null cells as an explanation for a decrease in cells showing loss of XCI, we think that the normal development of *Rnf12*$^{-/Y}$ and the high contribution of *Rnf12*$^{-/-}$ ES cells to male chimaeras argues against this option. We therefore conclude that in the developing *Rnf12*$^{-/-}$ embryo, XCI is incomplete in cells or a pool of cells that initiate XCI on the wild type X chromosome. In time, cells subject to loss of XCI involving dose sensitive genes will be selected against. In addition, cells which properly established an Xi may have a proliferative advantage, and both processes may lead to a near normal dosage of X-encoded genes in older *Rnf12*$^{+/-}$ mice. Several questions remain to be addressed, for instance do the *Rnf12*$^{+/-}$ mice show a phenotype? So far, we have not noticed any behavioral or other abnormalities, but a more thorough examination is required to address this question. The fact that mice do survive with loss of XCI of at least a few genes that we tested so far, hint at possible therapies to alleviate X-linked disorders in heterozygous phenotypic woman by reactivation of the inactive X chromosome.

Material and Methods

Mice

All animal experiments were in accordance with the legislation of the Erasmus MC Animal Experimental Commission. To generate *Rnf12* mutant mice, *Rnf12*+/- and *Rnf12*-/- ES cells were used for blastocyst injections, and constituted embryos were transferred to pseudopregnant mice. For genotyping of *Rnf12* mutant mice, the following primers were used: Nhe GenA F (gccttcgaacatctctgagc), Nhe GenA R (gagccggactaatccaaaca), Puro detect R (agcaaaaacaggaaggcaaa), Neo detect F (acatttccccgaaaagtgc). To assess Cast/Ei contribution, RFLP PCR was performed using primers m*Xist*I 1-3L (cagtggtagctcgagcctttt) and m*Xist*I 1-3R (ccagaagagggagtcagacg), followed by digestion with BsrgI. Results were confirmed using primers detecting length polymorphisms distinguishing between C57Bl/6 and Cast/Ei: DXMit55f (ctgcttccagaatattatcactactcc), DXMit55rev (aaaacatccatttatgttaacacaca), DXMit44for (tctaaaagcatgccaaattgg) DXMit44 rev (ttcctatcgctcaggtttttg), *Xist* LP 1445 (actgggtcttcagcgtga) and *Xist* LP 1446 (gcaacaacgaattagacaacac).

Embryo collection, DNA and RNA from single embryos

All procedures were performed according to the institutional animal care and approved animal use committee protocols. In brief, female mice were synchronized with Follugon and Chorulon, mated and sacrificed the day following mating. Zygotes were isolated from the ampulla and cultured in KSOM until they reached the blastocyst stage. Blastocysts were collected for RNA and DNA analysis between 96 and 108h post Chorulon administration. Individual blastocysts were transferred to 0.2 ml PCR tubes and stored in lysis buffer (Stratagene) at -80°C until further processing. RNA and DNA was extracted using the Absolutely RNA Nanoprep Kit (Stratagene, #400753). To enable genotyping, DNase treatment was omitted from the manufacturer's protocol. One tenth of the RNA/DNA elute was utilized for genotyping, whereas the remainder was reverse transcribed into cDNA using random hexamers and Superscript III reverse transcriptase (Invitrogen, #18080-051) following the manufacturer's protocol. Allele specific discrimination for *Xist* expression between the two polymorphic X-chromosomes was performed as described previously [174], using the primers described above. For the quantitative analysis of *Actin*, *Tsix* and *Xist* expression, all samples were analyzed in triplicate in a 10 µl final reaction volume using the BioRad CFX 384 Real-time System. The reaction mixture contained SYBR Green PCR Master Mix (Applied Biosystems, #4309155), primer (either *Actin*, *Tsix* or *Xist*) and 2.5 µl of cDNA. After an initial hold at 94°C for 2 min, reaction mixtures underwent 40 cycles of 30 sec at 94°C, 30 sec at 60°C and 30 sec at 72°C. Standard curves were generated using mouse ES cell cDNA. All samples were normalized against *Actin* expression and compared to mean expression levels of three female wildtype blastocysts.

RT-PCR and qRT-PCR analysis of mice tissues

To assess XCI skewing, hybrid female mice were sacrificed by cervical dislocation, parts of organs were collected, snap-frozen and triturated using micro-pestils in 1 ml of Trizol reagent (Invitrogen). After an additional centrifugation to clear debris, 700 µl was added to 300 µl fresh Trizol, and RNA was purified following manufacturer's instructions. RNA was reverse-transcribed with SuperScript II (Invitrogen), using random hexamers. Allele specific *Xist* expression was analyzed by RT-PCR using the primers mentioned above. To determine allele specific X-linked gene expression of *Atp7a*, *Mecp2* and *G6pdx*, primers 335 moF3930 (agggcaaacgtgtagcaatggtag) and 336 moF4812 (agagcttgttctaactcactgttct) were used for *Atp7a* amplifying a length polymorphism, [995], primers (catggtagctgggatgttagg) and (gcaatcaattctactttagagcg), for *Mecp2* amplifying a DdeI RFLP in *MeCP2*, and primers (ggagtgatgaactcagggaagc) and (atgtagctgggtttactggtgg) to amplify a ScrFI RFLP in *G6PD*. PCR products were gel purified and digested with the indicated restriction enzymes and analyzed on a 2% agarose gel stained with ethidium bromide. Allele specific expression was determined by measuring relative band intensities using a Typhone image scanner and ImageQuant software. qRT-PCR was performed as described before [911]

Chapter 9

X inactivation in human iPS and ES cells

Tahsin Stefan Barakat, Mehrnaz Ghazvini, Tracy Li, Bert Eussen, Bas de Hoon, Hannie Douben, Annelies de Klein, Robert-Jan Galjaard, Niels Geijssen, J. Anton Grootegoed and Joost Gribnau

(Work in progress)

X inactivation in human iPS and ES cells

Tahsin Stefan Barakat[1], Mehrnaz Ghazvini[1,2], Tracy Li[1,2], Bert Eussen[3], Bas de Hoon[1], Hannie Douben[3], Annelies de Klein[3], Robert-Jan Galjaard[3], Niels Geijssen[4,5,6], J. Anton Grootegoed[1] and Joost Gribnau[1,7]

[1]Department of Reproduction and Development, Erasmus MC, University Medical Center, Rotterdam, The Netherlands.
[2]Erasmus Stem Cell Institute, Erasmus MC, University Medical Center, Rotterdam, The Netherlands.
[3]Department of Clinical Genetics, Erasmus MC, University Medical Center, Rotterdam, The Netherlands.
[4]Hubrecht Institute-KNAW& University Medical Center Utrecht, Utrecht, The Netherlands
[5]Center for Regenerative Medicine, Harvard Medical School, Massachusetts General Hospital, Boston, MA, USA
[6]Harvard Stem Cell Institute, Harvard University, Boston, MA, USA
[7]corresponding author

Contact details:
Joost Gribnau
Department of Reproduction and Development
Erasmus MC
Room Ee 09-71
PO Box 2040
3000 CA Rotterdam
The Netherlands
Phone +31-10-7043069
Fax +31-10-7044736
Email: j.gribnau@erasmusmc.nl

Abstract

Balanced expression of X-linked genes in male and female placental mammals, is accomplished by inactivation of one of the two X chromosomes in female somatic cells. In mice, X chromosome inactivation (XCI) is regulated by the X-transcribed non-coding *Xist* RNA, and spreading of *Xist* results in silencing of X-linked genes in *cis*. *Xist* gene transcription is under control of inhibitors and activators of XCI which coordinate the proper expression of *Xist* in the epiblast of the developing female embryo, or upon differentiation of female ES cells in culture. In contrast to the mouse, initiation of XCI in human is less well studied, because human embryos are rightly protected from such studies and human ES cells (hES) appear to represent a post-XCI state. Studies on XCI in human induced pluripotent stem (hiPS) cells might provide an option to study XCI. However, using human iPS cells, conflicting results have been obtained, some investigators reporting reactivation of the inactive somatic X chromosome during reprogramming, whereas other studies concluded that the inactive X (Xi) remains silent. Here, we have generated a series of hiPS cell lines from female fibroblasts heterozygous for large X-chromosomal deletions, subject to skewed inactivation favoring inactivation of the deletion carrying X chromosome. XCI analysis of the iPS cell lines showed that approximately 70% of the cells have lost markers of the Xi. Single cell RT-PCR on iPS cells revealed bi-allelic expression of several X-linked genes, in most cells within each cell line. We also found a large population of hiPS cells carrying the X-chromosomal deletion expressing *XIST* from the wild type X chromosome, which is not expressed in the fibroblasts used to generate the hiPS cells. Analysis of allele specific methylation at the X-linked *androgen receptor* locus in the hiPS cells showed initiation of XCI on the X that is active in the founder fibroblast cell line. Taken together, these findings indicate robust reactivation of the inactive X chromosome in hiPS cell lines, under the present experimental conditions. However, it is also indicated that these, and other, culture conditions may not allow various hES and hiPS cell lines to maintain two X chromosomes active.

Introduction

XCI is required in eutherian females to compensate for potential dosage differences of X chromosomal genes between female XX and male XY cells [30]. In mice, XCI is first initiated in the pre-implantation embryo, where it is imprinted, leading to inactivation of the paternal X chromosome. Imprinted XCI is reversed in the inner cell mass (ICM), prior to subsequent random XCI in the differentiating cells developing from the epiblast, in which either the maternal or paternal X chromosome is silenced [987]. XCI is an epigenetic process, and a key factor controlling XCI is the *Xist* gene, which is transcribed into a functional but non-coding RNA [74, 84-85]. Transcribed from the X-linked gene, *Xist* RNA is able to spread along the X chromosome in *cis*, thereby attracting chromatin modifiers which induce heterochromatization and silencing of the X chromosome [97-99]. Mono-allelic expression of *Xist* is accomplished by the action of X-encoded XCI-activators and autosomally encoded XCI-inhibitors. A two-fold increased expression of XCI-activators in female cells results in stochastic activation of XCI [174, 911]. Several ES cell pluripotency

factors have been identified as inhibitors of XCI and the interplay of the pluripotency factor network [191, 1009] ensures proper developmental control of XCI (for review [910, 987]).

Most of the insights in XCI regulation have been obtained from studies using mouse ES cells. These cells, which are derived from the ICM of a blastocyst, contain two active X chromosomes when female, and undergo XCI upon *in vitro* differentiation. For studies on human XCI, a good model system for XCI is lacking. Although recently novel insights have been obtained using human embryos [368, 379], these experiments are difficult to perform, and, for ethical reasons, the use of human embryos for research purposes has been widely restricted. Contrary to mouse ES (mES) cells, most human ES (hES) cell lines are in a post-XCI state, and are prone to epigenetic fluidity [361]. Although several hES cell lines show two active X chromosomes and undergo XCI upon differentiation (Class I cells), these cells are prone to undergo XCI even in the undifferentiated state (Class II cells), and a remarkable variation exists between cell lines and different subclones, even among different laboratories [359-364, 1015]. Peculiar, some hES lines have lost *XIST* expression, but do not show evidence of X reactivation (Class III cells) [361, 363]. These findings might have implications for differentiation potential and disease modelling [361], and can likely be influenced by the derivation conditions, as hES cell lines with two active X chromosomes have been obtained under low oxygen conditions [1016], and with the addition of chemical compounds [1017-1018]. Therefore, it seems likely that the variation observed regarding the XCI state in hES cells is a reflection of suboptimal culture conditions, in which from the derivation onwards, cells having two active X chromosomes are lost and gradually progress to a more progressed state, in which XCI has been initiated. Alternatively, hES cells might represent a more advanced and differentiated state compared to mouse ES cells, so that XCI in the hES cells has occurred already prior to or during ES cell derivation [394]. Human ES cells show striking similarities, regarding morphology, culture conditions and gene expression, to mouse epiblast stem cells (mEpiSCs), which are developmentally more advanced than mES cells, and are characterised by the presence of an Xi, suggesting that hES cells might also represent a more differentiated state compared to mouse ES cells [386-387].

In 2006, Takahashi and Yamanaka discovered that over-expression of defined pluripotency factors in fibroblasts can result in reprogramming towards a pluripotent state, which they referred to as induced pluripotent stem (iPS) cells [61]. These cells share all key properties with ES cells, including self-renewal and differentiation potential, and have a similar gene expression profile as hES cells [61, 63]. The derivation of these cells from human fibroblasts [64-66] offers the promise of generating patient-specific stem cells which might be used in future cell replacement-based therapies and disease modelling. Besides these potential advantages for translational medicine, hiPS cells offer opportunities for basic research on establishment and maintenance of pluripotency, and might offer a useful novel model to study XCI in human cells, as in the mouse, it has been shown that the Xi of fibroblasts becomes reactivated during the reprogramming process, followed by random XCI upon differentiation of these mouse iPS cells [67-68].

Recently, several studies have investigated the XCI state of female hiPS cells. The first systematic analysis of multiple female hiPS cell lines derived from four different fibroblast populations under two reprogramming strategies, using either polycistronic lentiviral or retroviral vectors expressing OCT4, SOX2, KLF4 and C-MYC, has shown that

all these hiPS cell lines retain the Xi derived from the starting fibroblasts [1019]. Analysis by RNA-FISH and RT-PCR of several fully reprogrammed female hiPS cell lines did not detect evidence for bi-allelic gene expression from the X chromosomes. It was therefore concluded that during reprogramming of human cells the Xi is not reactivated, resulting in the non-random XCI observed in the hiPS cell lines due to clonal outgrowth of a single fibroblast which started the reprogramming process. Similar results have been obtained in studies of Rett syndrome hiPS cells established from female patients, were non-random XCI in the hiPS cells enabled the derivation of isogenic hiPS cells, in which either the mutant or wild type X chromosome was inactive [1020-1022]. Another study found that all hiPS cell lines derived from one and the same fibroblast population with random XCI, always showed inactivation of the same X chromosome, which indicated that activity of a particular X chromosome might have a selective advantage during the reprogramming process [1023]. In contrast to these findings, another study of Rett syndrome hiPS cells showed that the Xi can be reactivated during reprogramming of fibroblasts, as all cells in a population of undifferentiated hiPS cells from a heterozygous Rett mutation carrier expressed the intact X-encoded MECP2 protein (*MECP2* mutations are the cause of most cases of Rett syndrome), and did not show markers for inactive heterochromatin [1024]. Upon neural differentiation, these cells underwent random X chromosome inactivation, resulting in a mosaic population of cells with or without expression of MECP2, which also showed the presence of *XIST* clouds, indicative of an Xi. Another study even reported that different hiPS cell lines with signs of either reactivation or maintenance of XCI could be obtained from the same fibroblasts [1025]. These lines only seem to differ based on expression of X-linked genes, whereas the level of reprogramming as assessed by gene expression analysis and the ability to form teratomas was similar. Studies investigating the global gene expression of the X chromosome in hiPS cells further support that at least some hiPS cell lines might reactivate the somatic Xi [1026].

Taking together, it is still not clear whether iPS reprogramming can result in reactivation of the inactive X chromosome in human cells. Here we analyze established hiPS cell lines, and novel hiPS cell lines derived from female carriers of heterozygous large X chromosomal deletions showing non-random XCI, and from a patient with a 47,XXX karyotype. These hiPS cell lines were generated using a polycistronic lentiviral vector encoding OCT4, SOX2, KLF4 and C-MYC, and a dTomato transgene which becomes silenced upon complete reprogramming. Although XCI analysis at early passage showed that approximately 30%-40% of the cells have hallmarks of an Xi, including *XIST* cloud formation and heterochromatin markers, a significant portion of cells showed absence of these marks. This might be indicative of either loss of Xi markers comparable to Class III hES cells, or might reflect that X reactivation has occurred. Single cell expression analysis indicated gene transcription from both X chromosomes in many cells. As expected, the X chromosome harboring a deletion expressed *XIST* in the founder fibroblast population, but we detected *XIST* expression from the wild type X chromosome in a significant percentage of hiPS cells derived from these fibroblasts. Taken together, the present study provides evidence that X reactivation does occur during the course of reprogramming of human cells towards hiPS cell lines. However, this may not be a stable condition. Further research will be required to obtain hES and hiPS cell lines, and culture conditions, which can maintain two X chromosomes active.

Results

X chromosome inactivation in established hES, hiPS and hLR5 cells

Human ES and iPS cells may provide a suitable model system to study XCI, and we therefore decided to investigate the XCI state of established hES and hiPS cell lines. Immuno-RNA-FISH experiments on female hES cell line H9 showed that the majority of nuclei (>95%, N=200, data not shown) did not show markers of an Xi. Less then 5% of the nuclei analysed at passage 53 showed the presence of focal *XIST* accumulation (hereafter referred to as *XIST* clouds) (**Figure 1A**). These *XIST* clouds co-localized with a DAPI-dense, heterochromatic region (Barr body), enriched for H3K27me3, and depleted for H3K4me3 and H3K9-acetylation, which are hallmarks of an epigenetically silenced X chromosome. Although *XIST* was not detected in the majority of H9 nuclei, the remaining nuclei also showed a Barr body, suggesting the presence of an Xi. To further characterize the XCI state of H9, we performed the human androgen receptor (HUMARA) assay [480]. This assay makes use of the fact that inactivation of the X chromosome results in methylation of the *androgen receptor* gene. When undigested DNA is amplified by PCR with primers covering a polymorphic repeat in the *androgen receptor* gene, two peaks will be visible, representing the two different alleles. Upon digestion with a methylation-sensitive restriction enzyme, only the methylated and hence inactivated allele will be amplified by PCR. Therefore, after digestion, a randomly inactivated population of cells will still display two peaks, whereas a non-randomly inactivated population will show one dominant peak. Analysis of the methylation state at the human *androgen receptor* gene in H9, showed preferential methylation of a single allele in DNA obtained from the culture, indicating that all nuclei have a clonal origin with the same Xi (**Figure 1B**). These results suggest that H9 belongs to the Class III hES cell lines, in which the majority of cells have lost *XIST* expression, but maintained the Xi. The presence of Class III nuclei and the post-XCI state of the H9 cell line is in agreement with earlier reports on XCI in H9, which showed a high level of variation in XCI between laboratories [363-364, 1027-1028].

We next investigated the XCI state of a previously generated and characterized hiPS cell line derived from a female carrier heterozygous for a mutation of Lesch-Nyhan syndrome (HPRT deficiency, LN-hiPS) [1029]. This cell line was established using lentiviral transduction of fibroblasts with inducible vectors encoding OCT4, SOX2, KLF4, C-MYC and NANOG, and was propagated in the absence of expression of these exogenous factors. Immuno-RNA-FISH analysis detecting *XIST* and NANOG or *XIST* and KLF4 (**Figure 1C**) showed that more than 99% of all nuclei analyzed showed an *XIST* cloud (N=200). This indicated that this cell line also represents a post-XCI state, and similar results were obtained when this cell line was cultured under hypoxic conditions (5% O2) or in the presence of doxycylin for four weeks, to further induce reprogramming (data not shown). HUMARA analysis indicated that also this cell line was subject to complete non-random XCI, in which presumably the X harboring the mutant HPRT allele, was preferentially inactivated (data not shown).

We next analyzed whether we could establish a more naïve pluripotent state which might result in reactivation of the silent X chromosome. To this end, we differentiated the LN-hiPS cells by embryonic body (EB) formation in suspension culture for one week, and

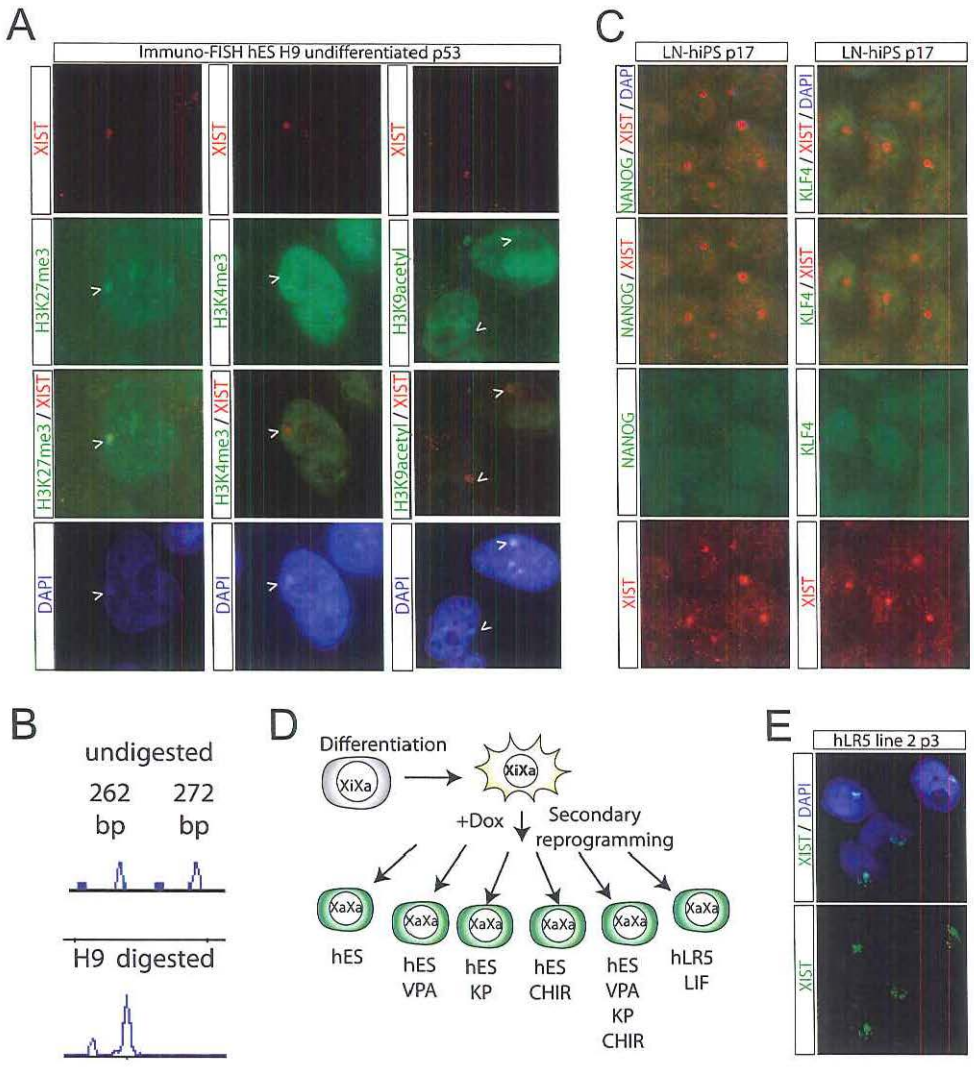

Figure 1: XCI in established human ES cell line H9, hiPS cells and hLR5 cells
A) Immuno-RNA-FISH detecting *XIST* (Rhodamine Red), and H3K27me3, H3K4me3, or H3K9 acetylation (all FITC) in human ES cell line H9 analyzed at passage 53. DNA is counterstained with DAPI (blue). Xi's are indicated with an arrow head. **B)** HUMARA analysis with DNA from the H9 hES cell line. Prior to HpaII digestion, PCR amplification of a polymorphic repeat in the *androgen receptor* gene detects both parental alleles (262 and 272 bp, respectively). After HpaII digestion, only the 262 bp allele is detected. A methylated allele will be protected against HpaII digestion and can be amplified, indicating that the 262 bp allele is preferentially inactivated in H9 ES cells. **C)** Immuno-RNA-FISH detecting *XIST* (Rhodamine Red), and either NANOG or KLF4 (all FITC) in LN-hiPS analyzed at passage 17. DNA is counterstained with DAPI (blue). **D)** Cartoon showing the strategy followed in the secondary reprogramming experiment. LN-hiPS cells were differentiated, and differentiated cells were subjected to a second round of reprogramming, by addition of doxycyclin (Dox) which induces

plated EBs on gelatinised culture dishes to allow outgrowth of differentiated cells. After a further 4 weeks of differentiation, differentiated progeny was obtained, which mainly consisted of terminally differentiated fibroblast-like cells which did no longer show expression of pluripotency factors, including *NANOG* and *OCT4* (data not shown). These cells were then subjected to a secondary round of reprogramming (**Figure 1D**), by the addition of doxycyclin, to induce expression of the 5 reprogramming factors which were originally used to generate the LN-hiPS cell line, aiming to obtain cells in a more naïve pluripotent state. This was done either under hypoxic (5% O2) or normoxic (20% O2) conditions, with either human ES cell medium (condition 1), human ES cell medium supplemented with the histone deacetylase inhibitor valproic acid [1030] (condition 2), human ES cell medium supplemented with Kenpaullone which replaces KLF4 [1031] (condition 3), human ES cell medium supplemented with the GSK3ß inhibitor CHIR (condition 4), human ES cell medium with valproic acid, Kenpaullone and CHIR (condition 5) or a medium supplemented with human LIF (condition 6), to obtain so-called hLR5 cells [973]. Using these conditions, we noted morphological changes within 2 weeks, and for most conditions colony-like structures emerged. No difference in colony formation was found between different oxygen conditions. After picking of colonies, only stable clones for conditions 1 and 6 could be obtained. Two cell lines obtained from condition 1, grown after withdrawal of doxycyclin, still showed all hallmarks of a post-XCI state, with more than 99% of the cells showing an *XIST* cloud (data not shown). Six female hLR5 cell lines were obtained from condition 6, of which three were derived under hypoxic conditions. These cells represent a metastable, more mouse-like state, which requires the continues expression of 5 exogenous pluripotency factors induced by doxycyclin in the presence of human LIF [973]. Previous work has shown that in this state, hLR5 cells grow in mouse-like, dome-shaped colonies, and show expression of mouse-specific pluripotency surface markers, and can be highly efficiently genetically modified. A switch in culture conditions towards standard human ES cell medium and withdrawal of doxycyclin can transfer these cells to a standard, basic FGF dependent hiPS cell state [973]. To investigate the XCI state of the generated hLR5 cells, RNA-FISH was performed, detecting *XIST* expression. Despite their mouse-like characteristics, more than 99% of cells still showed an *XIST* cloud (N=200 per cell line, 6 cell lines analyzed, **Figure 1E**), indicating that also these cells represent a post-XCI state.

Cell lines with non-random XCI for hiPS formation

Our experiments so far with established hiPS cells and hLR5 cells indicated that upon reprogramming the somatic inactivated X chromosome does not become reactivated. To exclude the possibility that this is due to a cell line specific effect (e.g. specific to the LN-hiPS cell line), or might be caused by the method used to reprogram this cell line (with 5 inducible factors), we decided to establish novel female hiPS cell lines. To this end, we screened cell repositories for cell lines harboring large deletions on one of the X chromosomes. Due to secondary selection, X chromosomes with large deletions are

Figure 1: continued
expression of the reprogramming factors. See text for details. E) RNA-FISH detecting *XIST* (FITC) in female hLR5 cell line 2 analyzed at passage 2. DNA is counterstained with DAPI (blue).

preferentially inactivated in female carriers of such deletions, because otherwise such a female cell would become nullisomic for genes which are located in the deleted area due to inactivation of the wild type allele, which is a cell lethal condition. This non-random XCI could help identifying cells which have reactivated the Xi in hiPS cells, as expression of an informative transcript in hiPS cells differing between the two X chromosomes not expressed in the skewed fibroblast population would be diagnostic for a reactivation event.

To obtain skewed fibroblast cell lines with large X chromosomal deletions, cell lines were collected through different sources, and the gene content was further characterized by MLPA analysis, SNP array and DNA-FISH. Results for this analysis are summarized in **Supplementary Table I**, and examples of the analysis are shown in **Figure 2**. Here we focus on fibroblast lines which were used to generate hiPS cell lines, namely X12, X14, and X15 (**Figure 2A**), and a cell line derived from a patient with triple X syndrome (47,XXX). The latter cell line was used as a control, but also could be an interesting model to study XCI initiation in case of X chromosomal aneuploidies. When analysed by RNA-FISH, 99% of all fibroblast of cell lines X12, X14 and X15 showed one *XIST* cloud per nucleus (**Figure 2C** and data not shown, N=200 cells analyzed per cell line). In the 47,XXX fibroblast, two inactive X chromosomes were found in almost every cell (**Figure 2C**), in agreement with the rule that all but one X chromosome become inactivated per diploid genome [163]. To analyse whether indeed a single X chromosome was preferentially inactivated in the fibroblast populations harboring large X chromosomal deletions, we performed the HUMARA assay. In all cell lines harboring large deletions, we detected almost exclusively one allele after digestion with the methylation sensitive enzyme HpaII, indicating non-random XCI favoring inactivation of one of the two X chromosomes (**Figure 2D** and data not shown). In the 47,XXX fibroblast cell line, random XCI was observed (data not shown). Preferential inactivation of one X chromosome in fibroblast lines X12, X14 and X15 was confirmed by RFLP RT-PCR analysis of an SNP in *XIST*, which always showed mono-allelic expression (**Figure 2E**). Also expression of several tested X-linked genes showed completely skewed XCI (data not shown). We conclude that the selected fibroblast lines are subject to non-random XCI, most likely silencing of the X carrying the deletion.

Generation of hiPS cell lines

To generate hiPS cells, X12, X15 and 47,XXX fibroblasts were transduced with a polycistronic lentiviral vector expressing OCT4, SOX2, KLF4 and C-MYC and a dTomato reporter [1032]. Upon transduction, transduced fibroblasts express dTomato (**Figure 3A, B**). These fibroblasts were plated on MEFs, and cultured in the presence of human ES medium. After approximately 10 days, small clusters of cells appeared which started to develop a human ES cell morphology. These clusters gradually lost the expression of the dTomato reporter (**Figure 3B**), which indicated proper silencing of the lentiviral transgene, required to establish fully reprogrammed hiPS cells. Six dTomato negative colonies were picked per cell line 22 days post-transduction, and expanded. The established cell lines showed a characteristic human ES cell morphology (**Figure 3C**), had a stable 46,XX karyotype (47,XXX in case of lines derived from the 47,XXX fibroblasts) and expressed key endogenous pluripotency factors including *NANOG* and *REX1* (**Figure 3D, E,** and data not shown).They also stained positive for the pluripotency associated surface markers CD9

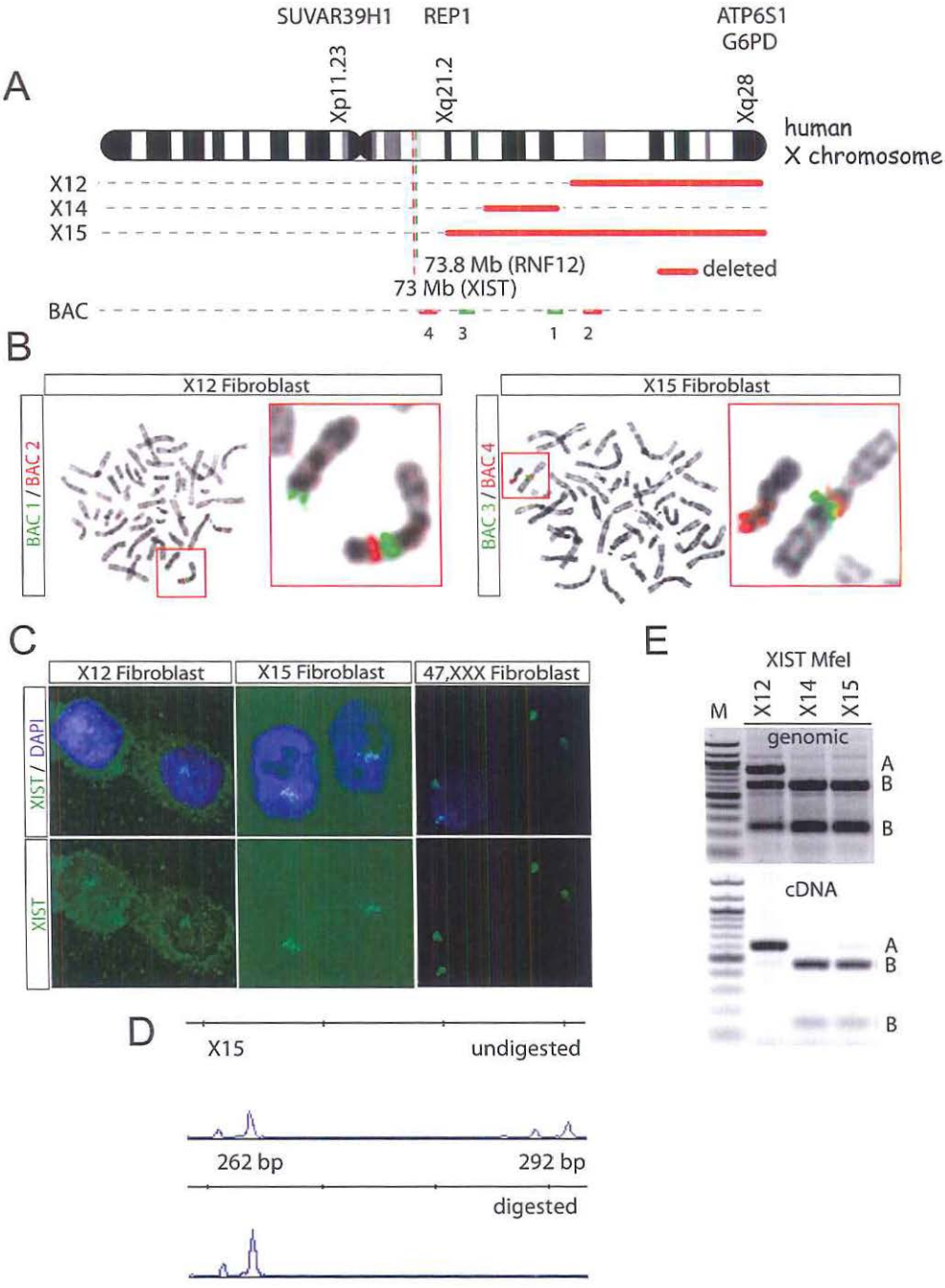

Figure 2: Fibroblast cell lines with skewed XCI

and GCTM2, as determined by FACS analysis (**Figure 3F**). Upon EB differentiation, all cell lines expressed markers of all germ layers (**Figure 3G**), confirming that these cells were completely reprogrammed and had differentiation potential (**Figure 3H**).

Early passage female hiPS cells show reactivation of the Xi

The established novel female hiPS cells from fibroblasts cell lines X12, X15 and 47,XXX were subjected to immuno-RNA-FISH analysis at passage 3-5 prior to cryopreservation, to investigate the XCI status of these cell lines. This analysis showed that only 30% of the nuclei within the various cell lines showed *XIST* expression (**Figure 4A, D, E**). Contrary to the results obtained with the LN-hiPS cell line described above, which showed more than 99% of nuclei with hallmarks of an Xi, more variation was observed in the low passage iPS cell lines, with many cells showing absence of *XIST* clouds (**Figure 4A, C, D**). In hiPS cell lines generated from 47,XXX fibroblasts, many cells did not show Xi markers, or only showed signs of one Xi (**Figure 4B, E**). In all cell lines, analysis of heterochromatin markers associated with the Xi, including enrichment of H3K27me3 and depletion of H3K4me3 and H3K9 acetylation, indicated variable staining, with many cells not displaying all characteristic Xi features (**Figure 4B**). Also, Barr bodies were detected in a minority of cells. Strikingly, in many colonies, cells with all Xi hallmarks were most often found at the edges or in the center of the colonies, were most of the differentiated cells are found. In contrast, cells without *XIST* and associated Xi markers were found in a donut shaped region surrounding the middle of the colonies (**Figure 4A, C**).

Figure 2: continued

A) Ideogram of the human X chromosome. Location of genes analyzed in this study is indicated. The red lines indicate the deletions in the X12, X14 and X15 fibroblast cell lines. Also the location of the four BAC probes, used in B, is indicated. **B)** DNA-FISH on metaphase chromosomes of X12 and X15 fibroblasts, using BAC probes 1, 2, 3 and 4. Magnification of X chromosomes is shown in the insert. Hybridization with BACs located in the deleted area results in a single signal, whereas hybridization with BACs located proximal to the deletion results in two signals. Note that deleted chromosomes are also shorter, compared to the wild type X chromosome. **C)** RNA-FISH detecting *XIST* (FITC) in X12, X15 and 47,XXX fibroblasts. DNA is counterstained with DAPI (blue). X12 and X15 showed a single *XIST* cloud in almost every cell, whereas two *XIST* clouds are observed in 47,XXX fibroblasts. **D)** HUMARA analysis with DNA from X15 fibroblasts. Prior to HpaII digestion, PCR amplification of a polymorphic repeat in the *androgen receptor* gene detects the two parental alleles (262 and 292 bp, respectively). After HpaII digestion, only the 262 bp allele is detected, indicating that this allele is preferentially inactivated in X15 fibroblasts, confirming skewed XCI in this fibroblast cell line. **E)** PCR and RT-PCR analysis with DNA and cDNA from X12, X14 and X15 fibroblast cell lines, amplifying an RFLP in *XIST*. PCR products were digested with MfeI, to discriminate between both alleles. Polymorphic alleles are present in X12, but not in X14 and X15. RT-PCR shows that *XIST* is mono-allelically expressed in X12 fibroblasts. Note: for genomic PCR primers are used that amplify a longer amplicon, compared to the RT-PCR.

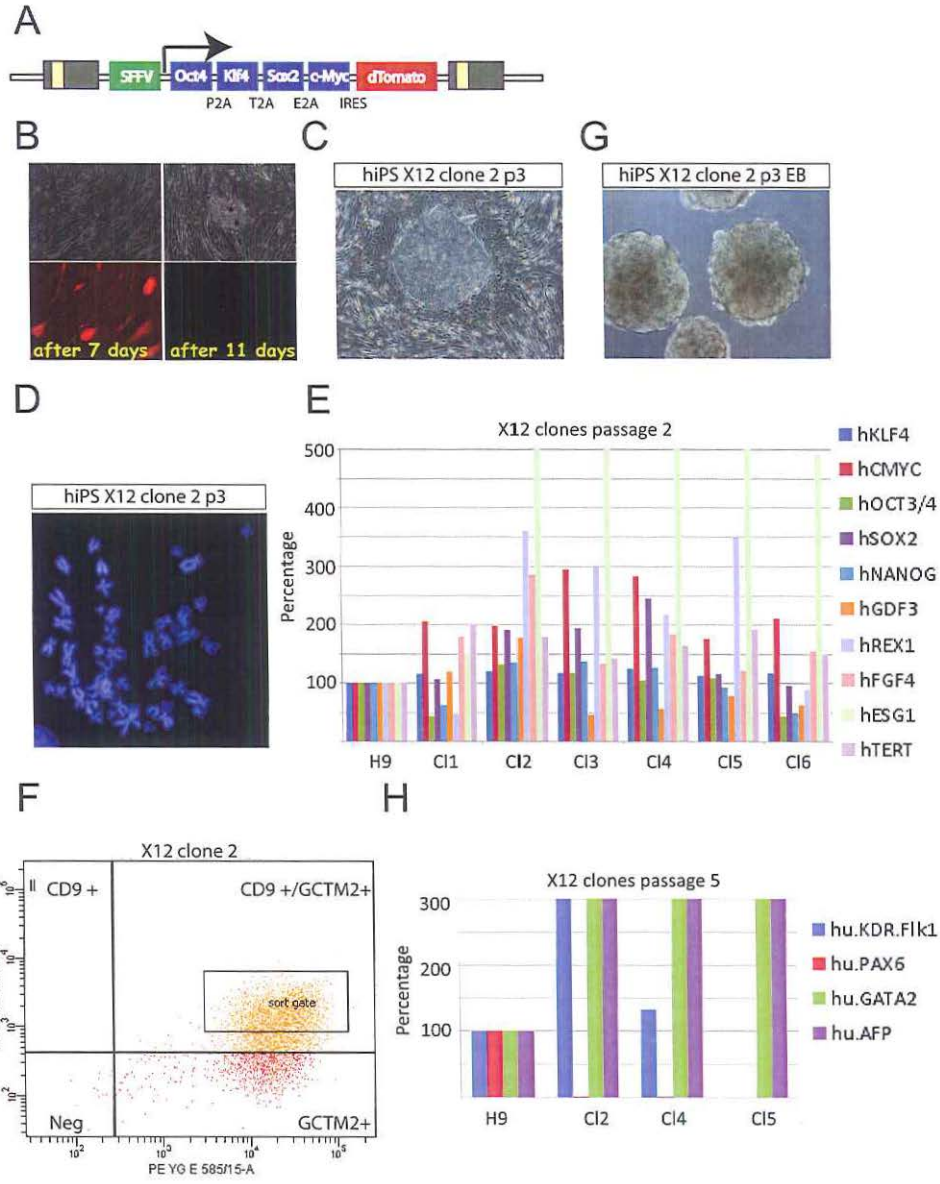

Figure 3: Generation of hiPS cell lines from skewed fibroblast populations and 47,XXX fibroblasts

A) Schematic overview of the lentiviral reprogramming cassette used. A multicistronic cassette consisting of *OCT4*, *KLF4*, *SOX2* and *C-MYC* is surrounded by self-cleavage sites, and under control of the Spleen Focus Forming Virus U3 promoter. dTomato is fused to this cassette using an IRES. Adapted from [1032]. **B)** Upon transduction of the reprogramming cassette, transduced fibroblasts express dTomato (left panel). Upon reprogramming, the lentiviral cassette becomes silenced, resulting

These results could be explained by: 1) loss of one of the X chromosomes; 2) loss of *XIST* expression and Xi markers in hiPS cell culture, similar to findings with hES lines; or 3) X reactivation, potentially only in a limited, more pluripotent sub-population. The first possibility was excluded by karyotyping, which did not detect a number of cells with X chromosome aneuploidies sufficiently high to explain lack of *XIST* in a high percentage of our hiPS cell lines (data not shown). To distinguish between the last two possibilities, we first analysed the methylation pattern of the inactive X chromosome by HUMARA analysis, focussing on lines derived from X12 and X15 fibroblasts. If the established hiPS cells still carry the same Xi present in the starting fibroblast, HUMARA analysis should detect completely skewed non-random methylation of the androgen receptor. In contrast, reactivation of the X chromosome in all cells would lead to an absence of methylation at the *androgen receptor* gene. Unfortunately, partial reactivation cannot be detected and will be masked by cells with an Xi. Nevertheless, if all or a sub-population of hiPS cells, after a transient reactivation, start another round of inactivation, for example due to spontaneous differentiation in the culture, methylation of the second allele might be detectable, as long as selection against these cells is not too strict and does not result in immediate elimination. HUMARA analysis with genomic DNA of undifferentiated X15 hiPS cell lines showed the initial 100:0 skewing ratio (**Figure 4G**), which was also observed for the original fibroblast cell line, compatible with either an absence of X chromosome reactivation, or reactivation of a portion of cells which cannot be detected by this method. However, in undifferentiated X12 hiPS cell lines, we also observed methylation, in some clones up to 12%, of the second *androgen receptor* allele located on the wild type X chromosome (**Figure 4F, G**). This finding indicates that the X12 hiPS cells have started XCI on the wild type X chromosome in a sub-population of cells. We next performed allele specific expression analysis of *XIST* with RFLP RT-PCR analysis on X12 hiPS cells, the only hiPS cell line with an informative *XIST* SNP. On a total population level we detected *XIST* expression from both X chromosomes (**Figure 4H**). This supported the findings with the HUMARA analysis, indicating that *XIST* up-regulation and X inactivation has occurred after initial X reactivation in X12 hiPS cell lines. The fact that we only detect this reversal of inactivation in clones derived from X12 and not X15 could indicate that selection against cells having inactivated the wild type X chromosome is less stringent in this cell line, which might correlate to the smaller deletion in X12 compared to X15 fibroblasts (**Figure 2A**).

Figure 3: continued
in the gradual loss of dTomato expression from emerging hiPS cells, indicating proper reprogramming. **C)** Representative picture of a hiPS cell colony from X12 hiPS cell line 2 obtained after reprogramming of the X12 fibroblast cell line. **D)** Karyogram of X12 hiPS cell line 2, showing no karyotypical abnormalities compared to the starting fibroblast cell line **E)** qRT-PCR analysis of pluripotency factors in X12 hiPS cell lines (Cl1-6). Expression of these factors in hES cell line (H9) served as a control, and was set at 100%. Results are normalized to *GAPDH*. Results for X15 and 47,XXX clones were similar (data not shown). **F)** FACS analysis of pluripotency associated surface markers CD9 and GCTM2 in X12 hiPS cell lines. Other generated cell lines showed similar results (data not shown). **G)** Representative picture of EBs derived from X12 hiPS cell line 2 after 8 days of differentiation. **H)** qRT-PCR analysis of differentiation associated markers in day 8 EBs from X12 hiPS cell lines (Cl2, 4 and 5). Differentiated hES cell line H9 served as a control, and its gene expression was set at 100%. Results are normalized for *GAPDH*. Other generated cell lines showed similar results (data not shown).

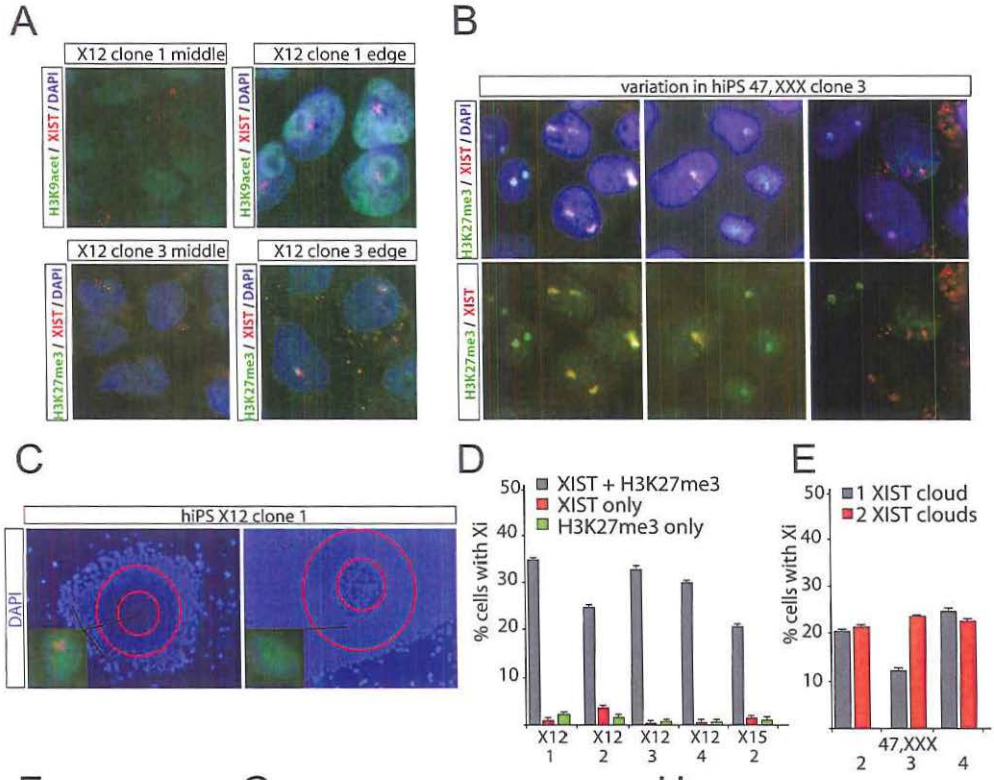

	Skewing ratio	
	% allele 1	% allele 2
X12 fibroblast	0,0	100,0
X12 clone 1 p3	2,6	97,4
X12 clone 2 p3	12,0	88,0
X12 clone 3 p3	5,3	94,7
X12 clone 4 p3	1,5	98,5
X12 clone 5 p3	2,6	97,4
X12 clone 6 p3	3,0	97,0
X15 fibroblast	100,0	0,0
X15 clone 1 p7	100,0	0,0
X15 clone 2 p7	100,0	0,0

Figure 4: XCI analysis of hiPS cells
A) Immuno-RNA-FISH analysis on X12 hiPS cell line 1 detecting *XIST* (Rhodamine Red) and H3K9 acetylation (FITC), and X12 hiPS cell line 3 detecting *XIST* (Rhodamine Red) and H3K27me3 (FITC). Shown are cells in the cell dense donut shape middle region of the colony, which most often do not show signs of an Xi, and cells from the edge of the colony, which have undergone XCI. **B)** Immuno-RNA-FISH analysis detecting *XIST* (Rhodamine Red) and H3K27me3 with 47,XXX hiPS cell line 3. Pictures indicate the variability in XCI and associated markers, with cells having inactivated only one X chromosome, cells showing only H3K27me3 staining without *XIST* signal, or only *XIST* staining without

Bi-allelic expression of X-linked loci, and reversal of XIST expression.

The presence of *XIST* negative cells within colonies at an early passage of the above hiPS cell lines supported our findings on the whole cell populations with the HUMARA assay and *XIST* expression analysis, and indicates the presence of undifferentiated hiPS cells with a reactivated Xi resulting in bi-allelic expression of X-linked loci. As these cells represent a sub-population of the complete culture, including spontaneous differentiated cells, undifferentiated XaXa hiPS cells might be underrepresented in the RT-PCR analysis of the complete culture. We therefore performed single cell RT-PCR analysis, in which we detected expression of RFLPs in the X-linked genes *XIST*, *SUVAR39H1* and *G6PD*, discriminating between the two X chromosomes. X12 hiPS cell line 2, X12 hiPS cell line 4 and 47,XXX hiPS cell line 4, which were at passage 25 and had been continuously in culture, were stained with antibodies against the pluripotency associated surface markers SSEA4 and Tra1-81, and double positive single cells were sorted in 96-well plates. The double positive fraction represented approximately 40% of the total viable cell fraction (**Figure 5A**), and qPCR analysis showed increased expression of the pluripotency markers in pooled double positive sorted cells (**Figure 5B**). Double positive cells were sorted in lysis buffer, and single cell RT-PCR was performed using a one step cDNA synthesis procedure using primers amplifying the pool of genes of interest. A nested PCR was then performed followed by restriction digestion to distinguish between expression from the different alleles. Interestingly, analysis of *XIST* in the X12 hiPS clones showed that up to 16% of all cells analysed (N=96 per cell line, 2 cell lines analysed) did not show expression of *XIST*, but did show expression of at least one other X-linked gene (**Figure 5C, D**). Interestingly, whereas in the original fibroblast population only *XIST* allele A was detected, which was detected in 41% of single hiPS cells analysed, up to 18% of analysed cells showed expression of *XIST* allele B. Since hiPS cells originate from a single transduced fibroblast, this reversal of *XIST* expression indicates that during the course of reprogramming the X chromosome must have been reactivated, after which *XIST* expression must have started from the alternative allele. Another 25% of cells even showed bi-allelic *XIST* expression.

Figure 4: continued
H3K27me3. **C)** Example of two colonies of X12 hiPS cell clone 1. Center part showing differentiation is delineated with the inner red circle. The middle part of the colony, between the two red circles, mainly contains cells which do not show signs of an Xi (see **A**). Left panel insert shows a typical cell found in the area with differentiating cells, whereas insert on the right shows a typical cell found in the middle of the colony. **D)** Quantification of immuno-RNA-FISH analysis of representative hiPS cell lines obtained from X12 (clones 1-4) and X15 (clone 2) fibroblasts. Percentage of cells with an *XIST* cloud and H3K27me3 accumulation, *XIST* cloud only, or H3K27me3 accumulation only is shown. **E)** Quantification of immuno-RNA-FISH analysis of representative hiPS cell lines (2-4) obtained from the 47,XXX fibroblast cell line. Percentage of cells with one *XIST* or two *XIST* clouds is plotted. **F)** HUMARA analysis with DNA from X12 hiPS cell line 2. Prior to HpaII digestion, PCR amplification of a polymorphic repeat in the *androgen receptor* gene detects both parental alleles (275 and 278 bp). After HpaII digestion, the larger allele is preferentially amplified, but the smaller allele is still detectable, showing that two different X chromosomes are subject to XCI in this population. **G)** Quantification of all HUMARA analyses performed with different hiPS cell lines. **H)** Allele-specific RT-PCR analysis of *XIST*. PCR products were digested using MfeI to distinguish between both parental alleles. X12 hiPS cell lines 2 and 4 show bi-allelic *XIST* expression, which was not found in the original fibroblast line (compare to **Figure 2E**).

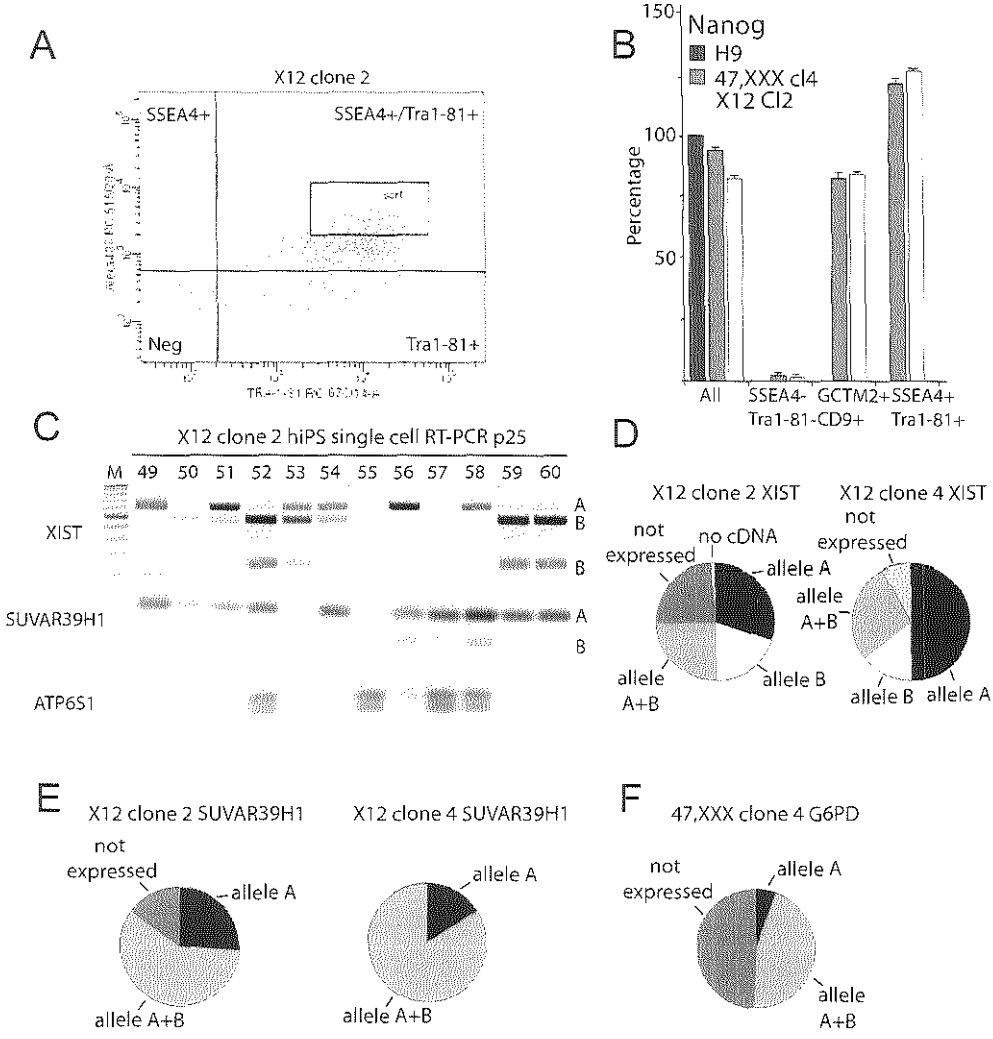

Figure 5: Single cell RT-PCR analysis on pluripotent hiPS cells
A) FACS analysis of hiPS cell stained for the pluripotency associated surface markers SSEA4 and Tra1-81. **B)** qRT-PCR analysis of the pluripotency factor NANOG in all living sorted cells, SSEA1-/Tra1-81 double negative cells, in CD9+/GCTM2+ double positive cells and in SSEA1+/Tra1-81+ double positive cells for 47,XXX clone 4 and X12 clone 2 hiPS cell lines. Results are normalized for *GAPDH*. Unsorted H9 served as positive control.
C) Single cell RT-PCR analysis of SSEA1+/Tra1-81+ sorted cells from X12 hiPS cell line 2, passage 25. Shown are the cells numbered 49-60. Allele-specific expression of *XIST* and *SUVAR39H1* was assessed. *ATP6S1* expression served as a control. PCR products for *XIST* and *SUVAR39H1* were digested with MfeI and MspI to distinguish between both parental alleles (indicated with A and B, respectively). **D)** Circle diagram showing the distribution of allele specific *XIST* expression for SSEA1+/Tra1-81+ sorted cells from X12 hiPS cell lines 2 and 4. N=96 cells per cell line. **E)** As for **D**, but now *SUVAR39H1* is assessed. **F)** As for **D**, but now *G6PD* is assessed in hiPS cell line 47,XXX clone 4.

Although we cannot exclude that part of this fraction consists of doublet cells, many of the same cells displayed mono-allelic expression of *SUVAR39H1* (17% of the bi-allelic *XIST* positive cells), which would not be possible if these samples would be a mixture of two cells with a different active X chromosome, since then also bi-allelic *SUV39H1* expression should be detected. Possibly, cells with bi-allelic *XIST* expression could represent cells with low level *XIST* transcription, as we did not observe a high percentage of cells with two *XIST* clouds by RNA-FISH analysis (**Figure 4**). These cells could also represent cells which have not yet reactivated the X chromosome, but have up-regulated *XIST* from two alleles. When allelic expression of *SUVAR39H1* was assessed, 54% and 77% of cells analysed of X12 hiPS cell line 2 and 4 respectively showed bi-allelic expression (**Figure 5E**). The remainder of the cells either did not express *SUVAR39H1* (13% and 0%), or expressed allele A (24% and 15%) which was also found in the fibroblast population, whereas expression of only allele B was not found. As *SUVAR39H1* was previously found to be subject to XCI [577], bi-allelic expression indicates that both X chromosomes are active in these cells. Similar results were obtained in the analysis of the 47,XXX clone 4 cell line, in which a considerable amount of cells showed bi-allelic expression of *G6PD* (41%) (**Figure 5F**). We conclude that reactivation of the Xi occurs during the reprogramming process and is detectable in hiPS cells. Future experiments need to establish whether differentiation of hiPS cells leads to initiation of XCI, which would make our hiPS cell lines a good *in vitro* model system to study human XCI.

Discussion

Here we have investigated the XCI state of female hiPS cells derived from fibroblast cultures with completely skewed non-random XCI. Our studies are the first to show that at the single cell level reprogramming of human cells into hiPS cells results in X chromosome reactivation. This reactivation is visible as a large percentage of nuclei which lost hallmarks of the Xi (e.g *XIST* expression and associated markers) and showed bi-allelic expression of X-linked loci. Bi-allelic expression of different X-linked loci indicates that the Xi is reactivated in at least a large fraction of our hiPS cell lines. In a significant fraction of cells we also detect *XIST* expression from the *XIST* allele which was not active in the starting fibroblast culture. Human iPS cell lines share a clonal origin, and therefore this switch in *XIST* expression indicates retrospectively that during the reprogramming process, reactivation most likely has occurred, followed by initiation of XCI on a different allele compared to the progenitor cell.

A recent study has shown that upon prolonged passaging of female hiPS cells *XIST* expression can be lost, which is accompanied by de-repression of dosage compensation, which the authors call "erosion of XCI" [1033]. This epigenetic erosion is irreversible, and is accompanied by a loss of differentiation characteristics, which might be important for disease modelling procedures, as results obtained with early and late passage hiPS cells might differ. It has also been shown that this erosion also results in a higher expression of cancer-related X chromosomal genes, which indicates that assessing the XCI state of hiPS cells should be a benchmark for future clinical applications [1034]. Similar results have been obtained with a large panel of hES and hiPS cells, which showed accumulation of

aberrant methylation of X-linked genes leading to gene activation [1035]. Derepression of genes located on the Xi has also been observed in hES cell lines upon loss of *XIST* expression [1016], and has been reported in studies involving gene expression profile comparison of multiple female hES and hiPS cell lines [1026]. The latter authors conclude that there are three different classes of hiPS cells, the first class which does not reactivate the X chromosome upon reprogramming, a second class which is completely reactivated, and a third class which shows partial reactivation of X-linked loci. The last group consists mainly of genes in the proximity of the X inactivation center, which may be most dependent on *XIST*. Global gene expression profiling assesses the complete heterogeneous population of cells, and partial reactivation processes could likely be explained by a minority of cells in the culture which are completely reactivated. Future studies should therefore focus on gene expression profiling on single, pluripotent hiPS cells, and our analysis of single cell RT-PCR of female hiPS cells sorted on the presence of pluripotency associated surface markers represents an important step in this direction.

At present, we cannot formally exclude that the bi-allelic gene expression of *SUV39H1* and *G6PD* which we report, is based on a progressive erosion of XCI, as we performed our single cell analysis at a relatively late passage (p25). To this end, we are currently repeating our analysis with novel lines derived from the same fibroblasts, at earlier stages of reprogramming, even in reprogramming cultures prior to the selection of colonies. Results of this ongoing analysis should provide us with a definitive answer whether bi-allelic gene expression is also found at earlier passages, or is only observed after erosion of epigenetic features of the Xi happening upon prolonged culturing. Despite these pitfalls, several lines of evidence argue that the bi-allelic gene expression we observe is a result of the reactivation process. First, in our immuno-FISH analysis performed at early passage (p3-5) we already noticed a high percentage of cells which lacked all hallmarks of an Xi. Although loss of *XIST* has also been observed at early passage in hES cells in one study [1015], such an observation has not previously been made in hiPS cells [1019, 1023]. XaXa cells were confined to areas of undifferentiated cells, which might indicate that the presence of Xi markers is more associated with (perhaps subtle) differentiation processes, and might indicate that at present culture conditions for hES and hiPS cells are not suitable to capture the most undifferentiated cells in the culture for a prolonged time period. Secondly, the switch in *XIST* expression between the different alleles in X12 hiPS cells which we observe unequivocally indicates that at a certain moment in time, both X chromosomes must have been reactivated, followed by initiation of XCI on a different allele compared to the starting fibroblast. The results obtained with HUMARA analysis at passage 3-5 support such an initiation of XCI after reactivation, since methylation was also detected in a fraction of cells on the alternative allele compared to the initial fibroblast population. *XIST* expression on the wild type X chromosome in combination with X-linked gene silencing would most likely be selected against to prevent the complete absence of gene expression from genes located in the deletion on one X chromosome. It will be interesting to test whether differentiation of the hiPS cells results in elimination of cells which have inactivated the wild type X chromosome, as under such conditions it can be expected that the selective pressure is more stringent. Although we were unable to investigate origin of *XIST* expression in X15 hiPS cells, due to a lack of polymorphisms, our methylation studies indicate that in X15 hiPS a reversal of XCI does not occur. This

might be explained by the larger deletion in X15 encompassing more genes compared to X12, resulting in a more stringent selection against cells having inactivated the wild type X chromosome.

Why was reactivation of the X chromosome upon reprogramming not noticed in some previous investigations [1019]? One explanation could be related to the skewing which is observed in human fibroblast cell lines [1023]. Activity of a particular X chromosome is favoured in some cell lines, maybe due to the presence of subtle mutations on X-linked genes, and therefore initial reactivation followed by XCI initiation on a particular X chromosome is not observed due to selection processes. This could explain why several previous investigations noted skewed XCI favoring a same X chromosome in hiPS cells and the founder fibroblast cell line, which was then interpreted as being evidence for the clonality of a female hiPS cell line [1021, 1023]. Alternatively it could be that differences in reprogramming techniques underlie the differences observed. Therefore, future studies should directly compare different reprogramming vectors and culture conditions regarding XCI.

Clear differences in XCI exist between mouse ES cells, with two active X chromosomes and hES cells, which most often retain an Xi. Based on differences in morphology, growth factor requirements and gene expression profiling, it has been argued that hES cells are more similar to primed EpiSCs, derived from a post-implantation epiblast of a mouse embryo, characterized by the presence of one inactive X chromosome. Therefore, it has been hypothesised that a more naïve, mouse-like state should also exist in humans, and this state might be characterized by the presence of two active X chromosomes. Indeed, two studies have recently reported that more mouse-like human cells can be obtained by iPS reprogramming, in the presence of human LIF, and either expression of five inducible reprogramming factors (hLR5 cells) [973], or exogenous expression of OCT4, KLF4 (or KLF2) in combination with GSK3ß inhibition and inhibition of the mitogen-activated protein kinase pathway [1017]. The latter study reported reactivation of both X chromosomes comparable to mouse ES cells. In our own experiments, culture of hiPS cells under these conditions did result in morphological changes, and growth characteristics that resembled mouse ES cells, but until now we were unable to reproduce results regarding X reactivation in hiPS cell lines (data not shown). Also in the hLR5 cells, for which XCI was not assessed before, we did not find evidence of X reactivation. These data argue that even a more mouse-like, naïve state might not be sufficient to obtain or maintain hES or hiPS cells in a state in which all X chromosomes are active. The same variation we observed in the hiPS cell lines, in which we found cells which have not reactivated the X chromosome, cells which have reactivated and show bi-allelic expression of X-linked genes, and even cells which have started XCI after reactivation might indicate that present culture conditions for hES and hiPS cells are not sufficient to bring or maintain cells in a state with two active X chromosomes. Indeed, a recent study argued that derivation of hiPS cells on SNL-feeder cells which produce LIF might result in a higher percentage of cells with X chromosome reactivation [1036]. In line with this, it has recently been shown that a switch in culture conditions towards human ES medium like conditions during the derivation of mouse ES cells can result in derivation of EpiSCs from pre-implantation embryos [1037], emphasizing that differences in culture conditions can remarkably change the cell characteristics. Also it has been found that

during the derivation of hES cell lines from the ICM of a blastocyst in culture, a transient, epiblast-like structure emerges called a post-ICM intermediate (PICMI), which is essential for the subsequent derivation of hES cells [1038]. This PICMI has undergone XCI, as assessed by H3K27me3 staining, and is followed by reactivation of the Xi in hES cells, when grown under hypoxic conditions. Reactivation might not occur, or is less efficient in hES and hiPS cells grown under standard conditions. Although the present data in principle show that reactivation can occur upon reprogramming, and appears to be remarkably efficient, future studies should address whether the activity of both X chromosomes in undifferentiated hiPS cells is stable under the described culture conditions. In addition, we will analyze if XCI is properly induced upon differentiation of our hiPS cell lines, which would make these lines a powerful model system to study human XCI.

Acknowledgements

We would like to thank Dr. Elisabeth M. de Jong for providing 47,XXX fibroblasts, and Dr. Konrad Hochedlinger for the Lesch-Nyhan iPS cell line. Dr. Suzanne Frynts and Dr. Walter Just are acknowledged for providing several fibroblast cell lines. We thank Dr. Dorota Kurek and Dr. Derk ten Berge for providing anti-GCTM2 antibody.

Supplemental data

Supplemental data contains one figure and two tables.

Materials and Methods

Cell lines

Fibroblast cell lines were obtained from the Corriel Cell repository, under the following accession numbers: GM07148 (X12), GM03923 (X14) and GM03827 (X15). 47,XXX fibroblasts were a gift from Dr. Elisabeth M. de Jong, Department of Clinical Genetics, Erasmus MC. All fibroblast were cultured in standard fibroblast medium. The Lesch-Nyhan hiPS cell line has been described [1029], and was a gift from Dr. Konrad Hochedlinger, Harvard Stem Cell Institute, Boston. All hES and hiPS cells were maintained in standard human ES cell culture medium, consisting of DMEM/F12 containing 20% knockout serum replacement, 2 mM L-glutamine, 1% NEAA, 100 U of penicillin, 100 mg of streptomycin (all Invitrogen), 0.1 mM b-mercaptoethanol (Sigma), and 5 ng/ml bFGF (Peprotech). For secondary reprogramming experiments, LN-hiPS cells were differentiated in suspension culture for 1 week in EB differentiation medium, consisting of IMDM-glutamax, 15% foetal calf serum, 100 U ml^{-1} penicillin, 100 mg ml^{-1} streptomycin, 1% non-essential amino acids (all Invitrogen), 37.8 ml l^{-1} monothioglycerol (Sigma) and 50 mg/ml ascorbic acid (Sigma), followed by culture in fibroblast medium for 4 weeks. Induction of reprogramming factors was achieved by addition of doxycylin (2 µg/ml, Sigma). Valproic acid (Calbiochem), Kenpaullone (Sigma) and CHIR99021 (Stemgent) were used at 0.5 mM, 5 µM, 3 µM, respectively. hLR5 medium consisted of DMEM/F12 containing 20% KOSR,100 U of penicillin, 100 mg of streptomycin, 2 mM L-glutamine, 1% NEAA (all Invitrogen), 0.1 mM b-mercaptoethanol (Sigma), 10 ng/ml human LIF (Sigma), and 2 µg/ml doxycycline (Sigma).

hiPS cell generation and culture

To generate iPSC, $1x10^5$ human fibroblasts from lines X12 (p12), X15 (p4) and 47,XXX (p14) were seeded in a well of a 6-well plate. The next day, cells were transduced with a polycistronic lentiviral reprogramming vector [1032] for 16 hours in the presence of 4µg/ml polybrene (Millipore). Cells were further cultured in standard fibroblast medium. At day 4 posttransduction, $5x10^4$ cells were seeded on irradiated MEFs in standard fibroblast medium. One day later, medium was changed to human ES medium including 5 ng/ml bFGF. From day 2 to 9 media were supplemented with 2 mmol/l valproic acid (Calbiochem) as described by Warlich et al. (2011) [1032]. iPS colonies were picked between day 22 to 25 and further propagated on MEFs. All analysis for characterization of iPSC was performed prior to cryopreservation.

Immuno-FISH and qPCR analysis

Detailed protocols and probes for RNA-FISH and immuno-RNA-FISH have been described [174, 911]. For immunostainings, the following antibodies were used: anti-Nanog (1:100, Abcam), anti-KLF4 (1:250, Abcam), anti-H3K27me3 (1:500, Diagenode), anti-H3K4me3 (1:1000, Upstate), anti-H3K9 acetylation (1:1000, Sigma), anti-CD9 (Invitrogen), anti-GCTM2 (BD), anti-SSEA4 (BD) and anti-Tra1-80 (BD).

RT-PCR and single cell RT-PCR

All primers used in this study are described in **Supplementary Table 2**. For RNA analysis of complete cultures, cells were lysed in Trizol (Invitrogen), RNA was prepared according to manufacturer's instructions, and cDNA was obtained through reverse transcription using SuperScriptII (Invitrogen). For single cell RT-PCR, SSEA1/Tra1-81 double positive cells were FACS sorted in 96-well plates containing 9 µl lysis buffer using a BD FACSAria apparatus. Lysis buffer consisted of 8 µl 2xReaction mix (SuperScript One-Step RT-PCR kit, Invitrogen), 10U RNAseOut (Invitrogen), and 0.15% IGEPAL CA-630 (Sigma). cDNA was prepared with gene specific outer primers (a combination for four different genes per cell line), using the one-step RT-PCR kit (Invitrogen), according to manufacturer's instructions in a total volume of 16 µl. After an initial amplification using the outer primers, nested PCR was performed using the internal primers, and Phusion PCR polymerase (Fynnzyme). PCR products were precipitated, and digested with the indicated restriction enzymes (New England Biolabs) to distinguish expression from the different alleles.

SNP array and HUMARA analysis

To map the deletions in our fibroblast cell lines, SNP array was performed using Human CYTO SNP 12 version 1 arrays (Illumina®, San Diego, CA, USA), aligned to human genome build 18. To determine skewing of XCI, allele specific methylation of the Androgen receptor was quantified using the HUMARA assay (Human Methylation of the Androgen Receptor Assay) [480]; 40ng of genomic DNA was double digested with DdeI and HpaII (New England Biolabs) at 37°C in an overnight reaction. 1µl of reaction product was used as a template for PCR using Phusion polymerase (Fynnzyme) using FAM-labelled primers GCTGTGAAGGTTGCTGTTCCTCAT and TCCAGAATCTGTTCCAGAGCGTGC. PCR products were visualized on a sequencer.

DNA-FISH analysis

To visualize the deletion in cell lines, DNA-FISH was performed according to standard procedures. Probes used were BAC CTD-3076O23 (BAC1, X12 FITC), RP11-799O20 (BAC2, X12 Rhodamine Red) RP1-75N13 (BAC3, X15 FITC) and RP1-279N11 (BAC4, X15 Rhodamine Red).

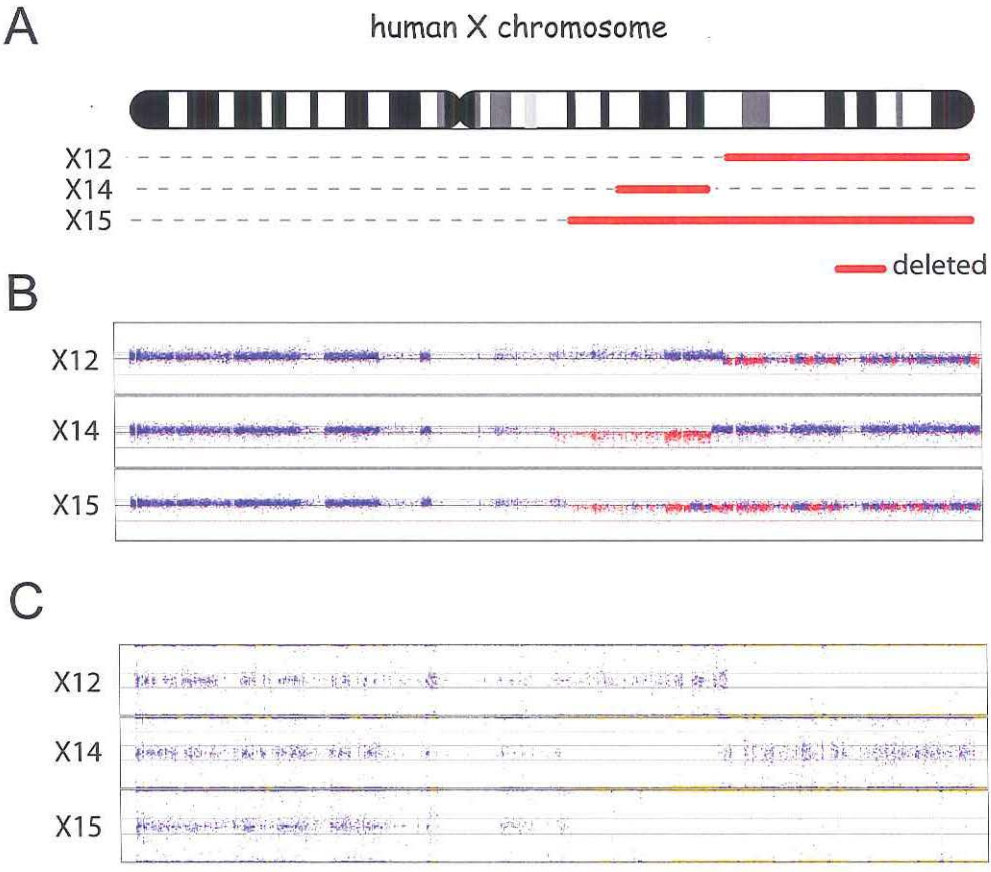

Supplementary Figure 1: SNP Array of fibroblasts used to generate hiPS cells
A) Ideogram of the human X chromosome. The deleted areas in the indicated cell lines are shown in red. **B)** SNP Array data showing the deleted areas in fibroblast cell line X12, X14 and X15. Every dot is representing a probe along the X chromosome. Deleted areas are indicated in red. **C)** SNP Array data showing loss of heterozygosity (areas marked in yellow) in the deleted regions.

Supplementary Table 1: Overview of collected cell lines harboring X chromosomal deletions

X	Original number	Source	Karyotype described by source	Cell line
1	A23952	Univ of Ulm	46, X,i(Xq)	fibroblast
2	G656	Univ of Ulm	46, X, del(Xq)	fibroblast
3	Gw176	Univ of Ulm	46, X,i(Xq)	fibroblast
4	Gw177	Univ of Ulm	46, X,i(Xq)	fibroblast
5	Gw178	Univ of Ulm	46, X,i(Xq)	fibroblast
6	Gw179	Univ of Ulm	46, X;(Xq), most likely X,i(Xq)	fibroblast
7	LB-Xq-	Univ of Ulm	46, X, del(Xq)	lymphoblastoid
8	I9	Univ of Ulm	46, X, Xq-, delX(q22/24>qter)	fibroblast
9	GM10254	Coriel	46, X, del(X)(pter>q13::q21>qter)	lymphoblastoid
10	GM09332	Coriel	46, X, del(X)(pter>q22::q26>qter)	lymphoblastoid
11	GM13277	Coriel	46, X, del(X)(pter>q13:)	lymphoblastoid
12	GM07148	Coriel	46, X,del(X)(pter>q22.3:)	fibroblast
13	GM06563	Coriel	45,X [36]/46 X r(X)(::p22.3>q24::)[14]	fibroblast
14	GM03923	Coriel	46, X,del(X)(pter>q13::q22>qter)	fibroblast
15	GM03827	Coriel	46, X,del(X)(pter>q21:)	fibroblast
16	AG03204	Coriel	normal, IMR-90 SV40 transformed	fetal lung fibroblast
17	DD2361	ECACC	ring X	only DNA
18	DD2694	ECACC	ring X	only DNA
19	AR0143	ECACC	ring X	only DNA
20	DD2799	ECACC	ring X	only DNA
21	DD2693	ECACC	ring X	only DNA
22	AR0134	ECACC	ring X	only DNA
23	D04-1938	Univ Maastricht	46,X,t(X;13)(p21;q22)	only DNA
24	D04-2042	Univ Maastricht	46,X,inv(X)(p22.3q21.1)	only DNA
25	D04-2330	Univ Maastricht	46,X,inv(x)(p22.1q21.2)	only DNA
26	D09-1228	Univ Maastricht	46,X,t(X;9)(p23;q13)	only DNA
27	D06-0899	Univ Maastricht	45,X0 [35], 46,X,r(X) [65]	only DNA
28	D05-2530	Univ Maastricht	46,X,t(X;14)(q13;q32.1)	only DNA
29	D05-2536	Univ Maastricht	46,XX	only DNA
30	D06-1835	Univ Maastricht	46,XX	only DNA
31	D06-1255	Univ Maastricht	not determined	only DNA
32	D06-1132	Univ Maastricht	not determined	only DNA
33	D91-0080	Univ Maastricht	46,XX,Xp22 duplication (array CGH)	only DNA
34	D91-0081	Univ Maastricht	46,XX,Xp22 duplication (MLPA)	only DNA
35	01PA2559	Erasmus MC	45,X/46,X,ring(X)	only DNA
36	05PA0545	Erasmus MC	45,X [8](STC)/46,X,del(X)(q24?)[6]/45,X [16] (LTC)	only DNA
37	L02.1242	Erasmus MC	46,X, del(X)(q23)	only DNA
38	L79.0766	Erasmus MC	46,X,t(X;X)(p22;22)	fibroblast
39	L88.0849	Erasmus MC	45,X/46,X,del(X)(q21) (27/23) (9/41) 2 times	fibroblast
40	L96.2149	Erasmus MC	46,X,dup(X)(q13q26)	only DNA
41	L97.1578	Erasmus MC	mos45,X[38]/46,X,r(X)[5]/46,XX[7]	only DNA
42	L01.0178	Erasmus MC	46,X,der(X).ish der(X)(wcpX+,75+),rev ish	only DNA

Supplementary Table 2: Primers used in this study

Primer	Forward	Purpose	Digest	ref
365 RNF12 LP F	CAACATAGTAACAAACACACC	LP RT-PCR	-	-
366 RNF12 LP R	CTTAATCTTCAACTGGTCTTT	LP RT-PCR	-	-
453 RNF12 LP nest fw	TTTTCCAATGCACTGTTGTATG	LP RT-PCR	-	-
454 RNF12 LP nest rv	CCCAACATGACTTTCAACAAA	LP RT-PCR	-	-
367 SUVAR39-F	GCATAGGGTTGAGGGGTGTA	RFLP RT-PCR	MspI	577
368 SUVAR39-R	TTTGTGCTCACCCTGGTTC	RFLP RT-PCR	MspI	577
369 SUVAR39 2192	AGGCACTGGGTAGAGCACCT	RFLP RT-PCR	MspI	-
370 SUVAR39 2710	TTTTATTGATGCCCACTCCA	RFLP RT-PCR	MspI	-
377 ATP6S1 F	GTGATGTTGTGCTAACAAGAAG	RFLP RT-PCR	MboII	-
378 ATP6S1 R	CATGGCGACCCGCGTTTA	RFLP RT-PCR	MboII	-
457 Atp6S1 nest for	ATCCCTGGCTGTGGATAGTG	RFLP RT-PCR	MboII	-
458 Atp6S1 nest rev	CGACCCGCGTTTATTTTATT	RFLP RT-PCR	MboII	-
383 G6PD-E10	GCTGGACCTGACCTACGGCAACA	RFLP RT-PCR	PvuI	-
384 G6PVPDPVU1	GAAGACGTCCAGGATGAGGCGATC	RFLP RT-PCR	PvuI	-
455 G6PD nest for	GAGGCCGTGTACACCAAGAT	RFLP RT-PCR		-
456 G6PD nest rev	GAATGTGCAGCTGAGGTCAA	RFLP RT-PCR		-
351 G6PD-1311R	GTGAAGCTCCCTGACGCGTA	RFLP RT-PCR	RsaI	577
352 G6PD-E	TTCTCCAGCTCAATCTGGTG	RFLP RT-PCR	RsaI	577
347 REP1–15	CCTGTCACTTCAGCACCATT	RFLP RT-PCR	HhaI	577
348 REP1–16	TTGCTCTTAGCAGGAAGGAC	RFLP RT-PCR	HhaI	577
349 REP1–14	GTTATGCCAGTCAGGATTTGC	RFLP RT-PCR	HhaI	577
350 REP1–11	TCGCTGCTTGGAGTTTGTTC	RFLP RT-PCR	HhaI	577
hXIST SNP1 for	AATGGGCAAAGTGGTTATGC	RFLP RT-PCR	MfeI	1019
hXIST SNP1 rev	AGGCCCCTTTCTCAAACTGT	RFLP RT-PCR	MfeI	1019
389 XIST SNP1 nested int F 6033	TTTCTTGGCCTCCCAATATG	RFLP RT-PCR	MfeI	-
390 XIST SNP1 nested int R 6610	CAGGAACCGGGACAAACA	RFLP RT-PCR	MfeI	-
h NANOG-S	CAGCCCCGATTCTTCCACCAGTCCC	qRT-PCR	-	65
h NANOG-AS	CGGAAGATTCCCAGTCGGGTTCACC	qRT-PCR	-	65
hGDF3-S243	CTTATGCTACGTAAAGGAGCTGGG	qRT-PCR	-	65
hGDF3-AS850	GTGCCAACCCAGGTCCCGGAAGTT	qRT-PCR	-	65
hREX1-RT-S	CAGATCCTAAACAGCTCGCAGAAT	qRT-PCR	-	65
hREX1-RT-AS	GCGTACGCAAATTAAAGTCCAGA	qRT-PCR	-	65
hFGF4-RT-S	CTACAACGCCTACGAGTCCTACA	qRT-PCR	-	65
hFGF4-RT-AS	GTTGCACCAGAAAAGTCAGAGTTG	qRT-PCR	-	65
h ESG1-S40	ATATCCCGCCGTGGGTGAAAGTTC	qRT-PCR	-	65
h ESG1-AS259	ACTCAGCCATGGACTGGAGCATCC	qRT-PCR	-	65
hTERT-S3234	CCTGCTCAAGCTGACTCGACACCGTG	qRT-PCR	-	65
hTERT-AS3713	GGAAAAGCTGGCCCTGGGGTGGAGC	qRT-PCR	-	65
hOCT3/4-S1165	GACAGGGGGAGGGGAGGAGCTAGG	qRT-PCR	-	65
hOCT3/4-AS1283	CTTCCCTCCAACCAGTTGCCCCAAAC	qRT-PCR	-	65
hSOX2-S1430	GGGAAATGGGAGGGGTGCAAAAGAGG	qRT-PCR	-	65
hSOX2-AS1555	TTGCGTGAGTGTGGATGGGATTGGTG	qRT-PCR	-	65
hu_KDR–Flk-1-F	CTGGCATGGTCTTCTGTGAAGCA	qRT-PCR	-	65
hu_KDR–Flk-1-R	AATACCAGTGGATGTGATGGCGG	qRT-PCR	-	65
hu_PAX6-F	TTTGCCCGAGAAAGACTAGC	qRT-PCR	-	65

hu_PAX6-R	CATTTGGCCCTTCGATTAGA	qRT-PCR	-	65
hu_GATA2-F	TGACTTCTCCTGCATGCACT	qRT-PCR	-	65
hu_GATA2-R	AGCCGGCACCTGTTGTGCAA	qRT-PCR	-	65
hu_AFP- F	GAAACCCACTGGAGATGAACA	qRT-PCR	-	65
hu_AFP- R	CTGCAGCAGTCTGAATGTCC	qRT-PCR	-	65
hu_Alb1-F	GCTACGGCACAGTGCTTG	qRT-PCR	-	65
hu_Alb1-R	CAGGATTGCAGACAGATAGTC	qRT-PCR	-	65
human endo_KLF4-F	TGATTGTAGTGCTTTCTGGCTGGGCTCC	qRT-PCR	-	65
human endo_KLF4-R	ACGATCGTGGCCCCGGAAAAGGACC	qRT-PCR	-	65
human endo_c-MYC-F	GCGTCCTGGGAAGGGAGTTCCGGAGC	qRT-PCR	-	65
human endo_c-MYC R	TTGAGGGGCATCGTCGCGGGAGGCTG	qRT-PCR	-	65
endo hGAPDH for	CTGCACCACCAACTGCTTAG	qRT-PCR	-	1019
endo hGAPDH rev	GTCTTCTGGGTGGCAGTGAT	qRT-PCR	-	1019

Chapter 10

General Discussion

Parts of this chapter have been published in

Tahsin Stefan Barakat and Joost Gribnau (2012)
"X chromosome inactivation in the cycle of life"
Development 139:2085-2089

In this thesis, we have focused on the initiation mechanism of XCI, and found that X-encoded RNF12 exerts an essential function during this process. As an X-linked activator of XCI, RNF12 is required for XCI to occur, and mediates its *trans* acting function by ubiquitination of REX1. This results in inhibition of the repression of the *Xist* gene, which will become activated upon *Rnf12* up-regulation. Other genes and elements located in proximity to *Xist*, including *Jpx*, *Ftx*, and the *Xpr* region are important for *cis* regulation of the *Xist* locus. A transient X chromosome pairing process is observed during the initiation phase of XCI, but is not functionally required for XCI to occur. Rather, the XCI initiation process is regulated by *cis* and *trans* acting factors, which determine the activity of the *Xist* gene. *Rnf12* is also required for XCI *in vivo*, as we have learned from the generation and analysis of a mouse model mutant for *Rnf12*, which shows signs of a failure of X dosage compensation.

The following discussion elaborates on the roles of RNF12 in XCI and other processes, and aims to integrate our obtained knowledge from this thesis work with other recently published work, resulting in a description of a novel view on the X inactivation center. Then, the role of RNF12 in imprinted XCI is discussed. We also speculate on a potential role for RNF12 in the reactivation of the X chromosome occurring *in vivo* during reactivation of imprinted XCI in the inner cell mass, in primordial germ cells and *ex vivo* during somatic reprogramming with defined factors. Furthermore, the observations made in the adult heterozygous *Rnf12* knockout mouse and in human induced pluripotent stem cells, and the potential clinical relevance these observations may have, brings us to the question whether we can live with two active X chromosomes.

Rnf12, an important player in X chromosome inactivation

In our BAC transgenesis screen described in Chapter 2 we identified X-encoded RNF12 as the first known XCI-activator [174]. Over-expression of *Rnf12* resulted in XCI initiation on the single X chromosome in male ES cells, and on two X chromosomes in a significant portion of female ES cells. Endogenous *Rnf12* becomes up-regulated upon differentiation of ES cells, and a two-fold higher dosage has been found in female compared to male ES cells. This two-fold higher dosage of RNF12 explains female specific initiation of XCI, as only in female cells a threshold will be reached upon differentiation which is needed to overcome repression of XCI by XCI-inhibitors, resulting in *Xist* accumulation. These XCI-inhibitors are mainly pluripotency associated factors, which either repress *Xist* directly, or indirectly, via stimulation of *Tsix* expression or repression of XCI-activators. In line with this, over-expression of RNF12 even leads to initiation of XCI in undifferentiated cells, indicating that absence of XCI-activator activity is important in preventing XCI in undifferentiated cells. The importance of *Rnf12* in activating XCI is emphasized by the fact that a removal of one of the two copies of *Rnf12* in female cells results in delayed XCI initiation, favoring inactivation of the X chromosome harboring the *Rnf12* deletion. Even more importantly, in the complete absence of RNF12 in female *Rnf12*-/- ES cells, XCI is no longer initiated, as described in Chapter 5 where it is shown that RNF12 is essential for XCI to occur [911]. Genetic experiments performed as described in that Chapter indicated that the XCI-activating function of RNF12 works mainly on *Xist*, as *Xist* transgenes were higher expressed when *Rnf12* was over-expressed, whereas the expression of *Tsix*

transgenes was not affected. As RNF12 is an E3 ubiquitin ligase, it was likely that such activation of *Xist* should involve an indirect mechanism, in which RNF12 would target a repressor of *Xist* for proteasomal degradation. Indeed, studies to determine the interaction partners of RNF12 described in Chapter 6 indicated that RNF12 targets REX1 for degradation [1009]. REX1, a pluripotency associated transcription factor involved in repression of differentiation associated genes, was found to bind the *Xist* promoter and distal region, and the *Tsix* regulatory region *Dxpas34*. This indicated that REX1 serves a dual role in repression of XCI in undifferentiated cells, by direct repression of *Xist*, and possibly by enhancing expression of *Tsix*, which is a negative regulator of *Xist*. Therefore, upon differentiation, *Rnf12* will become up-regulated, and this will result in a dose-dependent catalysis and breakdown of REX1, which will result in loss of repression of *Xist*, and might result in a loss of stimulation of *Tsix*, and hence will lead to initiation of XCI. The initiation itself is a stochastic process, as described in Chapter 4, in which *Xist* will become up-regulated on one of the X chromosomes [910]. Accumulation of *Xist* will result in spreading along the X chromosome and associated silencing of X-linked genes. As *Rnf12* is one of the first genes to be silenced, a drop in the RNF12 level will occur, which will prevent XCI initiation on the second X chromosome. RNF12 itself is also continuously required during XCI initiation for proper establishment of the Xi, as we have shown in Chapter 7. This explains why *Rnf12* activity from the active X chromosome is further required, until the XCI process is finished, and explains the observed skewing of XCI in *Rnf12*+/- cells. *Rnf12* is also essential for XCI initiation *in vivo*, as analysis of our *Rnf12* mutant mouse model described in Chapter 8 shows. In summary, initiation of XCI is regulated by a dose-dependent (depending on the number of X chromosomes per diploid genome and therefore female-specific) up-regulation of *Rnf12*, leading to *Xist* accumulation through dose-dependent breakdown of the *Xist* repressor and *Tsix* stimulator REX1.

What are the other processes in which RNF12 is involved? RNF12 has first been identified as an ubiquitously expressed and highly conserved E3 ubiquitin ligase involved in the negative regulation of LIM-homeodomain containing transcription factors by targeting the LIM-interacting proteins LDB1 and LDB2 (together referred to as CLIM) for degradation [893, 984, 1039-1040]. In the developing mouse brain, RNF12 and CLIM are ubiquitously expressed at the mRNA level, whereas protein levels are more specifically found in various cell types, indicating that *Rnf12* is subject to post-transcriptional regulation [1041]. In addition to its repressive function on LIM-homeodomain transcription factors, RNF12 can enhance the transcriptional activation of endogenous estrogen receptor α target genes [895]. By targeting TRF1, a negative regulator of telomere length, for proteasomal degradation, RNF12 can positively modulate telomere length homeostasis [894]. Since RNF12 protein is recognized by autologous antibodies in patients with renal cell carcinoma [1042], and is one of the genes differentially expressed between adenomas and normal intestinal mucosa in a cross-species comparison between human and mouse intestinal tumors [1043], altered expression of *Rnf12* might contribute to carcinogenesis. Together with the laboratory of Prof.dr. Peter ten Dijke we recently identified RNF12 as an important regulator of the TGF-ß signalling pathway [1044]. RNF12 enhances TGF-ß signalling pathways by targeting SMAD7, a potent antagonist of the pathway, for proteasomal degradation. Therefore, RNF12 seems to be involved in many key processes in vertebrates. Surprisingly, the absence of RNF12 protein is compatible with adult life in male mice, as

shown in Chapter 8, indicating that in many of these processes redundant pathways must exist which can substitute the function of RNF12. An important candidate for this *in vivo* can be RNF6, which has a high sequence homology to RNF12 [1045-1047]. Apparently, only in the XCI process the crucial function of RNF12 cannot be replaced, as RNF12 is essential for this important epigenetic process both *in vitro*, as shown in Chapters 2, 5, 6 and 7, as *in vivo*, as described in Chapter 8.

A novel picture of the X inactivation center is emerging

The Xic, or the minimal region of the X chromosome required for XCI to occur, has been traditionally defined on the basis of patients and mutant mice having various translocations and deletions on the X chromosome [71-73] (reviewed in Chapter 1), mapping the region of interest to a 10 Mb interval in mice, and a 700 kb region in humans. This analysis has shown that at least two Xic's are needed in a diploid cell to start X chromosome inactivation, as males having a single Xic do not undergo XCI. Initially, the Xic was proposed to be able to bind a blocking factor, which would prevent XCI [72]. As a diploid genome could only produce enough blocking factor to rescue a single Xic from inactivation, XCI would occur on every supernumerary Xic, thereby explaining XCI initiation in females (46,XX), Klinefelter patients (47,XXY) or triple X females (47,XXX) or their respective mouse counterparts. The initial discovery of *Xist* [74, 84-85], a gene being expressed from the inactive X chromosome and also located on the Xic candidate region both in mouse and human, raised the possibility that *Xist* might be the Xic itself [167]. However, deletion of *Xist* still results in XCI occurring on the wild type X chromosome in females and showed that *Xist* itself works in *cis* [93-94]. Hence, *Xist* alone cannot be the Xic or the blocking factor binding side itself. Subsequent discoveries of *Tsix* [118] and *Xite* [136] provided novel candidates to be, together with *Xist*, sufficient to fulfill all requirements for the Xic, namely the ability to count the number of X chromosomes present and the ability to induce silencing. However, the combined deletion of all three genes, performed in our laboratory [179], and the experiments using *Xist* and *Tsix* BAC transgenes described in Chapter 2, showed that also this combination of genes is insufficient to represent the Xic. This, together with data obtained from tetraploid [179] and triploid ES cells [189] having different X-to-autosome ratios, also indicated that initiation of XCI is a stochastic process, in which each X chromosome has an independent probability to become inactivated which becomes higher the more X chromosomes are present (see Chapter 4 for a detailed description of this model). Our discovery of *Rnf12* described in Chapter 2, supports this model, as RNF12 was found to be an X-linked activator of the XCI process, and is required for XCI to occur (Chapters 5 and 7).

The region surrounding the *Xist* locus has been thoroughly investigated in recent years, either by studies focusing on screens of candidate genes [174, 187, 1005-1007], or by chromatin confirmation capture studies to determine genome wide interactions [1004, 1008, 1012]. As described in Chapter 2, our BAC screen to identify *trans*-acting factors acting as XCI-activators identified RNF12 [174]. In a similar BAC screen, the *Xpr* region was identified [187]. This region, when located on an autosome in female cells is able to induce pairing between the autosomal region containing the transgene and an X chromosome, thereby disrupting normal XCI kinetics. When such a transgene was transfected in male

cells, this was strictly selected against, rendering it possible that the presence of such a transgene could induce ectopic pairing and XCI in these male transgenic cells. As the *Xpr* is the first region to show pairing behavior during the initiation phase of XCI, this region was proposed to be important in the regulation of X chromosome pairing and hence counting and regulation of mono-allelic *Xist* expression. Another study proposed an important role of the non-coding RNA *Jpx* in the regulation of *Xist* expression [1006]. Cells in which *Jpx* was deleted on one allele did no longer initiate XCI, which resulted in massive cell death, which was not observed in male *Jpx* mutant cells. This phenotype could be rescued to certain extend by *Jpx* transgenes, arguing that *Jpx* could work in *trans*, although also evidence for a *cis* acting function was provided. Another non-coding gene located in the telomeric proximity of *Xist* is *Ftx*, which was also shown to influence expression of *Xist* and neighboring genes [1007]. Since the phenotype of an *Ftx* mutation was only analyzed in male cells, it was not possible to distinguish between a *cis* or *trans* acting effect. Beside genes acting on *Xist*, also genes involved in the regulation of *Tsix* have been found in close proximity to the *Xist/Tsix* locus. *Tsx* has been shown to activate the expression of *Tsix* [1005]. A knockout of this gene in ES cells resulted in lower *Tsix* expression, which resulted in a low percentage of ectopic *Xist* clouds upon differentiation. Another gene acting on *Tsix* is the non-coding RNA *Linx*, of which transcription is initiated 50 kb upstream of the *Ppnx* promoter [1004]. Only when *Tsix* transgenes harbor *Linx* sequences, expression of *Tsix* was observed in transgenic mice, and *Tsix* and *Linx* were often co-expressed from the same allele, arguing for an important role for *Linx* in *Tsix* regulation.

Genome wide interactions studies have shown that there are two different topological associated domains (TADs) surrounding the *Xist/Tsix* locus, with one encompassing a region up to 500 kb telomeric to, and including *Xist*, whereas the other includes *Tsix* and 200 kb of sequence towards the centromere [1004, 1008, 1012]. The biological relevance of the TADs is indicated by the presence of a functional boundary site, located between *Xist* and *Tsix* [1008]. Interactions between genes are mainly found within the domains, but not between the two different domains [1004]. This indicates that potential *cis* regulatory elements for both *Xist* and *Tsix* must be located on different sides of the boundary elements.

To address the question whether the genes and regions located between *Rnf12* and *Xist* would harbor all missing activating factors for XCI, we have generated a cell line in which the complete *Xist* interaction domain is deleted. The analysis of this cell line, transgene rescue experiments and different extensions of the deletion described in Chapter 7, all have shown that *Jpx*, *Ftx* and the *Xpr* region are important for the *cis* regulation of the *Xist* locus. In the absence of this genomic region, *Xist* expression from the mutated X chromosome is compromised. It seems that in the absence of this region, the threshold to initiate XCI is much higher on the mutated allele, compared to the wild type allele, and this is supported by the finding that a *Tsix* mutation in *cis* can almost completely rescue the phenotype. When we performed rescue experiments in which we brought back transgenes harboring *Jpx/Ftx*, the *Xpr* or *Rnf12* into the cell line with the deleted chromatin interaction domain, we were only able to observe a *trans* acting effect for the *Rnf12* gene. This, together with the BAC transgenesis experiments described in Chapter 2, unequivocally shows that the *Jpx*, *Ftx* and *Xpr* region acts in *cis* on the *Xist* locus, contrasting previous findings in which *Jpx* was proposed to act in *trans* [1006]. Also, X chromosome pairing

does not seem to be required for the initiation of XCI, as XCI was observed in male nuclei of differentiating experimental XY-XX heterokaryons and in the absence of all elements known to be involved in pairing. Therefore, in Chapter 7 we have proposed to divide the Xic in a *cis*-acting Xic, and a *trans*-acting Xic. In this model, the *cis*-Xic consists of all genes and regions which regulate the *Xist/Tsix* locus in *cis*, and this *cis*-Xic is likely be represented by the two TADs located around the *Xist/Tsix* locus and divided by a chromatin boundary. Therefore, genes located in the *Tsix* TAD are expected to be involved in *Tsix* regulation, and indeed for *Xite*, *Tsx* and *Linx* this has been reported to be the case [136, 1004-1005]. On the other hand, genes located in the *Xist* TAD will be important for *Xist* regulation. Indeed, our data presented in Chapter 7 indicate that this is the case for *Jpx*, *Ftx* and the *Xpr* region. This model does not exclude the possibility that other factors located elsewhere in the genome on autosomes act on genes within the *cis*-Xic. However, as these factors, for example pluripotency factors like REX1, act on their target and influence genes within the *cis*-Xic, the effect will be equal between males and females, and the result will be a *cis* effect acting on either *Xist* or *Tsix*. The content of the *cis*-Xic will be equal between males and females, so that *cis* acting elements will not be able to count the number of X chromosomes and to decide how many of them need to be inactivated. For this, *trans*-acting factors are required, and at present, the only known gene within the *trans*-Xic is *Rnf12*.

What is the delineation of the *trans*-Xic and how many other *trans*-acting factors can be involved? Initial experiments with female *Rnf12*+/- ES cells, described in Chapter 2, indicated that additional XCI-activators must be involved in the regulation of XCI initiation, as these cells still initiated XCI in contrast to male ES cells [174]. These potential novel activators of XCI could in principal be located everywhere on the X chromosome, without a need to be located within the Xic candidate region defined by the translocation and deletion studies mentioned above [72-73], although a proximity to *Xist* would help to assure a fast feedback system. However, the results obtained in Chapter 5, showing that RNF12 is essential for XCI initiation, and the results described in Chapter 7, showing that the continued expression of RNF12 is also essential for establishment of the Xi, could also argue that no additional activators are required. In female ES cell lines which have a compound mutation of both *Rnf12* and *Xist* on a single X chromosome, we did not detect robust XCI initiation on the wild type X chromosome. Sporadic spots of *Xist* accumulation were found to be diffuse, and this is likely to be caused by the fact that upon XCI on the wild type X chromosome, *Rnf12* will become silenced. Absence of RNF12 is not compatible with XCI initiation, as seen in female *Rnf12*-/- ES cells, and results in a high level of REX1. Hence, the silencing of the wild type *Rnf12* copy in the compound mutant cells (carrying a compound mutation of both *Rnf12* and *Xist* on a single X chromosome) will likely explain the absence of robust XCI initiation in this cell line. Indeed, rescuing *Rnf12* expression from a transgene resulted in robust XCI initiation in that cell line, confirming that RNF12 is also required for the full length of the XCI initiation process. To generate *Rnf12*+/- ES cells, we initially targeted the 129/Sv allele in wild type hybrid ES cells, harboring a Cast/Ei and a 129/Sv X chromosome (Chapter 2). Although these cells still initiated XCI, indicating that more activators are required, these cells always showed a skewed XCI favoring inactivation of the 129/Sv X chromosome. We later generated *Rnf12*+/- ES cells in which the Cast/Ei allele was targeted, as described in Chapter 7, and observed a reciprocal skewing, favoring inactivation of the Cast/Ei X chromosome. With

the knowledge obtained from the compound mutant *Rnf12/Xist* cell lines, we can now explain that skewing in *Rnf12*+/- ES cells is caused by the fact that XCI on the wild type allele will result in failure of XCI initiation, as soon as the wild type allele of *Rnf12* becomes silenced. This would result in up-regulation of REX1, and subsequent suppression of *Xist*. Therefore, only inactivation of the X chromosome harboring the *Rnf12* mutant allele will result in robust XCI initiation, as an active *Rnf12* copy will be maintained and will "lock-in" the initiation of XCI by continuous degradation of REX1, and hence expression of *Xist*. In male ES cells, which like female *Rnf12*+/- ES cells have only one copy of *Rnf12*, XCI initiation on the single X chromosome would also result in *Rnf12* silencing. This could explain why only a few male cells (< 0,1%) initiate XCI in wild type cells, compared to female wild type ES cells which have a twofold higher dosage of RNF12 (Chapter 2). Therefore, it is possible that indeed RNF12 is by far the main XCI-activator present, although this does not exclude that other factors with a more subtle role are involved as well.

What else could be different between male ES cells and *Rnf12*+/- ES cells? It will be interesting to investigate whether there are differences between RNF12 and REX1 kinetics in these cell lines. In line with this, in male ES cells we found a higher level of REX1 compared to female ES cells [1009] (Chapter 6). In female *Rnf12*+/- ES cells, the absence of one functional *Rnf12* allele also results in a higher REX1 level, although there is no linear twofold increase compared to *Rnf12*-/- ES cells which have the highest REX1 level. The REX1 level has not been directly compared between male ES cells and *Rnf12*+/- ES cells. Although in principle the REX1 level should be equal between these cells, because both cells have only one copy of *Rnf12*, it is possible that female-specific regulation of *Rnf12* could result in higher *Rnf12* expression from a single allele in females compared to a single allele in males, thereby resulting in an even lower REX1 level in *Rnf12*+/- ES cells. Hence, this could explain why in male cells it is even more difficult to up-regulate *Xist* compared to female cells, even before *Rnf12* silencing in *cis*. Potentially, other X-linked factors could therefore be involved in the regulation of *Rnf12*, and these could be the subtle acting remaining factors to be identified. This is supported by the finding that *Rnf12* immuno-staining intensity measured in differentiating female ES cells is more than two-fold higher compared to the intensity in differentiating male ES cells (Chapter 5).

If RNF12 would be the only, or main activator of XCI, this could also explain some findings in male ES cells in which NANOG or OCT4 was down-regulated by doxycylin induction [191]. In these experiments, down-regulation of NANOG or OCT4 resulted in up-regulation of *Xist* expression, and since binding sites for these pluripotency factors were found within *Xist* intron 1, these data were interpreted as providing evidence for a direct suppression of *Xist* by pluripotency factors in undifferentiated cells. We have addressed the role of the *Xist* intron 1 region in Chapter 5, and found that genetic ablation of this region both in ES cells as in mice does not result in a dramatic XCI phenotype, making it unlikely that this region is directly involved in the suppression of *Xist*. But how then can *Xist* up-regulation upon forced NANOG and OCT4 repression be explained? An intriguing hypothesis could be that upon loss of these factors, REX1 will become down-regulated, allowing loss of repression of the *Xist* locus, and enabling up-regulation of *Xist*. Down-regulation of REX1 upon down-regulation of NANOG and OCT4 seems likely, as

the expression of many pluripotency factors is interconnected by reciprocal binding to their gene regulatory sequences [1048]. *Rnf12* might also become up-regulated in this situation, as it has been proposed that *Rnf12* is under control of the pluripotency factor network [990], thereby enhancing the effect on REX1 down-regulation. Indeed, we have described a negative correlation between RNF12 and NANOG expression in Chapter 5. Although our preliminary results of a targeted deletion of proposed pluripotency factor binding sites in the *Rnf12* upstream region [990] do not provide evidence for an important direct repressive function of NANOG and OCT4 (data not shown), it reinforces the role of REX1, which is likely to be involved in direct RNF12 regulation through a binding site close to the transcriptional start site of *Rnf12*. Therefore, forced down-regulation of NANOG and OCT4 could result in drastic up-regulation of RNF12 and down-regulation of REX1 normally not observed in wild type male ES cells, thereby explaining the ectopic *Xist* induction.

Would the novel division of the Xic in a *cis*-Xic and a *trans*-Xic which we propose in Chapter 7 fit to the original data delineating the Xic candidate region? Both the *cis*-Xic, consisting of all genes from *Linx* till the *Xpr* region, as well as the *trans*-Xic, consisting solely of *Rnf12*, lie well between the borders delineated by the Searle's translocation and HD3 truncation originally defining the Xic [72-73]. Based on ring X chromosomes in human patients with severe forms of Turner syndrome, the Xic candidate region can likely be even further defined (**Figure 1**). Ring X chromosomes are small, ring like remnants of truncated X chromosomes, which have a centromere, but miss telomeric sequences [863]. Some Turner patients (45,X) have mosaicisms of cells carrying an additional ring X chromosome, and it has been shown that activity of these rings correlate to a severe clinical phenotype [871-873]. Indeed, the majority of ring X chromosomes are active due to the fact that *XIST* sequences are lacking [873, 875-877]. However, in some of these rings, *XIST* is present, but not expressed [1049-1050]. Analysis of breakpoints in these rings often shows that the distal breakpoint is located in close proximity to *RNF12*. This could indicate that these ring X chromosomes do not undergo XCI due to a lack of XCI activation.

How could we further determine whether all known elements and genes in the *cis*- and *trans*-Xic as known today are sufficient to fulfill all functions required for counting and initiation of XCI? BAC and YAC transgenesis experiments are unlikely to resolve this question, as it will be technically difficult to engineer transgenes covering all sequences known to be involved right now. Therefore, further removal of X chromosomal sequences will be necessary. Most ideally, the complete 10 Mb candidate region defined by the Searle's translocation and HD3 truncation [72-73] should be removed from a single X chromosome, leaving the region from upstream of *Linx* till telomeric to *Rnf12* intact. If such a cell line would still undergo XCI with normal kinetics, most likely preferring inactivation of the mutated allele due to secondary selection, all long standing questions on the content of the Xic and the initiation mechanisms for XCI would be solved.

Rnf12 and imprinted X chromosome inactivation

In the female mouse pre-implantation embryo, XCI is imprinted leading to exclusive inactivation of the paternally inherited X chromosome (Xp). The Xp has been reported to be inherited in a partially inactive state [51], but other evidence suggests that both X chromosomes are active in female embryos after zygotic genome activation followed by

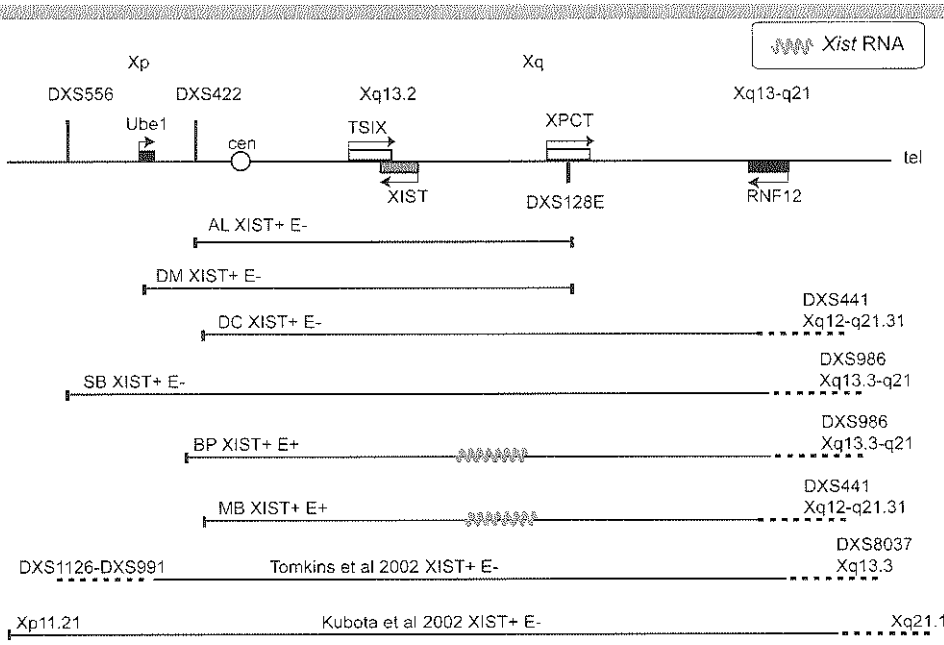

Figure 1: Ring X chromosomes in patients with Turner syndrome
At the top, a simplified map of the human X chromosome is shown. The locations of *UBE1*, *XIST*, *TSIX*, *XPCT* and *RNF12* and polymorphic markers used in molecular characterization of ring X chromosomes are indicated. Xp: short arm of the X chromosome; Xq: long arm of X chromosome; Cen: centromere; Tel: telomeric. Below the map, the genetic content of ring X chromosomes described in literature is shown. XIST+E-: *XIST* locus present, but no expression of XIST; XIST+E+: *XIST* locus and expression of XIST are present. Abbreviations in front of the rings correspond to the names of patients, as mentioned in the literature (Jani et al., 1995) or the authors (Kubota et al., 2002; Tomkins et al., 2002). Dots indicate that breakpoint are not precisely defined. Most breakpoints of rings which do not express *XIST* do not have *RNF12*, or have breakpoints in close proximity. Further characterization of ring X chromosomes by array-CGH would be required to definitively delineate the deletions.

initiation of imprinted XCI at the 4-8 cell stage [52, 311, 986]. Probably, parental-specific epigenetic modifications, which are set during gametogenesis, regulate imprinted XCI, and these likely involve an imprint that represses *Xist* on the maternally inherited Xm. This is supported by transgene studies, which indicated that all the epigenetic information required for imprinted XCI is located within a 220 kb region that includes *Xist* and *Tsix* [986].

The molecular mechanisms used by placental mammals to silence an X chromosome in imprinted XCI versus random XCI might partly overlap, with both processes requiring *Xist*. In contrast, in the imprinted XCI process, repression of *Xist* on the Xm is independent of *Tsix*, and was proposed to involve OCT4- and SOX2-mediated repression of *Xist*, by binding of these pluripotency factors to the *Xist* intron 1 region [993]. However, our analysis of *Xist* intron 1 mutant mice described in Chapter 5, where we did not notice any failure of imprinted XCI in the offspring obtained, argues against an

important role of this region in the regulation of imprinted XCI *in vivo*. *Tsix* mediated repression of *Xist* starts to play an important role on the Xm somewhat later in embryonic development, around the morula stage. This can be concluded from the observation that a maternally inherited *Tsix* null allele is embryonic lethal due to aberrant initiation of XCI on the Xm [354, 988].

A recent study revealed an important role for RNF12 in imprinted XCI, in addition to its role in random XCI which we discovered as described in Chapters 2 and 8. A maternally transmitted *Rnf12* knockout allele caused embryonic lethality only in female offspring, due to defects in the development of extra-embryonic tissues [981]. Female Δ*Rnf12*/+ embryos with the deletion on the Xm failed to initiate imprinted XCI on the wild type Xp at the early cleavage stage. From this, the maternal storage of RNF12 protein in the oocyte was suggested to play an important role in imprinted XCI [981]. In our *Rnf12* mutant mouse model described in Chapter 8, we also observed that a maternally transmitted knockout allele is unlikely to give viable female offspring. From the 118 pups obtained from crosses with a heterozygous $Rnf12^{+/-}$ mother, of which 81 were males and 37 were female, only a single heterozygous $Rnf12^{-/+}$ female was born, whereas the *Rnf12* mutant allele was effectively transmitted to 27 males. If we take processes occurring during meiosis into account, it seems unlikely that all features of this failure of imprinted XCI can be explained by the maternal storage of RNF12 protein. As a consequence of meiotic recombination, it can be expected that many haploid oocytes generated by the first meiotic division (the reduction division) of $Rnf12^{+/-}$ oocytes, which occurs at the time of ovulation, will contain both wild type and *Rnf12* mutated alleles on the recombined sister chromatids. Hence, we foresee that there will be ongoing expression of *Rnf12* in a high percentage of oocytes transmitting the mutated *Rnf12* allele, until fertilization triggers meiotic division II. Therefore, the recombined wild type and mutant alleles which are present within the same haploid oocyte, will be exposed to the same maternal storage of RNF12. Since $Rnf12^{+/-}$ oocytes did not give rise to female offspring carrying the mutant allele, whereas female offspring carrying the wild type allele were obtained at the expected Mendelian ratio from these oocytes, this argues against an important role for maternal storage in imprinted XCI. But how then can failure of maternal transmission of the knockout allele to female offspring be explained? It seems likely that the same continuous requirement of RNF12 which we observe during random XCI in ES cells (Chapter 7) is also required during imprinted XCI *in vivo*. During imprinted XCI the paternal X chromosome is inactivated, so that an embryo inheriting a maternal *Rnf12* knockout allele would become deficient of RNF12 upon imprinted XCI. Therefore, it seems likely that in this situation XCI cannot be maintained. When the *Rnf12* mutant allele is derived from the father, this paternal X chromosome will become inactivated during the imprinted XCI. In that scenario, maternal RNF12 is still available, and this explains why females are normally born in matings with an *Rnf12* mutant father. This suggests that, ongoing *de novo* synthesis of RNF12 may be required for persistent expression of *Xist* both for imprinted and random XCI. To definitively address the need for maternal storage in imprinted XCI, one could make use of a nuclear transfer experiment. In such an experiment, the nucleus of a fertilized two-cell stage embryo derived from a cross of a wild type male and an oocyte conditionally homozygously deleted for RNF12, could be transferred to an enucleated wild type oocyte, or to an RNF12 depleted oocyte. If maternal storage would be required and sufficient for

imprinted XCI to occur, transferring the *Rnf12* mutant nucleus to the wild type oocyte should restore initiation of imprinted XCI.

Of note, *Rnf12* becomes reactivated in round spermatids after the process of meiotic sex chromosome inactivation (MSCI), which would be compatible with rapid onset of expression of the paternal allele following fertilization [1051]. This indicates that from the moment of fertilization onwards, some portion of RNF12 protein in the zygote might be derived from mRNA transcribed from the paternal *Rnf12* allele, when the maternal derived genome is still inactive. Indeed, although not significant, at the 2-cell stage more cells displayed a paternally derived *Rnf12* primary transcript compared to the maternal derived one, as determined by RNA-FISH [311]. Therefore, it could be that imprinted XCI is initiated, at least in part, by this paternal derived fraction. As in a female embryo, the Xm allele harbors an imprint which makes it impossible for *Xist* RNA to accumulate, paternally derived RNF12 together with RNF12 present in the oocyte might be sufficient to trigger *Xist* accumulation on the paternal *Xist* allele, which is devoid of an imprint and hence might be prone to become expressed. Spreading of *Xist* would result in silencing of *Rnf12* in *cis*, and maternally stored RNF12 which has a short half-life will become diluted over the cell divisions. Consequently, zygotic genome activation occurring at the 2-cell stage might be sufficient to maintain the initiation of inactivation of the Xp, after *Rnf12* transcription from the maternally transmitted allele would become activated. Indeed, in line with this, *Rnf12* on the paternal X chromosome is one of the first genes to become silenced [311], already at the 4-cell stage. In case of a paternally transmitted *Rnf12* knockout allele, such a paternally programmed *Rnf12* expression could not play a role, but initiation of imprinted XCI might be rescued by RNF12 present in the oocyte or upon production of RNF12 from the maternally derived allele. Therefore, it should be tested whether imprinted XCI is occurring at exactly the same time in development in wild type and paternally *Rnf12* mutant embryos. Future studies should also address the question whether paternal *Rnf12* is already active directly after the fertilization, or whether sperm cells might perhaps carry a significant amount of *Rnf12* mRNA, produced after MSCI. This could provide important insights in unraveling the initiation mechanisms of imprinted XCI.

Rnf12 and reactivation of the X chromosome

The tight connection between the pluripotency factor network and suppression of XCI provides a mechanism for proper developmental timing of random XCI in the early female embryo, but might also be instrumental in the observed reactivation of the Xi in the ICM and in PGCs. In female mouse embryos, imprinted XCI of the Xp is reversed in the late blastocyst at embryonic day 4.5 (E4.5) of development. From the late morula stage onwards, NANOG is expressed, and its expression is maintained throughout formation and expansion of the ICM. At day E3.5, NANOG is together with OCT4 expressed in the ICM, whereas at day E4.5, NANOG expression is restricted to the emerging epiblast, and its expression is lost in hypoblast cells expressing GATA4 and GATA6. Interestingly, only ICM cells with prolonged NANOG expression show reactivation of the Xi [367], indicating that X reactivation is indeed linked to pluripotency factor expression. A possible direct function for these pluripotency factors in reactivating the Xp after imprinted XCI involved the binding of these factors to the *Xist* intron 1 region, which was proposed to be involved

in direct suppression of *Xist* [191, 993]. However, our detailed analysis of genetic ablation of this region in ES cells and in mice described in Chapter 5 showed that this region does not play a role in *Xist* suppression both *in vitro* as *in vivo*. Since NANOG, OCT4 and SOX2 are already present prior to E4.5, but only at this developmental stage imprinted XCI is reversed in a subset of epiblast cells, it is tempting to speculate that activators of XCI which could play a role in imprinted XCI are down-regulated at this point, thereby enabling the X reactivation in collaboration with the pluripotency factors. Indeed, *Rnf12* expression seems to be influenced by pluripotency factors, as binding sites have been found in the *Rnf12* upstream region [983, 990], and NANOG and RNF12 expression is mutually exclusive in differentiating ES cells, as described in Chapter 5. Although our preliminary results of targeted deletion of pluripotency factor binding sites 3.8 and 5.3 kb upstream of the transcriptional start site of *Rnf12* did not show an effect on *Rnf12* expression and *Rnf12* regulation seems to be mainly regulated by the minimal promoter region harboring a REX1 binding site (data not shown), it is expected that *Rnf12* will become down-regulated in NANOG expressing cells in the epiblast. This down-regulation will be accompanied with an up-regulation of REX1, which might have a role in *Xist* suppression at the epibast stage. Up-regulation of pluripotency factors including NANOG in the epiblast cells could also result in indirect mechanisms, leading to higher REX1 expression, and hence repression of *Rnf12* expression.

Xist repression in the ICM may be required for reactivation of the X. However, such a repression is not sufficient, as is illustrated by studies involving NANOG over-expression in the ICM, which results in repression of *Xist* at an earlier stage of development, but does not lead to premature X reactivation [1052]. This is an interesting finding, because it indicates that up-regulation of *Nanog* expression, possibly in conjunction with the down-regulation of XCI-activators, is involved in *Xist* shut-down, but also that at least one additional mechanism is involved in the reactivation process. The order of events during this reactivation process need to be further characterized, but we anticipate that *Rnf12* and its direct and indirect connections to the pluripotency factor network will be important for this process (**Figure 2**).

A second wave of Xi reactivation is initiated in developing female germ cells. PGCs arise in the epiblast around E7.5 and subsequently migrate through the hindgut to reach the genital ridge at E11.5. In the mouse embryo, XCI is random in the epiblast cells that give rise to the PGCs, and reactivation of the Xi happens during migration or around the time PGCs enter the genital ridge [1053-1055]. Reactivation of the randomly inactivated Xi in PGCs seems to require a longer time window than resetting of imprinted XCI in the ICM, which may reflect differences in the composition of the Xi heterochromatin formed during the random XCI and imprinted XCI processes. OCT4, SOX2, NANOG and REX1 are highly expressed in PGCs and are therefore candidate factors involved in the direct repression of *Xist* in the germ line cells, possibly supported by a low level of expression of XCI-activators including RNF12 [1056]. Also here, high expression of pluripotency factors could result in indirect mechanisms leading to a low level of XCI-activators, which would facilitate reactivation of the X chromosome.

Reactivation of the Xi can also be artificially induced during formation of induced pluripotent stem (iPS) cells [67], or by fusion of somatic cells with embryonic carcinoma (EC) cells [1057]. Forced expression of *Oct4*, *Sox2*, *Klf4* and *c-Myc* to generate iPS cells, or

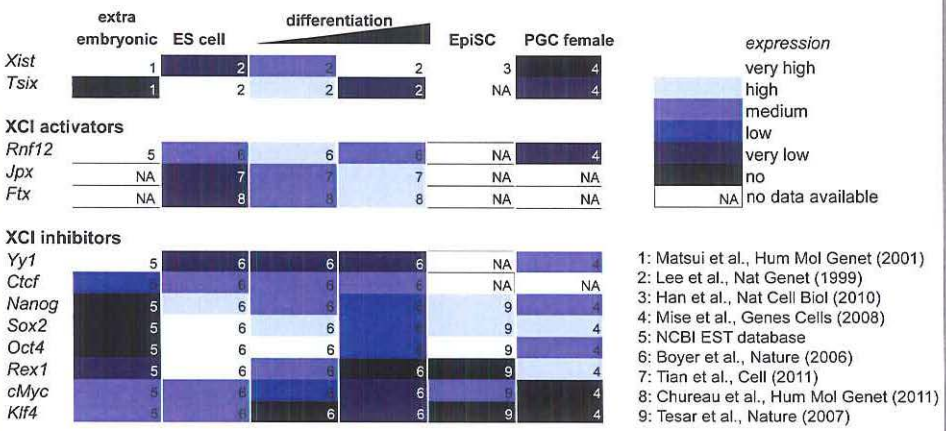

Figure 2: Expression profile of factors involved in XCI
An overview of the expression profile of genes encoding important players in the XCI process at different steps of embryonic development, and in different cell types. The data was obtained and compiled from different studies using different platforms to assess expression levels, and therefore inter-study comparisons should be interpreted with caution.

Adapted from Barakat and Gribnau, Development 2012.

expression of EC-specific pluripotency genes in hybrid cells, is not sufficient to reactivate the Xi instantly [67, 1058]. In both cases, reactivation of an X-linked GFP reporter gene on the Xi happens late during the reprogramming process, most likely because several layers of epigenetic silencing mechanisms have to be erased in conjunction with a shut-down of the *Xist* promoter. Epiblast stem cells (EpiSCs) are post-XCI pluripotent stem cells isolated from the epiblast of an E5.5 embryo. Reprogramming of EpiSCs into ES cells by sustained culture in the presence of LIF, or by forced expression of *Klf2*, *Klf4* and *Nr5a*, also leads to reactivation of the Xi [391-392, 1059]. Furthermore, the Xi is reactivated in embryos obtained through somatic cell nuclear transfer (SCNT) [1060]. In SCNT, a somatic cell nucleus is reprogrammed by insertion to an enucleated oocyte, which results in the fast, and complete reprogramming of the somatic nucleus towards a pluripotent state. Extra-embryonic tissues of cloned female embryos obtained through SCNT retain the Xi that was also inactive in the donor cell, which suggests that the information required for proper imprinted XCI may be reminiscent of the epigenetic marks acquired during random XCI.

Interestingly, a recent publication has linked aberrant *Xist* expression to reprogramming by SCNT [1061]. This process, which can give rise to complete cloned mammals, is however also highly inefficient, and often results in faulty reprogramming. Inoue et al. (2010) could show that faulty reprogrammed SCNT mouse embryos, both male and female, are characterized by aberrant *Xist* expression, and that genetic ablation of *Xist* could increase the efficiency of SCNT-based reprogramming. SCNT and iPS-based reprogramming could make use of similar mechanisms, which leads to an attractive, but not yet tested, hypothesis, that hindering *Xist* expression might also facilitate iPS reprogramming. It will certainly be interesting to explore the role of *Rnf12* in these reprogramming processes. Since REX1 is an important pluripotency factor, and expression

of REX1 is a key-event for complete reprogramming, an attractive hypothesis could be that hindering RNF12 mediated proteasomal degradation of REX1 might facilitate somatic cell reprogramming. Therefore, down-regulating *Rnf12* during reprogramming might facilitate more efficient iPS cell derivation and, due to its XCI-activator activity, might also help in preventing aberrant *Xist* expression during this process. RNF12 involvement in regulation of TGF-ß signalling [1044] could likewise facilitate reprogramming, as inhibition of TGF-ß signalling has been shown to result in more efficient iPS reprogramming in mice [1062]. Whether all these possible functions for *Rnf12* might also help in generating hiPS cells which maintain their X chromosomes active more efficiently remains to be determined.

Living with two X chromosomes

The analysis of our *Rnf12* mutant mouse model described in Chapter 8 clearly shows that *Rnf12* has an important role in XCI initiation *in vivo*. Whereas males deficient for *Rnf12* are readily born, female homozygous knockout animals could not be obtained. Also a maternally transmitted knockout allele is strictly selected against, most likely due to the continuous requirement of RNF12 during imprinted XCI. Surprisingly, when we analyzed tissues of adult heterozygous *Rnf12*$^{+/-}$ animals, obtained from crosses of *Rnf12* mutant mice harboring a Cast/Ei X chromosome and wild type females harboring C57Bl/6 X chromosomes, we observed that XCI skewing ratios based on *Xist* and X-linked gene expression were no longer correlating, implicating that these animals may have a defect in dosage compensation. Based on our results obtained with ES cells, we expected to find complete XCI skewing in these animals, rendering the paternal Cast/Ei X chromosome harboring the *Rnf12* mutant allele inactive. Hence X-linked gene expression should only be observed from the maternally derived C57Bl/6 X chromosome. However, as our analysis of many organs in several animals has shown, we do find variable expression of *Xist* derived either from the Cast/Ei or the C57Bl/6 X chromosome. The allelic gene expression of several X-linked genes was analyzed, which in wild type mice shows a reciprocal pattern compared to the *Xist* expression. However, this reciprocal expression of *Xist* and X-linked genes normally subject to XCI was not observed in the *Rnf12* mutant mice. This might indicate that these animals harbor many cells which did not undergo the XCI process properly.

How can this be explained? To answer this intriguing question, we should take a look at the hypothetical events happening in these animals during the embryonic stages. These *Rnf12*$^{+/-}$ female animals will survive the imprinted XCI phase during pre-implantation development, as the paternally transmitted *Rnf12* knockout allele will become inactivated, rendering the maternally derived wild type copy of *Rnf12* active. After reactivation of imprinted XCI in the epiblast, random XCI will occur. As we have shown for *Rnf12*+/- ES cells, in Chapter 2, lacking one copy of *Rnf12* will result in a lower XCI initiation rate, with a delayed up-regulation of *Xist* expression. When these cells finally up-regulate *Xist*, and by a stochastic event choose to inactivate the paternally derived Cast/Ei chromosome harboring the *Rnf12* mutant allele, these cells will still have *Rnf12* expression from the maternally derived allele, will maintain *Xist* expression and will therefore be properly silenced. However, when these cells choose to inactivate the maternally derived C57Bl/6 X chromosome harboring the wild type *Rnf12* allele, these cells will most likely

not be able to maintain robust *Xist* expression, as *Rnf12* expression is continuously required for this, as we have shown in Chapter 7. Therefore these cells will, from the moment that *Rnf12* becomes silenced on the C57Bl/6 X chromosome, stop accumulating *Xist* RNA, which might result in reactivation of the one X chromosome which was still in the process of becoming completely silenced. After reactivation of *Rnf12* from the C57Bl/6 X chromosome, these cells could in principle undergo a new round of *Xist* accumulation, again at a lower rate, as one copy of *Rnf12* is lacking. When these cells now choose to inactivate the Cast/Ei X chromosome, they might be on time to establish robust silencing of XCI, since their maternal *Rnf12* copy will still be active. However, as these cells might alternatively choose to try to inactivate the C57Bl/6 X chromosome again, they might end up with the same reactivation process described above, since *Xist* accumulation will not be maintained upon silencing of *Rnf12*. Of note, it has been shown that both *in vitro* as *in vivo* *Xist* accumulation can result in gene silencing only when expressed during a certain time frame, within 48h of differentiation of ES cells [261, 273]. Therefore, the combination of delayed XCI kinetics due to the presence of only one *Rnf12* copy, in combination with potentially several rounds of unsuccessful attempts to establish XCI, will result in cells which will accumulate *Xist* too late. These cells will be expected to have a failure of XCI, perhaps only silencing several X-chromosomal genes in a random fashion. As some of these cells might end up in lineages in which a less strict selection on correct dosage compensation is applied, the presence of these cells could explain the aberrant gene expression observed in the adult heterozygous *Rnf12* females.

The above hypothetical scenario concerns a highly interesting phenomenon, and we need to find out if lack of XCI really is compatible with viability, as observed in the present mouse model. To this end, we are currently applying several approaches. In a first attempt, we started profiling the complete X-chromosomal allele-specific expression profile by RNAseq for several organs derived from *Rnf12*$^{-/-}$ females. This should provide data on the extent of the failure of XCI in these animals. Using gene-specific probes and RNA-FISH technology, we will investigate whether cells showing bi-allelic X-linked gene expression are found during the stages that random XCI is initiated, and in the adult tissues. Finally, further generation of reporter mice in which expression from both X chromosomes can be detected in a direct manner will further help in deciphering the phenotype of these *Rnf12*$^{-/-}$ animals.

When it is confirmed that mice can develop and live with two active X chromosomes, we will be looking at the next question, how this might at all be compatible with life? All studies investigating XCI during the last 51 years after Mary Lyon's postulation of XCI in females [30] have assumed that successful inactivation of one of the two X chromosomes through XCI is required for a female to live. It is a fact that an inactive X chromosome is found in all adult women with a 46,XX karyotype who have been investigated, and the severe phenotype of Turner patients carrying active ring X chromosomes indicates that a twofold dosage of X-linked genes will result in a physiology which is doomed to fail. However, what is really the evidence that correct X dosage compensation is required for all cells, in any of the placental mammals? If we look at the results obtained for mice mutant for *Xist* [93-94], which indicated that a failure of X dosage compensation is embryonic lethal, these studies showed that a correct dosage compensation is needed in extra-embryonic tissues. Although the embryonic parts are also affected in *Xist*

mutant embryos, this could be a secondary effect, due to a failure of proper nutrition of the embryo caused by a placental defect, as has also been observed in the analysis of embryos carrying a wild type X chromosome and a Searle's translocation X chromosome [1063]. A female embryo with a paternally transmitted mutant *Xist* allele will die, due to a failure of imprinted XCI. In contrast, a maternally transmitted *Xist* knockout allele will result in living female offspring, but with skewed XCI in all adult tissues, as only the paternal X chromosome can be inactivated. Evidently, animals with a *Xist* mutant allele inherited from both the mother and the father are not viable, which prohibits investigation whether there is a requirement for X dosage compensation in all adult tissues, so that this remains a very important open question. A relatively simple experiment can be performed, to test the requirement for X dosage compensation in embryonic cell lineages, by using *Xist*-/- ES cells in a tetraploid embryo complementation assay. In such an assay, all extra-embryonic tissues are formed from the tetraploid donor embryo, and it can be investigated where cells deficient of X dosage compensation turn up, in which cell lineages and tissues during subsequent steps of development.

All available *Xist* mutant mouse models will have an extra-embryonic phenotype, which limits the investigation of the effect of loss of *Xist* on the embryonic parts of the embryo. In this regard, our *Rnf12* mutant mouse model could be a unique tool for further investigations. *Rnf12*$^{+/-}$ female mice will survive the imprinted XCI stages when the mutant *Rnf12* allele is inherited from the father, so that these animals allow, for the first time, a functional dissection of the effects on dysregulation of either imprinted XCI in the pre-implantation embryo or random XCI in the epiblast. Therefore, we can now address key questions regarding the life-long need for dosage compensation. Interestingly, when we take a look at our *Rnf12*-/- ES cells, these cells differentiate normally despite the presence of two active X chromosomes. This indicates that at least in certain cell lineages, a two-fold dosage of X-linked genes is tolerated. Maybe a strict dosage compensation is required in particular in extra-embryonic tissues. To a certain extent, two active X chromosomes are tolerated also in human iPS cells, as shown in Chapter 9. Until now, no clear disease phenotype is observed in *Rnf12*$^{+/-}$ females. Therefore, it is possible that living with cells with two active X chromosomes is compatible with life, at least in mice, although we need to find out if this concerns many cells in many tissues. If this might be true for humans, it certainly promises to have important clinical implications. As discussed in Chapter 1, many X-linked genes cause disease in humans. In some X-linked diseases affecting females, often a single mutant allele is sufficient to cause severe disease, despite the presence of a mosaicism with cells expressing a wild type allele. If in such diseases a reactivation of the inactive X chromosome harboring a wild type allele in affected cells could be achieved, this would open new ways to therapies. In line with this, it has been shown that reactivation of a silent *Mecp2* allele in adult mice, for example, can alleviate the symptoms of Rett syndrome [1064-1065], and similar observations have been made in case of fragile X syndrome [1066]. Therefore, now that many questions regarding the initiation of XCI in mice may have reached an advanced stage of mechanistic explanation, a new important area of research will try to answer the question whether it is feasible to live with two active X chromosomes.

References

1. Darwin, E., Phytologia, 1800. **115**: p. 103.
2. Sarre, S.D., T. Ezaz, and A. Georges, *Transitions between sex-determining systems in reptiles and amphibians.* Annu Rev Genomics Hum Genet, 2011. **12**: p. 391-406.
3. Rhen, T. and A. Schroeder, *Molecular mechanisms of sex determination in reptiles.* Sex Dev, 2010. **4**(1-2): p. 16-28.
4. Ohno, S., *Sex chromosomes and Sex-linked genes.* 1967, Berlin: Springer.
5. Muller, H.J., *A gene for the fourth chromosome in Drosophila.* J. Exp. Zool., 1914. **17**: p. 325-336.
6. Charlesworth, B., *The evolution of sex chromosomes.* Science, 1991. **251**(4997): p. 1030-3.
7. Graves, J.A., *The origin and function of the mammalian Y chromosome and Y-borne genes--an evolving understanding.* Bioessays, 1995. **17**(4): p. 311-20.
8. Graves, J.A., E. Koina, and N. Sankovic, *How the gene content of human sex chromosomes evolved.* Curr Opin Genet Dev, 2006. **16**(3): p. 219-24.
9. Graves, J.A., *Sex chromosome specialization and degeneration in mammals.* Cell, 2006. **124**(5): p. 901-14.
10. Marshall Graves, J.A., *Weird animal genomes and the evolution of vertebrate sex and sex chromosomes.* Annu Rev Genet, 2008. **42**: p. 565-86.
11. Sutton, E., et al., *Identification of SOX3 as an XX male sex reversal gene in mice and humans.* J Clin Invest, 2011. **121**(1): p. 328-41.
12. Skaletsky, H., et al., *The male-specific region of the human Y chromosome is a mosaic of discrete sequence classes.* Nature, 2003. **423**(6942): p. 825-37.
13. Koopman, P., et al., *Male development of chromosomally female mice transgenic for Sry.* Nature, 1991. **351**(6322): p. 117-21.
14. Ross, M.T., et al., *The DNA sequence of the human X chromosome.* Nature, 2005. **434**(7031): p. 325-37.
15. Wang, P.J., et al., *An abundance of X-linked genes expressed in spermatogonia.* Nat Genet, 2001. **27**(4): p. 422-6.
16. Zhang, Y.E., et al., *Chromosomal redistribution of male-biased genes in mammalian evolution with two bursts of gene gain on the X chromosome.* PLoS Biol, 2010. **8**(10).
17. Khil, P.P., et al., *The mouse X chromosome is enriched for sex-biased genes not subject to selection by meiotic sex chromosome inactivation.* Nat Genet, 2004. **36**(6): p. 642-6.
18. Mueller, J.L., et al., *The mouse X chromosome is enriched for multicopy testis genes showing postmeiotic expression.* Nat Genet, 2008. **40**(6): p. 794-9.
19. Saifi, G.M. and H.S. Chandra, *An apparent excess of sex- and reproduction-related genes on the human X chromosome.* Proc Biol Sci, 1999. **266**(1415): p. 203-9.
20. Bellott, D.W., et al., *Convergent evolution of chicken Z and human X chromosomes by expansion and gene acquisition.* Nature, 2010. **466**(7306): p. 612-6.
21. Delgado, C.L., et al., *Physical mapping of the elephant X chromosome: conservation of gene order over 105 million years.* Chromosome Res, 2009. **17**(7): p. 917-26.
22. Mohandas, T.K., et al., *Role of the pseudoautosomal region in sex-chromosome pairing during male meiosis: meiotic studies in a man with a deletion of distal Xp.* Am J Hum Genet, 1992. **51**(3): p. 526-33.
23. Burgoyne, P.S., et al., *Fertility in mice requires X-Y pairing and a Y-chromosomal "spermiogenesis" gene mapping to the long arm.* Cell, 1992. **71**(3): p. 391-8.
24. Helena Mangs, A. and B.J. Morris, *The Human Pseudoautosomal Region (PAR): Origin, Function and Future.* Curr Genomics, 2007. **8**(2): p. 129-36.
25. Freije, D., et al., *Identification of a second pseudoautosomal region near the Xq and Yq telomeres.* Science, 1992. **258**(5089): p. 1784-7.

26. Kuhl, H., et al., *Loss of the Y chromosomal PAR2-region in four familial cases of satellited Y chromosomes (Yqs).* Chromosome Res, 2001. **9**(3): p. 215-22.
27. Birchler, J.A., et al., *Dosage balance in gene regulation: biological implications.* Trends Genet, 2005. **21**(4): p. 219-26.
28. Veitia, R.A., S. Bottani, and J.A. Birchler, *Cellular reactions to gene dosage imbalance: genomic, transcriptomic and proteomic effects.* Trends Genet, 2008. **24**(8): p. 390-7.
29. Deng, X. and C.M. Disteche, *Genomic responses to abnormal gene dosage: the X chromosome improved on a common strategy.* PLoS Biol, 2010. **8**(2): p. e1000318.
30. Lyon, M.F., *Gene action in the X-chromosome of the mouse (Mus musculus L.).* Nature, 1961. **190**: p. 372-3.
31. Lyon, M.F., R.J. Phillips, and A.G. Searle, *A test for mutagenicity of caffeine in mice.* Z Vererbungsl, 1962. **93**: p. 7-13.
32. Lyon, M.F., *Sex chromatin and gene action in the mammalian X-chromosome.* Am J Hum Genet, 1962. **14**: p. 135-48.
33. Davidson, R.G., H.M. Nitowsky, and B. Childs, *Demonstration of Two Populations of Cells in the Human Female Heterozygous for Glucose-6-Phosphate Dehydrogenase Variants.* Proc Natl Acad Sci U S A, 1963. **50**: p. 481-5.
34. Shapiro, L.J., et al., *Non-inactivation of an x-chromosome locus in man.* Science, 1979. **204**(4398): p. 1224-6.
35. Prothero, K.E., J.M. Stahl, and L. Carrel, *Dosage compensation and gene expression on the mammalian X chromosome: one plus one does not always equal two.* Chromosome Res, 2009. **17**(5): p. 637-48.
36. Adler, D.A., et al., *Evidence of evolutionary up-regulation of the single active X chromosome in mammals based on Clc4 expression levels in Mus spretus and Mus musculus.* Proc Natl Acad Sci U S A, 1997. **94**(17): p. 9244-8.
37. Nguyen, D.K. and C.M. Disteche, *Dosage compensation of the active X chromosome in mammals.* Nat Genet, 2006. **38**(1): p. 47-53.
38. Lin, H., et al., *Dosage compensation in the mouse balances up-regulation and silencing of X-linked genes.* PLoS Biol, 2007. **5**(12): p. e326.
39. Birchler, J.A., H.R. Fernandez, and H.H. Kavi, *Commonalities in compensation.* Bioessays, 2006. **28**(6): p. 565-8.
40. Johnston, C.M., et al., *Large-scale population study of human cell lines indicates that dosage compensation is virtually complete.* PLoS Genet, 2008. **4**(1): p. e9.
41. Xiong, Y., et al., *RNA sequencing shows no dosage compensation of the active X-chromosome.* Nat Genet, 2010. **42**(12): p. 1043-7.
42. Casci, T., *What dosage compensation?* Nat Rev Genet, 2011. **12**(1): p. 2.
43. Deng, X., et al., *Evidence for compensatory upregulation of expressed X-linked genes in mammals, Caenorhabditis elegans and Drosophila melanogaster.* Nat Genet, 2011.
44. Lin, H., et al., *Relative overexpression of X-linked genes in mouse embryonic stem cells is consistent with Ohno's hypothesis.* Nat Genet, 2011. **43**(12): p. 1169-70.
45. Pessia, E., et al., *Mammalian X chromosome inactivation evolved as a dosage-compensation mechanism for dosage-sensitive genes on the X chromosome.* Proc Natl Acad Sci U S A, 2012. **109**(14): p. 5346-51.
46. Gelbart, M.E. and M.I. Kuroda, *Drosophila dosage compensation: a complex voyage to the X chromosome.* Development, 2009. **136**(9): p. 1399-410.
47. Straub, T. and P.B. Becker, *Dosage compensation: the beginning and end of generalization.* Nat Rev Genet, 2007. **8**(1): p. 47-57.
48. Maenner, S., M. Muller, and P.B. Becker, *Roles of long, non-coding RNA in chromosome-wide transcription regulation: Lessons from two dosage compensation systems.* Biochimie, 2012.
49. Meyer, B.J., et al., *Sex and X-chromosome-wide repression in Caenorhabditis elegans.* Cold Spring Harb Symp Quant Biol, 2004. **69**: p. 71-9.
50. Meyer, B.J., *Targeting X chromosomes for repression.* Curr Opin Genet Dev, 2010. **20**(2): p. 179-89.
51. Huynh, K.D. and J.T. Lee, *Inheritance of a pre-inactivated paternal X chromosome in early mouse embryos.* Nature, 2003. **426**(6968): p. 857-62.
52. Okamoto, I., et al., *Epigenetic dynamics of imprinted X inactivation during early mouse development.* Science, 2004. **303**(5658): p. 644-9.

53. Takagi, N. and M. Sasaki, *Preferential inactivation of the paternally derived X chromosome in the extraembryonic membranes of the mouse.* Nature, 1975. **256**(5519): p. 640-2.
54. Mak, W., et al., *Reactivation of the paternal X chromosome in early mouse embryos.* Science, 2004. **303**(5658): p. 666-9.
55. Evans, M.J. and M.H. Kaufman, *Establishment in culture of pluripotential cells from mouse embryos.* Nature, 1981. **292**(5819): p. 154-6.
56. Martin, G.R., *Isolation of a pluripotent cell line from early mouse embryos cultured in medium conditioned by teratocarcinoma stem cells.* Proc Natl Acad Sci U S A, 1981. **78**(12): p. 7634-8.
57. Thomson, J.A., et al., *Embryonic stem cell lines derived from human blastocysts.* Science, 1998. **282**(5391): p. 1145-7.
58. Keller, G., *Embryonic stem cell differentiation: emergence of a new era in biology and medicine.* Genes Dev, 2005. **19**(10): p. 1129-55.
59. Leahy, A., et al., *Use of developmental marker genes to define temporal and spatial patterns of differentiation during embryoid body formation.* J Exp Zool, 1999. **284**(1): p. 67-81.
60. Monk, M., *A stem-line model for cellular and chromosomal differentiation in early mouse-development.* Differentiation, 1981. **19**(2): p. 71-6.
61. Takahashi, K. and S. Yamanaka, *Induction of pluripotent stem cells from mouse embryonic and adult fibroblast cultures by defined factors.* Cell, 2006. **126**(4): p. 663-76.
62. Nakagawa, M., et al., *Generation of induced pluripotent stem cells without Myc from mouse and human fibroblasts.* Nat Biotechnol, 2008. **26**(1): p. 101-6.
63. Wernig, M., et al., *In vitro reprogramming of fibroblasts into a pluripotent ES-cell-like state.* Nature, 2007. **448**(7151): p. 318-24.
64. Yu, J., et al., *Induced pluripotent stem cell lines derived from human somatic cells.* Science, 2007. **318**(5858): p. 1917-20.
65. Takahashi, K., et al., *Induction of pluripotent stem cells from adult human fibroblasts by defined factors.* Cell, 2007. **131**(5): p. 861-72.
66. Park, I.H., et al., *Reprogramming of human somatic cells to pluripotency with defined factors.* Nature, 2008. **451**(7175): p. 141-6.
67. Maherali, N., et al., *Directly reprogrammed fibroblasts show global epigenetic remodeling and widespread tissue contribution.* Cell Stem Cell, 2007. **1**(1): p. 55-70.
68. Stadtfeld, M., et al., *Defining molecular cornerstones during fibroblast to iPS cell reprogramming in mouse.* Cell Stem Cell, 2008. **2**(3): p. 230-40.
69. Tam, P.P., S.X. Zhou, and S.S. Tan, *X-chromosome activity of the mouse primordial germ cells revealed by the expression of an X-linked lacZ transgene.* Development, 1994. **120**(10): p. 2925-32.
70. Turner, J.M., *Meiotic sex chromosome inactivation.* Development, 2007. **134**(10): p. 1823-31.
71. Russell, L.B., *Mammalian X-chromosome action: inactivation limited in spread and region of origin.* Science, 1963. **140**: p. 976-8.
72. Rastan, S., *Non-random X-chromosome inactivation in mouse X-autosome translocation embryos--location of the inactivation centre.* J Embryol Exp Morphol, 1983. **78**: p. 1-22.
73. Rastan, S. and E.J. Robertson, *X-chromosome deletions in embryo-derived (EK) cell lines associated with lack of X-chromosome inactivation.* J Embryol Exp Morphol, 1985. **90**: p. 379-88.
74. Brown, C.J., et al., *A gene from the region of the human X inactivation centre is expressed exclusively from the inactive X chromosome.* Nature, 1991. **349**(6304): p. 38-44.
75. Therman, E., G.E. Sarto, and K. Patau, *Center for Barr body condensation on the proximal part of the human Xq: a hypothesis.* Chromosoma, 1974. **44**(4): p. 361-6.
76. Therman, E., et al., *Position of the human X inactivation center on Xq.* Hum Genet, 1979. **50**(1): p. 59-64.
77. Pettigrew, A.L., et al., *Isodicentric X chromosome in a patient with Turner syndrome--implications for localization of the X-inactivation center.* Hum Genet, 1991. **87**(4): p. 498-502.
78. Mattei, M.G., et al., *Structural anomalies of the X chromosome and inactivation center.* Hum Genet, 1981. **56**(3): p. 401-8.
79. Flejter, W.L., D.L. Van Dyke, and L. Weiss, *Bends in human mitotic metaphase chromosomes, including a bend marking the X-inactivation center.* Am J Hum Genet, 1984. **36**(1): p. 218-26.
80. Flejter, W.L., D.L. Van Dyke, and L. Weiss, *Location of the X inactivation center in primates and other mammals.* Hum Genet, 1986. **74**(1): p. 63-6.
81. Brown, C.J., et al., *Localization of the X inactivation centre on the human X chromosome in Xq13.* Nature, 1991. **349**(6304): p. 82-4.

82. Rastan, S. and S.D. Brown, *The search for the mouse X-chromosome inactivation centre.* Genet Res, 1990. **56**(2-3): p. 99-106.
83. Heard, E. and P. Avner, *Role play in X-inactivation.* Hum Mol Genet, 1994. **3 Spec No**: p. 1481-5.
84. Borsani, G., et al., *Characterization of a murine gene expressed from the inactive X chromosome.* Nature, 1991. **351**(6324): p. 325-9.
85. Brockdorff, N., et al., *Conservation of position and exclusive expression of mouse Xist from the inactive X chromosome.* Nature, 1991. **351**(6324): p. 329-31.
86. Brockdorff, N., et al., *The product of the mouse Xist gene is a 15 kb inactive X-specific transcript containing no conserved ORF and located in the nucleus.* Cell, 1992. **71**(3): p. 515-26.
87. Brown, C.J., et al., *The human XIST gene: analysis of a 17 kb inactive X-specific RNA that contains conserved repeats and is highly localized within the nucleus.* Cell, 1992. **71**(3): p. 527-42.
88. Sheardown, S.A., et al., *Stabilization of Xist RNA mediates initiation of X chromosome inactivation.* Cell, 1997. **91**(1): p. 99-107.
89. Sun, B.K., A.M. Deaton, and J.T. Lee, *A transient heterochromatic state in Xist preempts X inactivation choice without RNA stabilization.* Mol Cell, 2006. **21**(5): p. 617-28.
90. Panning, B., J. Dausman, and R. Jaenisch, *X chromosome inactivation is mediated by Xist RNA stabilization.* Cell, 1997. **90**(5): p. 907-16.
91. Clemson, C.M., et al., *XIST RNA paints the inactive X chromosome at interphase: evidence for a novel RNA involved in nuclear/chromosome structure.* J Cell Biol, 1996. **132**(3): p. 259-75.
92. Jonkers, I., et al., *Xist RNA is confined to the nuclear territory of the silenced X chromosome throughout the cell cycle.* Mol Cell Biol, 2008. **28**(18): p. 5583-94.
93. Penny, G.D., et al., *Requirement for Xist in X chromosome inactivation.* Nature, 1996. **379**(6561): p. 131-7.
94. Marahrens, Y., et al., *Xist-deficient mice are defective in dosage compensation but not spermatogenesis.* Genes Dev, 1997. **11**(2): p. 156-66.
95. Csankovszki, G., et al., *Conditional deletion of Xist disrupts histone macroH2A localization but not maintenance of X inactivation.* Nat Genet, 1999. **22**(4): p. 323-4.
96. Kay, G.F., et al., *Expression of Xist during mouse development suggests a role in the initiation of X chromosome inactivation.* Cell, 1993. **72**(2): p. 171-82.
97. Plath, K., et al., *Role of histone H3 lysine 27 methylation in X inactivation.* Science, 2003. **300**(5616): p. 131-5.
98. Silva, J., et al., *Establishment of histone h3 methylation on the inactive X chromosome requires transient recruitment of Eed-Enx1 polycomb group complexes.* Dev Cell, 2003. **4**(4): p. 481-95.
99. Zhao, J., et al., *Polycomb proteins targeted by a short repeat RNA to the mouse X chromosome.* Science, 2008. **322**(5902): p. 750-6.
100. Pillet, N., C. Bonny, and D.F. Schorderet, *Characterization of the promoter region of the mouse Xist gene.* Proc Natl Acad Sci U S A, 1995. **92**(26): p. 12515-9.
101. Sheardown, S.A., et al., *Regulatory elements in the minimal promoter region of the mouse Xist gene.* Gene, 1997. **203**(2): p. 159-68.
102. Komura, J., et al., *In vivo ultraviolet and dimethyl sulfate footprinting of the 5' region of the expressed and silent Xist alleles.* J Biol Chem, 1997. **272**(16): p. 10975-80.
103. Newall, A.E., et al., *Primary non-random X inactivation associated with disruption of Xist promoter regulation.* Hum Mol Genet, 2001. **10**(6): p. 581-9.
104. Nesterova, T.B., et al., *Skewing X chromosome choice by modulating sense transcription across the Xist locus.* Genes Dev, 2003. **17**(17): p. 2177-90.
105. Korotkova, A.M., E.A. Elisafenko, and S.M. Zakiian, *[Functional analysis of the Xist promoter region in mouse Mus musculus].* Genetika, 2011. **47**(1): p. 140-4.
106. Johnston, C.M., et al., *Developmentally regulated Xist promoter switch mediates initiation of X inactivation.* Cell, 1998. **94**(6): p. 809-17.
107. Warshawsky, D., N. Stavropoulos, and J.T. Lee, *Further examination of the Xist promoter-switch hypothesis in X inactivation: evidence against the existence and function of a P(0) promoter.* Proc Natl Acad Sci U S A, 1999. **96**(25): p. 14424-9.
108. Hendrich, B.D., R.M. Plenge, and H.F. Willard, *Identification and characterization of the human XIST gene promoter: implications for models of X chromosome inactivation.* Nucleic Acids Res, 1997. **25**(13): p. 2661-71.
109. Norris, D.P., et al., *Evidence that random and imprinted Xist expression is controlled by preemptive methylation.* Cell, 1994. **77**(1): p. 41-51.

110. Hendrich, B.D., C.J. Brown, and H.F. Willard, *Evolutionary conservation of possible functional domains of the human and murine XIST genes.* Hum Mol Genet, 1993. **2**(6): p. 663-72.
111. Navarro, P., et al., *Tsix transcription across the Xist gene alters chromatin conformation without affecting Xist transcription: implications for X-chromosome inactivation.* Genes Dev, 2005. **19**(12): p. 1474-84.
112. Ohhata, T., et al., *Crucial role of antisense transcription across the Xist promoter in Tsix-mediated Xist chromatin modification.* Development, 2008. **135**(2): p. 227-35.
113. Panning, B. and R. Jaenisch, *DNA hypomethylation can activate Xist expression and silence X-linked genes.* Genes Dev, 1996. **10**(16): p. 1991-2002.
114. Beard, C., E. Li, and R. Jaenisch, *Loss of methylation activates Xist in somatic but not in embryonic cells.* Genes Dev, 1995. **9**(19): p. 2325-34.
115. Wutz, A., T.P. Rasmussen, and R. Jaenisch, *Chromosomal silencing and localization are mediated by different domains of Xist RNA.* Nat Genet, 2002. **30**(2): p. 167-74.
116. Elisaphenko, E.A., et al., *A dual origin of the Xist gene from a protein-coding gene and a set of transposable elements.* PLoS ONE, 2008. **3**(6): p. e2521.
117. Nesterova, T.B., et al., *Characterization of the genomic Xist locus in rodents reveals conservation of overall gene structure and tandem repeats but rapid evolution of unique sequence.* Genome Res, 2001. **11**(5): p. 833-49.
118. Lee, J.T., L.S. Davidow, and D. Warshawsky, *Tsix, a gene antisense to Xist at the X-inactivation centre.* Nat Genet, 1999. **21**(4): p. 400-4.
119. Lee, J.T. and N. Lu, *Targeted mutagenesis of Tsix leads to nonrandom X inactivation.* Cell, 1999. **99**(1): p. 47-57.
120. Clerc, P. and P. Avner, *Role of the region 3' to Xist exon 6 in the counting process of X-chromosome inactivation.* Nat Genet, 1998. **19**(3): p. 249-53.
121. Shibata, S. and J.T. Lee, *Characterization and quantitation of differential Tsix transcripts: implications for Tsix function.* Hum Mol Genet, 2003. **12**(2): p. 125-36.
122. Marks, H., et al., *High-resolution analysis of epigenetic changes associated with X inactivation.* Genome Res, 2009. **19**(8): p. 1361-73.
123. Luikenhuis, S., A. Wutz, and R. Jaenisch, *Antisense transcription through the Xist locus mediates Tsix function in embryonic stem cells.* Mol Cell Biol, 2001. **21**(24): p. 8512-20.
124. Ohhata, T., et al., *Lineage-specific function of the noncoding Tsix RNA for Xist repression and Xi reactivation in mice.* Genes Dev, 2011. **25**(16): p. 1702-15.
125. Navarro, P., et al., *Tsix-mediated epigenetic switch of a CTCF-flanked region of the Xist promoter determines the Xist transcription program.* Genes Dev, 2006. **20**(20): p. 2787-92.
126. Sado, T., Y. Hoki, and H. Sasaki, *Tsix silences Xist through modification of chromatin structure.* Dev Cell, 2005. **9**(1): p. 159-65.
127. Vigneau, S., et al., *An essential role for the DXPas34 tandem repeat and Tsix transcription in the counting process of X chromosome inactivation.* Proc Natl Acad Sci U S A, 2006. **103**(19): p. 7390-5.
128. Cohen, D.E., et al., *The DXPas34 repeat regulates random and imprinted X inactivation.* Dev Cell, 2007. **12**(1): p. 57-71.
129. Debrand, E., et al., *Functional analysis of the DXPas34 locus, a 3' regulator of Xist expression.* Mol Cell Biol, 1999. **19**(12): p. 8513-25.
130. Prissette, M., et al., *Methylation profiles of DXPas34 during the onset of X-inactivation.* Hum Mol Genet, 2001. **10**(1): p. 31-8.
131. Boumil, R.M., et al., *Differential methylation of Xite and CTCF sites in Tsix mirrors the pattern of X-inactivation choice in mice.* Mol Cell Biol, 2006. **26**(6): p. 2109-17.
132. Ogawa, Y., B.K. Sun, and J.T. Lee, *Intersection of the RNA interference and X-inactivation pathways.* Science, 2008. **320**(5881): p. 1336-41.
133. Nesterova, T.B., et al., *Dicer regulates Xist promoter methylation in ES cells indirectly through transcriptional control of Dnmt3a.* Epigenetics Chromatin, 2008. **1**(1): p. 2.
134. Kanellopoulou, C., et al., *X chromosome inactivation in the absence of Dicer.* Proc Natl Acad Sci U S A, 2009. **106**(4): p. 1122-7.
135. Shibata, S. and J.T. Lee, *Tsix transcription- versus RNA-based mechanisms in Xist repression and epigenetic choice.* Curr Biol, 2004. **14**(19): p. 1747-54.
136. Ogawa, Y. and J.T. Lee, *Xite, X-inactivation intergenic transcription elements that regulate the probability of choice.* Mol Cell, 2003. **11**(3): p. 731-43.

137. Stavropoulos, N., R.K. Rowntree, and J.T. Lee, *Identification of developmentally specific enhancers for Tsix in the regulation of X chromosome inactivation.* Mol Cell Biol, 2005. **25**(7): p. 2757-69.
138. Rogner, U.C., et al., *Control of neurulation by the nucleosome assembly protein-1-like 2.* Nat Genet, 2000. **25**(4): p. 431-5.
139. Rougeulle, C. and P. Avner, *Cloning and characterization of a murine brain specific gene Bpx and its human homologue lying within the Xic candidate region.* Hum Mol Genet, 1996. **5**(1): p. 41-9.
140. Chureau, C., et al., *Comparative sequence analysis of the X-inactivation center region in mouse, human, and bovine.* Genome Res, 2002. **12**(6): p. 894-908.
141. Gamer, L.W. and C.V. Wright, *Murine Cdx-4 bears striking similarities to the Drosophila caudal gene in its homeodomain sequence and early expression pattern.* Mech Dev, 1993. **43**(1): p. 71-81.
142. Simmler, M.C., et al., *Localization and expression analysis of a novel conserved brain expressed transcript, Brx/BRX, lying within the Xic/XIC candidate region.* Mamm Genome, 1997. **8**(10): p. 760-6.
143. Simmler, M.C., et al., *A 94 kb genomic sequence 3' to the murine Xist gene reveals an AT rich region containing a new testis specific gene Tsx.* Hum Mol Genet, 1996. **5**(11): p. 1713-26.
144. Cunningham, D.B., et al., *The mouse Tsx gene is expressed in Sertoli cells of the adult testis and transiently in premeiotic germ cells during puberty.* Dev Biol, 1998. **204**(2): p. 345-60.
145. Sebastiano, V., et al., *Cloned pre-implantation mouse embryos show correct timing but altered levels of gene expression.* Mol Reprod Dev, 2005. **70**(2): p. 146-54.
146. Johnston, C.M., et al., *Enox, a novel gene that maps 10 kb upstream of Xist and partially escapes X inactivation.* Genomics, 2002. **80**(2): p. 236-44.
147. Chow, J.C., et al., *Characterization of expression at the human XIST locus in somatic, embryonal carcinoma, and transgenic cell lines.* Genomics, 2003. **82**(3): p. 309-22.
148. Lafreniere, R.G., L. Carrel, and H.F. Willard, *A novel transmembrane transporter encoded by the XPCT gene in Xq13.2.* Hum Mol Genet, 1994. **3**(7): p. 1133-9.
149. Debrand, E., E. Heard, and P. Avner, *Cloning and localization of the murine Xpct gene: evidence for complex rearrangements during the evolution of the region around the Xist gene.* Genomics, 1998. **48**(3): p. 296-303.
150. Friesema, E.C., et al., *Identification of monocarboxylate transporter 8 as a specific thyroid hormone transporter.* J Biol Chem, 2003. **278**(41): p. 40128-35.
151. Schwartz, C.E., et al., *Allan-Herndon-Dudley syndrome and the monocarboxylate transporter 8 (MCT8) gene.* Am J Hum Genet, 2005. **77**(1): p. 41-53.
152. Friesema, E.C., et al., *Association between mutations in a thyroid hormone transporter and severe X-linked psychomotor retardation.* Lancet, 2004. **364**(9443): p. 1435-7.
153. Koina, E., et al., *Isolation, X location and activity of the marsupial homologue of SLC16A2, an XIST-flanking gene in eutherian mammals.* Chromosome Res, 2005. **13**(7): p. 687-98.
154. Sugiura, M., et al., *Overexpression of MCT8 enhances the differentiation of ES cells into neural progenitors.* Biochem Biophys Res Commun, 2007. **360**(4): p. 741-5.
155. Trajkovic, M., et al., *Abnormal thyroid hormone metabolism in mice lacking the monocarboxylate transporter 8.* J Clin Invest, 2007. **117**(3): p. 627-35.
156. Heard, E., et al., *Methylation of histone H3 at Lys-9 is an early mark on the X chromosome during X inactivation.* Cell, 2001. **107**(6): p. 727-38.
157. Rougeulle, C., et al., *Differential histone H3 Lys-9 and Lys-27 methylation profiles on the X chromosome.* Mol Cell Biol, 2004. **24**(12): p. 5475-84.
158. Jacobs, P.A., et al., *Evidence for the existence of the human "super female".* Lancet, 1959. **2**(7100): p. 423-5.
159. Maclean, N. and J.M. Mitchell, *A survey of sex-chromosome abnormalities among 4514 mental defectives.* Lancet, 1962. **1**(7224): p. 293-6.
160. Grumbach, M.M., A. Morishima, and J.H. Taylor, *Human Sex Chromosome Abnormalities in Relation to DNA Replication and Heterochromatinization.* Proc Natl Acad Sci U S A, 1963. **49**(5): p. 581-9.
161. Carr, D.H., *Chromosome studies in selected spontaneous abortions. 1. Conception after oral contraceptives.* Can Med Assoc J, 1970. **103**(4): p. 343-8.
162. Webb, S., T.J. de Vries, and M.H. Kaufman, *The differential staining pattern of the X chromosome in the embryonic and extraembryonic tissues of postimplantation homozygous tetraploid mouse embryos.* Genet Res, 1992. **59**(3): p. 205-14.
163. Harnden, D.G., *Nuclear sex in triploid XXY human cells.* Lancet, 1961. **2**(7200): p. 488.
164. Nicodemi, M. and A. Prisco, *Symmetry-breaking model for X-chromosome inactivation.* Phys Rev Lett, 2007. **98**(10): p. 108104.

165. Nicodemi, M. and A. Prisco, *Self-assembly and DNA binding of the blocking factor in x chromosome inactivation.* PLoS Comput Biol, 2007. **3**(11): p. e210.
166. Lee, J.T., et al., *A 450 kb transgene displays properties of the mammalian X-inactivation center.* Cell, 1996. **86**(1): p. 83-94.
167. Herzing, L.B., et al., *Xist has properties of the X-chromosome inactivation centre.* Nature, 1997. **386**(6622): p. 272-5.
168. Lee, J.T. and R. Jaenisch, *Long-range cis effects of ectopic X-inactivation centres on a mouse autosome.* Nature, 1997. **386**(6622): p. 275-9.
169. Lee, J.T., N. Lu, and Y. Han, *Genetic analysis of the mouse X inactivation center defines an 80-kb multifunction domain.* Proc Natl Acad Sci U S A, 1999. **96**(7): p. 3836-41.
170. Migeon, B.R., et al., *Human X inactivation center induces random X chromosome inactivation in male transgenic mice.* Genomics, 1999. **59**(2): p. 113-21.
171. Migeon, B.R., et al., *Low-copy-number human transgene is recognized as an X inactivation center in mouse ES cells, but fails to induce cis-inactivation in chimeric mice.* Genomics, 2001. **71**(2): p. 156-62.
172. Heard, E., et al., *Transgenic mice carrying an Xist-containing YAC.* Hum Mol Genet, 1996. **5**(4): p. 441-50.
173. Matsuura, S., et al., *Xist expression from an Xist YAC transgene carried on the mouse Y chromosome.* Hum Mol Genet, 1996. **5**(4): p. 451-9.
174. Jonkers, I., et al., *RNF12 is an X-Encoded dose-dependent activator of X chromosome inactivation.* Cell, 2009. **139**(5): p. 999-1011.
175. Heard, E., et al., *Xist yeast artificial chromosome transgenes function as X-inactivation centers only in multicopy arrays and not as single copies.* Mol Cell Biol, 1999. **19**(4): p. 3156-66.
176. Gribnau, J., et al., *X chromosome choice occurs independently of asynchronous replication timing.* J Cell Biol, 2005. **168**(3): p. 365-73.
177. Marahrens, Y., J. Loring, and R. Jaenisch, *Role of the Xist gene in X chromosome choosing.* Cell, 1998. **92**(5): p. 657-64.
178. Sado, T., E. Li, and H. Sasaki, *Effect of TSIX disruption on XIST expression in male ES cells.* Cytogenet Genome Res, 2002. **99**(1-4): p. 115-8.
179. Monkhorst, K., et al., *X inactivation counting and choice is a stochastic process: evidence for involvement of an X-linked activator.* Cell, 2008. **132**(3): p. 410-21.
180. Lee, J.T., *Homozygous Tsix mutant mice reveal a sex-ratio distortion and revert to random X-inactivation.* Nat Genet, 2002. **32**(1): p. 195-200.
181. Mlynarczyk-Evans, S., et al., *X chromosomes alternate between two states prior to random X-inactivation.* PLoS Biol, 2006. **4**(6): p. e159.
182. Bacher, C.P., et al., *Transient colocalization of X-inactivation centres accompanies the initiation of X inactivation.* Nat Cell Biol, 2006. **8**(3): p. 293-9.
183. Xu, N., C.L. Tsai, and J.T. Lee, *Transient homologous chromosome pairing marks the onset of X inactivation.* Science, 2006. **311**(5764): p. 1149-52.
184. Masui, O., et al., *Live-cell chromosome dynamics and outcome of X chromosome pairing events during ES cell differentiation.* Cell, **145**(3): p. 447-58.
185. Xu, N., et al., *Evidence that homologous X-chromosome pairing requires transcription and Ctcf protein.* Nat Genet, 2007. **39**(11): p. 1390-6.
186. Donohoe, M.E., et al., *The pluripotency factor Oct4 interacts with Ctcf and also controls X-chromosome pairing and counting.* Nature, 2009. **460**(7251): p. 128-32.
187. Augui, S., et al., *Sensing X chromosome pairs before X inactivation via a novel X-pairing region of the Xic.* Science, 2007. **318**(5856): p. 1632-6.
188. Takagi, N., *Variable X chromosome inactivation patterns in near-tetraploid murine EC x somatic cell hybrid cells differentiated in vitro.* Genetica, 1993. **88**(2-3): p. 107-17.
189. Monkhorst, K., et al., *The probability to initiate X chromosome inactivation is determined by the X to autosomal ratio and X chromosome specific allelic properties.* PLoS One, 2009. **4**(5): p. e5616.
190. Monk, M. and M.I. Harper, *Sequential X chromosome inactivation coupled with cellular differentiation in early mouse embryos.* Nature, 1979. **281**(5729): p. 311-3.
191. Navarro, P., et al., *Molecular coupling of Xist regulation and pluripotency.* Science, 2008. **321**(5896): p. 1693-5.
192. Navarro, P. and P. Avner, *An embryonic story: analysis of the gene regulative network controlling Xist expression in mouse embryonic stem cells.* Bioessays, 2010. **32**(7): p. 581-8.

193. Donohoe, M.E., et al., *Identification of a Ctcf cofactor, Yy1, for the X chromosome binary switch.* Mol Cell, 2007. **25**(1): p. 43-56.
194. Ma, Z., et al., *Sequence-specific regulator Prdm14 safeguards mouse ESCs from entering extraembryonic endoderm fates.* Nat Struct Mol Biol, 2011. **18**(2): p. 120-7.
195. Marson, A., et al., *Wnt signaling promotes reprogramming of somatic cells to pluripotency.* Cell Stem Cell, 2008. **3**(2): p. 132-5.
196. Barr, M.L. and E.G. Bertram, *A morphological distinction between neurones of the male and female, and the behaviour of the nucleolar satellite during accelerated nucleoprotein synthesis.* Nature, 1949. **163**(4148): p. 676.
197. Ohno, S. and T.S. Hauschka, *Allocycly of the X-chromosome in tumors and normal tissues.* Cancer Res, 1960. **20**: p. 541-5.
198. Chaumeil, J., et al., *A novel role for Xist RNA in the formation of a repressive nuclear compartment into which genes are recruited when silenced.* Genes Dev, 2006. **20**(16): p. 2223-37.
199. Clemson, C.M., et al., *The X chromosome is organized into a gene-rich outer rim and an internal core containing silenced nongenic sequences.* Proc Natl Acad Sci U S A, 2006. **103**(20): p. 7688-93.
200. Goto, Y., et al., *Differential patterns of histone methylation and acetylation distinguish active and repressed alleles at X-linked genes.* Cytogenet Genome Res, 2002. **99**(1-4): p. 66-74.
201. Mak, W., et al., *Mitotically stable association of polycomb group proteins eed and enx1 with the inactive x chromosome in trophoblast stem cells.* Curr Biol, 2002. **12**(12): p. 1016-20.
202. Boggs, B.A., et al., *Differentially methylated forms of histone H3 show unique association patterns with inactive human X chromosomes.* Nat Genet, 2002. **30**(1): p. 73-6.
203. Mermoud, J.E., et al., *Histone H3 lysine 9 methylation occurs rapidly at the onset of random X chromosome inactivation.* Curr Biol, 2002. **12**(3): p. 247-51.
204. Peters, A.H., et al., *Histone H3 lysine 9 methylation is an epigenetic imprint of facultative heterochromatin.* Nat Genet, 2002. **30**(1): p. 77-80.
205. Kohlmaier, A., et al., *A chromosomal memory triggered by Xist regulates histone methylation in X inactivation.* PLoS Biol, 2004. **2**(7): p. E171.
206. de Napoles, M., et al., *Polycomb group proteins Ring1A/B link ubiquitylation of histone H2A to heritable gene silencing and X inactivation.* Dev Cell, 2004. **7**(5): p. 663-76.
207. Fang, J., et al., *Ring1b-mediated H2A ubiquitination associates with inactive X chromosomes and is involved in initiation of X inactivation.* J Biol Chem, 2004. **279**(51): p. 52812-5.
208. Costanzi, C. and J.R. Pehrson, *Histone macroH2A1 is concentrated in the inactive X chromosome of female mammals.* Nature, 1998. **393**(6685): p. 599-601.
209. Lock, L.F., N. Takagi, and G.R. Martin, *Methylation of the Hprt gene on the inactive X occurs after chromosome inactivation.* Cell, 1987. **48**(1): p. 39-46.
210. Norris, D.P., N. Brockdorff, and S. Rastan, *Methylation status of CpG-rich islands on active and inactive mouse X chromosomes.* Mamm Genome, 1991. **1**(2): p. 78-83.
211. Mohandas, T., R.S. Sparkes, and L.J. Shapiro, *Reactivation of an inactive human X chromosome: evidence for X inactivation by DNA methylation.* Science, 1981. **211**(4480): p. 393-6.
212. Senner, C.E., et al., *Disruption of a conserved region of Xist exon 1 impairs Xist RNA localisation and X-linked gene silencing during random and imprinted X chromosome inactivation.* Development, 2011. **138**(8): p. 1541-50.
213. Beletskii, A., et al., *PNA interference mapping demonstrates functional domains in the noncoding RNA Xist.* Proc Natl Acad Sci U S A, 2001. **98**(16): p. 9215-20.
214. Sarma, K., et al., *Locked nucleic acids (LNAs) reveal sequence requirements and kinetics of Xist RNA localization to the X chromosome.* Proc Natl Acad Sci U S A, 2010. **107**(51): p. 22196-201.
215. Fackelmayer, F.O., *A stable proteinaceous structure in the territory of inactive X chromosomes.* J Biol Chem, 2005. **280**(3): p. 1720-3.
216. Hasegawa, Y., et al., *The matrix protein hnRNP U is required for chromosomal localization of Xist RNA.* Dev Cell, 2010. **19**(3): p. 469-76.
217. Helbig, R. and F.O. Fackelmayer, *Scaffold attachment factor A (SAF-A) is concentrated in inactive X chromosome territories through its RGG domain.* Chromosoma, 2003. **112**(4): p. 173-82.
218. Pullirsch, D., et al., *The Trithorax group protein Ash2l and Saf-A are recruited to the inactive X chromosome at the onset of stable X inactivation.* Development, 2010. **137**(6): p. 935-43.
219. Roshon, M.J. and H.E. Ruley, *Hypomorphic mutation in hnRNP U results in post-implantation lethality.* Transgenic Res, 2005. **14**(2): p. 179-92.

220. Jeon, Y. and J.T. Lee, *YY1 tethers Xist RNA to the inactive X nucleation center.* Cell, 2011. **146**(1): p. 119-33.
221. Ganesan, S., et al., *BRCA1 supports XIST RNA concentration on the inactive X chromosome.* Cell, 2002. **111**(3): p. 393-405.
222. Silver, D.P., et al., *Further evidence for BRCA1 communication with the inactive X chromosome.* Cell, 2007. **128**(5): p. 991-1002.
223. Vincent-Salomon, A., et al., *X inactive-specific transcript RNA coating and genetic instability of the X chromosome in BRCA1 breast tumors.* Cancer Res, 2007. **67**(11): p. 5134-40.
224. Xiao, C., et al., *The XIST noncoding RNA functions independently of BRCA1 in X inactivation.* Cell, 2007. **128**(5): p. 977-89.
225. Russell, L.B. and C.S. Montgomery, *Comparative studies on X-autosome translocations in the mouse. II. Inactivation of autosomal loci, segregation, and mapping of autosomal breakpoints in five T (X;1) S.* Genetics, 1970. **64**(2): p. 281-312.
226. Duthie, S.M., et al., *Xist RNA exhibits a banded localization on the inactive X chromosome and is excluded from autosomal material in cis.* Hum Mol Genet, 1999. **8**(2): p. 195-204.
227. Keohane, A.M., et al., *H4 acetylation, XIST RNA and replication timing are coincident and define x;autosome boundaries in two abnormal X chromosomes.* Hum Mol Genet, 1999. **8**(2): p. 377-83.
228. Popova, B.C., et al., *Attenuated spread of X-inactivation in an X;autosome translocation.* Proc Natl Acad Sci U S A, 2006. **103**(20): p. 7706-11.
229. Gartler, S.M. and A.D. Riggs, *Mammalian X-chromosome inactivation.* Annu Rev Genet, 1983. **17**: p. 155-90.
230. Lyon, M.F., *X-chromosome inactivation: a repeat hypothesis.* Cytogenet Cell Genet, 1998. **80**(1-4): p. 133-7.
231. Lyon, M.F., *LINE-1 elements and X chromosome inactivation: a function for "junk" DNA?* Proc Natl Acad Sci U S A, 2000. **97**(12): p. 6248-9.
232. Lyon, M.F., *Do LINEs Have a Role in X-Chromosome Inactivation?* J Biomed Biotechnol, 2006. **2006**(1): p. 59746.
233. Lyon, M.F., *No longer 'all-or-none'.* Eur J Hum Genet, 2005. **13**(7): p. 796-7.
234. Wichman, H.A., et al., *Transposable elements and the evolution of genome organization in mammals.* Genetica, 1992. **86**(1-3): p. 287-93.
235. Furano, A.V., *The biological properties and evolutionary dynamics of mammalian LINE-1 retrotransposons.* Prog Nucleic Acid Res Mol Biol, 2000. **64**: p. 255-94.
236. Parish, D.A., et al., *Distribution of LINEs and other repetitive elements in the karyotype of the bat Carollia: implications for X-chromosome inactivation.* Cytogenet Genome Res, 2002. **96**(1-4): p. 191-7.
237. Waters, P.D., et al., *LINE-1 distribution in Afrotheria and Xenarthra: implications for understanding the evolution of LINE-1 in eutherian genomes.* Chromosoma, 2004. **113**(3): p. 137-44.
238. Bailey, J.A., et al., *Molecular evidence for a relationship between LINE-1 elements and X chromosome inactivation: the Lyon repeat hypothesis.* Proc Natl Acad Sci U S A, 2000. **97**(12): p. 6634-9.
239. Dobigny, G., et al., *Viability of X-autosome translocations in mammals: an epigenomic hypothesis from a rodent case-study.* Chromosoma, 2004. **113**(1): p. 34-41.
240. Carrel, L. and H.F. Willard, *X-inactivation profile reveals extensive variability in X-linked gene expression in females.* Nature, 2005. **434**(7031): p. 400-4.
241. Wang, Z., et al., *Evidence of influence of genomic DNA sequence on human X chromosome inactivation.* PLoS Comput Biol, 2006. **2**(9): p. e113.
242. White, W.M., et al., *The spreading of X inactivation into autosomal material of an x;autosome translocation: evidence for a difference between autosomal and X-chromosomal DNA.* Am J Hum Genet, 1998. **63**(1): p. 20-8.
243. Sharp, A., D.O. Robinson, and P. Jacobs, *Absence of correlation between late-replication and spreading of X inactivation in an X;autosome translocation.* Hum Genet, 2001. **109**(3): p. 295-302.
244. Solari, A.J., et al., *The behavior of sex chromosomes in two human X-autosome translocations: failure of extensive X-inactivation spreading.* Biocell, 2001. **25**(2): p. 155-66.
245. Hall, L.L., et al., *Unbalanced X;autosome translocations provide evidence for sequence specificity in the association of XIST RNA with chromatin.* Hum Mol Genet, 2002. **11**(25): p. 3157-65.
246. Sharp, A.J., et al., *Molecular and cytogenetic analysis of the spreading of X inactivation in X;autosome translocations.* Hum Mol Genet, 2002. **11**(25): p. 3145-56.

247. Ke, X. and A. Collins, *CpG islands in human X-inactivation.* Ann Hum Genet, 2003. **67**(Pt 3): p. 242-9.
248. Cantrell, M.A., B.C. Carstens, and H.A. Wichman, *X chromosome inactivation and Xist evolution in a rodent lacking LINE-1 activity.* PLoS One, 2009. **4**(7): p. e6252.
249. Tang, Y.A., et al., *Efficiency of Xist-mediated silencing on autosomes is linked to chromosomal domain organisation.* Epigenetics Chromatin, 2010. **3**(1): p. 10.
250. Chow, J.C., et al., *LINE-1 activity in facultative heterochromatin formation during X chromosome inactivation.* Cell, 2010. **141**(6): p. 956-69.
251. Hansen, R.S., *X inactivation-specific methylation of LINE-1 elements by DNMT3B: implications for the Lyon repeat hypothesis.* Hum Mol Genet, 2003. **12**(19): p. 2559-67.
252. Cao, R. and Y. Zhang, *SUZ12 is required for both the histone methyltransferase activity and the silencing function of the EED-EZH2 complex.* Mol Cell, 2004. **15**(1): p. 57-67.
253. de la Cruz, C.C., et al., *Developmental regulation of Suz 12 localization.* Chromosoma, 2005. **114**(3): p. 183-92.
254. Kaneko, S., et al., *Phosphorylation of the PRC2 component Ezh2 is cell cycle-regulated and up-regulates its binding to ncRNA.* Genes Dev, 2010. **24**(23): p. 2615-20.
255. Kanhere, A., et al., *Short RNAs are transcribed from repressed polycomb target genes and interact with polycomb repressive complex-2.* Mol Cell, 2010. **38**(5): p. 675-88.
256. Wang, J., et al., *Imprinted X inactivation maintained by a mouse Polycomb group gene.* Nat Genet, 2001. **28**(4): p. 371-5.
257. Kalantry, S. and T. Magnuson, *The Polycomb group protein EED is dispensable for the initiation of random X-chromosome inactivation.* PLoS Genet, 2006. **2**(5): p. e66.
258. Schoeftner, S., et al., *Recruitment of PRC1 function at the initiation of X inactivation independent of PRC2 and silencing.* Embo J, 2006. **25**(13): p. 3110-22.
259. Hoki, Y., et al., *A proximal conserved repeat in the Xist gene is essential as a genomic element for X-inactivation in mouse.* Development, 2009. **136**(1): p. 139-46.
260. Royce-Tolland, M.E., et al., *The A-repeat links ASF/SF2-dependent Xist RNA processing with random choice during X inactivation.* Nat Struct Mol Biol, 2010. **17**(8): p. 948-54.
261. Wutz, A. and R. Jaenisch, *A shift from reversible to irreversible X inactivation is triggered during ES cell differentiation.* Mol Cell, 2000. **5**(4): p. 695-705.
262. Hoki, Y., et al., *Incomplete X-inactivation initiated by a hypomorphic Xist allele in the mouse.* Development, 2011. **138**(13): p. 2649-59.
263. Landeira, D., et al., *Jarid2 is a PRC2 component in embryonic stem cells required for multi-lineage differentiation and recruitment of PRC1 and RNA Polymerase II to developmental regulators.* Nat Cell Biol, 2010. **12**(6): p. 618-24.
264. Peng, J.C., et al., *Jarid2/Jumonji coordinates control of PRC2 enzymatic activity and target gene occupancy in pluripotent cells.* Cell, 2009. **139**(7): p. 1290-302.
265. Shen, X., et al., *Jumonji modulates polycomb activity and self-renewal versus differentiation of stem cells.* Cell, 2009. **139**(7): p. 1303-14.
266. Casanova, M., et al., *Polycomblike 2 facilitates the recruitment of PRC2 Polycomb group complexes to the inactive X chromosome and to target loci in embryonic stem cells.* Development, 2011. **138**(8): p. 1471-82.
267. Fischle, W., et al., *Molecular basis for the discrimination of repressive methyl-lysine marks in histone H3 by Polycomb and HP1 chromodomains.* Genes Dev, 2003. **17**(15): p. 1870-81.
268. Min, J., Y. Zhang, and R.M. Xu, *Structural basis for specific binding of Polycomb chromodomain to histone H3 methylated at Lys 27.* Genes Dev, 2003. **17**(15): p. 1823-8.
269. Wang, L., et al., *Hierarchical recruitment of polycomb group silencing complexes.* Mol Cell, 2004. **14**(5): p. 637-46.
270. Leeb, M., et al., *Polycomb complexes act redundantly to repress genomic repeats and genes.* Genes Dev, 2010. **24**(3): p. 265-76.
271. Tavares, L., et al., *RYBP-PRC1 complexes mediate H2A ubiquitylation at polycomb target sites independently of PRC2 and H3K27me3.* Cell, 2012. **148**(4): p. 664-78.
272. Arrigoni, R., et al., *The Polycomb-associated protein Rybp is a ubiquitin binding protein.* FEBS Lett, 2006. **580**(26): p. 6233-41.
273. Savarese, F., et al., *Hematopoietic precursor cells transiently reestablish permissiveness for X inactivation.* Mol Cell Biol, 2006. **26**(19): p. 7167-77.

274. Agrelo, R., et al., *SATB1 defines the developmental context for gene silencing by Xist in lymphoma and embryonic cells.* Dev Cell, 2009. **16**(4): p. 507-16.
275. Han, H.J., et al., *SATB1 reprogrammes gene expression to promote breast tumour growth and metastasis.* Nature, 2008. **452**(7184): p. 187-93.
276. Alvarez, J.D., et al., *The MAR-binding protein SATB1 orchestrates temporal and spatial expression of multiple genes during T-cell development.* Genes Dev, 2000. **14**(5): p. 521-35.
277. Britanova, O., et al., *Satb2 haploinsufficiency phenocopies 2q32-q33 deletions, whereas loss suggests a fundamental role in the coordination of jaw development.* Am J Hum Genet, 2006. **79**(4): p. 668-78.
278. Dobreva, G., et al., *SATB2 is a multifunctional determinant of craniofacial patterning and osteoblast differentiation.* Cell, 2006. **125**(5): p. 971-86.
279. Hernandez-Munoz, I., et al., *Stable X chromosome inactivation involves the PRC1 Polycomb complex and requires histone MACROH2A1 and the CULLIN3/SPOP ubiquitin E3 ligase.* Proc Natl Acad Sci U S A, 2005. **102**(21): p. 7635-40.
280. Nusinow, D.A., et al., *Poly(ADP-ribose) polymerase 1 is inhibited by a histone H2A variant, MacroH2A, and contributes to silencing of the inactive X chromosome.* J Biol Chem, 2007. **282**(17): p. 12851-9.
281. Kim, M.Y., T. Zhang, and W.L. Kraus, *Poly(ADP-ribosyl)ation by PARP-1: 'PAR-laying' NAD+ into a nuclear signal.* Genes Dev, 2005. **19**(17): p. 1951-67.
282. Rouleau, M., R.A. Aubin, and G.G. Poirier, *Poly(ADP-ribosyl)ated chromatin domains: access granted.* J Cell Sci, 2004. **117**(Pt 6): p. 815-25.
283. Hassa, P.O., et al., *Nuclear ADP-ribosylation reactions in mammalian cells: where are we today and where are we going?* Microbiol Mol Biol Rev, 2006. **70**(3): p. 789-829.
284. Kim, M.Y., et al., *NAD+-dependent modulation of chromatin structure and transcription by nucleosome binding properties of PARP-1.* Cell, 2004. **119**(6): p. 803-14.
285. Chadwick, B.P. and H.F. Willard, *Histone H2A variants and the inactive X chromosome: identification of a second macroH2A variant.* Hum Mol Genet, 2001. **10**(10): p. 1101-13.
286. Mietton, F., et al., *Weak but uniform enrichment of the histone variant macroH2A1 along the inactive X chromosome.* Mol Cell Biol, 2009. **29**(1): p. 150-6.
287. Rasmussen, T.P., et al., *Expression of Xist RNA is sufficient to initiate macrochromatin body formation.* Chromosoma, 2001. **110**(6): p. 411-20.
288. Costanzi, C., et al., *Histone macroH2A1 is concentrated in the inactive X chromosome of female preimplantation mouse embryos.* Development, 2000. **127**(11): p. 2283-9.
289. Changolkar, L.N., et al., *Developmental changes in histone macroH2A1-mediated gene regulation.* Mol Cell Biol, 2007. **27**(7): p. 2758-64.
290. Boulard, M., et al., *Histone variant macroH2A1 deletion in mice causes female-specific steatosis.* Epigenetics Chromatin, 2010. **3**(1): p. 8.
291. Costanzi, C. and J.R. Pehrson, *MACROH2A2, a new member of the MARCOH2A core histone family.* J Biol Chem, 2001. **276**(24): p. 21776-84.
292. Rasmussen, T.P., et al., *Messenger RNAs encoding mouse histone macroH2A1 isoforms are expressed at similar levels in male and female cells and result from alternative splicing.* Nucleic Acids Res, 1999. **27**(18): p. 3685-9.
293. Tanasijevic, B. and T.P. Rasmussen, *X chromosome inactivation and differentiation occur readily in ES cells doubly-deficient for macroH2A1 and macroH2A2.* PLoS One, 2011. **6**(6): p. e21512.
294. Cotton, A.M., et al., *Chromosome-wide DNA methylation analysis predicts human tissue-specific X inactivation.* Hum Genet, 2011. **130**(2): p. 187-201.
295. Weber, M., et al., *Chromosome-wide and promoter-specific analyses identify sites of differential DNA methylation in normal and transformed human cells.* Nat Genet, 2005. **37**(8): p. 853-62.
296. Hellman, A. and A. Chess, *Gene body-specific methylation on the active X chromosome.* Science, 2007. **315**(5815): p. 1141-3.
297. Sado, T., et al., *X inactivation in the mouse embryo deficient for Dnmt1: distinct effect of hypomethylation on imprinted and random X inactivation.* Dev Biol, 2000. **225**(2): p. 294-303.
298. Sado, T., et al., *De novo DNA methylation is dispensable for the initiation and propagation of X chromosome inactivation.* Development, 2004. **131**(5): p. 975-82.
299. Blewitt, M.E., et al., *An N-ethyl-N-nitrosourea screen for genes involved in variegation in the mouse.* Proc Natl Acad Sci U S A, 2005. **102**(21): p. 7629-34.
300. Blewitt, M.E., et al., *SmcHD1, containing a structural-maintenance-of-chromosomes hinge domain, has a critical role in X inactivation.* Nat Genet, 2008. **40**(5): p. 663-9.

301. Kanno, T., et al., *A structural-maintenance-of-chromosomes hinge domain-containing protein is required for RNA-directed DNA methylation.* Nat Genet, 2008. **40**(5): p. 670-5.
302. Garrick, D., et al., *Loss of Atrx affects trophoblast development and the pattern of X-inactivation in extraembryonic tissues.* PLoS Genet, 2006. **2**(4): p. e58.
303. Baumann, C. and R. De La Fuente, *ATRX marks the inactive X chromosome (Xi) in somatic cells and during imprinted X chromosome inactivation in trophoblast stem cells.* Chromosoma, 2009. **118**(2): p. 209-22.
304. Brown, C.J. and H.F. Willard, *The human X-inactivation centre is not required for maintenance of X-chromosome inactivation.* Nature, 1994. **368**(6467): p. 154-6.
305. Al Nadaf, S., et al., *A cross-species comparison of escape from X inactivation in Eutheria: implications for evolution of X chromosome inactivation.* Chromosoma, 2012. **121**(1): p. 71-8.
306. Disteche, C.M., *Escape from X inactivation in human and mouse.* Trends Genet, 1995. **11**(1): p. 17-22.
307. Disteche, C.M., *Escapees on the X chromosome.* Proc Natl Acad Sci U S A, 1999. **96**(25): p. 14180-2.
308. Disteche, C.M., G.N. Filippova, and K.D. Tsuchiya, *Escape from X inactivation.* Cytogenet Genome Res, 2002. **99**(1-4): p. 36-43.
309. Brown, C.J. and J.M. Greally, *A stain upon the silence: genes escaping X inactivation.* Trends Genet, 2003. **19**(8): p. 432-8.
310. Yen, Z.C., et al., *A cross-species comparison of X-chromosome inactivation in Eutheria.* Genomics, 2007. **90**(4): p. 453-63.
311. Patrat, C., et al., *Dynamic changes in paternal X-chromosome activity during imprinted X-chromosome inactivation in mice.* Proc Natl Acad Sci U S A, 2009. **106**(13): p. 5198-203.
312. Yang, F., et al., *Global survey of escape from X inactivation by RNA-sequencing in mouse.* Genome Res, 2010. **20**(5): p. 614-22.
313. Carrel, L., et al., *Genomic environment predicts expression patterns on the human inactive X chromosome.* PLoS Genet, 2006. **2**(9): p. e151.
314. Gaszner, M. and G. Felsenfeld, *Insulators: exploiting transcriptional and epigenetic mechanisms.* Nat Rev Genet, 2006. **7**(9): p. 703-13.
315. Phillips, J.E. and V.G. Corces, *CTCF: master weaver of the genome.* Cell, 2009. **137**(7): p. 1194-211.
316. Filippova, G.N., et al., *Boundaries between chromosomal domains of X inactivation and escape bind CTCF and lack CpG methylation during early development.* Dev Cell, 2005. **8**(1): p. 31-42.
317. Ciavatta, D., et al., *A DNA insulator prevents repression of a targeted X-linked transgene but not its random or imprinted X inactivation.* Proc Natl Acad Sci U S A, 2006. **103**(26): p. 9958-63.
318. Li, N. and L. Carrel, *Escape from X chromosome inactivation is an intrinsic property of the Jarid1c locus.* Proc Natl Acad Sci U S A, 2008. **105**(44): p. 17055-60.
319. Chan, K.M., et al., *Diverse factors are involved in maintaining X chromosome inactivation.* Proc Natl Acad Sci U S A, 2011. **108**(40): p. 16699-704.
320. Bininda-Emonds, O.R., et al., *The delayed rise of present-day mammals.* Nature, 2007. **446**(7135): p. 507-12.
321. Rens, W., et al., *Resolution and evolution of the duck-billed platypus karyotype with an X1Y1X2Y2X3Y3X4Y4X5Y5 male sex chromosome constitution.* Proc Natl Acad Sci U S A, 2004. **101**(46): p. 16257-61.
322. Rens, W., et al., *The multiple sex chromosomes of platypus and echidna are not completely identical and several share homology with the avian Z.* Genome Biol, 2007. **8**(11): p. R243.
323. Grutzner, F., et al., *The monotreme genome: a patchwork of reptile, mammal and unique features?* Comp Biochem Physiol A Mol Integr Physiol, 2003. **136**(4): p. 867-81.
324. Grutzner, F. and J.A. Graves, *A platypus' eye view of the mammalian genome.* Curr Opin Genet Dev, 2004. **14**(6): p. 642-9.
325. Grutzner, F., et al., *In the platypus a meiotic chain of ten sex chromosomes shares genes with the bird Z and mammal X chromosomes.* Nature, 2004. **432**(7019): p. 913-7.
326. Veyrunes, F., et al., *Bird-like sex chromosomes of platypus imply recent origin of mammal sex chromosomes.* Genome Res, 2008. **18**(6): p. 965-73.
327. Rens, W., et al., *Epigenetic modifications on X chromosomes in marsupial and monotreme mammals and implications for evolution of dosage compensation.* Proc Natl Acad Sci U S A, 2010. **107**(41): p. 17657-62.
328. Deakin, J.E., et al., *Unravelling the evolutionary origins of X chromosome inactivation in mammals: insights from marsupials and monotremes.* Chromosome Res, 2009. **17**(5): p. 671-85.

329. Deakin, J.E., et al., *The status of dosage compensation in the multiple X chromosomes of the platypus.* PLoS Genet, 2008. **4**(7): p. e1000140.
330. Mahadevaiah, S.K., et al., *Key features of the X inactivation process are conserved between marsupials and eutherians.* Curr Biol, 2009. **19**(17): p. 1478-84.
331. Cooper, D.W., *Directed genetic change model for X chromosome inactivation in eutherian mammals.* Nature, 1971. **230**(5292): p. 292-4.
332. Sharman, G.B., *Late DNA replication in the paternally derived X chromosome of female kangaroos.* Nature, 1971. **230**(5291): p. 231-2.
333. Richardson, B.J., A.B. Czuppon, and G.B. Sharman, *Inheritance of glucose-6-phosphate dehydrogenase variation in kangaroos.* Nat New Biol, 1971. **230**(13): p. 154-5.
334. Cooper, D.W., et al., *Phosphoglycerate kinase polymorphism in kangaroos provides further evidence for paternal X inactivation.* Nat New Biol, 1971. **230**(13): p. 155-7.
335. Kaslow, D.C. and B.R. Migeon, *DNA methylation stabilizes X chromosome inactivation in eutherians but not in marsupials: evidence for multistep maintenance of mammalian X dosage compensation.* Proc Natl Acad Sci U S A, 1987. **84**(17): p. 6210-4.
336. Graves, J.A., *DNA synthesis in chromosomes of cultured leucocytes from two marsupial species.* Exp Cell Res, 1967. **46**(1): p. 37-57.
337. Koina, E., et al., *Specific patterns of histone marks accompany X chromosome inactivation in a marsupial.* Chromosome Res, 2009. **17**(1): p. 115-26.
338. Wakefield, M.J., et al., *Histone underacetylation is an ancient component of mammalian X chromosome inactivation.* Proc Natl Acad Sci U S A, 1997. **94**(18): p. 9665-8.
339. Chaumeil, J., et al., *Evolution from XIST-independent to XIST-controlled X-chromosome inactivation: epigenetic modifications in distantly related mammals.* PLoS One, 2011. **6**(4): p. e19040.
340. Piper, A.A., et al., *Isolation of a clone partially encoding hill kangaroo X-linked hypoxanthine phosphoribosyltransferase: sex differences in methylation in the body of the gene.* Somat Cell Mol Genet, 1993. **19**(2): p. 141-59.
341. Loebel, D.A. and P.G. Johnston, *Methylation analysis of a marsupial X-linked CpG island by bisulfite genomic sequencing.* Genome Res, 1996. **6**(2): p. 114-23.
342. Duret, L., et al., *The Xist RNA gene evolved in eutherians by pseudogenization of a protein-coding gene.* Science, 2006. **312**(5780): p. 1653-5.
343. Hore, T.A., et al., *The region homologous to the X-chromosome inactivation centre has been disrupted in marsupial and monotreme mammals.* Chromosome Res, 2007. **15**(2): p. 147-61.
344. Grant, J., et al., *Rsx is a metatherian RNA with Xist-like properties in X-chromosome inactivation.* Nature, 2012.
345. Kolesnikov, N.N. and E.A. Elisafenko, *[Exon-intron structure of the Xist gene in elephant, armadillo, and the ancestor of placental mammals].* Genetika, 2010. **46**(10): p. 1379-85.
346. Nishihara, H., S. Maruyama, and N. Okada, *Retroposon analysis and recent geological data suggest near-simultaneous divergence of the three superorders of mammals.* Proc Natl Acad Sci U S A, 2009. **106**(13): p. 5235-40.
347. Gribnau, J. and J.A. Grootegoed, *Origin and evolution of X chromosome inactivation.* Curr Opin Cell Biol, 2012.
348. Shevchenko, A.I., et al., *Genes flanking Xist in mouse and human are separated on the X chromosome in American marsupials.* Chromosome Res, 2007. **15**(2): p. 127-36.
349. Davidow, L.S., et al., *The search for a marsupial XIC reveals a break with vertebrate synteny.* Chromosome Res, 2007. **15**(2): p. 137-46.
350. Flynn, M., O. Saha, and P. Young, *Molecular evolution of the LNX gene family.* BMC Evol Biol, 2011. **11**: p. 235.
351. Caparros, M.L., et al., *Functional analysis of the highly conserved exon IV of XIST RNA.* Cytogenet Genome Res, 2002. **99**(1-4): p. 99-105.
352. Horvath, J.E., et al., *Comparative analysis of the primate X-inactivation center region and reconstruction of the ancestral primate XIST locus.* Genome Res, 2011. **21**(6): p. 850-62.
353. Michalak, P., *Coexpression, coregulation, and cofunctionality of neighboring genes in eukaryotic genomes.* Genomics, 2008. **91**(3): p. 243-8.
354. Sado, T., et al., *Regulation of imprinted X-chromosome inactivation in mice by Tsix.* Development, 2001. **128**(8): p. 1275-86.
355. Looijenga, L.H., et al., *X inactivation in human testicular tumors. XIST expression and androgen receptor methylation status.* Am J Pathol, 1997. **151**(2): p. 581-90.

356. Migeon, B.R., et al., *Identification of TSIX, encoding an RNA antisense to human XIST, reveals differences from its murine counterpart: implications for X inactivation.* Am J Hum Genet, 2001. **69**(5): p. 951-60.
357. Chow, J.C., et al., *Ectopic XIST transcripts in human somatic cells show variable expression and localization.* Cytogenet Genome Res, 2002. **99**(1-4): p. 92-8.
358. Hall, L.L., et al., *An ectopic human XIST gene can induce chromosome inactivation in postdifferentiation human HT-1080 cells.* Proc Natl Acad Sci U S A, 2002. **99**(13): p. 8677-82.
359. Hall, L.L., et al., *X-inactivation reveals epigenetic anomalies in most hESC but identifies sublines that initiate as expected.* J Cell Physiol, 2008. **216**(2): p. 445-52.
360. Shen, Y., et al., *X-inactivation in female human embryonic stem cells is in a nonrandom pattern and prone to epigenetic alterations.* Proc Natl Acad Sci U S A, 2008. **105**(12): p. 4709-14.
361. Silva, S.S., et al., *X-chromosome inactivation and epigenetic fluidity in human embryonic stem cells.* Proc Natl Acad Sci U S A, 2008. **105**(12): p. 4820-5.
362. Enver, T., et al., *Cellular differentiation hierarchies in normal and culture-adapted human embryonic stem cells.* Hum Mol Genet, 2005. **14**(21): p. 3129-40.
363. Hoffman, L.M., et al., *X-inactivation status varies in human embryonic stem cell lines.* Stem Cells, 2005. **23**(10): p. 1468-78.
364. Dhara, S.K. and N. Benvenisty, *Gene trap as a tool for genome annotation and analysis of X chromosome inactivation in human embryonic stem cells.* Nucleic Acids Res, 2004. **32**(13): p. 3995-4002.
365. Takagi, N., *Imprinted X-chromosome inactivation: enlightenment from embryos in vivo.* Semin Cell Dev Biol, 2003. **14**(6): p. 319-29.
366. West, J.D., et al., *Preferential expression of the maternally derived X chromosome in the mouse yolk sac.* Cell, 1977. **12**(4): p. 873-82.
367. Silva, J., et al., *Nanog is the gateway to the pluripotent ground state.* Cell, 2009. **138**(4): p. 722-37.
368. van den Berg, I.M., et al., *X chromosome inactivation is initiated in human preimplantation embryos.* Am J Hum Genet, 2009. **84**(6): p. 771-9.
369. Looijenga, L.H., et al., *Heterogeneous X inactivation in trophoblastic cells of human full-term female placentas.* Am J Hum Genet, 1999. **64**(5): p. 1445-52.
370. Ropers, H.H., G. Wolff, and H.W. Hitzeroth, *Preferential X inactivation in human placenta membranes: is the paternal X inactive in early embryonic development of female mammals?* Hum Genet, 1978. **43**(3): p. 265-73.
371. Daniels, R., et al., *XIST expression in human oocytes and preimplantation embryos.* Am J Hum Genet, 1997. **61**(1): p. 33-9.
372. Ray, P.F., R.M. Winston, and A.H. Handyside, *XIST expression from the maternal X chromosome in human male preimplantation embryos at the blastocyst stage.* Hum Mol Genet, 1997. **6**(8): p. 1323-7.
373. Bamforth, F., G. Machin, and M. Innes, *X-chromosome inactivation is mostly random in placental tissues of female monozygotic twins and triplets.* Am J Med Genet, 1996. **61**(3): p. 209-15.
374. Migeon, B.R., et al., *Incomplete X chromosome dosage compensation in chorionic villi of human placenta.* Proc Natl Acad Sci U S A, 1985. **82**(10): p. 3390-4.
375. Migeon, B.R., J. Axelman, and P. Jeppesen, *Differential X reactivation in human placental cells: implications for reversal of X inactivation.* Am J Hum Genet, 2005. **77**(3): p. 355-64.
376. Goto, T., E. Wright, and M. Monk, *Paternal X-chromosome inactivation in human trophoblastic cells.* Mol Hum Reprod, 1997. **3**(1): p. 77-80.
377. Harrison, K.B., *X-chromosome inactivation in the human cytotrophoblast.* Cytogenet Cell Genet, 1989. **52**(1-2): p. 37-41.
378. Harrison, K.B. and D. Warburton, *Preferential X-chromosome activity in human female placental tissues.* Cytogenet Cell Genet, 1986. **41**(3): p. 163-8.
379. Okamoto, I., et al., *Eutherian mammals use diverse strategies to initiate X-chromosome inactivation during development.* Nature, 2011. **472**(7343): p. 370-4.
380. Liu, W. and X. Sun, *Skewed X chromosome inactivation in diploid and triploid female human embryonic stem cells.* Hum Reprod, 2009. **24**(8): p. 1834-43.
381. Sato, N., et al., *Molecular signature of human embryonic stem cells and its comparison with the mouse.* Dev Biol, 2003. **260**(2): p. 404-13.
382. Ginis, I., et al., *Differences between human and mouse embryonic stem cells.* Dev Biol, 2004. **269**(2): p. 360-80.

383. Xu, R.H., et al., *Basic FGF and suppression of BMP signaling sustain undifferentiated proliferation of human ES cells.* Nat Methods, 2005. **2**(3): p. 185-90.
384. Ying, Q.L., et al., *BMP induction of Id proteins suppresses differentiation and sustains embryonic stem cell self-renewal in collaboration with STAT3.* Cell, 2003. **115**(3): p. 281-92.
385. Boyer, L.A., et al., *Core transcriptional regulatory circuitry in human embryonic stem cells.* Cell, 2005. **122**(6): p. 947-56.
386. Brons, I.G., et al., *Derivation of pluripotent epiblast stem cells from mammalian embryos.* Nature, 2007. **448**(7150): p. 191-5.
387. Tesar, P.J., et al., *New cell lines from mouse epiblast share defining features with human embryonic stem cells.* Nature, 2007. **448**(7150): p. 196-9.
388. Rossant, J., *Stem cells and early lineage development.* Cell, 2008. **132**(4): p. 527-31.
389. Lovell-Badge, R., *Many ways to pluripotency.* Nat Biotechnol, 2007. **25**(10): p. 1114-6.
390. Xu, R.H., et al., *BMP4 initiates human embryonic stem cell differentiation to trophoblast.* Nat Biotechnol, 2002. **20**(12): p. 1261-4.
391. Guo, G., et al., *Klf4 reverts developmentally programmed restriction of ground state pluripotency.* Development, 2009. **136**(7): p. 1063-9.
392. Bao, S., et al., *Epigenetic reversion of post-implantation epiblast to pluripotent embryonic stem cells.* Nature, 2009. **461**(7268): p. 1292-5.
393. Hanna, J., et al., *Metastable pluripotent states in NOD-mouse-derived ESCs.* Cell Stem Cell, 2009. **4**(6): p. 513-24.
394. Nichols, J. and A. Smith, *Naive and primed pluripotent states.* Cell Stem Cell, 2009. **4**(6): p. 487-92.
395. Zvetkova, I., et al., *Global hypomethylation of the genome in XX embryonic stem cells.* Nat Genet, 2005. **37**(11): p. 1274-9.
396. Lagarkova, M.A., et al., *Diverse epigenetic profile of novel human embryonic stem cell lines.* Cell Cycle, 2006. **5**(4): p. 416-20.
397. Rugg-Gunn, P.J., A.C. Ferguson-Smith, and R.A. Pedersen, *Epigenetic status of human embryonic stem cells.* Nat Genet, 2005. **37**(6): p. 585-7.
398. Allegrucci, C., et al., *Restriction landmark genome scanning identifies culture-induced DNA methylation instability in the human embryonic stem cell epigenome.* Hum Mol Genet, 2007. **16**(10): p. 1253-68.
399. Boklage, C.E., *The epigenetic environment: secondary sex ratio depends on differential survival in embryogenesis.* Hum Reprod, 2005. **20**(3): p. 583-7.
400. Han, T.L., et al., *Detection of X- and Y-bearing human spermatozoa after motile sperm isolation by swim-up.* Fertil Steril, 1993. **60**(6): p. 1046-51.
401. Hassold, T., S.D. Quillen, and J.A. Yamane, *Sex ratio in spontaneous abortions.* Ann Hum Genet, 1983. **47**(Pt 1): p. 39-47.
402. Hassold, T., et al., *Cytogenetic and molecular studies of trisomy 13.* J Med Genet, 1987. **24**(12): p. 725-32.
403. Jacobs, P.A., et al., *Trisomy 13 ascertained in a survey of spontaneous abortions.* J Med Genet, 1987. **24**(12): p. 721-4.
404. Rasmussen, S.A., et al., *Population-based analyses of mortality in trisomy 13 and trisomy 18.* Pediatrics, 2003. **111**(4 Pt 1): p. 777-84.
405. Miller, J.F., et al., *Fetal loss after implantation. A prospective study.* Lancet, 1980. **2**(8194): p. 554-6.
406. Ellish, N.J., et al., *A prospective study of early pregnancy loss.* Hum Reprod, 1996. **11**(2): p. 406-12.
407. Wilcox, A.J., et al., *Incidence of early loss of pregnancy.* N Engl J Med, 1988. **319**(4): p. 189-94.
408. Jacobs, P.A. and T.J. Hassold, *The origin of numerical chromosome abnormalities.* Adv Genet, 1995. **33**: p. 101-33.
409. CBS, C.b.v.d.S. 21 April 2012; Available from: www.CBS.nl.
410. Childs, B., *GENETIC ORIGIN OF SOME SEX DIFFERENCES AMONG HUMAN BEINGS.* Pediatrics, 1965. **35**: p. 798-812.
411. Verbrugge, L.M., *Sex differentials in health.* Public Health Rep, 1982. **97**(5): p. 417-37.
412. Crimmins, E.M., J.K. Kim, and A. Sole-Auro, *Gender differences in health: results from SHARE, ELSA and HRS.* Eur J Public Health, 2011. **21**(1): p. 81-91.
413. Gissler, M., et al., *Boys have more health problems in childhood than girls: follow-up of the 1987 Finnish birth cohort.* Acta Paediatr, 1999. **88**(3): p. 310-4.
414. Cui, W., et al., *Sex differences in birth defects: a study of opposite-sex twins.* Birth Defects Res A Clin Mol Teratol, 2005. **73**(11): p. 876-80.

415. Lary, J.M. and L.J. Paulozzi, *Sex differences in the prevalence of human birth defects: a population-based study.* Teratology, 2001. **64**(5): p. 237-51.
416. Cartwright, R.A., K.A. Gurney, and A.V. Moorman, *Sex ratios and the risks of haematological malignancies.* Br J Haematol, 2002. **118**(4): p. 1071-7.
417. Horner, J.F., *Die Erblichkeit des Daltonismus. Amtlicher Bericht ueber die Verwaltung des Medizinalwesens des Kantons Zurich vom Jahr 1876.* 1876, Zurich: Druck der Genossenschaftbuchdruckerei.
418. Otto, J.C., *An account of an haemorrhagic disposition existing in certain families.* Medical Repository, 1803. **6**: p. 1-4.
419. Jaeger, W., *Horner's law. The first step in the history of the understanding of X-linked disorders.* Ophthalmic Paediatr Genet, 1992. **13**(2): p. 49-56.
420. Dobyns, W.B., *The pattern of inheritance of X-linked traits is not dominant or recessive, just X-linked.* Acta Paediatr Suppl, 2006. **95**(451): p. 11-5.
421. Morgan, T., *Sex-linked inheritance in Drosophila.* Science, 1910. **32**: p. 120-122.
422. Morgan, T., et al., *The mechanism of Mendelian heredity.* 1915, New York: Henry Holt & Company.
423. Morgan, T., et al., *The mechanism of Mendelian heredity.* 1922, New York: Henry Holt & Company.
424. Strachan, T. and A. Read, *Human Molecular Genetics 3.* 3rd ed. 2004, New York: Garland Science.
425. Lyon, M.F., *X-chromosome inactivation and human genetic disease.* Acta Paediatr Suppl, 2002. **91**(439): p. 107-12.
426. Chabas, A. and R. Happle, *Understanding the biology of X-linked diseases.* Acta Paediatr Suppl, 2006. **95**(451): p. 9-10.
427. Migeon, B.R., *Why females are mosaics, X-chromosome inactivation, and sex differences in disease.* Gend Med, 2007. **4**(2): p. 97-105.
428. Dobyns, W.B., et al., *Inheritance of most X-linked traits is not dominant or recessive, just X-linked.* Am J Med Genet A, 2004. **129A**(2): p. 136-43.
429. Migeon, B.R., *Selection and cell communication as determinants of female phenotype.* Basic Life Sci, 1978. **12**: p. 417-32.
430. Fratantoni, J.C., C.W. Hall, and E.F. Neufeld, *Hurler and Hunter syndromes: mutual correction of the defect in cultured fibroblasts.* Science, 1968. **162**(3853): p. 570-2.
431. Dewey, M.J., et al., *Mosaic mice with teratocarcinoma-derived mutant cells deficient in hypoxanthine phosphoribosyltransferase.* Proc Natl Acad Sci U S A, 1977. **74**(12): p. 5564-8.
432. Migeon, B.R., *Studies of skin fibroblasts from 10 families with HGPRT deficiency, with reference in X-chromosomal inactivation.* Am J Hum Genet, 1971. **23**(2): p. 199-210.
433. Filosa, S., et al., *Somatic-cell selection is a major determinant of the blood-cell phenotype in heterozygotes for glucose-6-phosphate dehydrogenase mutations causing severe enzyme deficiency.* Am J Hum Genet, 1996. **59**(4): p. 887-95.
434. Migeon, B.R., et al., *Adrenoleukodystrophy: evidence for X linkage, inactivation, and selection favoring the mutant allele in heterozygous cells.* Proc Natl Acad Sci U S A, 1981. **78**(8): p. 5066-70.
435. Maier, E.M., et al., *Symptoms in carriers of adrenoleukodystrophy relate to skewed X inactivation.* Ann Neurol, 2002. **52**(5): p. 683-8.
436. Wieland, I., et al., *Mutations of the ephrin-B1 gene cause craniofrontonasal syndrome.* Am J Hum Genet, 2004. **74**(6): p. 1209-15.
437. Twigg, S.R., et al., *Mutations of ephrin-B1 (EFNB1), a marker of tissue boundary formation, cause craniofrontonasal syndrome.* Proc Natl Acad Sci U S A, 2004. **101**(23): p. 8652-7.
438. Makarov, R., et al., *The impact of CFNS-causing EFNB1 mutations on ephrin-B1 function.* BMC Med Genet, 2010. **11**: p. 98.
439. Davy, A., J.O. Bush, and P. Soriano, *Inhibition of gap junction communication at ectopic Eph/ephrin boundaries underlies craniofrontonasal syndrome.* PLoS Biol, 2006. **4**(10): p. e315.
440. Amos-Landgraf, J.M., et al., *X chromosome-inactivation patterns of 1,005 phenotypically unaffected females.* Am J Hum Genet, 2006. **79**(3): p. 493-9.
441. Sharp, A., D. Robinson, and P. Jacobs, *Age- and tissue-specific variation of X chromosome inactivation ratios in normal women.* Hum Genet, 2000. **107**(4): p. 343-9.
442. Puck, J.M., C.C. Stewart, and R.L. Nussbaum, *Maximum-likelihood analysis of human T-cell X chromosome inactivation patterns: normal women versus carriers of X-linked severe combined immunodeficiency.* Am J Hum Genet, 1992. **50**(4): p. 742-8.
443. Monteiro, J., et al., *Commitment to X inactivation precedes the twinning event in monochorionic MZ twins.* Am J Hum Genet, 1998. **63**(2): p. 339-46.

444. Belmont, J.W., *Genetic control of X inactivation and processes leading to X-inactivation skewing.* Am J Hum Genet, 1996. **58**(6): p. 1101-8.
445. Cattanach, B.M. and J.H. Isaacson, *Controlling elements in the mouse X chromosome.* Genetics, 1967. **57**(2): p. 331-46.
446. Cattanach, B.M. and C.E. Williams, *Evidence of non-random X chromosome activity in the mouse.* Genet Res, 1972. **19**(3): p. 229-40.
447. Cattanach, B.M., *Control of chromosome inactivation.* Annu Rev Genet, 1975. **9**: p. 1-18.
448. Simmler, M.C., et al., *Mapping the murine Xce locus with (CA)n repeats.* Mamm Genome, 1993. **4**(9): p. 523-30.
449. Chadwick, L.H., et al., *Genetic control of X chromosome inactivation in mice: definition of the Xce candidate interval.* Genetics, 2006. **173**(4): p. 2103-10.
450. Avner, P., et al., *Molecular correlates of the murine Xce locus.* Genet Res, 1998. **72**(3): p. 217-24.
451. Plenge, R.M., et al., *A promoter mutation in the XIST gene in two unrelated families with skewed X-chromosome inactivation.* Nat Genet, 1997. **17**(3): p. 353-6.
452. Pugacheva, E.M., et al., *Familial cases of point mutations in the XIST promoter reveal a correlation between CTCF binding and pre-emptive choices of X chromosome inactivation.* Hum Mol Genet, 2005. **14**(7): p. 953-65.
453. Naumova, A.K., et al., *Heritability of X chromosome--inactivation phenotype in a large family.* Am J Hum Genet, 1996. **58**(6): p. 1111-9.
454. Busque, L., et al., *Nonrandom X-inactivation patterns in normal females: lyonization ratios vary with age.* Blood, 1996. **88**(1): p. 59-65.
455. Naumova, A.K., et al., *Genetic mapping of X-linked loci involved in skewing of X chromosome inactivation in the human.* Eur J Hum Genet, 1998. **6**(6): p. 552-62.
456. Ropers, H.H., et al., *Evidence for preferential X-chromosome inactivation in a family with Fabry disease.* Am J Hum Genet, 1977. **29**(4): p. 361-70.
457. Migeon, B.R. and C. Haisley-Royster, *Familial skewed X inactivation and X-linked mutations: unbalanced X inactivation is a powerful means to ascertain X-linked genes that affect cell proliferation.* Am J Hum Genet, 1998. **62**(6): p. 1555-7; author reply 1557-8.
458. Marcus, S., et al., *Mutation analysis and prenatal diagnosis in a Lesch-Nyhan family showing non-random X-inactivation interfering with carrier detection tests.* Hum Genet, 1992. **89**(4): p. 395-400.
459. Ruttum, M.S., M.F. Lewandowski, and J.B. Bateman, *Affected females in X-linked congenital stationary night blindness.* Ophthalmology, 1992. **99**(5): p. 747-52.
460. Orstavik, K.H., et al., *Inheritance of skewed X chromosome inactivation in a large family with an X-linked recessive deafness syndrome.* Am J Med Genet, 1996. **64**(1): p. 31-4.
461. Bolduc, V., et al., *No evidence that skewing of X chromosome inactivation patterns is transmitted to offspring in humans.* J Clin Invest, 2008. **118**(1): p. 333-41.
462. Lau, A.W., et al., *Skewed X-chromosome inactivation is common in fetuses or newborns associated with confined placental mosaicism.* Am J Hum Genet, 1997. **61**(6): p. 1353-61.
463. Goodship, J., J. Carter, and J. Burn, *X-inactivation patterns in monozygotic and dizygotic female twins.* Am J Med Genet, 1996. **61**(3): p. 205-8.
464. Richards, C.S., et al., *Skewed X inactivation in a female MZ twin results in Duchenne muscular dystrophy.* Am J Hum Genet, 1990. **46**(4): p. 672-81.
465. Lupski, J.R., et al., *Discordance of muscular dystrophy in monozygotic female twins: evidence supporting asymmetric splitting of the inner cell mass in a manifesting carrier of Duchenne dystrophy.* Am J Med Genet, 1991. **40**(3): p. 354-64.
466. Abbadi, N., et al., *Additional case of female monozygotic twins discordant for the clinical manifestations of Duchenne muscular dystrophy due to opposite X-chromosome inactivation.* Am J Med Genet, 1994. **52**(2): p. 198-206.
467. Winchester, B., et al., *Female twin with Hunter disease due to nonrandom inactivation of the X-chromosome: a consequence of twinning.* Am J Med Genet, 1992. **44**(6): p. 834-8.
468. Tiberio, G., *MZ female twins discordant for X-linked diseases: a review.* Acta Genet Med Gemellol (Roma), 1994. **43**(3-4): p. 207-14.
469. Redonnet-Vernhet, I., et al., *Uneven X inactivation in a female monozygotic twin pair with Fabry disease and discordant expression of a novel mutation in the alpha-galactosidase A gene.* J Med Genet, 1996. **33**(8): p. 682-8.
470. Bennett, C.M., E. Boye, and E.J. Neufeld, *Female monozygotic twins discordant for hemophilia A due to nonrandom X-chromosome inactivation.* Am J Hematol, 2008. **83**(10): p. 778-80.

471. Costa, T., et al., *Monozygotic twins discordant for Aicardi syndrome.* J Med Genet, 1997. **34**(8): p. 688-91.
472. Burn, J., et al., *Duchenne muscular dystrophy in one of monozygotic twin girls.* J Med Genet, 1986. **23**(6): p. 494-500.
473. Marguery, M.C., et al., *Fabry's disease: heterozygous form of different expression in two monozygous twin sisters.* Dermatology, 1993. **187**(1): p. 9-15.
474. Nance, W.E., *Do twin Lyons have larger spots?* Am J Hum Genet, 1990. **46**(4): p. 646-8.
475. Lubinsky, M.S. and J.G. Hall, *Genomic imprinting, monozygous twinning, and X inactivation.* Lancet, 1991. **337**(8752): p. 1288.
476. Chitnis, S., et al., *X chromosome-inactivation patterns confirm the late timing of monoamniotic-MZ twinning.* Am J Hum Genet, 1999. **65**(2): p. 570-1.
477. Puck, J.M., *The timing of twinning: more insights from X inactivation.* Am J Hum Genet, 1998. **63**(2): p. 327-8.
478. Fisk, N.M., et al., *X-chromosome inactivation patterns do not implicate asymmetric splitting of the inner cell mass in the aetiology of twin-twin transfusion syndrome.* Mol Hum Reprod, 1999. **5**(1): p. 52-6.
479. Kristiansen, M., et al., *Twin study of genetic and aging effects on X chromosome inactivation.* Eur J Hum Genet, 2005. **13**(5): p. 599-606.
480. Allen, R.C., et al., *Application of carrier testing to genetic counseling for X-linked agammaglobulinemia.* Am J Hum Genet, 1994. **54**(1): p. 25-35.
481. Li, S.L., et al., *Carrier identification in X-linked immunodeficiency diseases.* J Paediatr Child Health, 1998. **34**(3): p. 273-9.
482. Moschese, V., et al., *X-chromosome inactivation and mutation pattern in the Bruton's tyrosine kinase gene in patients with X-linked agammaglobulinemia. Italian XLA Collaborative Group.* Mol Med, 2000. **6**(2): p. 104-13.
483. Hendriks, R.W., et al., *Inactivation of Btk by insertion of lacZ reveals defects in B cell development only past the pre-B cell stage.* Embo J, 1996. **15**(18): p. 4862-72.
484. Hendriks, R.W., M.E. Kraakman, and R.K. Schuurman, *Patterns of X chromosome inactivation in haematopoietic cells of female carriers of X linked severe combined immunodeficiency.* Immunodeficiency, 1993. **4**(1-4): p. 263-5.
485. Hendriks, R.W., M.E. Kraakman, and R.K. Schuurman, *X chromosome inactivation patterns in haematopoietic cells of female carriers of X-linked severe combined immunodeficiency determined by methylation analysis at the hypervariable DXS255 locus.* Clin Genet, 1992. **42**(3): p. 114-21.
486. Wengler, G., et al., *Nonrandom inactivation of the X chromosome in early lineage hematopoietic cells in carriers of Wiskott-Aldrich syndrome.* Blood, 1995. **85**(9): p. 2471-7.
487. Gealy, W.J., J.M. Dwyer, and J.B. Harley, *Allelic exclusion of glucose-6-phosphate dehydrogenase in platelets and T lymphocytes from a Wiskott-Aldrich syndrome carrier.* Lancet, 1980. **1**(8159): p. 63-5.
488. Prchal, J.T., et al., *Wiskott-Aldrich syndrome: cellular impairments and their implication for carrier detection.* Blood, 1980. **56**(6): p. 1048-54.
489. Goodship, J., et al., *Carrier detection in Wiskott-Aldrich syndrome: combined use of M27 beta for X-inactivation studies and as a linked probe.* Blood, 1991. **77**(12): p. 2677-81.
490. Fearon, E.R., et al., *Carrier detection in the Wiskott Aldrich syndrome.* Blood, 1988. **72**(5): p. 1735-9.
491. Mantuano, E., et al., *Analysis of X-chromosome inactivation in bone marrow precursors from carriers of Wiskott-Aldrich syndrome and X-linked severe combined immunodeficiency: evidence that the Wiskott-Aldrich gene is expressed prior to granulocyte-macrophage colony-forming-unit.* Immunodeficiency, 1993. **4**(1-4): p. 271-6.
492. Greer, W.L., et al., *X-chromosome inactivation in the Wiskott-Aldrich syndrome: a marker for detection of the carrier state and identification of cell lineages expressing the gene defect.* Genomics, 1989. **4**(1): p. 60-7.
493. Puck, J.M., R.L. Nussbaum, and M.E. Conley, *Carrier detection in X-linked severe combined immunodeficiency based on patterns of X chromosome inactivation.* J Clin Invest, 1987. **79**(5): p. 1395-400.
494. Goodship, J., et al., *Use of X chromosome inactivation analysis to establish carrier status for X-linked severe combined immunodeficiency.* Lancet, 1988. **1**(8588): p. 729-32.
495. Winkelstein, J.A. and E. Fearon, *Carrier detection of the X-linked primary immunodeficiency diseases using X-chromosome inactivation analysis.* J Allergy Clin Immunol, 1990. **85**(6): p. 1090-7.

496. Wong, C.C., et al., *A longitudinal twin study of skewed X chromosome-inactivation.* PLoS One, 2011. **6**(3): p. e17873.
497. Christensen, K., et al., *X-linked genetic factors regulate hematopoietic stem-cell kinetics in females.* Blood, 2000. **95**(7): p. 2449-51.
498. Hatakeyama, C., et al., *The dynamics of X-inactivation skewing as women age.* Clin Genet, 2004. **66**(4): p. 327-32.
499. Sandovici, I., et al., *A longitudinal study of X-inactivation ratio in human females.* Hum Genet, 2004. **115**(5): p. 387-92.
500. Knudsen, G.P., et al., *Increased skewing of X chromosome inactivation with age in both blood and buccal cells.* Cytogenet Genome Res, 2007. **116**(1-2): p. 24-8.
501. Fey, M.F., et al., *Clonality and X-inactivation patterns in hematopoietic cell populations detected by the highly informative M27 beta DNA probe.* Blood, 1994. **83**(4): p. 931-8.
502. Cotter, P.D., et al., *Late-onset X-linked sideroblastic anemia. Missense mutations in the erythroid delta-aminolevulinate synthase (ALAS2) gene in two pyridoxine-responsive patients initially diagnosed with acquired refractory anemia and ringed sideroblasts.* J Clin Invest, 1995. **96**(4): p. 2090-6.
503. Cazzola, M., et al., *Familial-skewed X-chromosome inactivation as a predisposing factor for late-onset X-linked sideroblastic anemia in carrier females.* Blood, 2000. **96**(13): p. 4363-5.
504. Manco, L., et al., *Chronic hemolytic anemia is associated with a new glucose-6-phosphate dehydrogenase in-frame deletion in an older woman.* Blood Cells Mol Dis, 2011. **46**(4): p. 288-93.
505. Au, W.Y., et al., *Glucose 6-phosphate dehydrogenase (G6PD) deficiency in elderly Chinese women heterozygous for G6PD variants.* Am J Med Genet A, 2004. **129A**(2): p. 208-11.
506. Au, W.Y., et al., *Glucose-6-phosphate dehydrogenase deficiency in female octogenarians, nanogenarians, and centenarians.* J Gerontol A Biol Sci Med Sci, 2006. **61**(10): p. 1086-9.
507. Gale, R.E., et al., *Acquired skewing of X-chromosome inactivation patterns in myeloid cells of the elderly suggests stochastic clonal loss with age.* Br J Haematol, 1997. **98**(3): p. 512-9.
508. Mengel-From, J., et al., *Skewed X inactivation and survival: a 13-year follow-up study of elderly twins and singletons.* Eur J Hum Genet, 2012. **20**(3): p. 361-4.
509. Vickers, M.A., et al., *Assessment of mechanism of acquired skewed X inactivation by analysis of twins.* Blood, 2001. **97**(5): p. 1274-81.
510. Abkowitz, J.L., et al., *An X chromosome gene regulates hematopoietic stem cell kinetics.* Proc Natl Acad Sci U S A, 1998. **95**(7): p. 3862-6.
511. Coleman, R., et al., *Interaction of incontinentia pigmenti and factor VIII mutations in a female with biased X inactivation, resulting in haemophilia.* J Med Genet, 1993. **30**(6): p. 497-500.
512. Gibbons, R.J., et al., *X-linked alpha-thalassemia/mental retardation (ATR-X) syndrome: localization to Xq12-q21.31 by X inactivation and linkage analysis.* Am J Hum Genet, 1992. **51**(5): p. 1136-49.
513. Wada, T., et al., *Non-skewed X-inactivation may cause mental retardation in a female carrier of X-linked alpha-thalassemia/mental retardation syndrome (ATR-X): X-inactivation study of nine female carriers of ATR-X.* Am J Med Genet A, 2005. **138**(1): p. 18-20.
514. Orstavik, K.H., et al., *X chromosome inactivation in carriers of Barth syndrome.* Am J Hum Genet, 1998. **63**(5): p. 1457-63.
515. Ferraris, A.M., et al., *Nonrandom X-chromosome inactivation in hemopoietic cells from carriers of dyskeratosis congenita.* Am J Hum Genet, 1997. **61**(2): p. 458-61.
516. Devriendt, K., et al., *Skewed X-chromosome inactivation in female carriers of dyskeratosis congenita.* Am J Hum Genet, 1997. **60**(3): p. 581-7.
517. Vulliamy, T.J., et al., *Skewed X-inactivation in carriers of X-linked dyskeratosis congenita.* Blood, 1997. **90**(6): p. 2213-6.
518. Orstavik, K.H., et al., *Novel splicing mutation in the NEMO (IKK-gamma) gene with severe immunodeficiency and heterogeneity of X-chromosome inactivation.* Am J Med Genet A, 2006. **140**(1): p. 31-9.
519. Van Esch, H., et al., *Duplication of the MECP2 region is a frequent cause of severe mental retardation and progressive neurological symptoms in males.* Am J Hum Genet, 2005. **77**(3): p. 442-53.
520. Jiang, Y.H., et al., *Molecular characterization of co-occurring Duchenne muscular dystrophy and X-linked oculo-facio-cardio-dental syndrome in a girl.* Am J Med Genet A, 2009. **149A**(6): p. 1249-52.
521. Azofeifa, J., et al., *X-chromosome methylation in manifesting and healthy carriers of dystrophinopathies: concordance of activation ratios among first degree female relatives and skewed inactivation as cause of the affected phenotypes.* Hum Genet, 1995. **96**(2): p. 167-76.

522. Yoshioka, M., T. Yorifuji, and I. Mituyoshi, *Skewed X inactivation in manifesting carriers of Duchenne muscular dystrophy.* Clin Genet, 1998. **53**(2): p. 102-7.
523. Parolini, O., et al., *X-linked Wiskott-Aldrich syndrome in a girl.* N Engl J Med, 1998. **338**(5): p. 291-5.
524. Puck, J.M. and H.F. Willard, *X inactivation in females with X-linked disease.* N Engl J Med, 1998. **338**(5): p. 325-8.
525. Inoue, H., et al., *X-linked thrombocytopenia in a girl.* Br J Haematol, 2002. **118**(4): p. 1163-5.
526. Andreu, N., et al., *Wiskott-Aldrich syndrome in a female with skewed X-chromosome inactivation.* Blood Cells Mol Dis, 2003. **31**(3): p. 332-7.
527. Conley, M.E., et al., *Atypical Wiskott-Aldrich syndrome in a girl.* Blood, 1992. **80**(5): p. 1264-9.
528. Russell, S.J. and P.D. Nisen, *Random X chromosome inactivation in a female with a variant of Wiskott-Aldrich syndrome.* Br J Haematol, 1995. **90**(1): p. 210-2.
529. Lutskiy, M.I., et al., *Wiskott-Aldrich syndrome in a female.* Blood, 2002. **100**(8): p. 2763-8.
530. Orstavik, K.H., R.E. Orstavik, and M. Schwartz, *Skewed X chromosome inactivation in a female with haemophilia B and in her non-carrier daughter: a genetic influence on X chromosome inactivation?* J Med Genet, 1999. **36**(11): p. 865-6.
531. Knobe, K.E., et al., *Female haemophilia A caused by skewed X inactivation.* Haemophilia, 2008. **14**(4): p. 846-8.
532. Tanner, S.M., et al., *Skewed X-inactivation in a manifesting carrier of X-linked myotubular myopathy and in her non-manifesting carrier mother.* Hum Genet, 1999. **104**(3): p. 249-53.
533. Jungbluth, H., et al., *Early and severe presentation of X-linked myotubular myopathy in a girl with skewed X-inactivation.* Neuromuscul Disord, 2003. **13**(1): p. 55-9.
534. Kristiansen, M., et al., *X-inactivation patterns in carriers of X-linked myotubular myopathy.* Neuromuscul Disord, 2003. **13**(6): p. 468-71.
535. Roos, D., et al., *Molecular basis and enzymatic properties of glucose 6-phosphate dehydrogenase volendam, leading to chronic nonspherocytic anemia, granulocyte dysfunction, and increased susceptibility to infections.* Blood, 1999. **94**(9): p. 2955-62.
536. Badens, C., et al., *ATRX syndrome in a girl with a heterozygous mutation in the ATRX Zn finger domain and a totally skewed X-inactivation pattern.* Am J Med Genet A, 2006. **140**(20): p. 2212-5.
537. Morrone, A., et al., *Fabry disease: molecular studies in Italian patients and X inactivation analysis in manifesting carriers.* J Med Genet, 2003. **40**(8): p. e103.
538. Mattei, M.G., et al., *X-autosome translocations: cytogenetic characteristics and their consequences.* Hum Genet, 1982. **61**(4): p. 295-309.
539. Schmidt, M. and D. Du Sart, *Functional disomies of the X chromosome influence the cell selection and hence the X inactivation pattern in females with balanced X-autosome translocations: a review of 122 cases.* Am J Med Genet, 1992. **42**(2): p. 161-9.
540. Orstavik, K.H., et al., *Severe hypohidrotic ectodermal dysplasia in a girl caused by a de novo 9;X insertion that includes XIST and disrupts the EDA gene.* Am J Med Genet A, 2007. **143A**(13): p. 1510-3.
541. Hodgson, S.V., et al., *A balanced de novo X/autosome translocation in a girl with manifestations of Lowe syndrome.* Am J Med Genet, 1986. **23**(3): p. 837-47.
542. Punnett, H.H., *Simpson-Golabi-Behmel syndrome (SGBS) in a female with an X-autosome translocation.* Am J Med Genet, 1994. **50**(4): p. 391-3.
543. Imai, K., et al., *Female hyper IgM syndrome type 1 with a chromosomal translocation disrupting CD40LG.* Biochim Biophys Acta, 2006. **1762**(3): p. 335-40.
544. Monaco, A.P., et al., *Isolation of candidate cDNAs for portions of the Duchenne muscular dystrophy gene.* Nature, 1986. **323**(6089): p. 646-50.
545. Boyd, Y., et al., *Muscular dystrophy in girls with X;autosome translocations.* J Med Genet, 1986. **23**(6): p. 484-90.
546. Boyd, Y., et al., *Mapping of 12 translocation breakpoints in the Xp21 region with respect to the locus for Duchenne muscular dystrophy.* Cytogenet Cell Genet, 1988. **48**(1): p. 28-34.
547. Jacobs, P.A., et al., *Duchenne muscular dystrophy (DMD) in a female with an X/autosome translocation: further evidence that the DMD locus is at Xp21.* Am J Hum Genet, 1981. **33**(4): p. 513-8.
548. Bodrug, S.E., et al., *Mapping of four translocation breakpoints within the Duchenne muscular dystrophy gene.* Genomics, 1989. **4**(1): p. 101-4.
549. Billuart, P., et al., *Oligophrenin-1 encodes a rhoGAP protein involved in X-linked mental retardation.* Nature, 1998. **392**(6679): p. 923-6.

550. Bienvenu, T., et al., *Mapping of the X-breakpoint involved in a balanced X;12 translocation in a female with mild mental retardation.* Eur J Hum Genet, 1997. **5**(2): p. 105-9.
551. Bawle, E., et al., *Aarskog syndrome: full male and female expression associated with an X-autosome translocation.* Am J Med Genet, 1984. **17**(3): p. 595-602.
552. Hodgson, S.V., et al., *Two cases of X/autosome translocation in females with incontinentia pigmenti.* Hum Genet, 1985. **71**(3): p. 231-4.
553. Royer-Pokora, B., et al., *Cloning the gene for an inherited human disorder--chronic granulomatous disease--on the basis of its chromosomal location.* Nature, 1986. **322**(6074): p. 32-8.
554. Baehner, R.L., et al., *DNA linkage analysis of X chromosome-linked chronic granulomatous disease.* Proc Natl Acad Sci U S A, 1986. **83**(10): p. 3398-401.
555. Orstavik, K.H., *X chromosome inactivation in clinical practice.* Hum Genet, 2009. **126**(3): p. 363-73.
556. Franco, B. and A. Ballabio, *X-inactivation and human disease: X-linked dominant male-lethal disorders.* Curr Opin Genet Dev, 2006. **16**(3): p. 254-9.
557. Morleo, M. and B. Franco, *Dosage compensation of the mammalian X chromosome influences the phenotypic variability of X-linked dominant male-lethal disorders.* J Med Genet, 2008. **45**(7): p. 401-8.
558. Bahi-Buisson, N., et al., *Key clinical features to identify girls with CDKL5 mutations.* Brain, 2008. **131**(Pt 10): p. 2647-61.
559. Thauvin-Robinet, C., et al., *Clinical, molecular, and genotype-phenotype correlation studies from 25 cases of oral-facial-digital syndrome type 1: a French and Belgian collaborative study.* J Med Genet, 2006. **43**(1): p. 54-61.
560. Robertson, S.P., et al., *Localized mutations in the gene encoding the cytoskeletal protein filamin A cause diverse malformations in humans.* Nat Genet, 2003. **33**(4): p. 487-91.
561. Parrish, J.E., et al., *Selection against mutant alleles in blood leukocytes is a consistent feature in Incontinentia Pigmenti type 2.* Hum Mol Genet, 1996. **5**(11): p. 1777-83.
562. Shirahama, S., et al., *Skewed X-chromosome inactivation causes intra-familial phenotypic variation of an EBP mutation in a family with X-linked dominant chondrodysplasia punctata.* Hum Genet, 2003. **112**(1): p. 78-83.
563. Hedera, P. and J.L. Gorski, *Oculo-facio-cardio-dental syndrome: skewed X chromosome inactivation in mother and daughter suggest X-linked dominant Inheritance.* Am J Med Genet A, 2003. **123A**(3): p. 261-6.
564. Fusco, F., et al., *Molecular analysis of the genetic defect in a large cohort of IP patients and identification of novel NEMO mutations interfering with NF-kappaB activation.* Hum Mol Genet, 2004. **13**(16): p. 1763-73.
565. Kristiansen, M., et al., *Phenotypic variation in Melnick-Needles syndrome is not reflected in X inactivation patterns from blood or buccal smear.* Am J Med Genet, 2002. **108**(2): p. 120-7.
566. Knudsen, G.P., et al., *Increased skewing of X chromosome inactivation in Rett syndrome patients and their mothers.* Eur J Hum Genet, 2006. **14**(11): p. 1189-94.
567. Robertson, S.P., et al., *Frontometaphyseal dysplasia: mutations in FLNA and phenotypic diversity.* Am J Med Genet A, 2006. **140**(16): p. 1726-36.
568. Lcoyklang, P., et al., *Three novel mutations in the PORCN gene underlying focal dermal hypoplasia.* Clin Genet, 2008. **73**(4): p. 373-9.
569. Blinkenberg, E.O., et al., *Angioma serpiginosum with oesophageal papillomatosis is an X-linked dominant condition that maps to Xp11.3-Xq12.* Eur J Hum Genet, 2007. **15**(5): p. 543-7.
570. Amir, R.E., et al., *Rett syndrome is caused by mutations in X-linked MECP2, encoding methyl-CpG-binding protein 2.* Nat Genet, 1999. **23**(2): p. 185-8.
571. Chahrour, M. and H.Y. Zoghbi, *The story of Rett syndrome: from clinic to neurobiology.* Neuron, 2007. **56**(3): p. 422-37.
572. Dayer, A.G., et al., *MECP2 mutant allele in a boy with Rett syndrome and his unaffected heterozygous mother.* Brain Dev, 2007. **29**(1): p. 47-50.
573. Huppke, P., et al., *Very mild cases of Rett syndrome with skewed X inactivation.* J Med Genet, 2006. **43**(10): p. 814-6.
574. Allanson, J. and S. Richter, *Linear skin defects and congenital microphthalmia: a new syndrome at Xp22.2.* J Med Genet, 1991. **28**(2): p. 143-4.
575. Lindsay, E.A., et al., *Microphthalmia with linear skin defects (MLS) syndrome: clinical, cytogenetic, and molecular characterization.* Am J Med Genet, 1994. **49**(2): p. 229-34.

576. Ogata, T., et al., *Microphthalmia with linear skin defects syndrome in a mosaic female infant with monosomy for the Xp22 region: molecular analysis of the Xp22 breakpoint and the X-inactivation pattern.* Hum Genet, 1998. **103**(1): p. 51-6.
577. Carrel, L., et al., *A first-generation X-inactivation profile of the human X chromosome.* Proc Natl Acad Sci U S A, 1999. **96**(25): p. 14440-4.
578. de Conciliis, L., et al., *Characterization of Cxorf5 (71-7A), a novel human cDNA mapping to Xp22 and encoding a protein containing coiled-coil alpha-helical domains.* Genomics, 1998. **51**(2): p. 243-50.
579. Ferrante, M.I., et al., *Identification of the gene for oral-facial-digital type I syndrome.* Am J Hum Genet, 2001. **68**(3): p. 569-76.
580. Ferrante, M.I., et al., *Oral-facial-digital type I protein is required for primary cilia formation and left-right axis specification.* Nat Genet, 2006. **38**(1): p. 112-7.
581. Cai, X.H., et al., *Female hemophilia A heterozygous for a de novo frameshift and a novel missense mutation of factor VIII.* J Thromb Haemost, 2006. **4**(9): p. 1969-74.
582. Windsor, S., et al., *Severe haemophilia A in a female resulting from two de novo factor VIII mutations.* Br J Haematol, 1995. **90**(4): p. 906-9.
583. David, D., et al., *Female haemophiliac homozygous for the factor VIII intron 22 inversion mutation, with transcriptional inactivation of one of the factor VIII alleles.* Haemophilia, 2003. **9**(1): p. 125-30.
584. Vencesla, A., et al., *Severe haemophilia A in a female resulting from an inherited gross deletion and a de novo codon deletion in the F8 gene.* Haemophilia, 2008. **14**(5): p. 1094-8.
585. Radhakrishna, U., et al., *Novel homozygous, heterozygous and hemizygous FRMD7 gene mutations segregated in the same consanguineous family with congenital X-linked nystagmus.* Eur J Hum Genet, 2012.
586. Nagtzaam, I.F., et al., *Clinically manifest X-linked recessive ichthyosis in a female due to a homozygous interstitial 1.6-Mb deletion of Xp22.31.* Br J Dermatol, 2012. **166**(4): p. 905-7.
587. Saito, T., et al., *A patient with hypophosphatemic rickets and ossification of posterior longitudinal ligament caused by a novel homozygous mutation in ENPP1 gene.* Bone, 2011. **49**(4): p. 913-6.
588. Fujii, K., et al., *Homozygous female Becker muscular dystrophy.* Am J Med Genet A, 2009. **149A**(5): p. 1052-5.
589. Israels, M.C., H. Lempert, and E. Gilbertson, *Haemophilia in the female.* Lancet, 1951. **1**(6670): p. 1375-80.
590. Merskey, C., *The occurrence of haemophilia in the human female.* Q J Med, 1951. **20**(79): p. 299-312.
591. Quan, F., et al., *Uniparental disomy of the entire X chromosome in a female with Duchenne muscular dystrophy.* Am J Hum Genet, 1997. **60**(1): p. 160-5.
592. Solomon, I.L. and E.J. Schoen, *Sex-linked ichthyosis in XO gonadal dysgenesis.* Lancet, 1971. **1**(7712): p. 1304-5.
593. Chelly, J., et al., *De novo DNA microdeletion in a girl with Turner syndrome and Duchenne muscular dystrophy.* Hum Genet, 1986. **74**(2): p. 193-6.
594. Gilgenkrantz, S., et al., *A case of female hemophilia with a 46,XXr karyotype studied with X-chromosome DNA probes.* Hum Genet, 1986. **72**(2): p. 157-9.
595. Panarello, C., et al., *Concomitant Turner syndrome and hemophilia A in a female with an idic(X)(p11) heterozygous at locus DXS52.* Cytogenet Cell Genet, 1992. **59**(4): p. 241-2.
596. Gilchrist, G.S., D. Hammond, and J. Melnyk, *Hemophilia A in a phenotypically normal female with XX-XO mosaicism.* N Engl J Med, 1965. **273**(26): p. 1402-6.
597. Chuansumrit, A., et al., *Inversion of intron 22 of the factor VIII gene in a girl with severe hemophilia A and Turner's syndrome.* Thromb Haemost, 1999. **82**(4): p. 1379.
598. Weinspach, S., et al., *Intracranial hemorrhage in a female leading to the diagnosis of severe hemophilia A and Turner syndrome.* Klin Padiatr, 2009. **221**(3): p. 167-71.
599. Katayama, Y., et al., *Co-occurrence of mutations in both dystrophin- and androgen-receptor genes is a novel cause of female Duchenne muscular dystrophy.* Hum Genet, 2006. **119**(5): p. 516-9.
600. Nilsson, I.M., et al., *Haemophilia A in a "girl" with male sex-chromatin pattern.* Lancet, 1959. **2**(7097): p. 264-6.
601. Huisse, M.G., et al., *Hemophilia A in a phenotypic female with normal male karyotype associated with a low factor XII level.* Ann Genet, 1980. **23**(1): p. 31-4.
602. Sitalakshmi, S., et al., *An unusual case of haemophilia--a case report.* Indian J Pathol Microbiol, 2001. **44**(3): p. 367-8.
603. Andrejev, N.J., et al., *Haemophilia A in a patient with testicular feminization.* Thromb Diath Haemorrh, 1975. **33**(2): p. 208-16.

604. Witkowski, R., *Germinal "mosaicism"--germline mutation or chimerism?* Hum Genet, 1992. **88**(3): p. 359-60.
605. Malan, V., M. Vekemans, and C. Turleau, *Chimera and other fertilization errors.* Clin Genet, 2006. **70**(5): p. 363-73.
606. Wieacker, P., J. Zimmer, and H.H. Ropers, *X inactivation patterns in two syndromes with probable X-linked dominant, male lethal inheritance.* Clin Genet, 1985. **28**(3): p. 238-42.
607. Neidich, J.A., et al., *Heterogeneity of clinical severity and molecular lesions in Aicardi syndrome.* J Pediatr, 1990. **116**(6): p. 911-7.
608. Hoag, H.M., et al., *Evidence that skewed X inactivation is not needed for the phenotypic expression of Aicardi syndrome.* Hum Genet, 1997. **100**(3-4): p. 459-64.
609. Eble, T.N., et al., *Non-random X chromosome inactivation in Aicardi syndrome.* Hum Genet, 2009. **125**(2): p. 211-6.
610. Canueto, J., et al., *Clinical, molecular and biochemical characterization of nine Spanish families with Conradi-Hunermann-Happle syndrome: new insights into X-linked dominant chondrodysplasia punctata with a comprehensive review of the literature.* Br J Dermatol, 2012. **166**(4): p. 830-8.
611. Konig, A., et al., *A novel missense mutation of NSDHL in an unusual case of CHILD syndrome showing bilateral, almost symmetric involvement.* J Am Acad Dermatol, 2002. **46**(4): p. 594-6.
612. Schluth, C., et al., *Phenotype in X chromosome rearrangements: pitfalls of X inactivation study.* Pathol Biol (Paris), 2007. **55**(1): p. 29-36.
613. Baroncini, A., et al., *Terminal osseous dysplasia with pigmentary defects: clinical description of a new family.* Am J Med Genet A, 2007. **143(1)**: p. 51-7.
614. Cutler, J.A., et al., *Germline mosaicism resulting in the transmission of severe hemophilia B from a grandfather with a mild deficiency.* Am J Med Genet A, 2004. **129A**(1): p. 13-5.
615. Leuer, M., et al., *Somatic mosaicism in hemophilia A: a fairly common event.* Am J Hum Genet, 2001. **69**(1): p. 75-87.
616. Youssoufian, H. and R.E. Pyeritz, *Mechanisms and consequences of somatic mosaicism in humans.* Nat Rev Genet, 2002. **3**(10): p. 748-58.
617. Kasper, C.K. and C.H. Buzin, *Mosaics and haemophilia.* Haemophilia, 2009. **15**(6): p. 1181-6.
618. Rogaev, E.I., et al., *Genotype analysis identifies the cause of the "royal disease".* Science, 2009. **326**(5954): p. 817.
619. Stevens, R.F., *The history of haemophilia in the royal families of Europe.* Br J Haematol, 1999. **105**(1): p. 25-32.
620. Orstavik, K.H., et al., *Absence of correlation between X chromosome inactivation pattern and plasma concentration of factor VIII and factor IX in carriers of haemophilia A and B.* Thromb Haemost, 2000. **83**(3): p. 433-7.
621. Song, M.J., et al., *Molecular characterization of female hemophilia A by multiplex ligation-dependent probe amplification analysis and X-chromosome inactivation study.* Blood Coagul Fibrinolysis, 2011. **22**(3): p. 211-4.
622. Luzzatto, L., et al., *Imbalance in X-chromosome expression: evidence for a human X-linked gene affecting growth of hemopoietic cells.* Science, 1979. **205**(4413): p. 1418-20.
623. Usanga, E.A. and L. Luzzatto, *Adaptation of Plasmodium falciparum to glucose 6-phosphate dehydrogenase-deficient host red cells by production of parasite-encoded enzyme.* Nature, 1985. **313**(6005): p. 793-5.
624. Cappadoro, M., et al., *Early phagocytosis of glucose-6-phosphate dehydrogenase (G6PD)-deficient erythrocytes parasitized by Plasmodium falciparum may explain malaria protection in G6PD deficiency.* Blood, 1998. **92**(7): p. 2527-34.
625. Green, A.M. and G.M. Kupfer, *Fanconi anemia.* Hematol Oncol Clin North Am, 2009. **23**(2): p. 193-214.
626. Harigae, H. and K. Furuyama, *Hereditary sideroblastic anemia: pathophysiology and gene mutations.* Int J Hematol, 2010. **92**(3): p. 425-31.
627. Kacena, M.A., et al., *GATA1-Related X-Linked Cytopenia.* 1993.
628. Holden, S.T., et al., *Fanconi anaemia complementation group B presenting as X linked VACTERL with hydrocephalus syndrome.* J Med Genet, 2006. **43**(9): p. 750-4.
629. McCauley, J., et al., *X-linked VACTERL with hydrocephalus syndrome: further delineation of the phenotype caused by FANCB mutations.* Am J Med Genet A, 2011. **155A**(10): p. 2370-80.
630. Aivado, M., N. Gattermann, and S. Bottomley, *X chromosome inactivation ratios in female carriers of X-linked sideroblastic anemia.* Blood, 2001. **97**(12): p. 4000-2.

631. Aivado, M., et al., *X-linked sideroblastic anemia associated with a novel ALAS2 mutation and unfortunate skewed X-chromosome inactivation patterns.* Blood Cells Mol Dis, 2006. **37**(1): p. 40-5.
632. Ducamp, S., et al., *Sideroblastic anemia: molecular analysis of the ALAS2 gene in a series of 29 probands and functional studies of 10 missense mutations.* Hum Mutat, 2011. **32**(6): p. 590-7.
633. Freson, K., et al., *Different substitutions at residue D218 of the X-linked transcription factor GATA1 lead to altered clinical severity of macrothrombocytopenia and anemia and are associated with variable skewed X inactivation.* Hum Mol Genet, 2002. **11**(2): p. 147-52.
634. Fish, E.N., *The X-files in immunity: sex-based differences predispose immune responses.* Nat Rev Immunol, 2008. **8**(9): p. 737-44.
635. Thompson, D.J., et al., *Excess risk of staphylococcal infection and disease in newborn males.* Am J Epidemiol, 1966. **84**(2): p. 314-28.
636. Green, M.S., *The male predominance in the incidence of infectious diseases in children: a postulated explanation for disparities in the literature.* Int J Epidemiol, 1992. **21**(2): p. 381-6.
637. Purtilo, D.T. and J.L. Sullivan, *Immunological bases for superior survival of females.* Am J Dis Child, 1979. **133**(12): p. 1251-3.
638. Butterworth, M., B. McClellan, and M. Allansmith, *Influence of sex in immunoglobulin levels.* Nature, 1967. **214**(5094): p. 1224-5.
639. Aspinall, R., *Longevity and the immune response.* Biogerontology, 2000. **1**(3): p. 273-8.
640. Libert, C., L. Dejager, and I. Pinheiro, *The X chromosome in immune functions: when a chromosome makes the difference.* Nat Rev Immunol, 2010. **10**(8): p. 594-604.
641. Morris, J.A. and L.M. Harrison, *Hypothesis: increased male mortality caused by infection is due to a decrease in heterozygous loci as a result of a single X chromosome.* Med Hypotheses, 2009. **72**(3): p. 322-4.
642. Spolarics, Z., *The X-files of inflammation: cellular mosaicism of X-linked polymorphic genes and the female advantage in the host response to injury and infection.* Shock, 2007. **27**(6): p. 597-604.
643. Selmi, C., et al., *The X chromosome and the sex ratio of autoimmunity.* Autoimmun Rev, 2011.
644. Gleicher, N. and D.H. Barad, *Gender as risk factor for autoimmune diseases.* J Autoimmun, 2007. **28**(1): p. 1-6.
645. Koker, M.Y., et al., *Skewing of X-chromosome inactivation in three generations of carriers with X-linked chronic granulomatous disease within one family.* Eur J Clin Invest, 2006. **36**(4): p. 257-64.
646. Notarangelo, L.D., et al., *Analysis of X-chromosome inactivation in X-linked immunodeficiency with hyper-IgM (HIGM1): evidence for involvement of different hematopoietic cell lineages.* Hum Genet, 1991. **88**(2): p. 130-4.
647. Hendriks, R.W., et al., *Evidence that in X-linked immunodeficiency with hyperimmunoglobulinemia M the intrinsic immunoglobulin heavy chain class switch mechanism is intact.* Eur J Immunol, 1990. **20**(12): p. 2603-8.
648. Tommasini, A., et al., *X-chromosome inactivation analysis in a female carrier of FOXP3 mutation.* Clin Exp Immunol, 2002. **130**(1): p. 127-30.
649. van den Bogaard, R., et al., *Molecular characterisation of 10 Dutch properdin type I deficient families: mutation analysis and X-inactivation studies.* Eur J Hum Genet, 2000. **8**(7): p. 513-8.
650. Woon, S.T., et al., *Follicular lymphoma in a X-linked lymphoproliferative syndrome carrier female.* Scand J Immunol, 2008. **68**(2): p. 153-8.
651. Marsh, R.A., et al., *A rapid flow cytometric screening test for X-linked lymphoproliferative disease due to XIAP deficiency.* Cytometry B Clin Cytom, 2009. **76**(5): p. 334-44.
652. Ozcelik, T., *X chromosome inactivation and female predisposition to autoimmunity.* Clin Rev Allergy Immunol, 2008. **34**(3): p. 348-51.
653. Kast, R.E., *Predominance of autoimmune and rheumatic diseases in females.* J Rheumatol, 1977. **4**(3): p. 288-92.
654. Stewart, J.J., *The female X-inactivation mosaic in systemic lupus erythematosus.* Immunol Today, 1998. **19**(8): p. 352-7.
655. Uz, E., et al., *Increased frequency of extremely skewed X chromosome inactivation in juvenile idiopathic arthritis.* Arthritis Rheum, 2009. **60**(11): p. 3410-2.
656. Broen, J.C., et al., *Skewed X chromosomal inactivation impacts T regulatory cell function in systemic sclerosis.* Ann Rheum Dis, 2010. **69**(12): p. 2213-6.
657. Brix, T.H., et al., *High frequency of skewed X-chromosome inactivation in females with autoimmune thyroid disease: a possible explanation for the female predisposition to thyroid autoimmunity.* J Clin Endocrinol Metab, 2005. **90**(11): p. 5949-53.

658. Ozbalkan, Z., et al., *Skewed X chromosome inactivation in blood cells of women with scleroderma.* Arthritis Rheum, 2005. **52**(5): p. 1564-70.
659. Ozcelik, T., et al., *Evidence from autoimmune thyroiditis of skewed X-chromosome inactivation in female predisposition to autoimmunity.* Eur J Hum Genet, 2006. **14**(6): p. 791-7.
660. Uz, E., et al., *Skewed X-chromosome inactivation in scleroderma.* Clin Rev Allergy Immunol, 2008. **34**(3): p. 352-5.
661. Scofield, R.H., et al., *Klinefelter's syndrome (47,XXY) in male systemic lupus erythematosus patients: support for the notion of a gene-dose effect from the X chromosome.* Arthritis Rheum, 2008. **58**(8): p. 2511-7.
662. Knudsen, G.P., et al., *X chromosome inactivation in females with multiple sclerosis.* Eur J Neurol, 2007. **14**(12): p. 1392-6.
663. Chitnis, S., et al., *The role of X-chromosome inactivation in female predisposition to autoimmunity.* Arthritis Res, 2000. **2**(5): p. 399-406.
664. Lu, Q., et al., *Demethylation of CD40LG on the inactive X in T cells from women with lupus.* J Immunol, 2007. **179**(9): p. 6352-8.
665. Forsdyke, D.R., *X chromosome reactivation perturbs intracellular self/not-self discrimination.* Immunol Cell Biol, 2009. **87**(7): p. 525-8.
666. Zhou, Y., et al., *T cell CD40LG gene expression and the production of IgG by autologous B cells in systemic lupus erythematosus.* Clin Immunol, 2009. **132**(3): p. 362-70.
667. Brooks, W.H., *X chromosome inactivation and autoimmunity.* Clin Rev Allergy Immunol, 2010. **39**(1): p. 20-9.
668. Ranke, M.B. and P. Saenger, *Turner's syndrome.* Lancet, 2001. **358**(9278): p. 309-14.
669. Elsheikh, M., J.A. Wass, and G.S. Conway, *Autoimmune thyroid syndrome in women with Turner's syndrome--the association with karyotype.* Clin Endocrinol (Oxf), 2001. **55**(2): p. 223-6.
670. Sybert, V.P. and E. McCauley, *Turner's syndrome.* N Engl J Med, 2004. **351**(12): p. 1227-38.
671. Invernizzi, P., et al., *X chromosome monosomy: a common mechanism for autoimmune diseases.* J Immunol, 2005. **175**(1): p. 575-8.
672. Invernizzi, P., et al., *Frequency of monosomy X in women with primary biliary cirrhosis.* Lancet, 2004. **363**(9408): p. 533-5.
673. Invernizzi, P., et al., *X monosomy in female systemic lupus erythematosus.* Ann N Y Acad Sci, 2007. **1110**: p. 84-91.
674. Chiurazzi, P., et al., *XLMR genes: update 2007.* Eur J Hum Genet, 2008. **16**(4): p. 422-34.
675. Bonnet, C., et al., *Exploring the potential role of disease-causing mutation in a gene desert: duplication of noncoding elements 5' of GRIA3 is associated with GRIA3 silencing and X-linked intellectual disability.* Hum Mutat, 2012. **33**(2): p. 355-8.
676. Yonath, H., et al., *X inactivation testing for identifying a non-syndromic X-linked mental retardation gene.* J Appl Genet, 2011. **52**(4): p. 437-41.
677. Plenge, R.M., et al., *Skewed X-chromosome inactivation is a common feature of X-linked mental retardation disorders.* Am J Hum Genet, 2002. **71**(1): p. 168-73.
678. Bittel, D.C., et al., *Comparison of X-chromosome inactivation patterns in multiple tissues from human females.* J Med Genet, 2008. **45**(5): p. 309-13.
679. van de Kamp, J.M., et al., *Clinical features and X-inactivation in females heterozygous for creatine transporter defect.* Clin Genet, 2011. **79**(3): p. 264-72.
680. Oostra, B.A. and R. Willemsen, *The X chromosome and fragile X mental retardation.* Cytogenet Genome Res, 2002. **99**(1-4): p. 257-64.
681. Kirchgessner, C.U., S.T. Warren, and H.F. Willard, *X inactivation of the FMR1 fragile X mental retardation gene.* J Med Genet, 1995. **32**(12): p. 925-9.
682. Fryns, J.P., et al., *Inactivation pattern of the fragile X in heterozygous carriers.* Hum Genet, 1984. **65**(4): p. 400-1.
683. Schmidt, M., et al., *Unusual X chromosome inactivation in a mentally retarded girl with an interstitial deletion Xq27: implications for the fragile X syndrome.* Hum Genet, 1990. **84**(4): p. 347-52.
684. Martinez, R., et al., *Skewed X inactivation of the normal allele in fully mutated female carriers determines the levels of FMRP in blood and the fragile X phenotype.* Mol Diagn, 2005. **9**(3): p. 157-62.
685. Martorell, L., et al., *Four sisters compound heterozygotes for the pre- and full mutation in fragile X syndrome and a complete inactivation of X-functional chromosome: implications for genetic counseling.* J Hum Genet, 2011. **56**(1): p. 87-90.

686. Heine-Suner, D., et al., *Fragile-X syndrome and skewed X-chromosome inactivation within a family: a female member with complete inactivation of the functional X chromosome.* Am J Med Genet A, 2003. **122A**(2): p. 108-14.
687. Nolin, S.L., et al., *Mosaicism in fragile X affected males.* Am J Med Genet, 1994. **51**(4): p. 509-12.
688. de Vries, B.B., et al., *Variable FMR1 gene methylation of large expansions leads to variable phenotype in three males from one fragile X family.* J Med Genet, 1996. **33**(12): p. 1007-10.
689. Willemsen, R., et al., *Twin sisters, monozygotic with the fragile X mutation, but with a different phenotype.* J Med Genet, 2000. **37**(8): p. 603-4.
690. Garcia-Alegria, E., et al., *Analysis of FMR1 gene expression in female premutation carriers using robust segmented linear regression models.* RNA, 2007. **13**(5): p. 756-62.
691. Ramocki, M.B., et al., *Autism and other neuropsychiatric symptoms are prevalent in individuals with MeCP2 duplication syndrome.* Ann Neurol, 2009. **66**(6): p. 771-82.
692. del Gaudio, D., et al., *Increased MECP2 gene copy number as the result of genomic duplication in neurodevelopmentally delayed males.* Genet Med, 2006. **8**(12): p. 784-92.
693. Meins, M., et al., *Submicroscopic duplication in Xq28 causes increased expression of the MECP2 gene in a boy with severe mental retardation and features of Rett syndrome.* J Med Genet, 2005. **42**(2): p. e12.
694. Ramocki, M.B., Y.J. Tavyev, and S.U. Peters, *The MECP2 duplication syndrome.* Am J Med Genet A, 2010. **152A**(5): p. 1079-88.
695. Kernohan, K.D., et al., *ATRX partners with cohesin and MeCP2 and contributes to developmental silencing of imprinted genes in the brain.* Dev Cell, 2010. **18**(2): p. 191-202.
696. Honda, S., et al., *Concomitant microduplications of MECP2 and ATRX in male patients with severe mental retardation.* J Hum Genet, 2011.
697. De La Fuente, R., C. Baumann, and M.M. Viveiros, *Role of ATRX in chromatin structure and function: implications for chromosome instability and human disease.* Reproduction, 2011. **142**(2): p. 221-34.
698. Grasshoff, U., et al., *De novo MECP2 duplication in two females with random X-inactivation and moderate mental retardation.* Eur J Hum Genet, 2011. **19**(5): p. 507-12.
699. Mayo, S., et al., *De novo interstitial triplication of MECP2 in a girl with neurodevelopmental disorder and random X chromosome inactivation.* Cytogenet Genome Res, 2011. **135**(2): p. 93-101.
700. Pichavant, C., et al., *Current status of pharmaceutical and genetic therapeutic approaches to treat DMD.* Mol Ther, 2011. **19**(5): p. 830-40.
701. Schanzer, A., et al., *Duchenne Muscular Dystrophy in a 4-Year-Old Girl due to Heterozygous Frame Shift Deletion of the Dystrophin Gene and Skewed X-Inactivation.* Klin Padiatr, 2012.
702. Soltanzadeh, P., et al., *Clinical and genetic characterization of manifesting carriers of DMD mutations.* Neuromuscul Disord, 2010. **20**(8): p. 499-504.
703. Lesca, G., et al., *[Symptomatic carriers of dystrophinopathy with chromosome X inactivation bias].* Rev Neurol (Paris), 2003. **159**(8-9): p. 775-80.
704. Melacini, P., et al., *Cardiac transplantation in a Duchenne muscular dystrophy carrier.* Neuromuscul Disord, 1998. **8**(8): p. 585-90.
705. Yoon, J., et al., *Carrier woman of Duchenne muscular dystrophy mimicking inflammatory myositis.* J Korean Med Sci, 2011. **26**(4): p. 587-91.
706. Seemann, N., et al., *Symptomatic dystrophinopathies in female children.* Neuromuscul Disord, 2011. **21**(3): p. 172-7.
707. Takeda, A., et al., *Eponym: Barth syndrome.* Eur J Pediatr, 2011. **170**(11): p. 1365-7.
708. Grogan, P.M., et al., *Myopathy with skeletal asymmetry and hemidiaphragm elevation is caused by myotubularin mutations.* Neurology, 2005. **64**(9): p. 1638-40.
709. Hedberg, C., et al., *Myopathy in a woman and her daughter associated with a novel splice site MTM1 mutation.* Neuromuscul Disord, 2012. **22**(3): p. 244-51.
710. Sutton, I.J., et al., *Limb girdle and facial weakness in female carriers of X-linked myotubular myopathy mutations.* Neurology, 2001. **57**(5): p. 900-2.
711. Drouet, A., et al., *[Unilateral presentation of X-linked myotubular myopathy (XLMTM) in two out of three female carriers in a family with no affected male].* Rev Neurol (Paris), 2008. **164**(2): p. 169-76.
712. Finsterer, J., *Perspectives of Kennedy's disease.* J Neurol Sci, 2010. **298**(1-2): p. 1-10.
713. Mariotti, C., et al., *Phenotypic manifestations associated with CAG-repeat expansion in the androgen receptor gene in male patients and heterozygous females: a clinical and molecular study of 30 families.* Neuromuscul Disord, 2000. **10**(6): p. 391-7.

714. Sobue, G., et al., *Subclinical phenotypic expressions in heterozygous females of X-linked recessive bulbospinal neuronopathy.* J Neurol Sci, 1993. **117**(1-2): p. 74-8.
715. Chen, R.S., et al., *Random X chromosome methylation patterns in the carriers with clinical phenotypic expressions of X-linked recessive bulbospinal neuronopathy.* Acta Neurol Scand, 1999. **100**(4): p. 249-53.
716. Ishihara, H., et al., *Clinical features and skewed X-chromosome inactivation in female carriers of X-linked recessive spinal and bulbar muscular atrophy.* J Neurol, 2001. **248**(10): p. 856-60.
717. Paradas, C., et al., *Highly skewed inactivation of the wild-type X-chromosome in asymptomatic female carriers of spinal and bulbar muscular atrophy (Kennedy's disease).* J Neurol, 2008. **255**(6): p. 853-7.
718. Yang, Z. and M. Vatta, *Danon disease as a cause of autophagic vacuolar myopathy.* Congenit Heart Dis, 2007. **2**(6): p. 404-9.
719. Majer, F., et al., *Danon disease: a focus on processing of the novel LAMP2 mutation and comments on the beneficial use of peripheral white blood cells in the diagnosis of LAMP2 deficiency.* Gene, 2012. **498**(2): p. 183-95.
720. Fanin, M., et al., *Generalized lysosome-associated membrane protein-2 defect explains multisystem clinical involvement and allows leukocyte diagnostic screening in Danon disease.* Am J Pathol, 2006. **168**(4): p. 1309-20.
721. Yiu, E.M., et al., *A retrospective review of X-linked Charcot-Marie-Tooth disease in childhood.* Neurology, 2011. **76**(5): p. 461-6.
722. Lin, G.S., et al., *A unique mutation in connexin32 associated with severe, early onset CMTX in a heterozygous female.* Ann N Y Acad Sci, 1999. **883**: p. 481-4.
723. Siskind, C.E., et al., *Phenotype expression in women with CMT1X.* J Peripher Nerv Syst, 2011. **16**(2): p. 102-7.
724. Murphy, S.M., et al., *X inactivation in females with X-linked Charcot-Marie-Tooth disease.* Neuromuscul Disord, 2012.
725. Yorifuji, T., et al., *X-inactivation pattern in the liver of a manifesting female with ornithine transcarbamylase (OTC) deficiency.* Clin Genet, 1998. **54**(4): p. 349-53.
726. Gale, R.E., et al., *Tissue specificity of X-chromosome inactivation patterns.* Blood, 1994. **83**(10): p. 2899-905.
727. Pinto, L.L., et al., *Expression of the disease on female carriers of X-linked lysosomal disorders: a brief review.* Orphanet J Rare Dis, 2010. **5**: p. 14.
728. Zarate, Y.A. and R.J. Hopkin, *Fabry's disease.* Lancet, 2008. **372**(9647): p. 1427-35.
729. Kaneski, C.R., et al., *Use of lissamine rhodamine ceramide trihexoside as a functional assay for alpha-galactosidase A in intact cells.* J Lipid Res, 2010. **51**(9): p. 2808-17.
730. Wang, R.Y., et al., *Heterozygous Fabry women are not just carriers, but have a significant burden of disease and impaired quality of life.* Genet Med, 2007. **9**(1): p. 34-45.
731. Giacomini, P.S., et al., *Fabry's disease presenting as stroke in a young female.* Can J Neurol Sci, 2004. **31**(1): p. 112-4.
732. Dobrovolny, R., et al., *Relationship between X-inactivation and clinical involvement in Fabry heterozygotes. Eleven novel mutations in the alpha-galactosidase A gene in the Czech and Slovak population.* J Mol Med (Berl), 2005. **83**(8): p. 647-54.
733. Maier, E.M., et al., *Disease manifestations and X inactivation in heterozygous females with Fabry disease.* Acta Paediatr Suppl, 2006. **95**(451): p. 30-8.
734. Elstein, D., et al., *X-inactivation in Fabry disease.* Gene, 2012.
735. Menkes, J.H., et al., *A sex-linked recessive disorder with retardation of growth, peculiar hair, and focal cerebral and cerebellar degeneration.* Pediatrics, 1962. **29**: p. 764-79.
736. Vulpe, C., et al., *Isolation of a candidate gene for Menkes disease and evidence that it encodes a copper-transporting ATPase.* Nat Genet, 1993. **3**(1): p. 7-13.
737. Mercer, J.F., et al., *Isolation of a partial candidate gene for Menkes disease by positional cloning.* Nat Genet, 1993. **3**(1): p. 20-5.
738. Chelly, J., et al., *Isolation of a candidate gene for Menkes disease that encodes a potential heavy metal binding protein.* Nat Genet, 1993. **3**(1): p. 14-9.
739. Desai, V., et al., *Favorably skewed X-inactivation accounts for neurological sparing in female carriers of Menkes disease.* Clin Genet, 2011. **79**(2): p. 176-82.
740. Sirleto, P., et al., *Lyonization effects of the t(X;16) translocation on the phenotypic expression in a rare female with Menkes disease.* Pediatr Res, 2009. **65**(3): p. 347-51.

741. Lazoff, S.G., et al., *Skeletal dysplasia, occipital horns, diarrhea and obstructive uropathy- a new hereditary syndrome.* Birth Defects Orig Artic Ser, 1975. **11**(5): p. 71-4.
742. Kaler, S.G., et al., *Occipital horn syndrome and a mild Menkes phenotype associated with splice site mutations at the MNK locus.* Nat Genet, 1994. **8**(2): p. 195-202.
743. Yamaguchi, S., et al., *Mutations and polymorphisms in the human ornithine transcarbamylase (OTC) gene.* Hum Mutat, 2006. **27**(7): p. 626-32.
744. Klein, O.D., et al., *Acute fatal presentation of ornithine transcarbamylase deficiency in a previously healthy male.* Hepatol Int, 2008. **2**(3): p. 390-4.
745. Trivedi, M., et al., *Ornithine transcarbamylase deficiency unmasked because of gastrointestinal bleeding.* J Clin Gastroenterol, 2001. **32**(4): p. 340-3.
746. Schimanski, U., et al., *A novel two-nucleotide deletion in the ornithine transcarbamylase gene causing fatal hyperammonia in early pregnancy.* Hepatology, 1996. **24**(6): p. 1413-5.
747. Pridmore, C.L., J.T. Clarke, and S. Blaser, *Ornithine transcarbamylase deficiency in females: an often overlooked cause of treatable encephalopathy.* J Child Neurol, 1995. **10**(5): p. 369-74.
748. Felig, D.M., S.W. Brusilow, and J.L. Boyer, *Hyperammonemic coma due to parenteral nutrition in a woman with heterozygous ornithine transcarbamylase deficiency.* Gastroenterology, 1995. **109**(1): p. 282-4.
749. Migeon, B.R., *X inactivation, female mosaicism, and sex differences in renal diseases.* J Am Soc Nephrol, 2008. **19**(11): p. 2052-9.
750. Rheault, M.N., et al., *X-inactivation modifies disease severity in female carriers of murine X-linked Alport syndrome.* Nephrol Dial Transplant, 2010. **25**(3): p. 764-9.
751. Kashtan, C.E., *Alport syndrome and the X chromosome: implications of a diagnosis of Alport syndrome in females.* Nephrol Dial Transplant, 2007. **22**(6): p. 1499-505.
752. Rheault, M.N., *Women and Alport syndrome.* Pediatr Nephrol, 2012. **27**(1): p. 41-6.
753. Guo, C., et al., *Severe alport phenotype in a woman with two missense mutations in the same COL4A5 gene and preponderant inactivation of the X chromosome carrying the normal allele.* J Clin Invest, 1995. **95**(4): p. 1832-7.
754. Cau, M., et al., *A locus for familial skewed X chromosome inactivation maps to chromosome Xq25 in a family with a female manifesting Lowe syndrome.* J Hum Genet, 2006. **51**(11): p. 1030-6.
755. Demura, M., et al., *Surgical stress-induced transient nephrogenic diabetes insipidus (NDI) associated with decreased Vasopressin receptor2 (AVPR2) expression linked to nonsense-mediated mRNA decay and incomplete skewed X-inactivation in a female patient with a heterozygous AVPR2 mutation (c. 89-90 delAC).* Clin Endocrinol (Oxf), 2004. **60**(6): p. 773-5.
756. Nomura, Y., et al., *Detection of skewed X-inactivation in two female carriers of vasopressin type 2 receptor gene mutation.* J Clin Endocrinol Metab, 1997. **82**(10): p. 3434-7.
757. van Lieburg, A.F., et al., *Clinical phenotype of nephrogenic diabetes insipidus in females heterozygous for a vasopressin type 2 receptor mutation.* Hum Genet, 1995. **96**(1): p. 70-8.
758. Satoh, M., S. Ogikubo, and A. Yoshizawa-Ogasawara, *Correlation between clinical phenotypes and X-inactivation patterns in six female carriers with heterozygote vasopressin type 2 receptor gene mutations.* Endocr J, 2008. **55**(2): p. 277-84.
759. Oohashi, T., et al., *Clonal overgrowth of esophageal smooth muscle cells in diffuse leiomyomatosis-Alport syndrome caused by partial deletion in COL4A5 and COL4A6 genes.* Matrix Biol, 2011. **30**(1): p. 3-8.
760. Orstavik, K.H., et al., *X chromosome inactivation pattern in female carriers of X linked hypophosphataemic rickets.* J Med Genet, 1996. **33**(8): p. 700-3.
761. Owen, C.J., et al., *Discordance for X-linked hypophosphataemic rickets in identical twin girls.* Horm Res, 2009. **71**(4): p. 237-44.
762. Faerch, M., et al., *Skewed X-chromosome inactivation causing diagnostic misinterpretation in congenital nephrogenic diabetes insipidus.* Scand J Urol Nephrol, 2010. **44**(5): p. 324-30.
763. Decaux, G., et al., *Nephrogenic syndrome of inappropriate antidiuresis in adults: high phenotypic variability in men and women from a large pedigree.* J Am Soc Nephrol, 2007. **18**(2): p. 606-12.
764. De Gregorio, L., et al., *Lesch-Nyhan disease in a female with a clinically normal monozygotic twin.* Mol Genet Metab, 2005. **85**(1): p. 70-7.
765. Rinat, C., et al., *Molecular, biochemical, and genetic characterization of a female patient with Lesch-Nyhan disease.* Mol Genet Metab, 2006. **87**(3): p. 249-52.

766. Blaschko, A., *Die Nervenverteilung in der Haut in ihrer Beziehung zu den Erkrankungen der Haut. Beilage zu den Verhandlungen der Deutschen Dermatologischen Gesellschaft.* 1901, Wien Leipzig: Braumüller.
767. Happle, R., *Lyonization and the lines of Blaschko.* Hum Genet, 1985. **70**(3): p. 200-6.
768. Happle, R., *X-chromosome inactivation: role in skin disease expression.* Acta Paediatr Suppl, 2006. **95**(451): p. 16-23.
769. Lexner, M.O., et al., *X-linked hypohidrotic ectodermal dysplasia. Genetic and dental findings in 67 Danish patients from 19 families.* Clin Genet, 2008. **74**(3): p. 252-9.
770. Balmer, R., et al., *Enamel defects and Lyonization in focal dermal hypoplasia.* Oral Surg Oral Med Oral Pathol Oral Radiol Endod, 2004. **98**(6): p. 686-91.
771. Witkop, C.J., Jr., *Partial expression of sex-linked recessive amelogenesis imperfecta in females compatible with the Lyon hypothesis.* Oral Surg Oral Med Oral Pathol, 1967. **23**(2): p. 174-82.
772. Rott, H.D., *Extracutaneous analogies of Blaschko lines.* Am J Med Genet, 1999. **85**(4): p. 338-41.
773. Thomas, G.A., D. Williams, and E.D. Williams, *The demonstration of tissue clonality by X-linked enzyme histochemistry.* J Pathol, 1988. **155**(2): p. 101-8.
774. Tan, S.S. and S. Breen, *Radial mosaicism and tangential cell dispersion both contribute to mouse neocortical development.* Nature, 1993. **362**(6421): p. 638-40.
775. Konig, A., et al., *Mutations in the NSDHL gene, encoding a 3beta-hydroxysteroid dehydrogenase, cause CHILD syndrome.* Am J Med Genet, 2000. **90**(4): p. 339-46.
776. Jurkiewicz, D., et al., *Four novel RSK2 mutations in females with Coffin-Lowry syndrome.* Eur J Med Genet, 2010. **53**(5): p. 268-73.
777. Wang, Y., et al., *A novel RSK2 (RPS6KA3) gene mutation associated with abnormal brain MRI findings in a family with Coffin-Lowry syndrome.* Am J Med Genet A, 2006. **140**(12): p. 1274-9.
778. Simensen, R.J., et al., *Cognitive function in Coffin-Lowry syndrome.* Clin Genet, 2002. **61**(4): p. 299-304.
779. Aten, E., et al., *Keratosis Follicularis Spinulosa Decalvans is caused by mutations in MBTPS2.* Hum Mutat, 2010. **31**(10): p. 1125-33.
780. Graham, J.M., Jr., et al., *Behavior of 10 patients with FG syndrome (Opitz-Kaveggia syndrome) and the p.R961W mutation in the MED12 gene.* Am J Med Genet A, 2008. **146A**(23): p. 3011-7.
781. Yano, S., et al., *Familial Simpson-Golabi-Behmel syndrome: studies of X-chromosome inactivation and clinical phenotypes in two female individuals with GPC3 mutations.* Clin Genet, 2011. **80**(5): p. 466-71.
782. Hernandez-Martin, A., R. Gonzalez-Sarmiento, and P. De Unamuno, *X-linked ichthyosis: an update.* Br J Dermatol, 1999. **141**(4): p. 617-27.
783. Happle, R., *Cutaneous manifestation of X-linked genes escaping inactivation.* Clin Exp Dermatol, 1992. **17**(1): p. 69.
784. Simunovic, M.P., *Colour vision deficiency.* Eye (Lond), 2010. **24**(5): p. 747-55.
785. Martinez-Garcia, M., et al., *Identification of a novel deletion in the OA1 gene: report of the first Spanish family with X-linked ocular albinism.* Clin Experiment Ophthalmol, 2010. **38**(5): p. 489-95.
786. Kondo, H., et al., *Novel mutations in Norrie disease gene in Japanese patients with Norrie disease and familial exudative vitreoretinopathy.* Invest Ophthalmol Vis Sci, 2007. **48**(3): p. 1276-82.
787. Sato, M., et al., *Three novel mutations in the X-linked juvenile retinoschisis (XLRS1) gene in 6 Japanese patients, 1 of whom had Turner's syndrome.* Ophthalmic Res, 2003. **35**(5): p. 295-300.
788. Mendoza-Londono, R., et al., *A Colombian family with X-linked juvenile retinoschisis with three affected females finding of a frameshift mutation.* Ophthalmic Genet, 1999. **20**(1): p. 37-43.
789. Rodriguez, F.J., et al., *X-linked retinoschisis in three females from the same family: a phenotype-genotype correlation.* Retina, 2005. **25**(1): p. 69-74.
790. Watkins, R.J., et al., *The Role of FRMD7 in Idiopathic Infantile Nystagmus.* J Ophthalmol, 2012. **2012**: p. 460956.
791. Zhang, Q., et al., *FRMD7 mutations in Chinese families with X-linked congenital motor nystagmus.* Mol Vis, 2007. **13**: p. 1375-8.
792. Kaplan, Y., et al., *Skewed X inactivation in an X linked nystagmus family resulted from a novel, p.R229G, missense mutation in the FRMD7 gene.* Br J Ophthalmol, 2008. **92**(1): p. 135-41.
793. Self, J.E., et al., *Allelic variation of the FRMD7 gene in congenital idiopathic nystagmus.* Arch Ophthalmol, 2007. **125**(9): p. 1255-63.
794. Terai, N. and F. Raiskup, *[Bilateral visual loss in a young male patient].* Ophthalmologe, 2012. **109**(5): p. 487-90.

795. Callea, M., et al., *Infantile bilateral glaucoma in a child with ectodermal dysplasia.* Ophthalmic Genet, 2012.
796. *ACOG practice bulletin. Management of recurrent pregnancy loss. Number 24, February 2001. (Replaces Technical Bulletin Number 212, September 1995). American College of Obstetricians and Gynecologists.* Int J Gynaecol Obstet, 2002. **78**(2): p. 179-90.
797. Lanasa, M.C., et al., *Highly skewed X-chromosome inactivation is associated with idiopathic recurrent spontaneous abortion.* Am J Hum Genet, 1999. **65**(1): p. 252-4.
798. Sangha, K.K., et al., *Extremely skewed X-chromosome inactivation is increased in women with recurrent spontaneous abortion.* Am J Hum Genet, 1999. **65**(3): p. 913-7.
799. Robinson, W.P., et al., *Skewed X inactivation and recurrent spontaneous abortion.* Semin Reprod Med, 2001. **19**(2): p. 175-81.
800. Uehara, S., et al., *Preferential X-chromosome inactivation in women with idiopathic recurrent pregnancy loss.* Fertil Steril, 2001. **76**(5): p. 908-14.
801. Su, M.T., S.H. Lin, and Y.C. Chen, *Association of sex hormone receptor gene polymorphisms with recurrent pregnancy loss: a systematic review and meta-analysis.* Fertil Steril, 2011. **96**(6): p. 1435-1444 e1.
802. Bagislar, S., et al., *Extremely skewed X-chromosome inactivation patterns in women with recurrent spontaneous abortion.* Aust N Z J Obstet Gynaecol, 2006. **46**(5): p. 384-7.
803. Kuo, P.L., et al., *Association of extremely skewed X-chromosome inactivation with Taiwanese women presenting with recurrent pregnancy loss.* J Formos Med Assoc, 2008. **107**(4): p. 340-3.
804. Kim, J.W., et al., *X-chromosome inactivation patterns in Korean women with idiopathic recurrent spontaneous abortion.* J Korean Med Sci, 2004. **19**(2): p. 258-62.
805. Aruna, M., et al., *Role of androgen receptor CAG repeat polymorphism and X-inactivation in the manifestation of recurrent spontaneous abortions in Indian women.* PLoS One, 2011. **6**(3): p. e17718.
806. Dasoula, A., et al., *Skewed X-chromosome inactivation in Greek women with idiopathic recurrent miscarriage.* Fetal Diagn Ther, 2008. **23**(3): p. 198-203.
807. Beever, C.L., et al., *Skewed X-chromosome inactivation is associated with trisomy in women ascertained on the basis of recurrent spontaneous abortion or chromosomally abnormal pregnancies.* Am J Hum Genet, 2003. **72**(2): p. 399-407.
808. Bretherick, K., J. Gair, and W.P. Robinson, *The association of skewed X chromosome inactivation with aneuploidy in humans.* Cytogenet Genome Res, 2005. **111**(3-4): p. 260-5.
809. Warburton, D., et al., *Skewed X chromosome inactivation and trisomic spontaneous abortion: no association.* Am J Hum Genet, 2009. **85**(2): p. 179-93.
810. Toniolo, D. and F. Rizzolio, *X chromosome and ovarian failure.* Semin Reprod Med, 2007. **25**(4): p. 264-71.
811. Ferreira, S.I., et al., *X-chromosome terminal deletion in a female with premature ovarian failure: Haploinsufficiency of X-linked genes as a possible explanation.* Mol Cytogenet, 2010. **3**: p. 14.
812. Bertini, V., et al., *Molecular cytogenetic definition of a translocation t(X;15) associated with premature ovarian failure.* Fertil Steril, 2010. **94**(3): p. 1097 e5-8.
813. Layman, L.C., *Editorial: BMP15--the first true ovarian determinant gene on the X-chromosome?* J Clin Endocrinol Metab, 2006. **91**(5): p. 1673-6.
814. Di Pasquale, E., P. Beck-Peccoz, and L. Persani, *Hypergonadotropic ovarian failure associated with an inherited mutation of human bone morphogenetic protein-15 (BMP15) gene.* Am J Hum Genet, 2004. **75**(1): p. 106-11.
815. Allingham-Hawkins, D.J., et al., *Fragile X premutation is a significant risk factor for premature ovarian failure: the International Collaborative POF in Fragile X study--preliminary data.* Am J Med Genet, 1999. **83**(4): p. 322-5.
816. Sato, K., et al., *Genetic significance of skewed X-chromosome inactivation in premature ovarian failure.* Am J Med Genet A, 2004. **130A**(3): p. 240-4.
817. Bretherick, K.L., et al., *Skewed X-chromosome inactivation is associated with primary but not secondary ovarian failure.* Am J Med Genet A, 2007. **143A**(9): p. 945-51.
818. Rodriguez-Revenga, L., et al., *Premature ovarian failure and fragile X female premutation carriers: no evidence for a skewed X-chromosome inactivation pattern.* Menopause, 2009. **16**(5): p. 944-9.
819. Tejada, M.I., et al., *Analysis of the molecular parameters that could predict the risk of manifesting premature ovarian failure in female premutation carriers of fragile X syndrome.* Menopause, 2008. **15**(5): p. 945-9.

820. Yoon, S.H., et al., *X chromosome inactivation patterns in patients with idiopathic premature ovarian failure.* Hum Reprod, 2008. **23**(3): p. 688-92.
821. Spath, M.A., et al., *X chromosome inactivation does not define the development of premature ovarian failure in fragile X premutation carriers.* Am J Med Genet A, 2010. **152A**(2): p. 387-93.
822. Pu, D., J. Wu, and J. Liu, *Skewed X chromosome inactivation may be not associated with premature ovarian failure.* Gynecol Endocrinol, 2010. **26**(6): p. 423-8.
823. Medema, R.H. and B.M. Burgering, *The X factor: skewing X inactivation towards cancer.* Cell, 2007. **129**(7): p. 1253-4.
824. Kido, T., J.H. Ou, and Y.F. Lau, *The X-linked tumor suppressor TSPX interacts and promotes degradation of the hepatitis B viral protein HBx via the proteasome pathway.* PLoS One, 2011. **6**(7): p. e22979.
825. Liu, R., M. Kain, and L. Wang, *Inactivation of X-linked tumor suppressor genes in human cancer.* Future Oncol, 2012. **8**(4): p. 463-81.
826. Rivera, M.N., et al., *An X chromosome gene, WTX, is commonly inactivated in Wilms tumor.* Science, 2007. **315**(5812): p. 642-5.
827. Zuo, T., et al., *FOXP3 is an X-linked breast cancer suppressor gene and an important repressor of the HER-2/ErbB2 oncogene.* Cell, 2007. **129**(7): p. 1275-86.
828. Wang, L., et al., *FOXP3 as an X-linked tumor suppressor.* Discov Med, 2010. **10**(53): p. 322-8.
829. Knudson, A.G., Jr., *Mutation and cancer: statistical study of retinoblastoma.* Proc Natl Acad Sci U S A, 1971. **68**(4): p. 820-3.
830. Weakley, S.M., et al., *Expression and function of a large non-coding RNA gene XIST in human cancer.* World J Surg, 2011. **35**(8): p. 1751-6.
831. Kawakami, T., et al., *The roles of supernumerical X chromosomes and XIST expression in testicular germ cell tumors.* J Urol, 2003. **169**(4): p. 1546-52.
832. Lind, G.E., R.I. Skotheim, and R.A. Lothe, *The epigenome of testicular germ cell tumors.* APMIS, 2007. **115**(10): p. 1147-60.
833. Sirchia, S.M., et al., *Misbehaviour of XIST RNA in breast cancer cells.* PLoS One, 2009. **4**(5): p. e5559.
834. Huang, K.C., et al., *Relationship of XIST expression and responses of ovarian cancer to chemotherapy.* Mol Cancer Ther, 2002. **1**(10): p. 769-76.
835. Kawakami, T., et al., *Characterization of loss-of-inactive X in Klinefelter syndrome and female-derived cancer cells.* Oncogene, 2004. **23**(36): p. 6163-9.
836. McDonald, H.L., et al., *Involvement of the X chromosome in non-Hodgkin lymphoma.* Genes Chromosomes Cancer, 2000. **28**(3): p. 246-57.
837. Sirchia, S.M., et al., *Loss of the inactive X chromosome and replication of the active X in BRCA1-defective and wild-type breast cancer cells.* Cancer Res, 2005. **65**(6): p. 2139-46.
838. Wang, N., et al., *Two identical active X chromosomes in human mammary carcinoma cells.* Cancer Genet Cytogenet, 1990. **46**(2): p. 271-80.
839. van Leenders, G.J., et al., *Polycomb-group oncogenes EZH2, BMI1, and RING1 are overexpressed in prostate cancer with adverse pathologic and clinical features.* Eur Urol, 2007. **52**(2): p. 455-63.
840. Simon, J.A. and C.A. Lange, *Roles of the EZH2 histone methyltransferase in cancer epigenetics.* Mutat Res, 2008. **647**(1-2): p. 21-9.
841. Laird, P.W. and R. Jaenisch, *The role of DNA methylation in cancer genetic and epigenetics.* Annu Rev Genet, 1996. **30**: p. 441-64.
842. Iacobuzio-Donahue, C.A., *Epigenetic changes in cancer.* Annu Rev Pathol, 2009. **4**: p. 229-49.
843. Pageau, G.J., L.L. Hall, and J.B. Lawrence, *BRCA1 does not paint the inactive X to localize XIST RNA but may contribute to broad changes in cancer that impact XIST and Xi heterochromatin.* J Cell Biochem, 2007. **100**(4): p. 835-50.
844. Klinefelter, H.F., E.C. Reifenstein, and F. Albright, *Syndrome characterized by gynecomastia, aspermatogenesis without Leydigism, increased excretion of follicle stimulating hormone.* J Clin Endocrinol 1942. **2**: p. 615-627.
845. Jacobs, P.A. and J.A. Strong, *A case of human intersexuality having a possible XXY sex-determining mechanism.* Nature, 1959. **183**(4657): p. 302-3.
846. Tuttelmann, F. and J. Gromoll, *Novel genetic aspects of Klinefelter's syndrome.* Mol Hum Reprod, 2010. **16**(6): p. 386-95.
847. Morris, J.K., et al., *Is the prevalence of Klinefelter syndrome increasing?* Eur J Hum Genet, 2008. **16**(2): p. 163-70.

848. Iitsuka, Y., et al., *Evidence of skewed X-chromosome inactivation in 47,XXY and 48,XXYY Klinefelter patients.* Am J Med Genet, 2001. **98**(1): p. 25-31.
849. Zitzmann, M., et al., *X-chromosome inactivation patterns and androgen receptor functionality influence phenotype and social characteristics as well as pharmacogenetics of testosterone therapy in Klinefelter patients.* J Clin Endocrinol Metab, 2004. **89**(12): p. 6208-17.
850. Bojesen, A., J.M. Hertz, and C.H. Gravholt, *Genotype and phenotype in Klinefelter syndrome - impact of androgen receptor polymorphism and skewed X inactivation.* Int J Androl, 2011. **34**(6 Pt 2): p. e642-8.
851. Kanaka-Gantenbein, C., et al., *Tall stature, insulin resistance, and disturbed behavior in a girl with the triple X syndrome harboring three SHOX genes: offspring of a father with mosaic Klinefelter syndrome but with two maternal X chromosomes.* Horm Res, 2004. **61**(5): p. 205-10.
852. Prendiville, J.S., et al., *Incontinentia pigmenti in a male infant with Klinefelter syndrome.* J Am Acad Dermatol, 1989. **20**(5 Pt 2): p. 937-40.
853. Ormerod, A.D., et al., *Incontinentia pigmenti in a boy with Klinefelter's syndrome.* J Med Genet, 1987. **24**(7): p. 439-41.
854. Buinauskaite, E., et al., *Incontinentia pigmenti in a male infant with Klinefelter syndrome: a case report and review of the literature.* Pediatr Dermatol, 2010. **27**(5): p. 492-5.
855. Kenwrick, S., et al., *Survival of male patients with incontinentia pigmenti carrying a lethal mutation can be explained by somatic mosaicism or Klinefelter syndrome.* Am J Hum Genet, 2001. **69**(6): p. 1210-7.
856. Cho, S.Y., C.K. Lee, and B.K. Drummond, *Surviving male with incontinentia pigmenti: a case report.* Int J Paediatr Dent, 2004. **14**(1): p. 69-72.
857. Turner, H.H., *A syndrome of infantilism, congenital webbed neck and cubitus valgus.* Endocrinology, 1938. **23**: p. 566-574.
858. Ford, C.E., et al., *A sex-chromosome anomaly in a case of gonadal dysgenesis (Turner's syndrome).* Lancet, 1959. **1**(7075): p. 711-3.
859. Zinn, A.R., D.C. Page, and E.M. Fisher, *Turner syndrome: the case of the missing sex chromosome.* Trends Genet, 1993. **9**(3): p. 90-3.
860. Rao, E., et al., *Pseudoautosomal deletions encompassing a novel homeobox gene cause growth failure in idiopathic short stature and Turner syndrome.* Nat Genet, 1997. **16**(1): p. 54-63.
861. Shears, D.J., et al., *Mutation and deletion of the pseudoautosomal gene SHOX cause Leri-Weill dyschondrosteosis.* Nat Genet, 1998. **19**(1): p. 70-3.
862. Speed, R.M., *The possible role of meiotic pairing anomalies in the atresia of human fetal oocytes.* Hum Genet, 1988. **78**(3): p. 260-6.
863. Cohen, M.M., et al., *Autoradiographic investigations of centric fragments and rings in patients with stigmata of gonadal dysgenesis.* Cytogenetics, 1967. **6**(3): p. 254-67.
864. Kushnick, T., et al., *45X/46X,r(X) with syndactyly and severe mental retardation.* Am J Med Genet, 1987. **28**(3): p. 567-74.
865. Lindgren, V., et al., *Cytogenetic and molecular characterization of marker chromosomes in patients with mosaic 45,X karyotypes.* Hum Genet, 1992. **88**(4): p. 393-8.
866. Van Dyke, D.L., et al., *Mental retardation in Turner syndrome.* J Pediatr, 1991. **118**(3): p. 415-7.
867. Van Dyke, D.L., et al., *Ullrich-Turner syndrome with a small ring X chromosome and presence of mental retardation.* Am J Med Genet, 1992. **43**(6): p. 996-1005.
868. Dennis, N.R., et al., *Three patients with ring (X) chromosomes and a severe phenotype.* J Med Genet, 1993. **30**(6): p. 482-6.
869. Grompe, M., et al., *45,X/46,X,+r(X) can have a distinct phenotype different from Ullrich-Turner syndrome.* Am J Med Genet, 1992. **42**(1): p. 39-43.
870. El Abd, S., et al., *Social, communicational, and behavioral deficits associated with ring X turner syndrome.* Am J Med Genet, 1999. **88**(5): p. 510-6.
871. Kubota, T., et al., *The proportion of cells with functional X disomy is associated with the severity of mental retardation in mosaic ring X Turner syndrome females.* Cytogenet Genome Res, 2002. **99**(1-4): p. 276-84.
872. Migeon, B.R., et al., *The severe phenotype of females with tiny ring X chromosomes is associated with inability of these chromosomes to undergo X inactivation.* Am J Hum Genet, 1994. **55**(3): p. 497-504.
873. Migeon, B.R., et al., *Deficient transcription of XIST from tiny ring X chromosomes in females with severe phenotypes.* Proc Natl Acad Sci U S A, 1993. **90**(24): p. 12025-9.

874. Shchelochkov, O.A., et al., *Mosaicism for r(X) and der(X)del(X)(p11.23)dup(X)(p11.21p11.22) provides insight into the possible mechanism of rearrangement.* Mol Cytogenet, 2008. **1**: p. 16.
875. Wolff, D.J., et al., *Small marker X chromosomes lack the X inactivation center: implications for karyotype/phenotype correlations.* Am J Hum Genet, 1994. **55**(1): p. 87-95.
876. Cole, H., et al., *Mental retardation and Ullrich-Turner syndrome in cases with 45,X/46X,+mar: additional support for the loss of the X-inactivation center hypothesis.* Am J Med Genet, 1994. **52**(2): p. 136-45.
877. Stavropoulou, C., et al., *Severe phenotype resulting from an active ring X chromosome in a female with a complex karyotype: characterisation and replication study.* J Med Genet, 1998. **35**(11): p. 932-8.
878. Otter, M., C.T. Schrander-Stumpel, and L.M. Curfs, *Triple X syndrome: a review of the literature.* Eur J Hum Genet, 2010. **18**(3): p. 265-71.
879. Tartaglia, N.R., et al., *A review of trisomy X (47,XXX).* Orphanet J Rare Dis, 2010. **5**: p. 8.
880. Ratcliffe, S.G., H. Pan, and M. McKie, *The growth of XXX females: population-based studies.* Ann Hum Biol, 1994. **21**(1): p. 57-66.
881. Alvesalo, L., E. Tammisalo, and E. Therman, *47,XXX females, sex chromosomes, and tooth crown structure.* Hum Genet, 1987. **77**(4): p. 345-8.
882. Gropman, A.L., et al., *Clinical variability and novel neurodevelopmental findings in 49, XXXXY syndrome.* Am J Med Genet A, 2010. **152A**(6): p. 1523-30.
883. Monheit, A., et al., *The penta-X syndrome.* J Med Genet, 1980. **17**(5): p. 392-6.
884. Linden, M.G., B.G. Bender, and A. Robinson, *Sex chromosome tetrasomy and pentasomy.* Pediatrics, 1995. **96**(4 Pt 1): p. 672-82.
885. Visootsak, J., et al., *Behavioral phenotype of sex chromosome aneuploidies: 48,XXYY, 48,XXXY, and 49,XXXXY.* Am J Med Genet A, 2007. **143A**(11): p. 1198-203.
886. Therman, E., et al., *X chromosome constitution and the human female phenotype.* Hum Genet, 1980. **54**(2): p. 133-43.
887. Sarto, G.E., et al., *What causes the abnormal phenotype in a 49,XXXXY male?* Hum Genet, 1987. **76**(1): p. 1-4.
888. Moraes, L.M., et al., *Detailed analysis of X chromosome inactivation in a 49,XXXXX pentasomy.* Mol Cytogenet, 2009. **2**: p. 20.
889. Stochholm, K., et al., *Criminality in men with Klinefelter's syndrome and XYY syndrome: a cohort study.* BMJ Open, 2012. **2**(1): p. e000650.
890. Freyne, A. and A. O'Connor, *XYY genotype and crime: 2 cases.* Med Sci Law, 1992. **32**(3): p. 261-3.
891. Ross, J.L., et al., *Behavioral and social phenotypes in boys with 47,XYY syndrome or 47,XXY Klinefelter syndrome.* Pediatrics, 2012. **129**(4): p. 769-78.
892. Wutz, A. and J. Gribnau, *X inactivation Xplained.* Curr Opin Genet Dev, 2007. **17**(5): p. 387-93.
893. Bach, I., et al., *RLIM inhibits functional activity of LIM homeodomain transcription factors via recruitment of the histone deacetylase complex.* Nat Genet, 1999. **22**(4): p. 394-9.
894. Her, Y.R. and I.K. Chung, *Ubiquitin Ligase RLIM Modulates Telomere Length Homeostasis through a Proteolysis of TRF1.* J Biol Chem, 2009. **284**(13): p. 8557-66.
895. Johnsen, S.A., et al., *Regulation of estrogen-dependent transcription by the LIM cofactors CLIM and RLIM in breast cancer.* Cancer Res, 2009. **69**(1): p. 128-36.
896. Kalantry, S., et al., *Evidence of Xist RNA-independent initiation of mouse imprinted X-chromosome inactivation.* Nature, 2009. **460**(7255): p. 647-51.
897. Becker, T., et al., *Comparing protein stabilities during zebrafish embryogenesis.* Methods Cell Sci, 2003. **25**(1-2): p. 85-9.
898. Sado, T., Y. Hoki, and H. Sasaki, *Tsix defective in splicing is competent to establish Xist silencing.* Development, 2006. **133**(24): p. 4925-31.
899. Cline, T.W. and B.J. Meyer, *Vive la difference: males vs females in flies vs worms.* Annu Rev Genet, 1996. **30**: p. 637-702.
900. Lee, E.C., et al., *A highly efficient Escherichia coli-based chromosome engineering system adapted for recombinogenic targeting and subcloning of BAC DNA.* Genomics, 2001. **73**(1): p. 56-65.
901. Capecchi, M.R., *Altering the genome by homologous recombination.* Science, 1989. **244**(4910): p. 1288-92.
902. Deng, C. and M.R. Capecchi, *Reexamination of gene targeting frequency as a function of the extent of homology between the targeting vector and the target locus.* Mol Cell Biol, 1992. **12**(8): p. 3365-71.
903. Hasty, P., et al., *Target frequency and integration pattern for insertion and replacement vectors in embryonic stem cells.* Mol Cell Biol, 1991. **11**(9): p. 4509-17.

904. te Riele, H., E.R. Maandag, and A. Berns, *Highly efficient gene targeting in embryonic stem cells through homologous recombination with isogenic DNA constructs.* Proc Natl Acad Sci U S A, 1992. **89**(11): p. 5128-32.
905. Valenzuela, D.M., et al., *High-throughput engineering of the mouse genome coupled with high-resolution expression analysis.* Nat Biotechnol, 2003. **21**(6): p. 652-9.
906. Yang, Y. and B. Seed, *Site-specific gene targeting in mouse embryonic stem cells with intact bacterial artificial chromosomes.* Nat Biotechnol, 2003. **21**(4): p. 447-51.
907. Song, H., S.K. Chung, and Y. Xu, *Modeling disease in human ESCs using an efficient BAC-based homologous recombination system.* Cell Stem Cell, 2010. **6**(1): p. 80-9.
908. Osoegawa, K., et al., *Bacterial artificial chromosome libraries for mouse sequencing and functional analysis.* Genome Res, 2000. **10**(1): p. 116-28.
909. Frazer, K.A., et al., *A sequence-based variation map of 8.27 million SNPs in inbred mouse strains.* Nature, 2007. **448**(7157): p. 1050-3.
910. Barakat, T.S., et al., *X-changing information on X inactivation.* Exp Cell Res, 2010. **316**(5): p. 679-87.
911. Barakat, T.S., et al., *RNF12 activates Xist and is essential for X chromosome inactivation.* PLoS Genet, 2011. **7**(1): p. e1002001.
912. Eggan, K., et al., *Hybrid vigor, fetal overgrowth, and viability of mice derived by nuclear cloning and tetraploid embryo complementation.* Proc Natl Acad Sci U S A, 2001. **98**(11): p. 6209-14.
913. Bradley, A., et al., *Formation of germ-line chimaeras from embryo-derived teratocarcinoma cell lines.* Nature, 1984. **309**(5965): p. 255-6.
914. Thomas, K.R. and M.R. Capecchi, *Site-directed mutagenesis by gene targeting in mouse embryo-derived stem cells.* Cell, 1987. **51**(3): p. 503-12.
915. Mansour, S.L., K.R. Thomas, and M.R. Capecchi, *Disruption of the proto-oncogene int-2 in mouse embryo-derived stem cells: a general strategy for targeting mutations to non-selectable genes.* Nature, 1988. **336**(6197): p. 348-52.
916. Smithies, O., et al., *Insertion of DNA sequences into the human chromosomal beta-globin locus by homologous recombination.* Nature, 1985. **317**(6034): p. 230-4.
917. Doetschman, T., et al., *Targetted correction of a mutant HPRT gene in mouse embryonic stem cells.* Nature, 1987. **330**(6148): p. 576-8.
918. Koller, B.H., et al., *Normal development of mice deficient in beta 2M, MHC class I proteins, and CD8+ T cells.* Science, 1990. **248**(4960): p. 1227-30.
919. Schwartzberg, P.L., S.P. Goff, and E.J. Robertson, *Germ-line transmission of a c-abl mutation produced by targeted gene disruption in ES cells.* Science, 1989. **246**(4931): p. 799-803.
920. Zijlstra, M., et al., *Germ-line transmission of a disrupted beta 2-microglobulin gene produced by homologous recombination in embryonic stem cells.* Nature, 1989. **342**(6248): p. 435-8.
921. International Mouse Knockout, C., et al., *A mouse for all reasons.* Cell, 2007. **128**(1): p. 9-13.
922. Austin, C.P., et al., *The knockout mouse project.* Nat Genet, 2004. **36**(9): p. 921-4.
923. Auwerx, J., et al., *The European dimension for the mouse genome mutagenesis program.* Nat Genet, 2004. **36**(9): p. 925-7.
924. Pardo, M., et al., *An expanded Oct4 interaction network: implications for stem cell biology, development, and disease.* Cell Stem Cell, 2010. **6**(4): p. 382-95.
925. Ciotta, G., et al., *Recombineering BAC transgenes for protein tagging.* Methods, 2011. **53**(2): p. 113-9.
926. Zhang, P., M.Z. Li, and S.J. Elledge, *Towards genetic genome projects: genomic library screening and gene-targeting vector construction in a single step.* Nat Genet, 2002. **30**(1): p. 31-9.
927. Testa, G., et al., *Engineering the mouse genome with bacterial artificial chromosomes to create multipurpose alleles.* Nat Biotechnol, 2003. **21**(4): p. 443-7.
928. Cotta-de-Almeida, V., et al., *A new method for rapidly generating gene-targeting vectors by engineering BACs through homologous recombination in bacteria.* Genome Res, 2003. **13**(9): p. 2190-4.
929. Testa, G., et al., *BAC engineering for the generation of ES cell-targeting constructs and mouse transgenes.* Methods Mol Biol, 2004. **256**: p. 123-39.
930. Shizuya, H., et al., *Cloning and stable maintenance of 300-kilobase-pair fragments of human DNA in Escherichia coli using an F-factor-based vector.* Proc Natl Acad Sci U S A, 1992. **89**(18): p. 8794-7.
931. Ioannou, P.A., et al., *A new bacteriophage P1-derived vector for the propagation of large human DNA fragments.* Nat Genet, 1994. **6**(1): p. 84-9.
932. Marra, M.A., et al., *High throughput fingerprint analysis of large-insert clones.* Genome Res, 1997. **7**(11): p. 1072-84.

933. Kelley, J.M., et al., *High throughput direct end sequencing of BAC clones.* Nucleic Acids Res, 1999. **27**(6): p. 1539-46.
934. Osoegawa, K. and P.J. de Jong, *BAC library construction.* Methods Mol Biol, 2004. **255**: p. 1-46.
935. Mozo, T., et al., *A complete BAC-based physical map of the Arabidopsis thaliana genome.* Nat Genet, 1999. **22**(3): p. 271-5.
936. Hoskins, R.A., et al., *A BAC-based physical map of the major autosomes of Drosophila melanogaster.* Science, 2000. **287**(5461): p. 2271-4.
937. McPherson, J.D., et al., *A physical map of the human genome.* Nature, 2001. **409**(6822): p. 934-41.
938. Kim, U.J., et al., *Construction and characterization of a human bacterial artificial chromosome library.* Genomics, 1996. **34**(2): p. 213-8.
939. Frengen, E., et al., *A modular, positive selection bacterial artificial chromosome vector with multiple cloning sites.* Genomics, 1999. **58**(3): p. 250-3.
940. Frengen, E., et al., *Modular bacterial artificial chromosome vectors for transfer of large inserts into mammalian cells.* Genomics, 2000. **68**(2): p. 118-26.
941. Hejna, J.A., et al., *Functional complementation by electroporation of human BACs into mammalian fibroblast cells.* Nucleic Acids Res, 1998. **26**(4): p. 1124-5.
942. Jessen, J.R., et al., *Modification of bacterial artificial chromosomes through chi-stimulated homologous recombination and its application in zebrafish transgenesis.* Proc Natl Acad Sci U S A, 1998. **95**(9): p. 5121-6.
943. Muyrers, J.P., et al., *ET recombination: DNA engineering using homologous recombination in E. coli.* Methods Mol Biol, 2004. **256**: p. 107-21.
944. Muyrers, J.P., et al., *Rapid modification of bacterial artificial chromosomes by ET-recombination.* Nucleic Acids Res, 1999. **27**(6): p. 1555-7.
945. Narayanan, K., et al., *Efficient and precise engineering of a 200 kb beta-globin human/bacterial artificial chromosome in E. coli DH10B using an inducible homologous recombination system.* Gene Ther, 1999. **6**(3): p. 442-7.
946. Chan, W., et al., *A recombineering based approach for high-throughput conditional knockout targeting vector construction.* Nucleic Acids Res, 2007. **35**(8): p. e64.
947. Adams, D.J., et al., *Mutagenic insertion and chromosome engineering resource (MICER).* Nat Genet, 2004. **36**(8): p. 867-71.
948. Yang, X.W., P. Model, and N. Heintz, *Homologous recombination based modification in Escherichia coli and germline transmission in transgenic mice of a bacterial artificial chromosome.* Nat Biotechnol, 1997. **15**(9): p. 859-65.
949. Lalioti, M. and J. Heath, *A new method for generating point mutations in bacterial artificial chromosomes by homologous recombination in Escherichia coli.* Nucleic Acids Res, 2001. **29**(3): p. E14.
950. Zhang, Y., et al., *A new logic for DNA engineering using recombination in Escherichia coli.* Nat Genet, 1998. **20**(2): p. 123-8.
951. Murphy, K.C., *Use of bacteriophage lambda recombination functions to promote gene replacement in Escherichia coli.* J Bacteriol, 1998. **180**(8): p. 2063-71.
952. Sharan, S.K., et al., *Recombineering: a homologous recombination-based method of genetic engineering.* Nat Protoc, 2009. **4**(2): p. 206-23.
953. Copeland, N.G., N.A. Jenkins, and D.L. Court, *Recombineering: a powerful new tool for mouse functional genomics.* Nat Rev Genet, 2001. **2**(10): p. 769-79.
954. Wu, S., et al., *A protocol for constructing gene targeting vectors: generating knockout mice for the cadherin family and beyond.* Nat Protoc, 2008. **3**(6): p. 1056-76.
955. Gong, S., L. Kus, and N. Heintz, *Rapid bacterial artificial chromosome modification for large-scale mouse transgenesis.* Nat Protoc, 2010. **5**(10): p. 1678-96.
956. Hofemeister, H., et al., *Recombineering, transfection, Western, IP and ChIP methods for protein tagging via gene targeting or BAC transgenesis.* Methods, 2011. **53**(4): p. 437-52.
957. Narayanan, K. and Q. Chen, *Bacterial artificial chromosome mutagenesis using recombineering.* J Biomed Biotechnol, 2011. **2011**: p. 971296.
958. Barakat, T.S., et al., *Precise BAC targeting of genetically polymorphic mouse ES cells.* Nucleic Acids Res, 2011 Oct;39(18):e121.
959. Beck, J.A., et al., *Genealogies of mouse inbred strains.* Nat Genet, 2000. **24**(1): p. 23-5.
960. Abremski, K. and R. Hoess, *Bacteriophage P1 site-specific recombination. Purification and properties of the Cre recombinase protein.* J Biol Chem, 1984. **259**(3): p. 1509-14.

961. Abremski, K., R. Hoess, and N. Sternberg, *Studies on the properties of P1 site-specific recombination: evidence for topologically unlinked products following recombination.* Cell, 1983. **32**(4): p. 1301-11.
962. Zhang, Z. and B. Lutz, *Cre recombinase-mediated inversion using lox66 and lox71: method to introduce conditional point mutations into the CREB-binding protein.* Nucleic Acids Res, 2002. **30**(17): p. e90.
963. Oberdoerffer, P., et al., *Unidirectional Cre-mediated genetic inversion in mice using the mutant loxP pair lox66/lox71.* Nucleic Acids Res, 2003. **31**(22): p. e140.
964. Hogan B, B.R., Costantini F, Lacy E, ed. *Manipulating the Mouse Embryo.* 1994, Cold Spring Harbor Laboratory Press: Cold Spring Harbor, New York.
965. Eakin, G.S. and A.K. Hadjantonakis, *Production of chimeras by aggregation of embryonic stem cells with diploid or tetraploid mouse embryos.* Nat Protoc, 2006. **1**(3): p. 1145-53.
966. Eggan, K., et al., *Male and female mice derived from the same embryonic stem cell clone by tetraploid embryo complementation.* Nat Biotechnol, 2002. **20**(5): p. 455-9.
967. Zhao, X.Y., et al., *Production of mice using iPS cells and tetraploid complementation.* Nat Protoc, 2010. **5**(5): p. 963-71.
968. Sambrook J, *Molecular Cloning: A Laboratory Manual* third edition ed. 2000, Cold Spring Harbor, New York: Cold Spring Harbor Laboratory Press
969. Lin, S. and P. Talbot, *Methods for culturing mouse and human embryonic stem cells.* Methods Mol Biol, 2011. **690**: p. 31-56.
970. Meissner, A., S. Eminli, and R. Jaenisch, *Derivation and manipulation of murine embryonic stem cells.* Methods Mol Biol, 2009. **482**: p. 3-19.
971. Nichols, J. and Q.L. Ying, *Derivation and propagation of embryonic stem cells in serum- and feeder-free culture.* Methods Mol Biol, 2006. **329**: p. 91-8.
972. Laird, P.W., et al., *Simplified mammalian DNA isolation procedure.* Nucleic Acids Res, 1991. **19**(15): p. 4293.
973. Buecker, C., et al., *A murine ESC-like state facilitates transgenesis and homologous recombination in human pluripotent stem cells.* Cell Stem Cell, 2010. **6**(6): p. 535-46.
974. Lyon, M.F., et al., *A Mouse Translocation Suppressing Sex-Linked Variegation.* Cytogenetics, 1964. **15**: p. 306-23.
975. Chow, J. and E. Heard, *X inactivation and the complexities of silencing a sex chromosome.* Curr Opin Cell Biol, 2009. **21**(3): p. 359-66.
976. Lee, J.T., *Regulation of X-chromosome counting by Tsix and Xite sequences.* Science, 2005. **309**(5735): p. 768-71.
977. Xu, M. and P.R. Cook, *The role of specialized transcription factories in chromosome pairing.* Biochim Biophys Acta, 2008. **1783**(11): p. 2155-60.
978. Hailesellasse Sene, K., et al., *Gene function in early mouse embryonic stem cell differentiation.* BMC Genomics, 2007. **8**: p. 85.
979. Burgoyne, P.S., et al., *The genetic basis of XX-XY differences present before gonadal sex differentiation in the mouse.* Philos Trans R Soc Lond B Biol Sci, 1995. **350**(1333): p. 253-60 discussion 260-1.
980. Lee, J.T., *Functional intergenic transcription: a case study of the X-inactivation centre.* Philos Trans R Soc Lond B Biol Sci, 2003. **358**(1436): p. 1417-23; discussion 1423.
981. Shin, J., et al., *Maternal Rnf12/RLIM is required for imprinted X-chromosome inactivation in mice.* Nature, 2010. **467**(7318): p. 977-81.
982. Ahn, J.Y. and J.T. Lee, *Retinoic acid accelerates downregulation of the Xist repressor, Oct4, and increases the likelihood of Xist activation when Tsix is deficient.* BMC Dev Biol, 2010. **10**: p. 90.
983. Kim, J., et al., *An extended transcriptional network for pluripotency of embryonic stem cells.* Cell, 2008. **132**(6): p. 1049-61.
984. Ostendorff, H.P., et al., *Functional characterization of the gene encoding RLIM, the corepressor of LIM homeodomain factors.* Genomics, 2000. **69**(1): p. 120-30.
985. Takagi, N., *Differentiation of X chromosomes in early female mouse embryos.* Exp Cell Res, 1974. **86**(1): p. 127-35.
986. Okamoto, I., et al., *Evidence for de novo imprinted X-chromosome inactivation independent of meiotic inactivation in mice.* Nature, 2005. **438**(7066): p. 369-73.
987. Barakat, T.S. and J. Gribnau, *X chromosome inactivation in the cycle of life.* Development, 2012. **139**(12): p. 2085-9.

988. Lee, J.T., *Disruption of imprinted X inactivation by parent-of-origin effects at Tsix.* Cell, 2000. **103**(1): p. 17-27.
989. Navarro, P., et al., *Molecular coupling of Tsix regulation and pluripotency.* Nature, 2010. **468**(7322): p. 457-60.
990. Navarro, P., et al., *The X-inactivation trans-activator Rnf12 is negatively regulated by pluripotency factors in embryonic stem cells.* Hum Genet, 2011. **130**(2): p. 255-64.
991. Gillich, A., et al., *Epiblast stem cell-based system reveals reprogramming synergy of germline factors.* Cell Stem Cell, 2012. **10**(4): p. 425-39.
992. Tsai, C.L., et al., *Higher order chromatin structure at the X-inactivation center via looping DNA.* Dev Biol, 2008. **319**(2): p. 416-25.
993. Navarro, P. and P. Avner, *When X-inactivation meets pluripotency: an intimate rendezvous.* FEBS Lett, 2009. **583**(11): p. 1721-7.
994. Nesterova, T.B., et al., *Pluripotency factor binding and Tsix expression act synergistically to repress Xist in undifferentiated embryonic stem cells.* Epigenetics Chromatin, 2011. **4**(1): p. 17.
995. Cecchi, C. and P. Avner, *Genomic organization of the mottled gene, the mouse homologue of the human Menkes disease gene.* Genomics, 1996. **37**(1): p. 96-104.
996. Hosler, B.A., et al., *Expression of REX-1, a gene containing zinc finger motifs, is rapidly reduced by retinoic acid in F9 teratocarcinoma cells.* Mol Cell Biol, 1989. **9**(12): p. 5623-9.
997. Scotland, K.B., et al., *Analysis of Rex1 (zfp42) function in embryonic stem cell differentiation.* Dev Dyn, 2009. **238**(8): p. 1863-77.
998. Kim, J.D., et al., *Rex1/Zfp42 as an epigenetic regulator for genomic imprinting.* Hum Mol Genet, 2011. **20**(7): p. 1353-62.
999. Masui, S., et al., *Rex1/Zfp42 is dispensable for pluripotency in mouse ES cells.* BMC Dev Biol, 2008. **8**: p. 45.
1000. Kim, J.D., C. Faulk, and J. Kim, *Retroposition and evolution of the DNA-binding motifs of YY1, YY2 and REX1.* Nucleic Acids Res, 2007. **35**(10): p. 3442-52.
1001. van den Berg, D.L., et al., *An Oct4-centered protein interaction network in embryonic stem cells.* Cell Stem Cell, 2010. **6**(4): p. 369-81.
1002. Soler, E., et al., *A systems approach to analyze transcription factors in mammalian cells.* Methods, 2011. **53**(2): p. 151-62.
1003. Dignam, J.D., R.M. Lebovitz, and R.G. Roeder, *Accurate transcription initiation by RNA polymerase II in a soluble extract from isolated mammalian nuclei.* Nucleic Acids Res, 1983. **11**(5): p. 1475-89.
1004. Nora, E.P., et al., *Spatial partitioning of the regulatory landscape of the X-inactivation centre.* Nature, 2012. **485**(7398): p. 381-5.
1005. Anguera, M.C., et al., *Tsx produces a long noncoding RNA and has general functions in the germline, stem cells, and brain.* PLoS Genet, 2011. **7**(9): p. e1002248.
1006. Tian, D., S. Sun, and J.T. Lee, *The long noncoding RNA, Jpx, is a molecular switch for X chromosome inactivation.* Cell, 2011. **143**(3): p. 390-403.
1007. Chureau, C., et al., *Ftx is a non-coding RNA which affects Xist expression and chromatin structure within the X-inactivation center region.* Hum Mol Genet, 2011. **20**(4): p. 705-18.
1008. Spencer, R.J., et al., *A boundary element between Tsix and Xist binds the chromatin insulator Ctcf and contributes to initiation of X-chromosome inactivation.* Genetics, 2011. **189**(2): p. 441-54.
1009. Gontan, C., et al., *RNF12 initiates X-chromosome inactivation by targeting REX1 for degradation.* Nature, 2012. **485**(7398): p. 386-90.
1010. Schoenfelder, S., et al., *Preferential associations between co-regulated genes reveal a transcriptional interactome in erythroid cells.* Nat Genet, 2010. **42**(1): p. 53-61.
1011. Augui, S., E.P. Nora, and E. Heard, *Regulation of X-chromosome inactivation by the X-inactivation centre.* Nat Rev Genet, 2011. **12**(6): p. 429-42.
1012. Dixon, J.R., et al., *Topological domains in mammalian genomes identified by analysis of chromatin interactions.* Nature, 2012. **485**(7398): p. 376-80.
1013. Nesterova, T.B., et al., *Loss of Xist imprinting in diploid parthenogenetic preimplantation embryos.* Dev Biol, 2001. **235**(2): p. 343-50.
1014. Wang, Z. and R. Jaenisch, *At most three ES cells contribute to the somatic lineages of chimeric mice and of mice produced by ES-tetraploid complementation.* Dev Biol, 2004. **275**(1): p. 192-201.
1015. Dvash, T., N. Lavon, and G. Fan, *Variations of X chromosome inactivation occur in early passages of female human embryonic stem cells.* PLoS One, 2010. **5**(6): p. e11330.

1016. Lengner, C.J., et al., *Derivation of pre-X inactivation human embryonic stem cells under physiological oxygen concentrations.* Cell, 2010. **141**(5): p. 872-83.
1017. Hanna, J., et al., *Human embryonic stem cells with biological and epigenetic characteristics similar to those of mouse ESCs.* Proc Natl Acad Sci U S A, 2010. **107**(20): p. 9222-7.
1018. Diaz Perez, S.V., et al., *Derivation of new human embryonic stem cell lines reveals rapid epigenetic progression in vitro that can be prevented by chemical modification of chromatin.* Hum Mol Genet, 2012. **21**(4): p. 751-64.
1019. Tchieu, J., et al., *Female human iPSCs retain an inactive X chromosome.* Cell Stem Cell, 2010. **7**(3): p. 329-42.
1020. Ananiev, G., et al., *Isogenic pairs of wild type and mutant induced pluripotent stem cell (iPSC) lines from Rett syndrome patients as in vitro disease model.* PLoS One, 2011. **6**(9): p. e25255.
1021. Cheung, A.Y., et al., *Isolation of MECP2-null Rett Syndrome patient hiPS cells and isogenic controls through X-chromosome inactivation.* Hum Mol Genet, 2011. **20**(11): p. 2103-15.
1022. Amenduni, M., et al., *iPS cells to model CDKL5-related disorders.* Eur J Hum Genet, 2011. **19**(12): p. 1246-55.
1023. Pomp, O., et al., *Unexpected X chromosome skewing during culture and reprogramming of human somatic cells can be alleviated by exogenous telomerase.* Cell Stem Cell, 2011. **9**(2): p. 156-65.
1024. Marchetto, M.C., et al., *A model for neural development and treatment of Rett syndrome using human induced pluripotent stem cells.* Cell, 2010. **143**(4): p. 527-39.
1025. Kim, K.Y., E. Hysolli, and I.H. Park, *Neuronal maturation defect in induced pluripotent stem cells from patients with Rett syndrome.* Proc Natl Acad Sci U S A, 2011. **108**(34): p. 14169-74.
1026. Bruck, T. and N. Benvenisty, *Meta-analysis of the heterogeneity of X chromosome inactivation in human pluripotent stem cells.* Stem Cell Res, 2011. **6**(2): p. 187-93.
1027. Sperger, J.M., et al., *Gene expression patterns in human embryonic stem cells and human pluripotent germ cell tumors.* Proc Natl Acad Sci U S A, 2003. **100**(23): p. 13350-5.
1028. Mitjavila-Garcia, M.T., et al., *Partial reversal of the methylation pattern of the X-linked gene HUMARA during hematopoietic differentiation of human embryonic stem cells.* J Mol Cell Biol, 2010. **2**(5): p. 291-8.
1029. Park, I.H., et al., *Disease-specific induced pluripotent stem cells.* Cell, 2008. **134**(5): p. 877-86.
1030. Huangfu, D., et al., *Induction of pluripotent stem cells from primary human fibroblasts with only Oct4 and Sox2.* Nat Biotechnol, 2008. **26**(11): p. 1269-75.
1031. Lyssiotis, C.A., et al., *Reprogramming of murine fibroblasts to induced pluripotent stem cells with chemical complementation of Klf4.* Proc Natl Acad Sci U S A, 2009. **106**(22): p. 8912-7.
1032. Warlich, E., et al., *Lentiviral vector design and imaging approaches to visualize the early stages of cellular reprogramming.* Mol Ther, 2011. **19**(4): p. 782-9.
1033. Mekhoubad, S., et al., *Erosion of dosage compensation impacts human iPSC disease modeling.* Cell Stem Cell, 2012. **10**(5): p. 595-609.
1034. Anguera, M.C., et al., *Molecular signatures of human induced pluripotent stem cells highlight sex differences and cancer genes.* Cell Stem Cell, 2012. **11**(1): p. 75-90.
1035. Nazor, K.L., et al., *Recurrent variations in DNA methylation in human pluripotent stem cells and their differentiated derivatives.* Cell Stem Cell, 2012. **10**(5): p. 620-34.
1036. Tomoda, K., et al., *Derivation conditions impact x-inactivation status in female human induced pluripotent stem cells.* Cell Stem Cell, 2012. **11**(1): p. 91-9.
1037. Najm, F.J., et al., *Isolation of epiblast stem cells from preimplantation mouse embryos.* Cell Stem Cell, 2011. **8**(3): p. 318-25.
1038. O'Leary, T., et al., *Tracking the progression of the human inner cell mass during embryonic stem cell derivation.* Nat Biotechnol, 2012. **30**(3): p. 278-82.
1039. Ostendorff, H.P., et al., *Ubiquitination-dependent cofactor exchange on LIM homeodomain transcription factors.* Nature, 2002. **416**(6876): p. 99-103.
1040. Hiratani, I., et al., *Selective degradation of excess Ldb1 by Rnf12/RLIM confers proper Ldb1 expression levels and Xlim-1/Ldb1 stoichiome' y in Xenopus organizer functions.* Development, 2003. **130**(17): p. 4161-75.
1041. Ostendorff, H.P., et al., *Dynamic expression of LIM cofactors in the developing mouse neural tube.* Dev Dyn, 2006. **235**(3): p. 786-91.
1042. Scanlan, M.J., et al., *Antigens recognized by autologous antibody in patients with renal-cell carcinoma.* Int J Cancer, 1999. **83**(4): p. 456-64.

1043. Gaspar, C., et al., *Cross-species comparison of human and mouse intestinal polyps reveals conserved mechanisms in adenomatous polyposis coli (APC)-driven tumorigenesis.* Am J Pathol, 2008. **172**(5): p. 1363-80.
1044. Zhang, L., et al., *RNF12 Controls Embryonic Stem Cell Fate and Morphogenesis in Zebrafish Embryos by Targeting Smad7 for Degradation.* Mol Cell, 2012. **46**(5): p. 650-61.
1045. Macdonald, D.H., et al., *Cloning and characterization of RNF6, a novel RING finger gene mapping to 13q12.* Genomics, 1999. **58**(1): p. 94-7.
1046. Lo, H.S., et al., *Identification of somatic mutations of the RNF6 gene in human esophageal squamous cell carcinoma.* Cancer Res, 2002. **62**(15): p. 4191-3.
1047. Lopez, P., et al., *Gene control in germinal differentiation: RNF6, a transcription regulatory protein in the mouse sertoli cell.* Mol Cell Biol, 2002. **22**(10): p. 3488-96.
1048. Jaenisch, R. and R. Young, *Stem cells, the molecular circuitry of pluripotency and nuclear reprogramming.* Cell, 2008. **132**(4): p. 567-82.
1049. Jani, M.M., et al., *Molecular characterization of tiny ring X chromosomes from females with functional X chromosome disomy and lack of cis X inactivation.* Genomics, 1995. **27**(1): p. 182-8.
1050. Tomkins, D.J., et al., *Lack of expression of XIST from a small ring X chromosome containing the XIST locus in a girl with short stature, facial dysmorphism and developmental delay.* Eur J Hum Genet, 2002. **10**(1): p. 44-51.
1051. Namekawa, S.H., et al., *Postmeiotic sex chromatin in the male germline of mice.* Curr Biol, 2006. **16**(7): p. 660-7.
1052. Williams, L.H., et al., *Transcription precedes loss of Xist coating and depletion of H3K27me3 during X-chromosome reprogramming in the mouse inner cell mass.* Development, 2011. **138**(10): p. 2049-57.
1053. Chuva de Sousa Lopes, S.M., et al., *X chromosome activity in mouse XX primordial germ cells.* PLoS Genet, 2008. **4**(2): p. e30.
1054. de Napoles, M., T. Nesterova, and N. Brockdorff, *Early loss of Xist RNA expression and inactive X chromosome associated chromatin modification in developing primordial germ cells.* PLoS One, 2007. **2**(9): p. e860.
1055. Sugimoto, M. and K. Abe, *X chromosome reactivation initiates in nascent primordial germ cells in mice.* PLoS Genet, 2007. **3**(7): p. e116.
1056. Mise, N., et al., *Differences and similarities in the developmental status of embryo-derived stem cells and primordial germ cells revealed by global expression profiling.* Genes Cells, 2008. **13**(8): p. 863-77.
1057. Takagi, N., et al., *Reversal of X-inactivation in female mouse somatic cells hybridized with murine teratocarcinoma stem cells in vitro.* Cell, 1983. **34**(3): p. 1053-62.
1058. Do, J.T., et al., *Erasure of cellular memory by fusion with pluripotent cells.* Stem Cells, 2007. **25**(4): p. 1013-20.
1059. Guo, G. and A. Smith, *A genome-wide screen in EpiSCs identifies Nr5a nuclear receptors as potent inducers of ground state pluripotency.* Development, 2010. **137**(19): p. 3185-92.
1060. Eggan, K., et al., *X-Chromosome inactivation in cloned mouse embryos.* Science, 2000. **290**(5496): p. 1578-81.
1061. Inoue, K., et al., *Impeding Xist expression from the active X chromosome improves mouse somatic cell nuclear transfer.* Science, 2010. **330**(6003): p. 496-9.
1062. Maherali, N. and K. Hochedlinger, *Tgfbeta signal inhibition cooperates in the induction of iPSCs and replaces Sox2 and cMyc.* Curr Biol, 2009. **19**(20): p. 1718-23.
1063. Takagi, N. and K. Abe, *Detrimental effects of two active X chromosomes on early mouse development.* Development, 1990. **109**(1): p. 189-201.
1064. Guy, J., et al., *Reversal of neurological defects in a mouse model of Rett syndrome.* Science, 2007. **315**(5815): p. 1143-7.
1065. Gadalla, K.K., M.E. Bailey, and S.R. Cobb, *MeCP2 and Rett syndrome: reversibility and potential avenues for therapy.* Biochem J, 2011. **439**(1): p. 1-14.
1066. Michalon, A., et al., *Chronic pharmacological mGlu5 inhibition corrects fragile X in adult mice.* Neuron, 2012. **74**(1): p. 49-56.

Appendix

Abbreviations
Summary
Samenvatting
Curriculum Vitae
List of publications
PhD portfolio
Acknowledgments

Abbreviations

BAC: Bacterial Artificial Chromosome
BF: Blocking Factor
CF: Competence Factor
(h)ES cell: (human) Embryonic Stem cell
EpiSC: Epiblast derived Stem Cell
FISH: Fluorescent *In Situ* Hybridization
ICM: Inner Cell Mass
(h)iPS cell: (human) induced Pluripotent Stem cell
iXCI: imprinted X Chromosome Inactivation
Mb: Mega base
MSCI: Meiotic Sex Chromosome Inactivation
MYA: Million Years Ago
OMIM: Online Mendelian Inheritance in Man database
PAR: Pseudoautosomal Region
PGCs: Primordial Germ Cells
rXCI: random X Chromosome Inactivation
TBP: TATA Binding Protein
Xa: active X chromosome
XAR: X Added Region
Xce: X controlling element
XCI: X Chromosome Inactivation
XCR: X Conserved Region
Xi: inactive X chromosome
Xic: X inactivation center
XicHR: X inactivation center Homologous Region
Xist: X inactive specific transcript
Xm: maternally derived X chromosome
Xp: paternally derived X chromosome, or short art of the human X chromosome
Xpr: X pairing region
Xq: long arm of the human X chromosome
YAC: Yeast Artificial Chromosome

Summary

The evolution of placental mammals has resulted in a genetic mechanism of sex determination with X and Y sex chromosomes, where females of most species have two X chromosomes and the males have a single X chromosome and a small Y chromosome. These sex chromosomes originated from a non-sex-specific pair of autosomes. In males the deterioration of the Y chromosome resulted in a loss of genes, compared to the X chromosome. To balance this loss, the single X chromosome in males became transcriptionally up-regulated, resulting in a dosage compensation mechanism between genes located on the sex chromosomes and genes on autosomes. In females, this up-regulation of X-linked genes resulted in a subsequent dosage problem, as two copies of X chromosomes are present. Therefore, in females, an additional dosage compensation mechanism was required, which results in the transcriptional silencing of a single X chromosome in females. This silencing of an X chromosome in females, leaving one active X chromosome per diploid genome, is called X chromosome inactivation (XCI), and is the central topic in this thesis work.

XCI occurs during early female embryonic development, and results in transcriptional silencing of one X chromosome in females, thereby equalizing the dosage of X-linked genes between both sexes and between the sex chromosomes and autosomes. This is needed for proper biochemical and physiological functioning of cells in the body, as gene products derived from the X chromosome need to interact with gene products from autosomal genes. Aberrations of the crucial XCI process are believed to be lethal, as no healthy females are observed having more than one active X chromosome, and females in which parts of both X chromosomes are fully active suffer from severe phenotypes. The XCI process itself is random regarding the choice of the X chromosome that will be inactivated, resulting in silencing of either the X chromosome derived from the father or the X chromosome derived from the mother, in the cells forming the embryo. Therefore, growing and adult females consist of a mosaic of two different cell populations, which can have profound impacts on health and disease manifestations in females, as described in the Introduction in Chapter 1. Many genes located on the X chromosome can cause diseases when mutated. In general, females suffer less from X-chromosomal diseases, due to the presence of the mosaic, in which some cells will express the mutant gene, whereas others will express the non-mutated backup copy from the healthy X chromosome. Such a backup mechanism is not possible in males carrying a single X chromosome, who therefore always show expression of an X-linked mutation. Besides this advantage for females, of having two X chromosomes, there is also a disadvantage. The XCI process seems to be difficult to establish properly in all female cells, which might explain higher female lethality during peri-implantation development. Furthermore, the presence of mosaicism can sometimes cause a disease, when the choice of inactivation is not random between the X chromosomes present. Therefore, insight in the mechanisms resulting in epigenetic silencing of a single X chromosome in females is needed, and XCI is an important subject to study.

Following the initial discovery of the XCI process in 1961 by Mary Lyon, many investigations have tried to unravel the mechanisms leading to the shut-down of one X chromosome in females. Most of these studies have been performed in mice, by making use of either genetic mouse models or embryonic stem (ES) cells. ES cells are pluripotent cells derived from early embryos, and can be used to study several aspects of the XCI process in a culture dish, as undifferentiated female ES cells have two active X chromosomes, and upon differentiation to more specialized cells these cells engage in XCI, similar to what happens in early embryonic development. By making use of these models, studies have shown that a small region of the X chromosome, the X inactivation center (Xic), is crucial for XCI to occur, as this process is only initiated in cells having two copies of this regulatory region on two distinct X chromosomes. The Xic harbors several conserved genes, of which the *X inactive transcript* (*Xist*) is crucial for XCI to occur. *Xist* is the only gene which is specifically expressed from the inactive X chromosome, and transcription of this gene results in a non-coding RNA, which spreads along the X chromosome and induces silencing. Another non-coding gene, *Tsix*, has been found in the Xic, and this gene is transcribed in the opposite direction to *Xist* and functions as a negative regulator of *Xist*.

During female embryonic development, or upon ES cell differentiation, *Xist* is specifically up-regulated on a single X chromosome, thereby starting the XCI process. Even 20 years after the discovery of *Xist*, a longstanding question has remained how this gene is specifically up-regulated on a single X chromosome in cells having more than one X chromosome. Several models have tried to explain this female specific initiation of XCI, and in the past, we have proposed that sex-specific initiation of XCI is regulated by a stochastic process. In this model, autosomally-encoded XCI-inhibitors prevent XCI in undifferentiated cells or cells in early embryos, by directly inhibiting *Xist* or stimulating *Tsix*. These XCI-inhibitors are encoded by genes located on autosomes, in both sexes, so that an identical level of XCI repression will be present. In contrast, X-encoded activators of XCI will stimulate the XCI process. These activators are encoded by X-linked genes, which implies that in females a two-fold higher dosage of XCI-activators will be present compared to males. These activators are most likely developmentally regulated, with low or absent expression in undifferentiated cells. Therefore, in undifferentiated cells, XCI will be absent, and will only be initiated during differentiation, as XCI activators will become up-regulated. This up-regulation will most likely occur in both sexes, but only in females the level of activation will be high enough to reach a threshold which is set by the combined action of the XCI-inhibitors. In this model, XCI-activators work in *trans*, meaning that they can activate XCI on all X chromosomes in a cell nucleus, independent from which X chromosome they are derived, resulting in a stochastic choice which *Xist* allele will become up-regulated. Once up-regulation has occurred, silencing of the XCI-activator gene in *cis*, thus on the same X chromosome where *Xist* will spread, will also silence the XCI-activator gene. Hence, the level of XCI-activator will drop, to a level which is now similar to that of a male cell harboring a single X chromosome. This simple mechanism ensures that XCI initiation on the other X chromosome will be prevented. *Tsix* is also silenced in *cis*, so that XCI can be maintained on the X chromosome which has started inactivation despite the lower level of the XCI-activators. Therefore, in this model, initiation of XCI is regulated by a sex-specific dosage difference in XCI-activators.

Although this model could principally explain all features of the XCI initiation mechanism, the identity of the XCI-activator genes remained illusive. We therefore set out to identify genes encoding such activators. By making use of a Bacterial Artificial Chromosome (BAC) transgenesis screen in ES cells, described in Chapter 2, we identified X-encoded RNF12 as the first known XCI activator. When *Rnf12* was over-expressed in male ES cells, this resulted in XCI initiation on the single X chromosome, and over-expression in female ES cells resulted in XCI on both X chromosomes in a significant portion of cells. During differentiation of ES cells, endogenous *Rnf12* becomes up-regulated, and a two-fold higher dose of RNF12 has been found in female compared to male ES cells prior to and during XCI initiation. After XCI has occurred, expression levels are equal between male and female cells. This two-fold higher dosage of RNF12 explains female specific initiation of XCI, as only in female cells a threshold will be reached upon differentiation which is needed to overcome repression of XCI by XCI-inhibitors, resulting in *Xist* accumulation. These XCI-inhibitors are mainly pluripotency associated factors, which either repress *Xist* directly, or indirectly, via stimulation of *Tsix* expression, or they might even work via repression of XCI-activators. In line with this, over-expression of *Rnf12* even leads to initiation of XCI in undifferentiated cells, indicating that absence of XCI-activator activity is important in preventing XCI in undifferentiated cells. More evidence for an important role of RNF12 in the initiation of XCI was obtained when one of the two copies of *Rnf12* was removed from female ES cells, as this resulted in delayed XCI initiation in these cells, favoring inactivation of the X chromosome harboring the *Rnf12* deletion. To generate this and other genetic modifications of ES cells described throughout this thesis work, we developed a new BAC targeting strategy described in Chapter 3, which makes use of polymorphic ES cells. Chapter 4 discusses the identification of RNF12 as an XCI-activator, and describes this discovery in more detail in the context of the stochastic model of XCI initiation. We next asked the question whether RNF12 is essential for XCI to occur, by generation and analysis of *Rnf12* knockout ES cells, described in Chapter 5. These cells were found to be devoid of XCI, providing evidence that XCI is not occurring in the absence of this crucial activator. Additional genetic experiments performed indicated that the XCI-activating function of RNF12 works mainly on *Xist*, as *Xist* transgenes were higher expressed when *Rnf12* was over-expressed, whereas the expression of *Tsix* transgenes was not affected. As RNF12 is an E3 ubiquitin ligase, it seems likely that such *Xist* activation should involve an indirect mechanism, in which RNF12 would target a repressor of *Xist* for proteasomal degradation. Indeed, studies aiming to identify the interaction partners of RNF12, described in Chapter 6, indicated that RNF12 targets the pluripotency associated transcription factor REX1 for degradation. REX1 was found to bind the *Xist* promoter and distal region, thereby repressing *Xist* expression in undifferentiated cells. Upon differentiation, *Rnf12* will become up-regulated, leading to a dose-dependent catalysis of the breakdown of REX1, which will result in loss of repression of *Xist*, and hence will lead to initiation of XCI. The *Rnf12* gene is located in the near vicinity of *Xist*, which ensures rapid silencing of *Rnf12* transcription in *cis* shortly after initiation of XCI. Chapter 7 addresses the question whether other genes located between *Xist* and *Rnf12* are also functional in the regulation of the XCI process. We found that *Jpx*, *Ftx* and the *Xpr* region have a *cis* regulatory role, in which these regions likely create an active environment, which is needed to enable activation of *Xist* by the *trans* action of

RNF12. We propose to divide the Xic in a *cis*-Xic, composed of all genes and elements involved in the regulation of *Xist* and *Tsix* expression in *cis*, and a *trans*-Xic, which is required for *trans* regulation of the *cis*-Xic, and hence for counting the number of X chromosomes present. We also provide evidence which suggest that direct interaction between the two X chromosomes in a female nucleus, referred to as X-pairing, is not functionally required for XCI to occur. Rather, more evidence was obtained supporting an indispensible role for the *trans* action of RNF12, even for the maintenance of XCI initiation.

We next proceeded to test the role of RNF12 *in vivo*, by generating an *Rnf12* knockout mouse model, described in Chapter 8. As expected from the observations showing loss of XCI in *Rnf12* homozygous knockout ES cells, homozygous *Rnf12* knockout females are not born, suggesting that RNF12 has an important role in XCI initiation during *in vivo* development. Females heterozygous for the *Rnf12* mutation also have an XCI phenotype, with transcriptional activity from two X chromosomes in some cells from adult tissues representing loss of XCI. This surprising and remarkable phenotype might make it necessary to change the dogma that living with two active X chromosomes is not possible. This awaits detailed investigation, but promises to have important implications for the understanding and future therapies of X-linked diseases in humans. Finally, in Chapter 9, we proceeded to translate the newly obtained knowledge on the regulation of XCI initiation from mouse to human. We studied XCI in female human induced pluripotent stem cells, and provide evidence that the X chromosome that is inactivated in a founder human fibroblast becomes reactivated upon somatic reprogramming. This might allow future generation of novel model systems to study XCI in humans. The General Discussion, Chapter 10, aims to integrate our current views on the initiation of XCI with previously published observations, and provides an outlook for future investigations.

In conclusion, the work described in this thesis has allowed us to obtain novel insights in the mechanisms controlling the initiation of XCI, including the role of RNF12, and provides a framework for future studies investigating the possibility to live with two active X chromosomes.

Samenvatting

De evolutie van zoogdieren heeft geresulteerd in een genetisch mechanisme van geslachtsdeterminatie waarbij vrouwen van de meeste soorten twee X geslachtschromosomen hebben, in tegenstelling tot mannen met een enkel X chromosoom en daarnaast een Y geslachtschromosoom. De X en Y geslachtschromosomen zijn ontstaan uit een niet-geslachtsgebonden chromosomenpaar. Het snelle verlies van genen van het Y chromosoom, in tegenstelling tot een geleidelijke toename van het aantal genen op het X chromosoom, heeft geresulteerd in een situatie waarbij het X chromosoom verreweg de meeste genen bevat. Het Y-chromosomale verlies van genen werd gecompenseerd door een verhoging van de gen-transcriptie van het enkele X chromosoom in mannen, zodat een vergelijkbare dosis van geslachtsgebonden en niet-geslachtsgebonden genen behouden werd. Aangezien vrouwen twee X chromosomen hebben, zou een dergelijke verhoogde transcriptie van X-chromosomale genen tot een nieuw gendosis-probleem in vrouwen leiden. Dit werd voorkomen door een mechanisme, waarbij één van beide X chromosomen van de vrouw wordt uitgeschakeld. Dit proces, genaamd X-chromosoom-inactivatie (XCI), resulteert in niet meer dan één actief X chromosoom per vrouwelijk diploid genoom, en is het centrale onderwerp van dit proefschrift.

XCI vindt plaatst tijdens de vroege embryonale ontwikkeling van vrouwen, en resulteert in het uitschakelen van één van beide X chromosomen, waardoor de juiste dosis van X-gebonden genen tussen de geslachten, en tussen de geslachts- en de niet-geslachtsgebonden chromosomen behouden blijft. Dit is noodzakelijk om belangrijke processen in cellen goed te kunnen laten verlopen, aangezien veel genproducten van het X chromosoom in de juiste verhouding moeten kunnen samenwerken met genproducten van andere chromosomen. Afwijkingen in het cruciale XCI proces zijn dan ook embryonaal lethaal. Er zijn geen gezonde vrouwen waarbij volledige activiteit van beide X chromosomen werd vastgesteld, en zelfs de dubbele activiteit van kleine delen van het X chromosoom kan leiden tot aanzienlijke ziekteprocessen. Het XCI proces zelf kent een aspect van toeval, waarbij in cellen van het vrouwelijke embryo het X chromosoom verkregen van moeder of het X chromosoom verkregen van vader wordt uitgeschakeld. Door dit willekeurige proces zijn vrouwen een mozaïek van twee verschillende celpopulaties, hetgeen een aanzienlijk effect kan hebben op de manifestatie van ziekten, zoals beschreven in de Inleiding in Hoofdstuk 1. Vele genen gelokaliseerd op het X chromosoom kunnen ziekten veroorzaken indien zij afwijkend zijn, maar over het algemeen zijn ziekteverschijnselen bij vrouwen dankzij dit mozaïek milder vergeleken met mannen, aangezien veel cellen in vrouwen het intacte gen tot expressie zullen brengen. In mannen is een dergelijk back-up mechanisme niet mogelijk, en daarom zullen afwijkingen op het enkele X chromosoom altijd tot uitdrukking komen. Afgezien van deze voordelen voor vrouwen, zijn er ook nadelen verbonden aan het bezit van twee X chromosomen. Er zijn aanwijzingen dat het moeilijk is om het XCI proces goed te laten verlopen in alle vrouwelijke cellen tijdens de embryonale ontwikkeling, hetgeen de hogere sterfte van vrouwelijke embryo's tijdens de vroege embryonale ontwikkeling voorafgaand aan en rondom de implantatie fase zou kunnen verklaren. Tevens kan de aanwezigheid van een mozaïek soms ook problemen veroorzaken, in het bijzonder als de keus tussen het inactiveren van één van de X chromosomen niet willekeurig is. Daardoor is het van belang

om meer over dit belangrijke proces, dat kan worden gekenmerkt als een epigenetisch proces, te weten te komen.

Sinds de ontdekking van het XCI proces door Mary Lyon in 1961, zijn vele studies gewijd aan het ontrafelen van de mechanismen die er toe leiden dat in vrouwen één X chromosoom wordt uitgeschakeld. Het merendeel van deze studies heeft gebruik gemaakt van muismodellen of muis embryonale stamcellen (ES cellen). ES cellen zijn pluripotente cellen, nog niet gedifferentieerd, verkregen uit embryo's, die gebruikt kunnen worden om het XCI proces in een kweekschaal te bestuderen. Ongedifferentieerde vrouwelijke ES cellen hebben twee actieve X chromosomen, maar ondergaan het XCI proces als deze cellen naar andere, meer gespecialiseerde celtypen worden gedifferentieerd, waarbij deze cellen een eerste differentiatiestap tijdens de vroege embryonale ontwikkeling simuleren. Door gebruik te maken van deze modellen hebben studies laten zien dat een klein gedeelte van het X chromosoom, het zogenaamde X inactivatie centrum (Xic), vereist is om XCI plaats te laten vinden. Meerdere, in verschillende soorten geconserveerde, genen zijn gelokaliseerd in dit Xic, en het meest belangrijke is het *X inactieve transcript* (*Xist*) gen *Xist* is het enige gen dat specifiek actief is op het inactieve X chromosoom, en transcriptie van dit gen resulteert in een niet-coderend RNA, hetgeen over het X chromosoom kan spreiden en daardoor het X chromosoom kan uitschakelen. Een ander gen, *Tsix*, is tevens gelokaliseerd in de buurt van *Xist*. *Tsix* wordt in de tegenovergestelde richting afgeschreven in vergelijking met *Xist*, en is een negatieve regulator van het *Xist* gen.

Tijdens de vroege embryonale ontwikkeling van vrouwen of tijdens ES cel-differentiatie wordt het XCI proces gestart met de specifieke verhoging van transcriptie van het *Xist* gen. Ondanks dat het reeds 20 jaar geleden is dat *Xist* ontdekt werd, blijft een belangrijke vraag hoe het komt dat dit gen alleen wordt geactiveerd als meer dan één X chromosoom aanwezig is in de celkern. Verschillende modellen hebben geprobeerd om dit te verklaren, en wij hebben een stochastisch model voorgesteld. In dit model wordt XCI in ongedifferentieerde ES cellen of vroege embryo's voorkomen door de werking van XCI-remmers, die gecodeerd worden door niet-geslachtsgebonden chromosomen. Deze remmen *Xist* direct, of stimuleren de negatieve regulator *Tsix*. Aangezien in dit model de XCI-remmers afkomstig zijn van genen op niet-geslachtsgebonden chromosomen, zal de mate van repressie in vrouwelijke en mannelijke cellen gelijk zijn. In tegenstelling tot deze XCI-remmers, leiden XCI-activatoren tot activatie van het XCI proces. Indien deze XCI-activatoren gecodeerd worden door genen gelokaliseerd op het X chromosoom, zal in ongedifferentieerde vrouwelijke cellen met nog twee actieve X chromosomen een tweevoudige dosis van activatoren aanwezig zijn vergeleken met mannelijke cellen die maar één X chromosoom hebben. Naar verwachting zijn XCI-activatoren ontwikkelingsbiologisch gereguleerd, zodat ze tijdens ongedifferentieerde celstadia laag, of zelfs geheel niet, tot expressie komen. Hierdoor zal het proces van XCI in ongedifferentieerde cellen niet op gang komen. Echter tijdens differentiatie en verdere ontwikkeling van de cellen zal de expressie van deze XCI-activator genen toenemen, in beide geslachten. De twee actieve X chromosomen in vrouwelijke cellen zorgen voor een hoge dosis XCI-activatoren, voldoende om de remming van het XCI proces door de XCI-remmers te overkomen. De XCI-activatoren werken in *trans*, hetgeen betekend dat ze zowel XCI op het X chromosoom van waar zij geproduceerd worden als ook op alle andere X chromosomen in de celkern kunnen activeren. Dit heeft tot gevolg dat het een

willekeurige keuze zal zijn, welke kopie van *Xist* geactiveerd wordt. Eenmaal geactiveerd, zal *Xist* RNA over het X chromosoom spreiden, in *cis*, en X chromosomale genen op datzelfde X chromosoom uitschakelen. Hierdoor worden ook vrij snel de XCI-activator genen uitgeschakeld, hetgeen er voor zal zorgen dat de concentratie van XCI-activatoren in de celkern weer zal afnemen, zodat XCI niet plaats kan vinden op het tweede X chromosoom in dezelfde celkern. Aangezien de negatieve regulator *Tsix* ook wordt uitgeschakeld, zal de lagere dosis XCI-activator, die nu vergelijkbaar is met de dosis in mannelijke cellen, voldoende zijn om initiatie van XCI te behouden. Samengevat, in dit model wordt initiatie van het XCI proces dus gereguleerd door een geslachtsspecifiek verschil in de dosis van XCI-activatoren.

Hoewel dit model in principe alle eigenschappen van het XCI proces zou kunnen beschrijven, was de identiteit van de XCI-activator nog onbekend. We hebben daarom dit onderzoek gestart met een zoek-strategie om deze XCI-activatoren te identificeren, waarbij we gebruik maakten van bacteriële artificiële chromosomen (BACs) die we tot hoge expressie brachten in ES cellen. Door deze strategie, die beschreven staat in Hoofdstuk 2, ontdekten wij dat het door het X-chromosoom gecodeerde RNF12 eiwit de functie van XCI-activator kan uitoefenen. Wanneer het *Rnf12* gen tot hoge expressie werd gebracht in mannelijke ES cellen, resulteerde dit in XCI initiatie van het enkele X chromosoom in deze mannelijke cellen, en hoge expressie in vrouwelijke ES cellen resulteerde in XCI van beide X chromosomen in een hoog percentage van de cellen. Tijdens differentiatie van ES cellen komt het normaal aanwezige X-gebonden *Rnf12* gen ook hoger tot expressie, en een tweevoudige dosis van RNF12 werd gevonden in vrouwelijke cellen, vergeleken met mannelijke cellen, voor en tijdens XCI initiatie. Nadat de initiatie van het XCI proces is afgerond, is de hoeveelheid RNF12 gelijk tussen cellen van beide geslachten. Met dit dosis-afhankelijke mechanisme kan worden verklaard dat initiatie van XCI plaatsvindt in vrouwelijke cellen. De XCI-remmers zijn met name betrokken bij het in stand houden van de pluripotente staat van ongedifferentieerde cellen, en remmen *Xist* direct, of indirect via stimulatie van *Tsix* expressie. Tevens zouden zij kunnen werken via remming van de XCI-activatoren. Dit laatste wordt ondersteund door de vinding dat hoge expressie van RNF12 reeds tot activatie van XCI leidt in ongedifferentieerde cellen, hetgeen erop wijst dat remming van XCI-activatoren een belangrijk mechanisme zou kunnen zijn om XCI in ongedifferentieerde cellen te voorkomen. Meer bewijs voor een belangrijke rol van RNF12 bij de initiatie van XCI werd verkregen door het genetisch verwijderen van één van de twee X-gebonden *Rnf12* genen in vrouwelijke ES cellen. Dit resulteerde in vertraagde initiatie van XCI in deze cellen, die bij voorkeur het X chromosoom waarop het gemuteerde *Rnf12* gen was gelokaliseerd uitzetten. Om deze en andere genetische modificaties van ES cellen te bewerkstelligen, ontwikkelden wij een nieuwe BAC targeting strategie, die beschreven staat in Hoofdstuk 3 van dit proefschrift, en die gebruik maakt van polymorfe ES cellen verkregen door kruisingen van verschillende muizenstammen. In Hoofdstuk 4 bespreken we meer uitvoerig de bevindingen verkregen uit de *Rnf12* proeven, en zetten we deze uiteen in de context van het stochastische model van XCI. In het vervolg vroegen wij ons af of RNF12 een essentiële rol heeft in het XCI proces. Om dit te beantwoorden genereerden wij *Rnf12* knockout ES cellen, zoals beschreven in Hoofdstuk 5. In deze cellen bleek XCI niet op te treden tijdens differentiatie, hetgeen bevestigd dat RNF12 een cruciale rol bij het tot stand brengen van dit XCI proces speelt. Andere experimenten lieten zien dat de XCI-

activerende functie van RNF12 voornamelijk via *Xist* activatie werkt, aangezien *Xist* transgenen hoger tot expressie kwamen wanneer *Rnf12* tot hoge expressie werd gebracht, terwijl expressie van *Tsix* transgenen niet werd beïnvloed. RNF12 is een E3 ubiquitine ligase, een enzym dat betrokken is bij proteasomale eiwit-afbraak, en het is daarom aannemelijk dat deze *Xist* activatie verloopt via een indirect mechanisme, waarbij RNF12 een remmer van *Xist* zou markeren voor afbraak. Inderdaad lieten studies beschreven in Hoofdstuk 6 zien dat RNF12 de pluripotentie-geassocieerde transcriptiefactor REX1 target voor deze vorm van afbraak. We vonden dat REX1 bindt aan de *Xist* promotor, waardoor het de expressie van *Xist* remt in ongedifferentieerde cellen. Tijdens differentiatie komt RNF12 hoger tot expressie, hetgeen zal leiden tot een dosis-afhankelijke afbraak van REX1, waardoor de rem op *Xist* expressie verdwijnt en het XCI proces op gang zal komen. Op het X chromosoom is *Rnf12* dicht bij *Xist* gelokaliseerd. Dit zorgt ervoor dat na XCI initiatie *Rnf12* spoedig wordt uitgeschakeld in *cis*. In Hoofdstuk 7 behandelen wij de vraag of ook andere genen in de buurt van *Xist* en *Rnf12* betrokken zijn bij het XCI proces. Hier vonden wij dat *Jpx*, *Ftx* en de *Xpr* regio een rol spelen in de *Xist* regulatie in *cis*, hetgeen nodig zal zijn om RNF12 in staat te stellen om *Xist* in *trans* te kunnen activeren. Daarom stellen wij een nieuwe indeling van het Xic voor, waarbij we spreken van een *cis*-Xic, een regio die alle genen en elementen bevat die noodzakelijk zijn voor de *cis* regulatie van *Xist* en *Tsix*, en een *trans*-Xic, die nodig is voor de *trans* regulatie van de *cis*-Xic, met andere woorden voor het tellen van de hoeveelheid X chromosomen die aanwezig zijn. Verder vonden wij in experimenten beschreven in hetzelfde Hoofdstuk dat directe interactie tussen de beide X chromosomen, aangeduid met *X-pairing*, niet noodzakelijk is voor normale regulatie van XCI. In tegenstelling daarvan brachten deze experimenten verder inzicht in de belangrijke rol van RNF12 ook tijdens het in stand houden van de XCI. Om vast te stellen of RNF12 inderdaad een belangrijke rol *in vivo* speelt hebben wij een *Rnf12* deficiënt muismodel ontwikkeld, hetgeen beschreven staat in Hoofdstuk 8. Zoals reeds verwacht aan de hand van de *Rnf12* knockout ES cellen die geen XCI meer initiëren, bleken vrouwelijke *Rnf12* knockout muizen niet levensvatbaar, hetgeen suggereert dat RNF12 ook een belangrijke rol speelt tijdens de embryonale ontwikkeling *in vivo*. Heterozygote $Rnf12^{+/-}$ vrouwtjes hebben ook een XCI fenotype, waarbij in volwassen muizen cellen aanwezig zijn die twee actieve X chromosomen hebben. Deze verrassende vinding dient verder te worden onderzocht, en zou belangrijke nieuwe inzichten kunnen verschaffen over onze kennis en mogelijk nieuwe behandelingen van X-chromosomale ziekten. Tevens kan aan de hand van dit muismodel wellicht het dogma worden bijgesteld, waarbij ervan wordt uitgegaan dat de aanwezigheid van twee actieve X chromosomen niet levensvatbaar is. Tenslotte, in Hoofdstuk 9 proberen we onze nieuwe inzichten in de XCI regulatie in muizen te vertalen naar de mens, waarbij we XCI hebben bestudeerd in vrouwelijke humane geïnduceerde pluripotente stamcellen. Hier vonden wij dat het geïnactiveerde X chromosoom in humane fibroblasten tijdens het reprogrammeren gereactiveerd wordt. Dit kan mogelijk helpen om toekomstige modelsystemen te genereren om humane XCI te bestuderen. De Algemene Discussie in Hoofdstuk 10 vat de gevonden data samen, integreert deze met eerder gepubliceerde studies en biedt een vooruitzicht op toekomstige studies. Concluderend heeft het werk beschreven in dit proefschrift bijgedragen aan nieuwe inzichten in de regulatie van XCI en de rol van RNF12 hierin, en biedt het een basis voor toekomstige studies die zullen onderzoeken in hoeverre het mogelijk is om met twee actieve X chromosomen te leven.

Curriculum Vitae

Name: Tahsin Stefan Barakat
Born: 25 May 1984
City of Birth: Meerbusch, Germany
Place of Living: Wissenkerke, The Netherlands

Educational Background:

2008-2012	PhD student Erasmus MC, University Medical Center, Rotterdam Department of Reproduction and Development
2004-2008	Master of Science in Molecular Medicine Erasmus MC, University Medical Center, Rotterdam
2007-2008	Department of Reproduction and Development Master thesis "*Searching for an X-linked activator of X chromosome inactivation*", supervisor Prof.dr. Joost Gribnau
2006-2007	Department of Experimental Pathology Internship, "*Characterization of tumor-microenvironment derived effects on Wnt/β-catenin signalling and invasiveness of colorectal cancer cells*", supervisor Prof.dr. Riccardo Fodde
2006	Short lab rotations Department of Cell Biology, supervisor Prof.dr. Elaine Dzierzak Department of Experimental Pathology, supervisor Dr. Ron Smits
2003-2007	Medicine study, Erasmus MC, University Medical Center, Rotterdam
2004-2007	Doctoral exam (*cum laude*)
2003-2004	Propaedeutic exam
1997-2003	Gymnasium, Pontes Scholengemeenschap, Locatie Het Goese Lyceum, Goes
2003	Voorbereidend Wetenschappelijk onderwijs (VWO) exam (*cum laude*)
1990-1997	Primary education in Germany and The Netherlands

Curriculum Vitae

Tahsin Stefan Barakat was born on the 25th May of 1984 in Meerbusch, West-Germany. After primary school in Germany and The Netherlands, he graduated *cum laude* for his *Voorbereidend Wetenschappelijk Onderwijs (VWO)* exam in 2003 at the *Pontes Scholengemeenschap, Locatie Het Goese Lyceum*, Goes. In 2003 he started his medical study at the Erasmus MC / Erasmus University, Rotterdam. In 2004 he graduated for his Propaedeutic exam, and was elected for the Master of Science in Molecular Medicine programme at the Erasmus MC. After following several courses belonging to the programme, he performed in 2006 short laboratory rotations at the Departments of Cell Biology (Prof.dr. Elaine Dzierzak) and Experimental Pathology (Dr. Ron Smits). In 2007 he performed a six month research project at the Department of Experimental Pathology under supervision of Prof.dr. Riccardo Fodde, entitled *Characterization of tumor-microenvironment derived effects on Wnt/β-catenin signalling and invasiveness of colorectal cancer cells.* In 2007 he graduated for his Medical Doctoral exam (*cum laude*). From September 2007 until summer 2008 he was at the Department of Reproduction and Development under supervision of Dr. Joost Gribnau, were he performed the studies described in his Master Thesis, entitled *Searching for an X-linked activator of X chromosome inactivation.* From 2008 onwards, he continued his research in the same laboratory as a PhD student, performing the studies described in this thesis, with Prof.dr. J.Anton Grootegoed and Prof.dr. Joost Gribnau as promotors. In July 2012, he visited the laboratory of Prof.dr. Edith Heard in Paris, to perform FISH experiments on post-implantation embryos. After his public thesis defence in September 2012, he will continue his medical study with the clinical internships to obtain the degree of Medical Doctor, to be followed by a further scientific research career as a post-doctoral fellow.

List of publications

1. Iris Jonkers*, **Tahsin Stefan Barakat***, Eskeatnaf Mulugeta Achame, Kim Monkhorst, Annegien Kenter, Eveline Rentmeester, Frank Grosveld, J. Anton Grootegoed and Joost Gribnau (2009) "RNF12 is an X-Encoded dose-dependent activator of X chromosome inactivation" *Cell* 139(5):999-1011
   * both authors contributed equally
2. **Tahsin Stefan Barakat**, Iris Jonkers, Kim Monkhorst and Joost Gribnau (2010) "X-changing information on X inactivation" *Exp Cell Res* 10;316(5):679-87
3. Christa Buecker, Hsu-Hsin Chen, Jose Maria Polo, Laurence Daheron, Lei Bu, **Tahsin Stefan Barakat**, Patricia Okwieka, Andrew Porter, Joost Gribnau, Konrad Hochedlinger, and Niels Geijsen (2010) "A murine ESC-like state facilitates transgenesis and homologous recombination in human pluripotent stem cells" *Cell Stem Cell* 6:535-46.
4. **Tahsin Stefan Barakat** and Joost Gribnau (2010) "X chromosome inactivation and embryonic stem cells" *Adv Exp Med Biol* 695: 132-154.
5. **Tahsin Stefan Barakat**, Nilhan Gunhanlar, Cristina Gontan Pardo, Eskeatnaf Mulugeta Achame, Mehrnaz Ghazvini, Ruben Boers, Annegien Kenter, Eveline Rentmeester, J.Anton Grootegoed and Joost Gribnau (2011) "RNF12 activates *Xist* and is essential for X chromosome inactivation" *PLoS Genet.* 2011;7(1):e1002001
6. **Tahsin Stefan Barakat**, Eveline Rentmeester, Frank Sleutels, J. Anton Grootegoed and Joost Gribnau (2011) "Precise BAC targeting of genetically polymorphic mouse ES cells" *Nucleic Acids Res* 2011 Oct;39(18):e121
7. Long Zhang, Huizhe Huang, Fang Fang Zhou, Joost Schimmel, Cristina Gontan Pardo, Tingting Zhang, **Tahsin Stefan Barakat**, Kelly-Ann Sheppard, Craig Mickanin, Jeff A. Porter, Alfred C.O. Vertegaal, Hans van Dam, Joost Gribnau, Chris X. Lu, and Peter ten Dijke (2012) "RNF12 Controls Embryonic Stem Cell Fate and Morphogenesis in Zebrafish Embryos by Targeting SMAD7 for Degradation" *Mol Cell* 46:650-61.
8. Cristina Gontan, Eskeatnaf Mulugeta Achame, Jeroen Demmers, **Tahsin Stefan Barakat**, Eveline Rentmeester, Wilfred van IJcken, J. Anton Grootegoed and Joost Gribnau (2012) "RNF12 initiates X chromosome inactivation by targeting REX1 for degradation" *Nature* 2012 **485**(7398): p. 386-90
9. **Tahsin Stefan Barakat** and Joost Gribnau (2012) "X chromosome inactivation in the cycle of life" *Development* 139 (12): 2085-2089
10. **Tahsin Stefan Barakat** and Joost Gribnau (2012) "A Restriction Fragment Length Polymorphism based Bacterial Artificial Chromosome targeting strategy for efficient and fast generation of knockout alleles in polymorphic mouse Embryonic Stem cells" (*Manuscript in preparation*)
11. Erwin Brosens, Elisabeth M. de Jong, **Tahsin Stefan Barakat**, Bert H Eussen, Barbara D'haene, Elfride de Baere, Pino P Poddighe, Robert-Jan Galjaard, Joost Gribnau, Alice S Brooks, Dick Tibboel, and Annelies de Klein (2012) "Congenital malformations of the gastro-intestinal tract and Triple X syndrome" *(Submitted)*

12. **Tahsin Stefan Barakat**, Selma van Staveren, Friedemann Loos, Elvira Myronova, Mehrnaz Ghazvini, J. Anton Grootegoed and Joost Gribnau (2012) "Initiation of X inactivation is regulated by *trans*-acting activators and *cis*-acting elements: no evidence for a functional involvement of X-pairing" *(Submitted)*

PhD portfolio

General Academic Skills:
From Development to Disease course, 2009
Article 9 Animal Experimentation course, 2010

Presentations:

2009
BSIK Stem Cells in Development and Disease Conference, Rotterdam
7th Winter School of the International Graduiertenkolleg, Kleinwalsertal, Austria
2nd Dutch Stem Cell Meeting, Rotterdam
1st Erasmus Stem Cell Institute (ESI) meeting, Rotterdam
16th MGC PhD Student Workshop, Brugge, Belgium (Best Oral Presentation)
3rd SCDD International Symposium "Stem Cells, Development and Regulation" Amsterdam

2010
8th Winter School of the International Graduiertenkolleg, Kleinwalsertal, Austria

2011
Winter Symposium, "Epigenetics in Development and Disease", Miami, United States of America
4th Dutch Stem Cell Meeting, Leiden
18th MGC PhD Student Workshop, Maastricht
3rd X inactivation Conference, "50 years of X inactivation research", EMBO-workshop, Oxford, United Kingdom

2012
2nd Winter School of the Collaborative Research Center (TRR 81), "Chromatin Changes in Differentiation and Malignancies", Kleinwalsertal, Austria
Paris-Rotterdam X chromosome inactivation meeting, Spetses, Greece
10th Annual meeting of the International Society for Stem Cell Research (ISSCR), Yokohama, Japan

Awards:

Travel grant of the International Society for Stem Cell Research (ISSCR) for the 10th Annual meeting in Yokohama, Japan, 2012

International seminars, workshops and conferences:

2008
Stem Cell Symposium, "Stem Cell, Development and Regulation", Amsterdam

2009
European Molecular Biology Organisation (EMBO) meeting, Amsterdam
MGC day 2009, Rotterdam
Stem Cell Symposium, "Stem Cell, Development and Regulation", Amsterdam
JNI Symposium, "The stem of cancer", Rotterdam

2010
Epigenome Network of Excellence meeting: "Imprinting and X inactivation", Emmetten, Switserland
3rd Dutch Stem Cell meeting, Utrecht
Erasmus Stem Cell Institute Opening Symposium, Rotterdam (poster contribution)
Stem Cell Symposium, "Stem Cell, Development and Regulation", Amsterdam
8th Annual Meeting of the International Society for Stem Cell Research (ISSCR), San Francisco, United States of America

2011
6th International meeting, Stem Cell Network North-Rhine-Westphalia, Essen, Germany (Poster contribution)
International Symposium "Chromatin Changes in Differentiation and Malignancies", Giessen, Germany (Poster contribution)

Teaching activities:

Junior Science Program:
Supervision lab rotation Junior Science program, October 2009
Supervision Profielwerkstuk Junior Science student 2010-2011

Teaching Medical Curriculum Erasmus MC:
Course "Development of internal and external genitalia", November 2008
Course "Development of internal and external genitalia", December 2009
Course "Early embryos, cloning and transgenesis" November 2010
Course Embryology 2nd year Medicine/Master of Science programme, January 2010

Master of Science in Molecular Medicine Program:
Supervision lab rotation MSc Mol Med student, February 2009
Supervision lab rotation MSc Mol Med student, October 2009
Supervision lab rotation MSc Mol Med student, January 2010
Supervision MSc Thesis Selma van Staveren, "Initiation of X chromosome Inactivation" 2010-2011
Supervision MSc Thesis Elvira Myronova, 2011-2012

Acknowledgements

Finally, after a long journey, I'm arriving at the finish. For sure it has been a long journey, in which I travelled approximately 516780 km or 12.9 times around the earth; that's the distance you travel if you live in Zeeland and study and work in Rotterdam, during 5 years of study and 4 years of PhD. If I just look back at the last 4 years, many things have happened during that period, here just a small selection of the "really important" things:

The layout of the faculty changed completely and we also changed a bit the view on X chromosome inactivation; unnecessary wars have unfortunately been characterizing the politics in the world, we arrived in a economical crisis, the 7 billions human being has been born, a mad person with colored hair tried to come up for the rights of *Henk* and *Ingrid* in Dutch politics, but instead yet another round of new elections is upcoming. A nuclear catastrophe was necessary to finally result in a different view on nuclear energy. And two Olympic Games and several football tournaments passed by, with the only constant being that in every important football match I look at, my favorite team does not win.

So a lot has happened and changed in the world, and for sure also I changed due to the many positive but sometimes also negative events which happened during this journey. I came across many people during that exciting trip, and to all of them I would like to say thank you!

In particular, my special acknowledgements go to the following people:

Beste Joost, mijn promotor, of te wel Prof.dr. Gribnau! Er zijn heel veel dingen waarvoor ik jou zou willen bedanken, waar moet ik nu mee starten? Misschien gewoon eens bij het begin, in de tijd dat je nog gewoon Joost was. Voor het eerst heb ik jou ontmoet tijdens het keuzeonderwijs geneeskunde, ver terug in het tweede jaar van mijn studie, toen je mij en een groepje andere Master studenten begeleidde. Toen viel jij al op als een man die vrijwel altijd een glimlach op zijn gezicht heeft, en die eigenlijk altijd goed gehumeurd is, met een ontzettend uitgebreide lach. Later heb ik jou wat beter leren kennen met het Academische Jaarprijs team, en toen was eigenlijk voor mij snel de keuze gemaakt om naar jouw lab te komen. Dank je wel dat je mij toen hebt aangenomen als eigenwijze student, en mij tijdens mijn Master jaar veel kansen en vrijheden hebt gegeven, waardoor ik veel ruimte kreeg om mijn eigen ideeën in te brengen. En dat jaar was vrij bijzonder, met onze *Rnf12* ontdekking, die ons hele onderzoek in een stroomversnelling liet terecht komen. Het was toen dan ook een soort van logische beslissing dat ik bleef hangen om ook nog mijn promotieonderzoek bij je te doen, en ook voor dat wil ik je graag bedanken! De afgelopen 4 jaren waren een fantastische periode, waarin ik veel van je heb kunnen leren, en waarin we veel gedaan gekregen hebben. Het was bijzonder en ook erg leerzaam om mee te maken hoe een klein

labje met een handvol mensen uitgroeide tot het Imperium Gribnau, met bijna teveel mensen en ruimtegebrek. En ineens muteerde je dan ook nog van Joost tot bijzonder hoogleraar Joost. Je familie, Suzanne, Caroline, Willem en Thijs kunnen trots op je zijn! Bedankt dat ik dit allemaal heb kunnen meemaken, en ook bedankt voor het feit dat je mij altijd de ruimte die ik nodig heb, hebt gegeven, en mij altijd gesteund hebt. Het was een plezier om voor je te werken, en ik hoop dat we ook nog in de toekomst veel dingen met elkaar kunnen doen.

Professor Grootegoed, beste Anton, mijn andere promotor! Ook jou wil ik bedanken voor veel dingen. Allereerst voor je enthousiasme waarmee je gewone geneeskunde studenten dankzij jouw Master of Science in Molecular Medicine programma transformeert in echte wetenschappers. Natuurlijk ook voor het feit dat je mij binnen je afdeling hebt laten werken, en voor het vele nuttige commentaar gedurende de laatste jaren. Bij heel veel Monday Morning meetings heb ik jou (en waarschijnlijk ook anderen) lastig gevallen met lange presentaties met veel data, maar jij wist ondanks dat toch altijd weer essentiële opmerkingen te maken, die belangrijk waren voor de richting in mijn onderzoek. Ook was jij zeer belangrijk voor het schrijven van artikelen, waarbij je altijd weer door je net wat andere kijk op de dingen belangrijke suggesties kon doen, en deze hebben ook de afgelopen maanden erg bijgedragen aan het tot stand komen van dit proefschrift. Bedankt hiervoor! Ook al vroeg je volgens mij bij elk gesprek wat we buiten het werk om hadden hoe laat mijn laatste bus naar Zeeland zou vertrekken, ik vond het altijd heel leuk om met jou te kletsen.

Mijn dank geldt ook de leden van de kleine commissie voor het lezen van mijn manuscript, en het geven van de nodige suggesties. Frank Grosveld en Robert-Jan Galjaard, heel erg bedankt hiervoor. Dear Edith Heard, thank you so much for reading my manuscript, and giving me important feedback. Although we of course don't agree on everything, it's important to see someone else view on the thinks.

Niels Geijssen en Ruud Delwel, bedankt dat jullie de tijd hebben genomen om vandaag naar mijn verdediging te komen. Dat waardeer ik zeer.

Many people have worked in our group during the past years. To all of you, thank you!
Iris en Kim, bedankt voor de vele dingen die jullie mij in het begin hebben geleerd. Dankzij jullie werd ik ingewijd in de geheimen van de FISH, PCR en andere labtrucjes. Eskeww, you were there from the beginning onwards, and it was always great fun with you. Also scientifically, you contributed a lot with your bioinformatics knowhow. Thanks for the many printing related answers you could provide me recently during the preparation of this book. Good luck with your future career, and with Artemis and Helen. Cristina, thanks for all your contributions. Although we sometimes had our problems, I always appreciated your scientific input. I wish you all the best for your future, for Lara and Raymond, but unfortunately not for the Spanish football team... Eveline, bedankt voor de MEFs. Cathérine, er is waarschijnlijk niemand waarmee ik zoveel gelachen heb als met jou! Dank je voor de vele leuke tijd die we in en na San Francisco met elkaar hadden. Wat mij betreft staat onze afspraak, om elkaar daar over nu nog 38 jaar terug te zien, nog steeds.

Friedemann, dank Dir für die Verdoppelung des Deutschen Anteills im Labor, und Deine Hilfe. Vielleicht wirst Du ja doch noch einmal ein Fän eines richtigem Fussballvereins... Viel Erfolg die nächsten Jahre! Agnese thank you for being as you are! It was a pleasure for me to be your personal information desk, and remember, when it's closed, you can always ask Ballotelli... I'm happy for you, you found a different farmer than the one we saw in Oxford. Mehrnaz, dank je voor het feit dat je de afgelopen jaren een goede vriendin geworden bent! We kennen elkaar al lang uit ons vorige lab, en ik vond het erg leuk dat we uiteindelijk zoveel met iPS cellen samen konden werken. We hebben over heel veel dingen (soms heftig) gesproken de afgelopen jaren, en al die gesprekken hebben mij vaak zeer geholpen. Japan met jou was een bijzondere belevenis! Hai! Ook bedankt voor het bijstaan tijdens mijn verdediging. Veel geluk voor de toekomst, en voor Arjen en Saeed. Tracy, ook jou bedankt voor je vele hulp! Annegien, Bas, Cheryl, Daphne, Ruben en Zeli, ook jullie bedankt!

I was lucky to get a lot of help from several talented Master students. Nilhan, although you were not my student, I saw you often passing by with that one famous question of you ("I have a question"). It was always fun answering them, and it was really nice to start to collaborate even more at the end of your project. Good luck with your own PhD! Selma! Mijn eerste "echte" student! Het was erg bijzonder om jouw begeleider te zijn. Ik zal maar niet weer over de generatiekloof beginnen... Wat heb ik met jou gelachen! Het was heel erg indrukwekkend wat je allemaal in een jaar gedaan hebt, en het was een groot plezier om met jou samen te werken. Op een gegeven moment konden we elkaar echt blind begrijpen, en ook buiten het werk om hadden we snel een goede draad gevonden. Het was en is een plezier! Veel succes met je co-schappen, waarin je nu mijn voorbeeld kunt zijn. Elvira, mijn tweede student! Jij bent compleet anders, maar toch niet minder leuk! Het duurde even een beetje voordat ik doorhad hoe jij werkt, maar ook met jou heb ik vele grappige momenten meegemaakt, die ik niet zou willen missen. Bedankt voor al je hulp, en succes voor je toekomst! Selma en Elvira, jullie ook nog een keer beiden bedankt voor het feit dat jullie mij ook tijdens mijn verdediging als Paranimfen bijstaan, ik ben trots op jullie!

Then there was also the second half of the lab:
Marja, bedankt voor al jouw hulp. Jij bent echt een bijzonder mens, en ik heb zelden iemand ontmoet die zo behulpzaam is als jij. Daarnaast ben je altijd op de hoogte van alle sportuitslagen en nieuwsmomenten, dus dat heeft tot de nodige leuke gesprekken geleid in de loop der jaren. Jij bent echt de goede ziel van het lab! Jos, ook jij bent uniek! Dank je voor de vele humoristische momenten en diepgaande conversaties met jou. Succes met je clubje! Aristea, thank you for giving me the opportunity to improve my 5 words of Greek. It was really nice to have you in the lab! Nathalie, je bent een hele bijzondere vriendin geworden!

Then all the others: Albert, Akiko, Benno, Esther, Evelyne, Fabrizia, Federica, Gerd, Godfried, Jeannette, Marjolein, Maureen, Peng, Sam, Willy. You all contributed in the one or other way during the last years, thank you for that!

Of course, the Erasmus MC is larger then only lab 9.02. One social meeting club is for sure the 10th floor (cell culture), where I met many nice persons. Fanny, thanks for the many nice things we did together at the start of our PhDs. I still didn't manage to convince you that there is nice weather in the Netherlands. Let's meet again soon! Gerben, dank je voor je gezelligheid en al je adviezen over spiercellen. Vind het nog steeds heel grappig dat we door een toevalsbevinding nu zelfs een collaboratie hebben, en natuurlijk, speciale dank voor de kooien, je weet waar ik het over heb... Alvin, ook jij maakt de celkweek tot een special environment. Also all the others, you are special as well: Polynikis, Parham, Thomas, Jessica, Carol, Jean-Charles, Catherine R, Dorota, Derk, Frank S, Parissa, Melodi, Jeffrey, Reinier, Siska, Dies, and Elaine. Also in the rest of the building, I found many nice people: Xiao, Tiana, Katharina amongst many others. Sahar (icecream), good luck in Amsterdam! Sabrina, viel Erfolg mit Deinem Medizin Studium! Bin mir sicher Du meisterst es mit Bravour! En ook niet onbelangrijk, Ron Smits, dank je dat je mij hebt leren pipetteren!

Then of course, research would not be possible without collaborations.
Niels Geijssen en Christa Buecker, thanks for letting us being part of the hLR5 story, and for sharing a lot of knowhow on iPS cells. Laurens, dank je voor de hulp met de Btk experimenten; het blijft komisch dat onze wegen elkaar blijven kruisen: Biologie Olympiade, Geneeskunde, Master, PhD voor co-schappen, en nu op het einde beginnen we nog samen te werken ook. Ben benieuwd naar de toekomst! Annelies en Bert, dank jullie voor de hulp met het in kaart brengen en verzamelen van onze patiënten fibroblast lijnen. Suzanne Frynts, bedankt voor de patiënten samples. Peter ten Dijke and Long Zhang, thank you for the fruitful collaboration on RNF12 and Tgf-ß signalling. Dear Catherine Corbel, Patricia Diabangouaya and Edith Heard, thanks for the post-implantation embryo FISH experiments in Paris. Looking forward to our future collaborations!

Carmen, Rebecca, Caroline, Clara, Elena, Famous en Merle, danke für Eure grosse Freundschaft!

Und last but not least, die Person die mir am meisten am Herzen liegt, meine Mama. Nun ist es bald soweit, Du hast "deinen" Dokter! Die vielen Jahre der harten Arbeit haben sich ausgezahlt. In all den Jahren hast Du mich immer moralisch unterstützt, zu mir gehalten und aufgebaut in schweren Stunden. Du warst immer für mich da, und dass werde ich Dir nie vergessen! Hab' Dich lieb!

Tahsin Stefan Barakat, August 2012